



*University of Cambridge
Department of Archaeology*

Geological reconnaissance and provenancing of potential Neolithic lithic sources in the Maltese Islands



This Thesis is submitted for the degree of Doctor of Philosophy

Petros Chatzimpaloglou
Magdalene College
Cambridge, March 2019

Declaration

This thesis is the result of my own work and includes nothing which is the outcome of work done in collaboration except as specified in the text.

It is not substantially the same as any that I have submitted, or, is being concurrently submitted for a degree or diploma or other qualification at the University of Cambridge or any other University or similar institution except as specified in the text. I further state that no substantial part of my thesis has already been submitted, or, is being concurrently submitted for any such degree, diploma or other qualification at the University of Cambridge or any other University or similar institution except as specified in the text.

It does not exceed the prescribed word limit (80,000 words) for the relevant Degree Committee.

Title: Geological reconnaissance and provenancing of potential Neolithic lithic sources in the Maltese Islands

Name: Petros Chatzimpaloglou

Abstract

This study aims to identify the petrological characteristics of Neolithic chert artefacts associated with the Temple Period (c. 4000-2500 cal BC) and their probable sources from the local Maltese chert formation as well as the main possible chert sources in Sicily. Were the chert and flint materials used by prehistoric Maltese peoples obtained from local sources or imported from abroad? In particular, the archaeological literature just assumes that the chert/flint and cultural attributes of the Temple period came from Sicily; this assumption has never been tested or proved.

There are also a number of important subsidiary questions which will stem from the implications of this investigation. These include: 1) to what extent were the Maltese people isolated or part of an extended Mediterranean network through trade or exchange relationships; 2) if they were isolated, how would they be able to survive in such a seemingly restricted environment?; 3) if they were more connected to external cultural groups, what was the impact of these connections on Maltese identity?; 4) were they deliberately sourcing raw stone material for specific purposes?; 5) was there a link between the properties of the rocks (quality) with the usage of the rock artefact? and how did Neolithic Maltese people understand and assess rock 'quality'? This last question has further related implications: 6) is the chaîne opératoire the same for all raw stone materials or does the quality and the type of rock have a significant effect on the process? These questions are not all definitively answerable in this thesis, but have a significant bearing on the results of the ERC-funded FRAGSUS project and other archaeological projects dealing with the islands' cultural development.

In addition to the above thematic lines of inquiry, this research investigates to what extent a scientific perspective on sourcing lithic artefacts can provide conclusive evidence of resource exploitation sources. Traditional archaeological methodologies for stone sourcing (largely based on macroscopic qualitative assessments) are often subjective and unreliable, or produce un-verifiable results. Therefore, a more scientific methodology designed for examining rock outcrops is a necessary addition to this process, and is the reason why I have selected a methodology based on the geological and petrological properties derived from the geological formation of the rock outcrops. The approach consists of both traditional and new geological techniques, including: a) macroscopic examination, b) Optical and Scanning Electron Microscopy (SEM), c) Fourier-Transform Infrared Spectroscopy (FTIRS) d) X-ray Fluorescence (XRF), and e) Laser ablation - Inductively Coupled Plasma - Mass Spectrometry (LA-ICP-MS). All of these strands of evidence have contributed to an over-arching chaîne opératoire

approach to link source – choice - manufacturing process – tool – use – discard aspects of the life of chert artefacts recovered from several key Neolithic sites in Malta and Gozo, namely from Xagħra Circle, Ġgantija, Tač-Ċawla, Santa Verna, Kordin and Skorba. Thus a major outcome of this research is to propose a specific methodology for the analysis and sourcing of chert artefacts for the wider Mediterranean region, which can be reliably used in future archaeological projects. To date, the geological and archaeological literature has suggested a long list of potentially informative techniques for sourcing lithic assemblages. However, there has not yet been any investigation which indicates the most informative and reliable combination of appropriate techniques. It is believed that the chosen techniques as applied to the Maltese Islands have produced reliable results on sourcing chert assemblages, as each method approaches a different, yet related quality of the rock.

In conclusion, the macroscopic, microscopic and geochemical characteristics of the chert sources and artefact assemblages have suggested a combination of mainly local chert sources during the Temple period of the Neolithic, as well as a more minor component of imported material from Sicily and another unknown source altogether. Moreover, the type of tools and manufacturing techniques have provided strong evidence of a distinct local craft tradition employed on the Maltese Islands during the late Neolithic. It further confirms the interaction with neighbouring societies and gives a possible indication of cultural influence and exchange. Finally, this study has presented a beneficial methodology for lithic analysis for all archaeological researchers working on the provenance of lithic material elsewhere in the Mediterranean area and the wider world.

Acknowledgements

It has been almost four years that I now reach to the end of an amazing journey full of knowledge, wisdom, adventures. During these years, I have met some remarkable individuals who made my experience in Cambridge one that I will always remember. Although some did not have a direct input, without the encouragement, practical advice and friendship of several of them my PhD thesis could not have been finished in its present form.

First and foremost, I wish to thank my supervisor Professor Charly French and my advisor Dr. Simon Stoddart (Department of Archaeology, University of Cambridge) for their advice, insight, limitless efforts and support throughout my research project. They gave me the freedom to explore on my own, but also provided their guidance when I was diverging. They were always next to me but never in front or behind me. I was extremely fortunate to have both of you and will always have my gratitude.

I am truly thankful to Professor Caroline Malone (Principal Investigator of FRAGSUS project) from Queen's University Belfast who gave me the opportunity to work within this great project and allowed me to be a member of an incredible team with top researchers. She believed in my abilities from the very beginning and her role was crucial to the conduct my research.

Moreover, I will like to thank all the members of FRAGSUS project who have contributed, in one way or the other, to my work and helped me complete it under the best conditions possible. Special thanks must go to Dr. Rowan McLaughlin (full-time Research Fellow with FRAGSUS) and Dr. Catriona Brogan (Post-doctoral Research Assistant with FRAGSUS) for their constant support, help and guidance.

My successful and efficient fieldwork on Malta and Sicily would not have been possible without the contribution of Martyn Pedley (Emeritus Reader in Carbonate Sedimentology, University of Hull). Not only did he provide his knowledge on their geology, but also accompanied me on some fieldwork investigations which was more than I expected, and it is something I will always be grateful for.

My sincere gratitude must go to all the amazing Maltese people which made FRAGSUS project possible. My research in Malta would not be possible without their approval help and guidance. They showed great interest and appreciation to my work for the very beginning which made me feel welcome and happy with my choice to do PhD research in this wonderful place. Their respect and enthusiasm towards archaeology and their professionalism are remarkable, and for that they will always have my respect. Dr. Anthony Pace (The Superintendence of Cultural Heritage, Malta), Sharron Sultana (Curator of the Museum of Archaeology in Valletta), Professor Nicholas Vella (Department of Archaeology, University of Malta), Nathaniel Cutajar and Dr Maxine Anastasi are only some of these great people and to whom I will always be indebted. Without their contribution, experience, help and support my research would not have been reach its current level.

I wish to warmly thank Dr Tonko Rajkovaca for his endless help, support and guidance with every step of my research as a very experienced researcher archaeologist. Although he was not directly involved in my research, he provided the necessary “out of the box” perspective that allowed me to overcome many obstacles in my research and on a personal level. I will never forget the many coffee-break discussions we had, which have been an excellent positive boost with which to continue working. Furthermore, he and his wife Vida have opened their house to me and made feel part of their family, which I consider a great privilege.

I would also like to thank the members of the McBurney Laboratory, Department of Archaeology, and in particular Dr David Beresford-Jones, Dr. David Friesem and Sean Taylor who have helped to create an excellent environment in the laboratory and with whom I discussed several aspects of my research. Moreover, I would like to thank my amazing lab colleagues Ian Ostericher, David Kay, and Joanna Walker who have contributed greatly to my PhD experience and life. Also, I would like to thank them for their patience and help with my English skills.

Magdalene College, the McBurney Laboratory, the Department of Archaeology, the Anthony Wilkin Fund, Sir Richard Stapley Trusy, the Smuts Fund and the Archaeology and Anthropology Fund have provided small but significant funds with which to conduct my research. I have been a self-funded student, but their generosity and contributions helped me to cover the essential fieldwork and laboratory expenses of my research and for that they have my dearest gratitude. To that extent, I would like to thank Professor Paul Dupree (Graduate Tutor, Magdalene college) for his essential help and guidance on securing this funding.

I cannot forget the brilliant and sincere friends Chrysa Agapitou, Pedro Magalhães de Oliveira, and Michael Papageorgiou with whom we went through the best and also the hardest times together and I am really grateful that I have them by my side. Special acknowledgement must be given to Michael, who in a difficult time for me provided one of the most positive and inspiring pieces of advice which I quote: “All will be fine in the end and if there are not fine then the end is yet to come!”

It was also a pleasure and honour for me to meet and share a small but important part of my life with Roxine Staats, Ashley Hannay and Michael Lewis. They are unique individuals whose quality was shown during difficult times and their friendship in many beautiful moments. None could expect more and for that they will always have a special place in my heart.

I would like to give many thanks to Jess Thompson, Eoin Parkison, Jeremy Bennett and Ben Hinson. They were the very first people I met in Cambridge and created a safe and friendly environment around me which helped greatly to have a smooth transition into a new and different country. Moreover, I want to thank them for their kindness in answering all my archaeological questions.

My enormous gratitude must go to Harry Lamden, Antonia Symeonidou, Ashley Hannay, Cara Davinson, Maria Kotsovili, Sushana Cass and Michael Lewis. They were my proof-reading team, who first read my thesis and did an amazing job in raising its standard to proper English.

Most of all I want to thank my family which without their love, financial support and advice I would not have been able to reach to this stage and certainly not have done my PhD in Cambridge. This thesis is dedicated to my grandmother, Voula, who had always surrounded me with her crazy Greek style love and although she is not here to see me graduating, I know she is by my side. Additionally, this achievement goes to my grandfather, Othon, who in his 92 years still requires a monthly report of my whereabouts and when I am coming home.

Contents

Abstract	ii
Acknowledgements.....	iv
1 Introduction.....	1
2 Geology and Geo-environment	4
2.1 Geology and Geo-environment of the Maltese Islands	4
2.1.1 Geography	4
2.1.2 Geology	6
2.1.3 Stratigraphy of the Maltese Islands	10
2.1.4 Previous work.....	20
2.1.5 Structural and Tectonic Geology of the Maltese Islands	21
2.1.6 Geomorphology.....	23
2.2 Geology of the Sicily Island	24
2.2.1 Geology	24
2.2.2 Previous work.....	30
2.3 Chert rock formation	31
2.3.1 The origin of Chert.....	31
2.3.2 Chemical composition	32
2.3.3 Mineralogy and texture.....	32
2.3.4 Forms of Chert rocks	33
2.3.5 Varieties of Cherts	34
3 Archaeological Research.....	35
3.1 The Prehistory of Malta.....	35
3.1.1 Literature Review of the research on the Neolithic Period of Malta	36
3.2 The Archaeological Sites Investigated.....	39
3.2.1 Ġgantija (Temple Site).....	39
3.2.2 Brochtorff–Xagħra Circle (Burial Site)	41
3.2.3 Santa Verna (Temple Site).....	42
3.2.4 Taç-Ċawla (Settlement Site)	43
3.2.5 Skorba Temples (Stone Temple and Settlement Site).....	44
3.2.6 Kordin Temples (Temple Sites).....	45
3.3 Lithic provenance	47
3.3.1 Lithic provenance on a global scale.....	47
3.3.2 Malta	57
3.4 <i>Chaîne opératoire</i> approach.....	59
3.4.1 Literature review	60
4 Materials and Methods.....	61

4.1	Field Research.....	61
4.2	Laboratory research	62
5	Results.....	67
5.1.	Macroscopic Examination	75
5.1.1.	Chert Formations.....	75
5.1.1.1.	Maltese Islands	75
5.1.1.2.	Sicily	82
5.1.2.	Chert Assemblages	93
5.1.2.1.	The Brochtorff Xagħra Circle assemblage	93
5.1.2.2.	Kordin assemblage.....	99
5.1.2.3.	Taċ-Ċawla assemblage.....	104
5.1.2.4.	Santa Verna assemblage.....	109
5.1.2.5.	Ġgantija assemblage.....	114
5.1.2.6.	Skorba assemblage	119
5.1.3.	First remarks.....	130
5.2.	Optical Microscopy	132
5.2.1.	Chert Formations.....	132
5.2.1.1.	Maltese Islands	132
5.2.1.2.	Sicily	135
5.2.2.	First remarks.....	137
5.3.	Scanning Electron Microscopy (SEM)	138
5.3.1.	Chert Formations.....	138
5.4.	Fourier-Transform Infrared (FTIR) - Attenuated Total Reflectance (ATR) Spectroscopy ...	149
5.4.1.	Chert Formations.....	150
5.4.1.1.	Maltese Islands	150
5.4.1.2.	Sicily	153
5.4.2.	Chert Assemblages	156
5.4.2.1.	The Circle assemblage	156
5.4.2.2.	Kordin assemblage.....	156
5.4.2.3.	Taċ-Ċawla assemblage.....	158
5.4.2.4.	Santa Verna assemblage.....	158
5.4.2.5.	Ġgantija assemblage.....	161
5.4.2.6.	Skorba assemblage	161
5.4.3.	First remarks.....	163
5.5.	Portable X-ray Fluorescence (p-XRF)	164
5.5.1.	Chert Formations.....	164
5.5.2.	Chert Assemblages	166

5.5.3.	First remarks.....	170
5.6.	Laser ablation - Inductively Coupled Plasma - Mass Spectrometry (LA-ICP-MS).....	171
5.6.1.	Chert Formations.....	172
5.6.2.	Chert Assemblages	177
5.6.3.	First remarks.....	188
6	Discussion	189
6.1.	The location and geological background of chert sources.....	189
6.2.	Chert outcrops.....	191
6.2.1.	Chert source summary	198
6.3.	Chert artefacts.....	199
6.3.1.	First group of artefacts.....	200
6.3.2.	Second group of artefacts	209
6.3.3.	Third group of artefacts	219
6.3.3.1.	First sub-group	219
6.3.3.2.	Second sub-group	223
6.3.3.3.	Third sub-group	227
6.3.3.4.	Fourth sub-group	234
6.3.3.5.	Fifth sub-group	237
6.3.3.6.	Sixth sub-group	240
6.3.4.	Artefacts summary	244
6.4.	Chaîne opératoire.....	246
6.5.	Integrating with FRAGSUS.....	250
6.6.	Methodological remarks	252
7	Conclusion	256
8	Bibliography.....	260
	Appendix I.....	276
	Appendix II.....	460

List of figures

Figure 2-1: A general map of Maltese islands.....	5
Figure 2-2: Map of the central Mediterranean Sea and the location of Maltese Islands in the broader environment.....	5
Figure 2-3: Stratigraphic column of the geological formation reported on the Maltese Islands.....	7
Figure 2-4 : Geological map of the Maltese Islands.....	9
Figure 2-5: Typical coastal outcrops of Lower Coralline Limestone, forming sheer cliffs at the southwest of Malta.....	11
Figure 2-6: Characteristic geomorphological feature developed on Lower Coralline Limestone in western Gozo (Dwejra Point).....	11
Figure 2-7: The middle Globigerina Limestone at the Xwejni coastline.....	13
Figure 2-8: An overview of the area investigated in western Malta.....	15
Figure 2-9: The end of the major fault system of Malta (Victorian Lines) at Fomm-IR-RiĦ.....	15
Figure 2-10: An overview of the area in west of Gozo, where the chert outcrops were located.....	16
Figure 2-11: Chert outcrops.....	16
Figure 2-12: Characteristic exposures of the Blue Clay Formation at the Fomm-IR-RiĦ Bay.....	18
Figure 2-13: The Structural map of the Maltese Islands, showing the major faults (Pedley, 2002).....	22
Figure 2-14:Map of Sicily Island.....	25
Figure 2-15: Tectonic map of the central Mediterranean area.....	25
Figure 2-16: Modified Geological Map (Catalano, 2004).....	26
Figure 2-17: The Map of Sicily with the rock formations divided by age and the samples locations.....	27
Figure 2-18: Chert outcrops in Limestones of the Hyblean Plateau unit.....	28
Figure 2-19: Chert outcrops from the “European group”.....	29
Figure 3-1: The Gozo Island with the main cities and the archaeological sites.....	40
Figure 3-2: Overview of the Ġgantija Temples.....	40
Figure 3-3: Photographs of the Ġgantija Temples.....	40
Figure 3-4: Photographs of the Xagħra Circle.....	41
Figure 3-5: Photographs of the Santa Verna.....	42
Figure 3-6: Photographs of the Taċ-Ċawla.....	43
Figure 3-7: The island of Malta with the main cities and the archaeological sites investigated.....	44
Figure 3-8: Simplified plan of the Skorba Temples.....	45
Figure 3-9: General view of the Kordin III temple.....	46
Figure 3-10: <i>Chaîne opératoire</i> diagrams.....	60
Figure 4-1: Representative cross examining FTIR-ATR spectra.....	65
Figure 4-2: Geochemical models used in this PhD research and compare the results between the two LA-ICP-MS equipment employed in this research.....	66
Figure 5-1: A satellite image of Gozo with the locations of the investigations.....	76
Figure 5-2: Chert outcrops on Gozo.....	77
Figure 5-3: Chert outcrops on Malta.....	78

Figure 5-4: a) Bedded chert outcrops intercalated in bedded middle Globigerina Limestone, b) nodular chert with irregular shapes, c) Great exposure of chert outcrops and d) Nodular chert.	80
Figure 5-5: a) Overview of the Southwest cliffs with the middle Globigerina Limestone exposure, b) nodular chert, c) bedded siliceous formation and d) bedded chert intercalated in the bedded middle Globigerina Limestone.	80
Figure 5-6 A satellite image of Malta with the locations of investigations.	81
Figure 5-7: Map of SE Sicily recording the main towns and location of the area.	83
Figure 5-8: The Geological Map of SE Sicily by Age and the main sample locations.	83
Figure 5-9: a) An entrance of prehistoric mine, b) Chert outcrops close to the mine presented at a, c) Chert outcrops beside another prehistoric mine, and d) detail of c.	84
Figure 5-10: Chert and silicified limestone outcrops south of Modica Town in SE of Sicily.	86
Figure 5-11: Black to brownish chert lenses outcrops, which are found intercalating the Amerillo Formation (Eocene).	86
Figure 5-12: a) The road leading to Monterosso Almo town, where the man-made structures were found (on the left), b) The entrance of one of these structures, c) Detail of b where chert pieces were located (arrows), d) huge nodular chert with chalky residues, e and f) chert outcrops in lens form.	87
Figure 5-13: a) The Amerillo formation with the huge and thick chert outcrops, b) detail of a, focusing on a huge lens of brownish chert.	88
Figure 5-14: Chert outcrops in the broad Valona River area.	89
Figure 5-15: The exposure of the of the Radiolarian formation along the Valona River.	89
Figure 5-16: Map of West Sicily recording the main towns and location of the area.	91
Figure 5-17: The Geological Map of West Sicily by Age and the sample locations.	91
Figure 5-18: a) Fragmented nodular chert outcrops at "Madona del Balzo", b) Black bedded chert outcrop close to Santa Maria del Bosco (monastery). C) Pieces of the yellowish chert formation, d) greyish bedded chert outcrops intercalating with a highly silicified limestone.	92
Figure 5-19: Artefacts which have been allocated to the first group of chert source.	94
Figure 5-20: a) Artefacts included in the second group and related to local sources, b) Artefacts included in the third group and not related with local chert sources.	95
Figure 5-21: Example of a blade made from the Circle.	97
Figure 5-22: A scraper from in Xagħra Circle.	98
Figure 5-23: a) Artefacts included in the second group and related to local sources, b) Artefacts which have been allocated in the first group of chert source.	100
Figure 5-24: The diversity of macroscopic characteristics reported on the artefacts from the third group in the Kordin assemblage.	101
Figure 5-25: Scrapers of the Kordin assemblage.	103
Figure 5-26: An artefact which possibly is a burin with the characteristic feather edge.	103
Figure 5-27: Artefacts related with the first (a) and second group (b) of raw materials.	105
Figure 5-28: Foreign chert artefacts.	106
Figure 5-29: Unhafted biface tool.	108

Figure 5-30: Bimarginal flake that exhibits serration at its edge.	108
Figure 5-31: Artefacts related to the first (a) and second group (b) of raw materials.	110
Figure 5-32: 'Foreign' chert artefacts.	111
Figure 5-33: Debitage from the Santa Verna assemblages.....	113
Figure 5-34: Unimarginal flake of non-local chert.	113
Figure 5-35: Unimarginal flake tools.....	113
Figure 5-36: Representative artefacts of the different types of chert material.	115
Figure 5-37: The artefacts from context 1019 from Ġgantija assemblage.	116
Figure 5-38: Different flake types from context 1019.	118
Figure 5-39: The full layout of the lithic artefacts from context 11.....	119
Figure 5-40: A Harris matrix showing the order of the top-soil contexts of the 2016 Skorba excavation. A full matrix is found in the Appendix I.....	122
Figure 5-41: Representative samples of the different types of raw material found in context 12.	124
Figure 5-42: Representative samples of the different types of raw material found in context 13.	125
Figure 5-43: Representative samples of the different types of raw material found in context 23.	127
Figure 5-44: Representative samples of the different types of raw material found in context 26.	128
Figure 5-45: A Harris matrix of the main contexts of the 2016 Skorba excavation.	130
Figure 5-46: a) Laminae made of micro-quartz, under PPL, b) Micrite, micro-quartz and microcrystalline dolomite, c) Pores filled by micro-quartz and dolomite, d) Vein in the matrix filled with chalcedony, e) micrite matrix with silicified fossils and f) Radiolaria filled by micro-quartz.	133
Figure 5-47: a) Micrite matrix with sponge spicules and foraminifera, b) micro-quartz in the centre of the samples with microcrystalline -dolomite. c) Echinoderm fragments and feldspar crystals (red arrow) and d) Radiolarian filled with micro-quartz and chalcedony.	134
Figure 5-48: a) Chalcedony fills pores within the micro-quartz matrix, b) Calcite and dolomite crystals within the matrix, c) radiolarian filled with chalcedony, d) foraminifera and nummulites, filled with micro-quartz or retaining their original composition, e) cryptocrystalline (<math><5\mu\text{m}</math>) quartz matrix and f) Iron-oxide rich aggregate in the matrix.	136
Figure 5-49: SEM image and the semi-quantitative spot analyses.....	140
Figure 5-50: SEM image and the semi-quantitative spot analyses.....	141
Figure 5-51: SEM image and the semi-quantitative spot analyses.....	142
Figure 5-52: SEM image and the semi-quantitative spot analyses.....	143
Figure 5-53: SEM image and the semi-quantitative spot analyses.....	144
Figure 5-54: SEM image and the semi-quantitative spot analyses.....	145
Figure 5-55: SEM image and the semi-quantitative spot analyses.....	146
Figure 5-56: SEM image and the semi-quantitative spot analyses.....	147
Figure 5-57: SEM image and the semi-quantitative spot analyses.....	148
Figure 5-58: Representative FTIR spectra of the chert samples from Malta.	151
Figure 5-59: Representative FTIR spectra of the chert samples from Gozo.	152
Figure 5-60: Representative FTIR spectra of the chert samples from Sicily.	155

Figure 5-61: Representative ATR spectra of the artefact samples from the Circle and Kordin.....	157
Figure 5-62: Representative ATR spectra of the artefact samples from Taċ-Ċawla and Santa Verna.	160
Figure 5-63: Representative ATR spectra of the artefact samples from Ġgantija and Skorba.	162
Figure 5-64: Representative p-XRF spectra of the rock samples from Malta (a) and Sicily (b).	165
Figure 5-65: Representative p-XRF spectrum from the Circle.	168
Figure 5-66: Representative p-XRF spectrum from Kordin.....	168
Figure 5-67: Representative p-XRF spectrum from Taċ-Ċawla.....	168
Figure 5-68: Representative p-XRF spectrum from Santa Verna.....	169
Figure 5-69: Representative p-XRF spectrum from Ġgantija.....	169
Figure 5-70: Representative p-XRF spectrum from Skorba	169
Figure 5-71: Ternary diagram examining the type of the sediments related to the Maltese rock samples (left) and the Sicilian chert samples (right).	172
Figure 5-72: Binary diagram examining the type of depositional environment related to the Maltese chert samples (left) and the Sicilian chert samples (right).	173
Figure 5-73: Binary diagram examining the oxygen level of the depositional environment of the Maltese chert samples (left) and the Sicilian chert samples (right).	174
Figure 5-74: The normalised patterns of rare earth elements of the Maltese and the Sicilian chert samples. .	176
Figure 5-75: Ternary diagram examining the type of the sediments related to the Xagħra Circle artefact samples (left) and the Kordin artefact samples (right).....	177
Figure 5-76: Ternary diagram examining the type of the sediments related to the artefact samples of a) Taċ-Ċawla, b) Santa Verna, c) Ġgantija and d) Skorba.	178
Figure 5-77: Binary diagram examining the type of depositional environment related to the artefact samples of a) the Circle, b) Kordin, c) Taċ-Ċawla, d) Santa Verna, e) Ġgantija and f) Skorba.	179
Figure 5-78: Binary diagram examining the oxygen level of the depositional environment related to the artefact samples of a) the Circle, b) Kordin, c) Taċ-Ċawla and d) Santa Verna.	180
Figure 5-79: Binary diagram examining the oxygen level of the depositional environment related to the artefact samples of a) Ġgantija and f) Skorba.....	181
Figure 5-80: The normalised patterns of rare earth elements of the Circle artefact samples.....	184
Figure 5-81: The normalised patterns of rare earth elements of the Kordin artefact samples.	185
Figure 5-82: The normalised patterns of rare earth elements of the Taċ-Ċawla artefact samples.....	186
Figure 5-83: The normalised patterns of rare earth elements of the Santa Verna artefact samples. The red arrows point out the sample (SV15/S1/L98) with the distinct fluctuation.	186
Figure 5-84: The normalised patterns of rare earth elements of the Ġgantija artefact samples.	187
Figure 6-1: Ternary diagram examining the origin of the sediments of the investigated rock samples.	193
Figure 6-2: Binary diagram examining the depositional environment of the investigated rock samples.	194
Figure 6-3: Binary diagram examining the oxygen level of the depositional environment of the investigated rock samples.....	196
Figure 6-4: Representative samples of the fist group of artefacts found in the context 1019 at Ġgantija.	201
Figure 6-5: Satellite image with the investigated archaeological sites on Gozo Island.....	201

Figure 6-6: Comparison FTIR-ATR spectra between a representative artefact from the first group (above) and the chert sources of Malta (below).	203
Figure 6-7: Comparable p-XRF spectra between a representative artefact from the first group (above) and the chert sources of Malta (below).	204
Figure 6-8: Ternary diagram cross-examining the Sicilian cherts and the artefacts of the first group regarding the type of sediment.	205
Figure 6-9: Binary diagram cross-examining the Sicilian cherts and the artefacts of the first group regarding the depositional environment.	206
Figure 6-10: Spider plot with the REEs normalised concentrations of artefact samples from all the assemblages with the most similar pattern.	207
Figure 6-11: Comparable spider plot of the REEs concentrations between artefact samples of common origin and selective Sicilian chert outcrops.	207
Figure 6-12: Binary diagram cross-examining the Sicilian cherts and the artefacts of the first group regarding the oxygen level of the depositional environment.	208
Figure 6-13: Representative samples of the second group of artefacts. The purple arrows point out the characteristic spots.	210
Figure 6-14: Comparison FTIR-ATR spectra between a representative artefact (BR91/S566/L622) from the second group (above) and the chert sources (M1S3) of Malta (below).	211
Figure 6-15: Comparable p-XRF spectra between a representative artefact from the second group (above) and the chert sources of Malta (below).	212
Figure 6-16: Ternary diagram cross-examining the Maltese cherts and the artefacts of the second group regarding the type of sediment.	214
Figure 6-17: Binary diagram cross-examining the Sicilian cherts and the artefacts of the second group with respect to the depositional environment.	214
Figure 6-18: Comparable spider plot of the REE concentrations between representative artefact samples from all the examined assemblages which are considered of common local origin.	215
Figure 6-19: Comparable spider plot of the REE concentrations between representative Maltese chert samples and artefact samples of common local origin.	216
Figure 6-20: Comparable spider plot of the REE concentrations between representative artefact samples from the different layers of Skorba excavation, which are considered of common local origin.	216
Figure 6-21: Comparable spider plot of the REE concentrations between an artefact sample from Santa Verna that present a different pattern and a Maltese chert outcrop.	217
Figure 6-22: Binary diagram cross-examining the Maltese cherts and the artefacts of the second group with respect to the oxygen level of the depositional environment.	217
Figure 6-23: Representative FTIR-ATR and p-XRF spectra of the artefact included to this sub-group.	220
Figure 6-24: Ternary diagram cross-examining the Sicily cherts and the artefacts of this sub-group with respect to the type of sediment.	222
Figure 6-25: Binary diagram cross-examining the Sicilian cherts and the artefacts of this sub-group regarding the depositional environment.	222

Figure 6-26: Representative samples of this lithic sub-group.	223
Figure 6-27: Representative FTIR-ATR and p-XRF spectra for the artefact included to this sub-group.	224
Figure 6-28: Ternary diagram cross-examining the Sicily cherts and the artefacts of this sub-group with respect to the type of sediment.	226
Figure 6-29: Binary diagram cross-examining the Sicilian cherts and the artefacts of this sub-group with respect to the depositional environment.	226
Figure 6-30: Comparable spider plot of the REE concentrations between the radiolarian samples artefact samples of this sub-group.	227
Figure 6-31: Representative samples of this sub-group.	228
Figure 6-32: Representative p-XRF spectra of the artefacts included in this sub-group (top) and the chert sources of Gozo (below).	228
Figure 6-33: Comparative FTIR-ATR spectra between a representative artefact of this sub-group (above) and the chert sources of Gozo (below).	229
Figure 6-34: Ternary diagram cross-examining the Gozo chert outcrop (G2S6) and the artefacts of this sub-group with respect to the type of sediment.	231
Figure 6-35: Binary diagram cross-examining the Gozo chert outcrop and the artefacts of this sub-group with respect to the depositional environment.	231
Figure 6-36: Comparable spider plot of the REE concentrations of the artefacts included in this sub-group. ...	232
Figure 6-37: Binary diagram cross-examining the Gozo chert outcrop and the artefacts of this sub-group with respect to the oxygen level of the depositional environment.	232
Figure 6-38: Comparable spider plot of the REE concentrations between representative rock and artefact samples of common local origin.	233
Figure 6-39: The two members of this lithic sub-group.	234
Figure 6-40: Ternary diagram cross-examining the Sicilian cherts and the artefacts of this sub-group with respect to the type of sediment.	235
Figure 6-41: Binary diagram cross-examining the Sicilian cherts and the artefacts of this sub-group with respect to the depositional environment.	236
Figure 6-42: Comparable spider plot of the REE concentrations between representative rock and artefact samples of common local origin.	236
Figure 6-43: The two members of this lithic sub-group.	237
Figure 6-44: Ternary diagram cross-examining the Sicilian cherts and the artefacts of this sub-group with respect to the type of sediment.	239
Figure 6-45: Binary diagram cross-examining the Sicilian cherts and the artefacts of this sub-group with respect to the depositional environment.	239
Figure 6-46: Comparable spider plot of the REE concentrations between representative rock and artefact samples of common local origin.	240
Figure 6-47: FTIR-ATR (above) and p-XRF (below) spectra of a representative artefact of this sub-group (SV15/S2/L41).	242

Figure 6-48: Ternary diagram examining the artefacts of this sub-group with respect to the type of sediment. The black arrows show the two macroscopically similar artefacts of this group.	243
Figure 6-49: Binary diagram examining the artefacts of this sub-group with respect to the depositional environment.	243
Figure 6-50: Spider plot of the REE concentrations of the two macroscopically similar artefacts.	244

List of Tables

Table 2-1: Description of the geological formation found on the Maltese Islands.	8
Table 3-1: The cultural phases of Prehistoric Malta. Radiocarbon dates are quoted throughout the text as cal BC/AD dates unless otherwise stated.	35
Table 5-1: Summary of the main findings of all the samples recorded from each technique.	67
Table 5-2: The main and minor peaks of the minerals recorded with the FTIRS. These values derived from the Kimmel standards and the work of Parish (2013).	149
Table 5-3: The main and minor peaks of the minerals recorded with the ATR. These values derived from the work of Parish (2013) and Müller et al. (2012 and 2014).	149

1 Introduction

This PhD research investigates the origin of chert assemblages found within a number of well-known Neolithic sites on the Maltese Islands. A significant focus of the research investigates whether the cherts used for stone tools represent indigenous exploitation or results from longer-distance trade networks, such as from Sicily, as is often suggested. Furthermore, the research investigates to what extent the possible sources can be identified and how they were exploited in the past. The PhD forms part of a larger project (FRAGSUS) assessing the extent to which these islands were laboratories of human activity and their degree of connectivity with neighbouring areas in prehistoric times. In that respect, Sicily is considered the most probable location, as it is the closest land (90km) to the Maltese Islands. The project focuses on the period of the Stone Temples on Malta (between 4th and 3rd millennia BC) and identifies the circumstances under which these unique monuments were built. It involved several seasons of excavation at new sites, as well as re-evaluating previous excavations, a large scheme of radiocarbon dating, re-analysis of ceramic finds, extensive geoarchaeological research (e.g. landscape changes and utility of raw material), and a new phase of bioarchaeological analysis of the Xagħra Circle burial site (including DNA and isotope analyses and taphonomic analysis).

This research examines the chert assemblages recovered by the Cambridge Gozo Project of the late 1980s and early 1990s and by the FRAGSUS project (2013 – 2018) at six Neolithic sites in Malta and Gozo – Brochtorff Xagħra Circle, Ġgantija, Taċ-Ċawla, Santa Verna, Kordin and Skorba, as well as the naturally extant chert outcrops found in Malta and Sicily today. Although these Neolithic stone artefacts have been previously studied (Vella, 2008; Malone et al. 2009), the research conducted on their sources has been relatively cursory and at best inconclusive. Therefore, the findings of my work will resolve this uncertainty and contribute to the wider project results. Moreover, little is known about the characteristics (microscopic, geochemical, etc.) of the chert sources of the islands of Malta, Gozo and Sicily. Therefore, a comprehensive geological/petrological methodology was employed on both chert outcrops and artefacts to collect highly reliable results and correlate possible sources with a set of known lithic artefact assemblages. Thus, it becomes possible to establish, on a systematic, scientific basis by a trained geologist, whether the Maltese Neolithic people used the resources of their own islands, imported raw materials from elsewhere or undertook a combination of both strategies.

The findings of this work also contribute to our understanding of the impact of the Maltese landscape on the local population and the possible relationships with the broader central Mediterranean Sea. Indeed, the potential relationships with other areas are crucial since they most probably have not been confined to material exchange but have influenced other aspects of human life and have presumably shaped the distinctive cultural identity of the Maltese islands. To address these relationships, research is necessary to establish the extent of the travel and trade network of stone materials of the area. This can suggest possible influences on the late Neolithic society of the

Maltese Islands and their distinctive identity, at least by knowing and defining difference. Investigating the sources of the lithic assemblages and finding the origins of the raw materials is a promising method with which to address these issues. Nevertheless, provenancing chert artefacts cannot solely address these questions and will require the insight of the other members of FRAGSUS team. It is only by integrating the results of my work with the outcome of radiocarbon dating, ceramic typology and bioarchaeological and environmental research that the full spectrum of the late Neolithic Maltese society will be revealed.

This scientific investigation can work alongside and enhance the *chaîne opératoire* approach (Sellet, 1993), which analyses the technical processes and social acts involved in the step-by-step production, use and eventual disposal of artefacts, such as the chert assemblages found on the Maltese Islands. The main idea is that societies can be better understood through their material working techniques by virtue of the fact that operational sequences are steps organized according to an internal logic specific to a society (Plegrin et al., 1988). Understanding the processes and construction of tools, archaeologists can better determine the evolution of tool technology and the development of ancient cultures and lifestyles. Consequently, this research approach enables a better understanding not only of the society in which the technique originated but also of the social context, agencies and cognition that accompanied the production of an object. Merging these two methodologies provides evidence of a possible link between the types of chert rock (i.e. quality) and the usage of the artefacts which subsequently show to what extent the Neolithic Maltese people both understood and were able to assess rock 'quality'. Moreover, it can reveal the possible effect of this 'quality' on forming one or more *chaîne opératoire*. These studies should provide a much better understanding of the both society and the individual, which has created and used chert artefacts.

The selected methodology has identified the petrological profile of the probable chert sources from Malta and Sicily and the characteristics of the chert artefacts from the site-based Neolithic archaeological assemblages. The study has provided evidence of the chert resources of the Maltese Islands which would have been sufficient to sustain a robust local production of chert artefacts. Moreover, it has demonstrated that a substantial number of artefacts from the examined assemblages are petrologically identical with the local chert rocks, and scientifically confirmed their connections. However, it has also highlighted the existence of a similar number of artefacts to be related to non-local chert sources. Some of these artefacts provide strong evidence of a connection with specific sources in both East and West Sicily, while others are not associated with any known Sicilian source, such that their origin must be found elsewhere.

The type of tools and manufacturing techniques give a further understanding of the conditions under which these assemblages have been formed. The investigation has provided strong evidence of local *chaîne opératoire* which is recorded at all of the investigated Neolithic sites of the Maltese Islands. Moreover, this is not only employed on the local chert but also to ONE exotic chert material. There is

solid proof of foreign raw chert material being imported to the Maltese Islands rather than finished artefacts and locally modified. There are differences, but to what extent this is related to the quality of the material and/or the archaeological site is uncertain, and further research is necessary. Nevertheless, these findings provide strong evidence for the existence of a distinct local craft tradition employed on the Maltese Islands during the late Neolithic.

However, there is a small proportion of the assemblages that suggests a foreign and possibly different craft tradition. It is represented with small artefacts or fragments of such, which are also related to foreign chert sources. Their small size and the evidence of a constant retouch prevent the identification of the *chaîne opératoire* from which they emerge but, provide information on other aspects of past Maltese communities. The local population probably had restricted access to the sources of these artefacts, and these artefacts must have been of great value. Furthermore, they have been the tools of the local craftsmen during local *chaîne opératoire* which demonstrate the ability of the local community to understand and assess rock 'quality' of the different chert material and use them accordingly. In addition, it confirms the interaction with neighbouring societies and significantly gives a possible indication of cultural influence and exchange.

Moreover, it demonstrates that the petrological examination of these chert assemblages can lead to a re-appraisal of probable resources and the methods of exploitation of lithic sources in the Neolithic period of the Maltese Islands. Finally, this study has presented a beneficial methodology for lithic analysis for all archaeological researchers working on the provenance of lithic material, both elsewhere in the Mediterranean area and the wider world.

2 Geology and Geo-environment

2.1 Geology and Geo-environment of the Maltese Islands

This chapter sets the scene in terms of the geography and geology of the Maltese islands and the present-day geomorphology. The geology and faulting of the islands has had a huge influence on the topography, soils and vegetation of the islands, and, in turn, on the nature of human use and exploitation of the islands. All of these themes are giving time-depth to the sequences of climatic, environmental and landscape changes throughout the Holocene.

2.1.1 Geography

The modern state of Malta is made up of a small group of four principal islands (Malta, Gozo, Comino and Cominoto) (Fig. 2.1), with a total land surface of 316.75 km². It is characterised by high hills or plateaux (Ta' Dmejrek on Malta is 253m and Ta' Dbiegi on Gozo is 187m), separated by deeply incised valleys which are characteristically orientated southwest-northeast. Much of the remaining non-urban landscape is dominated by terraced fields. Although past water bodies have been reported on the surface of the islands, there are today no lakes, rivers or streams and only minor springs.

Malta and Gozo are the largest islands (respectively 246 km² and 67 km²), while Comino and Cominotto, which are found in the narrow space between the main islands, are far smaller at 3.5 km² and 0.25 km², respectively. The Maltese Islands lie in the middle of the Mediterranean Sea, with a southeast-northwest orientation, between the larger island of Sicily and the North African coast (Fig. 2.2). They are far from any mainland, located c. 80km south of Sicily, 300km east of Tunis and 350km north of the Libyan coast (Pedley et al. 1976). In spite of their small size, these islands occupy a very significant location within the broader Mediterranean region, once the Mediterranean was populated by state-organised societies (Stoddart, 1999). Their location in the Sicilian Channel, the main navigational seaway connection of the eastern and western Mediterranean, and the presence of exceptional, natural harbours, gave the Maltese Islands an indisputable strategic importance once written history began (Pedley et al. 2002). The key question is how different political conditions affected this strategic importance and how geography related to society in the earlier periods of occupation.



Figure 2-1: A general map of Maltese islands.

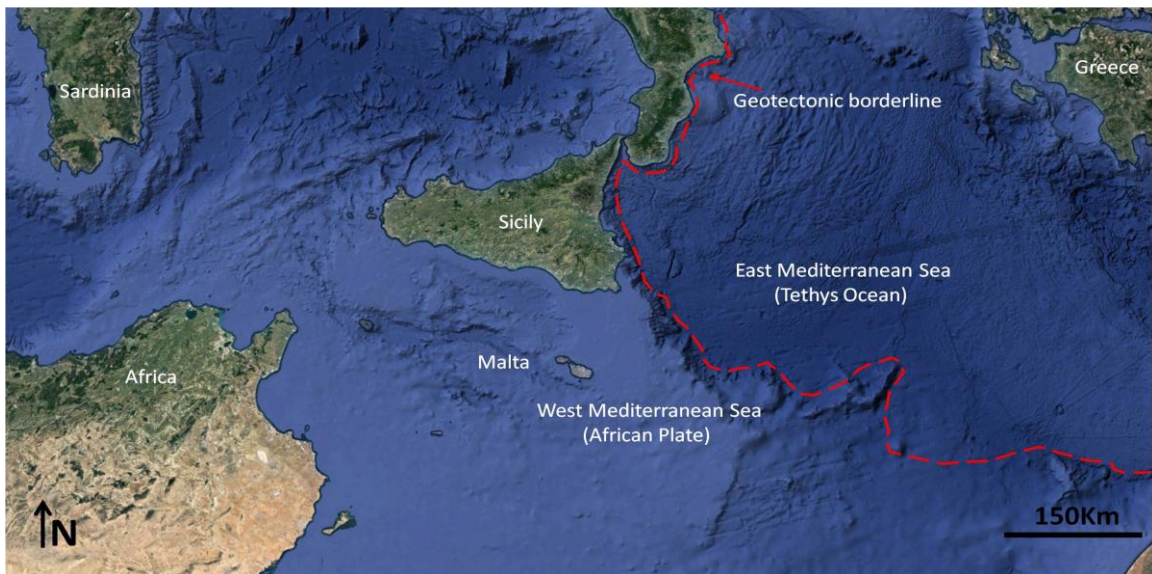


Figure 2-2: Map of the central Mediterranean Sea and the location of Maltese Islands in the broader environment (Map Copyright @2017 Google).

2.1.2 Geology

It is difficult to distinguish when exactly the basin which contains the Maltese Islands began to form. Some researchers place this at 150 million years (when Pangea began to break into continents), whilst others suggest 100 million years ago (when Europe split from North America and started moving towards North Africa) (Pedley 1974; Puglisi, 2014). Regardless of when exactly this was occurred, the progressive approach of the European and African continents transformed the intermediate zone (Tethys ocean) between them into the forerunner of the present-day Mediterranean Sea and set up the foundations of the Maltese Islands. This, however, was not a simple process, but included a variety of complex movements and caused many stresses to the continents' margins.

The movement of the African tectonic plate towards Europe resulted in the subduction of the African oceanic crust under the Eurasian continental crust followed by continent to continent collision and associated orogeny and volcanism (Galea, 2007, 2019; Puglisi, 2014). The plates are still approaching each other today and Mediterranean Sea is basically within two different types of basins. The western part of the Sea is in a continental basin (African plate) while the eastern part is on the remaining area of the Tethys ocean.

The Maltese Islands (or Maltese Archipelagos) have a key position in this environment as they lie on a shallow area (at a sea depth below 200m) that separates these two basins (Fig. 2.2). This area is called the "Sicilian-Tunisian Platform" and also known as 'Pelagian Block' represents the foreland margin of the African continental plate and consists of massive marine carbonate deposits (Pedley, 1974). Recent continental plate margin studies of the region suggest that the Maltese archipelago lies a short distance behind the leading margin of the African plate (Pedley, 1974). Extensional tectonics and the associated uplifting in the central parts of the Pelagian Block due to development of the Pantelleria Rift System in the Late Miocene gave rise to what today are the Maltese Islands to the northeast and the island of Lampedusa to the southwest of the rift (Reuther and Eisbacher, 1985; Dart et al. 1993; Galea, 2007 and 2019).

Inevitably, the location of the Maltese Islands in this broader geological environment has shaped the type of formations found on them. These are composed almost entirely of shallow marine sedimentary formations, mainly of the Oligo-Miocene age (c. 30-5Ma BP). They are most comparable with the mid-Tertiary carbonate limestones occurring in the Ragusa region of Sicily to the north, in the Pelagian Islands and in the Sirte Basin of Libya to the South (Pedley et al. 1978; Schembri, 1994). Previous research has reported five main rock formations, which are presented in a simple succession (Oil Exploration Directorate, 1993; Pedley et al. 1976, 2002; Schembri, 1993, 1994; Schembri et al. 2009). These, starting from the bottom, are: a) the Lower Coralline Limestone, b) the Globigerina Limestone, c) the Blue Clay, d) Greensand and e) the Upper Coralline Limestone (Fig. 2.3; Table 2-1).

Although the geology of the islands is simple with a similar stratigraphy throughout their extent, each formation does present different characteristics (Fig. 2.4). The stratigraphy of Malta is affected by normal faults, arranged as graben and half-graben. Gozo is structurally less complex, preserving a more or less layer-cake stratigraphy, but has a more varied geology than Malta. The centre of Gozo is dominated by the Upper Coralline Limestone, resting on Blue Clay, while the Globigerina Limestone and Lower Coralline Limestone out-crops in coastal locations. Here erosion has occurred low enough in the succession to expose these formations and create table-top plateaux or mesas of weathered and eroded Upper Coralline Limestone. Finally, the two smaller islands are composed of only the highest layers of the Upper Coralline Limestone Formation.

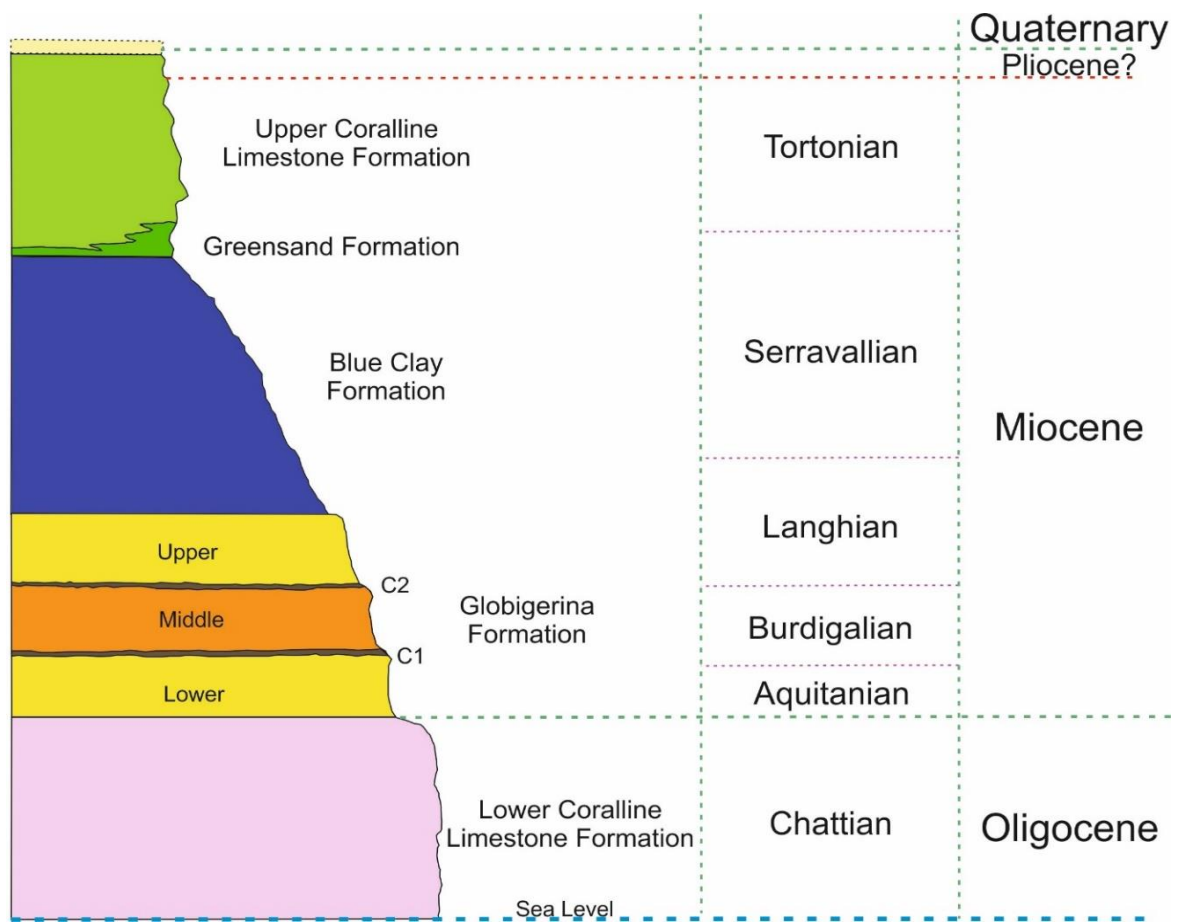
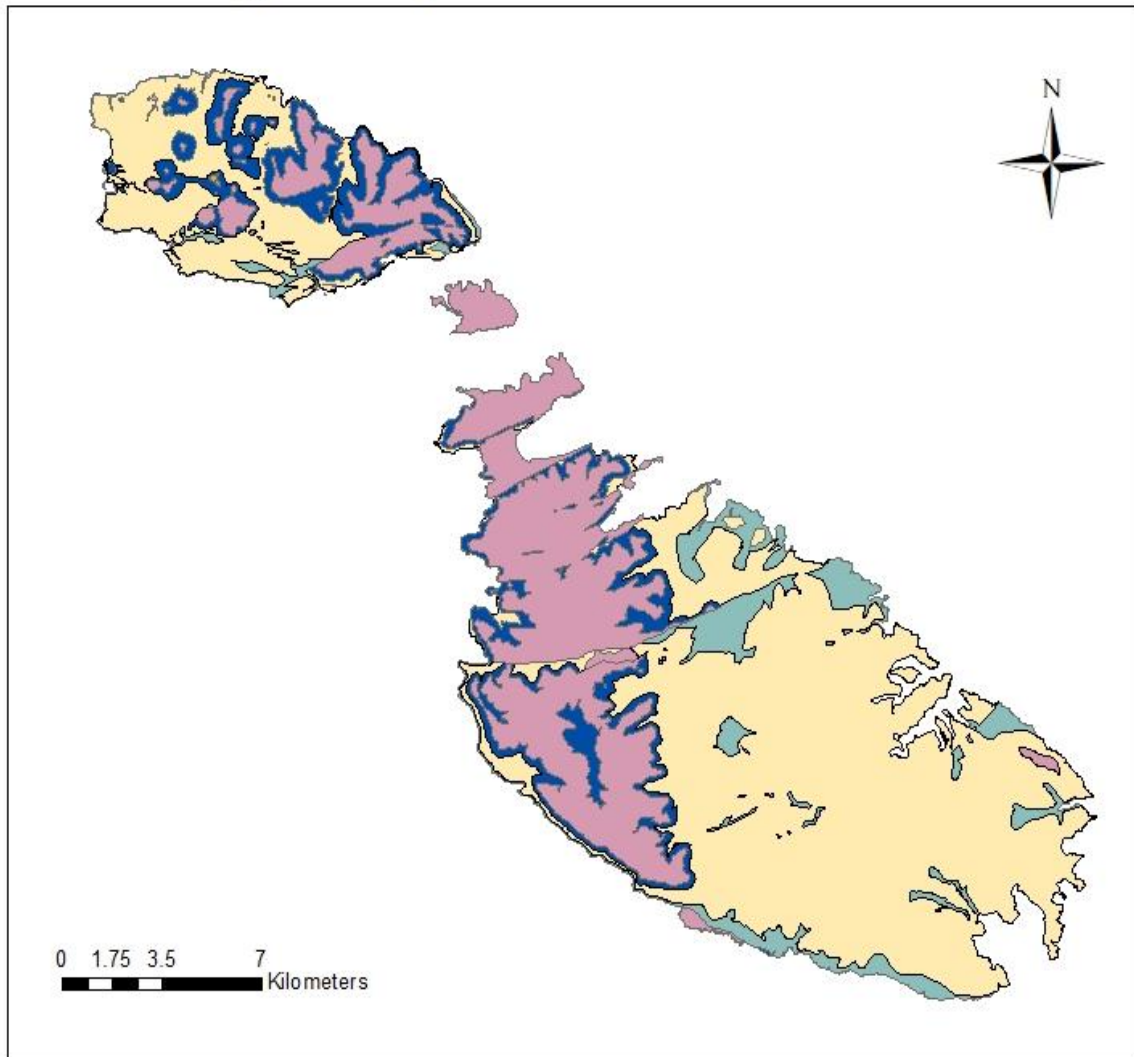


Figure 2-3: Stratigraphic column of the geological formation reported on the Maltese Islands.

Table 2-1: Description of the geological formation found on the Maltese Islands.

Geological time period (earliest to oldest)	Formation	Description	Thickness
Miocene	Upper Coralline Limestone	shallow marine limestone with abundant coral-algal mounds and reefs, commonly altered to micrite and sparite	0.70-100m; moderate to very high permeability (especially where karstified)
	Greensand	friable, glauconitic argillaceous sandstone, moderate permeability	0.5-15m
	Blue Clay	massive to bedded grey/blue shallow marine/offshore calcareous claystones with occasional to abundant marine fossils. Impermeable or an aquiclude	20-50m
	Globigerina Limestone	shallow marine, calcareous mudrocks with abundant fossils, poor permeability, phosphatised hardgrounds	20-60m
Oligocene	Lower Coralline Limestone	shallow marine limestones with spheroidal algal structures, abundant echinoid fossils. Well-cemented and permeable	100-140m

Geological Map Of The Maltese Islands



Legend

Geological Formations






-  Upper Coralline Limestone Formation
-  Greensand Formation
-  Blue Clay Formation
-  Globigerina Limestone Formation
-  Lower Coralline Limestone Formation

Figure 2-4 : Geological map of the Maltese Islands. Modified from original (Pedley, 1993).

2.1.3 Stratigraphy of the Maltese Islands

➤ *Lower Coralline Limestone Formation*

The Lower Coralline Limestone is the oldest visible unit of the rock formations on the Maltese Islands. It is a hard, pale grey limestone and contains beds with fossils such as corals and marine calcareous algae. Outcrops of this limestone are mainly restricted to coastal sections along the western coasts of Malta and Gozo (Fig. 2.5). It can be over 140 m. thick, forms sheer cliffs particularly on the southwest coasts of the islands and its base cannot be seen above the sea level. When found inland, this formation forms barren grey limestone-platform plateaux on which karst-land develops (Schembri, 1997). A characteristic geomorphological feature developed from this formation is the bare karstic plateau similar to these found in the west of Gozo (Fig. 2.6). The bedrocks comprising this formation are all indicative of sediments laid down in a shallow agitated sea and can be subdivided into five different facies¹ of limestones (Pedley, 2002). These facies are: a) the Reef Limestone, b) the fine-grained Shallow Lime Muds, c) the Cross-bedded lime sands, d) the Foraminiferal Limestones and e) the “Scutella Bed”. Felix (1973) suggested that the deposition of the Lower Coralline Limestone had initially been in a shallow gulf-type environment. In addition, succeeding beds provided evidence of increasingly open marine conditions during which algal rhodolites developed. Finally, a shallow marine shoal environment followed and was the dominant environment in all areas except southeastern Malta. In this area, calmer conditions prevailed in a protected deeper water environment (Pedley et al. 1976).

¹ “Facies” provides a specific characterisation of a group of rocks with distinct similar features. In sedimentary rocks, it embraces major features such as the main composition (e.g. quartz sand, clay or limestone facies), the sedimentary layering (e.g. cross bedded facies, etc.) or the main fossils. These are then related to an interpreted environment in which the sediments were deposited. Consequently, the rock can be referred to as beach-facies, lagoon facies, reef facies, and so on.



Figure 2-5: Typical coastal outcrops of Lower Coralline Limestone, forming sheer cliffs at the southwest of Malta.



Figure 2-6: Characteristic geomorphological feature developed on Lower Coralline Limestone in western Gozo (Dwejra Point). The picture shows different sub-circular collapsed karstic features (a and b), while the green arrow points the location of the chert outcrops (Map Copyright@2017 Google).

➤ *Globigerina Limestone Formation*

The Globigerina Limestone is a softer, yellowish fine-grained limestone that forms irregular slopes and is the most extensively exposed formation on these islands. It is named after a type of microscopic, planktonic foraminifera, fossil shell (*Globigerina*) which is abundant in this limestone. The formation varies in thickness from some 20 to over 200 m., a characteristic which possibly signifies the onset of the slow warping of the sea bed and possibly the formation of depressions due to the collapse of the sea bed above underlying caverns (Pedley et al. 2002). Moreover, the size of the fine grains and the content of fossils show that this formation was originally deposited in a deeper water below the level of wave action. Felix (1973) thought most of the Globigerina Limestones were deposited in water depths between 40 and 150 m. The unexpected occurrence of the planktonic foraminifera, such as *Globigerina*, in this shallow-water depositional environment may be explained by a drift that brought these organisms into this shallower basin from the surrounding deeper water seas.

The Globigerina Limestone is divided into three units (upper, middle and lower) by two layers of conglomerates (also referred as C1 and C2), which do not exceed one meter in thickness. The upper and lower units have a pale yellow colour, while the middle one is pale grey (Fig. 2.7). The latter unit is considered to have been deposited during the time that the sea basin reached the deepest level. This could also explain the presence of chert outcrops, which have been found intercalating with the middle Globigerina Limestone (see below). Although the sources providing the material are still not known, it is certain that only the middle Globigerina Limestone had the adequate conditions for these deposits to form.

The two conglomerate layers show evidence of erosion phases through the incorporation of many pebbles and cobbles of brown-colour limestones (Pedley et al. 2002). In addition, their presence indicates that the sea basin was influenced by water agitation and that the sea levels had probably fallen during the deposition of the formation. The colour of these layers is attributed to the concentration of the francolite (phosphatic mineral) in the cements. It was reported that francolite has replaced some fossils, the matrix of the pebbles and also the top surface of the limestone unit beneath the conglomerate layers. The presence of so much phosphate material in the cements suggests that the water streaming over this shallowed surface was rising from greater depths as an “upwelling” current (Pedley et al. 2002). Furthermore, the examination of the size of the pebbles in the conglomerates indicates that they become smaller moving to the east, implying that the currents had a direction from west to east. This suggests that high nutrient water was rising from the depths of the western Mediterranean basin (Pedley et al. 2002). It is possible that these inputs were also supplying material during the deposition of the middle Globigerina Limestone and contributed to the formation of the chert outcrops.

The fine-grained particles comprising the Globigerina Limestone formation (upper and lower) are only lightly cemented and therefore are easily worked as building stone. Indeed, the lower Globigerina Limestone unit, called 'Franka' locally, has proven to be the most suitable building stone. This is related to its uniform texture and can explain why most of the buildings of the Maltese Islands were built from this unit. Its texture, in addition to its extensive exposure on Malta and Gozo, has contributed to the smoothing of the topography of the islands. The thin soils produced from this formation are intensively cultivated and terraced.

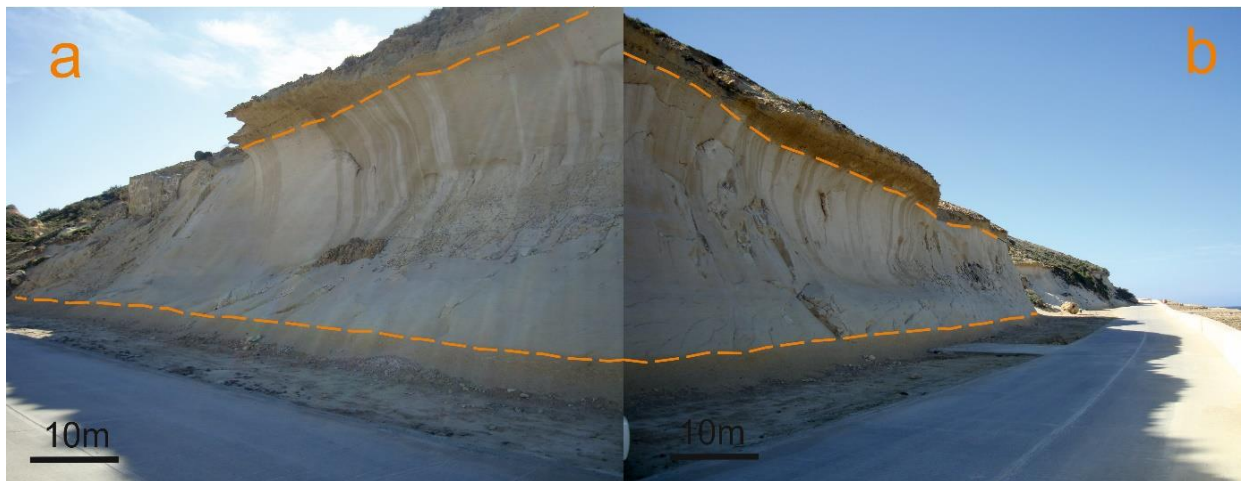


Figure 2-7: The middle Globigerina Limestone at the Xwejni coastline. It is one of the biggest outcrop of this unit and the orange lines highlight the two conglomerate layers, which are clearly presented in this location and signify the transition to the upper and lower Globigerina unit.

➤ *Chert outcrops*

The existence of the chert outcrops has been long reported (Cooke, 1893a), but little is known about their characteristics and the conditions under which they formed. Archaeological research has revealed that these chert rocks were used by the prehistoric inhabitants (Malone et al. 2009; Vella, 2009), and that a better understanding of these resources is necessary. The middle Globigerina has extensive exposures in both islands of Malta and Gozo, but not all of them present chert outcrops. The fieldwork surveys (conducted by Chatzimpaloglou in 2016 and 2017) on the islands revealed that chert outcrops were present only on the western parts of both islands. The exposures of middle Globigerina unit in these areas were in bedded form, which could possibly be attributed to the influence of tide cycles in a former shallow marine environment in this part of the Maltese basin.

The chert outcrops on Malta were located in the broader area of the Fomm-IR-RiĦ Bay area (Fig. 2.8) and are considered more extensive than on Gozo. It is probably not a coincidence that these exposures are located at the end of the Victoria Lines (Fig. 2.9), which is a major tectonic feature of the Maltese islands. The chert outcrops on Gozo were found at Dwejra Point, in an area close to Fungus Rock (Fig. 2.10). The area is characterised by massive karstic features (Fig. 2.6), which could have been enhanced by past tectonic activity. The investigation of both exposures showed that nodular chert was present at the top and bottom of the unit, while bedded chert and/or silicified limestone were found in the middle part of the unit (Fig. 2.11). Generally, the outcrops present similar macroscopic characteristics, but distinct outcrops have also been recorded. In addition, the bedded chert outcrops have a higher concentration of carbonate material than the nodules and are therefore softer.



Figure 2-8: An overview of the area investigated in western Malta. It presents the locations with the chert outcrops (yellow lines) and the areas investigated during fieldwork (green lines). The upper right figure shows Malta Island and the exact location of this area (Maps Copyright @2017 Google).



Figure 2-9: The end of the major fault system of Malta (Victorian Lines) at Fomm-IR-Riff, beside the location with the chert outcrops.

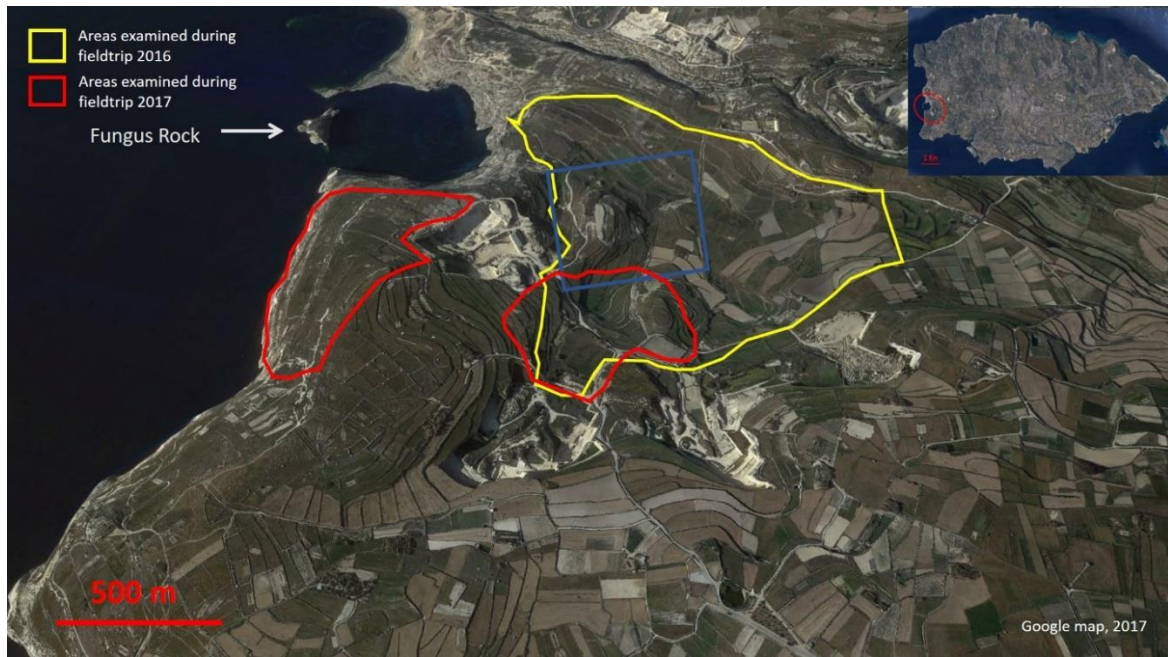


Figure 2-10: An overview of the area in west of Gozo, where the chert outcrops were located. The yellow line orientates the internal valley, close to Fungus Rock. The location with the chert outcrops is highlighted with the blue line and the areas investigated during the 2017 fieldwork are marked with red lines. The upper right figure shows Gozo Island and the exact location of this area (Maps Copyright @2017 Google).

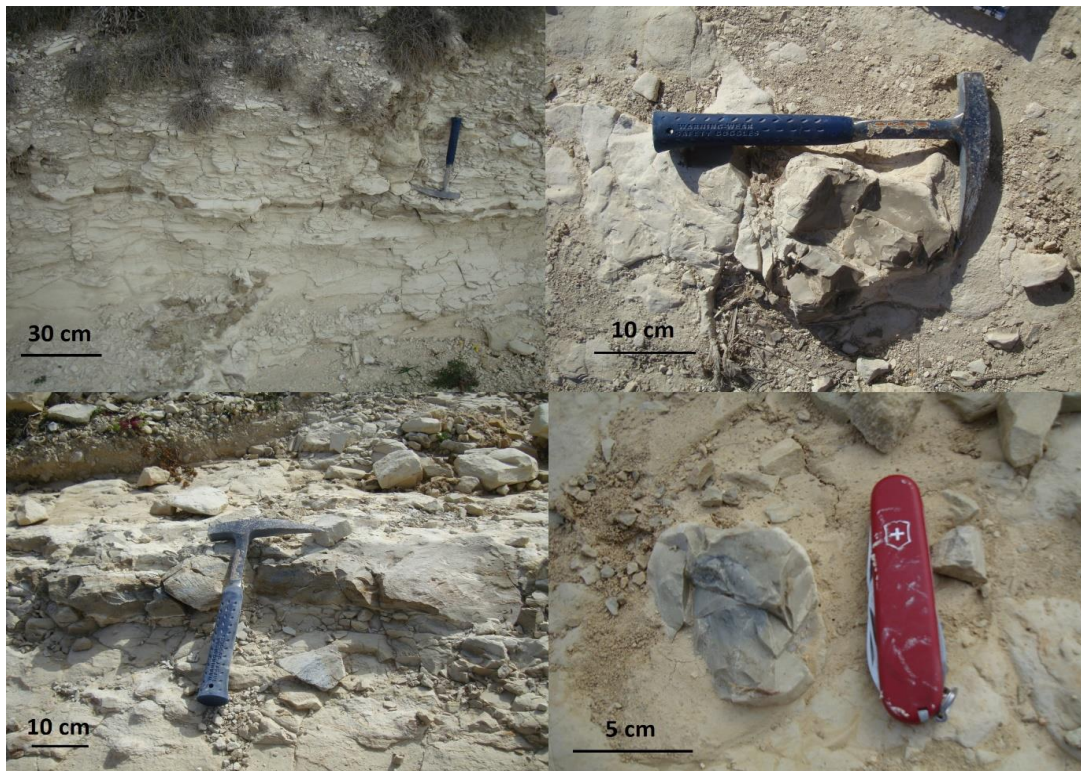


Figure 2-11: Chert outcrops. a) Bedded and b) Nodular chert from Malta, c) Bedded chert and d) Nodular chert from Gozo.

➤ *Blue Clay Formation*

The Blue Clay is a very soft formation and, when exposed on the surface, forms low or rounded slopes (Pedley et al. 2002). The thickness of the formation ranges from less than 20m to around 70m (at Fomm IR Bay), while the colour reported on the outcrops is bluish grey (Fig. 2.12). Although Blue Clay has macroscopic differences from the Globigerina Limestone, they have very similar characteristics. It is also composed of very fine-grained sediments, with a large proportion of them of carbonate origin. Hence, it can be suggested that this formation was originally deposited in a very similar deep-sea depositional setting (Pedley et al. 2002). It could be regarded as a continuation of the Globigerina limestone sedimentation in which clay material became progressively incorporated. This is also supported by the smooth and fast transition from the one formation to the other during sedimentation. There is only a small step in topography that highlights the change, and this transition is restricted to a layer just over one metre thick at the base of the Blue Clay Formation (Pedley et al. 1976).

Basically, the main factor that distinguishes the Blue Clay formation from the Globigerina limestone is the presence of clay minerals. This clay content can only have come from a land source, although the possibility that part of the clay fraction originates from volcanic ash of an active volcano should not be excluded (Pedley et al. 2002). The quality of clay material mixed with the planktonic calcium carbonate detritus prevented the formation from reaching the same level of hardness as the other limestones and this is the main reason that Blue Clay is considered the softest rock formation of the Maltese islands. Blue Clay formation is important for agriculture since it produces most of the important fertile and water retentive soils found across Gozo and Malta, provided there is the level of plough technology to work these heavier soils. This would have been more likely only in Roman and later historical times.

The upper parts of the formation show an increase in brown phosphatic sand grains and the green grains of the complex mineral glauconite. Finally, this passes up into sand made up almost entirely of these green grains together with lime-rich fossils fragments. This is known as the Greensand Formation. This change indicates that the sea was becoming shallower and was probably related to the uplift of the Maltese basin on the north flank of the Pantelleria Rift (Pedley et al. 2002).



Figure 2-12: Characteristic exposures of the Blue Clay Formation at the Fomm-IR-RiĦ Bay .

➤ *Greensand Formation*

The Greensand is lying between the Upper Coralline and the Blue Clay formations and was deposited under shallow-water, marine conditions. Moreover, much of the sediment was transported into the Maltese basin from foreign sources, which must have been areas of erosion (Pedley et al. 1976). The outcrops of this formation, when reported, are very thin and only in Gozo do they exceed the 10m (11m at Il-Gelmus).

The freshly exposed outcrops, mainly in man-made cuts, have a very characteristic green colour influenced by the presence of glauconite (a complex, silicate-based mineral). In contrast, the natural exposures have a chocolate brown colour, or the same mineral just altered by weathering (Pedley et al. 2002). These greensand outcrops have been upgraded to a Formation as they represent the residue of a long period of submarine erosion and winnowing of sediments (Pedley et al. 2002). The top part of the formation passes transitionally into the overlying Upper Coralline Formation and it acts simply as a base. However, lying above the Blue Clay, it acts as an important point of water seepage and springs in the stratigraphy of the Maltese Islands. The Greensand formation represents a final shallowing after the earlier deep-water situation and encompasses a period of active current activity. During that period, all the clay and fine carbonate particles were swept away, leaving behind the larger

particles, many of which were fossils or their fragments. The characteristic green Glauconite is typical of such winnowed marine environments bathed by upwelling water (Pedley et al. 2002).

➤ *Upper Coralline Limestone Formation*

The Upper Coralline limestone is situated at the top of the stratigraphic sequence of the Maltese Islands. It is a hard, pale grey limestone and very similar to the Lower Coralline limestone formation. This Coralline Limestone again forms sheer cliffs of varying height and includes a similar content of fossils such as corals and coralline alga. It can be over 160m thick, although it also forms thin hill cappings and limestone-platforms. Karstic geomorphological features have been reported on this formation, but not at the same scale as for the Lower Coralline limestone. The Upper Coralline Limestone is mostly comprised of shallow marine sediments which have characteristics of several different marine or intertidal environments (facies). Although there are five facies reported, these are slightly different in detail from those in the lowest formation. These facies are: a) the Reef Limestone, b) the Tidal Flat Limestone, c) the Oolitic Cross-bedded sands, d) the Muds with large Foraminiferal Limestones and e) the Planktonic muds. The Upper Coralline limestone is the only formation reported on Comino and Cominoto, while it is fully developed in western Malta and eastern Gozo (Pedley et al. 2002).

➤ *Quaternary Deposits*

Although the main sedimentation ended between the Miocene and Pliocene, geological research has recorded the presence of some Quaternary deposits (Trechmann, 1938). They are mainly reported as cavern, fissure infillings and thin hillside veneers of calcreted material (Pedley et al. 1976). The different layers of these sediments contain an abundant mammalian fauna, which provide insights into the climatic conditions of that period. These findings suggest a more temperate climate than today, with perennial stream-systems and abundant vegetation (Pedley et al. 1976). A land bridge with Sicily would have existed during part of this period, and indeed the separation of the Maltese islands only took place at about 14ka (Furlani et al. 2013). As sea level rose, the Maltese islands progressively formed broadly into their current configuration over the following 7000 years.

2.1.4 Previous work

The geological formations of Maltese Islands received the attention of scholars from a very early stage, mainly because they embodied very well-preserved fossils. However, whereas ancient Greek authors made the first surviving references to fossils elsewhere in the Mediterranean (e.g. Xenophanes of Colophon, born about 570 B.C. and Origen (A.D. 185-254)), the study of the Maltese islands had to await the nineteenth century. A number of early advances in the stratigraphic study of geology were made in Britain by scholars such as Smith (1769-1839). With the incorporation of Malta into the British Empire in 1800, there was then some focus and expertise on geological stratification. Indeed, Commander Spratt was the one who provided the first comprehensive geological descriptions (Spratt, 1843). Moreover, he was the first ever who reports the presence of chert outcrops on the Maltese Islands (1854):

“This deposit often contains nodules of a flinty texture, viz., chert, in which are fish-scales.”

Spratt was followed by Murray, who in 1890 produced a review of the geology of the islands. In this he wrote with great authority on oceanic sedimentation, having been on the Challenger Expedition, and his interpretations demand respect, even if they are often not entirely correct. Murray's work stimulated J. H. Cooke, a local resident, to produce a series of detailed studies on particular geological features (Cooke, 1891; 1893; 1893a; 1896; 1896a; 1896b). One of these was a very comprehensive investigation of the chert outcrops of the Maltese Islands (Cooke, 1893b), which, especially for the time, should be considered a high quality research. Although the work was mainly based on macroscopic examination, it presented a high level of detail and his interpretations were largely accurate. Indeed, Cooke is the only individual who ever undertook proper research on the chert formations of the islands, while the rest of the research on Maltese geology was restricted to some generic comments on the presence of these rocks. To be honest though, the low interest in the chert formations should be attributed to the limited exposures of the chert formation and the restricted area in which they are found.

Research on the geology of the Maltese Islands continued during the 20th century, when researchers focused on a range of features. A typical example was Hobbs (1914), who interpreted and described many of the faults and structures of the Islands. In addition, substantial detailed information, particularly on the structure of the islands, is contained in the study of water resources by Morris (1952) and Newbery (1968). The recent long-term research of Dr Martyn Pedley is of particular significance since he revealed the full spectrum of the Maltese geology. He exhaustively investigated many geological issues in the islands and, furthermore, his results are available in numerous publications (Pedley, 1974, 1975, 1993; Pedley et al. 1976, 2002), including the official Geological Map of the Maltese Islands (Pedley, 1993). However, even he did not provide much detail about the chert deposits on Malta and they remained an outstanding gap in the geology of Malta which this

dissertation has sought to fill. More recently there has been a focus on the now submerged continental shelf around the Maltese Islands, often associated with pre-Holocene archaeological and palaeo-environmental investigations around the coasts (Foglini et al. 2016; Harff et al. 2016; Hunt 1997; Micallef et al. 2013).

2.1.5 Structural and Tectonic Geology of the Maltese Islands

Tectonics have affected the geography of the Maltese islands and shaped them by a series of uplifts and subsidence, making the western side of Malta higher than the east, and forming dramatic cliffs on the western/northwestern shores (Alexander, 1988; Fenech, 2007; Ruffell et al. 2018). The main geological formations essentially lie horizontally, but are displaced at intervals by faults, which form the river valleys and coastlines, and, in turn, control the weathering and erosion of the exposed rock layers. These fault systems are dominated by those trending northeast-southwest, but also northwest-southeast (Schembri, 1994).

The Maltese Islands are situated on a shallow shelf or the Malta-Ragusa Rise, part of the submarine ridge that extends from Ragusa in Sicily southwards to the African coasts of Tunisia and Libya, and are generally regarded as forming part of the African continental plate (Alexander, 1988; Schembri, 1994, 1997; Schembri & Lanfranco, 1993; Pedley et al. 1976, 2002; Prampolini et al. 2017). This shelf is intersected by two main types of fault systems, where the dominant type is normal, arranged often as graben, and strike-slip structures (Prampolini et al. 2017). Gardiner et al. (1995) show the Malta-Ragusa Rise was intersected to the southwest of the islands by the northwest-southeast oriented Malta graben. This graben is possibly separate from, but in the same orientation and possibly associated with the Pantelleria graben to the northwest (Prampolini et al. 2017). Northwest of Gozo, the Malta Shelf (the northeastern portion of the Malta-Ragusa Rise) is split by the northeast-southwest orientated North Gozo graben, forming the southeastern margin of the Gela Basin, south of Sicily. More specifically for the Maltese Islands (Fig. 2.13), there is a major cut through the entire Oligocene-Miocene succession, and there is considerable evidence that movement has been continuous since Miocene times (Pedley, 1976). Malta, and Gozo to a lesser extent, are dominated by northeast-southwest orientated normal faults (Alexander 1988; Prampolini et al. 2017), arranged as horst and graben structures which are dominant in the north of the island (where the classic example is The Great Fault, or Victoria Lines along the Bingemma Valley, Malta). Gozo, by contrast, has no evidence of such strong structural control, although a strike-slip fault (the Scicli, Ragusa, Irmino Line) is conjectured by Gardiner et al. (1995) and Yellin-Dror et al. (1997) to run from southwest to northeast to the North of Gozo. The continental shelf around the Maltese Islands was progressively drowned by post-glacial sea levels rise such that there are well preserved terrestrial palaeo-landforms preserved on the present sea floor in depths shallower than c. -130m (Foglini et al. 2016; Micallef et al. 2013; Prampolin et al. 2017). The post-Quaternary tectonics are restricted mainly to more regional

movements which have resulted in the development of localised raised beaches, the submergence of 'cart-ruts' which enter the sea at St. George's Bay, St. Paul's Bay and Birzebbuga (Hyde, 1955), and the presence of stalagmites below the breakwater foundations of Valletta Harbour (Rizzo, 1932). Finally, Hyde (1955) recorded earthquakes in the region occurring intermittently between 1659 and 1856, and another was recorded in March 1972.

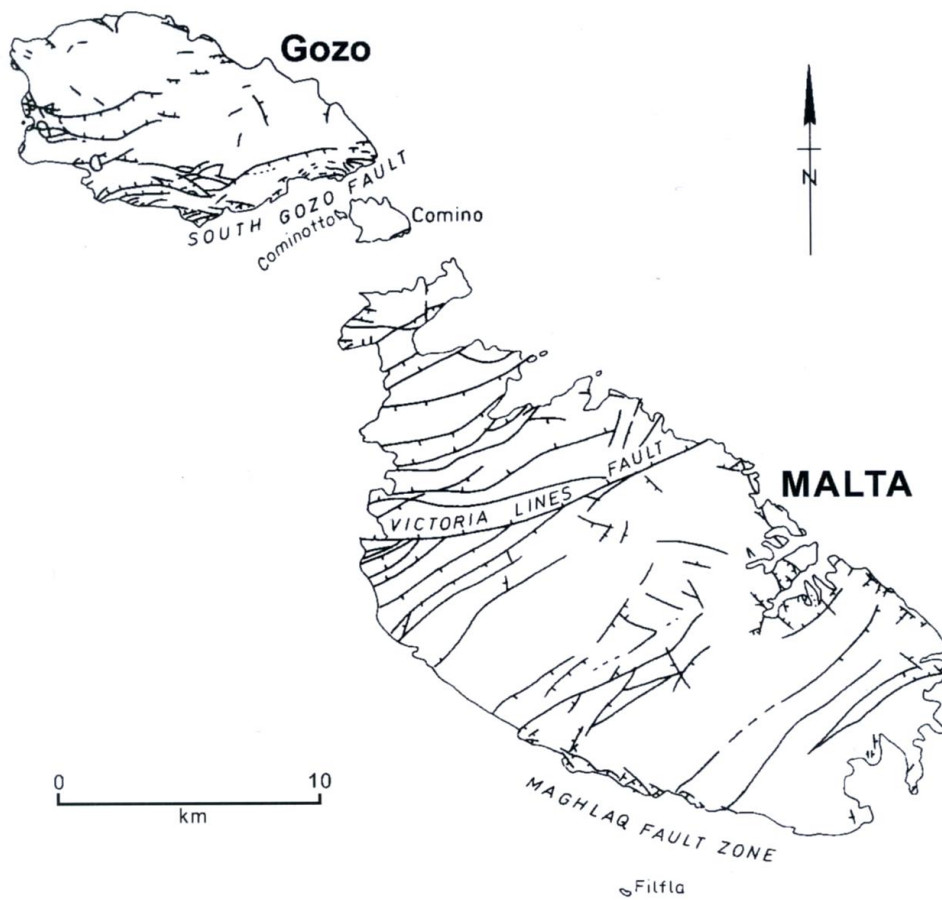


Figure 2-13: The Structural map of the Maltese Islands, showing the major faults (Pedley, 2002).

2.1.6 Geomorphology

The geomorphology of the Maltese Islands has been thoroughly described and discussed by a number of scholars, including Vossmerbäumer (1972), Guilcher and Paskoff, (1975), Ellenberg (1983), Reuther (1984), Alexander (1988), Schembri (1993, 1994, 1997) and Prampolini et al. (2017). The current geomorphological features of the Maltese Islands have been strongly influenced by the geological and tectonic status of the islands. Indeed, Malta presents a large scale gentle folding which is responsible for the characteristic topography of plains and shallow depressions separated by low hills (Schembri, 1997; Prampolini et al. 2017). By contrast, the Lower Coralline forms vertical cliff faces on the west of the islands, and table-topped plateaux in the interiors on which bare and scrubby karstland develops (Schembri, 1994; Prampolini et al. 2017). The Rabat-Dingli plateau is the only location on Malta, south of the Great Fault (Victorian Lines), where all five geological formations are presented, with much of its surface as exposed limestone pavement. Gozo, by comparison, consists of a series of hills, each topped by an Upper Coralline Limestone plateau and separated by low-lying plains where the rock has been eroded down to the Globigerina Limestone. The plateaux are also karstic, the hillsides are covered with clay taluses, and the plains between the hills are gently rolling in form.

Important and characteristic topographic features of the Maltese Islands are the *rdum* and *widien* (Schembri, 1994; 1997). *Rdum* are near vertical faces of rock formed either by erosion or by tectonic movements. Their bases are invariably surrounded by boulder scree eroded from the *rdum* edges. As they provide shelter and relative inaccessibility, the *rdum* sides and boulder screes provide important refuges for many species of Maltese flora and fauna, including many endemics. *Widien* are natural drainage channels formed either by stream erosion during a previous (Pleistocene) much wetter climatic regime, or by tectonism, or by a combination of the two processes. Most *widien* are now dry valleys and only carry water along their watercourses during the wet season. A few *widien* drain perennial springs and have some water flowing in them throughout the year, attaining the character of miniature river valleys. Sea level changes have often submerged the mouths of some *widien* causing the formation of headlands, creeks and bays. By virtue of the shelter provided by their sides and their water supply, *widien* are one of the richest habitats on the islands and are also extensively cultivated.

2.2 Geology of the Sicily Island

2.2.1 Geology

Sicily is part of modern Italy, located in the centre of Mediterranean Sea and it is the largest island of the Mediterranean (Fig.2.14). It developed along the African-European plate boundary and is a segment linking the African Maghrebides with the Southern Apennines across the Calabrian accretionary wedge (Fig. 2.15). In addition, the chain and its submerged western and northern extension are partly located between the Sardinia block and the Pelagian-Ionian sector and partly beneath the central southern Tyrrhenian sea (Fig. 2.15).

Sicily presents three main groups of geological formation (Catalano, 2004), which are: a) the formations of the African continental margin (Hyblean Plateau), b) the formations of the “European group” and c) the formations related with volcanic activity (Fig.2.16). The African rock units are the sedimentary successions which consist of Mesozoic – Lower Miocene deep-water carbonates and cherts (locally named Sicilide, Imerese, Sicanian) and the Meso–Cenozoic shelf carbonates. The “European group” consist of a Paleozoic – Mesozoic sedimentary succession and the ‘Tethyan’ rock units (ocean). The ‘Tethyan’ succession includes the Upper Jurassic–Oligocene sedimentary successions, characterized by basinal carbonates and sandy mudstones (Monte Soro Unit and Variegated Clays Auct.). These units also include the Upper Oligocene–Lower Miocene terrigenous turbiditic successions (internal Flyschs). The volcanic formations are divided in two groups, which are related with the two cycles of volcanic activity on the Island (Cretaceous–Jurassic the first cycle and Neocene–Quaternary the second).

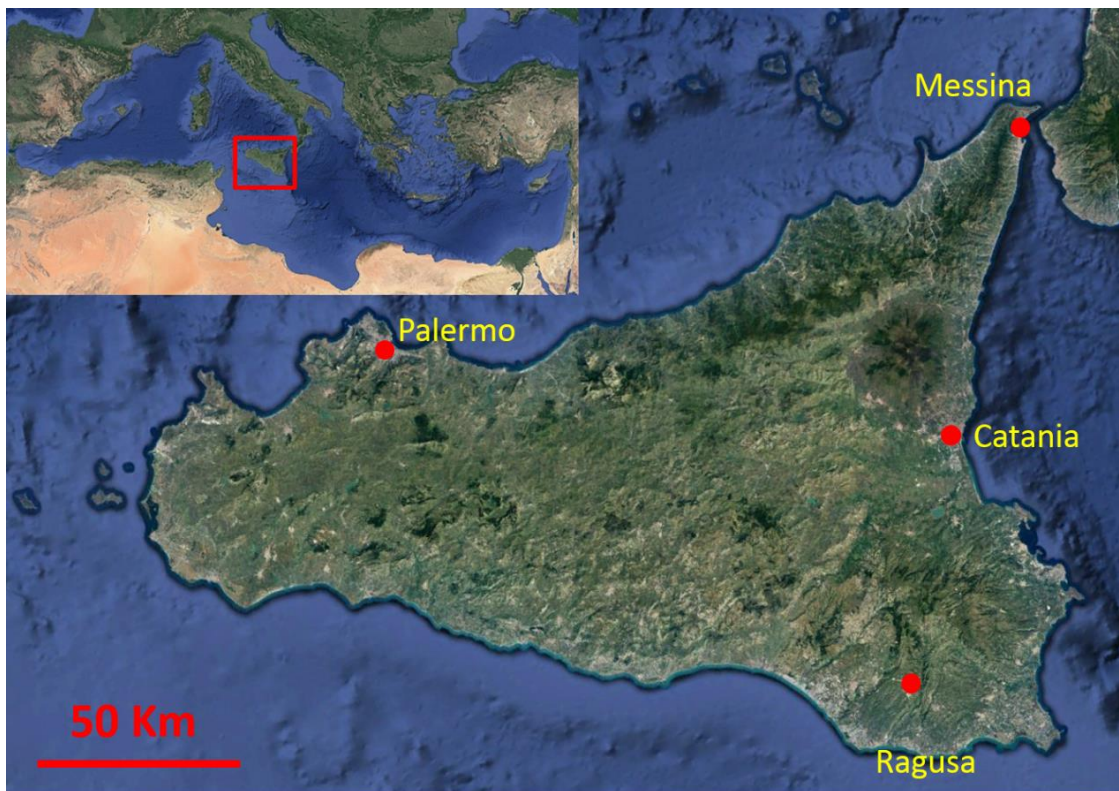


Figure 2-14: Map of Sicily Island with the map of Mediterranean Sea at the upper left corner (Maps Copyright @2016 Google).

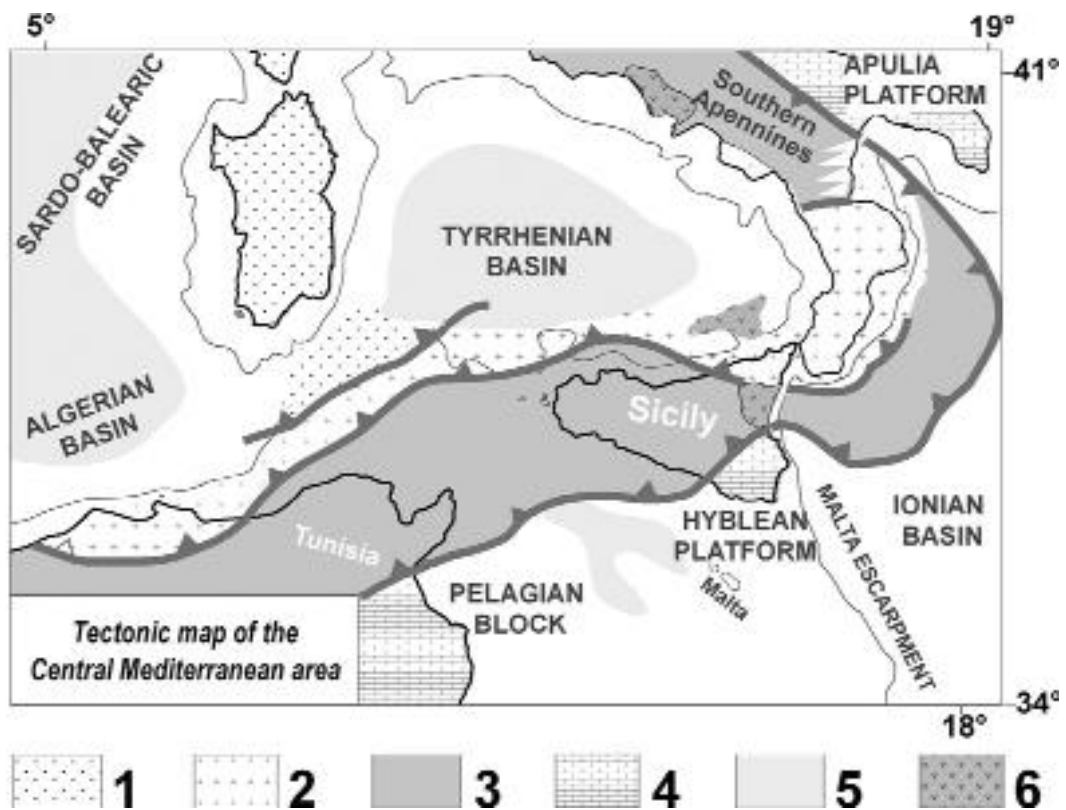


Figure 2-15: Tectonic map of the central Mediterranean area 1) Corsica-Sardinia; 2) Calabrian Arc and Kabylia; 3) Marghrebian- Sicilian-southern Apennine nappes and deformed foreland; 4) foreland and mildly folded foreland; 5) areas with superimposed extension; 6) Plio-Quaternary volcanoes.

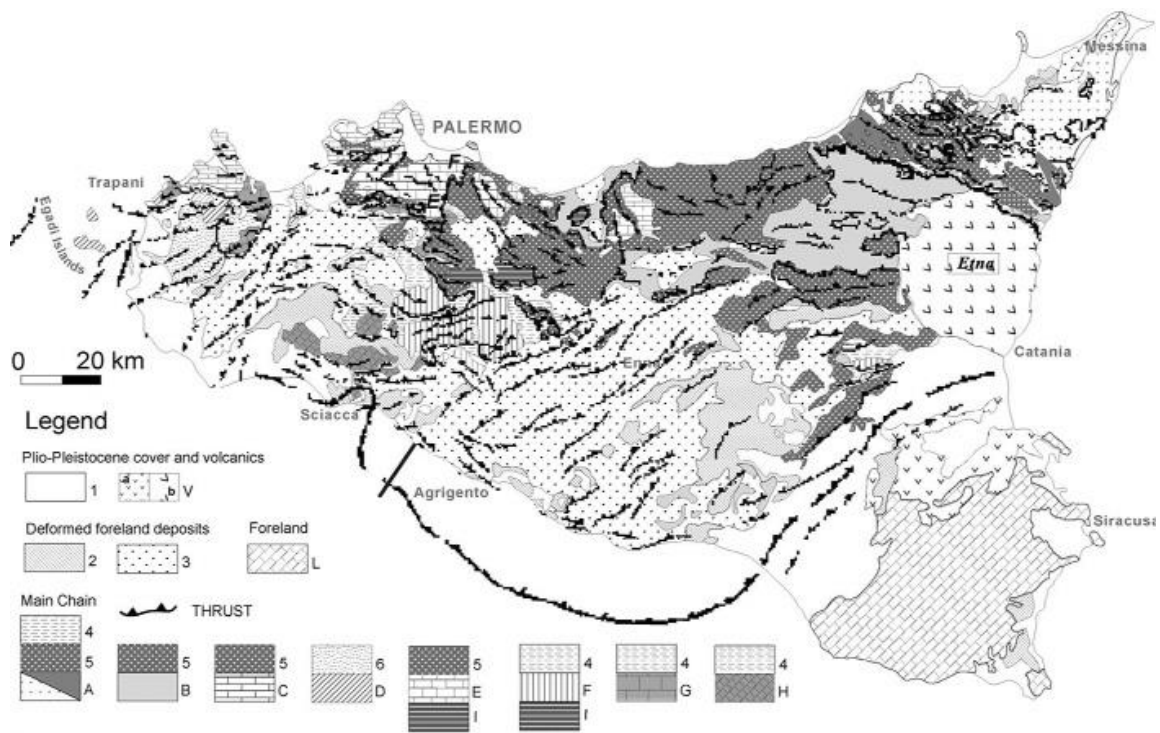


Figure 2-16: Modified Geological Map (Catalano, 2004). 1.Pleistocene; Deformed foreland basins (2.L. Pleistocene-U. Pliocene; 3.L. Pliocene-U. Tortonian; 4.M. to L. Miocene); Flysch units (5. L. Miocene-U. Oligocene); Shelf margin (6. L. Miocene-U. Oligocene); A. Calabrian tectonic units (Oligocene-Paleozoic); B. Sicilide units (Oligocene-U. Mesozoic); C. Panormide units (Oligocene-Trias); D. Pre-Panormide units (Oligocene-Trias); E. Imerese units (Oligocene-U. Mesozoic); F. Sicanian units (Oligocene-U. Mesozoic); G.. Trapanese units (Oligocene-Trias); H. Saccense units (Oligocene-Trias); I. L. Permian-Middle Triassic allochthons; L. Hyblean units (L.Pleistocene-Trias); V. Volcanics: (a) Pliocene, (b) Pleistocene.

➤ *Chert outcrops*

Chert formations were reported in all of these rock groups (e.g. Carbone et al., 1990; Lentini, 1984) and they presented a variety of form, characteristics and age (Fig. 2.17). The fieldwork survey (conducted by Chatzimpaloglou in 2017) on the island reported that chert outcrops were present in many areas of Sicily (Fig. 2.17). Starting from the southeast part of Sicily, the chert formations were intercalated with most of the limestone formations of the Hyblean Plateau unit (Fig. 2.18) from the Cretaceous (Campanian) to the Quaternary. The rest of the island was dominated from the “European group” which also presented a significant amount of chert outcrops (Fig. 2.19). They were intercalated with limestone formations (Triassic–Jurassic), but also forming the Radiolarian formation (Jurassic–Cretaceous) which presented extensive exposures in the East of Sicily (Fig. 2.19a-b). The first cycle of volcanic activity (Cretaceous–Jurassic) was reported in the west of Sicily (Palermo region) with some indications of chert outcrops, while the second cycle (Neocene–Quaternary) did not report any similar evidence. More details of the Sicilian chert outcrops and their characteristics will be presented below (Chapter 5).

The Age of the Rock Formations of Sicily

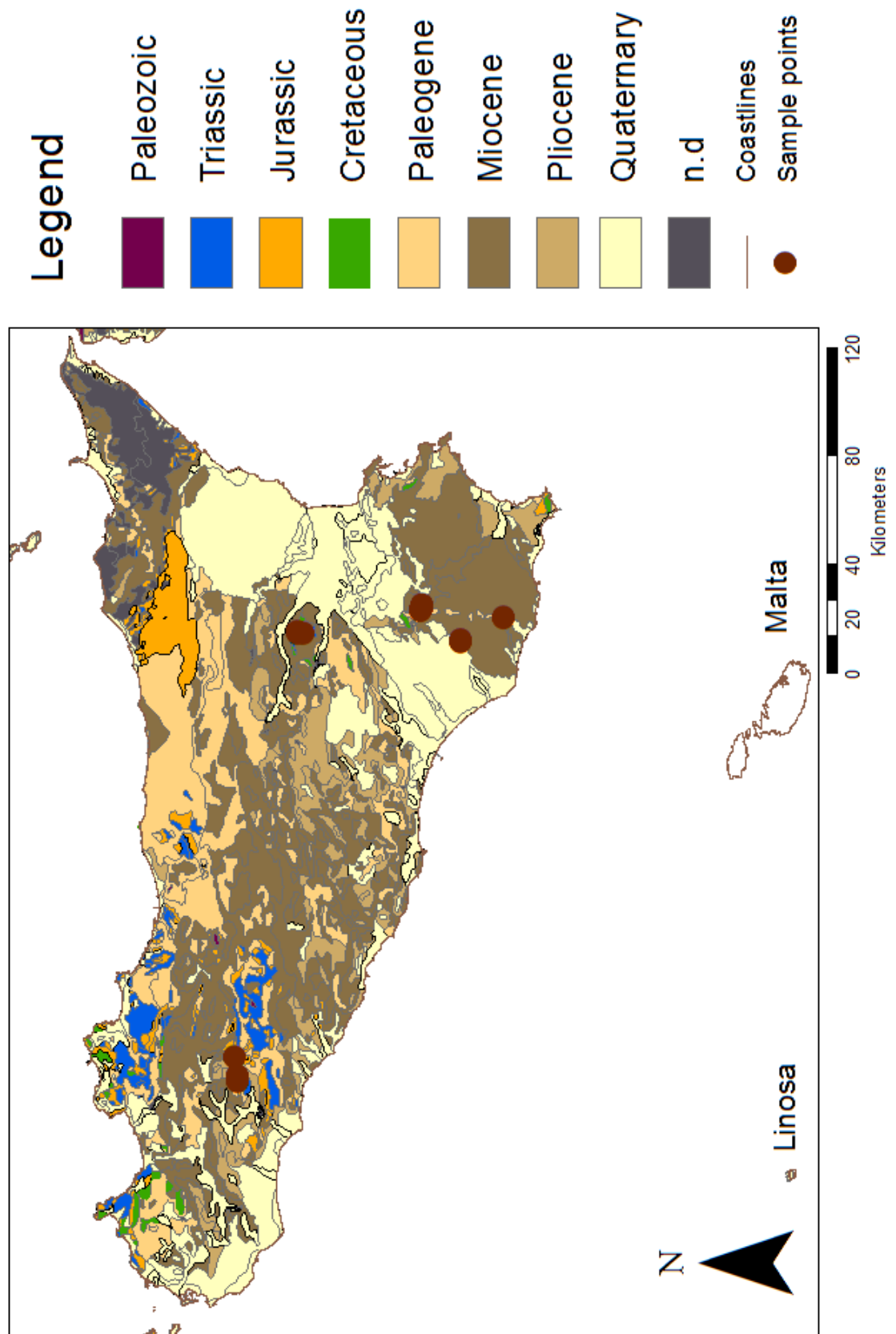


Figure 2-17: The Map of Sicily with the rock formations divided by age and the samples locations.

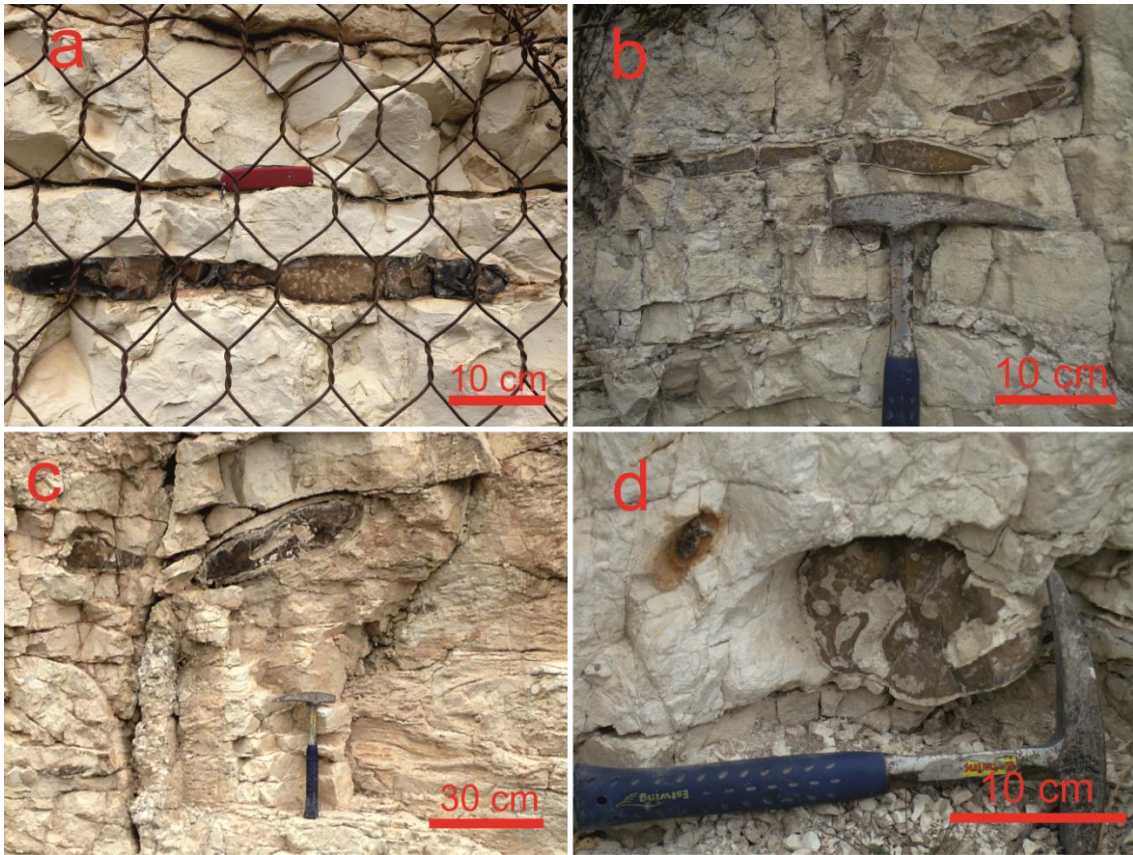


Figure 2-18: Chert outcrops in Limestones of the Hyblean Plateau unit. A) Black to brownish chert, b) chert lenses outcrops, c) brownish, huge lens and d) huge nodular chert with chalky residues.

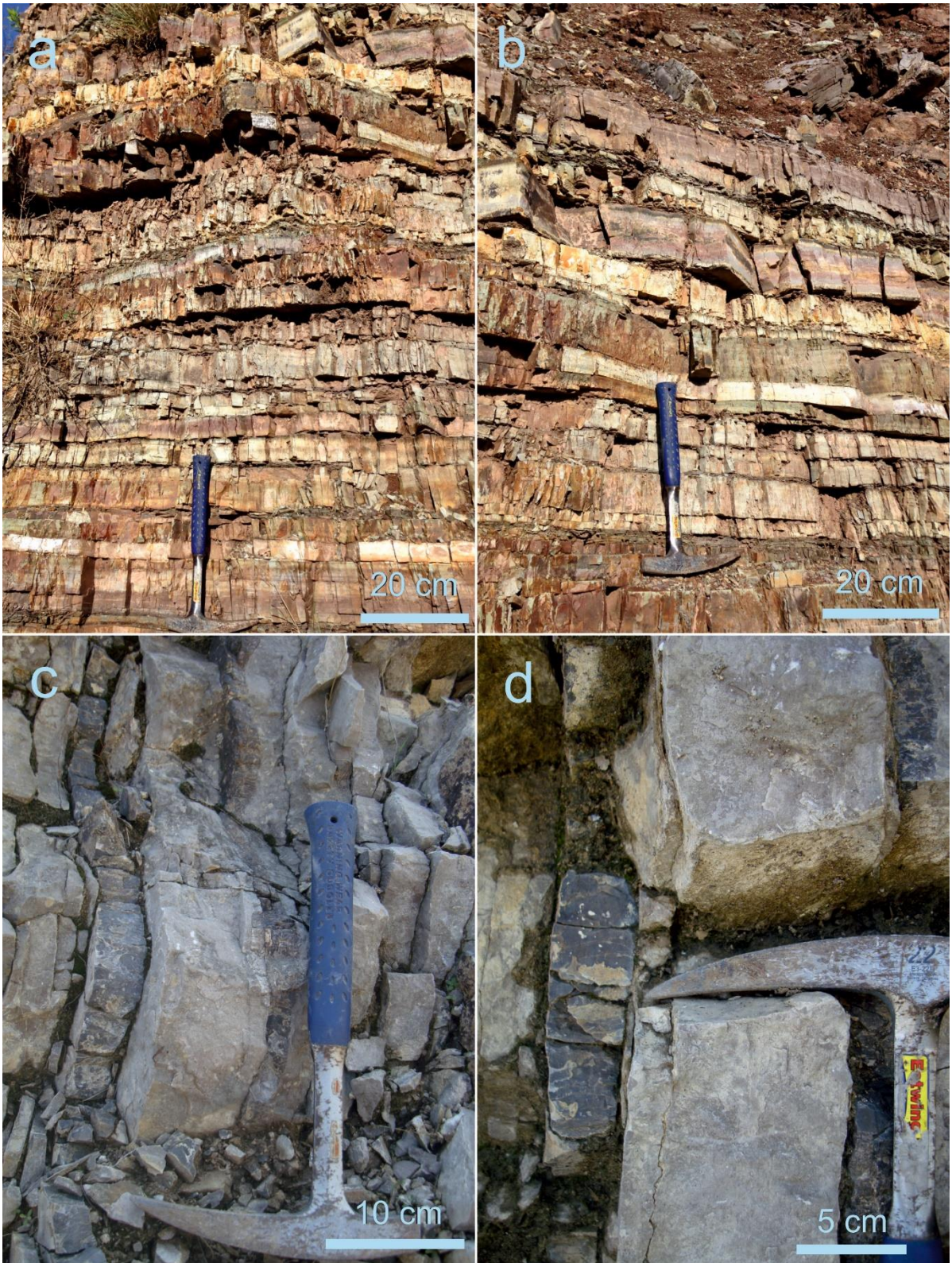


Figure 2-19: Chert outcrops from the “European group”. a and b) Different angles of the sequence of radiolarian beds on the riverbed of Valona River, c and d) Black bedded chert outcrops at the Monte Santo.

2.2.2 Previous work

In comparison with the Maltese islands, Sicily has a far more complex geology (which cannot be fully covered here) and consists of formations which vary significantly in origin, type and age. This diversity has possibly triggered the interest of many researchers of the 20th century to investigate the geology of the island. The first studies were mainly stratigraphic or palaeontological and carried out in a general framework of autochthony (Finetti, 2005). The first work on the regional structure of north-eastern Sicily was published by Ogniben (1960), which was based on the geosyncline model. This was followed by papers describing the geological features of the Calabrian–Peloritanean arc (e.g. Amodio Morelli et al., 1976).

Eastern Sicily has been intensively investigated and detailed geological maps have been created, which stated the current view of the geological structure of this part of Sicily (Carbone et al., 1984, 1986, 1990; CNR, 1991; Lentini, 2000). Furthermore, the structure of eastern Sicily was analyzed by Grasso and Lentini (1982); Ghisetti and Vezzani (1984); Lentini et al. (1996a); Lickorish et al. (1999). Bianchi et al. (1989) presented the geological structure between the Nebrodi Mountains (NE) and the Hyblean foreland (SE). However, his findings were later reinterpreted by Roure et al. (1990) and Lentini et al. (1996b). Finally, Bello & al. (2000), using several seismic sections, illustrated the most complete structural setting of Eastern Sicily.

The detailed investigation of western Sicily began only in the 1970s (Giunta and Liguori, 1973), presenting the first analysis of the Mesozoic carbonate and Neogene terrigenous deposits. Western and central Sicily was considered as a thin skinned imbricate wedge of mesocenozoic carbonate and siliciclastic rocks. This was suggested by many researchers such as: Catalano & D'Argenio (1978, 1982), Catalano & al. (1989), Roure & al. (1990), Giunta (1993), Lentini & al. (1995), Monaco & al. (1996). Recent papers (Lentini et al., 1996b, 1994; Finetti et al., 1996; Catalano et al., 2000; Del Ben and Guarnieri, 2000, Guarnieri et al., 2002;) used seismic lines and geological field data, in order to provide a more accurate description of the geo-tectonical structure of the western Sicily.

Although there has not been a research focused especially on chert formation, they have been reported in many surveys. Indeed, many of the investigation (e.g. Carbone et al., 1990; Catalano, 2004; Lentini, 1984) have recorded with great accuracy the presence and macroscopic characteristics of the chert formations of Sicily. Generally, in the past, the chert formations were always neglected, as they were not considered of equal importance to other formations (i.e. limestones). It was believed that chert could not provide much information about the geological history of an area and therefore they were never investigated in detail. Fortunately, the majority of the chert outcrops on Sicily is in the carbonate formations, which have been thoroughly investigated. This provided a respectable amount of information about the whereabouts and the volume of the chert sources on the island of Sicily. Nonetheless, there is a lack of knowledge on their exact mineralogical content and chemical

composition and more must be done on that aspect of the chert formations of Sicily. Once again, this dissertation has sought to fill this gap in knowledge.

2.3 Chert rock formation

It is essential before starting to investigate the lithic assemblages to have the background information for their rock sources. This is more than necessary in the case of sourcing chert assemblages, which has been proven to be difficult and problematic. Although the chert formations seem to be simple, they are actually very complex rocks with many aspects of them to be still unknown. In addition, there are no distinct characteristics which could clearly separate the chert varieties. Finally, the fields of Geology and Archaeology interpret differently the term chert causing a lot of confusion. Therefore, this chapter will present the main characteristics of the chert formations, which are going to be useful in examining the origin of chert assemblages. This will include the origin of the chert formations and their main varieties, in addition with their mineralogical and geochemical composition.

Cherts are fine-grained, dense, commonly very hard sedimentary rocks, which are composed predominantly of SiO_2 minerals (> 90%). They break with a conchoidal fracture, often producing very sharp edges and varying in colour. Cherts are common but not abundant rocks in the geologic record, while ranging in age from the Precambrian to the Quaternary (Boggs, 2009; Tucker, 2001).

2.3.1 The origin of Chert

The origin of silicon dioxide (SiO_2) is still not completely clear and until now two are the predominant versions (Tucker, 2001; Maliva et al. 2005; Shen, et al. 2018):

- a) The cherts are entirely biogenic in origin, unrelated to any hydrothermal activity;
- b) The cherts are a product of hydrothermal activity (e.g. submarine volcanism). This could be either directly through inorganic precipitation of silica derived from subaqueous magmas and hydrothermal activity or indirectly through plankton, which blooms in areas with submarine volcanism. Silica deposits can inorganically precipitate from solution, for example, siliceous sinter. In addition, on active ridges (e.g. oceanic ridges), metalliferous deposits derived from hydrothermal emanations usually prevail, and occasionally hydrothermal amorphous silica occurs. This must have been the main source of chert during Precambrian (Proterozoic), which was before the evolution of silica-secreting organisms (e.g. radiolarian).

Although the research on this matter is still inconclusive, a combination of these two factors should not be excluded especially for the chert formations after Precambrian era.

2.3.2 Chemical composition

Cherts are composed dominantly of SiO₂, but can include minor amounts of Al, Fe, Mn, Ca, Na, K, Mg, Ni, Cu, Ti, Sr, and Ba (Boogs, 2009). The amount of SiO₂ varies markedly in different types of cherts, ranging from more than 99 percent in very pure cherts such as the Arkansas Novaculite to less than 65% in some nodular cherts. Aluminum is commonly the second-most abundant element in cherts, followed by Fe, Mg or K, Ca and Na. Cherts may also contain trace amounts of rare-earth elements such as cerium (Ce) and europium (Eu).

Jones and Murchey (1986) suggest that the chemical elements in cherts are derived from four possible sources: biogenic, detrital, hydrogenous (precipitated or absorbed from seawater) and hydrothermal. Siliceous organisms furnish the major source of Si, and Ca may be derived in part from calcareous organisms. Detrital impurities furnish additional Si, as well as Al, Ti, Ca, Mg, K, and Na. In areas of high volcanic activity such as backarc basins and seamounts, significant amounts of K and Mg may be furnished in detrital components (Hein et al., 1983). The hydrogenous elements may include Fe, Mn, Ni, and Cu. Elements that may be contributed from hydrothermal fluids in areas of high heat flow such as oceanic spreading centers include Fe, Mn, and Ba.

2.3.3 Mineralogy and texture

The primary mineral of the chert formations is quartz and specifically the low temperature quartz. However, these formations could also present other SiO₂ minerals like :a) the amorphous biogenic silica (opal-A), b) the amorphous non-biogenic silica (opal-A'), c) the semi-crystalline opal with cristobalite and tridymite (opal-CT), d) the semi-crystalline opal with cristobalite (opal-C) and e) the chalcedony. Furthermore, a rock formation could be composed entirely from one mineral (e.g. Radiolarite – microcrystalline quartz) or from a combination of more than one.

The type of minerals found in a chert formation is related with the diagenetic maturity of the rock. Moreover, Kastner et al. (1983) suggested that when the diagenetic grade of chert formation is increased the normal course of the SiO₂ minerals is:

Opal-A → Opal-CT → Quartz.

Generally, all the SiO₂ minerals may be present in chert formations, from pure opal to pure quartz, depending upon the age of the deposits and the conditions of burial (Boogs, 2009). Nonetheless, SiO₂ minerals are not the only thing that can be found inside a chert formation. Calcite and dolomite are often found inside these rocks, especially in those recorded within carbonate formations such as limestones. In addition, constituents such as detrital clays and other siliciclastic minerals, pyroclastic particles, and organic matter have also been reported. Many of them contain recognizable remains of

siliceous organisms, including radiolarians, diatoms, silicoflagellates, and sponge spicules. The chert formations related to limestones, commonly include calcareous fossils such as foraminifera and echinoderm. The remaining fossils attributed to the host formation are considered indications that the chert rocks have been formed by replacing the host formation. Finally, authigenic minerals such as silica cement, clay minerals, hematite, pyrite, and magnetite are some of the other types of minerals found in a chert formation.

2.3.4 Forms of Chert rocks

The chert formations, based on their appearance on the field, can be found in bedded or nodular form.

2.3.4.1 *Bedded Cherts*

Bedded cherts consist of layers of nearly pure chert, ranging to several centimeters in thickness (3 – 10cm) and are commonly interbedded with thin layers or laminae of siliceous shale (Boggs, 2009). Moreover, they are commonly associated with ophiolitic rocks such as submarine volcanic flows, tuffs, pelagic limestones, shales, siliciclastic turbidites and many others. Bedded chert formations are considered as primary deposition and biogenic origin formations. They are composed dominantly of the remains of siliceous organisms, which are commonly altered to various degrees by solution and recrystallization. Finally, they can be subdivided on the basis of type and abundance of siliceous organic constituents into four principal types (Boggs, 2009): a) Diatomaceous deposits, b) Radiolarian deposits, c) Siliceous spicule deposits and d) Bedded cherts containing few or no siliceous skeletal remains.

2.3.4.2 *Nodular Cherts*

Nodular cherts are subspheroidal to irregular masses that range in size from a few centimeters to several tens of centimeters. Occasionally, these forms can be connected with each other and create almost continuous beds, which resemble to bedded cherts (Tucker, 2001). They are created mainly through the diagenetical replacement of their hosting rocks and they are commonly found in carbonate rocks. The diagenetic origin is clearly demonstrated in many nodules by the presence of a) partly or wholly silicified remains of calcareous fossils or ooids, b) burrow fillings, c) algal structures, etc. (e.g. Gao and Land, 1991). The nodular cherts normally lack internal structures, but some nodular cherts contain silicified fossils or relict structures from the preexisting formation. They typically occur in shelf-type carbonate rocks where they tend to be concentrated along certain horizons parallel to bedding. However, they could also occur in sandstones, mudrocks, lacustrine sediments and evaporites.

2.3.5 Varieties of Cherts

Although chert is the general group name for siliceous sedimentary rocks composed dominantly of SiO_2 minerals, several names are applied to various types of chert. **Flint** is used both as a synonym for chert and as a varietal name for chert, particularly chert that occurs as nodules in Cretaceous chalks. **Jasper** is a variety of chert colored red by impurities of disseminated hematite. Jasper that is interbedded with hematite in Precambrian iron formations is called jaspilite. **Novaculite** is a very dense, fine-grained, even-textured chert that occurs mainly in mid-Paleozoic rocks of the Arkansas, Oklahoma, Texas region of south-central United States. **Porcellanite** is a term used for fine-grained siliceous rocks with a texture and fracture resembling that of unglazed porcelain. The term is often used by chert workers for cherts having this character that are composed mainly of opal-CT. **Siliceous sinter** is porous, low-density, light-colored siliceous rock deposited by waters of hot springs and geysers. Although most siliceous rocks consist dominantly of chert, some have a high content of detrital clays or micrite. These impure cherts grade compositionally into siliceous shales or siliceous limestones.

3 Archaeological Research

3.1 The Prehistory of Malta

The prehistoric society that built the Megalithic Temple monuments of the Maltese Islands has been established as one of the most precocious pre-urban communities of the world (Malone et al., 2009). The earliest evidence for human occupation of the islands goes back to the early Neolithic period, which would now be placed at 5800 to 5500 BC thanks to the dating programme of the FRAGSUS project. This date is also considered the onset of the Pre-Temple period of the Maltese Islands, which lasted until 4100 B.C (Table 3.1).

The Pre-Temple period encapsulated the Għar Dalam, Grey Skorba, Red Skorba phases and the sites of human occupation were established in open areas and caves. The *Stone Temples* were constructed from the first half of the fourth millennium until their florescence in the mid-third millennium BC (Table 3.1). The Temple Period had a clear but not yet fully explained end at approximately 2500–2400 B.C, which also signified a possible break in the Neolithic sequence of the Maltese Islands. New activity on the islands was reported during the Tarxien Cemetery Phase (2400 B.C.), but there is a trace of continuity (Trump, 2010).

Although these monuments and the culture that erected them have been investigated for decades, there are many aspects of them that are still poorly understood. One of these is the origin of the chert/flint assemblages found in many prehistoric sites on the Maltese Islands. This study will try to investigate the origin of the chert/flint assemblages found in association with the archaeological sites of the: a) Ġgantija (temple site), b) Brochtorff–Xaghra Circle (funerary site), Taċ-Ċawla (settlement site) c), d) Kordin (temple site), e) Skorba (Temple and settlement) and f) Santa Verna (temple site). This chapter will present background information on these sites and their importance in the prehistory of Malta.

Table 3-1: The cultural phases of Prehistoric Malta. Radiocarbon dates are quoted throughout the text as cal BC/AD dates unless otherwise stated.

Maltese Chronological Sequence	
Early Neolithic Period	
<i>Phase</i>	<i>Approximate Date</i>
Għar Dalam	~5600 – 5000
Skorba	5000 – 4500
Temple Period	
<i>Phase</i>	<i>Approximate Date</i>
Żebbuġ/Mgarr	3800 – 3400
Ġgantija	3400 – 3000
Tarxien	3000 – 2300

Bronze Age	
<i>Phase</i>	<i>Approximate Date</i>
Tarxien Cemetery	2300 – 1500
Borġ in-Nadur	1500 – 1000
Baħrija	1000 – 800
Phoenician Period	
Phoenician	800 – 550
Punic	550 – 218
Roman	218 B.C. – A.D. 330

3.1.1 Literature Review of the research on the Neolithic Period of Malta

Recent work by the FRAGSUS project shows that the first Neolithic settlement on the Maltese Islands dates to at least 5500 BC and human impact recorded in the pollen record to even earlier in the sixth millennium BC (Farell et al. in press). The famous *Stone Temples* now appear to be part of the second cycle of human settlement reaching its peak between 3000 and 2350 BC. The remains of these huge constructions were known for millennia but were initially ascribed to incursive groups such as the Phoenicians (Houel 1782-7). The first certain records of prehistoric remains on the Maltese Islands were found in the work of Commendatore G. F. Abela (an official of the Knights of St. John in Malta), which was published in 1647. This was followed by the work of Houel (1782-7), which described some of the chief visible prehistoric remains. The author included detailed engravings of these monuments in the late 18th century and illustrated how these monuments appeared before they were excavated (Evans, 1959; Pecoraino 1989; Freller 2013).

One of the first monuments excavated was the Brochtorff–Xagħra Circle on Gozo, a project carried out by Otto Bayer in 1826. The excavation was conducted in the centre of the monument and revealed the megalithic structure and the burials below ground (Attard Tabone, 1999; Grima, 2004; Malone et al., 2009). Unfortunately, Bayer died without leaving any record of his work and nothing would have been known if it were not for the sketches of Charles de Brocktorff (Grima, 2004). The site was refilled and returned to its previous use as a field (a common practice at the time) and stayed hidden for more than a century. One year later (1827) Bayer was again the first to excavate the famous Ġgantija Temple, an archaeological site very close to the Circle. The decades that followed until the end of the 19th century were thronged with travellers (e.g. Sant Cassia, 1993) examining many Neolithic sites of the Maltese Islands (e.g. Ғaġar Qin, Kordin). Nonetheless, very few of these investigations (e.g. Vance, 1842) provided any records or published their findings and actually delayed the investigation into the prehistory of Malta. Therefore, it was no surprise that all the scholars until the 20th century believed that all of these sites were related to the Phoenician occupation (of approximately 1000 B.C.).

Thankfully the turn of the century initiated an increasing interest in Mediterranean prehistory and subsequently of the Maltese. During the first decades, a number of sites (e.g. Ғaġar Qim, Hypogeum) were excavated and investigated further. In 1901, the German scholar A. Mayr published his work with

the title: "Die vorgeschichtlichen Denkmäler von Malta". It was the first comprehensive work on the known prehistoric buildings and attempted to evaluate the content and significance of these monuments in the prehistory of the Mediterranean (Evans, 1959). In 1910 the work on the Ғал Саflieni Hypogeum, under the supervision of Magri and then Zammit, was published (Zammit, 1910) and provided a full description of the monument along with a plan of the temple/structure. The Hypogeum was initially found in 1902 and must be considered one of the most important discoveries of the Maltese prehistory. A major breakthrough was the work of Zammit initially with Ashby at Santa Verna and subsequently at Tarxien, establishing for the first time the importance of the Late Neolithic Period of Malta (Ashby et al., 1913; 1916; Zammit, 1915-1916). Special recognition must be given to Margaret Murray (1923–29), whose work remains, to date, the most easily quantifiable prehistoric excavations from the Maltese Islands. In addition, the work of Luigi Ugolini from 1924 to 1935 is considered an early systematic documentation of the prehistoric holdings in the archaeological museum in Malta and an architectural survey of monuments (Evans 1971). However, his unexpected death in 1936 and WWII led his archive to be forgotten for almost a century until it was finally rediscovered in 2000 (Pessina et al., 2005).

With the exception of the above, the two world wars did not have a significantly negative effect on the work carried out in Malta. Nevertheless, it was not before 1950 that the circumstances were right for advancement on the interpretation of prehistory. It was then that Professor John Evans was commissioned to produce a survey investigating the prehistory of the Maltese Islands, which proved to be a turning point in our understanding of these megalithic monuments. Indeed, in 1953 his major publication "The Prehistoric Culture–Sequence in the Maltese Archipelago" provided the foundation of all subsequent work on Maltese prehistory. Evans was fortunate enough to have Dr David Trump as the curator of the National and Archaeological Museum during the period 1958–63 and his work during the same period helped Evans' research greatly (1959; 1971). Indeed, Trump's excavations at Skorba, BaҒrija, Ta' ҒаҒrat, Kordin III (Malta) and Santa Verna (Gozo) in the 1960s provided the missing chronological links in the developing prehistoric sequence (Evans 1971). Trump was the first to employ the newly introduced radiocarbon dating technique on the Maltese islands, which provided scientific evidence for the exact dates of these prehistoric sites and it is still considered a major breakthrough in the archaeological research of the Maltese Islands (Malone et al., 2009; Renfrew, 1973). Trump's research is regarded as a great contribution to prehistoric Malta and has been presented in numerous publications (e.g. 1961a, b; 1966; 2002; 2015).

The next important discovery came from the investigation of the Brochtorff XaҒhra Circle (1987–1994), where a second hypogeum was conclusively found. The results of this excavation have been presented in the book of Malone et al. (2009) and it has been considered a counterbalance to the loss of data from Ғал Саflieni (Stoddart 1999; Trump, 2002; Sagona, 2015). The great importance of this excavation could be understood by the fact that it presented the first major analysis of human remains

from a mass burial ground of the prehistoric period (Sagona, 2015). Furthermore, the Skorba and Brochtorff Xagħra Circle excavations helped systematize the ceramic sequence of Maltese prehistory and the Skorba excavation gave Renfrew (1973) the opportunity to place these results in a broader European context (Sagona, 2015). In his work, he stressed the implications of calibrated dates, which suggested that the Maltese *Stone Temples* were some of the oldest free-standing monumental constructions in the world (Renfrew 1973; 1986a).

The FRAGSUS project (with which this dissertation is associated) has succeeded in taking the study of the patterns of human settlement in the Maltese Islands much further. Pollen evidence now suggests that humans had an impact on the islands as early as the beginning of the sixth millennium and that stable settlement was present from at least the middle of the same millennium. Furthermore, the application of hundreds of AMS radiocarbon dates has detected a possible absence of settlement and decline in agricultural activities between c. 4800 and 4100 BC, suggesting that the phase of settlement culminating in the *Stone Temples* may have represented a new Neolithic population. Most importantly, the recent excavations of Ġgantija, Santa Verna, Skorba and Kordin have been executed with greater rigour, recovering the archaeological samples of lithics analysed in this thesis, together with a more detailed analysis of materials from the earlier excavations at the Brochtorff Xagħra Circle. The research undertaken so far in the Maltese Islands has answered many questions about life and death rituals, the location and function of settlements and the degree of vegetational cover and erosion. An enduring question in much Maltese research is the degree of connectivity with neighbouring regions. The study of the Brochtorff Xagħra Circle added details to the study of exotic greenstones and the FRAGSUS project has added the study of isotopes and DNA to human remains. In this work, there has been no systematic sourcing of the lithic remains and this dissertation seeks to achieve this end from a strongly geological perspective.

3.2 The Archaeological Sites Investigated

3.2.1 Ġgantija (Temple Site)

Ġgantija temple is located on Gozo (Fig. 3.1), on the lip of the Xagħra plateau facing towards the South-East (a common characteristic for many temples). The name means “The Tower of the Giants” a nomenclature given by the locals because of its great size (Ugolini et. Al, 2012). This monument is actually two temples, which have been built close together and alongside each other (Fig. 3.2 and 3.3). They were constructed during the Ġgantija phase (Table 3.1) and enclosed within a single massive boundary wall (Trump, 2002; Ugolini et. al., 2012).

The southern temple is considered the oldest of the two temples and is also the largest and the better preserved (Trump, 2002; 2010). It is from this side of the archaeological site where the surviving height of the walls reaches just over 7m. The plan of this temple is simple; it consists of five large apses connected by a central corridor (Trump, 2002; 2010). The first pair of apses is smaller, while the inner apses are larger and the central one is slightly higher/raised. The façade between the two temples has crumbled, revealing the original outer wall of the southern temple. The evidence of the site suggested that, later in the Ġgantija phase, part of the first temple's north wall was removed to allow the rise of the second (Trump, 2002). This temple (northern) is placed a little further back from the front edge and has a slightly less elaborate structure. It has also five apses which are connected with a corridor, but the apse at the very end is extremely small. Moreover, the first pair of apses is larger than the second which is an inversion of the southern temple (Trump, 2010).

In terms of construction materials, the external walls were made of Coralline Limestone, while the internal walls and passages were made of Globigerina Limestone. These limestone types are local as they have both been reported in the geological sequence of the Maltese Islands (Chapter 2).

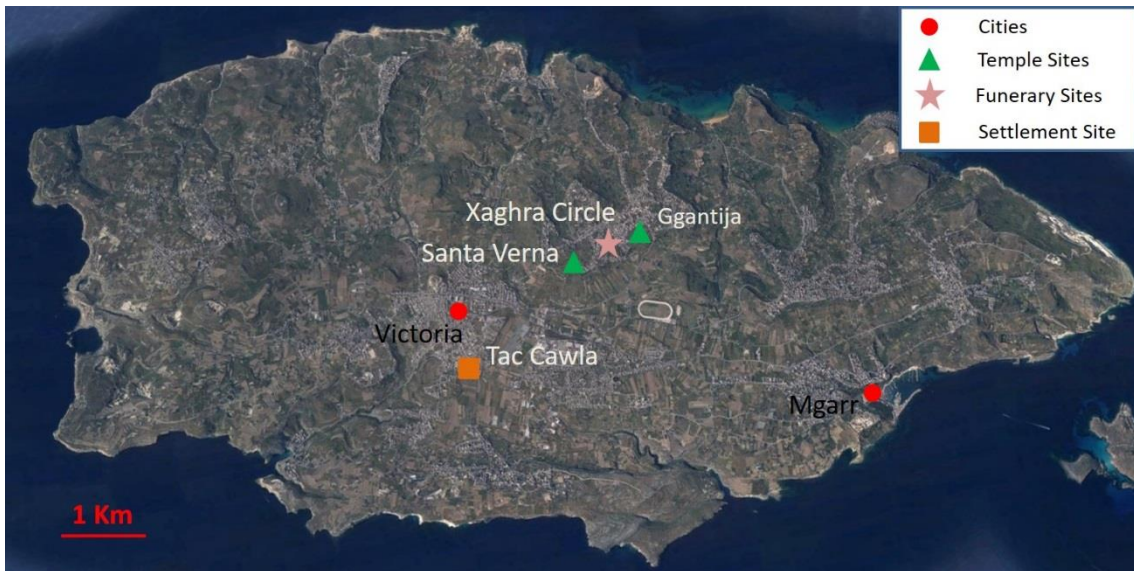


Figure 3-1: The Gozo Island with the main cities and the archaeological sites investigated (Maps Copyright @2018 Google).



Figure 3-2: Overview of the Ggantija Temples.



Figure 3-3: Photographs of the Ggantija Temples. a) The entrance of the north temple and b) The wall of the temples from the Northeast.

3.2.2 Brochtorff–Xagħra Circle (Burial Site)

The Brochtorff Xagħra Circle, also known as the Xagħra Stone Circle and the Gozo Stone Circle, is located on the southern crest of the Xagħra plateau, near the Ġgantija temple (Fig. 3.1). The Circle was recognized by 18th century antiquarian travelers, with Otto Bayer being the first to excavate the site (Malone et al., 2009). However, it was not until recently that the site was fully investigated and its importance recognized. An excavation project took place between 1987 and 1994, conducted by a joint team of the University of Malta and the University of Cambridge. Their efforts were supplemented by the Universities of York and Bristol and the Museums Department of Malta. The excavation led to the discovery that the Circle is an underground (cave) funerary complex (Fig. 3.4) containing more than 250,000 human bones and a rich collection of prehistoric artefacts (Malone et al., 2009).

The evidence collected from the excavation showed that the Circle was in use from the Ġgantija phase (Table 3.1) until the Tarxien Cemetery phase (approximately from 3400 BC to 2300 BC). The cultural use of the site (funeral use) was founded in the Żebbuġ phase (Table 3.1), reached its peak during the Tarxien phase and changed use in the Tarxien Cemetery phase to a domestic occupation.



Figure 3-4: Photographs of the site collected during the fieldwork in 2017.

3.2.3 Santa Verna (Temple Site)

The Santa Verna site is located 700m west of the Circle, near the southern tip of the Xagħra plateau (Fig. 3.1). Today, the remains of this site are nothing more than three shapeless blocks (Fig. 3.5) standing in an open field (Trump, 2002). The excavations conducted at the beginning of the 20th century (1908–1911) revealed a spread of torba alongside these standing stones, the shape of which suggested a small trefoil temple and these three blocks must have formed part of the façade.

Further work conducted on the site in 1960 (led by D. Trump) found deposits of a settlement that predated the temple. The settlement was established in the Pre-temple period, with the earliest pottery remains dating back to the Għar Dalam phase (Table 3.1). The temple was built at a much later stage and with current findings, the date of its construction can be placed in around 3800 B.C. It was not the first time that a temple was built over a settlement on the Maltese Islands as seen at a) Skorba, b) Kordin III and c) Ғaġrat (Trump, 2002). The site was more comprehensively excavated during the FRAGSUS project, and convincingly shown to be a temple of similar size and orientation as Ġgantija.



Figure 3-5: Photographs of the Santa Verna collected during fieldwork in 2017. These megalithic stones are pointing where the archaeological site is located.

3.2.4 Tač-Ċawla (Settlement Site)

The Tač-Ċawla site is a prehistoric settlement which is found on Gozo island (Fig. 3.1) in the southern suburbs of Victoria City (the capital of the island). The site was discovered in the late 1980s but only limited information was collected as it was never properly excavated. The first comprehensive investigation of the site was conducted in 2014 under the FRAGSUS project and is now in course of publication (2019). The first results of the soil deposits and the findings of this work suggest that Tač-Ċawla was a settlement from 3800 to 1800 B.C. The site is under the current ground level in the midst of the modern suburbs (Fig. 3.6).



Figure 3-6: Photographs of the Tač-Ċawla, under excavation in 2014 (Photograph S. Stoddart).

3.2.5 Skorba Temples (Stone Temple and Settlement Site)

This archaeological site is found in an area called Li Skorba, on the slope of a hill overlooking Żebbieh village outside Mġarr, which is located in the Northwest of Malta (Fig. 3.7). The existence of the site was first reported by Captain C.G. Zammit (then Curator of Archaeology) in 1937 and recorded as a suspected temple (Trump, 2015). Proper excavations were conducted by David Trump in the early 1960s (between 1961 and 1963), which revealed the full scale of the archaeological site. They were conducted using modern methods of dating and analysis, which provided reliable and significant data. Relatively small scale sampling was undertaken by the FRAGSUS project. Finally, the Skorba temples are one of the six megalithic temples in Malta listed as a UNESCO World Heritage Site.

The Skorba Temples are composed of two adjacent temples (West and East Temples) of the well-known Maltese prehistoric type (Trump, 2015). The West Temple is the oldest temple and its history can be separated/divided into five periods: a) pre-temple occupation, b) later erection alterations, c) ruins, d) re-occupation and e) final destruction. The East Temple was built during the Tarxien Phase (Table 3.1) and presents a different structure to the West Temple (Fig. 3.8). This structure is similar to temples constructed during the Ggantija Phase and in general in the Tarxien Phase (3000–2300 BC; Table 3.1). The early temples consist of three apses opening from a court, while the later ones are composed of four apses in two opposed pairs connected with a corridor (Trump, 2015).

During the excavation of the temples (1961-63), a settlement was discovered, which was established well before the erection of the temples. The importance of this settlement lies in the fact that it is one of the very few known Neolithic – Bronze Age site (Trump, 2015). This has provided detailed and informative insight into the earliest periods of Malta's Neolithic culture, allowing this study to consider the entire span of the Maltese Neolithic Period (5600-2300 BC).



Figure 3-7: The island of Malta with the main cities and the archaeological sites investigated (Maps Copyright @2018 Google).

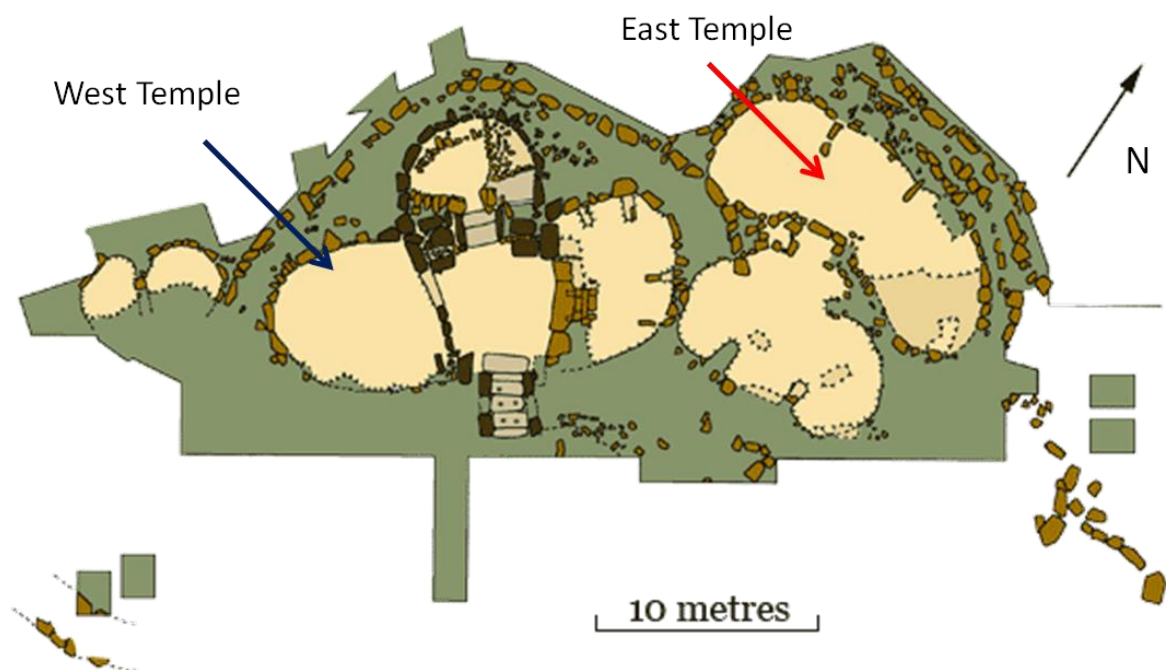


Figure 3-8: Simplified plan of the Skorba Temples.

3.2.6 Kordin Temples (Temple Sites)

Kordin is an area close to the harbour area of Valletta and it is also known as the Corradino plateau or Kordin Heights (Fig. 3.7). In 1896, Caruana mentioned the presence of five groups of megaliths at that location, but with no further information. The archaeological research of the 20th century has found and recorded three groups of sites in the Kordin area: a) Kordin I, b) Kordin II and c) Kordin III (Trump, 2010). Unfortunately, the bombardment of the islands in 1941 have destroyed the first two sites and only little information is known about them. Kordin I was possibly more of a small jumble of rooms than a temple, while Kordin II was more substantial but still smaller than the other known temples (Trump, 2002). These two megalithic sites were possibly complementary and contemporary establishments of the Kordin III (temple site).

On the contrary, Kordin III is in much better shape and enclosed in a high-walled structure between the Government Technical School and the church on its right (Fig. 3.9). The site was initially excavated by Dr Thomas Ashby of the British School of Rome in 1909 and further excavations took place in the period between 1953 and 1960 (Evans, 1971). The site is a standard trefoil temple of an early type, with the sherds beneath the floors and the forecourt placing it firmly in the Ġgantija Phase (Trump, 2010). Interestingly, this is the only stone-paved forecourt that has been found in a stone temple of the Maltese Islands. The cobbled court nestles into a typical concave façade, though the walls are now

very much reduced. The entrance passage leads into a central court with three separated apses, and is also paved (Trump, 2002). The three apses have walls which have probably been added during the Tarxien phase (Table 3.1), as documented at Skorba Temple (Trump, 2010). The most interesting feature of this site is the multiple massive quern lying across the entrance to the left apse. Although the exact time that this quern was put in the temple is unknown, it is contemporary with the site.



Figure 3-9: General view of the Kordin III temple.

3.3 Lithic provenance

The provenance of stone finds (also referred to as lithics) or the sourcing of raw materials is part of the lithic analysis. This analysis investigates stone tools and other chipped stone artefacts using basic scientific techniques (Ballin, 2000; Luedtke, 1992). Identifying the sources of lithics has proven to be a useful method for archaeological research. It contributes to the understanding of human behaviour in the past and the relationships between people and their environment, providing evidence for the reconstruction of movement systems of peoples and objects in landscapes. This includes patterns of mobility (e.g. migration routes), social boundaries, exchange systems, and trade routes. Furthermore, lithic analysis can also provide evidence for the locations of the resources used, the scale of exploitation and the extent of distribution of the products that may relate to social stratification, and the social and technical organisation of crafts and industries (Sellet, 1993).

The methods used are typical of those used in geological research (e.g. petrological and geochemical analysis) such as a) petrographic thin section analysis, b) X-ray fluorescence (XRF) and c) elementary analysis (Kempe, 1983; Luedtke, 1992). This procedure of investigating lithics does not have, until now, a fixed methodology and the techniques used are dependent on the type of material examined (e.g. obsidian, chert, etc), the goal of the research and the availability of resources. Although this is acceptable in a field with no boundaries as yet, some guidelines are necessary to avoid confusion and allow for comparison between similar research.

This chapter is divided into two parts, where the first presents the work on sourcing lithics at a global scale and the second the work on the Maltese Islands. The first part attempts to record how this discipline developed and evolved while simultaneously presenting the work conducted on a variety of lithics. The second is focused on the previous work of sourcing chert artefacts, which is the main interest of this research. This will highlight the importance of this work and how it will help reduce the broader uncertainties concerning Prehistoric Malta.

3.3.1 Lithic provenance on a global scale

The rock sources of stone artefacts were always under research, but only during the last decades have they been considered a distinctive field of study. Hence, it will always be very difficult to identify research on provenance before the 20th century and examples that are accurate before the 1960s. Additional obstacles for accurately reviewing and recording work conducted before the 1900s are the language barriers. The researchers of this period made records or publications which were commonly written in their local dialect. This is a problem common to all disciplines and if the researchers are not familiar with the specific language or have access to a translation then they fall in a dead end. Nonetheless, the investigation of the literature suggested that the earliest and possibly the first ever attempt of sourcing stone artefacts was made by Dugdale in 1656 (Shotton and Hendry, 1979). He

made a macroscopic examination of a chipped and polished flint axe and proposed that its source was not within a forty miles radius of the location where it was found (Dugdale, 1656). The next relevant work was possibly the research of Stukeley on the rocks of Stonehenge in 1740 (Shotton and Hendry, 1979). It was a work on the most famous and mysterious prehistoric site of Britain and finds have affected the interpretations regarding the monument and its significance. There were no records of other similar work until the end of the 19th century with the work of Ordonez (1892), who used petrographic methods to study obsidian in Mexico (Brothwell et al., 1969). It is important to highlight this research as possibly the first recorded attempt to use a geological technique (petrography) in an archaeological investigation and the first which did not depend only on macroscopic observations.

The advent of the 20th century had a significant impact on archaeological research and a radical change in the perspective of sourcing lithics. The connection of Archaeology and Geology was established at a research level (Brothwell et al., 1963; Rapp, 1977; Kempe et al., 1983), especially when the studies focused on the Pleistocene (approximately 2,588,000 to 11,700 BC). Especial interest was given to Petrology (a field in Geology) which investigated, among others, the origin, occurrence, structure and history of rocks (Bates and Jackson 1980). Hence, it was clear that the use of this discipline could provide evidence on the provenance of artefacts which subsequently could clarify exchange mechanisms and provide geographical and chronological evidence of man's activities (Kempe, 1983). The British were pioneers in this interdisciplinary activity, and in 1945 created a "Natural Science" Panel under the Council of British Archaeology (CBA). It was understood until then that many queries could not be answered with traditional methodology and new approaches were necessary (Clough and Cummins, 1979). A major task of this panel was to investigate the prospect of applying the petrological methodologies on sourcing stone implements. In the decades which followed, substantial work was produced by the Council on this matter with interesting results. Indeed, in 1979 Clough and Cummins published a report with several studies on sourcing stone artefacts/implements conducted by the Council, in Britain and elsewhere. The new developments also influenced researchers outside the Council and, in 1979, Shotton and Hendry presented a list of research investigating the provenance of British stone artefacts. The publications made by Brothwell et al. (1963; 1969) were similar, although he was aiming to highlight the general impact of science on archaeological research. The work of Smith et al. (1965; 1966) which presented an extensive amount of flint tools on Neolithic sites was also important in Britain. The author suggested that the dominance of flint in the assemblages should be related to the great flint deposits of Britain which were found in Chalk limestone. The work of Sieveking et al. (1970) was also exceptional, and he reported differences in the composition of trace elements between products that originated from the major British Neolithic flint mines and from those that originated from similar European examples.

This change, fortunately, was not restricted to Britain, but steadily expanded to the rest of the world. The advance in technology and communication allowed scientists all around the world to

communicate and exchange ideas and techniques. However, in my examination of the literature, I faced difficulties in recording provenance investigation at a global level. Firstly, few researchers reported reference of similar work that was conducted outside their area of investigation. The lack of research links between regions and continents (e.g. England, Europe) meant that I was forced to investigate each and every region separately which has taken a great amount of time. Secondly, much of the reported research was not accessible through the reference resources I had available. Additionally, most of the authors merely mentioned the previous surveys without providing any information about their content and therefore it was impossible to know if they were relevant to my research. In spite of these obstacles, I have tried to create an accurate and comprehensive literature review of this new discipline. I was motivated by the fact that this could possibly be the first attempt to gather in one place the previous investigations made on *Lithic provenancing* at a global scale.

Starting from the Scandinavian area, Carl Johan Becker (1952) made one of the first efforts to establish reliable criteria for differentiating the Scandinavian flint types. He believes that this was crucial in order to identify the origins of the Neolithic flint axe hoards found in northern Sweden (Hughes et al., 2010). The author relied on the appearance and physical qualities to narrow down the origin of the flint to the Senonian deposits of eastern Zealand or southwestern Scania (Becker 1952:69; Knutsson 1988:51). Moving to the Mediterranean region, Sayre and Dodson (1957) used Neutron activation analysis (NAA) to investigate the origin of pottery. This was followed by similar investigations of Catling (1963) and Harbottle (1970) on the provenance of Minoan and Mycenaean pottery. Meanwhile, Cann and Renfrew (1964) investigated the known obsidian sources of the region (e.g. Sardinia) and tried to outline the trade/exchange network of the Mediterranean during the Neolithic period. One year later, an interesting study was published by Gabel (1965) on a Later Stone Age site from Kafue (South Africa). The research concluded that most of the raw materials were local, except for the chalcedony and sandstone which were imported. The next relevant study appeared to be in the American continent where Lanning (1970) worked on Palaeo-Indian groups in South America, which used a variety of resources (e.g. chert, obsidian, basalt, etc.). The surprising outcome of this research was that the Palaeo-Indian groups were also exploiting silicified limestone sources. Returning briefly to Europe, there is the work of De Bruin et al. (1972) who used NAA to determine the trace element composition of flint material found in prehistoric mines and workshops from Netherlands, Denmark and France. Koztowski in 1973, published on Palaeolithic lithic material found in the Carpathian countries. This was possibly not the first attempt to source material from this region, but it was in English and accessible. The area of Carpathia and the Balkans are considered important for the movement of human groups between Europe and Asia in the Prehistoric period and so any research on lithic sources, movements and exchange should be considered important.

In 1974, Ward and Smith published possibly the first research on sourcing lithic material in the Pacific region. They investigated the geochemical content of chert sources from Australia, Papua New

Guinea, Solomon Islands and New Zealand and tried to identify patterns of trade in this region. One year later in Japan, Higashimura, and Warashina used X-ray Fluorescence Analysis (XRF) to source Sanukite Stone Implements. New research on obsidian was published in 1976 and the author (Dixon, 1976) became one of the first who attempted to characterize the obsidian sources of Mediterranean and Near East. Regarding chert sourcing in America, Luedtke (1978, 1979) did extensive research on the geochemical composition of chert sources and artefacts in the USA. This work was part of a larger trace-element analysis project conducted under the supervision of the University of Michigan Museum of Anthropology. The aim of this study was to investigate the trace elements and suggest which elements could be used as an identification marker of chert sources. In addition, the research tried to suggest which was the best method to assign artefacts to sources. Finally, before entering the 1980s Goodyear (1979) tried to use the raw material distribution to identify the geographic movements among Paleo-Indian populations of North America.

During the 20th century new and more effective equipment were developed (e.g. SEM, XRF, ICP-MS, etc.) and the mineralogical and geochemical content of the rock formations could be better examined. This consequently allowed the geologists and archaeologists to distinguish faster and more accurately the different types of rock sources. This had a positive impact on the archaeological research and the decades of the 1960s and 1970s thrived on research testing how these different techniques could contribute on sourcing stone artefacts. Although there was a variety of techniques employed, the main approaches found in the literature were XRF and NAA (e.g. Hall 1960; De Bruin et al, 1972). Moreover, an important amount of investigation surveys ignored or neglected the value of petrological methods and as a result, the geological content of many archaeological publications was not of the highest standards (Kempe, 1983). Their main problems were the lack of accurate terminology and the incorrect identification of rock and minerals. Furthermore, until the 1990s archaeologists (e.g. Caspar, 1984; S'eronie-Vivien & S'eronie-Vivien, 1987) still preferred to use visual methodologies for sourcing artefactual stones (Odell, 2000). The reason for that can be attributed to the unfamiliar terminology and lack of understanding the usage of these new techniques. To be fair the discipline of provenance was under constant development during the last two centuries and there have been fundamental changes in the terminology and the methods used. Hence, any criticism of research conducted in the previous centuries should only be in a frame of a theoretical academic discussion. Moreover, these developments set the foundations of Geoarchaeology, under whose aegis *Lithic provenance* can be placed (Odell, 2000). Criticism could be made only on the occasions that the archaeological research altered or did not record the context in which the artefacts were found or even worse when the finds were lost. This, however, was a more generic issue in the archaeological excavation of the past and cannot be restricted to the lithic content of the archaeological site.

This lack of knowledge or misunderstanding of the geological terminology and methods motivated some researchers to provide guidebooks to archaeologists who were interested in this new and

unfamiliar field. Among the many researchers who provided guidance on this issue, I have distinguished three whose work, I think, have a significant value. First is André Rosenfeld, who in 1965 published a book under the title *"The inorganic raw materials of Antiquity"*. The importance of this work was accurately described in the preface chapter of the book from which I quote: *"There is no book which adequately serves an introduction to the subject of identifying and understanding the mineral resources of antiquity"* and *"there is a real need for archaeologists in the field to be able to identify adequately the type of materials uncovered and to assess their possible significance before enlisting specialist examination"*. This was followed by the book of Kempe and Harvey (1983), which provided a more elaborate understanding of Petrology and how it could contribute on sourcing stone artefacts. They recorded the main varieties of raw materials, divided according to usage (e.g. artefacts, building material) and provided an update on the most frequently used methodologies. Last but not least, was the work of Luedtke (1992) under the title: *"An archaeologist's guide to chert and flint"*. This latter volume should be considered the most comprehensive work conducted on this type of raw material. It provided detailed information about the chert and flint raw materials and reported the methodologies that have been proven, up to that point in time, to be useful in sourcing flint and chert artefacts. Similar work was conducted on other raw materials (e.g. Obsidian - Shackley, 1998), but as the current study is focusing on chert and flint it seemed appropriate to distinguish this study. To that extent, it is important to report the work of Murray (1992; 1994) who did extensive work on chert formations from all around the world. Although his publications could be considered purely geological, they provided important information on chert resources, especially regarding their geochemical content. Furthermore, Murray provided significant interpretations of the geochemical results, which I consider to be extremely useful for sourcing chert/flint artefacts.

The different problems that emerged did not stop the development of provenance studies and the research continued. An important amount of research related to sourcing lithics was launched all around the world and the application of new techniques was investigated. Williams-Thorpe et. al (1979, 1984) investigated the sources and distribution of archaeological obsidian found in France and Italy. The importance of their work could easily be understood from the fact that all the subsequent research on the broader theme of obsidian provenancing referred to their research. Gale in 1981, used possibly for the first time strontium isotopes to characterize Mediterranean Obsidian Sources. In comparison, Francaviglia (1984) tried to achieve a similar outcome by using classical petrological methods. The writer of this study tried to highlight the problems and errors in previous similar research and that the basic geological methodology was the solution to source obsidian artefacts/tools accurately. Moreover, the author emphasized that the employment of all the available techniques with no consistency produced a great database of results which could not be compared. Bigazzi et al. (1986) used the rare earth and trace elements to link obsidian artefacts from Italy with sources of the broader Mediterranean area. Moving slightly to the Northeast of Europe, Biró (1986, 1992) made important

attempts to source prehistoric lithic finds from the Carpathians and central Europe. Meanwhile in 1984, Merrick and Brown published one of the few studies available from the region of Africa. They explored the movement of obsidian materials in Kenya and northern Tanzania. Sieveking and Newcomer in 1987, provided a very useful publication in which they gathered interesting results on chert and flint from all around the world. It was interesting to record that in books similar to this, which recorded research on provenance the majority of the articles were dealing with chert and flint.

In the last decade of the 20th-century research on the provenance of lithics flourished in America and presented an extensive amount of research. Moholy-Nagy and Nelson (1990) tried to demonstrate how inaccurate and subjective were the results of a visually based methodology. The experiment included a sample of 29 obsidian artefacts and 1 unworked nodule from Tikal. Initially, they sourced the stones using macroscopic/visual examination and then by X-ray fluorescence. The results showed that almost half of the sample was classified incorrectly by visual techniques, highlighting the unreliability of this method for distinguishing the substantial within-source variability of grey Mesoamerican obsidian (Odell,2000). Mesoamerica is a region with many obsidian sources which were linked with volcanic activity. Many researchers in the past (Trombold et al. 1993; Joyce et al. 1995) investigated these sources, mainly with instrumental NAA and confirmed the contact or exchange relationships between several Mexican areas and sites in the same period, Hofman et al. (1991) tried to explore the response of chert material under ultraviolet light and the possibility to discriminate successfully one chert type from another (Odell, 2000). Latham et al. (1992) developed a non-destructive XRF technique that did not require smooth surfaces. Furthermore, they employed this technique on basaltic artefacts from the California region. In 1993, Shelley tried to establish a suitable geoarchaeological approach to characterize non-igneous rocks. Additionally, he investigated which would be the proper means for assessing the variability of secondary deposits. This interesting work was conducted on prehistoric lithics from the southwest regions of USA (New Mexico). Shockey (1994), followed the work of Hofman and, curious about the effects that heating might have on this fluorescence effect, he tested three chert types from Oklahoma and Texas. Although no substantial results were found (Odell,200), he continued his experimentation into the effect of light by contrasting chert samples taken from primary versus secondary context (Shockey, 1995). Using polarized light, he found that cherts from primary contexts appear more anisotropic (polarized), whereas cherts from secondary contexts appear more isotropic (depolarized). Larson (1994) in comparison with the general trend suggested a relatively easy, heuristic way of measuring variability within an assemblage. This was originally proposed by Kelly (1985) and known as minimum nodule analysis, this method is also discussed under "piece refitting" (Odell, 2000). This practice though did not grasp the interest of other researchers and the focus of provenance studies remains on the geochemical composition of the lithics and their sources. Indeed, Hess (1996) tried to relate chert artefacts from the Mack Canyon Site (Oregon, USA) with the chert sources of the Columbian Plateau. This work was possibly the first that

used the inductively coupled plasma mass spectrometer (ICP-MS) to investigate the geochemical content of the samples.

One year later Hermes and Ritchie (1997a) developed a non-destructive, energy-dispersive XRF and applied it on felsitic rocks in New England. The inspiration and/or influence for this new version of XRF probably came from the work of Latham et al. (1992). In 1998, Shackley published a very useful synopsis and comparative study of the most commonly employed instrumental geochemical analyses, focusing on neutron activation analysis (NAA), X-ray fluorescence (XRF), and proton-induced X-ray emission/proton-induced gamma-ray emission (PIXE-PIGME) analysis. He stressed that the usage of these techniques requires a good understanding of Geology, the chemical variability presented in the source, and the nature of secondary depositional processes in the region of study. Moreover, this author was also the editor of the book "Archaeological Obsidian Studies" (1998), providing a review of the main geoarchaeological research conducted on obsidian finds. The same year, Malyk-Selivanova et al. (1998) presented a very interesting work on prehistoric artefacts from Alaska which was based on a geological approach. Finally, Odell (2000) made an excellent job by recording the main provenance research on stone artefacts, especially those conducted on the American continent.

Although America dominated the research on lithics during the 1990s, important investigations were also reported elsewhere. Biró et al. (1991), for example, published a very interesting comparative study of the raw material collection located at the national museum of Hungary. The importance of this research lies in the fact that it was one of the rare occasions where the archaeological research provided data on lithics from this part of the world. This region had political instability for decades, which did not allow the exchange of information. In central Europe, Bouard and Fedele (1993) did a petrographic examination on stone artefacts from different countries (e.g. France, Italy and Switzerland) and tried to connect them with the rock resources of the western Alps. Further west, Cooney and Mandai (1995) investigated the origin of Iris prehistoric stone axes. Using petrological techniques, they were able to confirm that the porcellanite was the dominant raw material used for the manufacture of these axes and that most of them were made in a limited number of production centres, which exploited a restricted range of resources (Odell, 2000). Petrological techniques were also used and successfully characterized material from Neolithic flint mines located in Belgium and the Netherlands (McDonnell et al., 1997). The successful application of these techniques was also demonstrated on heavy tools from southern England. Williams–Thorpe et al. (1999) employed both geochemical and petrological methods to determine the sources of glacial erratics. The correlation of these results with tools from archaeological sites provided evidence for movements of the preceding Pleistocene ice along established trails and human utilization of secondary deposits (Odell, 2000). In the same period special interest was recorded on the obsidian artefacts and sources, especially from the broader Mediterranean region. Among the many researchers, Ammerman et al. (1990, 1993, 1997) focused on the obsidian finds in many Neolithic sites of Italy, while Tykot

(1991, 1992, 1995, 1997) did extensive research on the sources and the distribution of obsidian in Sardinia and in the broader central and western Mediterranean area. Furthermore, Tykot et al. (1996) investigated the prospect that the ICP-MS method could have on sourcing obsidian material. Finally, Tykot and Ammerman (1997) combined forces and suggested that a combination of visual sorting and X-ray analysis could be the key to accurately sourcing obsidian finds in this region. A couple of years earlier, Williams-Thorpe (1995) published a review of the work conducted on the Mediterranean and Near East. The authors with this book tried to highlight the success that the provenance studies had on obsidian. Generally, the research on obsidian artefacts established that obsidian sources from the islands of Lipari, Palmarola, Pantelleria and Sardinia were exploited from the beginning of the Neolithic period and they were distributed to sites in southern France, the Italian mainland, Corsica, Sardinia, Sicily, Malta and North Africa. Although research on this field was conducted all around the world, it seemed that the focus was on America and Europe. The reason could be that the leading researchers were either European or Americans (mainly from USA universities).

The beginning of the new century found the provenance of lithics as an established discipline in the archaeological research and with a variety of suitable techniques to use. Therefore, it was no surprise that many archaeological projects all around the world had specialists for this task, especially when focusing on prehistory. The focus of these investigations was on the geochemical composition of the lithics in an attempt to distinguish the “signature” or “fingerprint”. These were terms found often in literature and aim to describe the investigation and identification of the distinctive characteristics of the stone tool and artefact. Possibly the very first work published was by Jan Apel (2001), who studied late Neolithic daggers from Scandinavian. This research followed Becker’s results (1952) to advance far-reaching conclusions about manufacturing centres and exchange systems. Similar studies focused on the availability and use of different flint sources and outcrops at a local or regional level (Högberg, 2002; Knarrström 2001; Turq, 2005). However, these studies were based on macroscopic characteristics. Furthermore, studies on SW Europe and more specifically the Pyrenees mountain range, have mostly focused on the analyses of textural and petrographic characteristics (Grégoire 2000; Terradas 2001; Ortega 2002; Foucher 2004; Briois, 2005) and only a few attempts to characterize chert artefacts geochemically have been done until now (Sánchez de la Torre, et. al., 2017). On the contrary, Costopoulos (2003) following the original work made by Matiskainen et al. (1989), used an electron microprobe and an energy dispersive spectrometer to distinguish different sources (Hughes et al. 2010). Delage (2003) published a great book which recorded an extensive list of research conducted on the procurement and exploitation of chert resources during prehistory. The author provided an abundant bibliography of this research field from all around the world for the period between 1870 and 2001. Although this work provided future researchers with the opportunity to examine the literature on chert artefacts through time, it showed also the problems of such a task.

Many of the publications recorded were in different languages and some could not be found even in the most updated databases.

Additional interest to the recent provenance surveys was the introduction of more non-destructive techniques in their methodology. Smith and Clark (2004) introduced the Raman microscopy and demonstrated the applications of this technique in archaeometric research. Their work has shown the significant advantages that Raman microscopy could have in archaeological research, but also presented the areas which required further experimentation. Furthermore, Tykot (2004) presented an extremely useful list of the scientific methods applied to provenance studies. The author attempted to explain the main principles, the type results and how they could contribute on sourcing stone artefacts and subsequently answering broader archaeological questions. Important also was the work of Moroni and Petrelli (2005), who investigated the prospect of using the LA-ICP-MS technique for sourcing flint artefacts. The test was made on flint formations from central Italy and on Palaeolithic to Neolithic flint artefacts from the collection of the national archaeological museum in Perugia. The laser ablation (LA) technique which was added to the ICP-MS converted this very useful technique into a non-destructive one and facilitated their usage in archaeological research. At the same time Andrefsky (2005) published the second edition of his work *"Lithics: Macroscopic Approaches to Analysis"*. The author tried to create a manual on lithic analysis and explain the importance of this discipline. The book was not focused on sourcing material, but, among other elements, introduced the readers to the lithic raw material and the related new techniques. It is a good book for student archaeologists who want to get an understanding of this discipline and the terminology employed. One year later, Crandell (2006) published a proposal for a standardized methodology to investigate chert materials. The methodology was based on recording specific macroscopic and microscopic characteristics which for the author could be indicators of the chert sources. The same year Negash et al. (2006) used geochemical methods to investigate the provenance of obsidian artefacts from Ethiopia. Although they used already tested techniques, it was one of the few known surveys which sourced prehistoric material from Africa. Useful also should be considered the work of Delage (2007) which revised the research of sourcing chert material in the region of Near East. The writer recorded the available chert sources of the area and tried to distinguish the previous attempts on sourcing stone artefact. He provided a good literature review of research conducted until then, but also highlighted their deficiencies. Another interesting review of previous research was published in 2009 by Blades and Adams. This recorded research on the procurement of lithic material, which could be considered as a type of sourcing investigation. The book included research focused mainly on the Palaeolithic period from all around the world. In 2010, Gijn published an interesting monograph on flint artefacts found in many prehistoric sites of the Netherlands. The author used, among other approaches, raw material sourcing and experimental archaeology techniques to prove the various and changing roles of these artefacts in prehistoric life. During the last two decades, research on sourcing stone artefacts continued to evolve and produced

many publications from all around the world. These either focus on exploring new non-destructive techniques (Hawkins et al., 2008; Olivares et al., 2009; Hughes et al., 2010; Olofsson et al., 2011; Forster 2012; Hogberg et al., 2012; Hassler et al. 2013; Parish et al. 2013; Speer, 2014) or employing these techniques to source lithics whose origin was still unclear (Bustillo et al., 2009; Milne et al., 2009; Pétrequin, et al., 2011; Pettitt et al. 2012; Gonzalez, et al., 2014; Ekshtain et al. 2014; Andreeva et al. 2014; Nazarov et al., 2015; Speer 2016; Bruggencate et al. 2016; Gurova et al. 2016; Sánchez de la Torre, et al., 2017).

In conclusion, the scientific sourcing of stone artefacts/tools have gone a long way and had already recorded an almost 400-year history. Initially, it was based mainly on subjective macroscopic characterization, while today there is a broader collection of techniques which are able to provide conclusive evidence. Moreover, archaeological research now has a better understanding of the role and importance of this new discipline and how they could contribute to broader archaeological questions. Finally, there is an evolving trend to standardize a fixed methodology which will provide great accuracy and efficiency, and at the same time be non-destructive to the archaeological finds. Nonetheless, this literature review also revealed the problems which still need to be resolved. Firstly, there are still a lot of archaeologists who prefer to employ only the macroscopic methods to source lithics. The argument of high cost is not valid today, because there is a couple of reliable and low-cost techniques available. Moreover, many of the new or modified traditional techniques are now considered non-destructive which allow the full preservation of the lithics. Possibly the reason for this preference lies in the difficult scientific terminology that follows these methods. Secondly, even now the terminology is unclear with a lot of confusion and miscommunication between researchers. Indeed, there is still a problem with the terms "flint" and "chert", and not just between disciplines (i.e. Archaeology, Geology) but also between areas (e.g. England, USA). Many researchers in the past tried to create a unified terminology or link between the vocabulary of the collaborating discipline but until now the problem has not been resolved. Thirdly, there is an absence of a fixed methodology which would secure consistency in collecting data and help the investigation to reach reliable and conclusive results. Through the years an enormous amount of data has been collected from a variety of techniques and methods. Although this is a positive outcome, there has never been any suggestion as to which of those were more efficient or useful. Different methods have been applied on different or the same lithic collections with no actual link or comparison between them. The literature review revealed some preference in techniques (e.g. XRF), but this is not connected with the effectiveness of the method and more with the availability of equipment. An additional problem to that there is an absence of guidelines on how the results from the different techniques should be treated, compared, integrated and processed to get to the correct results. In addition, there is the trend of archaeologists to treat the data as they were traditionally trained. However, the scientific data should be treated with

respect and even though there will be statistics involved, they should follow the appropriate theory not only in terms of process but in terms of outcome.

3.3.2 Malta

In the last two hundred years, the archaeology of the Maltese Islands has focused on the Neolithic monuments distributed throughout the islands (Vella, 2009). However, the archaeological research and its methods were not of the same standard as today. This resulted in the excavation of many monuments by inexperienced personnel and with an archaeological methodology that now is considered rudimentary. Focusing on the material culture and especially on lithics, they have been excavated from the sites unsystematically and a reevaluation of them is more than a necessity (Malone et al. 2009). Especially now, that the field of geoarchaeology and lithic studies have been given shape and play an important role in archaeological research (Pollard, 1999).

Nonetheless, it is equally important to present the work that has been performed until now on the lithics associated with the Neolithic monuments of Malta. The first scholarly publication referring to lithic tools was written by Murray in 1923, who published a brief article on selected lithic tools recovered at the Borg in-Nadur excavations (Murray, 1923). Although this article was written in such an early period, the author did an excellent job at annotating the location from which these lithic tools were recovered (Vella, 2009). Unfortunately, after this publication, no study was carried out on lithic finds and only rarely there were reports of flint knives and blades. The situation changed in the 1950s when Evans and Trump attempted to approach Maltese prehistoric material culture with a more quantitative methodology, focusing on ceramic and architectural typologies (Evans 1971; Trump 2002). However, the lithic finds were still considered of lesser importance and no further research was recorded. A great breakthrough in lithics research was done with the excavations of the Brochtorff Xaghra Circle from 1987 to 1994. The publication of this excavation (Malone, 2009) included a chapter dedicated to the material culture of the site. It was the first time that the lithics of a site were presented in detail and thoroughly investigated. Dixon studied axes made out of non-calcareous stone (Malone, 2009; 242) and Tykot looked at the obsidian (Malone, 2009; 250). Moreover, it was the time that an attempt was made to investigate the provenance, among others, of chert materials found in association with the Maltese Neolithic monuments. Cazzella and Moscoloni published (2005) a review of the prehistoric artefacts recovered by the Italians in the 1960s. The interest of this assemblage was that they belonged to the Bronze Age phase of Borg in-Nadur.

Special note must be made of Vella's work (2008–2012), which was focused on the chert materials found at many Neolithic sites of Maltese Islands and he is actually the only one who made an effort to investigate the possible sources. The investigation strategy of the author was based on some

distinctive macroscopic characteristics (i.e. colour, texture and translucency) and managed to distinguish between local and foreign material (Vella, 2009).

In the past, this level of investigation would have been more than sufficient and any archaeologists would have been content with the findings of such research. However, the recent developments on sourcing stone artefacts and the introduction of the scientific /geological approach have completely changed the procedure. The geological methodology examines and records a full spectrum of macroscopic characteristics, while Vella focused on three main characteristics (2009). One of them is colour, which has been suggested by many researchers (even Vella himself) as a very subjective characteristic (Luedtke, 1978). This allows many different interpretations, a high possibility of errors and causes a lack of credibility. Moreover, the new approach focusses more on the inner characteristics of the stone such as the mineralogical content and geochemical signature, which have provided more interesting and reliable results. Another problem with the previous research was the lack of geological knowledge about the chert outcrops of the Maltese Islands. There have not yet been any investigations on this matter and the actual locations, extent and characteristics of these formations are unclear. This lack of knowledge has been presented in the chapter above (see 1.21) and it is something that Vella mentioned previously (Vella, 2009). The information presented in previous publications on chert outcrops was retrieved from a literature review of the geological research of the Islands and there has not been any field investigation or sampling of the chert sources reported. To be fair in all his publications (Vella, 2008 – 2012), Vella made clear any lack of information or possible subjectivity in the results. Moreover, considering the period and conditions under which these investigations conducted and the availability of resources he did an excellent job. Although Vella is a pioneer in this field (not only in Malta), the current perspective and approach of sourcing stone artefacts suggest a re-evaluation on the origin of the chert artefacts related with the Neolithic monuments of the Maltese Islands is entirely justified.

3.4 *Chaîne opératoire* approach

The *chaîne opératoire* is a technological approach which investigates the succession of mental operations and technical gestures in order to satisfy a need (immediate or not) according to a preexisting project (Perles, 1989). Consequently, this approach aims to describe and understand all cultural transformations that a specific raw material had to go through (Fig. 3.10a). It is a chronological segment of the actions and mental processes required to manufacture an artefact and maintain the technical system of a prehistoric group. The initial stage of the chain is the raw material procurement and the final stage is the discard of the artefact (Sellet, 1993). The term *chaîne opératoire* is often used untranslated, although the terms 'work chain' or 'operational sequence' have also been proposed (Bar-Yosef et al., 2009).

The significance of this method in archaeological research is its ability to reveal the dynamics of a specific technical system (e.g. the lithic system) and the role of this system within the broader technology of a prehistoric group (Sellet, 1993). The different chains constitute the whole technical system of a prehistoric group at a given site (Plegrin et al., 1988). Such an approach provides a dynamic view of the stone tools because it takes the life trajectories of the tools into account (Fig. 3.10b). Moreover, it permits a reconstruction of the distinct technological strategies through an understanding of the relationship between raw material procurement, tool manufacture, tool use, maintenance and discard (Sellet, 1993).

The *chaîne opératoire* approach is a complementary method for this research on the provenance of prehistoric lithic assemblages of the Maltese Islands. It could be a beneficial methodology and provide useful information on the different sources of chert. Moreover, the identification of different technologies and craft traditions on the same or different raw material will have multiple implications for this research. This could possibly allow for the identification of different sources of chert, different levels of availability and different treatments. In addition, it could contribute to what the extent the raw materials define the employed technologies and vice versa.

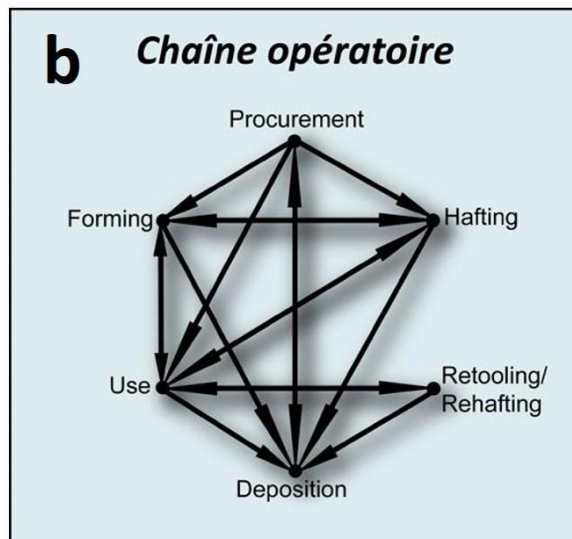
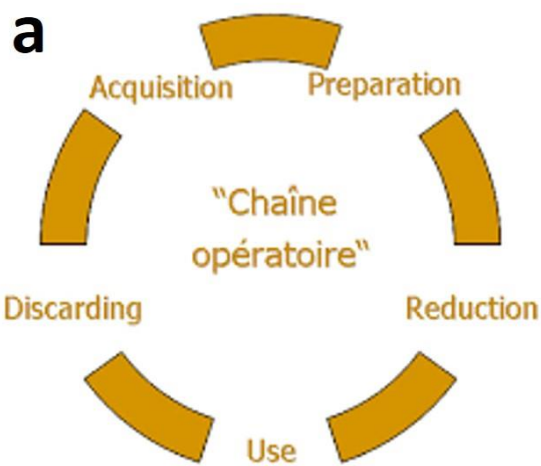


Figure 3-10: *Chaîne opératoire* diagrams. a) A simple diagram of a lithic *chaîne opératoire* (Pawlik, 2009), b) A diagram showing the life trajectories of the tools

3.4.1 Literature review

The *chaîne opératoire* was first used by Leroi-Gourhan (1964) and studied by R. Cresswell (1983, 1993). It was adopted by French prehistorians for the purpose of lithic analysis (e.g., Geneste 1985; Pelegrin 1990; Pigeot 1990; Sellet, 1993; Schlanger 1996; Inizan et al. 1999). The work of Tixier and his colleagues (e.g. Tixier et al., 1980) was extremely important as they defined the basic principles of this new method (Bar-Yosef et al., 2009; Soressi et al., 2011). They clarified that technology is different in scope from typology, and an assemblage of lithics is not a random but a methodically interconnected association of artefacts. Meanwhile, similar analytical methods were adopted by others elsewhere in Europe, the Near East and the United States (e.g., Crew 1975; Munday 1976; Fish 1979; Jelinek 1991; Van Peer 1992; Sellet 1993; Meignen 1995; Kerry et al., 2000). Indeed, Bleed (2001) has stressed similarities between the American concept of a reduction sequence and Japanese and French approaches to the analysis of production sequences. However, the concept of *chaîne opératoire* differs significantly from the reduction sequence found in the North American literature (Andrefsky 2005).

The beginning of the 21st century found the *chaîne opératoire* as a fully established methodology which was widely accepted by archaeologists. However, it also received a lot of criticism on the problems and limitations that this methodology presents. During the last two decades this methodology has been tested on different lithic assemblages all over the world, with interesting findings (e.g. Bar-Yosef et al., 2009; Pawlik, 2009; Strand, 2012). Researchers have also been focused on investigating the advantages, limitations and the future direction for this approach (e.g. Shott, 2003; Soressi et al., 2011; Tostevin, 2011).

4 Materials and Methods

4.1 Field Research

The fieldwork on the Maltese Islands was conducted over two consecutive years (2016 and 2017) during springtime, and each season lasted for three weeks. It was separated into two parts: a) indoor examination of the assemblages and b) fieldwork to investigate for chert outcrops and collect samples. The work included detailed mapping and macroscopic examination of the chert formations and assemblages. The outdoor investigation followed the baseline provided from the Geological Map of Malta (Pedley, 1993), and was aided by Martyn Pedley himself. Throughout the two field campaigns, 33 samples were collected for studying the mineralogy and geochemistry of the rocks. Meanwhile, the fieldwork on Sicily was conducted in September 2016, with the collaboration of Cambridge University, Martyn Pedley himself and the Universities of Catania and Palermo. The investigation focused on the different types of chert formations on the Island and the most important chert formations were examined. During this fieldwork, the macroscopic characteristics of the chert outcrops were recorded, and 29 representative samples were collected.

The examination of the assemblages was conducted in their storage locations and under the supervision of the appropriate authorities. Namely, the assemblage of Brochtorff Xagħra Circle and Taċ-Ċawla were stored in the Museum of Archaeology in Valletta, while the assemblages of Ġgantija, Kordin, Skorba and Santa Verna were housed in the University of Malta. 150 representative samples were selected from all of these collections for further laboratory investigation. In addition, these sites were visited to help understand the archaeological and cultural importance of late Neolithic Period on the Maltese Islands and better connect the archaeological background with my doctoral project.

The macroscopic examination in the field followed the baseline of the work provided by Crandell (2006) and Luedtke (1992). They suggested the examination of nine macroscopic characteristics: type of material, colour, fabric, translucency, texture, lustre, grain, pattern and cortex. The investigated assemblages included artefacts of different rock materials and were not restricted to the chert type. The scope of this research was the chert artefacts and the investigation focused only on this type of stone artefacts. The colour of the artefacts was described with the help of the Munsell rock colour book (2014). This increased the accuracy of the colour description and minimized the subjectivity of the researcher. The other seven features followed the terms and explanations provided in the work of Crandell (2006). The fabric could be homogenous or non-homogenous, while the translucency was described as highly translucent, translucent, sub-translucent or opaque. The lustre could be termed shiny, medium or dull and shine was further divided in silky, greasy, pearly or waxy. The texture (i.e. feel) of a rock material could be either rough or smooth and the intermediate situations labelled as semi-smooth. This feature was related to the size of the grains, which depending on the size, was

described as fine, medium or coarse. Pattern refers to the distribution (whether even or uneven) of colour, grain, lustre and translucency (Crandell, 2006). There could be many types of patterns, but generally, they were divided into categories of characteristics spots and lines (e.g. laminas). Finally, the last category recorded the existence of cortex residues on the samples, which indicated the host rock formation (e.g. limestone) of the original outcrops.

The selection of representative samples followed the macroscopic examination and covered the main chert groups that were identified at that stage. Although the sample-strategy intended to preserve the relative proportion of the different chert-groups within the assemblages, this was not always possible due to specific limitations. Many of the chert finds (30%) did not have the required size (<2mm) and shape (e.g. lack of flat surface) to be analysed with the proposed techniques. In addition, at least 15% of the chert artefacts in each assemblage were patinated and unsuitable for non-destructive analyses. Furthermore, there were assemblages (e.g. Taċ-Ċawla) with great heterogeneity and more samples was necessary to be collected. Also, there were other more homogeneous assemblages (e.g. Skorba) and less samples were necessary. Lastly, the sample strategy had a limit on the number of samples that could be exported. The Maltese authorities set a maximum limit of 150 samples and an additional limit of no more than 30 samples for export from the assemblages located in the Museum of Archaeology in Valletta. This combination of factors led to decisions that deviate from the original strategy (i.e. preserve relative proportion of raw material), but none of these choices put the representativeness of the samples under question. This stage was followed by employing a suite of laboratory methods (presented below) on the collected samples (geological and archaeological) in order to draw conclusions about the chert formations of Malta and Sicily and the chert assemblages.

4.2 Laboratory research

The laboratory work started with the preparation of 50 rock slices for macroscopic evaluation of the rock samples and re-evaluation of the macroscopic characteristics of the archaeological samples. Moreover, the most representative rock samples were selected, and 42 thin and polished-thin sections were prepared for examination using the Optical and SEM-EDS microscopes. The slices and the sections were prepared in the Charles McBurney Laboratory for Geoarchaeology. The laboratory is based in the Department of Archaeology (West Building) at the University of Cambridge. The optical microscopic examination and the FTIR-ATR analyses were conducted in the same laboratory, while the SEM-EDS investigation (Brothwell and Higgs, 1969) took place in the Department of Earth Science, also at the University of Cambridge. A Quanta 650F scanning electron microscope (QEMSCAN 650F) equipment was used, which had two energy dispersive spectrometers (EDS) detectors (Bruker SSD Flash 6|30 detectors). The EDS analysis carried out using the Bruker software, ESPRIT. The polished-thin sections were carbon-coated and investigated in low vacuum conditions. In addition, the analyses were acquire

having a working distance of 13mm (± 0.5 mm), HV set at 15.00 kV and the spot size of the analysis at 4s.

Representative FTIR spectra (McBurney Laboratory protocol; Appendix II) obtained from all rock samples ($n=62$) by grinding a few tens of micrograms of the sample using an agate mortar and pestle (Parish et al. 2013; Smith, B. C. 2011; Hawkins et al. 2008). About 0.1mg or less of the sample was mixed with about 80mg of KBr (IR-grade). A 7mm pellet was then made using a hand press and the spectra were collected between 4000 and 400cm^{-1} at 4cm^{-1} resolution, using a Thermo Nicolet 380 spectrometer. The interpretation of the spectra was based on an internal library of infrared spectra of archaeological materials (Weiner, 2010). Moreover, the rock samples were examined with the ATR method to have a solid cross-reference database between the two techniques (fig.4.1). Similar (0.1mg) or less sample was used to collect ATR spectra and compared them with the ones of the FTIR equipment. The spectra were also collected between 4000 and 400cm^{-1} at 4cm^{-1} resolution and the same internal library was used to identify the minerals. The cross-examination between the two methods (i.e. FTIR and ATR) reduced the errors and overcame the lack of mineral reference and secured an accurate interpretation of the ATR spectra. The ATR equipment was less invasive than FTIR but was lacking in accuracy and the results deviated from acceptable values. This method obtained all the spectra from the artefact samples ($n= 100$) with the ATR technique and minimized the impact of this technique. Representative ATR spectra have been obtained from 100 artefact samples, under the same conditions as the rock samples. In addition, representative XRF spectra were obtained from most rock ($n=60$) and artefact samples ($n=100$), with a Bruker portable XRF, the Tracer III-V analyser (Bruker, 2010; Shackley, 1998). It was a non-destructive technique, and the sample was placed on the top of the analyser without any preparation. The collection of the spectrum was controlled from the S1PXRF software (KeyMaster Technologies, Inc. 2001), through which the properties of the measurements were arranged. The Baud Rate was set at the highest level (i.e. 115200) and the “Back scatter” and “PC Trigger” options were activated. Moreover, the High Voltage was set at the 40kV, the Anode Current at 20mA and the length of each measurement was placed at 60 seconds. Before the measurements started, the equipment was standardised with the Duplex 2205 stainless steel standard and the standardisation repeated every 40 minutes. The equipment for both these techniques belongs to the Department of Archaeology at the University of Cambridge, on whose premises the analyses were performed.

Moreover, elementary analyses were performed using Laser Ablation- Inductively Coupled Plasma Mass Spectrometry (LA-ICP-MS) technique to determine the composition of the major, trace and rare earth elements (Speer, 2014; Neff, 2012). Through this method, 42 rock samples from Malta and Sicily and 129 archaeological samples from all the assemblages were examined. The equipment of this method is located in the Department of Earth Sciences, at the University of Cambridge. This high-resolution depth profiling technique initially employed an Analyte G2 excimer laser (Teledyne Photon

Machines Inc) coupled with Thermo i-CapQ ICPMS. The use of the Thermo i-CapQ ICPMS collision cell in kinetic energy discrimination (KED) minimized interferences on transitional mass elements (Tanner et al, 2002). The Laser Ablation system was optimized for high spatial resolution using an aperture slit of 60x20 μm to map the surface of the samples and 6Hz frequency with 1.8J/cm² laser fluence, while the laser speed scan along the tracks was set up at 2 $\mu\text{m}/\text{sec}$. In addition, approximately 1 μm of the top surface was removed using pre-ablation with 80x30 μm laser spot to avoid any potential surface contamination. The ICP-MS sensitivity was optimized using NIST612 reference glass material for maximum sensitivity. Data reduction involved initial screening of spectra for outliers, subtraction of the mean background intensities (measured with the laser turned off) from the analysed isotope intensities, internal standardisation to ⁴³Ca, and external standardisation using the NIST612 glass reference material. Finally, in-house NIST614 reference material was used to monitor long-term standards of reproducibility. However, this equipment was unable to perform elementary analyses on some of the Sicilian rock and artefact samples and therefore second type of equipment was employed. These samples were more resilient and prevented the laser from producing the necessary plasma for an accurate analysis. This was an unexpected outcome which was observed while monitoring the LA-ICP-MS measurements. The high resilience of those samples had a negative impact on the produced results which were characterised by low accuracy and high possibility of error (i.e. Error > 20%, RSD > 20% and 80% < REC < 120%). One suggested explanation might be the extremely high SiO₂ content that these samples had (>95%) and was recorded with another LA-ICP-MS equipment (see below).

The research used the ESI NWR193 excimer Laser Ablation system interfaced to the Nexion 350D ICP-MS, which was much stronger and succeeded in analysing the remaining samples. A 100 μm diameter laser beam and a laser repetition rate of 10 Hz and laser power of 8 J cm⁻¹ was used for the entire study. The ICP-MS data acquisition settings in the Syngistix version 1.1 software were 1 sweep per reading, 60 readings, 1 replicate, and total data acquisition lasted 44 seconds in peak hopping mode. The data was acquired at a rate of one point for each element every 0.75 seconds. For all analyses, NIST614 was used for calibration of element sensitivity using the "Preferred Values" Ref 1 published on the GEOREM database. Calibration accuracy was checked by repeatedly analysing NIST610, NIST614, and BCR-2G as unknowns and comparing to GEOREM values. Standards were analysed at the beginning, end, and periodically within each laser session. For data processing and calculation of concentrations, Glitter Software (GEMOC, Australia) was used to process the raw data files containing the signal intensity vs time data (the output from the Elan software). This allows precise selection of blanks, signals, and rapid visualisation of the intensity data. The calculated concentrations, 1 sigma error, and theoretical detection limits were exported to a statistical software and spreadsheet programs for further processing.

Special care was taken to secure consistency, precision and comparability between the results. In order to achieve this, samples were analysed with both equipment and the results of this cross-

examination is demonstrated below (fig.4.2). It is not expected to get the exact same values, especially when performing spot elementary analyses (LA-ICP-MS). Regardless of the measured values, prior geochemical analysis (e.g. Murray et al. 1992; Murray, 1994) have shown that the ratios between specific elements is consistent and it is based on these ratios that geochemical techniques are able to detect the features of the different rock samples.

The laboratory work was conducted in the Department of Earth Science at the University of Cambridge. The overall process of the results and the subsequent geochemical models were conducted with the use of the software GCDkit (ver. 3). It is the software that created the binary and ternary diagrams, and models used throughout the thesis.

Finally, the investigation of the typology and the craft techniques followed the work of Kowta (1980), Inizan et. al (1999), Andrefsky (2005), and Shea (2017). This method focused on the samples of the Brochtorff Xagħra Circle, Taç-Ċawla, Ġgantija, Santa Verna and Kordin, and was conducted in the McBurney Laboratory. The important characteristics were identified, and the typology of each artefact was recorded. These features have contributed to identify the techniques employed on these artefacts that led them to their final form (i.e. current form).

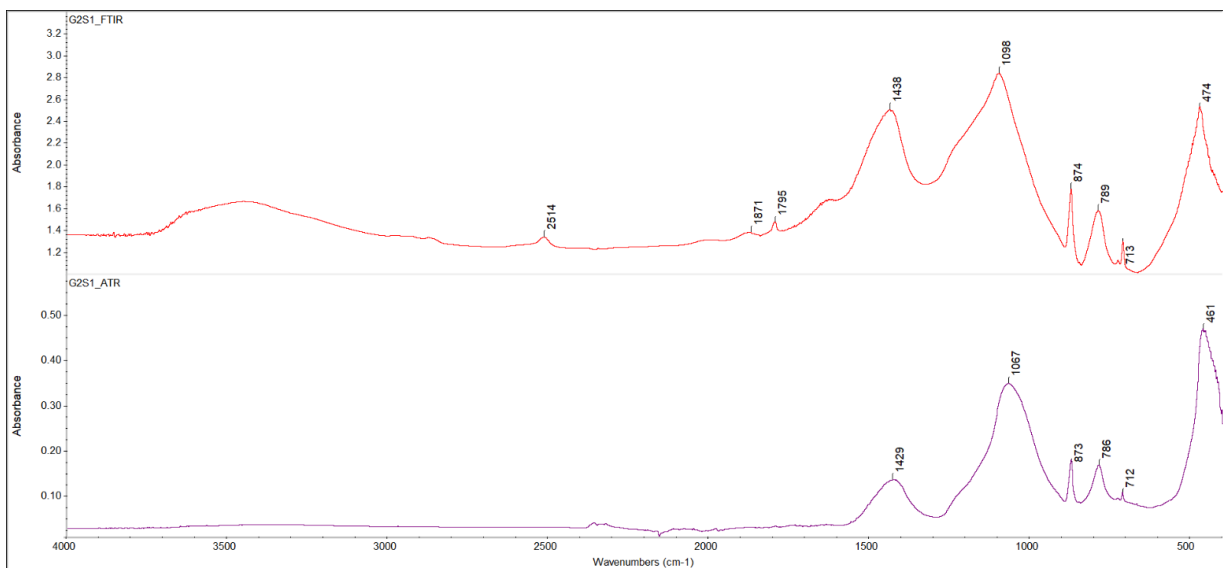


Figure 4-1: Representative cross-examining FTIR-ATR spectra. The chert-rock samples (e.g. G2S1) from Malta have been examined with the FTIR (above) and ATR (below) to reduce the errors in interpretation and overcome the lack of mineral reference of the ATR technique.

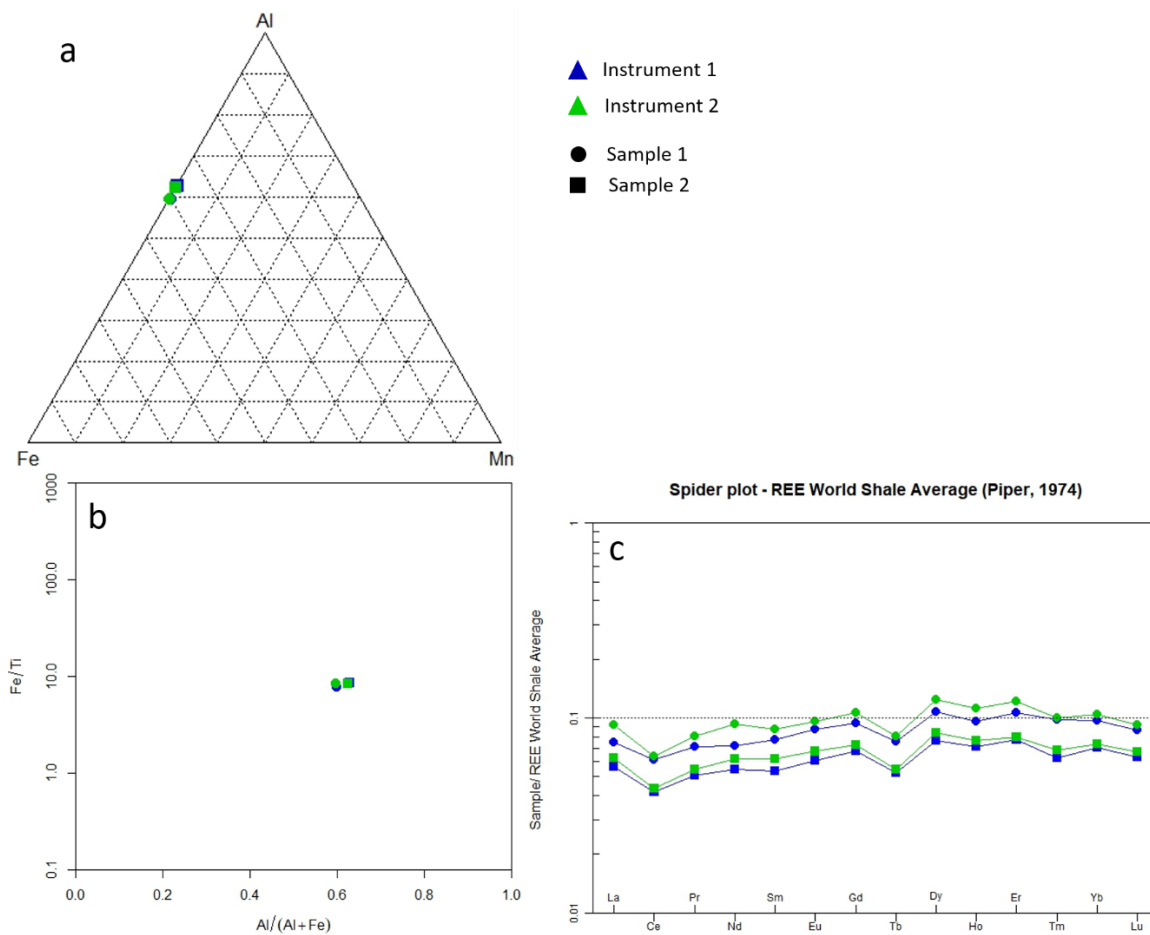


Figure 4-2: Geochemical models used in this PhD research and compare the results between the two LA-ICP-MS equipment employed in this research. a) Ternary model using the concentrations of Fe, Al and Mn, b) Binary model using the ratios of Fe/Ti and Al/(Al+Fe) and c) The concentrations of the REE normalised with the World average shales standard (Piper, 1974).

5 Results

This chapter presents all the results from the different techniques which have been employed and records some initial remarks. It is divided in subchapters for each technique of the methodology in which the collected results are recorded. Furthermore, important background information is given to explain the meaning of the findings and how the retrieved information contributes to the aims of this research. Initial remarks are recorded in each of these subchapters to help towards the better understanding of the results and how the chosen methodology contributes to the overall aims of this research. The detailed tables and diagrams of the data are found in the Appendix I, but a sufficient and representative selection are presented here to provide a better understanding of the results. The following table (Table 5.1) includes the main findings of the investigated samples recorded from each technique.

Table 5-1: Summary of the main findings of all the samples recorded from each technique. The Type indicates if the sample is rock source or artefact. The Location suggests the island from which the rock source was collected or the site from which the artefact was selected. The Microscopy and FTIR-ATR are recording the main minerals, while the p-XRF indicate the element with the highest peak. The LA-ICP-MS shows the element with the highest concentration. The indication N/A is inserted when a sample was not analysed with this method. Finally, the samples in blue font were analysed with the first LA-ICP-MS equipment and the ones in green were analysed with the second.

Samples	Type	Location	Macroscopy	Microscopy	FTIR-ATR	p-XRF	LA-ICP-MS
F1S4	Source rock	Gozo	Yellow chert	Calcite, quart	Opal-A	Ca	23.83% CaO
G1S1	Source rock	Gozo	Limestone	Calcite	Calcite	Ca	71.53% CaO
G1S2	Source rock	Gozo	Secondary calcite*	N/A	Calcite	Ca	68.07% CaO
G2S1	Source rock	Gozo	Brown, shiny chert	Calcite, quart	Opal-A	Ca	38.46% SiO ₂
G2S2	Source rock	Gozo	Grey, shiny chert	Calcite, quart	N/A	Ca	34.90% SiO ₂
G2S3	Source rock	Gozo	Grey chert	Calcite, quart	Opal-A	Ca	47.61% SiO ₂
G2S4	Source rock	Gozo	Grey, splotched chert	Calcite, quart	Opal-A	Ca	N/A
G2S5	Source rock	Gozo	Yellow chert	Calcite, quart	Opal-A	Ca	N/A
G2S6	Source rock	Gozo	White, shiny, translucent chert	Chalcedony, quartz	Opal-A	Si	94.69% SiO ₂
F1S2	Source rock	Malta	Yellow, laminated chert	Calcite, quart	Tridymite	N/A	9.05% CaO
F1S3	Source rock	Malta	Grey chert	Calcite, quart	Opal-A	N/A	7.84 CaO
M1S1b	Source rock	Malta	Yellow, laminated chert	Calcite, quart	Opal-A	Ca	47.68% SiO ₂
M1S2	Source rock	Malta	Brown, splotched chert	Calcite, quart	Opal-A	Ca	59.03% SiO ₂
M1S3	Source rock	Malta	Yellow, laminated chert	Calcite, quart	Opal-A	Ca	53.11% SiO ₂
M1S4	Source rock	Malta	Brown, spotted chert	Calcite, quart	Opal-A	N/A	48.96% SiO ₂

M1S5	Source rock	Malta	Brown, laminated chert	Calcite, quart	Opal-A	Ca	49.95% SiO ₂
M1S6	Source rock	Malta	Brown, laminated chert	Calcite, quart	N/A	Ca	32.01% SiO ₂
M1S7	Source rock	Malta	Brown, laminated chert	Calcite, quart	Opal-A	Ca	N/A
M1S8	Source rock	Malta	Brown, laminated chert	Calcite, quart	Opal-A	Ca	41.21% SiO ₂
M1S9	Source rock	Malta	Brown, laminated chert	Calcite, quart	Opal-A	Ca	37.54% SiO ₂
M1S10	Source rock	Malta	Brown, spotted chert	Calcite, quart	Opal-A	Ca	47.59% SiO ₂
M1S11	Source rock	Malta	Brown, laminated chert	Calcite, quart	N/A	Ca	39.02% SiO ₂
M2S1	Source rock	Malta	Brown, chert	Calcite, quart	Opal-A	Ca	N/A
M2S2	Source rock	Malta	Brown, shiny, laminated chert	Calcite, quart	Opal-A	Ca	25.35% SiO ₂
M2S3	Source rock	Malta	Olive-brown, laminated chert	N/A	Opal-A	Ca	N/A
M2S4	Source rock	Malta	Brown chert	Calcite, quart	N/A	Ca	38.04% SiO ₂
S1	Source rock	Sicily	Brown chert	Quartz	Quartz	N/A	N/A
S2	Source rock	Sicily	Silicified limestone	N/A	Calcite	Ca	N/A
S3	Source rock	Sicily	Black, shiny chert	Quartz	Quartz	Si	96.88% SiO ₂
S4	Source rock	Sicily	Grey, shiny, sub-translucent chert	Quartz	Quartz	Si	N/A
S5	Source rock	Sicily	Black chert	Quartz	Quartz	N/A	98.85% SiO ₂
S6a	Source rock	Sicily	Red, shiny chert	Quartz	N/A	Si	98.99% SiO ₂
S6b	Source rock	Sicily	Grey to red chert	Quartz	N/A	Fe, Si	87.98% SiO ₂
S7	Source rock	Sicily	Grey to red, shiny chert	N/A	Quartz	N/A	98.99% SiO ₂
S8	Source rock	Sicily	Grey to red chert	N/A	N/A	N/A	N/A
S9	Source rock	Sicily	Black chert	N/A	N/A	N/A	N/A
S10	Source rock	Sicily	Grey, shiny chert	Quartz	Quartz	Si	98.99% SiO ₂
S11	Source rock	Sicily	Black, shiny chert	Quartz	Quartz	Si	N/A
S12	Source rock	Sicily	Silicified limestone	N/A	N/A	Ca	N/A
S13	Source rock	Sicily	Grey, shiny chert	Quartz, calcite	N/A	Si	N/A
S14	Source rock	Sicily	Grey to brown, shiny chert	Quartz	N/A	Si	97.76% SiO ₂
S15	Source rock	Sicily	Grey, shiny chert	Quartz	Quartz	Si	98.79% SiO ₂
S16	Source rock	Sicily	Grey to brown shiny, sub-translucent chert	N/A	Quartz	N/A	95.12% SiO ₂

S17	Source rock	Sicily	Black, shiny chert	Quartz	Quartz	N/A	98.68% SiO ₂
S18	Source rock	Sicily	Black to brown, shiny, translucent chert	N/A	Quartz	Si	98.99% SiO ₂
S19	Source rock	Sicily	Black to brown, shiny, sub-translucent chert	N/A	Quartz	Si	98.99% SiO ₂
S20	Source rock	Sicily	Brown, shiny, sub-translucent chert	N/A	Quartz	Si	98.99% SiO ₂
S21	Source rock	Sicily	Red, shiny, sub-translucent chert	N/A	Quartz	Si	98.99% SiO ₂
S22r	Source rock	Sicily	Brown, shiny chert	N/A	N/A	Si	98.99% SiO ₂
S22p	Source rock	Sicily	Brown, sub-translucent chert	N/A	N/A	Si	98.99% SiO ₂
S23	Source rock	Sicily	Brown chert	Quartz	Quartz	Si	98.99% SiO ₂
S24	Source rock	Sicily	Orange to brown chert	N/A	Quartz	Fe	96.11% SiO ₂
S25	Source rock	Sicily	Grey, shiny, sub-translucent chert	Quartz	Quartz	Si	98.99% SiO ₂
BR88/ S110/L274	Artefact	Xaghra Circle	Brown, shiny flake	N/A	Quartz	Si	98.99% SiO ₂
BR89/ S291/L334	Artefact	Xaghra Circle	Orange, shiny blade	N/A	Quartz	Si	98.50% SiO ₂
BR89/ S395/L449	Artefact	Xaghra Circle	Brown, shiny, translucent flake	N/A	Quartz	Si	98.99% SiO ₂
BR91/ S564/L662	Artefact	Xaghra Circle	Brown, shiny, sub-translucent flake	N/A	Quartz	Si	98.99% SiO ₂
BR91/ S566/L662	Artefact	Xaghra Circle	Grey, prismatic flake	N/A	Opal-A	Ca	62.04% SiO ₂
BR91/ S611/L712	Artefact	Xaghra Circle	Brown, shiny, translucent flake	N/A	Quartz	Si	98.99% SiO ₂
BR91/ S745/L845	Artefact	Xaghra Circle	Brown, shiny scraper	N/A	Quartz	Si	97.77% SiO ₂
BR91/ S767/L783	Artefact	Xaghra Circle	Brown flake scraper	N/A	Quartz	Si	N/A
BR93/ S854/L897	Artefact	Xaghra Circle	Brown, translucent prismatic flake	N/A	Quartz	Si	98.75% SiO ₂
BR94/S1142 /L1279	Artefact	Xaghra Circle	Brown, shiny flake scraper	N/A	Quartz	Si	98.07% SiO ₂
BR93/ S843/L41	Artefact	Xaghra Circle	Orange, shiny, translucent flake debitage	N/A	Quartz	Si	98.99% SiO ₂
KRD15/L22/ S1/TR1A	Artefact	Kordin	Orange flake tool	N/A	Opal-A	Ca	61.45% SiO ₂
KRD15/L71/ S1/TRIA	Artefact	Kordin	Orange to brown, shiny, translucent flake debitage	N/A	Quartz	Si	98.99% SiO ₂
KRD15/ L201/S9	Artefact	Kordin	Brown, shiny, sub-translucent flake tool	N/A	N/A	Si	97.61% SiO ₂
KRD15/ S27/L203	Artefact	Kordin	Brown, shiny, sub-translucent flake	N/A	Quartz	Si	97.73% SiO ₂
KRD15/ S27/L207	Artefact	Kordin	Black, shiny proximal flake	N/A	Quartz	Si	97.73% SiO ₂

KRD15/ S34/L207	Artefact	Kordin	Brown, shiny, sub-translucent flake	N/A	Quartz	Si	98.99% SiO ₂
KRD15/ S42/L304	Artefact	Kordin	Grey, shiny, translucent flake tool	N/A	Quartz	Si	98.53% SiO ₂
KRD15/ S69/L211	Artefact	Kordin	Brown scraper	N/A	Quartz	Ca	97.85% SiO ₂
KRD15/ S98/L201	Artefact	Kordin	Brown, shiny burin	N/A	Quartz	Si	N/A
KRD15/ S133/L211	Artefact	Kordin	Brown, dull, sub-translucent scraper	N/A	Quartz	Si	N/A
KRD15/ S141/L150	Artefact	Kordin	Grey, shiny flake	N/A	Quartz	Si	93.55% SiO ₂
KRD15/ S144/L306	Artefact	Kordin	Orange, shiny shatter	N/A	Quartz	Si	98.16% SiO ₂
KRD15/ S156/L306	Artefact	Kordin	Brown to grey, shiny flake	N/A	Quartz	Si	N/A
KRD15/ S195/L209	Artefact	Kordin	Grey, shiny flake shatter	N/A	Quartz	Si	98.16% SiO ₂
TCC14/ S32A/L30	Artefact	Tač- Čawla	Brown, shiny flake shatter	N/A	Quartz	Si	N/A
TCC14/ S32B/L30	Artefact	Tač- Čawla	Brown, shiny flake tool	N/A	Quartz	Si	97.81% SiO ₂
TCC14/ S37/L30	Artefact	Tač- Čawla	Brown prismatic flake	N/A	Quartz	Ca	47.92% SiO ₂
TCC14/ S101/L85	Artefact	Tač- Čawla	Black, shiny flake tool	N/A	Quartz	Si	98.83% SiO ₂
TCC14/ S103/L85	Artefact	Tač- Čawla	Orange, shiny, sub-translucent blade	N/A	Tridymite	Si	98.90% SiO ₂
TCC14/S144	Artefact	Tač- Čawla	Brown, shiny flake tool	N/A	Quartz	Si	98.65% SiO ₂
TCC14/ S162/L155	Artefact	Tač- Čawla	Brown, shiny flake shatter	N/A	Quartz	Si	97.66% SiO ₂
TCC14/ S176/L100	Artefact	Tač- Čawla	Brown, shiny flake shatter	N/A	N/A	Si	81.88% SiO ₂
TCC14/ S193/L69	Artefact	Tač- Čawla	Brown, shiny, translucent flake tool	N/A	Quartz	Si	97.96% SiO ₂
TCC14/ S252/L179	Artefact	Tač- Čawla	Orange flake scraper	N/A	Quartz	Si	98.42% SiO ₂
TCC14/ S275/L208	Artefact	Tač- Čawla	Brown, shiny flake tool	N/A	Quartz	Si	98.84% SiO ₂
TCC14/ S316B/L63	Artefact	Tač- Čawla	Grey, shiny flake tool	N/A	Quartz	Si	94.09% SiO ₂
TCC14/ S416/L178	Artefact	Tač- Čawla	Black, shiny, translucent flake tool	N/A	Quartz	Si	97.89% SiO ₂
TCC14/ S460/L273	Artefact	Tač- Čawla	Brown, shiny shatter	N/A	Quartz	Si	98.51% SiO ₂
TCC14/ S502/L301	Artefact	Tač- Čawla	Brown flake tool	N/A	Quartz	Si	N/A
TCC14/ S513/L272	Artefact	Tač- Čawla	Brown flake tool	N/A	Opal-A	Ca	21.33% SiO ₂
TCC14/ S567/L206	Artefact	Tač- Čawla	Orange, shiny, translucent angular shatter	N/A	Calcite	Ca	61.57% CaO

TCC14/ S577/L131	Artefact	Tač- Čawla	Red, shiny, translucent flake tool	N/A	Quartz	Si	98.99% SiO ₂
TCC14/ S595/L81	Artefact	Tač- Čawla	Grey to brown, shiny, sub- translucent blade	N/A	Quartz	Si	N/A
SV15/ L4/S1	Artefact	Santa Verna	Brown, shiny, sub- translucent blade	N/A	Quartz	Ca	98.39% SiO ₂
SV15/ L16/S1	Artefact	Santa Verna	Brown, shiny blade	N/A	Quartz	Si	90.00% SiO ₂
SV15/S1/ L17/TRC	Artefact	Santa Verna	Grey, shiny flake shatter	N/A	Quartz	Si	98.90% SiO ₂
SV15/ L22/S1	Artefact	Santa Verna	Red, shiny, translucent flake tool	N/A	Quartz	Si	N/A
SV15/ L22/S2	Artefact	Santa Verna	Brown, shiny flake tool	N/A	Quartz	Si	N/A
SV15/ L33/S1	Artefact	Santa Verna	Brown proximal flake	N/A	Quartz	Si	96.84% SiO ₂
SV15/ L34/S1	Artefact	Santa Verna	Brown flake tool	N/A	Tridymite	Si	34.66% SiO ₂
SV15/S1/ L36/TRC	Artefact	Santa Verna	Grey, shiny, highly translucent flake tool	N/A	Quartz	Si	98.49% SiO ₂
SV15/ S2/L41	Artefact	Santa Verna	Brown, shiny, translucent flake tool	N/A	Quartz	Si	97.09% SiO ₂
SV15/ S1/L41	Artefact	Santa Verna	Brown, shiny, sub- translucent flake tool	N/A	Quartz	Si	98.39% SiO ₂
SV15/ S3/L41	Artefact	Santa Verna	Brown, shiny, translucent flake tool	N/A	Quartz	Si	98.99% SiO ₂
SV15/ L52/S1	Artefact	Santa Verna	Brown, shiny flake tool	N/A	Quartz	Si	68.70% SiO ₂
SV15/ L61/S1	Artefact	Santa Verna	Brown, shiny, translucent blade	N/A	Quartz	Si	98.35% SiO ₂
SV15/S1/ L68/TRG	Artefact	Santa Verna	Brown, shiny, sub- translucent flake tool	N/A	Quartz	Si	98.99% SiO ₂
SV15/ L80/S1	Artefact	Santa Verna	Brown, shiny, sub- translucent flake tool	N/A	Quartz	Si	98.99% SiO ₂
SV15/ S1/L98	Artefact	Santa Verna	Brown, shiny, sub- translucent flake tool	N/A	Quartz	Si	97.79% SiO ₂
SV15/ S32/L5	Artefact	Santa Verna	Black scraper	N/A	N/A	Si	98.40% SiO ₂
SV15/ S38/L8	Artefact	Santa Verna	Brown, shiny, translucent blade	N/A	Quartz	Si	98.99% SiO ₂
SV15/ S67/L34	Artefact	Santa Verna	Brown, sub- translucent flake tool	N/A	Quartz	Si	N/A
SV15/ S134/L58	Artefact	Santa Verna	Brown flake tool	N/A	Opal-A	Ca	55.62% SiO ₂
SV15/ S144/L42	Artefact	Santa Verna	Black, shiny flake	N/A	Tridymite	Ca	1.12% MgO

GG15/ L1004/S1	Artefact	Ġgantija	Orange flake	N/A	N/A	Si	98.19% SiO ₂
GG15/ L1004/S2	Artefact	Ġgantija	Grey, shiny, sub-translucent flake	N/A	Quartz	Si	98.00% SiO ₂
GGWC15/ L1012/S1	Artefact	Ġgantija	Grey, shiny shatter	N/A	Quartz	Ca	N/A
GGWC15/ L1012/S2	Artefact	Ġgantija	Brown, shiny, sub-translucent flake	N/A	Quartz	Si	N/A
GGWC15/ L1015/S1	Artefact	Ġgantija	Grey, shiny, sub-translucent blade	N/A	Quartz	Si	N/A
GGWC15/ L1015/S2	Artefact	Ġgantija	Brown, shiny, translucent flake	N/A	Quartz	Si	N/A
GGWC15/ L1015/S3	Artefact	Ġgantija	Brown, shiny, translucent flake	N/A	Quartz	Si	96.34% SiO ₂
GGWC15/ L1016/S1	Artefact	Ġgantija	Brown, shiny, translucent flake	N/A	Calcite	Ca	N/A
GGWC15/ L1016/S2	Artefact	Ġgantija	Brown, shiny, sub-translucent spall	N/A	Flint	Si	N/A
GGWC15/ L1016/S3	Artefact	Ġgantija	Brown, shiny, translucent blade	N/A	Quartz	Si	98.79% SiO ₂
GGWC15/ L1040/S1	Artefact	Ġgantija	Brown core	N/A	N/A	Si	N/A
GGWC15/ L008/S1/TRI	Artefact	Ġgantija	Brown, shiny, translucent flake	N/A	Quartz	Si	98.79% SiO ₂
GGWC15/ L12/S1	Artefact	Ġgantija	Brown flake	N/A	Opal-A	Ca	61.18% SiO ₂
GGWC15/ L1019/S1	Artefact	Ġgantija	Orange to brown proximal flake	N/A	Quartz	Si	N/A
GGWC15/ L1019/S2	Artefact	Ġgantija	Orange to brown blade	N/A	Quartz	Si	N/A
GGWC15/ L1019/S3	Artefact	Ġgantija	Orange to brown flake	N/A	Opal-A	Fe	N/A
GGWC15/L1 019/S4	Artefact	Ġgantija	Orange to brown flake	N/A	Quartz	Si	N/A
GGWC15/ L1019/S5/sb	Artefact	Ġgantija	Brown, sub-translucent blade tip	N/A	Quartz	Si	98.99% SiO ₂
GGWC15/ L1019/S6/sb	Artefact	Ġgantija	Brown, sub-translucent shatter	N/A	Quartz	Si	97.99% SiO ₂
GGWC15/ L1019/S7/sb	Artefact	Ġgantija	Brown, sub-translucent flake	N/A	Quartz	Si	98.79% SiO ₂
GGWC15/ L1019/S8/sb	Artefact	Ġgantija	Brown, sub-translucent flake	N/A	Quartz	Si	98.84% SiO ₂
SKB16/ L2/S1	Artefact	Skorba	Brown chert	N/A	Quartz	Fe	52.41% SiO ₂
SKB16/ L2/S4	Artefact	Skorba	Brown patinated chert	N/A	N/A	Fe	47.83% SiO ₂
SKB16/ L2/S5	Artefact	Skorba	Gray non-chert	N/A	Opal-A	Ca	48.51% SiO ₂
SKB16/ L2/S6	Artefact	Skorba	Gray, spotted chert	N/A	Opal-A	Fe	48.77% SiO ₂
SKB16/ L2/S7	Artefact	Skorba	Black, opaque non-chert	N/A	Quartz	N/A	51.77% SiO ₂
SKB16/ L2/S8	Artefact	Skorba	White, shiny, translucent chert	N/A	Quartz	N/A	98.40% SiO ₂
SKB16/ L5/S2	Artefact	Skorba	Gray chert	N/A	Quartz	Ca	62.61% SiO ₂

SKB16/ L5/S3	Artefact	Skorba	Black, shiny non-chert	N/A	Quartz	Ca	48.18% SiO ₂
SKB16/ L5/S4	Artefact	Skorba	Yellow chert	N/A	Tridymite	N/A	44.74% SiO ₂
SKB16/ L5/S5	Artefact	Skorba	Yellow, patinated chert	N/A	Quartz	N/A	47.50% SiO ₂
SKB16/ L10/S7	Artefact	Skorba	Patinated	N/A	Opal-A	N/A	50.70% SiO ₂
SKB16/ L10/S8	Artefact	Skorba	Yellow spotted chert	N/A	Quartz	N/A	55.41% SiO ₂
SKB16/ L10/S9	Artefact	Skorba	Orange, spotted chert	N/A	Opal-A	N/A	65.11% SiO ₂
SKB16/ L10/S10	Artefact	Skorba	Black non-chert	N/A	N/A	N/A	73.37% SiO ₂
SKB16/ L10/S11	Artefact	Skorba	Brown, spotted chert	N/A	Opal-A	N/A	60.97% SiO ₂
SKB16/ L10/S12	Artefact	Skorba	Gray chert	N/A	Quartz	N/A	58.51% SiO ₂
SKB16/ L10/S13	Artefact	Skorba	Black, shiny non-chert	N/A	Quartz	N/A	58.83% SiO ₂
SKB16/ L10/S14	Artefact	Skorba	Black, shiny chert	N/A	Quartz	N/A	77.87% SiO ₂
SKB16/ L10/S15	Artefact	Skorba	Orange, rough limestone	N/A	Calcite	N/A	59.68%Ca O
SKB16/ L10/S16	Artefact	Skorba	Yellow, spotted chert	N/A	Quartz	N/A	44.92% SiO ₂
SKB16/ L10/S18	Artefact	Skorba	Brown, rough limestone	N/A	Calcite	N/A	55.13%Ca O
SKB16/ L12/S6	Artefact	Skorba	Brown, spotted chert	N/A	Quartz	N/A	98.99% SiO ₂
SKB16/ L12b/S1	Artefact	Skorba	Black non-chert	N/A	Quartz	Ca	57.76% SiO ₂
SKB16/ L12b/S2	Artefact	Skorba	Brown non-chert	N/A	Quartz	Ca	44.60% SiO ₂
SKB16/ L12b/S3	Artefact	Skorba	Orange chert	N/A	Calcite	Ca	66.33%Ca O
SKB16/ L12b/S4	Artefact	Skorba	Brown, spotted chert	N/A	Tridymite	Ca	41.19% SiO ₂
SKB16/ L12b/S5	Artefact	Skorba	Grey chert	N/A	Quartz	Ca	52.52% SiO ₂
SKB16/ L13/S4	Artefact	Skorba	Black, spotted chert	N/A	Opal-A	Ca	51.49% SiO ₂
SKB16/ L13/S5	Artefact	Skorba	Pink limestone	N/A	Opal-A	Ca	50.08% SiO ₂
SKB16/ L13/S6	Artefact	Skorba	Black, spotted chert	N/A	Quartz	Ca	51.34% SiO ₂
SKB16/ L13/S7	Artefact	Skorba	Grey non-chert	N/A	Opal-A	Ca	49.01% SiO ₂
SKB16/ L13/S8	Artefact	Skorba	Black non-chert	N/A	Opal-A	Ca	54.41% SiO ₂
SKB16/ L13/S9	Artefact	Skorba	Brown, coarse limestone	N/A	Calcite	Ca	65.95%Ca O
SKB16/ L13/S10	Artefact	Skorba	Orange limestone	N/A	Calcite	Ca	65.16%Ca O
SKB16/ L13/S11	Artefact	Skorba	Brown chert	N/A	Tridymite	N/A	43.21% SiO ₂

SKB16/ L13/S12	Artefact	Skorba	Brown, shiny chert	N/A	Quartz	N/A	98.99% SiO ₂
SKB16/ L13/S13	Artefact	Skorba	Orange chert	N/A	Quartz	N/A	97.70% SiO ₂
SKB16/ L16/S1	Artefact	Skorba	Grey to yellow, spotted chert	N/A	Quartz	Ca	44.85% SiO ₂
SKB16/ L16/S2	Artefact	Skorba	Yellow, spotted chert	N/A	Opal-A	Si	48.70% SiO ₂
SKB16/ L16/S3	Artefact	Skorba	Yellow, shiny, sub- translucent chert	N/A	Quartz	Si	98.99% SiO ₂
SKB16/ L19/S2	Artefact	Skorba	Gray, spotted chert	N/A	Opal-A	Ca	89.03% SiO ₂
SKB16/ L19/S3	Artefact	Skorba	Gray, spotted chert	N/A	Tridymite	Ca	33.28% SiO ₂
SKB16/ L19/S4	Artefact	Skorba	Gray to brown, spotted chert	N/A	Opal-A	Ca	34.43% SiO ₂
SKB16/ L20/S2	Artefact	Skorba	Black, shiny non-chert	N/A	Tridymite	Ca	81.50% SiO ₂
SKB16/ L23/S1	Artefact	Skorba	Black non-chert	N/A	Quartz	Fe	24.57% SiO ₂
SKB16/ L23/S2	Artefact	Skorba	Gray, spotted chert	N/A	Tridymite	Ca	28.90% SiO ₂
SKB16/ L23/S3	Artefact	Skorba	Gray, spotted chert	N/A	Quartz	Ca	24.97% SiO ₂
SKB16/ L23/S4	Artefact	Skorba	Gray, spotted chert	N/A	Tridymite	Ca	25.63% SiO ₂
SKB16/ L23/S5	Artefact	Skorba	Gray, spotted chert	N/A	Tridymite	Fe	36.15% SiO ₂
SKB16/ L23/S7	Artefact	Skorba	Red, shiny, translucent chert	N/A	Quartz	N/A	98.99% SiO ₂
SKB16/ L23/S8	Artefact	Skorba	Brown, shiny, translucent chert	N/A	Quartz	N/A	98.99% SiO ₂
SKB16/ L26/S1	Artefact	Skorba	Brown, spotted chert	N/A	Quartz	Ca	69.63% SiO ₂
SKB16/ L26/S6	Artefact	Skorba	Gray, with spots chert	N/A	Quartz	N/A	53.12% SiO ₂
SKB16/ L26/S7	Artefact	Skorba	Gray to brown chert	N/A	Quartz	N/A	70.38% SiO ₂
SKB16/ L26/S8	Artefact	Skorba	Brown, spotted chert	N/A	Quartz	N/A	83.42% SiO ₂
SKB16/ L30/S1	Artefact	Skorba	Gray, spotted chert	N/A	Opal-A	Ca	43.68% SiO ₂
SKB16/ L30/S2	Artefact	Skorba	Gray limestone	N/A	Quartz	Ca	47.70% SiO ₂
SKB16/ L30/S3	Artefact	Skorba	Gray limestone	N/A	Opal-A	N/A	55.12% SiO ₂
SKB16/ L30/S4	Artefact	Skorba	Brown, shiny, translucent chert	N/A	Quartz	N/A	98.96% SiO ₂
SKB15/ S131/L211	Artefact	Skorba	Brown, shiny, sub- translucent flake scraper	N/A	Quartz	Si	98.90% SiO ₂

*it is a type of secondary deposit mostly related to limestone formations and found mainly within cracks, holes and caves. Erosion and weathering of the limestone creates the necessary material, that can be deposited mainly by supersaturated meteoric waters. It is named secondary calcite because it includes more than 90% calcite minerals.

5.1. Macroscopic Examination

The macroscopic examination included fieldwork and laboratory research and was first conducted on the Maltese Islands (Malta and Gozo) and Sicily. Further evaluation of the collected samples has been undertaken in the Geoarchaeological laboratory of the Department of Archaeology at the University of Cambridge. Moreover, the samples from the assemblages have been examined to identify the craft techniques employed and their typology (i.e. type of tools). The samples are also representative of the different typologies and craft techniques in the assemblages. The following sections present the investigation conducted on the field and the macroscopic evaluation of the chert outcrops and artefacts.

5.1.1. Chert Formations

5.1.1.1. Maltese Islands

It was well established from the literature (Pedley et al., 2002) and the reconnaissance fieldtrip (November 2015) that the chert outcrops are located in the middle Globigerina Limestone, the geological formation which is the focus for this research. The work on the Maltese Islands was mainly field exploration to investigate any possible chert sources present on the Islands. The first location investigated was the area of Ramla Valley, which is found at the northeast part of Gozo Island (Fig. 5.1). This valley is between Xaghra and Nadur Villages and extends from the Racetrack (south) to the Ir-Ramla Bay (north). There, an important exposure of middle Globigerina Limestone is reported, which might present chert outcrops. The limestone has a smooth and sandstone texture, white to beige colours, and is fine-grained. Although the whole exposure has been thoroughly examined, no indications have been found to support the presence of chert outcrops. Regardless of this, three samples of the area were collected to investigate this type of limestone exposure (i.e. G1S1, G1S2).

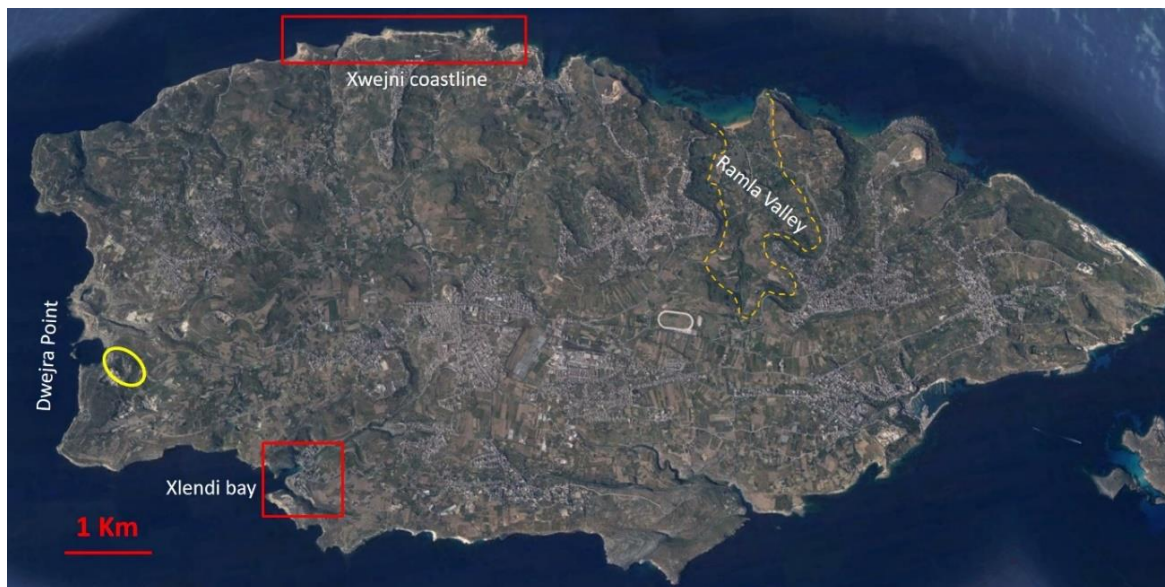


Figure 5-1: A satellite image of Gozo with the locations of the investigations (Map Copyright@2017 Google).

The next area of interest is on the west part of Gozo, at Dwejra Point in an area close to Fungus Rock (Fig. 5.1). This area is a small internal valley (Wied Pisklu) with exposures of middle Globigerina Limestone and the presence of siliceous deposits (Fig. 2.10). The Limestone has a maximum thickness of approximately 50m, white to beige in colour, and is bedded (Fig. 5.2a). The examination of the chert outcrops starts from the highest point and continues downwards. The cherts on the top of the formation are nodular in form, opaque and have greyish colour shades (Fig. 5.2b). In addition, they have a semi-smooth texture, medium lustre with greasy shine and homogenous fabric (G2S1, G2S2). They do not vary significantly in size (approximately 8cm in length and 5cm in width), some are fine-grained, while others have a medium coarse grain (G2S1). Continuing downhill, the silicate deposits increase in size and frequency, forming beds of approximately 4cm thick (maximum thickness is 7cm) and 3.6m long (Fig. 5.2c, d and e). This type of outcrop extends over a distance greater than 10m and four samples have been collected for laboratory investigation (G2S3, G2S4, G2S5 and F1S4). They are mainly heterogeneous, opaque and coarse-grained, with a significant presence of calcium carbonate (CaCO_3). They are olive-grey (5Y 3/2) or dusky-yellow (5Y 6/4) in colour, have dull lustre and rough texture and are occasionally laminated and splotched. At the lowest points, a change is noticed, since, at this point in the stratigraphy, the chert outcrops reshape into nodular forms. They are homogenous and fine-grained, but differ from the previous cherts (Fig. 5.2f). They have a white colour (N9), smooth texture, a pearly shine and are translucent (G2S6). The research of chert outcrops continued to other promising areas of Gozo Island to the north and to the south (Fig. 5.1). Starting from the North, at the Marsalforn Bay and the Xwejni coastline, there is a massive exposure of middle Globigerina Limestone. This exposure exceeds 2km in length, has a maximum thickness of 40m, smooth sandstone texture and is fine-grained (fig 2.7). In the south of Gozo, outcrops of this formation have been found near the

Xlendi Village, but the exposures are significantly smaller than the one in the north. Although these exposures have been thoroughly examined, no evidence of chert formations is reported.



Figure 5-2: Chert outcrops on Gozo. a) Bedded middle Globigerina Limestone, b) Nodular Chert, c,d,e) Bedded chert outcrops intercalated in middle Globigerina Limestone and f) Nodular Chert (G2S6).

The investigation of chert outcrops in Malta Island started from the Fomm-IR-RiĦ Bay (west), which is the only known location with siliceous formations (Fig. 2.8). The north part of the bay is composed mainly of the Blue Clay formations with no evidence of chert outcrops. The chert formations are found in the centre of the Bay, again within the middle Globigerina Limestone, which is in bedded form (Fig. 5.3a). The chert outcrops are in nodular form, dull, opaque, smooth, fine-grained, and presented with irregular shapes (M1S1 and M1S2). Some outcrops have yellowish colours, heterogeneous fabric and fine laminated lines (M1S1), while others have brownish colours, homogenous fabric and are splotted² (M1S2). There is no evidence for chert outcrops further inland (east), while 80m from this position there is the transition from the middle Globigerina Limestone to the upper Globigerina Limestone. More chert outcrops are reported to the West in a bedded form which are approximately 1.5cm thick. These outcrops extend north until the transition from the middle Globigerina Limestone to the Blue Clay. This transition is ruled by the tectonic status of the area, which is associated with the Victorian Lines (Fig. 2.9). These siliceous formations are thicker (5 to 7cm), but they might be silicified limestones and not cherts (M1S3 and M1S4). They present similarities in fabric, lustre, translucency and grain, but differ in colour, texture and pattern (Appendix, Table 3). Outcrops are also reported to West-Southwest until the transition from the middle Globigerina Limestone to the lower Globigerina Limestone. The beds are 10cm thick (M1S5 and F1S2) and the nodular cherts present more regular shapes and are approximately 7cm in width and 10 cm in length (Fig. 5.3c and d).



Figure 5-3: Chert outcrops on Malta. a) Nodular chert in middle Globigerina limestone, b) Chunky chert, c and d) b bedded shape chert outcrop.

² Irregular shape spot pattern that covers less than 30% of the sample's surface (Crandell, 2006).

The middle Globigerina Limestone re-appears to the south and along the main road and includes evidence of chert sources. Indeed, intact and unspoiled chunky nodular cherts are located on the top of a terrace sequence (Fig. 5.3b) and two representative samples were collected (M1S6 and M1S7). The first is 30 cm in length and 8cm in thickness, while the second is 27cm in length, 14cm in width and 4cm in thickness. Although they present some differences in colour and texture, they generally share the same macroscopic characteristics (Appendix I, Table 3). More chert outcrops have been found West-Southwest of the Fomm-IR-RiH bay, close (600m) to the Megalithic Temple and Punic Roman remains at Ras IR-Raheb (Fig. 2.8). There a small path/stream, which connects the cliffs with the main road, crosses the middle Globigerina Limestone and reveals the presence of chert formations (Fig. 5.4). The chert outcrops are both nodular and bedded, while some outcrops are agglomerates of small nodules. The bedded cherts are thin (2 to 3cm), olive-brown or yellowish in colour (M1S8) and they slowly disappear towards the south (Fig. 5.4a). The nodular cherts are opaque, brownish in colour, have irregular shapes and a size that varies (Fig. 5.4b and c). The smallest nodular chert is 5.5cm in length (M1S11), while the largest reach 60cm in size (M1S9). The search stopped just before the transition between the middle and the upper Globigerina Limestone, where one more sample (M1S10) was collected (Fig. 5.4d).

Walking along the exposures of the middle Globigerina Limestone to the Southwest (Fig. 2.8), more chert outcrops are found in this area alongside small paths and streams. They are again found in the part of the formation that has a bedded form and not in the exposures that resemble a sandstone formation. The chert outcrops are mainly nodular in form (M2S2 and M2S3) with their length exceeding 30cm and their width approximately 25cm (Fig. 5.5b). Although bedded cherts are also found (Fig. 5.5c) and were sampled (M2S4), they might be another type of siliceous deposits (e.g. silicified limestone or shale). Unfortunately, it has been impossible to investigate the outcrops further south, because of the steep cliffs and the huge rocks blocking the way to the South (Fig. 5.5a). In addition, all remaining paths lead downhill towards the steep cliffs without any alternative routes. This location has only the lowest parts of middle Globigerina Limestone which do not present any chert outcrops. Although this cul-de-sac area is far from any chert outcrop, it is full of scattered pieces of cherts. Thus, it was decided to collect samples (M2S1) as evidence of the presence of chert outcrops at a higher altitude and for further research. Finally, bedded chert outcrops are reported (Fig. 5.5d) and a sample was collected (F1S3) along the lane which connects the main road with the archaeological site at Ras IR-Raheb. The main macroscopic features of these outcrops are their brownish colour and the homogenous, opaque fabric.



Figure 5-4: a) Bedded chert outcrops intercalated in bedded middle Globigerina Limestone, b) nodular chert with irregular shapes, c) Great exposure of chert outcrops and d) Nodular chert.



Figure 5-5: a) Overview of the Southwest cliffs with the middle Globigerina Limestone exposure, b) nodular chert, c) bedded siliceous formation and d) bedded chert intercalated in the bedded middle Globigerina Limestone.

The search for chert sources continued in other locations in Malta where exposures of middle Globigerina Limestone were known (Fig. 5.6). Briefly, the places investigated were: a) the Gnejna Bay (north of the Fomm-IR-RIH bay), b) East of Rabat or on the hills opposite (south) the Skorba Temples, c) the area from Had – Dingli until the Blue Grotto (south part of Malta), d) the area from Mellieha Bay to Salina bay (north part of Malta), e) the area from Marsaskala bay until the St. Thomas Bay (east part of Malta), and f) the area from Marsaxlokk bay until Ghar Hasan (archaeological site). However, the field investigation did not detect any evidence supporting the presence of chert outcrops. The details with the exact location of the samples and their macroscopic characteristics can be found in the Appendix I (Fig.1; Table 1 and 3).



Figure 5-6 A satellite image of Malta with the locations of investigations (Map Copyright@2017 Google).

5.1.1.2. Sicily

The research on the Sicilian chert formations makes use of the baseline provided from the literature (Catalano et al. 1984, 1989; Lentini, 1984; Lentini et al. 1995) and follows the suggestions of Professor Pedley (University of Hull), Prof. Maniscalco (University of Catania) and Prof. Di Stefano (University of Palermo) who are experts on Sicilian geology. The search for chert sources was focused on three provinces: a) Ragusa, b) Enna and c) Palermo. The details with the exact location of the samples and their macroscopic characteristics can be found in the Appendix I (Table 2 and 4).

➤ Province of Ragusa

This province is located in the southeast part of Sicily and consists only of the formations of the Hyblean Plateau (Fig. 2.16). The chert outcrops are found in the Ragusa Formation and the investigation was conducted in a triangular area among the towns of Comiso, Monterosso Almo and Modica (Fig. 5.7). This area is also crucial for this fieldwork as it presents evidence of prehistoric mining activity (Vella, 2008) and it may have been a location from which chert material was exported to Malta. An established location with such activities is Monte Tabuto (mountain) which was the prime area investigated. Monte Tabuto is located between Comiso and Ragusa (Fig. 5.7-8) and the first prehistoric mines were found along the main road which leads to the top of the mountain (Fig. 5.9a). The fieldwork in this area revealed that the mining structures are not restricted along the road but spread across the whole west side of the mountain. The chert outcrops, however, are very limited and scattered, while no chert source has been reported in the mines. The first chert outcrops are in nodular form with a thickness between 6 to 8cm (sample S1) and were found beside a mine entrance (Fig. 5.9c, d). Further exploration of the area has shown that the chert outcrops vary in size and shape, while occasionally they form small layers (< 5 cm). They generally have a brownish colour but the greater nodules (reaching 35cm diameter) present black or dark olive-grey cores (Fig. 5.98b). Continuing away from the mines, downhill or uphill, the chert outcrops rapidly decrease and finally disappear within a couple of metres. The research continued into the area around the Ragusa Town, which on the geological map presented the same geological formation as at Monte Tabutto. However, the investigation in this area has not recorded any indication of chert outcrops and the research therefore moved to other locations. The next stop region was south of Modina Town (Fig. 5.7-8), which presented mainly the Irmino member (Lower Miocene) of the Ragusa Formation. The chert outcrops are in small nodular form, but they occasionally form beds of 5 to 10cm in thickness. They are described as fine-grained, translucent and present dark brownish colours.



Figure 5-7: Map of SE Sicily recording the main towns and location of the area (Maps Copyright ©2016 Google).

The geology of SE Sicily

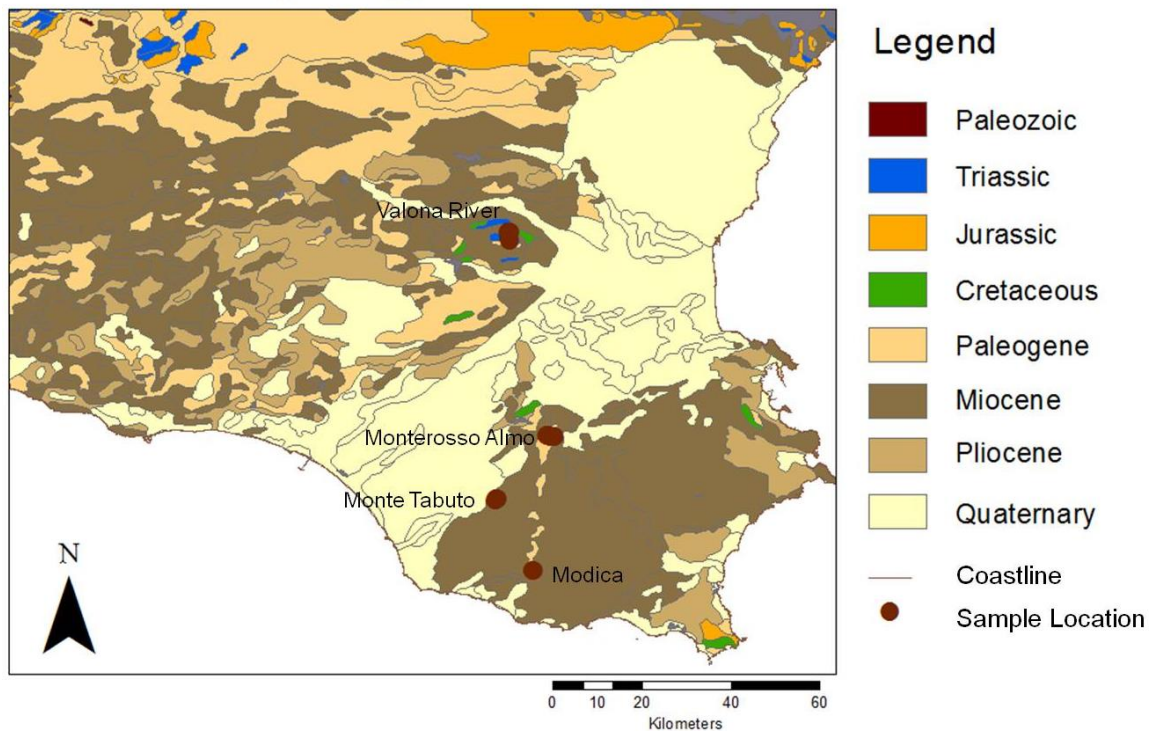


Figure 5-8: The Geological Map of SE Sicily by Age and the main sample locations.



Figure 5-9: a) An entrance of prehistoric mine, b) Chert outcrops close to the mine presented at a, c) Chert outcrops beside another prehistoric mine, and d) detail of c.

The final stop was near the town of Monterosso Almo (Fig. 5.7-8) which is located at the northern part of the province. This area has provided the opportunity to investigate almost the whole succession of the Hyblean Plateau. The geological formations which are found in this location extend from the Cretaceous (Campanian) to the Quaternary. The first chert outcrops are located in an old quarry along the road which connects the town with the Licodia Village. This quarry is in the lower part of the Armerillo Formation (Cretaceous) which is known to contain chert outcrops (Lentini, 1984). Starting from the entrance of the quarry (Fig. 5.10a), greyish nodular cherts intercalate with the limestone (Sample S15). These cherts vary in size and have chunky forms, while others form thin beds (2–3 cm). Moving to the inner parts of the quarry and following the left slope (Fig. 5.10b), these horizons become more distinct and are divided into two main groups. The lower group has greyish colours and a thickness between 3 to 6cm, while the upper group is thinner (2.5 cm), more fine-grained and has a dark brownish colour (Sample S14). The latter is not found in any other part of the quarry and is part of an exposure of several metres in length. The centre of the quarry presents an extensive profile (approximately 100m) of the Amerillo Formation (Fig. 5.10c) with multiple bedded chert outcrops (sample S13). Although they are very similar to the lower group of the previously described cherts, they are thicker (10 cm), denser and have a blackish colour on the upper parts (sample S17). During the investigation of the quarry, indications were recorded of another type of chert outcrop. This is

suggested from scattered pieces (cores and fragments) collected and examined in the quarry which are not *in situ* (sample S16). The investigation has not found their source and the *in situ* examination of the outcrops has not been possible. These pieces are thick (10cm), very strong (difficult to break even with the hammer), have a brownish grey colour and a completely different texture from the chert outcrops in the quarry.

The investigation for more chert sources continued along the road to Licodia Village, which presents exposures of the upper part (Eocene) of the Amerillo Formation. The examination of this Eocene limestone found very thin layers and lenses of chert (Fig. 5.11). These chert outcrops are divided into 3 or 4 distinctive horizons, which are 30 cm in length, 4 to 6cm in thickness and characterized by a brownish to black colour (Sample S18). The examination of this formation has been interrupted by the unexpected presence of a conglomerate outcrop. It is highly possible that it is an outcrop of the Pliocene brecciated formation (Pb), which has exposures in nearby locations (Lentini, 1984). Although this interruption is unexpected, it has provided some very interesting and new information. This conglomerate outcrop is a soft and sandy formation, with different sizes and shapes of breccias. Some of these breccias are actually chert pieces, which are easily extracted with the use of a lever. In addition, this formation presents man-made structures (Fig. 5.12a, b) similar to the prehistoric mines at Monde Tabuto. In fact, a chert sample was collected (Sample S19) for further investigation in precisely one of these structures (Fig. 5.12b, c).

Moving along the road, the Amerillo Formation (limestone) is found again, but this time presents slightly different chert outcrops. They are not divided into distinct horizons as before, but they form huge and irregular shaped nodular cherts (Fig. 5.12d; Sample S20). The majority of the nodular cherts are 7cm in thickness and 12cm in length, while the largest reaches 12cm in thickness and 15cm in length. Some lenses which exceed 45cm in length were also located, but they do not differ in any other macroscopic characteristic (Fig. 5.12e, f). The final stop was made just before the entrance of the active quarry, but again in the Armerillo formation. Important chert outcrops were located there, which are very different from the outcrops already examined. They are huge and thick cherts in nodular and lens forms with irregular shapes (Fig. 5.13) and are greyish-red to orange in colour (Sample S21). The investigation of the other formations in the area did not present anymore chert outcrops and therefore the investigation of the Ragusa province was completed.

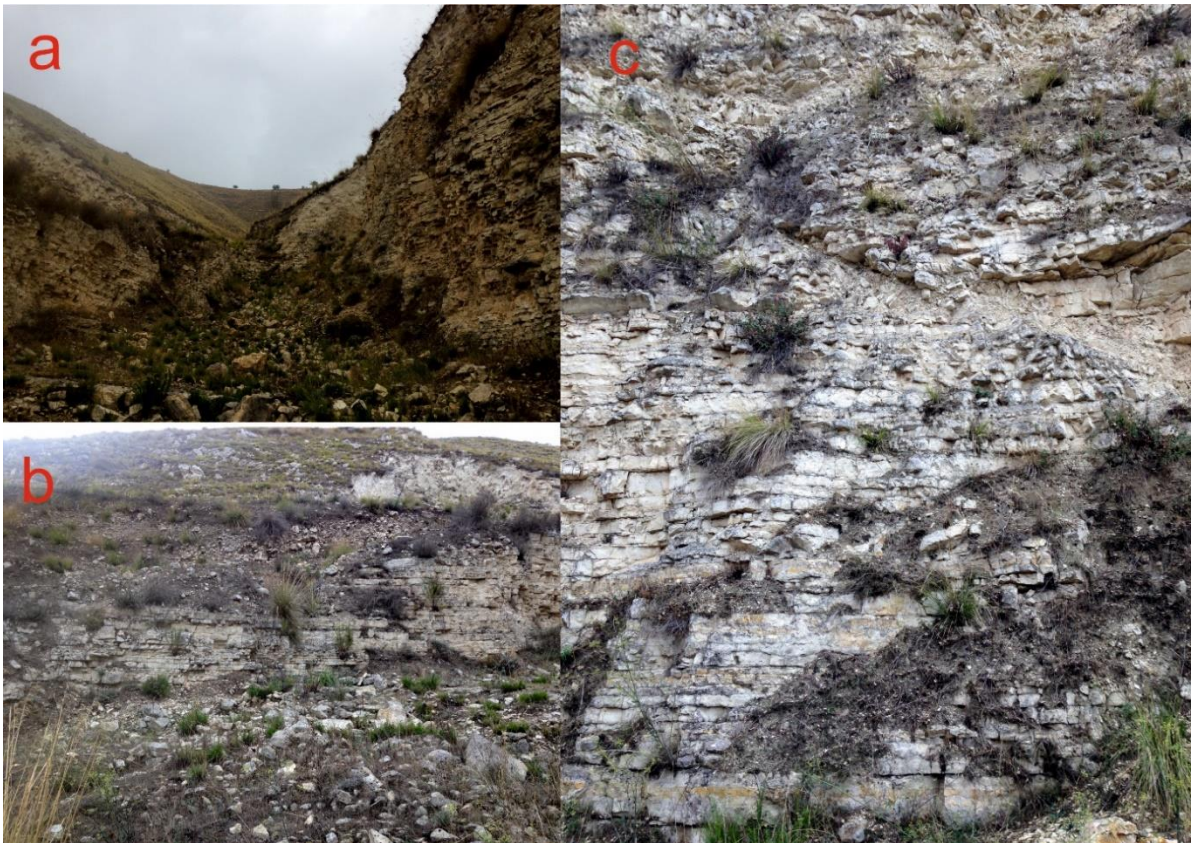


Figure 5-10: Chert and silicified limestone outcrops south of Modica Town in SE of Sicily.



Figure 5-11: Black to brownish chert lenses outcrops, which are found intercalating the Amerillo Formation (Eocene).



Figure 5-12: a) The road leading to Monterosso Almo town, where the man-made structures were found (on the left), b) The entrance of one of these structures, c) Detail of b where chert pieces were located (arrows), d) huge nodular chert with chalky residues, e and f) chert outcrops in lens form.



Figure 5-13: a) The Amerillo formation with the huge and thick chert outcrops, b) detail of a, focusing on a huge lens of brownish chert.

➤ Province of Enna

The next region is the province of Enna, which is located northwest of Ragusa province (Fig. 5.7-8) and has significant chert outcrops (Carbone et al., 1990). These outcrops are found in the formations of the Monte Judica unit (Carbone et al., 1990). Regarding their place in the geological time, they extend from Carnian (Triassic) to the Upper Serravallian (Miocene). The investigation started from a place called Contrada la Vina, which is close to the Valona River and presents significant exposures of the “Calcarei con Selce” formation. This Triassic limestone formation (Carnian to Upper Rhaetian) includes fragmented nodular cherts of different sizes and shapes (Fig. 5.14a, b) and two representative samples were collected (samples S4 and S5).

The next stop is at the Valona River riverbed, where exposures of the Radiolarian formation (Jurassic – Cretaceous) are found (Fig. 5.14c, d). The formation has huge exposures on both sides of the river which expand to several metres thick (Fig. 5.15). It consists of a sequence of radiolarian beds with different thicknesses and colours varying from red to green (Fig. 2.19a, b). Occasionally, the sequence is interrupted by thin intermediate layers/horizons of silicified limestone beds. The thin horizons have green or dark red colours, while the limestone has greyish to red colours and a thickness which varies from 5cm to 17cm. The lowest radiolarian bed is a solid and dense layer, which has a reddish colour and is 6cm thick (sample S6). This is followed by a thicker (12cm) red to green bed (sample S7), which is fragmented and weathered. Above that, the outcrop presents alterations of thinner radiolarian beds (2 to 5cm) and silicified limestones (5cm). The middle of the radiolarian succession consists of thicker beds with the silicified limestones reaching 17cm and the radiolarians 13cm in thickness, respectively. The radiolarian beds present distinct macroscopic characteristics and have been sampled (sample S8) for further investigation. The rest of the outcrop to the top is characterized by weathered, red and thick radiolarian beds alternating with thin silicified limestones.

The research then moved to a location called Monte Santo (Fig. 5.7-8), where more exposures of the “Calcarì con Selce” formation are found. This exposure differs from the previous one (Contrada la vina) because it presents well developed, black, bedded chert outcrops (Fig. 2.19c, d). Three samples were collected from the most representative zone (sample S9, S10, S11) and the stromatographical order (first sample from the lowest bed) was recorded.



Figure 5-14: Chert outcrops in the broad Valona River area. a and b) Fragmented Triassic nodular cherts, c and d) Bedded Radiolarian outcrops.

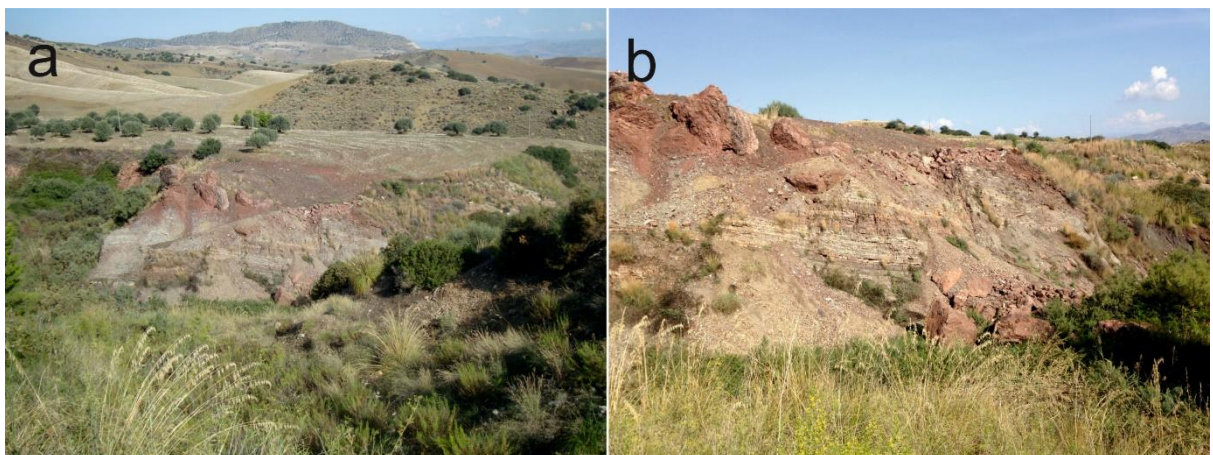


Figure 5-15: The exposure of the of the Radiolarian formation along the Valona River from a distance.

➤ Province of Palermo

The research continued into West Sicily and investigated the province of Palermo (West Sicily), which is geologically also known for chert outcrops (Catalano et al., 1978; Catalano 2004; Di Stefano et al. 1992; Di Stefano et al. 2013). The first stop was made at a sanctuary called “Madona del Balzo” (Fig. 5.16), located on the top of Triona Mountain (elevation 899cm). The sanctuary is built on a limestone formation (Formazione Scillato), which is part of the Del Bacino Sicano unit (Fig. 5.17) and is very similar to the “Calcari con Selce” formation of the Monte Judica unit (province of Enna). This limestone is of Upper Triassic age (Upper Carnian to Lower Rhaetian) and the exposure beside the sanctuary presents chert outcrops. They are small nodular or lenses outcrops, highly fragmented, with irregular shapes and very difficult to extract (Fig. 5.18a). Nonetheless, two representative samples (sample S22) were collected, which presented different macroscopic characteristics.

The next stop was located on the Genuardo Mountain (elevation 883m), very close to the Santa Maria del Bosco (monastery), and where the homonymous limestone formation (Calcari Di Santa Maria del Bosco) was examined for chert outcrops. The investigation found black bedded cherts (Fig. 5.18b) which are approximately 6 to 10cm in thickness (Sample S23). Continuing west of these black chert outcrops, indications of a new chert outcrop were found which differ significantly from any other chert formation previously examined. Plenty of scattered pieces of a dense, heavy and solid yellowish chert (Fig. 5.18c) were found lying on agricultural fields. The macroscopic characteristics of these pieces indicate that this chert formation must be related to the basaltic lavas which are recorded on the geological map (Di Stefano et al, 2013) of the area. These volcanic formations should be intercalating between the “Calcari Di Santa Maria del Bosco” (below) and the “Formazione Barracu” (above). The *in situ* examination of this outcrop was unsuccessful, mainly because the whole area is under private ownership which prevents any type of investigation. Therefore, it was decided to collect just one of the scattered pieces (Sample S24) as evidence and for further laboratory research.

Finally, moving along the same area, the research located several exposures of the “Formazione Barracu” (middle–upper Jurassic). It is a highly silicified limestone intercalating with greyish bedded chert (Fig. 5.18d). The chert outcrops present a significant amount of carbonate residues and the beds are 4 to 6cm in thickness (Sample S25).



Figure 5-16: Map of West Sicily recording the main towns and location of the area (Maps Copyright @2016 Google).

The geology of West Sicily

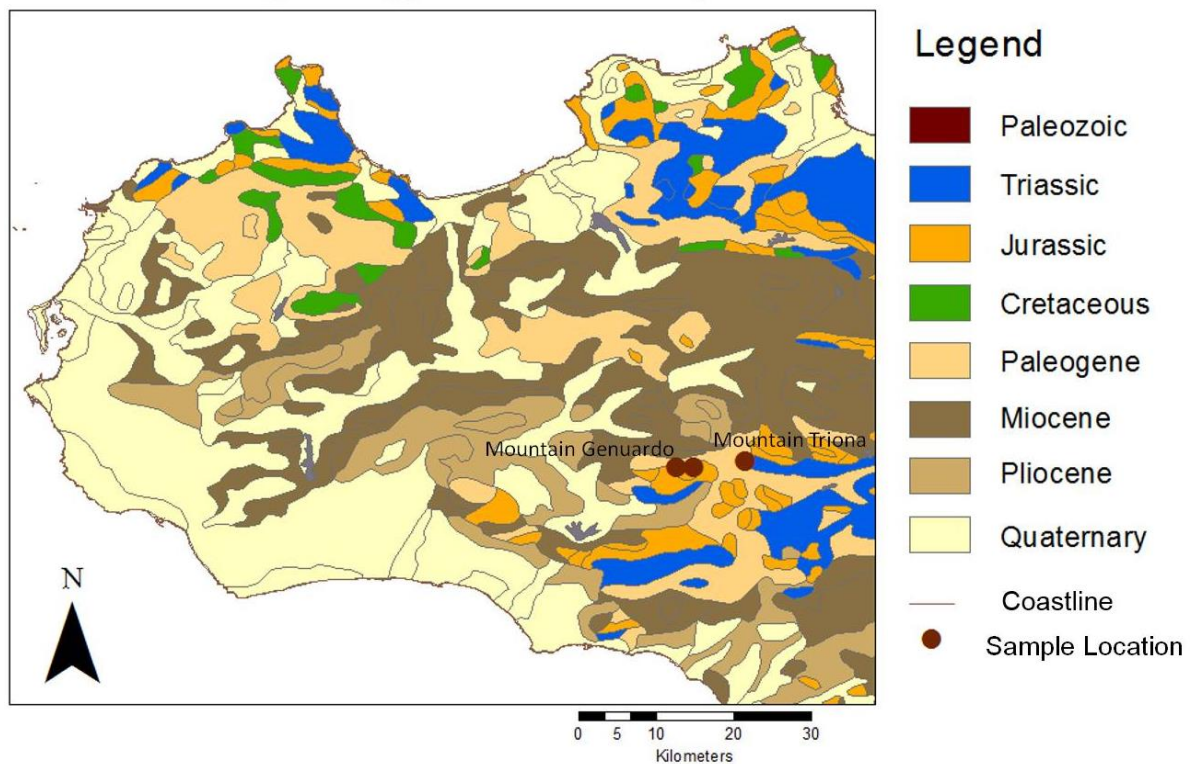


Figure 5-17: The Geological Map of West Sicily by Age and the sample locations.



Figure 5-18: a) Fragmented nodular chert outcrops at "Madona del Balzo", b) Black bedded chert outcrop close to Santa Maria del Bosco (monastery). C) Pieces of the yellowish chert formation, d) greyish bedded chert outcrops intercalating with a highly silicified limestone.

5.1.2. Chert Assemblages

The investigation of the assemblages has revealed that the artefacts are made from multiple lithic sources and are not restricted just to chert rocks (Appendix; Table 5). This consequently modified the initial strategy in order to address the challenge of examining lithic collections. The research has firstly recorded the total number of the finds and divided the lithics into three categories: a) chert, b) obsidian and c) "other". The chert category includes chert and flint materials because at this stage it is very difficult to distinguish between these two types. Moreover, it includes materials which are considered either chert cortex or highly silicified limestone. The "Other" category includes mainly limestone pieces and those which due to their macroscopic characteristics cannot be placed within any of the other two categories. Subsequently, the macroscopic characteristics of the chert materials were recorded (Appendix I, Table 7, 8) and representative samples from each assemblage were selected. These samples also represent the different type of artefacts found in the archaeological assemblages and demonstrate the main craft techniques (Appendix I; Table 9).

5.1.2.1. The Brochtorff Xagħra Circle assemblage

The assemblage of the Circle was collected during the excavations of the site between 1987 and 1994. It is an assemblage of 225 pieces and included artefacts which are made from a variety of rock materials (Appendix I; Table 5). Eight pieces are made from limestone, while one is made from calcite. Furthermore, there is a group of artefacts (n=18) of an unknown rock source, but clearly not related to chert rocks. Finally, there are a few chert artefacts which are patinated. It was decided to exclude the latter from further investigation as they are fully covered with patina (white or coloured) and their macroscopic characteristics cannot be easily distinguished. The finds related with this excavation have initials BR (Brochtorff) and further explanation of their coding is found in the Appendix (Table 6).

Focusing on the chert members of the assemblage in terms of sources, they are divided mainly into three main groups. The first group of artefacts (Fig.5.19) is mainly characterized by brown colours (10YR 4/2, 6/2 and 5YR 3/2), fine grain size and the absence of translucency (i.e. opaque) and shine (i.e. dull). Some differences have been recorded, but they are not at such a level to suggest different rock sources. The only exceptions are the small, brown and translucent artefacts (e.g. BR89/S395/L449), which always exhibit part of the cortex. The majority of the members of the assemblage are included in this group and are generally of greater size in comparison with artefacts of other chert materials.

Another important group included opaque, dull, spotted and grey coloured (e.g. 5Y 6/1) artefacts (Fig.5.20a). The artefacts of this group are described as spotted (Crandell, 2006) because they presented irregular shapes of white spots on their surface. The characteristics of this group are

compatible with the ones found in the Maltese chert formations. Additionally, the size of the artefacts of this group is substantial, but not on the same level as the ones in the first group.

The last group consists of artefacts exhibits a high level of translucency and similarities in lustre, texture and grain size. However, the diversity in colours (e.g. yellow, red and brown) and the fluctuation in the levels of translucency suggest that they are from different raw sources (Fig.5.20b). The artefacts of this group are actually fragments of bigger artefacts, which possibly explains their very small size.

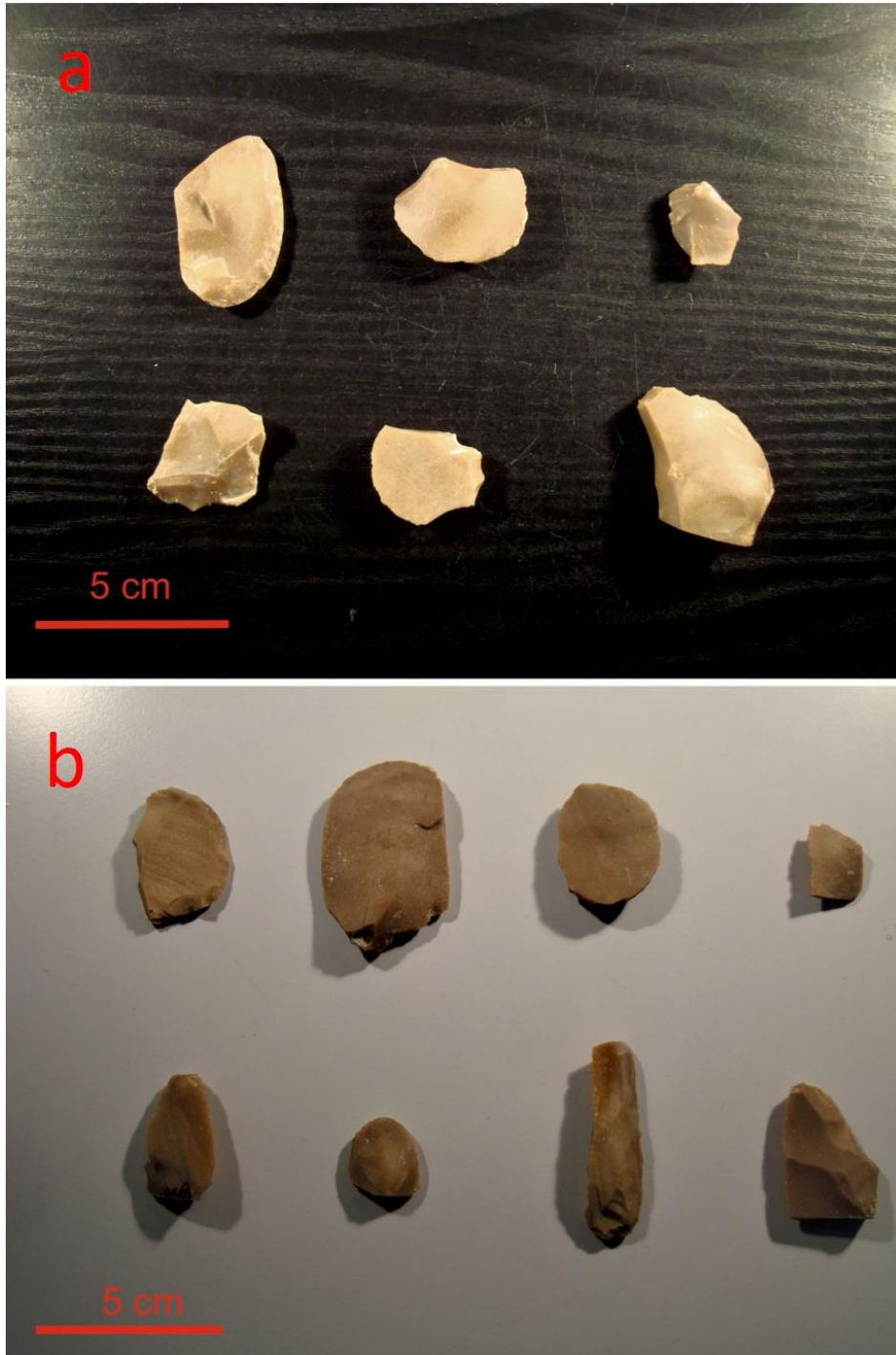


Figure 5-19: Artefacts which have been allocated to the first group of chert source. They include finds with different forms and tool types.

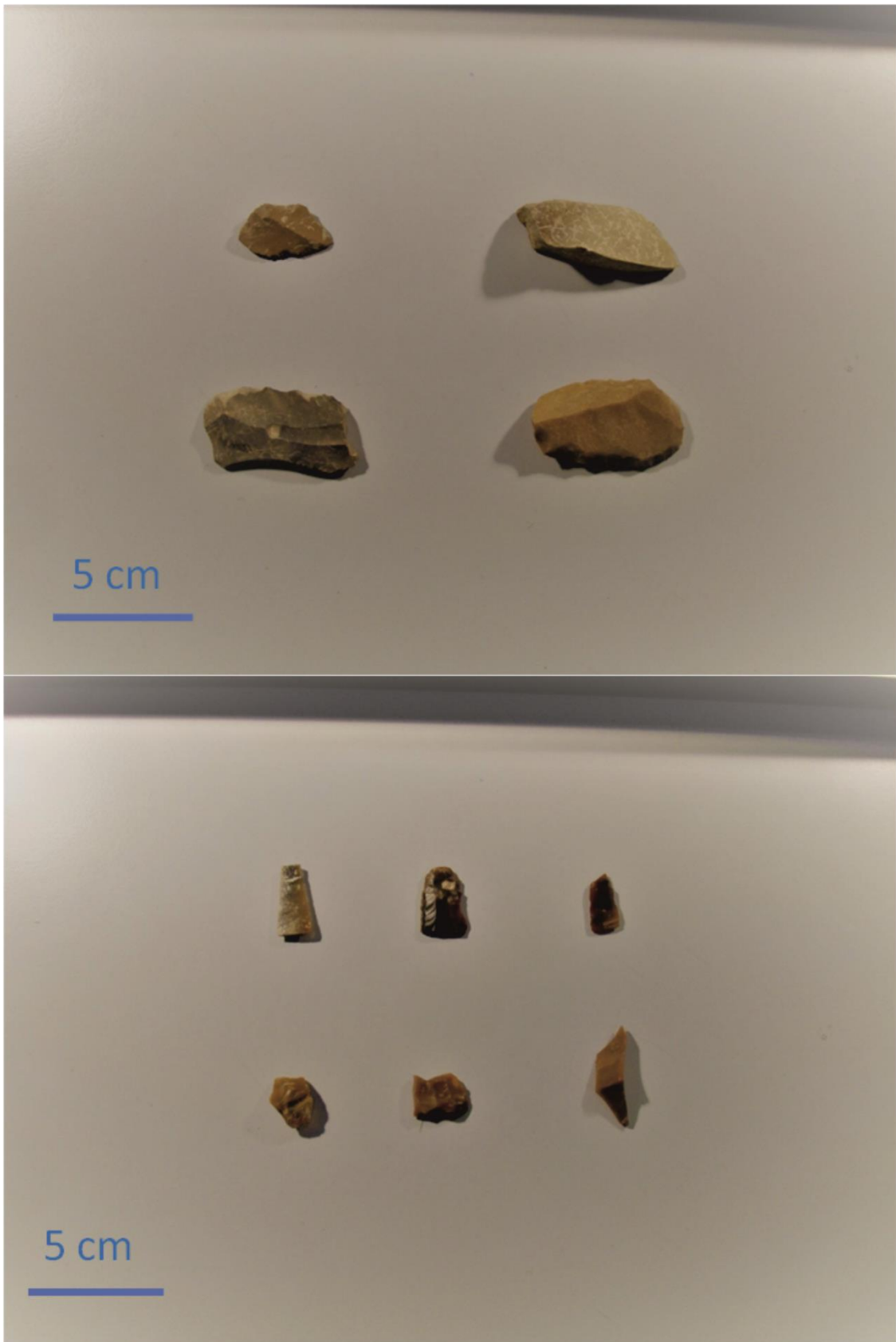


Figure 5-20: a) Artefacts included in the second group and related to local sources, b) Artefacts included in the third group and not related with local chert sources.

➤ *Types of tools*

The artefacts reported in the assemblage from the Circle are flakes, chips and indeterminate pieces, while cores and debitage are not reported (Table 7; Malone, 2009). The indeterminate pieces category includes those that present insufficiently identified features and therefore are unable to be categorized accurately. The majority of the artefacts are flakes, with further categories of flake scrapers or blades (Fig.5.21). The flake scrapers are partly modified on one of their sides (*unimarginal*³) and most of the blades are parts or fragments of a greater artefact (e.g. BR91/S611/L712, S110/L274). There are only some samples (Fig.5.22), which can be considered as scrapers, based on the extent of the modification (e.g. BR91/S745/L845).

➤ *Manufacturing techniques*

The examination of these artefacts has shown that percussion is the main technique used, especially to extract detached pieces from the original objective piece⁴. In addition, some samples have presented indications of flakes being extracted from their dorsal surface. Such flakes are considered evidence of the percussion technique and are called *Eraillure flakes*⁵. The sample BR93/S843/L4 constitutes an example of such a type of flake. There are artefacts presenting an *arris*⁶ feature which is created from modification or further flake extraction (Fig. 5.21). The pressure technique is used in the final or secondary flanking and especially for retouching the edges of the artefacts. All scrapers have some secondary modification on the edges, but no similar features are found on flakes and blades (e.g. BR88/S110/L274). The BR89/S291/L334 is a typical example of a microblade with secondary edge modification. The modification, where present, is only reported on the one side of the artefacts and classifies them as unimarginal flakes (Fig.5.21). There is one sample (Fig.5.22) which shows all the typical characteristics related with the *Levallois technique*⁷ (e.g. BR91/S745/L845). Furthermore, there are a few more samples that have similar characteristics to these artefacts, however safe conclusions cannot be drawn because of their small size.

³ A detached piece, mainly flakes, that have been modified only on one surface.

⁴ Objective pieces are stone items that have been hit, cracked, flaked or modified in some way (Andrefsky, 2005).

⁵ A small chip or flake on the bulb and it is produced during the original impact of the flake removal, caused from the striking force which results in the removal of a chip from bulb.

⁶ The intersection of flake scars produces a ridge, which is called an *arris*.

⁷ It is a distinctive type of stone knapping developed by precursors during the Palaeolithic period and creates lithic flakes from a prepared core. The striking platform is formed and then the core's edges are trimmed by flaking off pieces around the outline. A strike is performed on the striking platform and a lithic flake is separated with a distinctive profile and sharp edges by the earlier trimming works. Most of the time the extracted flake would be a scraper or a knife (Andrefsky, 2005).

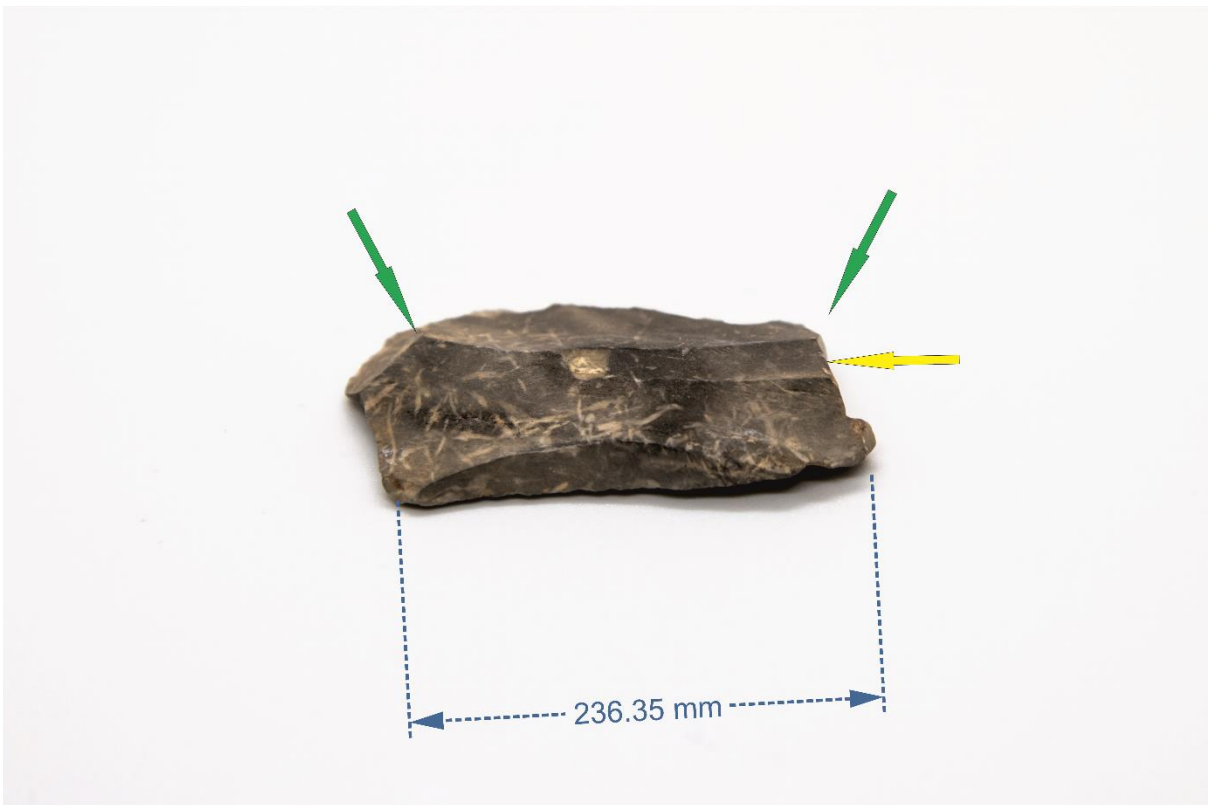


Figure 5-21: Example of a blade made from the Circle. The modifications are found only on the one side (purple arrow) and it is characterized as a unimarginal tool. Flakes have been extracted from this side (yellow arrow) which have resulted in an arris (green arrow) on its surface.

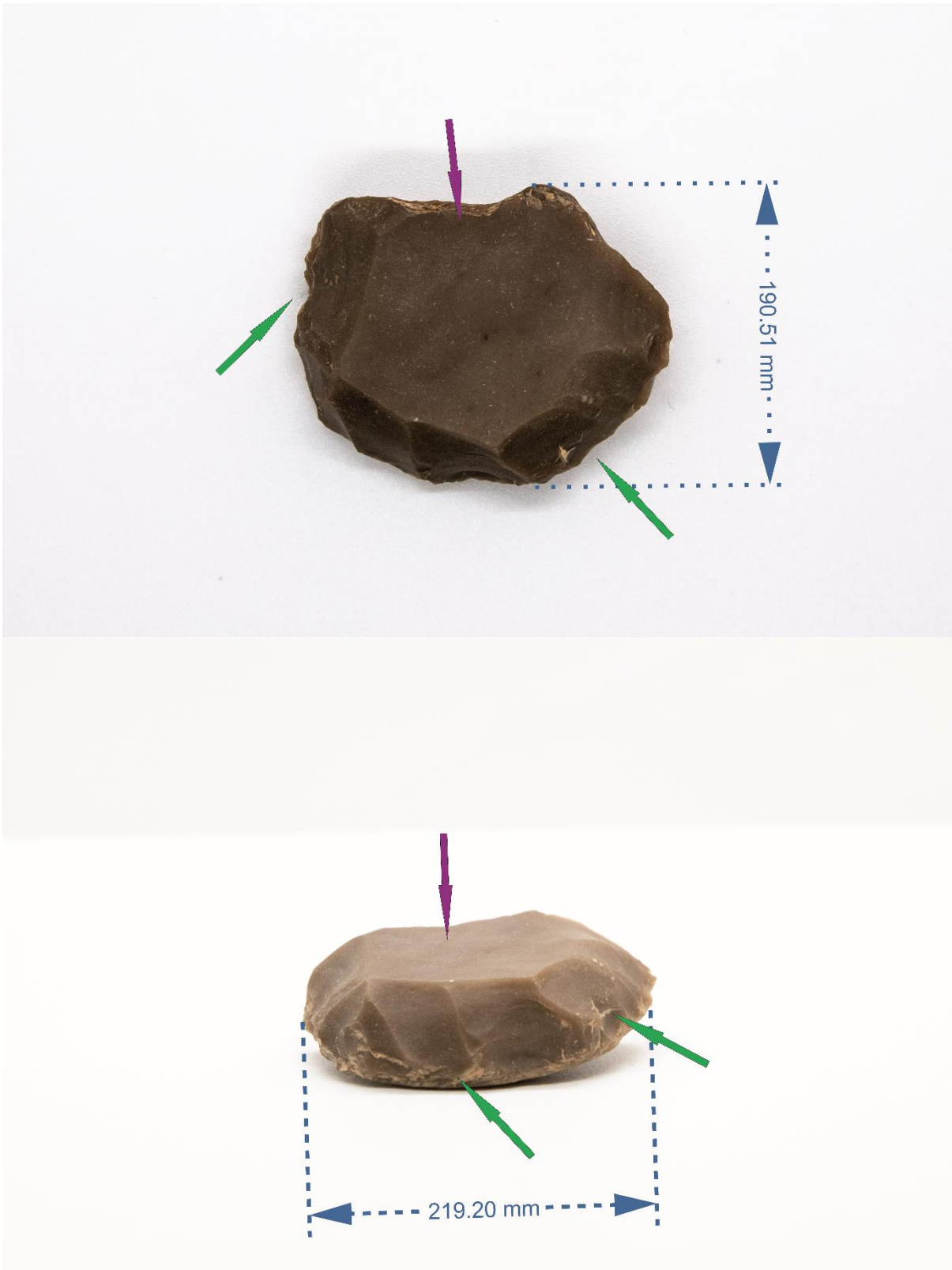


Figure 5-22: A scraper from in Xaghra Circle. It has a flat surface from which a flake has been extracted (purple arrow) and the edges have been trimmed (green arrows). It is most likely to be created with the Levallois technique (Andrefsky, 2005).

5.1.2.2. Kordin assemblage

The assemblage of Kordin Temple was collected during the excavations of the site in 2015 and consists of 215 pieces in total, of which 152 are chert, 23 obsidian and 40 “other”. It is a properly organised collection, with sample codes reported on the sample bags and only one or two pieces in each of them. The chert members of the assemblage are divided mainly into three main groups in terms of sources. The finds related with this excavation have initials KRD (Kordin) and further explanation of their coding is found in the Appendix I (Table 6).

The first big group of chert artefacts (Fig.5.23b) is mainly identified by brown colour shades (10YR 4/2 and 10YR 6/2) and substantial size (L and W > 3cm). Small differences in some macroscopic features (e.g. lustre, translucency, texture) are reported but, not to an extent that would support a different source. Furthermore, the macroscopic features of this group are similar to the first group of the Circle assemblage. In comparison with the Circle assemblage, this assemblage does not have artefacts with highly translucency (e.g. BR89/S395/L449) nor are they dull, opaque and rough (e.g. BR91/S767/L783). Lastly, there are some spotted artefacts (e.g. S69/L211), a characteristic recorded on the local chert, but the rest of their features are different from those reported for these outcrops.

Another important group includes yellowish (e.g. 10YR 6/6), heterogeneous, opaque, dull and spotted artefacts (Fig.5.23a). These features are identical with the ones found on some of the chert formations of the Maltese Islands. In comparison with the similar artefacts of the Circle, they are fewer in number and possibly related to different chert outcrops.

This assemblage has a number of artefacts made from completely different types of chert, which cannot be easily categorized (Fig.5.24). This can be explained by their macroscopic features which are diverse and support different chert sources. However, there are few artefacts (e.g. S1/L71, S62/L109) that present very similar macroscopic characteristics with each other and suggest a common origin. Furthermore, the macroscopic examination suggests that one artefact (i.e. S306/L306) might be related with one of the of the Circle assemblage (i.e. BR89/S291/L334). Additional, similarities are recorded between the artefact S27/L207 and the BR91/S701/L748 of the Circle assemblage. Lastly, there is an artefact (i.e. S42/L304) with very similar features to the unique chert outcrop which this research has found on Gozo (G2S6).



Figure 5-23: a) Artefacts included in the second group and related to local sources, b) Artefacts which have been allocated in the first group of chert source. They include finds with different forms and tool types.



Figure 5-24: The diversity of macroscopic characteristics reported on the artefacts from the third group in the Kordin assemblage.

➤ *Types of tools*

The majority of the artefacts in the Kordin assemblage (n=10; 71%) are flakes, and, depending on their features, can be proximal flakes or shatters (Table 7). Conchoidal flakes are found but they are less numerous than the ones reported in Circle assemblage. Scrapers and flake scrapers are recorded and many of them can be further categorized as *decortication flakes*⁸ (Fig. 5.25), mainly because they retain a portion of their cortex (e.g. S27/L203, S133/L211, S34/L207). These types of tool/artefact are abundant in this assemblage and all of them are characterized by modification to only one of the surfaces (unimaginal).

There are artefacts which can be categorized as blades, but because of their small size and the lack of sufficient indications they are recorded as shatters (e.g. S42/L304 and S141/L150). There is one sample (S98/L201) in the assemblage that has demonstrated typical characteristics of a burin⁹ (Fig. 5.26) e.g. feather edge at the distal end), which is a type of tool not reported in Circle assemblage.

⁸ Flakes that are struck from the outer surface of a core retain portions of the cortex.

⁹ A specialised tool mainly adapted for the working of antler and bone. Its characteristic feature is a short transverse cutting edge formed by striking the narrow edge of a flake or burin form to detach a spall.

➤ *Manufacturing techniques*

The examination of the assemblage shows that percussion is the main applied technique, especially to extract detached pieces from the original raw material (Fig. 5.25a, d). Further percussion is employed on the artefacts for modification or to extract more flakes. The samples from which flakes are extracted presented an *arris* on their surface, which is a very common feature on the artefacts of the Kordin assemblage. This characteristic is also reported on samples from the Circle assemblage but to a lesser extent. The pressure technique is used during the final or secondary flanking process, aiming to retouch the edges of the artefacts (Fig. 5.25b, c, e, f). This style of modification appears either on the dorsal or the ventral surface, but never on both or subsequently.

Unfortunately, many artefacts are small in size and it is difficult to identify the manufacturing techniques with great certainty (i.e. flake shatters). Nonetheless, the investigation has been able to identify some differences between the Circle and Kordin assemblages. Firstly, no artefact from the Kordin assemblage demonstrates any evidence of manufacture via the Levallois technique. Secondly, one sample (i.e. S1/L71) of this assemblage has indications of being extracted from the original core by a blow at an angle. It is possible that this artefact is produced during the core *rejuvenation process*¹⁰, evidence of which has not been found on any sample from the Circle assemblage.

¹⁰ A process during which flakes are removed from partially used cores to freshen up the striking platform edge and core rejuvenation flakes.

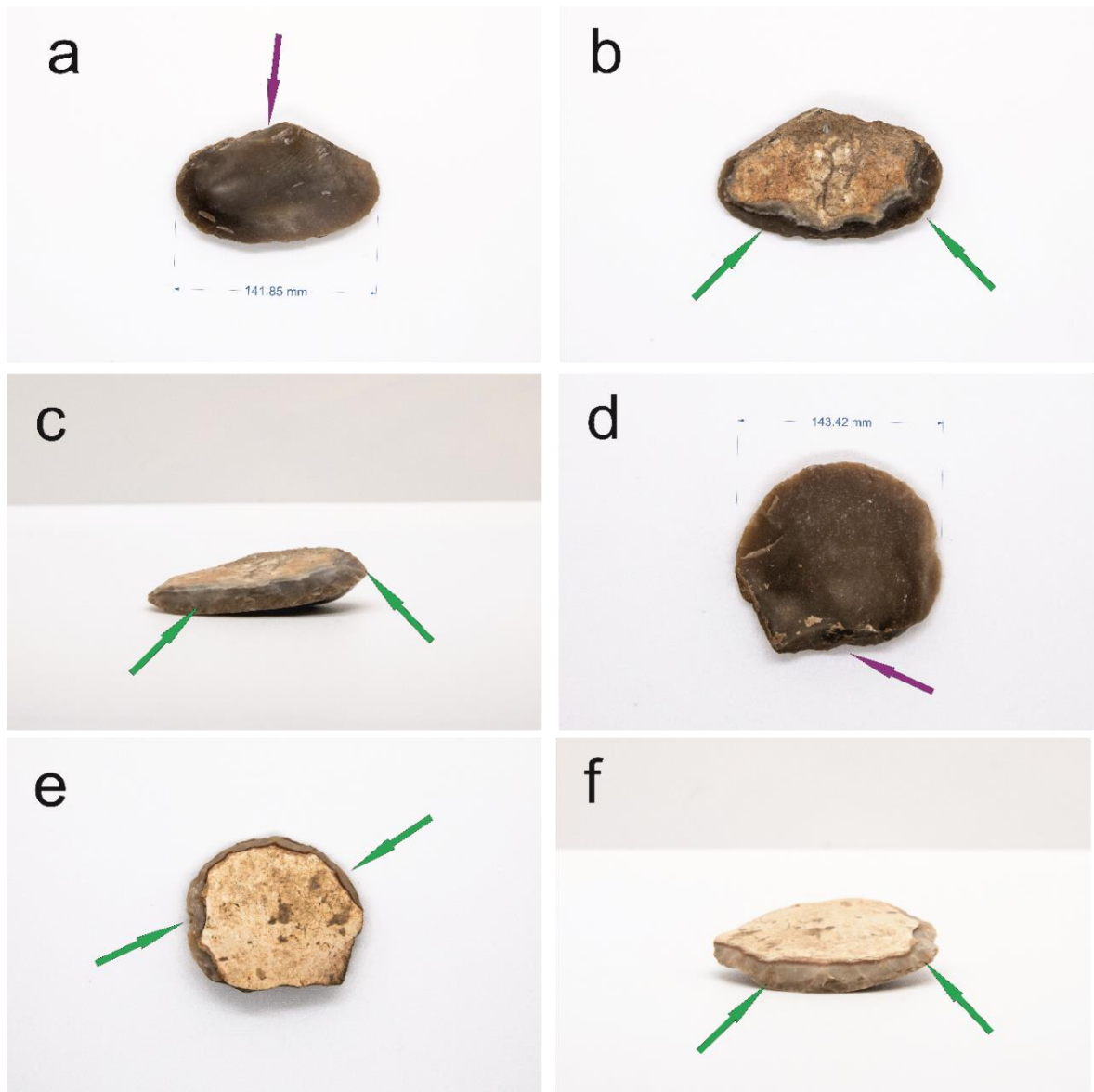


Figure 5-25: Scrapers of the Kordin assemblage; a and d show the sticking platform (purple arrows) and the size of these two samples. b and e show part of the cortex and suggest that they are decortication flakes and b, c, e and f show the retouched edges of these samples (green arrows).

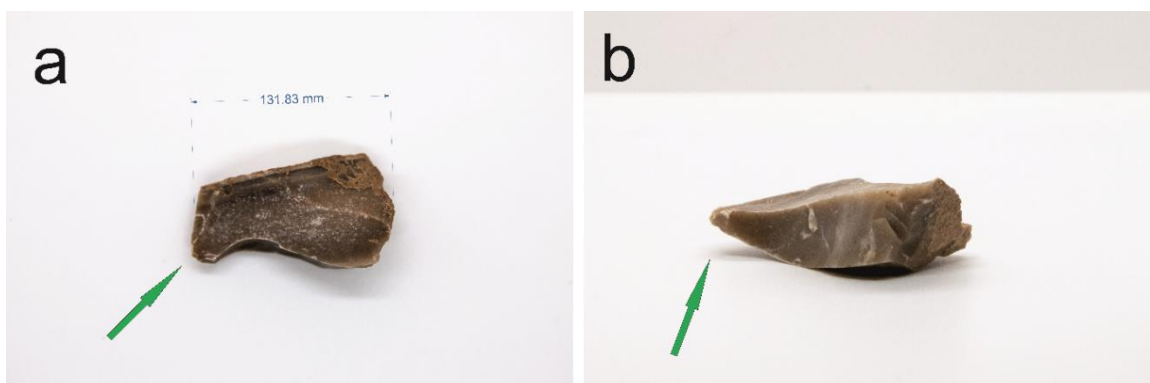


Figure 5-26: An artefact, which possibly is a burin with the characteristic feather edge (green arrows).

5.1.2.3. Tač-Ċawla assemblage

The Tač-Ċawla assemblage was collected during the excavation of 2014 and consists of 693 pieces in total of which 457 are chert, 111 obsidian and 125 “other” material. The examination suggests that the “other” material is mainly related to local limestone (possibly Coralline) and secondary calcite. The finds related with this excavation have initials TCC (Tač-Ċawla) and further explanation of their coding is found in the Appendix (Table 6).

Focusing on the chert members of the assemblage, they are also divided into three main groups in terms of sources. The first group is mainly identified by brown colour shades (10YR 4/2, 6/2 and 2/2). The artefacts of this group are further divided by the size of their grain (i.e. fine and medium) because the difference is so distinctive that it supports an origin from more than one source (see below). This type of material is used for a variety of artefacts and it is found in different shapes and sizes (Fig. 5.27a). Most of the artefacts in this group have part of the cortex and most likely the outcrop of the chert rock is intercalated with another rock formation. There are only a few dark brown artefacts (e.g. S176/S100) in comparison with the assemblages of the Circle (e.g. BR94/S1142/L1279) and Kordin (e.g. S68/L210). Nonetheless, the macroscopic examination suggests a possible common origin of an artefact from the Circle (i.e. BR94/S1142/L1279) and a member of this group (i.e. S176/S100). However, the assemblage of Tač-Ċawla has not presented any dark and translucent artefacts like the ones found in the Circle assemblage (e.g. BR89/S395/L449). Moreover, there are not any light brown artefacts similar to the ones reported in the Kordin assemblage (e.g. KRD15/S69/L211).

The second group includes artefacts with macroscopic features similar to the local chert sources (Fig. 5.27b). They are mainly identified from the characteristic brownish colour shades (Fig. 5.27b1,3,4 and 5) and the white spots on their surface (Fig. 5.27b1,2). In comparison with the other two assemblages, they are fewer in number and present less variety. The macroscopic characteristics of these artefacts are similar to those of a small outcrop in Gozo (Fig. 5.27b.2) or to the pale brown outcrop found on both Malta and Gozo (Fig. 5.27b5).

The final group includes all the multi-coloured and highly translucent artefacts that relate neither to the local resources nor to artefacts of the first group (Fig. 5.28). The only exception is one artefact (Fig. 5.28.2; TCC14/S193/L69) which has similarities with the distinct outcrop on Gozo (i.e. G2S6). Although the members of this group present a variety of colours, they are all highly translucent, shiny and fine-grained. It is the fluctuation in these characteristics which does not allow any safe conclusion on their sources at this stage. Nevertheless, it is possible to record the similarities between them, the artefacts of the other assemblages and the chert formations of Sicily. Indeed, the macroscopic characteristics of the artefact S193/L69 are very similar to a comparative example from the Kordin assemblages (i.e. KRD15/S42/L304). There are some artefacts (e.g. TCC14/S103/L85, S252/L179, S275/L208) which have a yellowish colour, but the rest of their features put in doubt the prospect of a

common origin. However, these yellowish artefacts have many similarities with artefacts found in the Circle (e.g. BR89/S291/L334) and Kordin assemblages (e.g. KRD15/S144/L306). In terms of rock sources, there is an artefact (Fig. 5.28.3; TCC14/S460/L273) which looks similar to a chert outcrop found in West Sicily (S22). Finally, an artefact (Fig. 5.28.1; TCC14/S416/L178) has very similar macroscopic characteristics with outcrops in SE Sicily (S18 and S19) and an artefact (i.e. BR91/S611/L712) of the Circle assemblage.

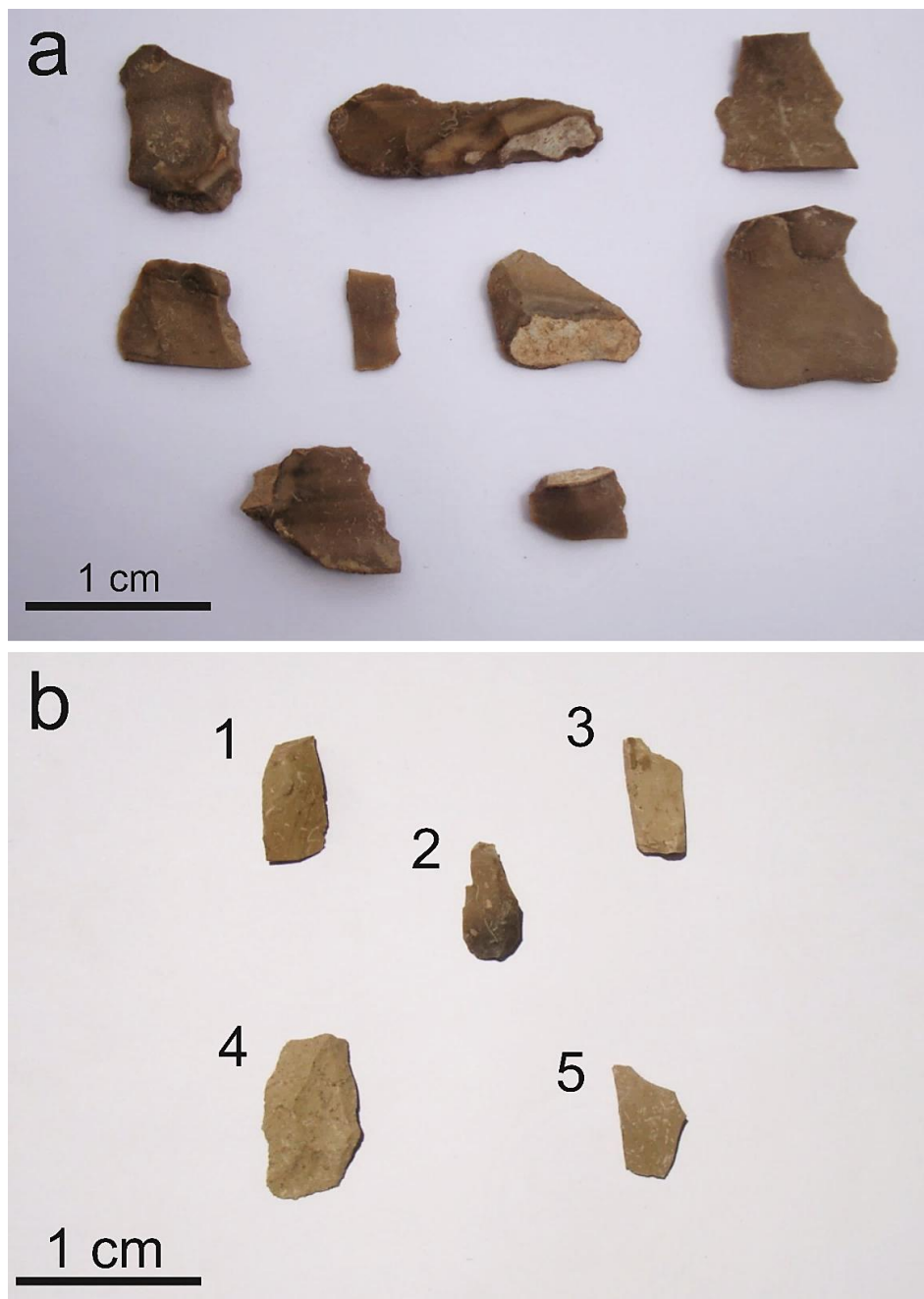


Figure 5-27: Artefacts related with the first (a) and second group (b) of raw materials.

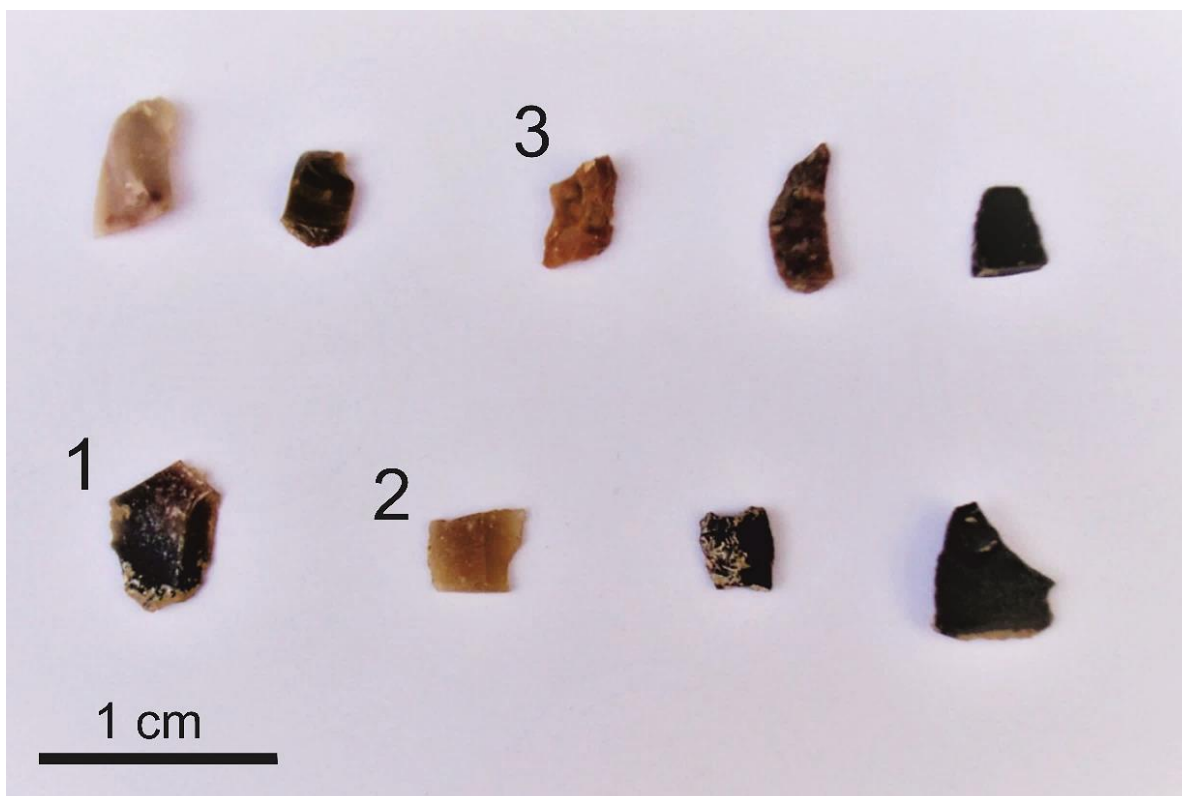


Figure 5-28: Foreign chert artefacts.

➤ *Types of tools*

Regarding the type of tools found in this Tač-Čawla assemblage, they are mainly debitage and flake tools. Some of them (n=5; 28%) can be further characterized as angular shatter because they do not present any additional features of flaking. The flake tools are the main type reported in this assemblage and, depending on the manufacturing process, are subdivided into different types. They are mostly unimarginally modified (e.g. S577/L131, S416/L178), but few have been modified on both their surfaces (e.g. S502/L301). These are characterized as *biface tools*¹¹ (e.g. TCC14/S275/L208, S37/L30), and because they lack any further characteristics, they are also considered unhafted¹² (Fig. 5.29). Furthermore, the examination found scrapers (e.g. TCC14/S252/L179) but they are fewer in number than the other assemblages and especially in comparison with the Circle. Restricted also is the number of blades reported in the Tač-Čawla assemblage (e.g. TCC14/S595/L81, S103/L85), although the shatter and debris (e.g. TCC14/S460/L273) pieces may have come from broken blades.

¹¹ An objective piece extensively modified by flakes removal across the facial surfaces. The two sides of these pieces are called faces and present evidence of flake removal. Some were primarily used as cores or sources for flakes. They may have been used as chopping or cutting tools. Others may be used for hafting or attachment to a handle to serve as a projecting point for arrows or spears (Andrefsky, 2005).

¹² Biface tools that are missing the haft element (Andrefsky, 2005). This includes preforms, point tips and bifacial knives. The haft element, when reported, is at the lower part of the artefact and considered to be articulated with a shaft or handle (attached to another element).

➤ *Manufacturing techniques*

The examination shows that the primary technique recorded on the artefacts of the Tač-Ćawla assemblage is percussion flaking. The bigger pieces of the collection do not have any modifications, but some have indications of flakes being extracted from their surfaces. The medium and small artefacts present additional manufacturing techniques, which relate to the type of material. Most of the artefacts, especially the smaller ones, have their edges retouched, but to a lesser extent than the retouch reported for the Circle and Kordin artefacts.

The artefacts which are similar to the local chert have indications of secondary percussion flaking, mainly for extracting more flakes. This technique is found either on one or both sides of these artefacts and subsequently categorises them as unimarginal or *bimarginal*¹³. Further investigation has reported that the bimarginal artefacts present evidence of more than one stick points. The artefacts of the first group present additional secondary percussion, but this is for retouching of the artefacts and not for extracting more flakes. Some of these artefacts present an *arris* feature which has resulted from the secondary flaking (Fig. 5.29b). The edges of these artefacts have been further retouched with pressure flaking. Moreover, it is the first assemblage in which an artefact (TCC14/S502/L301) has demonstrated the serration¹⁴ feature (Fig. 5.30).

The artefacts included in the last group are mainly of small size and the manufacturing techniques are difficult to be identified, especially the primary flaking. Regardless of this, the examination has managed to record important information and the techniques employed on them. There are some artefacts which present the sticking point of the primary flaking in a different position from the secondary flaking. In addition, the secondary flaking has been mainly conducted by employing pressure (e.g. TCC14/S275/L208, S144) rather than percussion (e.g. TCC14/S577/L131, S416/L178). Pressure flaking is mainly used to retouch and re-sharpen the artefacts, which subsequently causes their reduction (e.g. TCC14/S275/L208). The only uncertainty lies in one artefact (i.e. TCC14/S144) which has indications of a successive flake removal from its surface. This is a rare characteristic which suggests consistency and accuracy into the manufacturing process. The artefact coded as S577/L131 also presents similar features, but the flakes are extracted with percussion and not with pressure. The flake extraction has created an *arris* on almost all the artefacts, but it is unclear which is the exact extraction method or the strike angle. Finally, the artefact coded as S103/L85 has been additionally reworked and the flat surface close to the pointed tip is *polished*¹⁵ (Fig. 5.29a).

¹³ A flake modified on both surfaces at the same location (e.g. top or bottom).

¹⁴ Consecutive small teeth or barbs on the edge of a blade formed by removing pressure flakes. Biface serrations have flakes removed from both sides of the blade edge while uniface serrations have flakes removed from only one face of an edge.

¹⁵ Polish could be created by interactions among processed substances and the rock, and by chemical interactions between water and silica contained in the processed cereals and in the sandstone grinding surfaces.

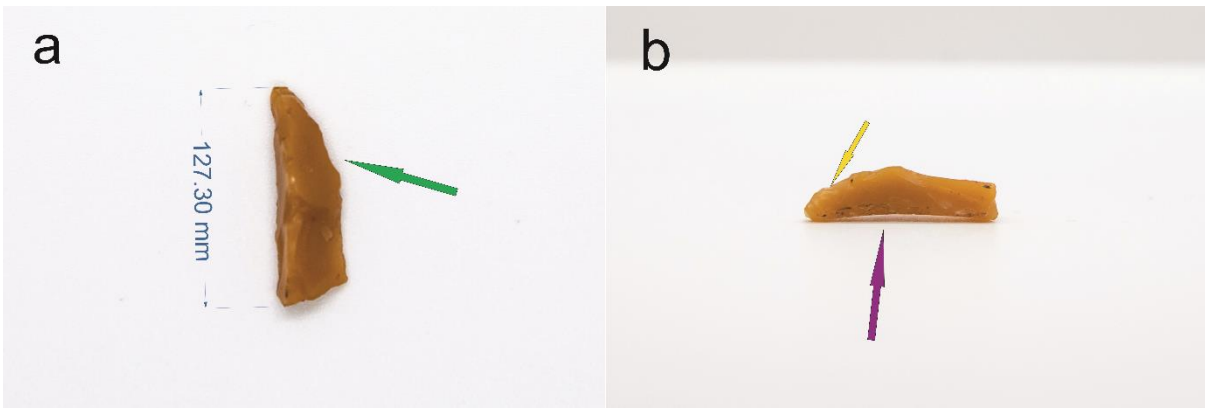


Figure 5-29: Unhafted biface tool. The a shows the polish surface (green arrow) and b shows evidence of retouch (yellow arrow) and arris (purple arrow).



Figure 5-30: Bimarginal flake that exhibits serration at its edge.

5.1.2.4. Santa Verna assemblage

The Santa Verna assemblage was collected during the excavation of 2015 and consisted of 723 pieces in total of which 284 are chert, 67 obsidian and 372 “other” material. The finds related with this excavation have initials SV (Santa Verna) and further explanation of their coding is found in the Appendix (Table 6).

Focusing on the chert members of the assemblage, they are divided into three main groups in terms of sources. The first group of chert artefacts is similar to the first one in all the previous assemblages. The artefacts are further subdivided based on the different shades of the brown colour (10YR 4/2, 6/2; 5YR 3/2 and 2/1), the level of translucency, lustre and grain size (e.g. medium, fine). The examination has recorded that more artefacts are made from the dull and medium-grain cherts (Fig. 5.31a) than the translucent and fine-grained. Furthermore, the artefacts of this material are far less than in the other assemblages and they actually do not exceed the 15% of the total assemblage. Additionally, no artefact is similar to the dark and translucent artefacts (e.g. SV15/S395/L449) or the artefacts of the Circle assemblage (i.e. BR91/S745/L845). In contrast, the characteristics of two artefacts (i.e. SV15/S67/L34 and S1/L22) suggest a common origin and they are possibly related to one artefact (i.e. TCC14/S502/L301) of the Tač-Ĉawla assemblage. In addition, the artefact coded as S1/L98 has similar characteristics with one artefact from the Tač-Ĉawla (i.e. TCC14/S32A/L30) and Kordin (i.e. KRD15/S34/L207) assemblages. One artefact from Tač-Ĉawla (i.e. TCC14/S32B/L30) has similar characteristics with the artefacts of this assemblage (i.e. SV15/S1/L16 and S1/L33). The latter artefact also has some similarities with an artefact coded from the Kordin assemblage (i.e. KRD15/S98/L201).

The second group, and possibly the biggest group of the assemblage, includes artefacts with macroscopic features identical to the local chert outcrops. The artefacts vary from brownish to greyish colour shades similar to those of the local material. They present a high uniformity of other macroscopic characteristics and are all dull, opaque and spotted (Fig. 5.31b). Moreover, this is the first assemblage that has debitage and pieces of the cortex related with this chert material group.

The last group includes artefacts of possibly non-local material and with a similar type of lustre and grain-size (Fig. 5.32). Their macroscopic characteristics do not show any relation with the Sicilian chert formations, except for one sample (i.e. SV15/S1/L68) which has some common characteristics with the radiolarian formation from the province of Enna. The examination of this group has recorded some artefacts (e.g. SV15/S1/L36 and S1/L41) that resemble the unique chert outcrop in Gozo (i.e. G2S6), but their small size does not allow safe conclusions. Similar pieces are found at Kordin (e.g. KRD15/S42/L304) and Tač-Ĉawla (e.g. TCC14/S193/L69), but not in the Circle. Moreover, a reddish flake is characterized by an unfamiliar colour-change, which is a feature only found on one artefact from the Kordin assemblages (e.g. SV15/S156/L306). Furthermore, this group includes a small subgroup of shiny, yellowish, chert artefacts which are also found in all the other assemblages. A

typical example is one artefact (i.e. SV15/S38/L8) which is similar to artefacts from Tač-Čawla (e.g. TCC14/S103/L85). In addition, some other artefacts (e.g. SV15/S3/L41) present similarities with artefacts from Kordin (e.g. KRD15/S144/L306) and Tač-Čawla (e.g. TCC14/S275/L208) assemblages. However, these characteristics are not enough to conclude whether they are made from the same chert formation. However, it is not possible at this stage to connect artefacts from the Circle with this subgroup, because they are either less translucent or exhibit lighter colours.

The examination has further recorded the absence of dark (e.g. dark red, grey or black) or greenish colours in comparison with other assemblages. There are some dark grey to black artefacts, but they do not present similar features either with the chert formations of Sicily or with artefacts from the other assemblages. Finally, there is an artefact (i.e. SV15/S1/L17) characterized by a greenish colour, pearly shine and fine-grain, which is not reported from any other assemblage.

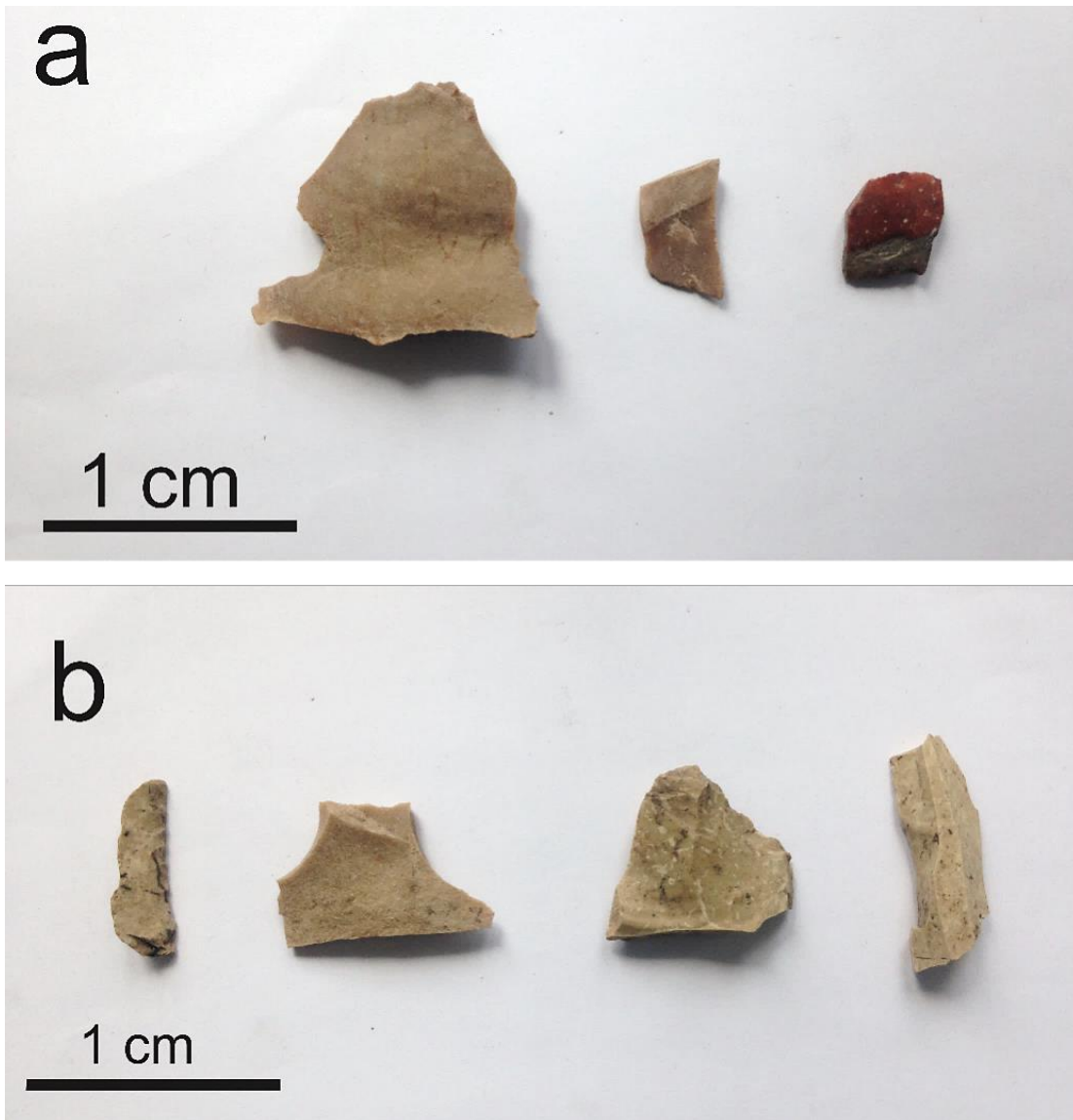


Figure 5-31: Artefacts related to the first (a) and second group (b) of raw materials.



Figure 5-32: 'Foreign' chert artefacts.

➤ *Types of tools*

As far as the type of tools found in this Santa Verna assemblage, they are mainly debitage and flake tools. The majority of the debitage (n=2; 66%) is of significant size (> 15cm) (Fig. 5.33), but small shatters are also reported (<2cm). This category is related to the local chert formations which occasionally exhibits part of the cortex of that chert (i.e. Globigerina Limestone). The flake tools are more difficult to categorize but bending¹⁶ (SV15/S1/L34) and conchoidal¹⁷ (e.g. SV15/S134/L58) types have been recorded in this collection. Unfortunately, the secondary flaking employed has altered most of the characteristics necessary to distinguish the type of flakes present. Generally, most of the flakes are unimarginally modified (Fig. 5.34 and 35), but some bimarginal tools are also reported (e.g. SV15/S3/L41). They are mostly blades (e.g. SV15/S1/L4) or blade fragments (e.g. SV15/S1/L36, S2/L22), while there are only a few scrapers (e.g. SV15/S32/L5) recorded in this assemblage. In addition, there are unimarginal flake tools which show indications of hafted element features (e.g. SV15/S1/L68 and S1/L34). The increased amount of blade tools and hafted elements are two characteristics that differentiate the Santa Verna material from the other assemblages.

¹⁶ Bending flakes are those formed by cracks that originate away from the point of applied force. Stresses are imposed upon the objective piece that attempt to "bend" brittle material. Some are produced as a result of applying force on the acute edge of an objective piece. The resulting bending flake will have a striking platform that is composed of a part of the original bifacial edge. Bending flakes are believed to originate as a result of soft hammers or pressure flakers (Andrefsky 2005).

¹⁷ Conchoidal flakes are initiated or started by the formation of a Hertzian cone at the point of applied force. It is a type of flake with a distinctive bulb of force and concentric undulations on the fracture surface which gives the inside surface of some flakes the appearance of a unionid shell. These flakes require a great deal of pressure to initiate and they are more easily produced with a hard hammer (Cotterell & Kamminga, 1987).

➤ *Manufacturing techniques*

The examination demonstrates that the primary technique used on the artefacts of the Santa Verna assemblage is percussion flaking. The main purpose of that technique is to extract detached pieces in the form of flakes from the original objective piece. The bigger pieces of the assemblage do not present any modifications, but some have indications of flake extraction on their surfaces. The medium and small artefacts also exhibit manufacturing techniques, which occasionally prevent them from distinguishing the primary flaking. An additional technique is secondary pressure flaking (Fig. 5.34), which aims to sharpen the artefacts or enhance their utility. Indeed, this particular technique is used on artefacts related to non-local chert rocks (Fig. 5.34) for a constant reshaping (e.g. S3/L41, S1/L80). This is better understood on the artefacts of the third chert group (e.g. SV15/S3/L41), which have been constantly modified with pressure flaking. Pressure flaking is also used at the final stage of manufacturing, mainly for retouching the edges (Fig. 5.34 and 5.35b). This technique on many occasions has created serration (Fig. 5.34a and 5.35a), especially on blades and unimarginal flake tools (e.g. S1/L80, S134/L58). A bimarginal serration is reported on a micro-blade (i.e. SV15/S1/L52), which however is not made from chert. There are indications of secondary percussion flaking, but there are not enough characteristics to support this technique being used. Evidence of polishing is recorded on two artefacts from Santa Verna (e.g. SV15/S144/L42, S1/L52). They are made from completely different raw materials, so there is no connection between the technique and a specific type of chert source.



Figure 5-33: Debitage from the Santa Verna assemblages.

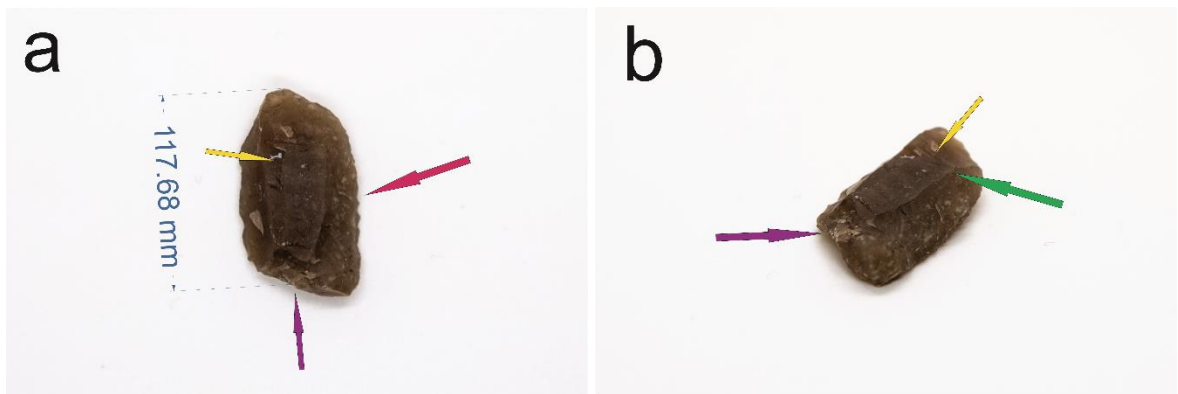


Figure 5-34: Unimarginal flake of non-local chert with the striking platform (purple arrow), secondary flaking (yellow arrows), arris (green arrow) and evidence of serration (red arrow).

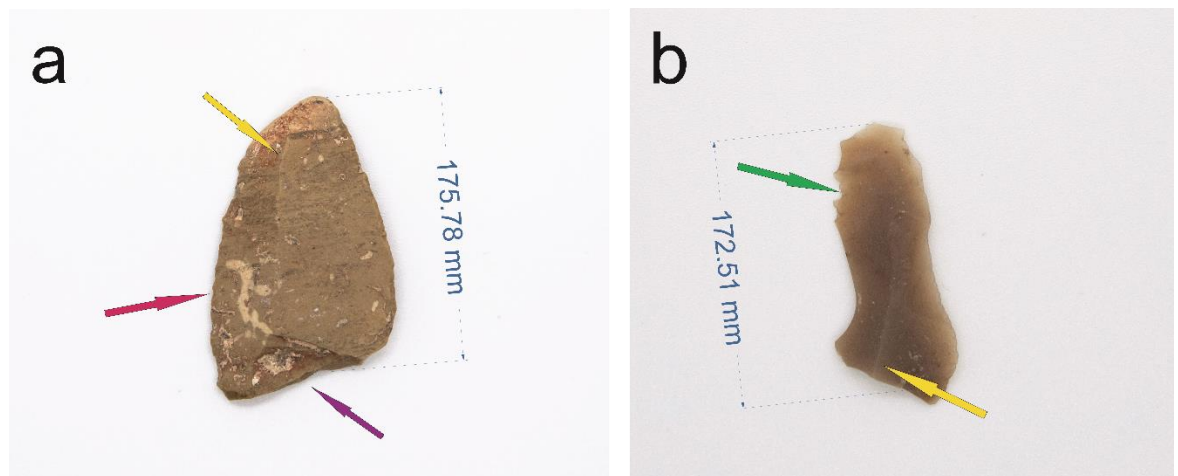


Figure 5-35: Unimarginal flake tools. A) Tool with a striking platform (purple arrow), arris feature (yellow arrow) and serration (red arrow). B) Tool with arris (yellow arrow) and retouched edges (green arrow).

5.1.2.5. Ġgantija assemblage

The Ġgantija assemblage was collected during the excavation of 2015 and consists of 170 pieces in total of which 85 are chert, 10 obsidian and 75 "other" material. The lithic material is in sample bags which recorded the archaeological context (soil layer) and a brief description of the material included. This description is not always accurate, because the bags contained many pieces which are usually of different lithic types. Nevertheless, the raw materials reported in this assemblage are restricted in terms of sources, in comparison with the previous assemblages. The finds related with this excavation have initials GG or GGWC (Ġgantija) and further explanation of their coding is found in the Appendix (Table 6).

The main group of chert artefacts is the one including all those with the brownish colour (10YR 7/4; 6/2; 4/2) of chert artefacts. The other common characteristics are homogeneity, the level of translucency and texture (Fig. 5.36). Occasionally, the individual characteristics varied but this is within the acceptable range of the natural exposure of a rock formation. The finds from context 1019 are very important because they provide strong evidence to support the common origin of the members of this group (Fig. 5.37). Moreover, the investigation revealed that they are made from the same piece of chert (e.g. nodule) and not just from similar raw materials. Throughout this context, the full range of the macroscopic characteristics of this chert source has been identified and enabled the research to establish a connection between the members of this group (e.g. S1/L1040, L1016, L1021(SF10), S1/L1040). This further allowed the comparison and the connection, in terms of raw material, with the similar groups found in the other assemblages (e.g. SV15/S1/L16, S1/L98, S1/L22; TCC14/S502/L301, S32A/L30; BR91/S767/L783; KRD15/S133/L211, S27/L203). An excellent example of such a connection between assemblages is the comparison of an artefact from this assemblage (i.e. GG15/S6/L1019) and an artefact from Santa Verna (i.e. SV15/S1/L16). However, this has also made clear that other chert outcrops are used with slightly different characteristics. There are artefacts of the Ġgantija assemblage (e.g. GG15/S2/L1015, L1030(SF6)) that are more translucent and shinier (pearly), similar to artefacts from other assemblages (SV15/S1/L33; TCC14/S32B/L30; KRD15/S98/L201). These differences suggest a different outcrop rather than a different chert source. Similar to the previous collection there has not been a member of this assemblage that is macroscopically similar to the distinctive artefacts of the Circle assemblage (i.e. BR89/L395/L449 and BR91/S745/L845).

The next group includes chert artefacts and debitage that present many similarities with the local chert sources (Fig. 5.36). They are brownish to greyish in colour, dull, with semi-smooth texture and spotted, all of which are typical characteristics of the local chert formations. The Ġgantija assemblage presents very limited artefacts related with these outcrops and the fewest among all the assemblages. Few are also debitage tools which present the characteristic cortex of a local chert source.

Equally restricted is the third group of artefacts which have macroscopic characteristic that are different from the ones of the other two groups. There are a couple of artefacts (i.e. S1/L1012 and S1/L1015) with the same olive-grey colour (5Y 3/2, 4/1), but with no other common macroscopic characteristic. The artefacts in this group have dark colours and are small in size, which causes difficulties linking them with artefacts from the other assemblages. The sample GG15/S1/L008 is a small red (10R 3/4), translucent and fine-grain artefact (Fig. 5.36), which has similar characteristics to the radiolarite outcrops in the province of Enna. Moreover, it has macroscopic similarities with artefacts from Santa Verna (e.g. SV15/S1/L68) and Skorba (e.g. SKB16/S12/L13). There is a small, homogeneous, shiny (pearly) and translucent artefact (i.e. GG15/S3/L1015) which has similar characteristics with artefacts from the other assemblages (e.g. SV15/S1/L36, S1/L41; TCC14/S193/L69; KRD15/S42/L304). On the contrary, there is one artefact with rare macroscopic features reported in this assemblage (i.e. S5/L1019) which has no equivalent from any of the other assemblages. Furthermore, the research has recorded a translucent, fine-grained artefact (e.g. GG15/S3/L1016) with a grey-brown colour, which cannot be linked with any of the examined chert sources. It may be related with artefacts from Kordin (i.e. KRD15/S144/L306), Tač-Ĉawla (i.e. TCC14/S275/L208) and Santa Verna (SV15/S3/L41), but further investigation is necessary.

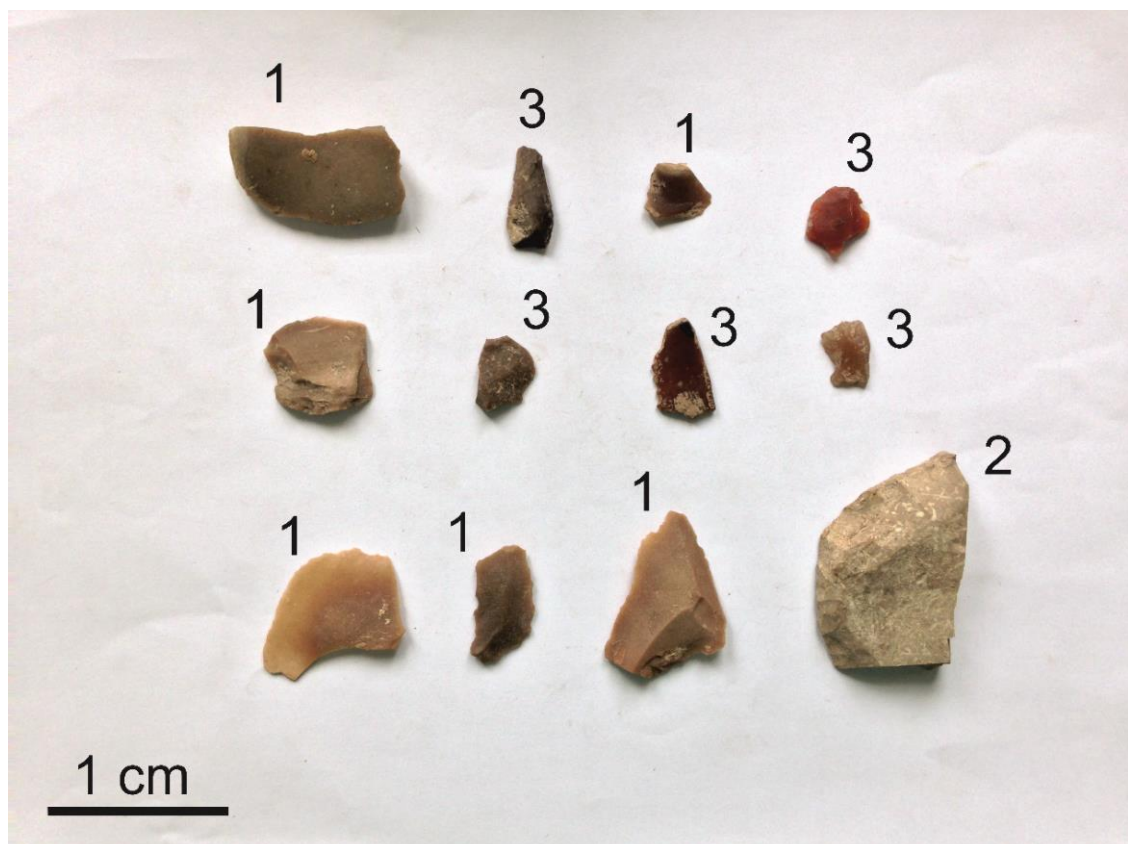


Figure 5-36: Representative artefacts of the different types of chert material. The number above each artefact indicates their source group.



Figure 5-37: The artefacts from context 1019 from Ġgantija assemblage.

➤ *Types of tools*

The Ġgantija assemblage is dominated by detached pieces, but some objective pieces are also reported. The latter are cores which can be further categorized as unidirectional or multidirectional, depending on the number of flat surfaces (i.e. striking platform). The detached pieces are mainly flake tools, but debitage and debris types of pieces are also recorded (Fig. 5.37).

This collection presents a great variety of flake tools, which were subsequently categorized according to their features. They are mainly in the form of prismatic flakes and occasionally they are further identified as blades (Fig. 5.38.2). Additional types of tool reported are: a) flake scrapper (e.g. S7/L1019), b) scraper (e.g. S2/L1012), decortication and/or rejuvenation flakes (Fig. 5.38.1). Some artefacts are characterized as bending flakes (e.g. S15/L1019), while others are unimarginal flake tools (Fig. 5.38.3) with no further classification. The investigation records the presence of a blade tip (i.e. GG15/S5/L1019) and a spall artefact (i.e. S2/L1016), which are new tool types and are not reported in the previous assemblages. The debitage pieces are classified either as proximal flakes (the proximal end is present), debris (fragments smaller than 1cm) or shatter (flake fragments with proximal end) according to their features.

➤ *Manufacturing techniques*

The main technique used on the artefacts of this assemblage is percussion, either primary or secondary. The primary flaking aims to detach pieces from the raw material (objective piece), while the secondary modifies the tool or creates more detached pieces. Many of the artefacts have indications (e.g. proximal end, raised hump) of both types of percussion, but occasionally only the secondary percussion is clearly recognizable. The latter is more common on the smaller artefacts or when flakes are extracted from the surface of the previous artefact. Some artefacts present more than one raised hump (a feature found below the striking platform) on the same surface, which made it difficult to distinguish which is the initial striking platform.

Pressure flaking is reported on many artefacts as a secondary and/or final action, aiming to retouch the edges or shape the artefact to the desirable form (e.g. triangle shape). The percussion technique is also used to shape some tools, but it is mainly focused on retouching their edges. Finally, a blade (i.e. GG15/S3/L1016) presents distinctive serrations on its one side, but it is unclear which technique was used.

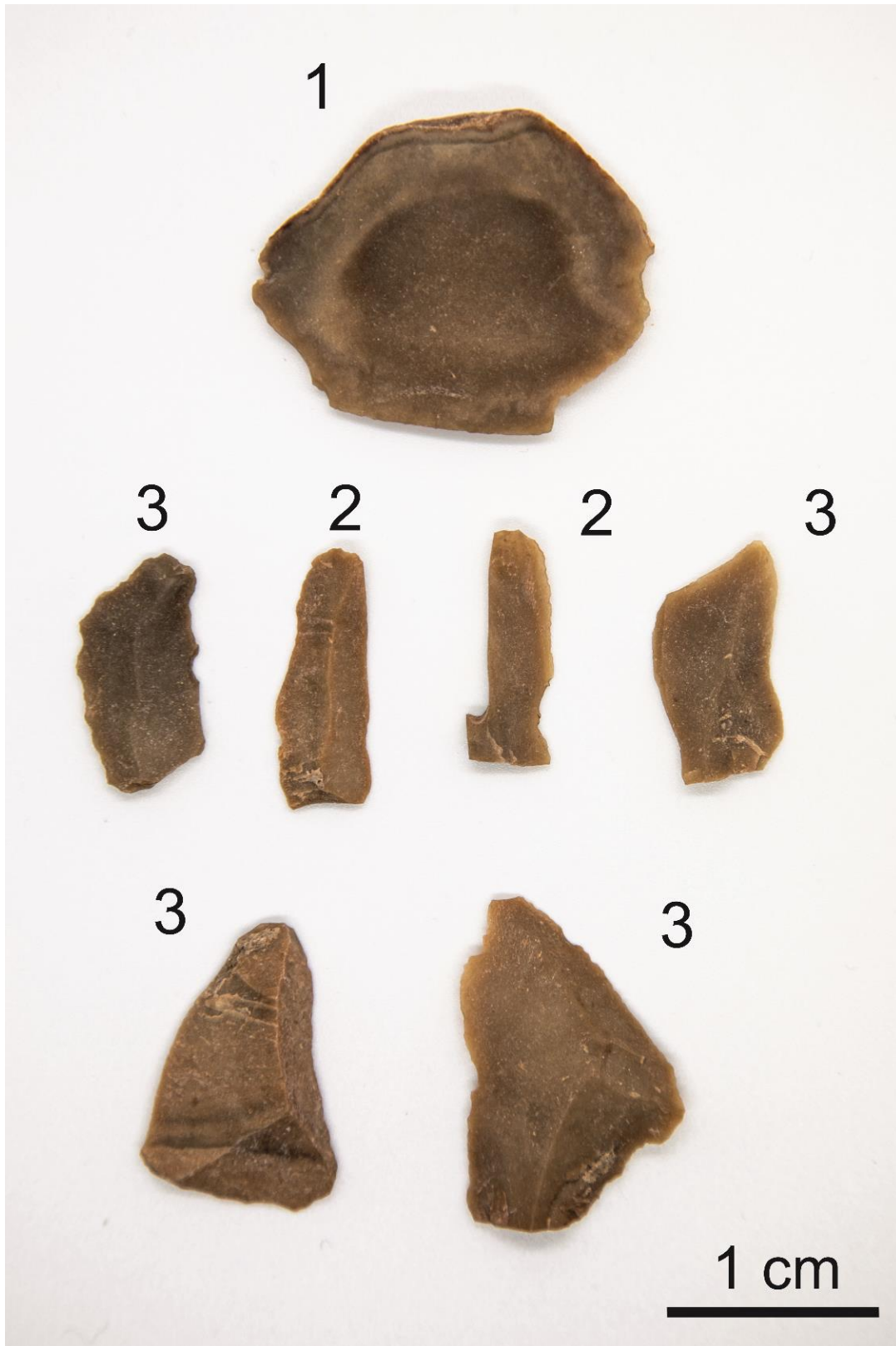


Figure 5-38: Different flake types from context 1019. The top artefact (1) is a decortication, the artefacts with number 2 are blades and the ones with number 3 are unimarginal flake tools.

5.1.2.6. Skorba assemblage

The Skorba assemblage was collected during the excavation of the prehistoric settlement, which is located on the west side of the Skorba Temple. The work on the site was conducted in 2016 and revealed a significant lithic assemblage of approximately 1200 pieces, including flakes, scrapers, cores and blades (Fig.5.39). The importance of this assemblage is that the finds are stratigraphically correlated and therefore chronologically secure in archaeological terms. The initial investigation showed that obsidian, chert (local and not local), limestone and other stones were used for tool crafting. However, there is no previous work or classification on them and it is a raw lithic assemblage which makes it impossible to follow the same strategy as in the previous ones. Research was focused on investigating the sources and composition of the material found. The finds related with this excavation have initials SKB (Skorba) and further explanation of their coding is found in the Appendix (Table 6).



Figure 5-39: The full layout of the lithic artefacts from context 11.

- Context 1

Context 1 is the topsoil of the trench (Fig. 5.40) and contained a large number of prehistoric pottery sherds from the Għar Dalam, Skorba, Żebbuġ and Ġgantija phases. This first horizon presents an important amount of lithic material (126 pieces), from which 20 samples were selected. The finds are mainly made of Coralline Limestone, chert and Globigerina Limestone, which are similar to the local rock formations. There are plenty of pieces (e.g. S2, S4, S6, S14) partly or fully patinated, but the recognized macroscopic features (e.g. fabric, texture) suggest a connection with the local chert rocks. There are some black (N1) or grey (N6), homogenous, dull, opaque and carbonated artefacts (e.g. S5, S9), which do not match any formation reported on the island. However, the spotted pattern recorded is very similar with the one on the chert and Globigerina Limestone formation of the islands. The homogeneous, dull artefacts (e.g. S7) with orange colour shades (e.g. 10YR 7/4) semi-smooth texture and medium-grain size are made from limestone and actually from the Coralline Limestone formation of the Maltese Islands. Some artefacts (e.g. S1, S3, S4) are heterogeneous, opaque, dull, fine-grained, spotted and with grey (e.g. 5Y 7/2, 5Y4/1) and brown colours (e.g. 10YR 6/2). They are of silicate origin and their characteristics are similar to the local chert outcrops. There is a small group of chert artefacts which present different characteristics from the local chert outcrops. They are fine-grained, shiny (pearly) and partly translucent, with colours from red (e.g. 5R 4/2; S10) to orange (e.g. 10 YR 6/6; S11) and brown (e.g. 10 YR 5/4; S13). One of these (i.e. S11) has similar features with artefacts from the Taċ-Ċawla and Santa Verna assemblages (e.g. TCC14/S103/L85; SV15/S38/L8). Finally, there is a group of very small artefacts from which it is not possible to record their macroscopic characteristics.

- Context 2

Context 2 is found below context 1 and is one of the upper topsoil layers (two in total) of the excavation (Fig. 5.40). Finds included pottery and lithic. 44 lithic artefacts from this horizon were excavated, of which, eight samples were selected for further investigation. Unfortunately, most of the artefacts are fully patinated and their macroscopic features are difficult to record. Nonetheless, the spotted characteristic is recognized on most of them, which suggests a possible connection with the local rock sources. Most of the carbonate artefacts are homogeneous, dull, with medium-grain size and dark colours (e.g. N1, 5YR 4/1 and 5Y 4/1). They are made from limestone, but some of their characteristics suggest more than one type of limestone source. The chert artefacts are heterogeneous, dull, opaque, smooth, fine-grained, spotted and with a grey colour (i.e. 5Y 4/1). They have similarities with the local chert formations and specifically with the outcrops of Gozo which have the same shades of grey (e.g. G2S3). The only exception in this layer is sample S8, which is a white, shiny (pearly) and highly translucent chert artefact. These characteristics are very similar with the ones

presented on the unique chert outcrop found on Gozo (G2S6). Finally, there is a group of very small artefacts whose macroscopic characteristics are impossible to describe.

- Context 3

Context 3 is again a top-soil layer (Fig. 5.40) and presents only 16 artefacts from which eight samples were selected for further investigation. The majority of them (n=12; 75%) is fully patinated and it is not possible to identify their macroscopic characteristics. There are some black (N1), homogeneous, dull and opaque artefacts, which possibly are made of carbonate rocks. However, their small size does not allow the research to record any further information about their origin. Most of the chert artefacts are mainly homogeneous, dull, opaque, smooth while there are some shiny (silky) artefacts with orange colours (i.e. 10YR 7/4).

- Context 5

From Context 5, (Fig. 5.40) 26 lithic artefacts were excavated, of which six samples were selected for further investigation. Once again most of the artefacts are fully patinated or weathered which prevented their macroscopic examination. In addition, there are some black (N1), homogeneous, opaque, smooth and fine-grained fragments of artefacts. Their small size has made it impossible to record any further information about their origin. Finally, the chert artefacts are mostly of brown colour (5YR 4/1), heterogeneous, dull, opaque, fine-grained and spotted. These characteristics are very similar to those of the chert formations of the Maltese Islands.

Top-soil and Upper strata of excavation

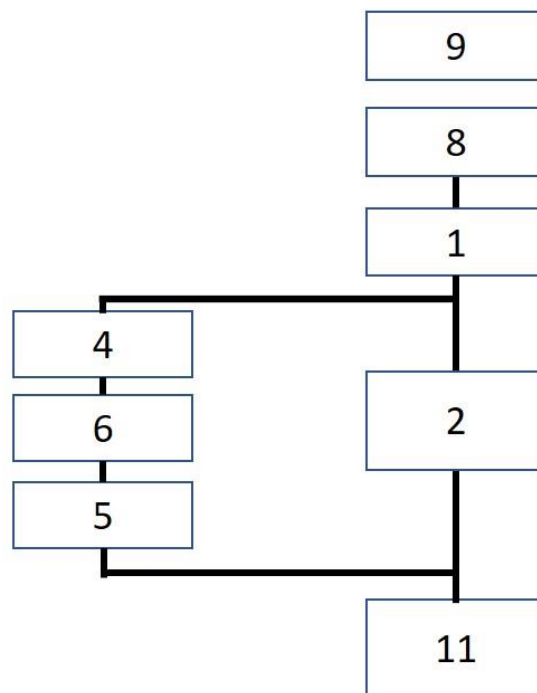


Figure 5-40: A Harris matrix showing the order of the top-soil contexts of the 2016 Skorba excavation. A full matrix is found in the Appendix I.

- Context 10

This context is located above the Temple Period wall located in the central sondage of the trench (Fig. 5.45). It contains 134 lithics of silicate and carbonate origin and from which 20 samples have been selected. The carbonate artefacts are mainly homogeneous and have black colour (N1), silky shine and semi-smooth texture. Some carbonate artefacts present brown (10R 4/6) or orange (10YR 8/6) colour shades and rough texture. The silicate artefacts presented a variety of colours from orange (10YR 7/4) and brown (10YR 4/2, 6/2) to grey (5Y 7/2, 4/1; 5YR 4/1) and black (5YR 2/1). They are homogeneous, dull, opaque, fine-grained, spotted and most of them have a smooth texture. These macroscopic characteristics are also reported on the chert outcrops of the Maltese Islands. On the contrary, there were only two artefacts with completely different characteristics which are different from the previous group of artefacts. The first (S19) is homogeneous, translucent, shiny (pearly), smooth, fine-grained and has a brown colour (5YR 2/2). These characteristics are not compatible with the local sources but are similar with characteristics of artefacts in the Circle and Ġgantija assemblages (e.g. BR98/S395/L449; GG15/S1/L1030/SF6). The second artefact (S21) is brown (10YR 6/2), homogeneous, opaque, fine-grained and with a silk shine. There are some patinated artefacts in this context and their features cannot be recorded, but they are correlated with similar artefacts from the previous layers which relate to the local chert formations.

- Context 11

This context is located above the Temple Period wall and on the same level as context 10 (Fig. 5.45). A total of 91 lithics were found in this context, mainly of silicate and carbonate origin, from which 17 samples have been selected. The majority of the finds are small, and the examination has been unable to record their macroscopic features. Nonetheless, the experience provided from the previous finds helped to identify and record useful information. Most of the artefacts are of silicate origin, grey (5Y 5/2), homogeneous, dull, opaque, smooth and fine-grained. There is only one exception (S4), which is brown (10YR 4/2), sub-translucent, smooth, fine-grained and has a pearly shine. These characteristics are similar with an artefact in layer 1 (i.e. S13/L1) and artefacts in the Kordin, Santa Verna and Ġgantija assemblages (e.g. KRD15/S27/L203; SV15/S2/L41 and GG15/S8/L109). In addition, there is a group of carbonate artefacts, which are homogeneous, dull, opaque and semi-smooth. Their colour varied from black (N1) to grey (N4), while they are medium-grained or fine-grained in size. Lastly, a few patinated pieces are recorded in this context, with macroscopic characteristics which are impossible to identify.

- Context 12

Context 12 is located at the eastern corner of the central sondage of the excavation and found below context 3 (Fig. 5.45). This horizon includes 123 lithic finds with 26 samples selected for further investigation (Fig. 5.40). A few small pieces are reported among this assemblage where it has been impossible to record their microscopical characteristics. An important number of these artefacts are made of a heterogeneous, dull, opaque, fine-grained and spotted silicate material. They fluctuate from brown (10YR 6/2, 4/2, 5/4) and grey (5Y 7/2; 5YR 4/1) to orange (10YR 8/6) colour shades, while their texture varies from smooth to semi-smooth. The only exception is a homogeneous, shiny (pearly), translucent, smooth and fine-grained chert artefact (S6). Macroscopically, this is similar with an artefact in layer 1 (i.e. S11/L1) and also with artefacts in the other assemblages (e.g. TCC14/S103/L85; SV15/S38/L8). Another group included dull, opaque and carbonated artefacts, but varies in its other macroscopic features. Moreover, there are lithics which macroscopically present the same characteristics with the cortex of the chert outcrops of Malta. Finally, an obsidian fragment (S12) was found in this context which has not been reported in the previous layers.

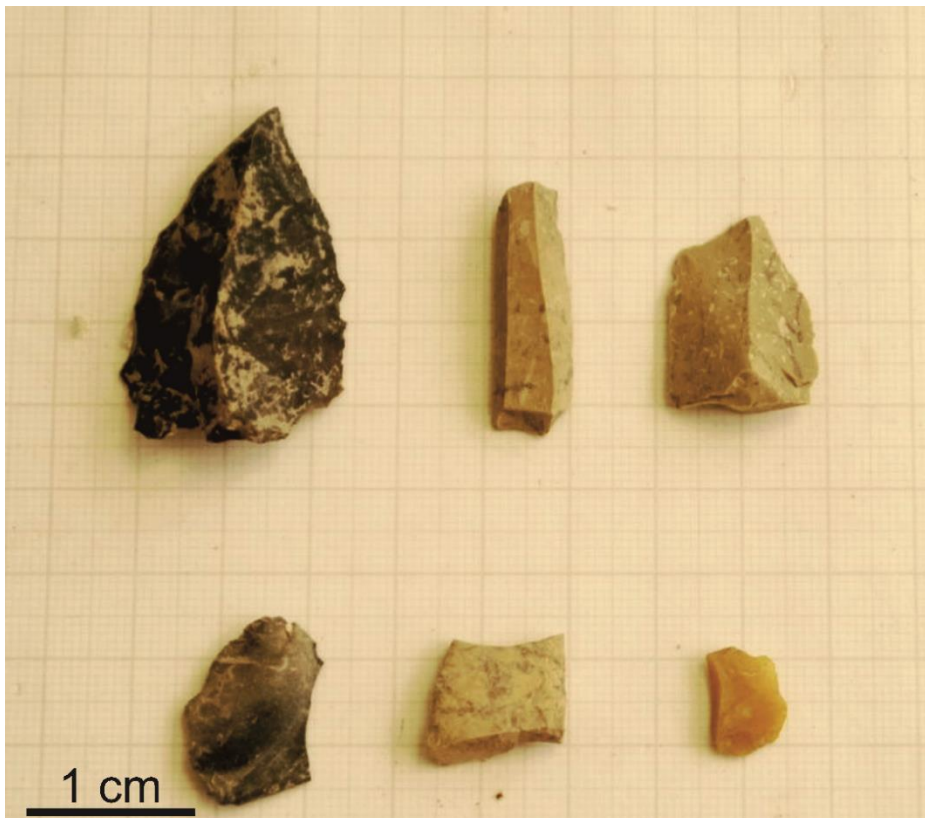


Figure 5-41: Representative samples of the different types of raw material found in context 12.

- Context 13

This horizon overlays contexts 22 and 23, and contains mixed Temple Period pottery (Fig. 5.45). It is the only strata from the 2016 excavations to bear a Tarxien-period finds. 58 lithic artefacts were found in this horizon with 13 samples selected for further investigation (Fig. 5.41). A few small pieces are reported among these finds which are impossible to be describe macroscopically. Most of the artefacts are made of a heterogeneous, dull, opaque, fine-grained and spotted chert material. There are mainly in brown colour shades (10YR 6/2; 4/2), but some of them presented a black colour (N1). A smaller group of artefacts are patinated, but their light brown colour (5Y 8/4) connects them with the local chert outcrops. There are two chert artefacts which presented different macroscopic characteristics from the above group. The first is a homogenous and opaque chipped stone artefact (i.e. S12) with a red colour (10R 3/4) and pearly shine that is similar to artefacts from the Ġgantija and Santa Verna assemblages (e.g. GG15/S1/L008 and SV15/S1/L68). Another artefact (i.e. S13) is homogeneous, dull opaque, semi-smooth, medium-grained and with an orange colour (10YR 7/4). Similar features have been reported on an artefact from the Ġgantija assemblage (GG14/S1/L1004).

A second group is recorded in this context, which includes carbonate, homogeneous, dull, opaque and fine-grain artefacts. Their colour ranged from black (N1, N2) and grey (N3) to brown (10YR 6/2), while only one presents a spotted pattern (S6). Finally, there are a couple of pieces made from limestone, but their macroscopic characteristics varied significantly from each other.



Figure 5-42: Representative samples of the different types of raw material found in context 13.

- Context 16

Context 16 lies below context 15, which has a radiocarbon date of 5190 to 4790 cal. BC (Fig. 5.45). 46 lithic finds were recorded from this context, mainly of silicate and carbonate origin and from which three samples were selected for further analysis. Unfortunately, most of these artefacts are weathered and their macroscopic characteristics are difficult to identify and record. Moreover, a few small pieces are reported among these finds which are impossible to be described macroscopically.

The artefacts that do not fall under the above groups were also examined and different subgroups were distinguished. Most of these artefacts are grey (5Y 7/2) and/or yellow (5Y 7/6, 10Y 8/2) in colour and have a heterogeneous fabric. They are dull, opaque, semi-smooth, fine-grained and spotted, but these features varied from artefact to artefact. In addition, some of these artefacts have a part of a cortex (e.g. S2), which is of limestone origin. There are other artefacts with a black (N1) colour, but the rest of the characteristics are impossible to distinguish. There is one heterogeneous, sub-translucent, shiny (silky), rough and coarse-grained artefact (S3) which has a yellow colour (i.e. 5Y 7/6) and white spots.

- Context 19

This context is found below context 16 and contains Żebbuġ-period and earlier Neolithic sherds (Fig. 5.40). A total of 51 lithics were found in this context, mainly of silicate and carbonate origin from which six samples have been selected for further analysis. The majority of the lithics are made from chert rocks and they are heterogeneous, dull, opaque, semi-smooth, fine-grained and spotted. They are mostly of grey colour (5Y 7/2), but artefacts with black (i.e. 5Y 2/1) and brown (i.e. 10YR 4/2) colours are also reported. Moreover, the investigation has distinguished one brown (i.e. 10YR 4/2), heterogeneous, sub-translucent, rough and coarse-grained artefact (i.e. S1/L19). The carbonate lithics of this layer are mainly made of limestone and have different black colour shades (e.g. N1, N2). They are homogeneous, opaque, semi-smooth, medium-grained and present waxy shine. Finally, a few small pieces are included among these finds which are impossible to be described macroscopically (patinated).

- Context 20

This context is located in the northern corner of the excavation and above an intact course of a Ġhar Dalam wall (Fig. 5.45). There are 26 lithics in this horizon, mainly of silicate and carbonate origin from which five samples were selected for further investigation. The main group of the artefacts is made from chert rocks and they are homogenous, dull, opaque, smooth, fine-grained, spotted and grey in colour (5Y 7/2). Furthermore, the investigation distinguished one brown (i.e. 10YR 5/4) heterogeneous, shiny (silky) sub-translucent, smooth, medium-grained artefact (i.e. S3/L20). A second group included carbonated artefacts which are mainly made of limestone and had black colour (i.e. N1). They are homogeneous, opaque, semi-smooth, fine-grained lithics and presented a silky shine. Finally, a few small pieces are included among these finds which are impossible to be described macroscopically (patinated).

- Context 23

Context 23 is one of the two horizons overlaying context 26 at the Central sondage, which contained Ġgantija, Mġarr and Żebbuġ pottery sherds (Fig. 5.45). 127 lithic artefacts were recovered from this context, mainly of silicate and carbonate origin and from which 12 samples have been selected. The main group of the artefacts is made from chert rocks and they are homogenous, dull, opaque, spotted and with grey colours (e.g. 5Y 5/2; 7/2). They are medium or fine-grained, have smooth or semi-smooth texture, while some artefacts present laminas¹⁸. Although patina covers the

¹⁸ Series of lines on the surface of the sample (Crandell, 2006).

external surface of many of the samples (e.g. S6), the observable macroscopic features indicate that they are compatible with local chert outcrops. Furthermore, the examination distinguished two artefacts (S7 and S8), which present different macroscopic characteristics in comparison with the other members of this group. They are homogenous, translucent, shiny (pearly), smooth and fine-grained artefacts. The only difference is their colour with the first (S7) red (5R 4/6) and the second (S8) reddish brown (10R 5/4). The macroscopic characteristics of these artefacts are very similar with the ones of the radiolarian outcrops of Sicily. Moreover, they present similarities with one artefact from layer 13 (i.e. S12/L13) and artefacts found in other assemblages (e.g. GG15/S1/L008 and SV15/S1/L68). A second group included homogenous, dull, opaque, smooth and fine-grained artefacts which had black colour shades (e.g. 5YR 2/1, N1). The examination suggests a limestone origin, but further investigation is necessary. Finally, a few small pieces are reported among these finds which are impossible to be described macroscopically.

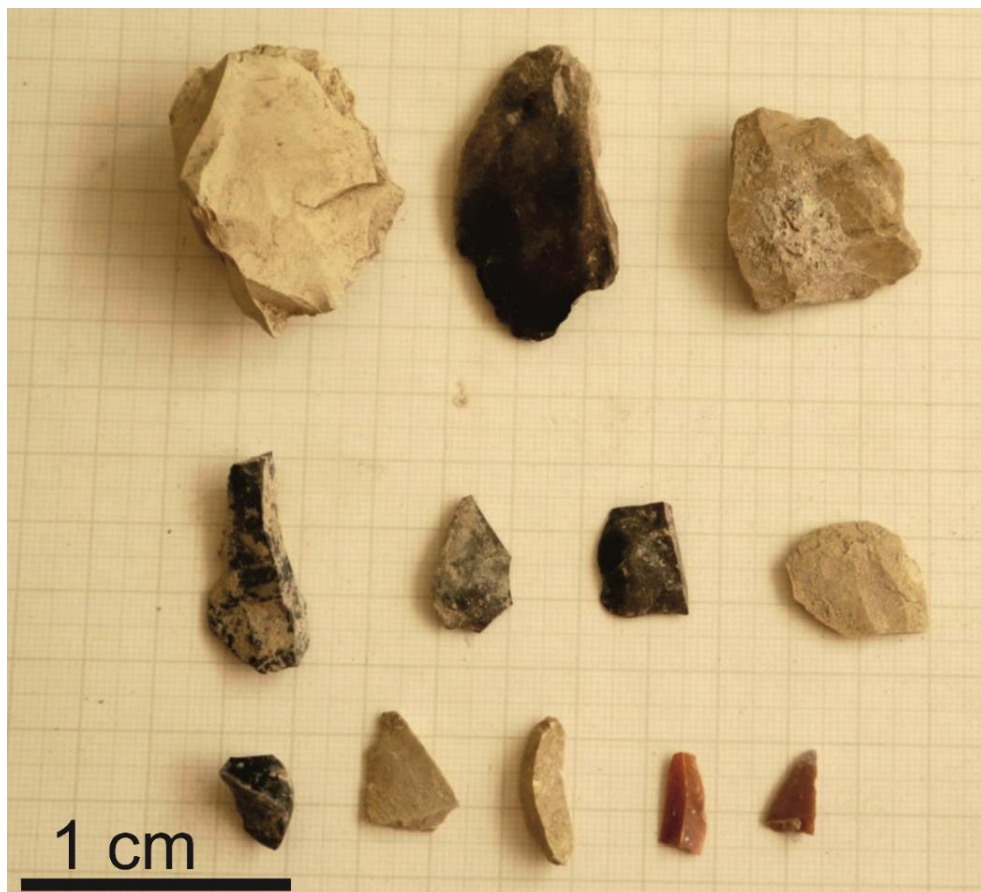


Figure 5-43: Representative samples of the different types of raw material found in context 23.

- Context 26

Context 26 overlays context 30 within the central sondage and contained Žebbuġ as well as earlier Neolithic sherds (Fig. 5.45). A total number of 263 lithics were found in this context, which is the highest recorded number in all the contexts of the Skorba excavation. They are mainly of silicate and carbonate origin and 13 samples have been selected for further investigation. The first group of the artefacts is made from chert rocks and they are homogenous, dull and opaque. They are grey (e.g. 5Y 7/2) or brown (e.g. 10YR 6/2; 4/2) in colour, smooth or semi-smooth in texture and medium or fine-grained in grain size. Some artefacts are spotted but they are generally fewer than the ones in the other horizons of the excavation. Although a patina covers the external surface of many of the samples (e.g. S3), the observable macroscopic features indicate that they are compatible with local chert outcrops. Furthermore, the examination distinguished three artefacts (i.e. S9, S10 and S11), which present different macroscopic characteristics in comparison with the other members of this group. The first artefact is homogenous, opaque, shiny (pearly), smooth, fine-grained and had brown colour (10YR 5/4). Similar macroscopic features are reported on artefacts in Santa Verna (e.g. SV15/S38/L8, S3/L41), Taċ-Ċawla (e.g. TCC14/S275/L208), the Circle (e.g. BR89/S291/L334) and Kordin (e.g. KRD15/S144/L306) assemblages. The second artefact is homogeneous, opaque, shiny (pearly), smooth, fine-grained and had reddish brown colour (i.e. 10R 5/4). The last one is pale red (10R 6/2), but the small size (<1cm) and the fact that it is partly patinated does allow other characteristics to be recorded. The second group included homogenous and opaque artefacts, which present grey colour shades (i.e. N2, N3). The rest of their macroscopic characteristics fluctuated, but not to such an extent as to suggest different sources. Finally, a few small pieces are included among these finds which are impossible to be described macroscopically.



Figure 5-44: Representative samples of the different types of raw material found in context 26.

- Context 30

Context 30 is the lowest (earliest) contexts from the central sondage (Fig. 5.45) and contained only Skorba and Ghar Dalam period pottery. 33 lithic artefacts were recovered mainly of silicate and carbonate origin and from which four samples were selected for further investigation. The first group of the artefacts is made from chert rocks and they are heterogeneous, dull and opaque. They vary from grey (e.g. 5Y 7/2) to brown (e.g. 10YR 6/2) colour, are semi-smooth, fine-grained and most of them are spotted. Although a patina covers the external surface of some of the samples (e.g. S3), the observable macroscopic features indicated they are compatible with local chert outcrops. Furthermore, the examination distinguished one artefact (S4), which presented different macroscopic characteristics in comparison with the other members of this group. It is brown (i.e. 10YR 5/4), homogenous, translucent, smooth, fine-grained and with a pearly shine. This artefact presented similar features to two other artefacts of the Skorba (i.e. S1/L13, and S4/L11), Santa Verna (i.e. SV15/S2/L41, S1/L80) and one of the Ġgantija (GG15/S6/L1019) assemblages.

The second group included dull, opaque, smooth and fine-grained artefacts of grey shades (i.e. N3, N6). The level of homogeneity of the fabric is influenced by the extent of the patterns (e.g. spotted) reported on samples. These samples are made of limestone, but their dark colour does not allow any further remarks regarding their origin at this stage.

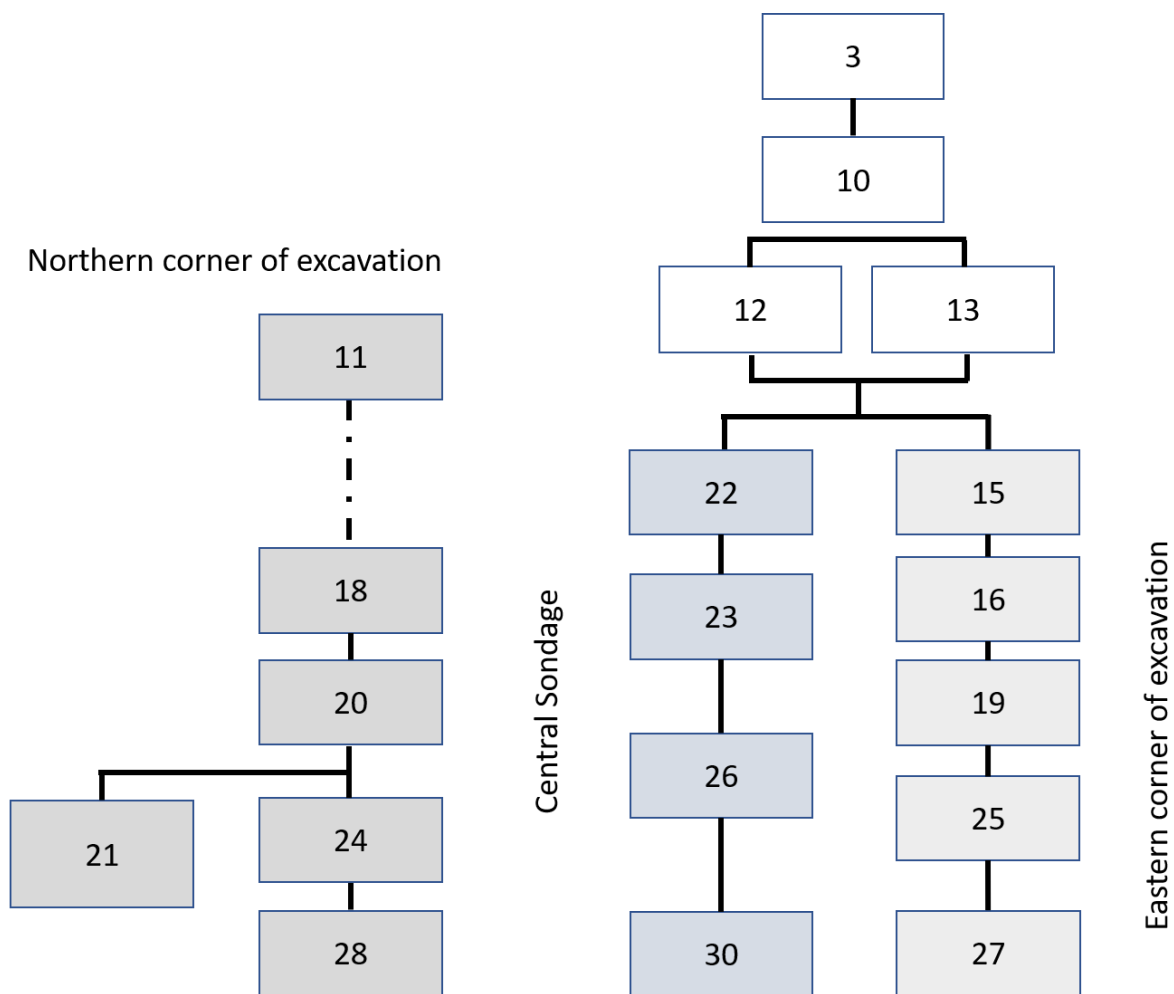


Figure 5-45: A Harris matrix showing the order of the main contexts of the 2016 Skorba excavation. A full matrix is found in the Appendix I. The white boxes show upper soils of the trenches. The dark grey boxes the northern corner, the blue the central sondage and light grey the eastern corner of the excavation.

5.1.3. First remarks

The macroscopic examination has enabled some initial observations regarding the type of raw material used, the type of techniques and the manufactured tools found at these late Neolithic sites. The assemblages contain artefacts from different types of rocks, but they are dominated by chert, obsidian and limestone. The chert artefacts can be further divided into three major groups with distinctive macroscopic features. The first group includes mainly brown, dull and opaque artefacts which have no similarities with the local resources. On the contrary, the second group has artefacts which present a combination of features that are almost identical with the ones reported on the Maltese chert outcrops. The third group contains members with great heterogeneity of macroscopic features which suggest an origin of multiple sources. They are in this group because they are completely different from the members of the other two groups. Moreover, they are not reported in all the assemblages nor have they the numbers to form a separated group.

Most of the artefacts in the examined assemblages are flakes which are subdivided into a variety of tools. The majority of flakes can be flake tools, flake scraper and blades, but many lack the evidence to allocate them accurately. Some of them have the characteristics of conchoidal flakes and bending flakes, but the second modification has eliminated the characteristic features of these flake types. Furthermore, in Santa Verna, some flakes have indications of hafted feature which is rare and not reported to the other assemblages. Another type of artefact in all the assemblages is the scrapers which are more abundant in the Circle assemblage. They are characterized by their retouched edges and most of them retain part of the cortex on one of their sides. The cortex might also suggest that these finds have originally served as decortication and/or rejuvenation flakes. Debitage and other types of detached pieces are limited and they are mainly reported in Tač-Ćawla and Santa Verna. Lastly, the research has recorded some typologically well-defined pieces (e.g. cores), but these are restricted in the assemblages of Tač-Ćawla and Ġgantija.

The main and primary technique recorded on the majority of the members of all the assemblages is Percussion flaking. It was used to extract detached pieces from the raw material or the detached piece which at a certain point served as an objective piece. The *arris* feature is related to this technique but mainly with secondary percussion flaking and not the primary. This feature is formed when flakes are removed from the dorsal surface of the artefact in different angles. The second recorded technique is Pressure flaking and is always employed after the Percussion flaking or as a final action for the modifying the edges of the artefacts. Occasionally this technique is employed to retouch the edges of artefacts in order to extend or enhance their utility. This is mostly found on scrapers and flake scrapers, but there are flake tools and blades that also have evidence of final Pressure flaking. The secondary modifications are principally limited to one of the sides of the artefact and they are characterized as unimarginal tools. However, the research recorded artefacts with modifications on both their sides. These two types of techniques are the dominant actions employed on these artefacts, but the research has found evidence of additional techniques. A blade in Santa Verna and another artefact in Tač-Ćawla have presented serration, a feature which has not been reported elsewhere. Possibly it has been created with pressure flaking, but there is insufficient evidence to support this technique. Moreover, a blade from Santa Verna has evidence of the polishing technique of one of its surfaces which is only reported on this sample. Finally, a scraper from the Circle assemblage has presented solid evidence of the Levallois technique. It is a well-established series of knapping actions to form artefacts in a specific manner and leaves specific features on the samples.

5.2. Optical Microscopy

Optical Microscopy is the best method to investigate the mineralogy and internal structure of a rock formation. It requires the preparation of thin sections from the samples in order to be examined under the polarizing microscope. This action is, unfortunately, the only disadvantage of this technique for archaeological research as it requires the destruction of the sample to create a thin section. Therefore, this method was only employed on the samples collected from the rock sources of the Maltese Islands and Sicily. For the purpose of this technique, 41 thin sections are created from the samples of the investigated chert sources. The results of the optical microscopy method are presented in the following subchapters.

5.2.1. Chert Formations

5.2.1.1. Maltese Islands

The cherts samples of Malta mainly present microcrystalline quartz and calcite (5-15 μ m), but chalcedony and dolomite crystal have also been reported. The external parts are a fine-grained matrix mainly consist of micro-calcite (Fig.5.46a), while the quartz is mostly concentrated in laminae of 0.5mm thick. Towards the centre of the samples, the laminae become denser and micro-quartz is the dominant mineral (Fig. 5.46b). Microcrystalline quartz and chalcedony are reported to fill pores and fragments within the thin sections (Fig. 5.46c, d). Many dolomite crystals (Fig.5.46c) are reported in the central part of the samples, which are between 0.2 to 0.8 mm in size. Most of these chert outcrops present only a few fossils, which are radiolarian (Fig. 5.46f), sponge spicules and/or foraminifera (Fig. 5.46e). Although some fossils retain their original composition, the majority is replaced with chalcedony, microcrystalline quartz or both.

The chert samples of Gozo present some additional features in comparison with the chert outcrops of Malta. They are more fine-grained and have more iron oxide which explains the brownish colour of the outcrops. The matrix of the samples (Fig. 5.47a) consists of a combination of micro-calcite (5-15 μ m) and cryptocrystalline silica material (<5 μ m). The microcrystalline quartz (5-15 μ m) is again reported in laminae (0.2 to 0.8 mm) which increase in thickness towards the centre of the outcrops. The outcrops in the lower parts of Globigerina formation present more micro-quartz and the lowest outcrop consists solely of micro-quartz. Small dolomite crystals are reported in many samples either in the matrix (Fig. 5.47b) or inside foraminifera fossil casts. The chert samples from Gozo present some apatite and feldspar crystals (Fig. 5.47c), which are minerals not found in the chert samples of Malta. Moreover, the Gozo samples have demonstrated more, and a greater variety of, fossils than the samples of Malta. The highest outcrops present few radiolarians and some foraminifera which are mainly found in the laminae. The radiolarians are filled with microcrystalline quartz (Fig. 5.47d), while the foraminifera are

filled with microcrystalline quartz and/or retained their original carbonate composition (Fig 5.47a). Sponge spicules are also found in this group of chert samples, which are mainly consisted of micro-quartz (Fig. 5.47a). The outcrops in the middle of the limestone present many globigerina and echinoderm fragments (Fig. 5.45c) that are clearly related to the host formation and are mainly filled with micro-quartz and/or chalcedony. Nevertheless, there are many of these two types of fossils that are dominated by microcrystalline calcite.

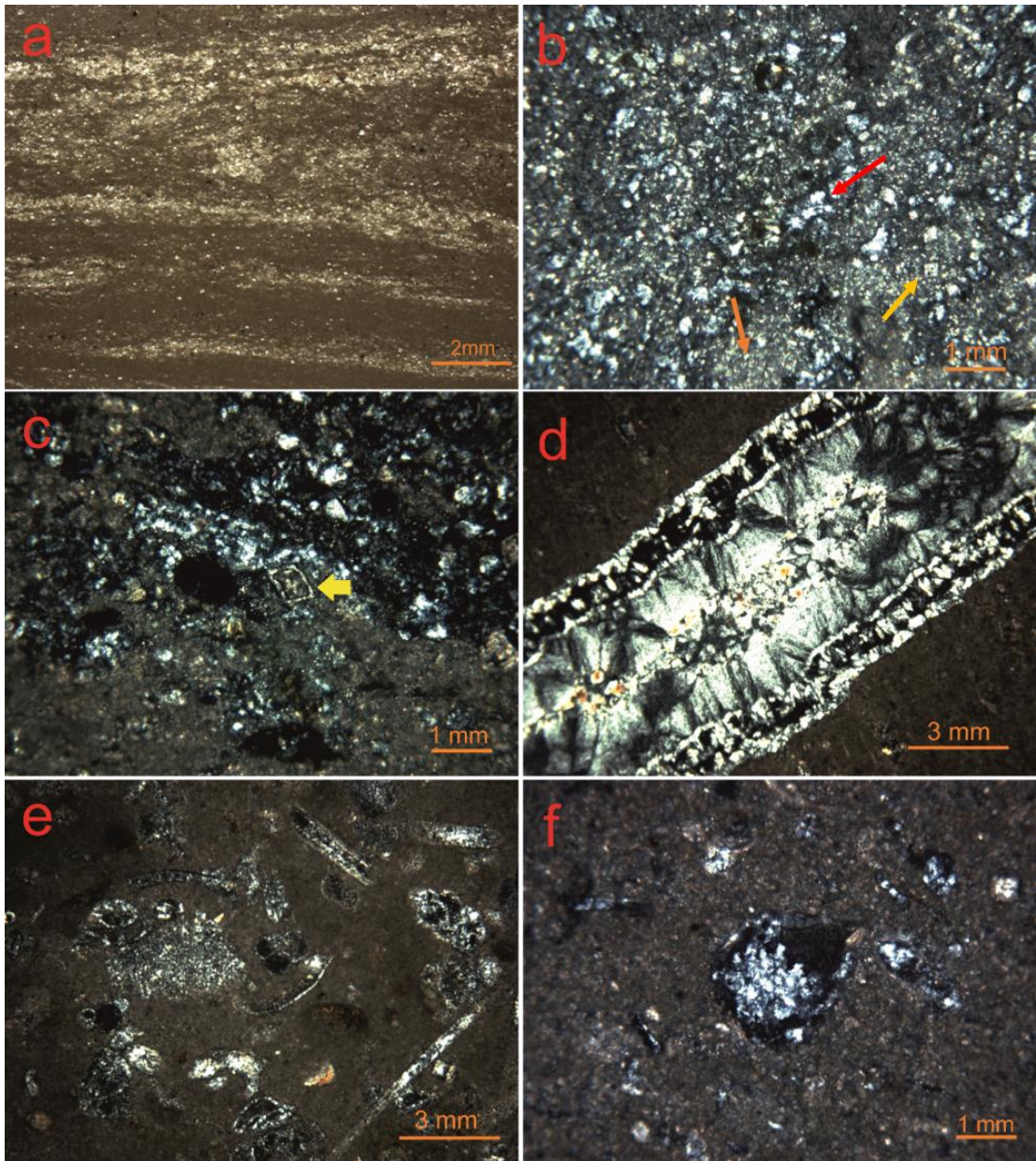


Figure 5-46: a) Laminae made of micro-quartz, under PPL , b) Micrite (orange arrow), micro-quartz (red arrow) and microcrystalline dolomite (yellow arrow), c) Pores filled by micro-quartz and dolomite (yellow arrow), d) Vein in the matrix filled with chalcedony , e) micrite matrix with silicified fossils (e.g. Foraminifera, echinoderm) and f) Radiolaria filled by micro-quartz.

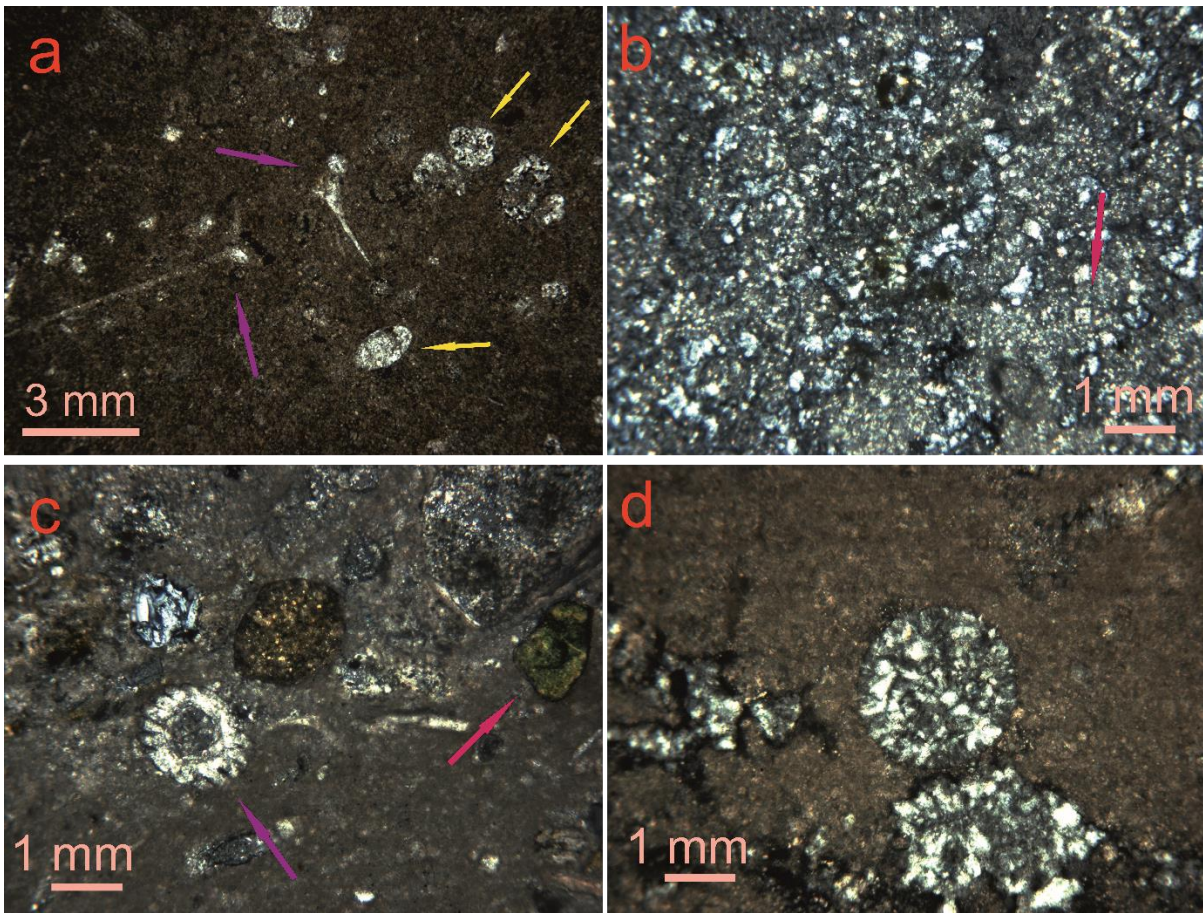


Figure 5-47: a) Micrite matrix with sponge spicules (purple arrows) and foraminifera (yellow arrows), b) micro-quartz in the centre of the samples with microcrystalline -dolomite (red arrow). c) Echinoderm fragments (purple arrow) and feldspar crystals (red arrow) and d) Radiolarian filled with micro-quartz and chalcedony. All images under are under XPL

5.2.1.2. Sicily

The cherts samples of southeastern Sicily present mainly microcrystalline quartz (5-15 μm), but crypto-quartz (<5 μm) have also been reported. Chalcedony crystals are mainly found to fill pores and fossils within the thin sections (Fig. 5.48a). Some of the samples (e.g. S5) present calcite and dolomite crystals within their matrix, which are 0.2 to 0.8mm in size (Fig. 5.48b). Calcite crystals are also found in cracks and veins and they range from microcrystalline (5-15 μm) to mega-crystalline (>20 μm) in size. Most of these chert samples present indications of iron minerals, but only residues of them are found. There are only a few fossils reported in these samples, mainly radiolarian (e.g. spoumelarian) filled with chalcedony (Fig. 5.48c). In some of the thin sections, the radiolarians retain residues of their original raw matter.

The chert samples from the Monterosso Almo area have a matrix consisting mainly of microcrystalline quartz (5-15 μm). Microcrystalline quartz and chalcedony are reported to fill pores and fragments within the thin sections. Carbonated residues are found in the matrix, but no calcite or dolomites crystals are reported. The chert samples from the old quarry have a great variety of fossils, but the other chert outcrops do not present the same feature. The fossils recorded are radiolarian, sponge spicules, foraminifera, cephalopods, nummulites, and echinoderms (Fig. 5.48d). They are filled with micro-quartz and/or chalcedony, but some retained their original composition.

The samples related to the Radiolarian formation present a cryptocrystalline (<5 μm) or microcrystalline (5-15 μm) quartz matrix (Fig. 5.48e). Microcrystalline quartz and chalcedony are reported to fill pores and fragments within the thin sections. There are indications of iron minerals, but only residues of them are recorded. Moreover, some calcite crystals are found to fill small fragments within the matrix. Radiolarians are the only type of fossils reported and they are filled with chalcedony or micro-quartz.

The chert samples from Monte Judica present a cryptocrystalline (<5 μm) to microcrystalline (5-15 μm) quartz matrix, in which few calcite microcrystals are reported. Microcrystalline quartz and calcite are also found to fill fragments within some of the thin sections. There are some fossil casts, mainly foraminifera, replaced with micro-quartz and/or chalcedony.

The chert samples from western Sicily present a matrix of microcrystalline quartz (5-15 μm) which includes calcite and hematite crystals. The calcite minerals are mainly in fragments, while hematite is gathered in small laminae (0.2 mm in thickness) or scattered in the matrix (Fig. 5.48f). There are only a few fossils reported in these chert samples and their cast is filled with chalcedony and/or micro-quartz.

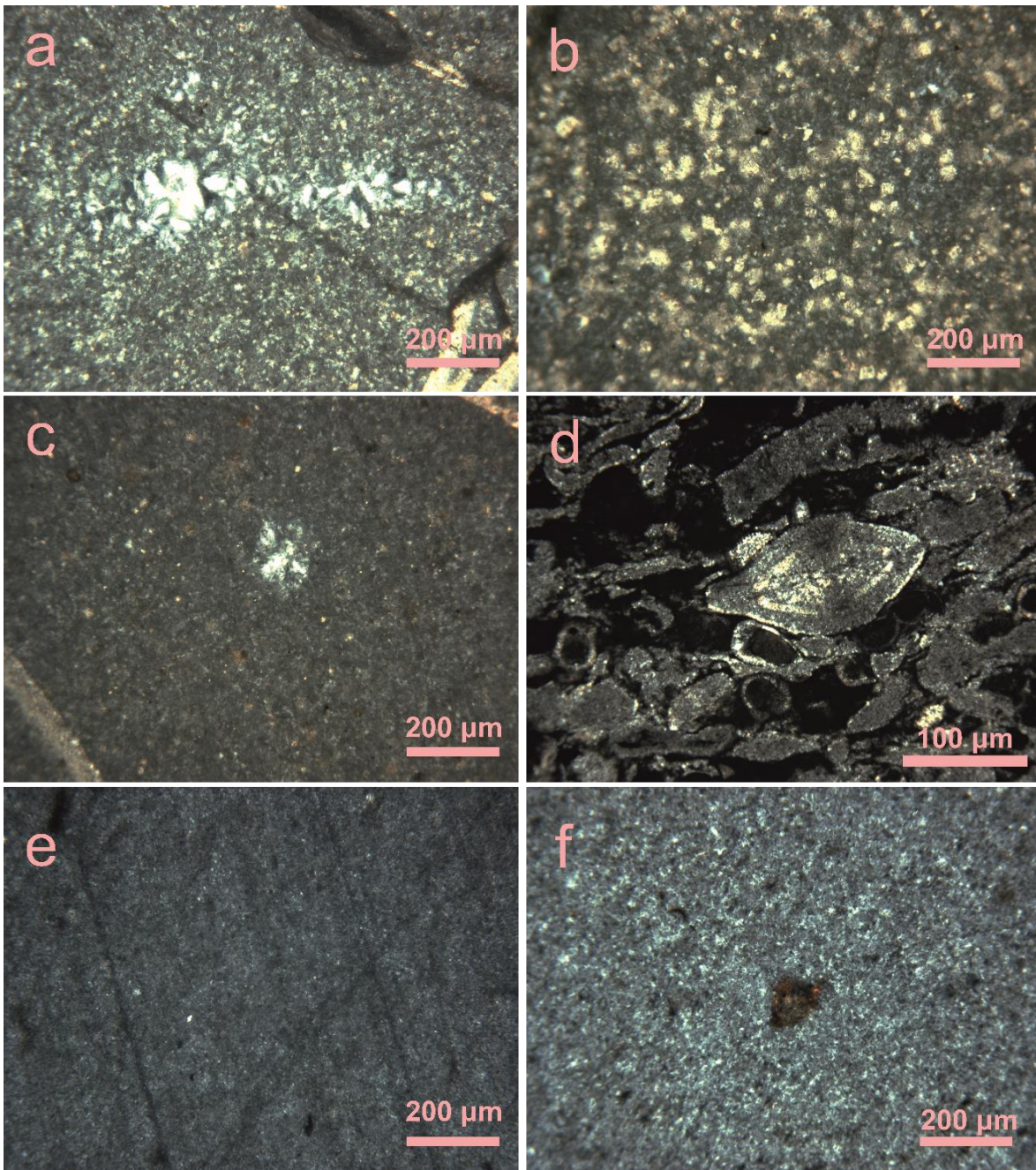


Figure 5-48: a) Chalcedony fills pores within the micro-quartz matrix, b) Calcite and dolomite crystals within the matrix, c) radiolarian filled with chalcedony, d) foraminifera and nummulites, filled with micro-quartz or retaining their original composition, e) cryptocrystalline (<5μm) quartz matrix and f) Iron-oxide rich aggregate in the matrix.

5.2.2. First remarks

The Maltese cherts consist of microcrystalline quartz and calcite (5-15 μ m) as well as chalcedony and dolomite. Quartz is mainly found in laminae although in the centre of the samples there is an increased concentration of quartz. In addition, quartz and chalcedony fill pores and fossils reported in the samples, while dolomite is found randomly within the matrix. The chert samples include many *radiolaria* and sponge spicules which are possibly the source of silica (Si), but also many foraminifera and echinoderm fragments which are associated with the host limestone formation (Globigerina Limestone). The noticeable differences between the Malta and Gozo are the higher number of carbonated fossils (e.g. foraminifera) and the apatite and feldspar reported in the Gozo cherts.

On the contrary, the Sicilian chert samples are dominated by microcrystalline (5-15 μ m) and cryptocrystalline (<5 μ m) quartz. Chalcedony is reported filling fossils, pores and cracks in the thin sections. Calcite and dolomite are found, but in lesser quantities than in the Maltese samples, while no apatite or feldspar have been recorded. Radiolarian and sponge spicules are the main type of fossils reported in the Sicilian cherts filled with quartz and chalcedony and possibly are the source of the silica (Si).

5.3. Scanning Electron Microscopy (SEM)

The SEM method works well in conjunction with optical microscopy and provides further details of the mineralogy and the internal structure of a rock formation. It allows the examination of the samples on a smaller scale and provides semi-quantitative elementary analysis of the minerals reported within the polished sections.

This technique was only employed on the Maltese chert rocks to collect the maximum data possible as there is insufficient geological literature on these sources. This is not the case with the Sicilian chert formations, therefore these formations are not examined using this technique. The artefacts samples were also not investigated because Scanning Electron Microscopy is a destructive technique. The thin section samples are the same as those used for optical microscopy, but at this stage do not have a coverslip (i.e. polished sections).

5.3.1. Chert Formations

The cherts samples of Malta present a microcrystalline matrix which predominantly consists of silica (Fig. 5.49-54). This contradicts the findings of the optical microscope and does not identify the type of the silicate minerals (e.g. Opal-A). Silicate minerals are also found filling the majority of the fossils in the matrix of these chert samples (Fig. 5.49a, 5.53a). Carbonate minerals are found in the matrix either in crystal form or filling fossils (Fig. 5.49-54). The semi-quantitative measurements show that calcite is mainly related to fossils but occasionally fragments of calcite crystals are recorded (Fig. 5.51b and 5.52b). Dolomite is the second carbonate mineral within these samples (Fig. 5.50c) but is not related to fossils. Apatite (a phosphatic mineral) is another type of mineral found in many of the chert samples of Malta which are mainly crystals within the matrix (Fig. 5.51c and 5.54c). Moreover, some feldspar minerals are found and a few of them are further distinguished as potassium feldspar (Fig. 5.52c). The SEM investigation has found two different types of minerals which are related to iron concentrations. The first are small (1-2 μ m), bright, white roundish crystals (Fig. 5.53c) which have the chemical composition of pyrite minerals (FeS_2). The second is greater in size but less clear in shape (Fig. 5.54d), mainly filling pores and has the chemical composition of ilmenite (FeTiO_3).

The chert samples of Gozo also present a matrix which is dominated by silica minerals (Fig. 5.55-57), but again the type is not identified. Silica minerals (e.g. quartz) are also found filling many of the fossils reported in these thin sections. Calcite and dolomite are the carbonate minerals found in the chert samples of Gozo (Fig. 5.55-57). The semi-quantitative measurements show that calcite is related to fossils (e.g. foraminifera), while dolomite crystals are reported in the matrix (Fig. 5.55c). Apatite (a phosphatic mineral) is another type of mineral found in many of the chert samples of Gozo and they could either be in crystals or filling fossils (Fig. 5.56b). The chert outcrops of Gozo are more abundant in feldspar minerals and they present two different categories. Potassium feldspar (KAlSi_3O_8) is the

main feldspar mineral, but plagioclase and especially anorthite minerals ($\text{CaAl}_2\text{Si}_2\text{O}_8$) are recorded (Fig. 5.55d). Pyrite (FeS_2) and ilmenite (FeTiO_3) are also found in the thin sections of the Gozo cherts (Fig. 5.55e and 5.57c.).

The structure and SEM analysis show that the matrix of all the Maltese chert samples consisted of silicate minerals (e.g. quartz), while carbonate minerals (e.g. calcite) have lesser importance. This was in contrast to observations made via optical microscopy. This might be explained by the present of cryptocrystalline or amorphous silicate minerals that cannot be recorded by the optical microscope. Nevertheless, this method supports the findings of the other minerals reported in the Maltese samples such as dolomite, apatite and feldspar.

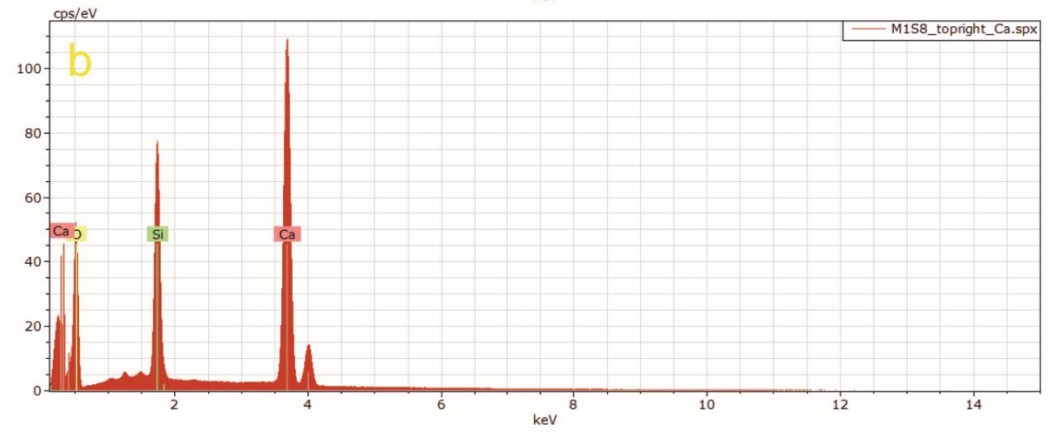
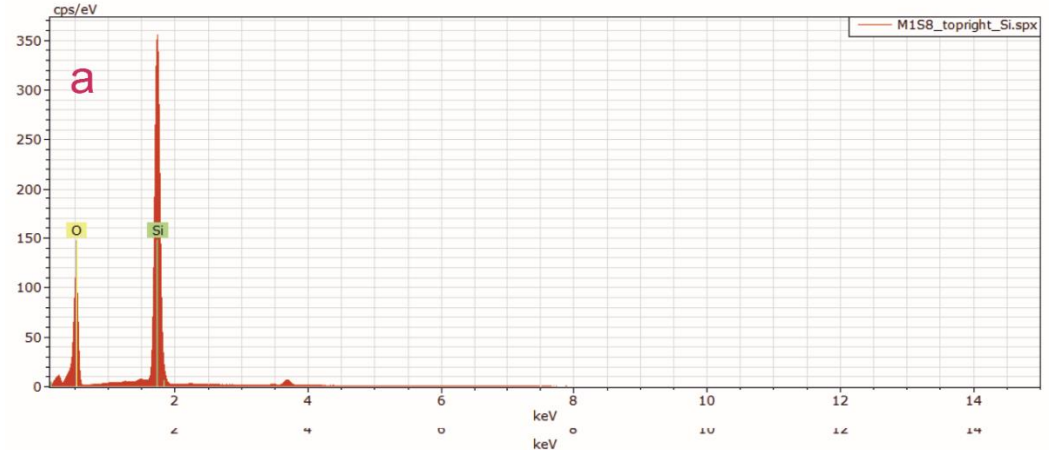
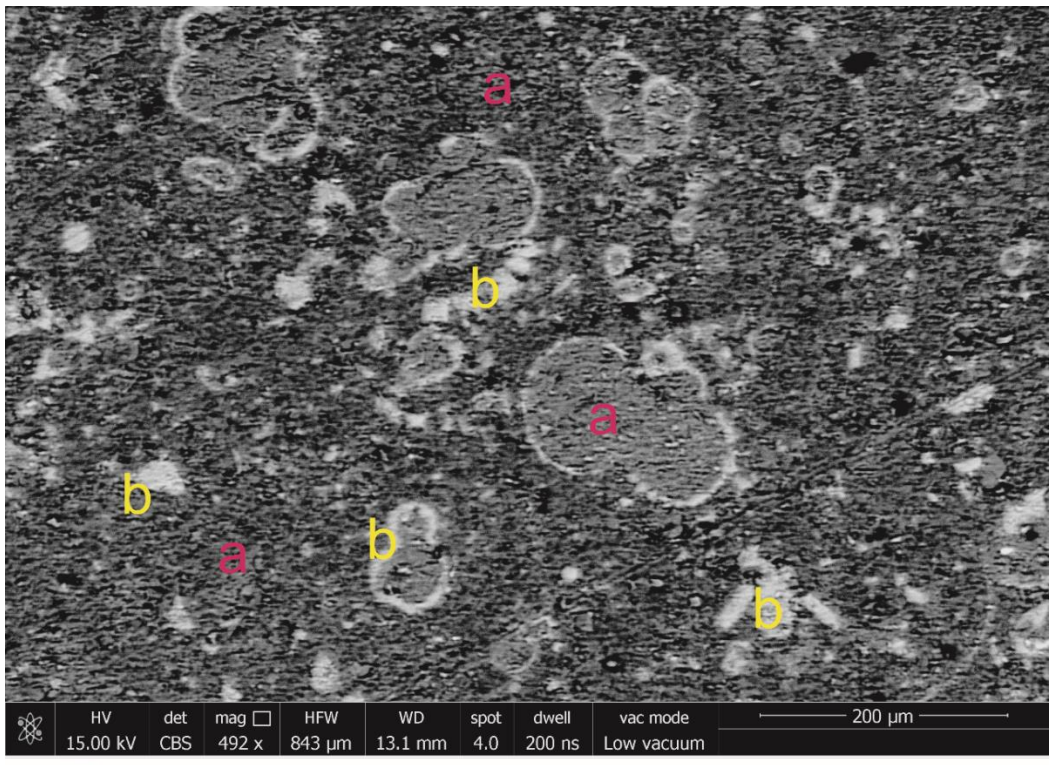


Figure 5-49: SEM image and the semi-quantitative spot analyses of a) Si and b) Ca and Si.

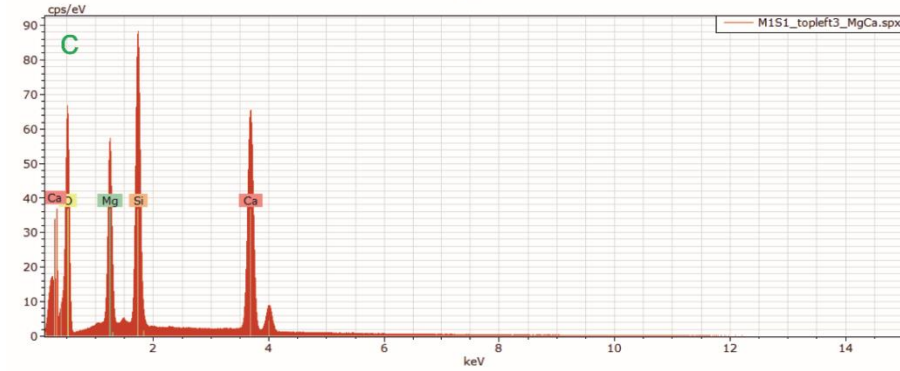
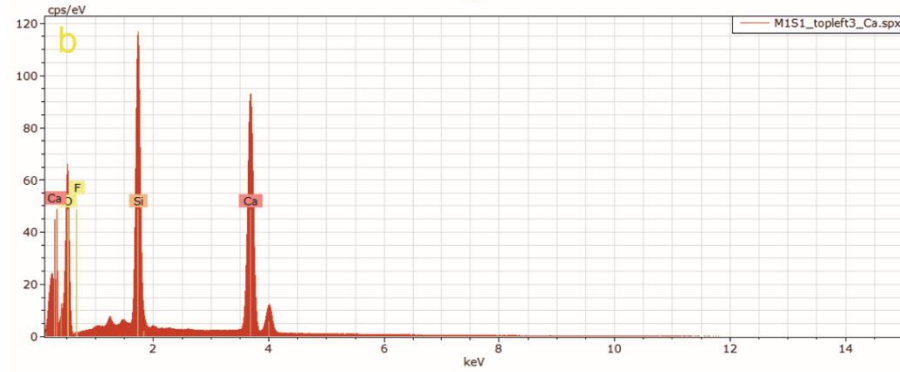
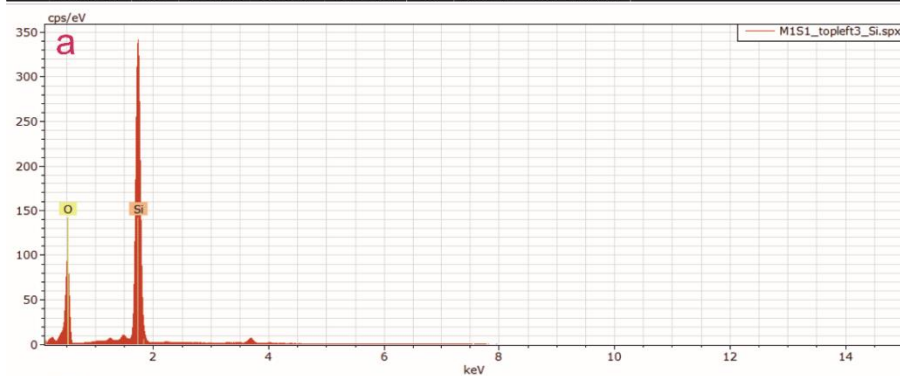
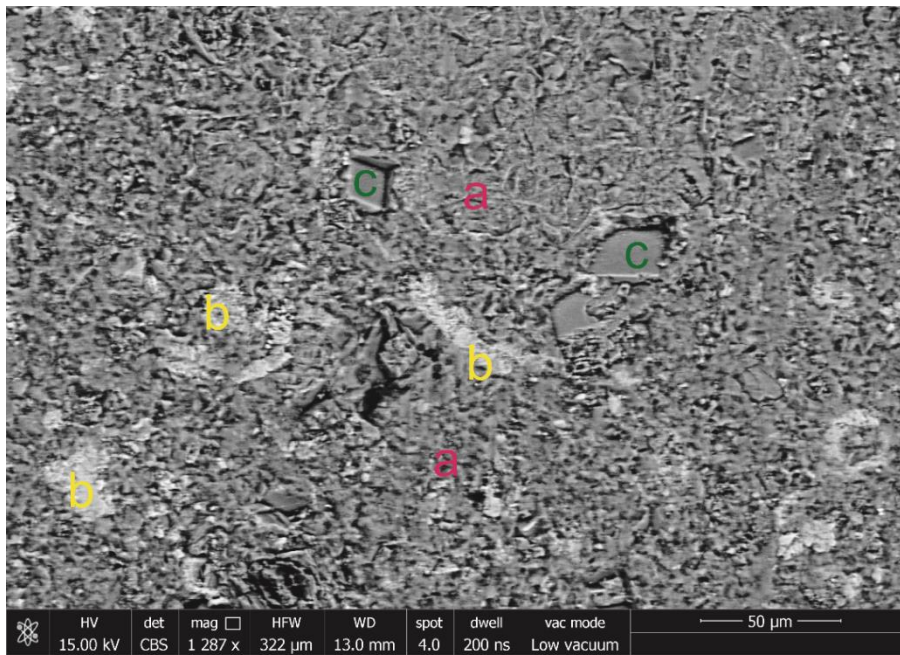


Figure 5-50: SEM image and the semi-quantitative spot analyses of a) Si, b) Si, and Ca and c) Si, Ca and Mg.

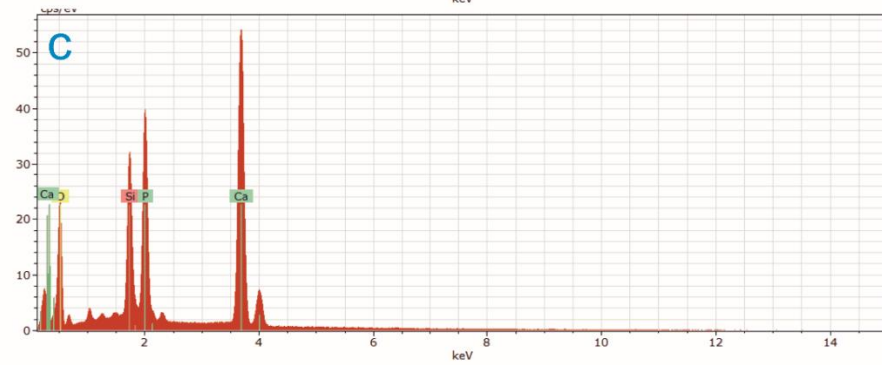
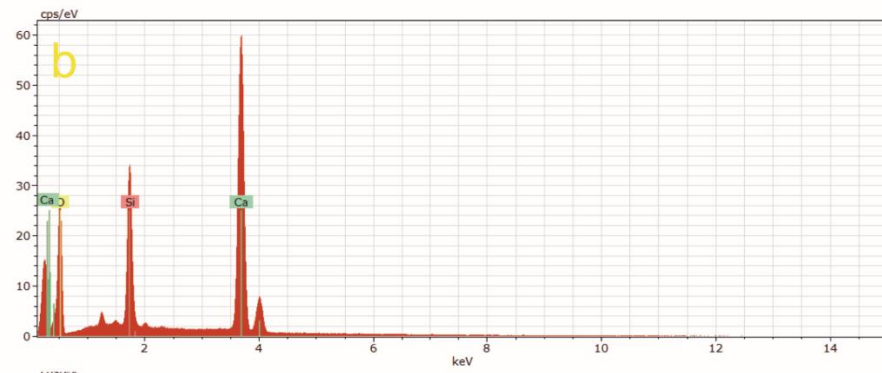
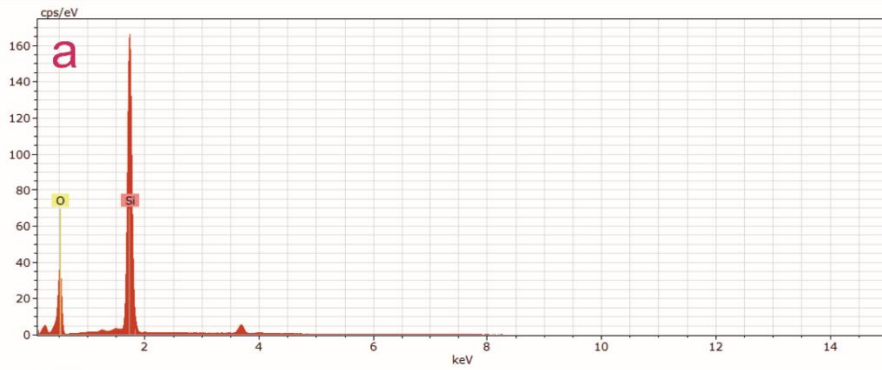
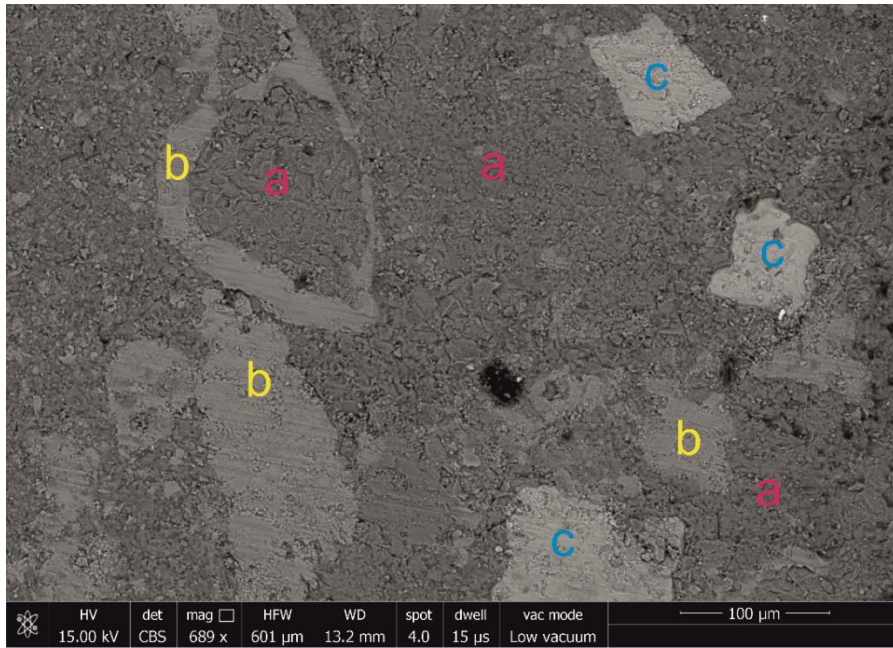


Figure 5-51: SEM image and the semi-quantitative spot analyses of a) Si, b) Si, and Ca and c) Si, Ca and P.

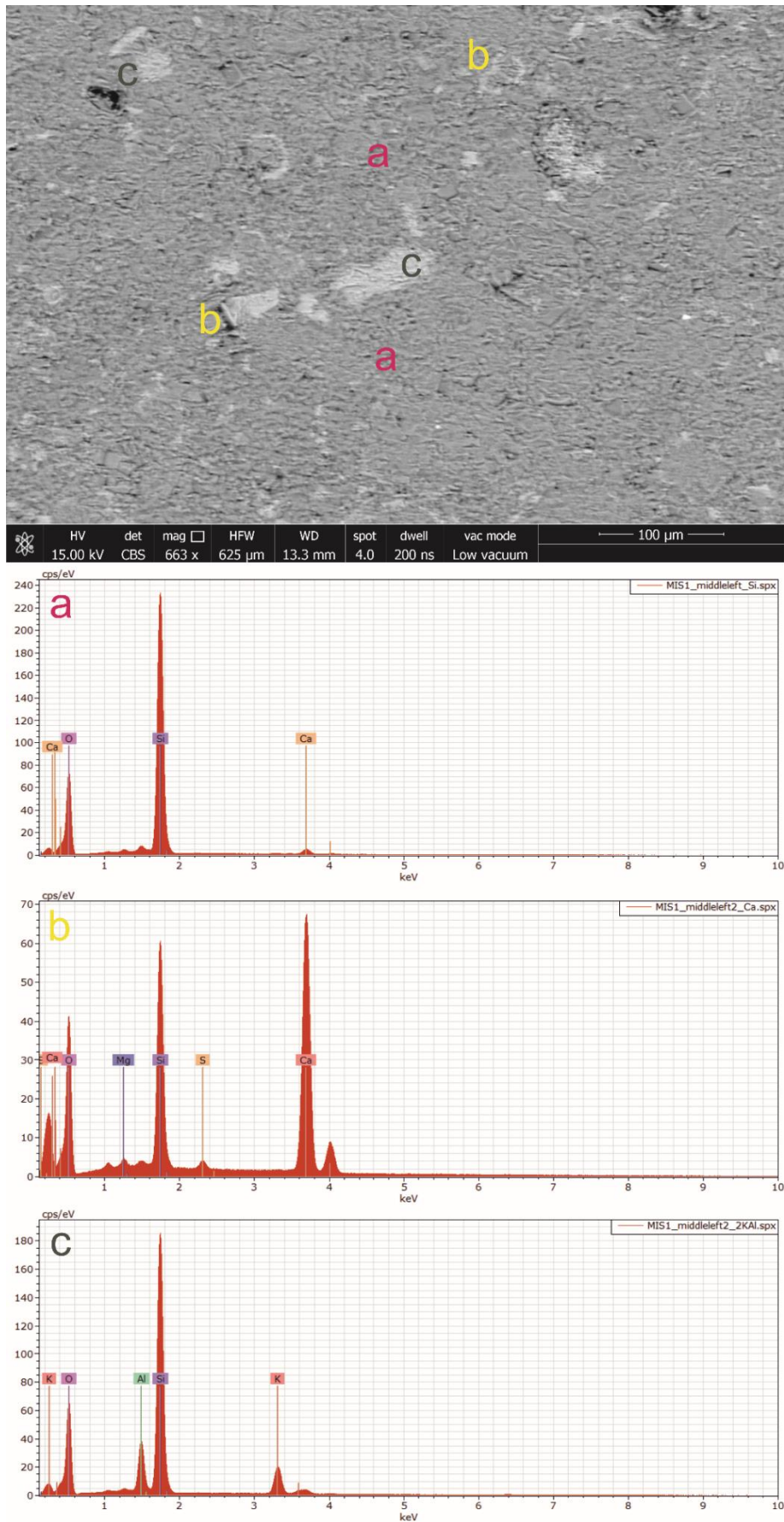


Figure 5-52: SEM image and the semi-quantitative spot analyses of a) Si and Ca, b) Si, Ca, S and Mg and c) Si, Al and K.

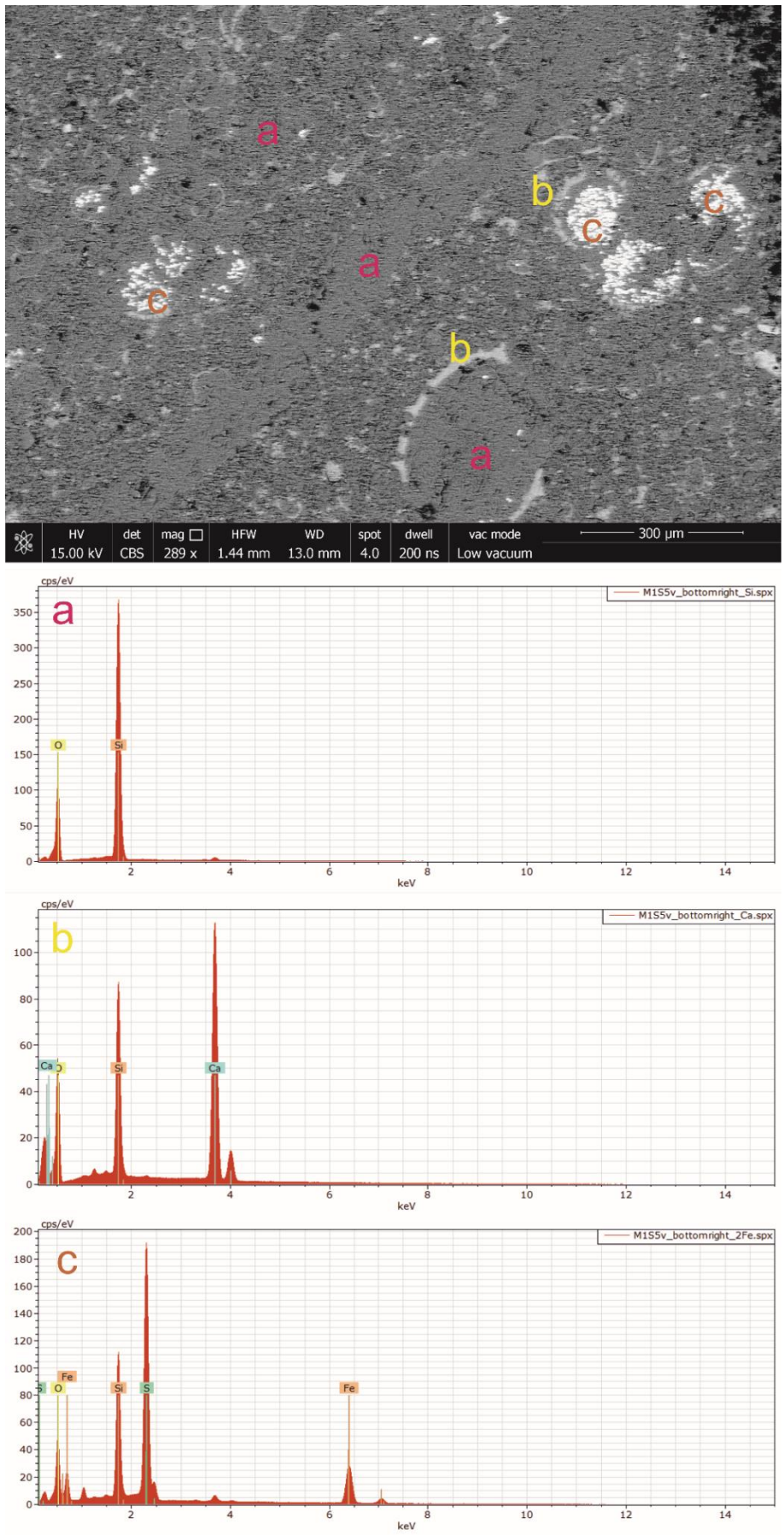


Figure 5-53: SEM image and the semi-quantitative spot analyses of a) Si, b) Si, and Ca and c) Si, S and Fe.

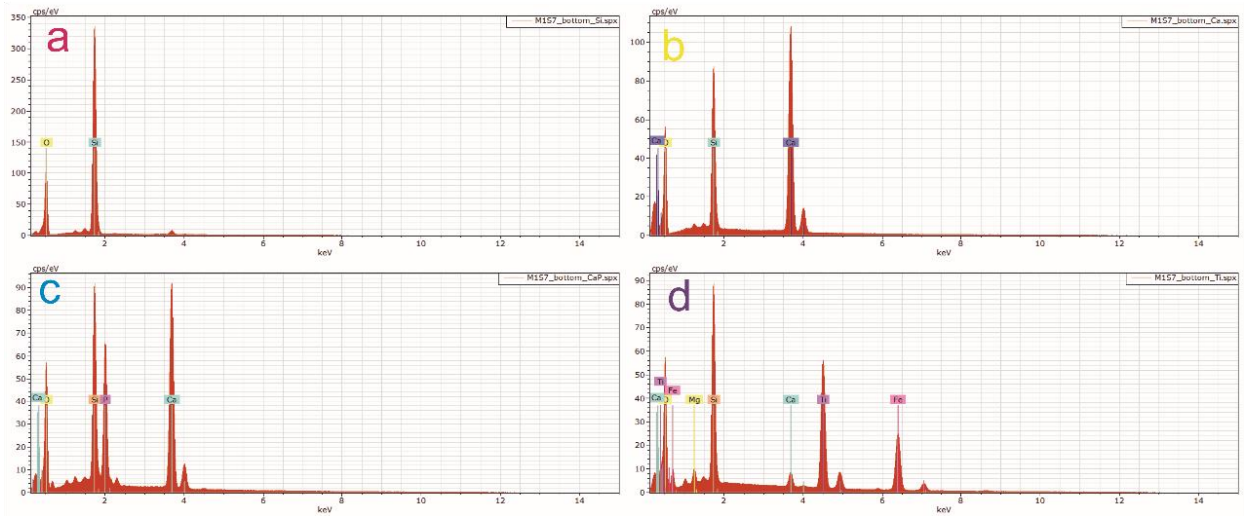
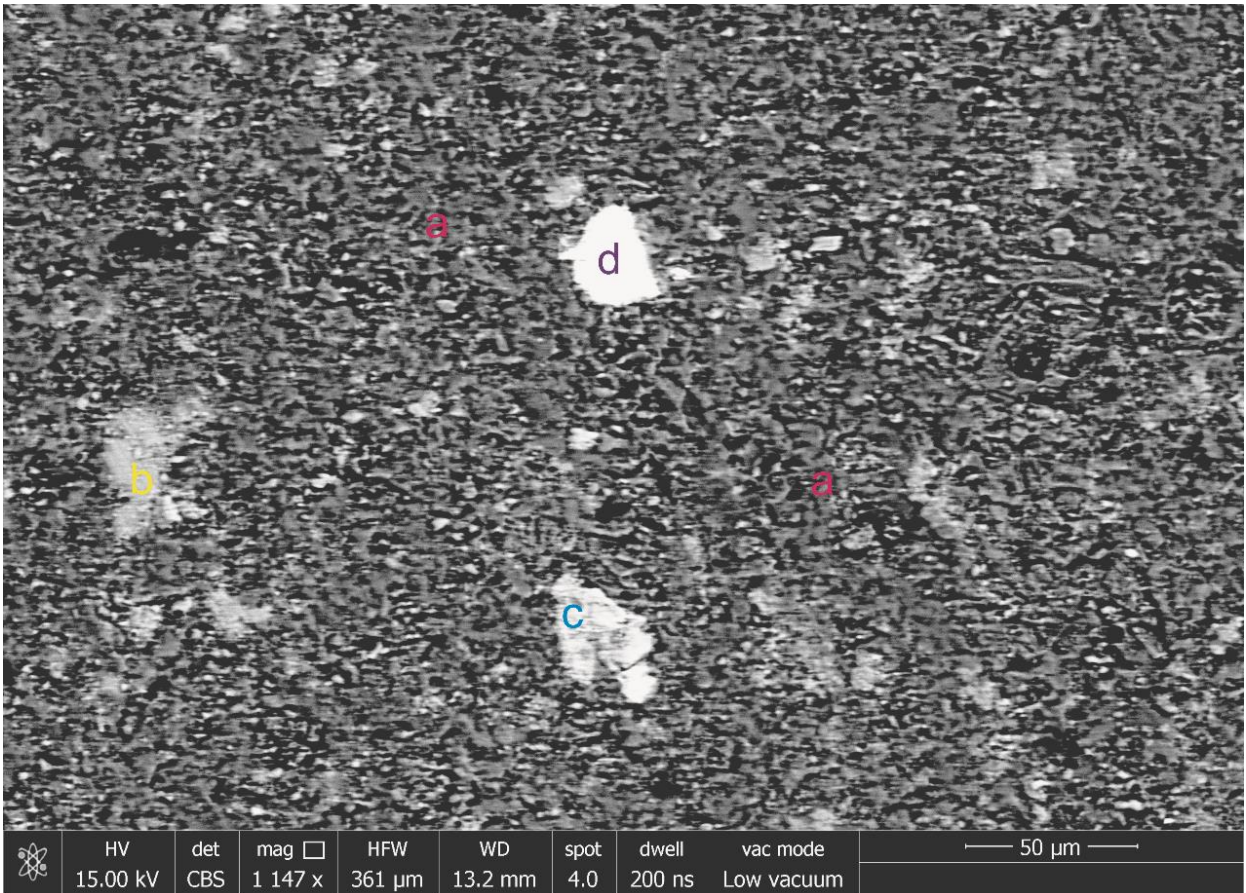


Figure 5-54: SEM image and the semi-quantitative spot analyses of a) Si, b) Si and Ca, c) Si, Ca and P and d) Si, Ti, Fe, Ca and Mg.

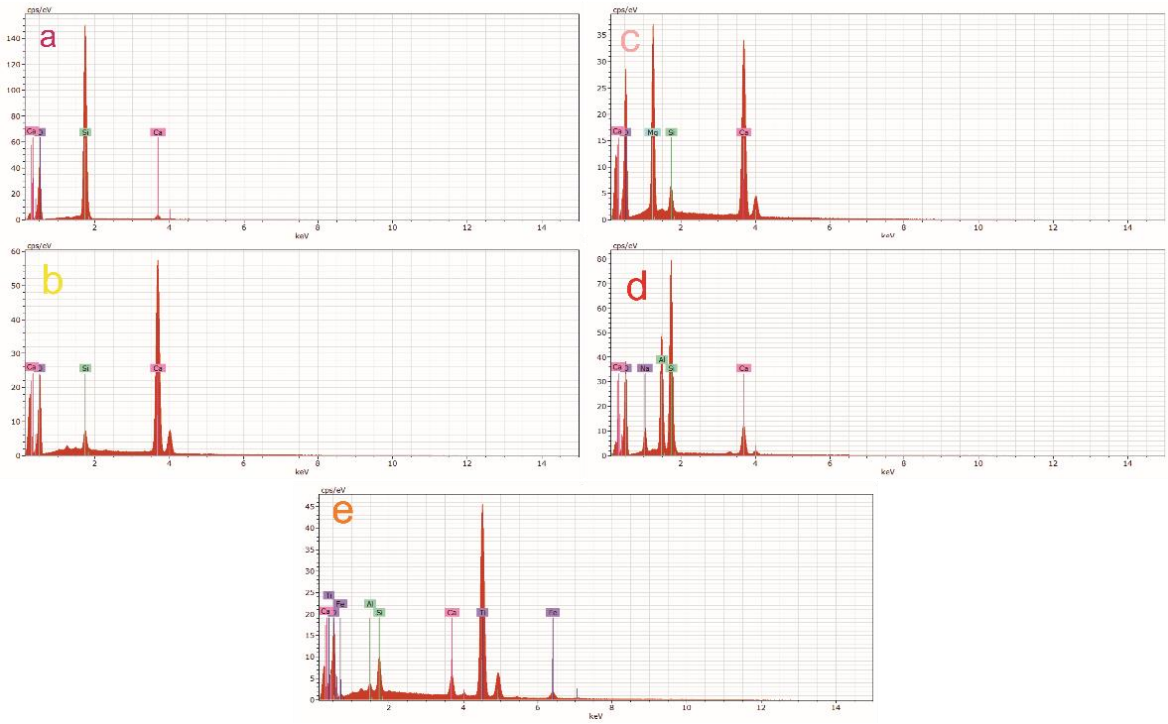
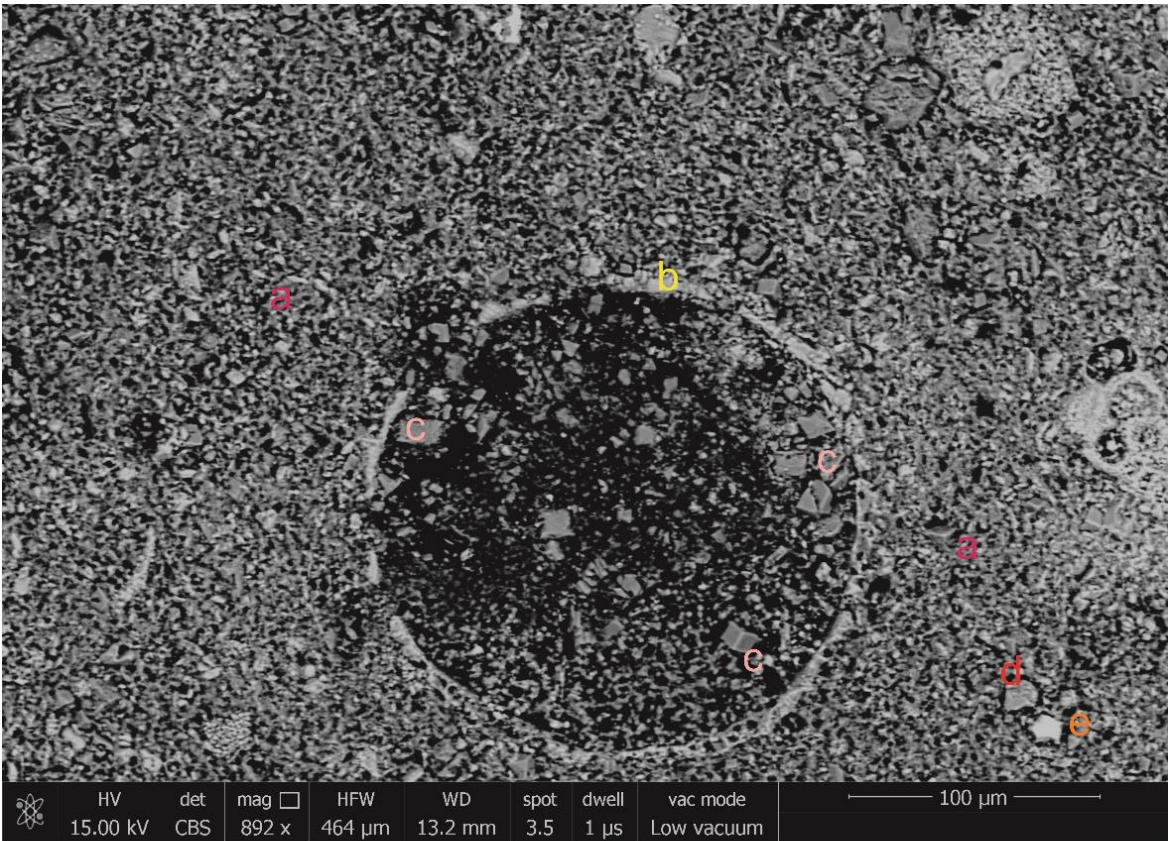


Figure 5-55: SEM image and the semi-quantitative spot analyses of a) Si, b) Si, and Ca, c) Si, Ca and Mg, d) Si, Al, Ca and Na and e) Ti, Si, Ca, Fe and Al.

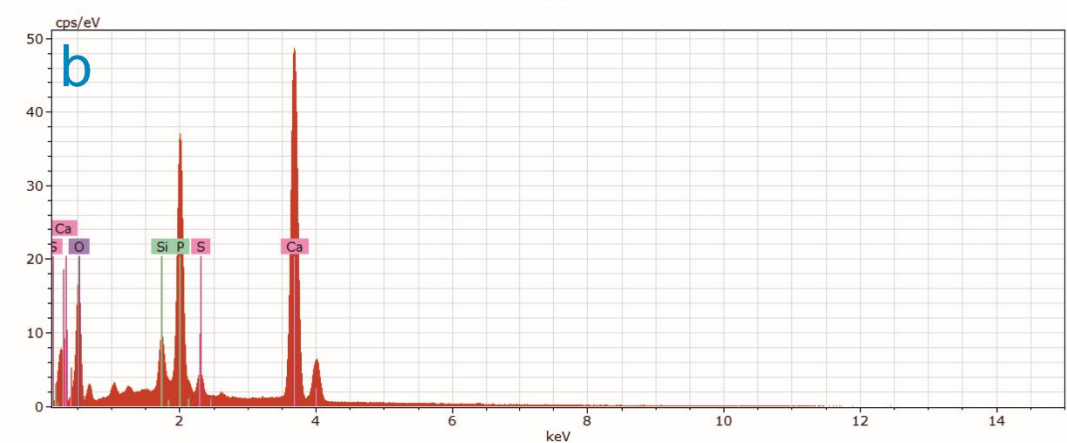
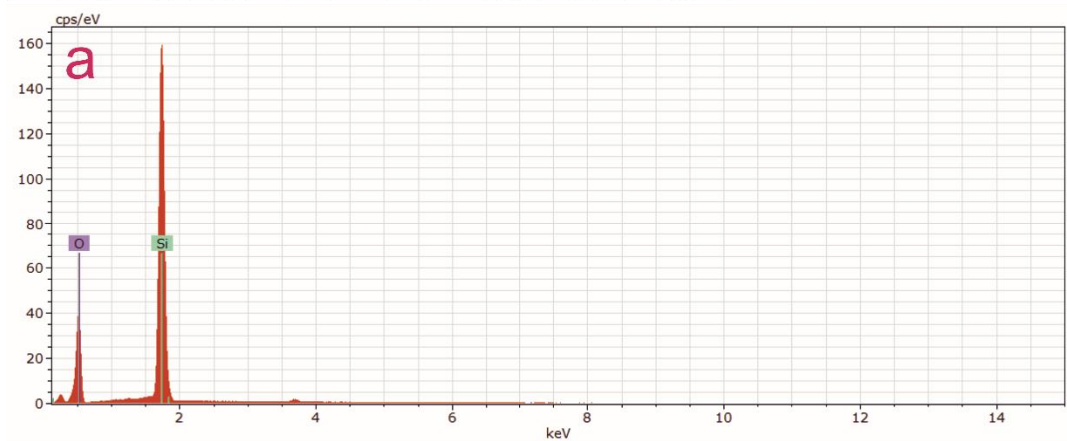
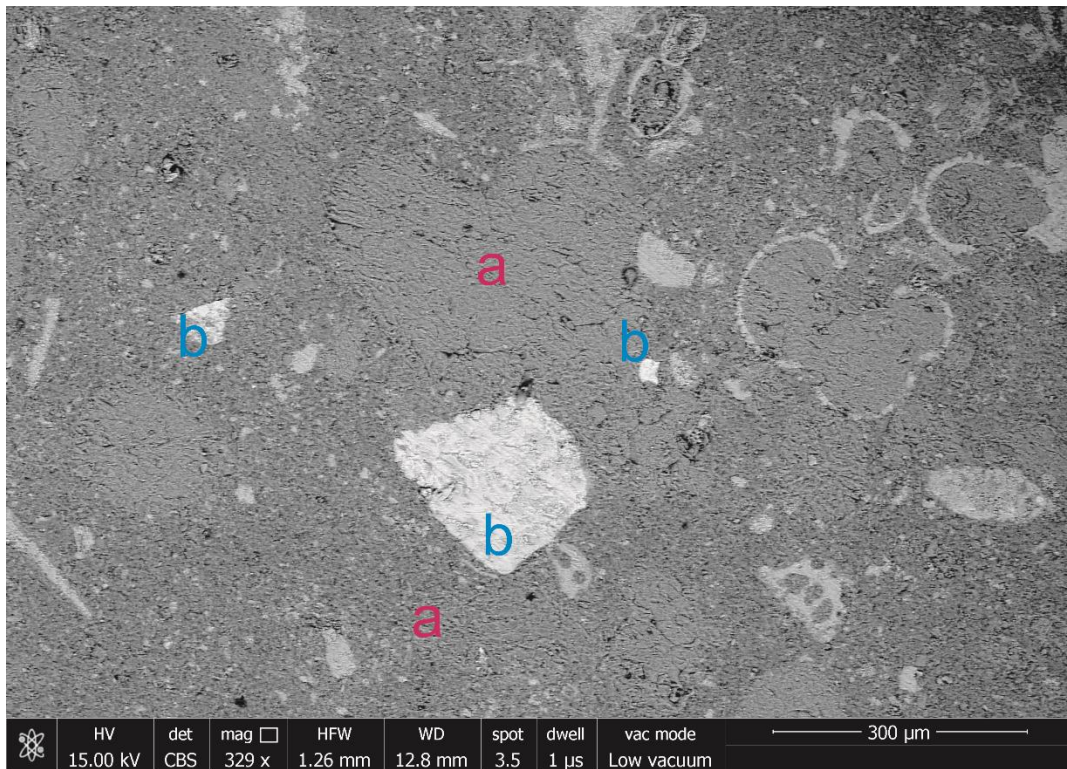


Figure 5-56: SEM image and the semi-quantitative spot analyses of a) Si and b) Si, Ca and P.

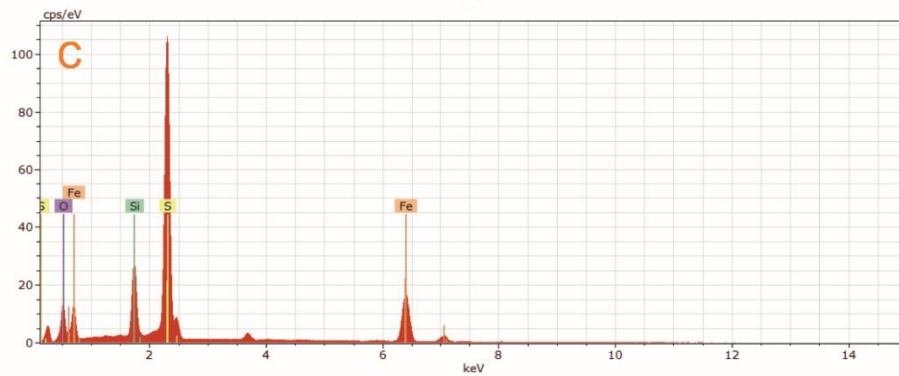
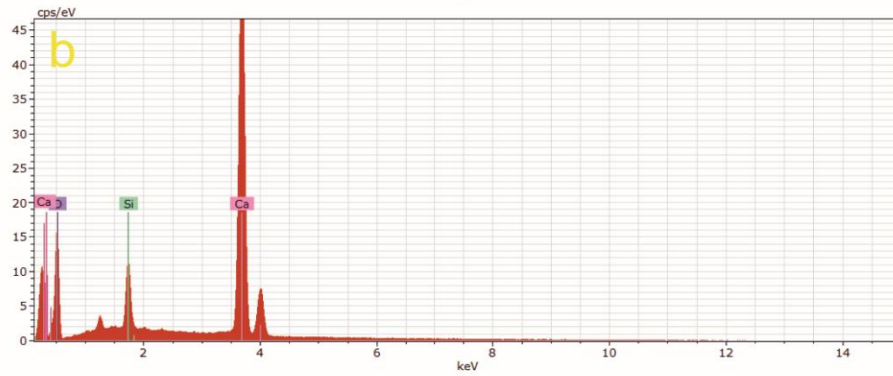
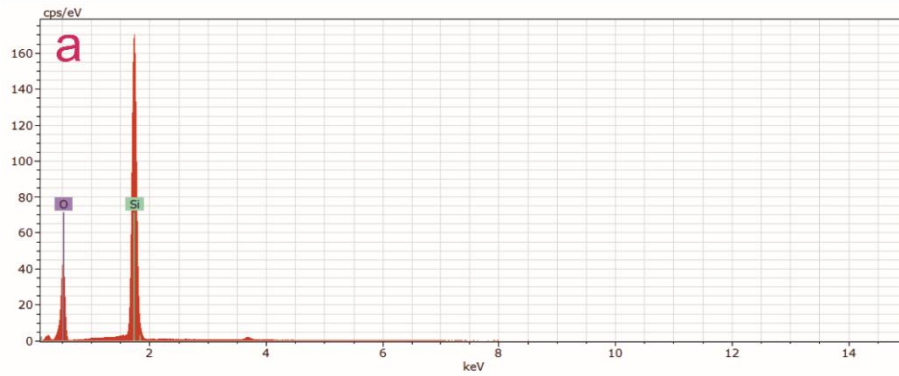
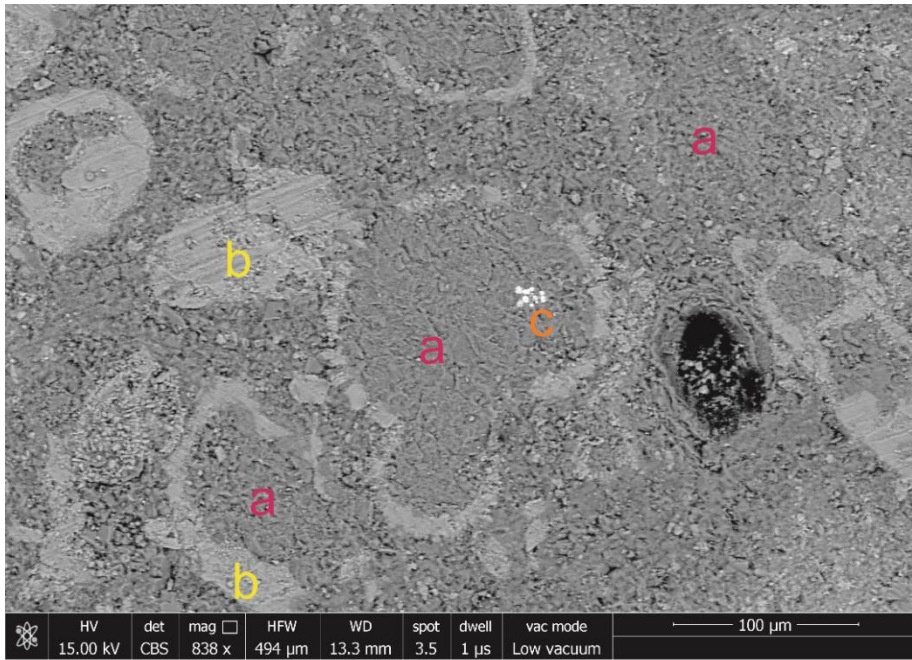


Figure 5-57: SEM image and the semi-quantitative spot analyses of a) Si, b) Si, and Ca and c) S, Si and Fe.

5.4. Fourier-Transform Infrared (FTIR) - Attenuated Total Reflectance (ATR) Spectroscopy

FTIR–ATR is an excellent method to identify the mineralogical content (Chukanov, 2014; Parish, 2013; Olivares et al. 2009; Guiliano et al. 2007) of the examined samples and does not require more than 1 gram of sample. Although it is an invasive technique, it is far less destructive than the two previous methods which required the preparation of thin sections. This method therefore is more appropriate for archaeological research where it is important to preserve the integrity of the archaeological sample. The opportunity to use FTIR-ATR equipment also minimised the need for microscopy, which was employed only on the rock samples. Nonetheless, microscopy is beneficial and necessary as it provides a reference point for the minerals reported in these rock sources and helps the efficient and accurate interpretation of the FTIR–ATR results.

FTIR and ATR are two different parts of the equipment used for this method, which present the same results (spectra). The basic differences are that ATR requires a smaller sample size and less preparation to conduct the analysis. The rock sources are examined with both FTIR and ATR, while the artefact samples are investigated only with ATR. The process followed for the chert rocks increased the accuracy of our results as it worked as an internal standardization of the method. All the FTIR and ATR spectra of the samples are found in the Appendix I (page 64).

Table 5-2: The main and minor peaks of the minerals recorded with the FTIR. These values derived from the Kimmel standards and the work of Parish (2013) and Chukanov (2014).

Minerals	Main Peaks (cm ⁻¹)										
Quartz		1880		1169	1086		798	776	698		517
Opal-CT	2926			1109			795				482
Opal-A			1632		~1099						473
Tridymite		1885	1631	1160	1105		791	668	568	535	480
Calcite	2516		1795	1420-40		875	713				
Dolomite	2372	2344	1810	1444		881	729				
Jasper		1872	1167		1085	798	779	695	557		459
Flint		1641		1166	1087				552	509	463

Table 5-3: The main and minor peaks of the minerals recorded with the ATR. These values derived from the work of Parish (2013) and Müller et al. (2012 and 2014).

Minerals	Main Peaks ATR (cm ⁻¹)										
Quartz		1879		1169	1080		798	779	695	514	450
Opal-A			1637		~1099						473
Tridymite		1885	1631		1105		791	668	568	535	480
Calcite	2516		1794	1400		875	712				
Dolomite	2372			1444		881	727				
Montmorillonite			1640			1040	885		530	467	

5.4.1. Chert Formations

5.4.1.1. Maltese Islands

The chert samples of Malta present spectra with peaks that relate predominantly to silicate and carbonate minerals. The main peak in most of the spectra falls within 1098 and 1100 cm^{-1} , which relate to the opal-A mineral (Fig. 5.58a). An additional smaller peak (about 472 cm^{-1}) within absorbance bands is also associated with this type of mineral. These findings suggest that opal-A is the predominant mineral of these chert outcrops. The secondary peaks (e.g. 1632, 789 cm^{-1}) which are recorded in the spectra signify the presence of tridymite minerals in most of the samples. There is one sample (F1S2) that also has the principal peak (1104 cm^{-1}) in the absorbance bands of tridymite minerals (Fig. 5.58b). This is the only sample of Malta, which is dominated by tridymite, while opal-A is recorded with minor peaks (i.e. 1632 and 472 cm^{-1}). Quartz has been only identified by a minor peak (1879 cm^{-1}), which however is not recorded in all the samples. The second highest peak (1437 cm^{-1}) of the FTIR spectra, signifies the presences of calcite in all the samples (Fig. 5.58). Moreover, minor peaks (e.g. 1793, 879 cm^{-1}) are in absorbent bands which are also related to calcite and suggest that this mineral is the second most abundant mineral after opal-A. Dolomite is the second carbonate mineral reported in the chert outcrops of Malta (Fig. 5.58b) and is identified by a minor peak (728 cm^{-1}). This mineral is found only in samples from the centre of Fomm-IR-RiĦ Bay (e.g. F1S2, M1S5) or close to the archaeological site (i.e. M1S9). Lastly, the FTIR examination records some minor peaks (e.g. 2854, 2003, 1869 cm^{-1}) which have not been connected with specific minerals.

The chert samples of Gozo also present spectra with peaks related to silicate and carbonate minerals. The main peak (e.g. 1098 cm^{-1}) is found within the absorbance bands of the opal-A mineral (Fig. 5.59). This in addition to the two smaller peaks (e.g. 1637, 472 cm^{-1}) confirms the dominance of opal-A minerals in these chert samples. Tridymite is reported in these chert samples (Fig. 5.59b), but only with one characteristic secondary peak (about 789 cm^{-1}). Additionally, the FTIR spectrum of only one sample (i.e. G2S6) presents peaks (i.e. 1879, 695 cm^{-1}) characteristic of quartz minerals (Fig. 5.59a). The second higher peak of almost all the spectra falls within the absorbance bands of 1030 and 1040 cm^{-1} . These peaks and the two minor peaks (i.e. 874, 713 cm^{-1}) signify the presence of calcite minerals. Dolomite minerals are reported only in the chert samples collected from the lower part of the Globigerina Limestone formation. The spectra of these samples show a secondary peak (728 cm^{-1}), which is within the expected absorbance bands for dolomite (Fig. 5.59b). The only exception is one chert sample (i.e. G2S6), which does not present any peak related to carbonate minerals (Fig. 5.59a). Finally, another sample (i.e. F1S4) presents some minor peaks (e.g. 2927 and 2002 cm^{-1}) which could not be connected with specific minerals.

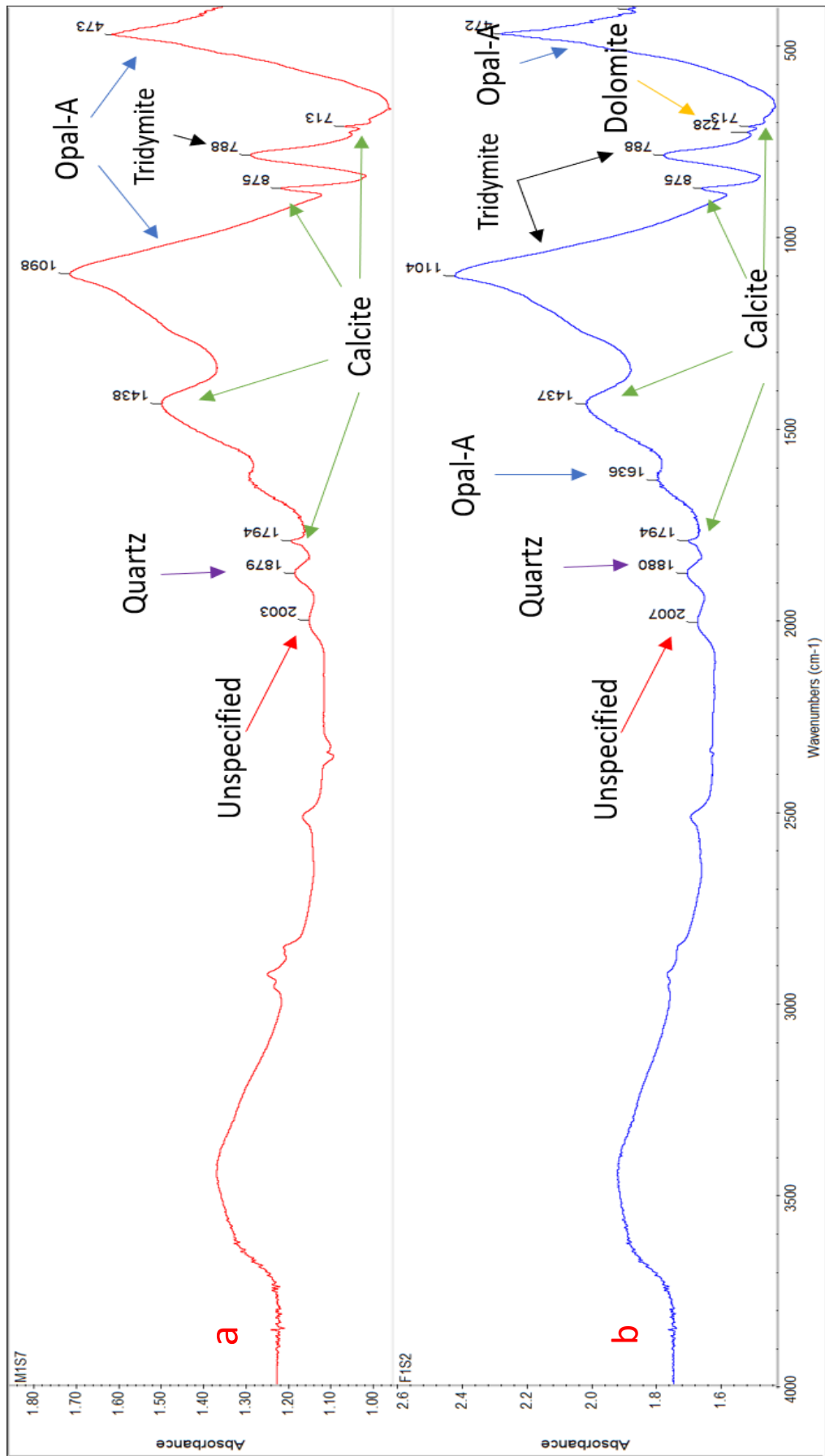


Figure 5-58: Representative FTIR spectra of the chert samples from Malta.

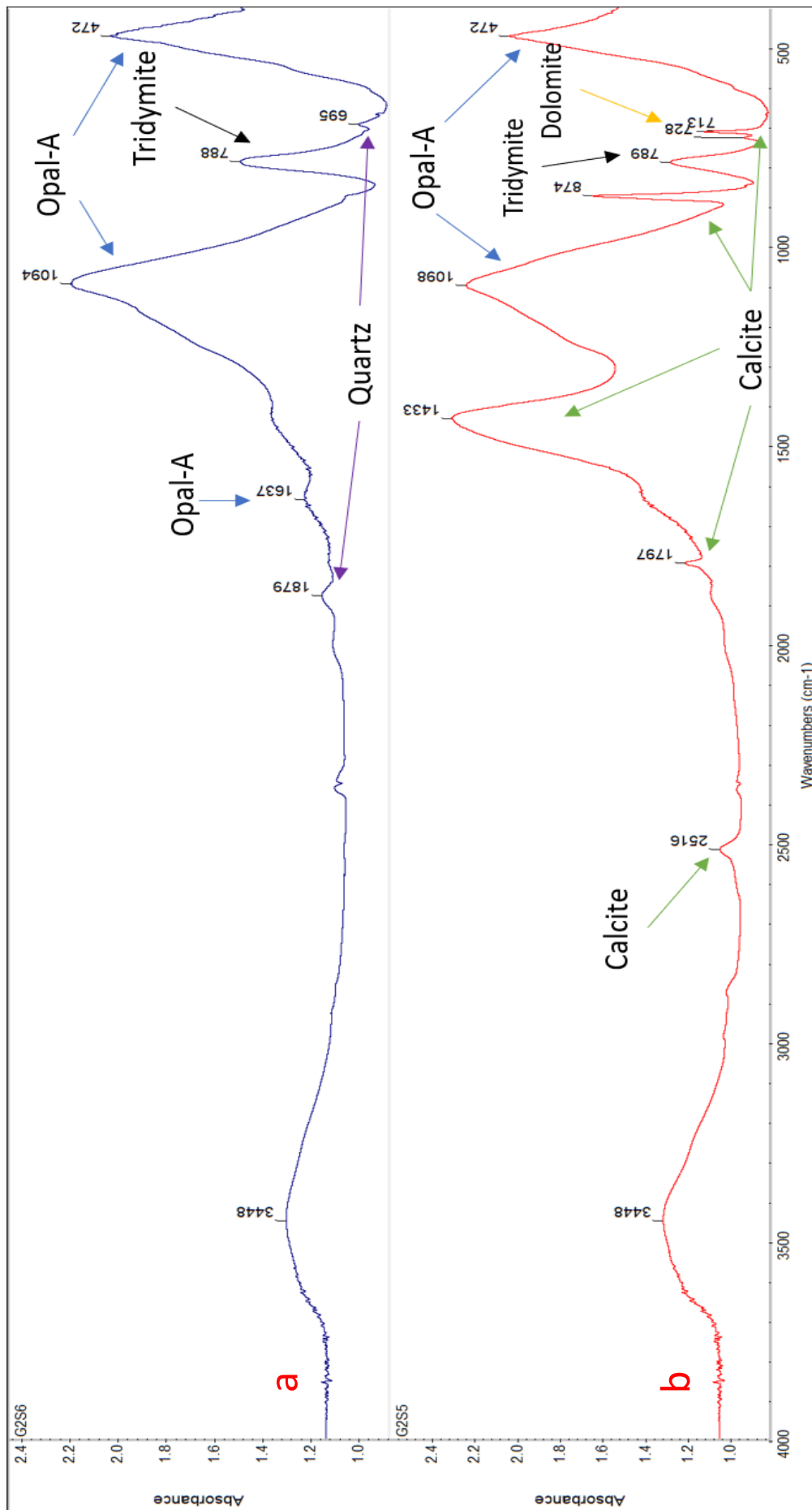


Figure 5-59: Representative FTIR spectra of the chert samples from Gozo.

5.4.1.2. Sicily

The spectrum of chert samples from Monte Tabuto presents three main peaks (e.g. 1084, 797, 778 cm^{-1}) which are within the absorbance bands of quartz minerals (Fig.5.60). Some minor peaks (e.g. 555 and 502 cm^{-1}) are recorded, but they are not directly related to minerals. The reference library (the Kimmel standards) of FTIR suggests that these peaks are within the absorbance bands of the flint and jasper rocks. This is considered as one more evidence of the dominance of silicate minerals in the samples. Nevertheless, some peaks are recorded to fall between 1420 and 1431 cm^{-1} which are values related to calcite (Fig. 5.60a). The chert samples from Modica area present similar spectra and quartz is the main mineral. The only exception lies in one sample (e.g. sample S2), which has a spectrum dominated by calcite. The main peaks are within the expected absorbance bands of calcite minerals while it has only a small peak (1099 cm^{-1}) which is related with opal-A. Finally, two samples (i.e. S1 and S3) have two minor peaks (i.e. 1611 and 613 cm^{-1}) which cannot be connected with specific minerals.

The chert samples from the Monterosso Almo area are dominated by quartz, but calcite is also recorded in the spectra. The samples from the old quarry present a main peak between 1082 and 1090 cm^{-1} , which is related to quartz. There are also other peaks (e.g. 1166, 797 and 778 cm^{-1}) within absorbance bands of quartz, which support the dominance of this mineral. The only exception is the spectrum of one sample (S15) which has a main peak value (1093 cm^{-1}) similar to the values of cristobalite. Furthermore, it has some minor peaks (e.g. 1870 and 472 cm^{-1}) within the absorbance bands of Jasper and opal-A. Calcite is reported in some of the samples, with minor peaks (e.g. 1794, 875 and 713 cm^{-1}), while the FTIR examination has recorded some other minor peaks which cannot be connected with specific minerals (e.g. 1993, 1617 and 612 cm^{-1}).

The samples (i.e. S18, S20, S21) of the Eocene chert outcrop present peaks (e.g. 1166, 797, 778, 694 and 457 cm^{-1}) within the expected absorbance bands of quartz (Fig. 5.60b). In addition, their main peak falls within 1083 and 1085 cm^{-1} which supports the dominance of this mineral in these samples. Some minor peaks (e.g. 1870, 558 and 508 cm^{-1}) are within the absorbance bands of the flint and jasper rock material. Calcite minerals are recorded with minor peaks (i.e. 1794, 1420 and 878 cm^{-1}), but only in some samples (Fig. 5.60b). Moreover, the FTIR examination has recorded some minor peaks which have not being connected with specific minerals (e.g. 1993, 1618 and 612 cm^{-1}) but can be compared to other Sicilian samples. The chert sample (i.e. S19) from the conglomerate outcrops has an almost identical spectrum with the Eocene cherts but does not have any peak related with calcite minerals.

The chert samples of the Triassic limestones consist mainly of silicate and carbonate minerals. The main peak has values (i.e. 1097 or 1101 cm^{-1}) related to opal-A or Tridymite. Moreover, secondary peaks (e.g. 1165, 798 and 777 cm^{-1}) are also attributed to the presence of quartz. Some minor peaks (e.g. 1870 and 505 cm^{-1}) are related to flint and jasper rocks which have a characteristic similar to the Tabuto chert samples. Calcite is identified in these samples with peaks (e.g. 1420, 876 and 713 cm^{-1})

within the expected absorbance bands. Furthermore, one sample (i.e. S4) presents a minor peak (i.e. 728 cm^{-1}) which suggest the presence of dolomite. This sample also presented peaks (e.g. 1048 cm^{-1}) within the absorbance bands of montmorillonite minerals.

The samples of the Radiolarian formation show peaks which are within the absorbance bands of quartz. Additionally, the actual values of these peaks (e.g. $1166, 1086, 798, 779, 695$ and 462 cm^{-1}) are almost identical with those of the FTIR quartz reference. These samples also present minor peaks (e.g. 1870 and 508 cm^{-1}) within the absorbance bands of jasper. Moreover, the FTIR examination has recorded some minor peaks which are not attributed to any specific mineral (e.g. 1617 cm^{-1}).

The chert samples from the area of Monte Santo (East Sicily) are dominated by quartz, but calcite minerals are also reported. The FTIR spectra present peaks (e.g. $1086, 797, 778\text{ cm}^{-1}$), which are within the absorbance bands of quartz (Fig. 5.60a). In addition, some secondary peaks (e.g. 1870 and 456 cm^{-1}) are reported within the absorbance bands of the jasper. Lastly, the calcite is recorded in the spectra with secondary peaks (e.g. $1794, 1420, 876$ and 713 cm^{-1}) in expected absorbance bands (Fig.5.60a).

The chert samples from the western Sicilian outcrops present spectra dominated by quartz minerals. The sample of the black chert outcrop has a main peak (1085 cm^{-1}) within the absorbance bands of quartz and in addition other smaller peaks (e.g. $1166, 797, 779, 694$ and 462 cm^{-1}) which also denote the dominance of quartz within this sample. Moreover, the spectrum presents one absorbance peak (i.e. 1870 cm^{-1}) which is related to jasper. The FTIR examination recorded only one minor absorbance peak (i.e. 1793 cm^{-1}) related to calcite. The investigation has further recorded some minor peaks (e.g. $1996, 1617$ and 613 cm^{-1}), which have not been connected with specific minerals. The chert samples related with volcanic formations (i.e. S24) demonstrate the main peak (i.e. 1082 cm^{-1}) suggesting the dominance of quartz. This is supported from additional smaller peaks (e.g. $1166, 797, 778, 694$ and 459 cm^{-1}) which are within the expected absorbance bands of this mineral. Additionally, it presents one absorbance peak (i.e. 1871 cm^{-1}) which is related to jasper. The spectrum of this sample has recorded only one minor peak (i.e. 1793 cm^{-1}) related to calcite minerals, while it has some minor peaks (e.g. 1993 and 1618 cm^{-1}) which have no connection with any specific minerals. The chert sample from the Jurassic outcrop (i.e. S25) presents the main peak (1086 cm^{-1}), which signifies the dominance of quartz. This is supported by additional smaller peaks (e.g. $1166, 797, 778, 693$ and 459 cm^{-1}) within the absorbance bands of this mineral. Furthermore, it presents one absorbance peak (i.e. 1871 cm^{-1}) which is related with jasper. Similarly, with the other samples of Western Sicily, it has one minor peak (i.e. 1794 cm^{-1}) which records the presence of calcite. Finally, it has also presented the same undefined minor peaks (e.g. $1993, 1618$ and 613 cm^{-1}).

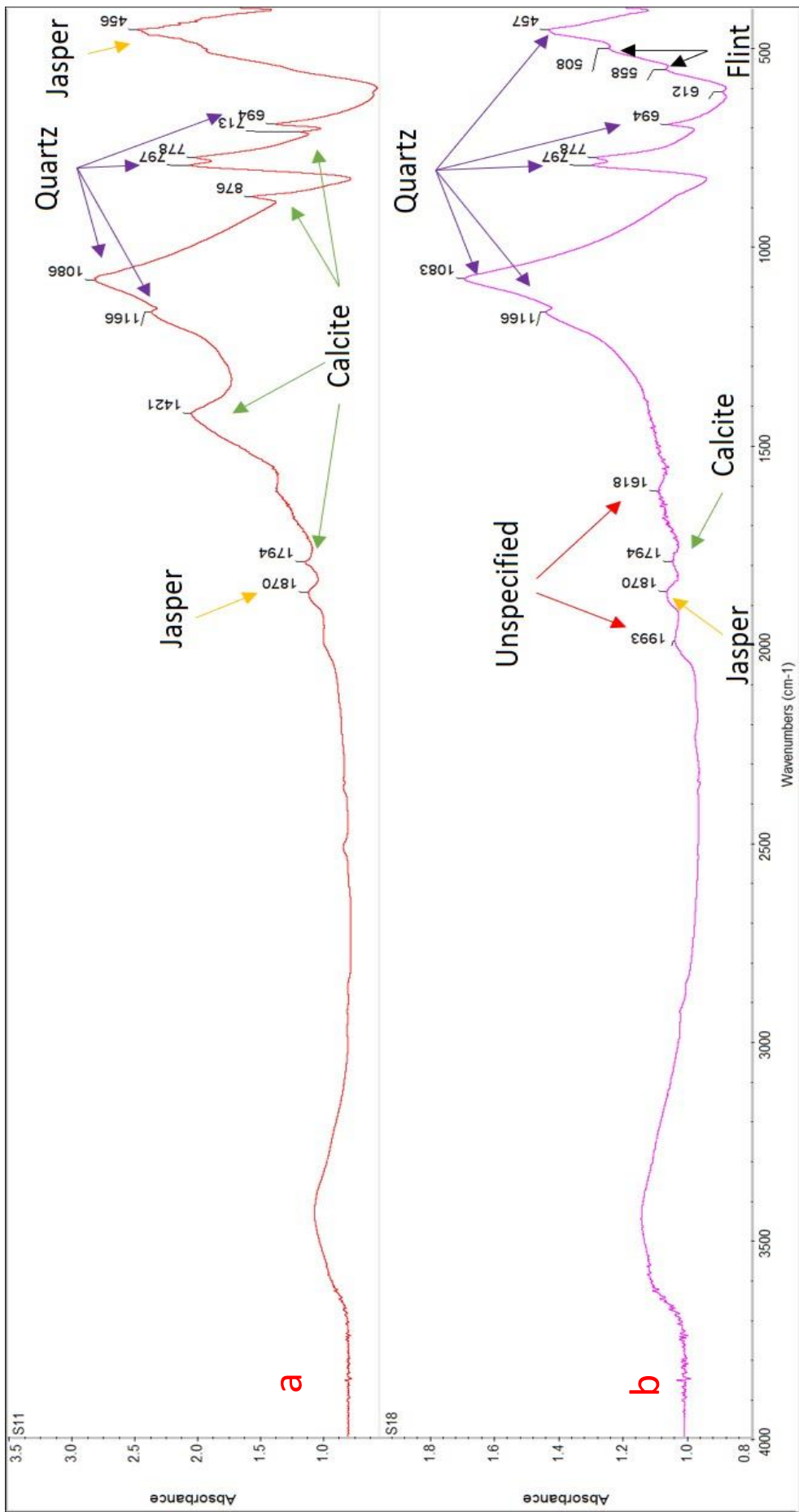


Figure 5-60: Representative FTIR spectra of the chert samples from Sicily.

5.4.2. Chert Assemblages

The samples of the assemblages are analysed only with the ATR equipment to reduce the negative effect of this method to the minimum. However, the literature (Parish et al., 2013; Müller et al. 2012 and 2014) suggests that the peak values of the minerals are slightly different from those discerned using FTIR. The rock samples have been examined with both sets of equipment to contribute towards the accurate interpretation of these ATR results. This cross-examination has shown that the peak values of a mineral are slightly shifted on the ATR spectra.

5.4.2.1. The Circle assemblage

The majority of the samples from this assemblage present spectra with peaks within the absorbance bands of quartz. Moreover, they have their main peak values close to 1080 cm^{-1} ($\pm 4\text{ cm}^{-1}$) which is characteristic for quartz (Fig. 5.61a). Another characteristic feature of these spectra is the two neighbouring peaks that also suggest the dominance of quartz. The one fell within the absorbance bands of 778 and 780 cm^{-1} , while the second is between 796 and 799 cm^{-1} (Fig. 5.61a). These samples also show peaks within absorbance bands that are related to flint (e.g. 1163 and 554 cm^{-1}). The only exception is one sample artefact (i.e. BR89/S566/L622) which presents the main peak (1070 cm^{-1}) and a minor peak (i.e. 461 cm^{-1}) within the restricted bands of the opal-A mineral (Fig. 5.61b). Furthermore, it presents a single peak (788 cm^{-1}) in the area that a quartz mineral has two peaks (Fig. 5.61b) which is attributed to tridymite. The examination of the spectra recorded two samples (i.e. BR89/S566/L622 and BR89/S767/L783) with peaks (e.g. 1435 , 874 and 712 cm^{-1}) which fall within the absorbance bands of calcite (Fig. 5.61b).

5.4.2.2. Kordin assemblage

Most of the samples from this assemblage present spectra with peaks within the absorbance bands of quartz. Moreover, they have their main peak values close to 1080 cm^{-1} ($\pm 4\text{ cm}^{-1}$) which is characteristic for quartz (Fig. 5.61c). They also have the two-neighbouring-peaks feature which indicate the dominance of Quartz. One falls within the absorbance bands of 778 and 780 cm^{-1} , while the second is between 795 and 799 cm^{-1} (Fig. 5.61c). In addition, these samples have peaks within absorbance bands which are related to flint (e.g. 1163 , 555 and 462 cm^{-1}). The only exception is one sample (i.e. KRD15/S1/L22) which shows a principal peak (i.e. 1071 cm^{-1}) and a minor peak (i.e. 464 cm^{-1}) within the restricted bands of the opal-A mineral (Fig. 5.61d). Furthermore, it also presents a single peak (i.e. 786 cm^{-1}) in the area where the quartz minerals have two peaks (Fig. 5.61d) which is attributed to the presence of tridymite in this sample. The examination of the spectra has recorded one sample (i.e. KRD15/S1/L22) with peaks (e.g. 1435 , 874 and 712 cm^{-1}) that fall within the absorbance bands of calcite (Fig. 5.61d).

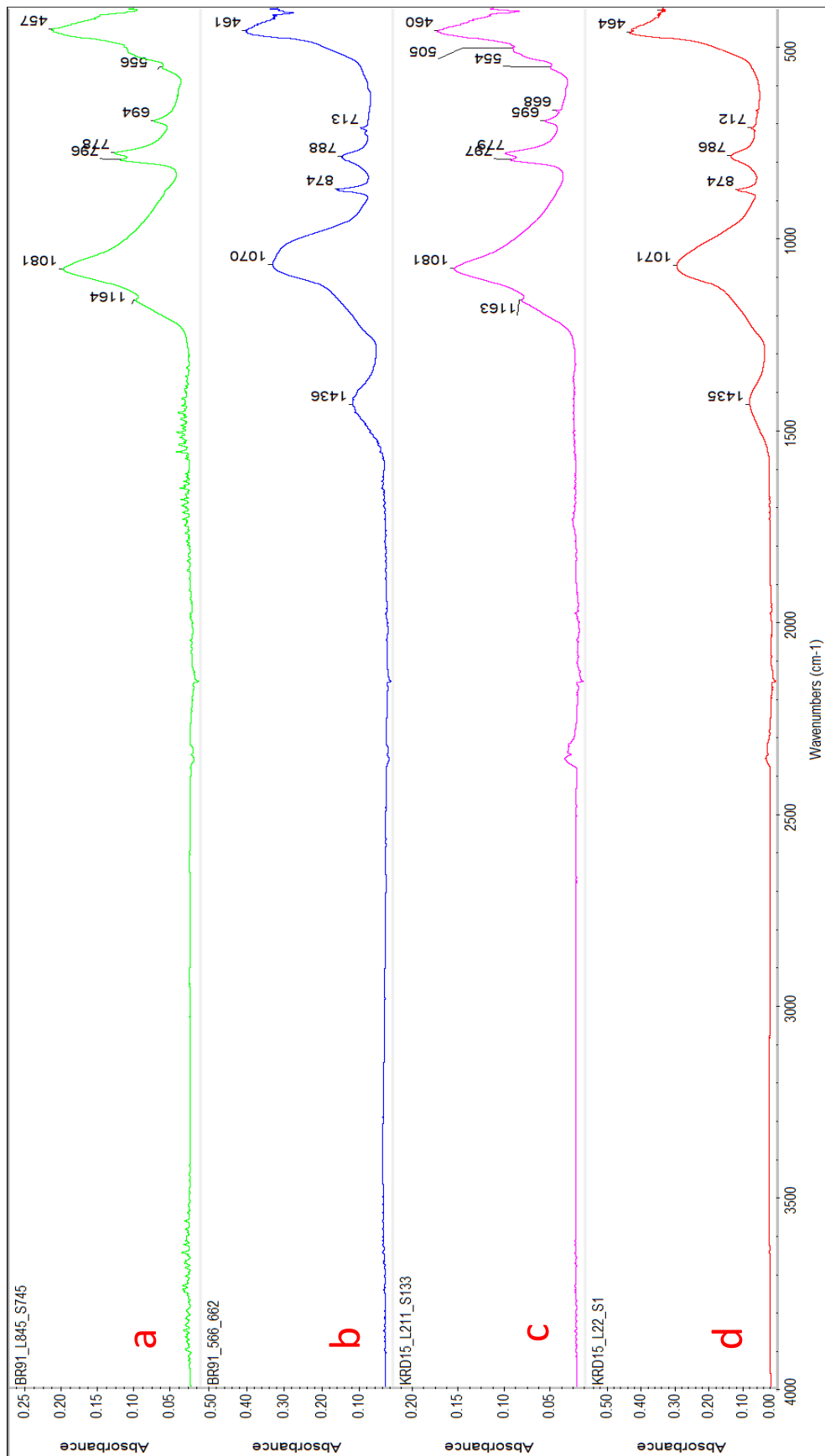


Figure 5-61: Representative ATR spectra of the artefact samples from the Circle and Kordin. Quartz is represented in these spectra with peaks around 1080 and 694 cm^{-1} , between 778 and 780 cm^{-1} and between 795 and 799 cm^{-1} . Flint is represented in these spectra with peak around 1163, 555 and 462 cm^{-1} . Opal-A is represented in these spectra with peak around 1070 cm^{-1} , 788 cm^{-1} and 464 cm^{-1} . Calcite is represented in these spectra with peak around 1435, 874 and 712 cm^{-1} .

5.4.2.3. Taç-Cawla assemblage

The samples from this assemblage present predominantly spectra with peaks within the absorbance bands of quartz. Moreover, they have a main peak with values close to 1080 cm^{-1} ($\pm 4\text{ cm}^{-1}$) which is characteristic of quartz (Fig. 5.62a). Another characteristic feature of these spectra is the two neighbouring peaks that also suggest the dominance of quartz. One falls within the absorbance bands of 777 and 780 cm^{-1} , while the second is between 795 and 799 cm^{-1} (Fig. 5.62a). These samples also show peaks within absorbance bands that are related to flint (e.g. 1163 and 554 cm^{-1}). There is one sample (i.e. TCC14/S513/L272) which has the main peak (i.e. 1074 cm^{-1}) and a minor peak (i.e. 464 cm^{-1}) within the restricted bands of the opal-A mineral (Fig. 5.62b). In addition, it presented a single peak (i.e. 787 cm^{-1}) in the area where the samples with quartz have two peaks (Fig. 5.62b) and is attributed to tridymite. This assemblage presented two samples (i.e. TCC14/S37/L30 and TCC14/S103/L85) with mixed results that make it difficult to identify conclusively their silicate minerals. Their main peak (i.e. 1074 cm^{-1}) is related with opal-A minerals, but at the same time, their spectrum has the two-neighbouring-peaks feature which is related to quartz minerals. The value of the main peak is on the borderline of the band for opal-A, but the cross-examination between FTIR and ATR suggested that such values can also be attributed to tridymite. They do not have the minor peak (e.g. 464 cm^{-1}) related with the opal-A mineral, but one of them (i.e. TCC14/S37/L30) has a peak at 668 cm^{-1} which is within the bands of the tridymite mineral. Therefore, it possible that these samples are consisted mainly of tridymite and quartz and with no opal-A minerals. Finally, the examination of the spectra records few samples (e.g. TCC14/S513/L272 and TCC14/S37/L30) with peaks (e.g. 1429 and 875 cm^{-1}) which fall within the absorbance bands of calcite (Fig. 5.62b).

5.4.2.4. Santa Verna assemblage

The majority of the samples from this assemblage present spectra with peaks within the absorbance bands of quartz. Moreover, they have a main peak with values close to 1080 cm^{-1} ($\pm 4\text{ cm}^{-1}$) which is characteristic of quartz minerals (Fig. 5.62c). They also have the two-neighbouring-peaks feature which indicates the dominance of quartz. One falls within the absorbance bands of 777 and 780 cm^{-1} , while the second is between 795 and 799 cm^{-1} (Fig. 5.62c). These samples also have peaks within absorbance bands that are related to flint (e.g. 1162 and 554 cm^{-1}). There are two samples (i.e. SV15/S144/L42, SV15/S134/L58) which present features and peaks suggesting their dominance of tridymite mineral (Fig. 5.62d) Moreover, they have a single peak (i.e. 786 cm^{-1}) in the area where the quartz related samples present two peaks. In addition, they have a peak at 668 cm^{-1} ($\pm 1\text{ cm}^{-1}$), while there is no minor peak at 462 cm^{-1} ($\pm 3\text{ cm}^{-1}$). The value of their main peak (e.g. 1074 cm^{-1}) is on the borderline between opal-A and Tridymite minerals. Furthermore, this assemblage also presents one sample (i.e. SV15/S1/L34) with a combination of two silicate minerals. The main peak (i.e. 1075 cm^{-1})

is related to tridymite, but at the same time, the spectrum has the two-neighbouring-peaks feature which is related to quartz minerals. Finally, these three samples are the only ones with peaks (e.g. 1419 and 874 cm^{-1}) falling within the absorbance bands of calcite (Fig. 5.62d).

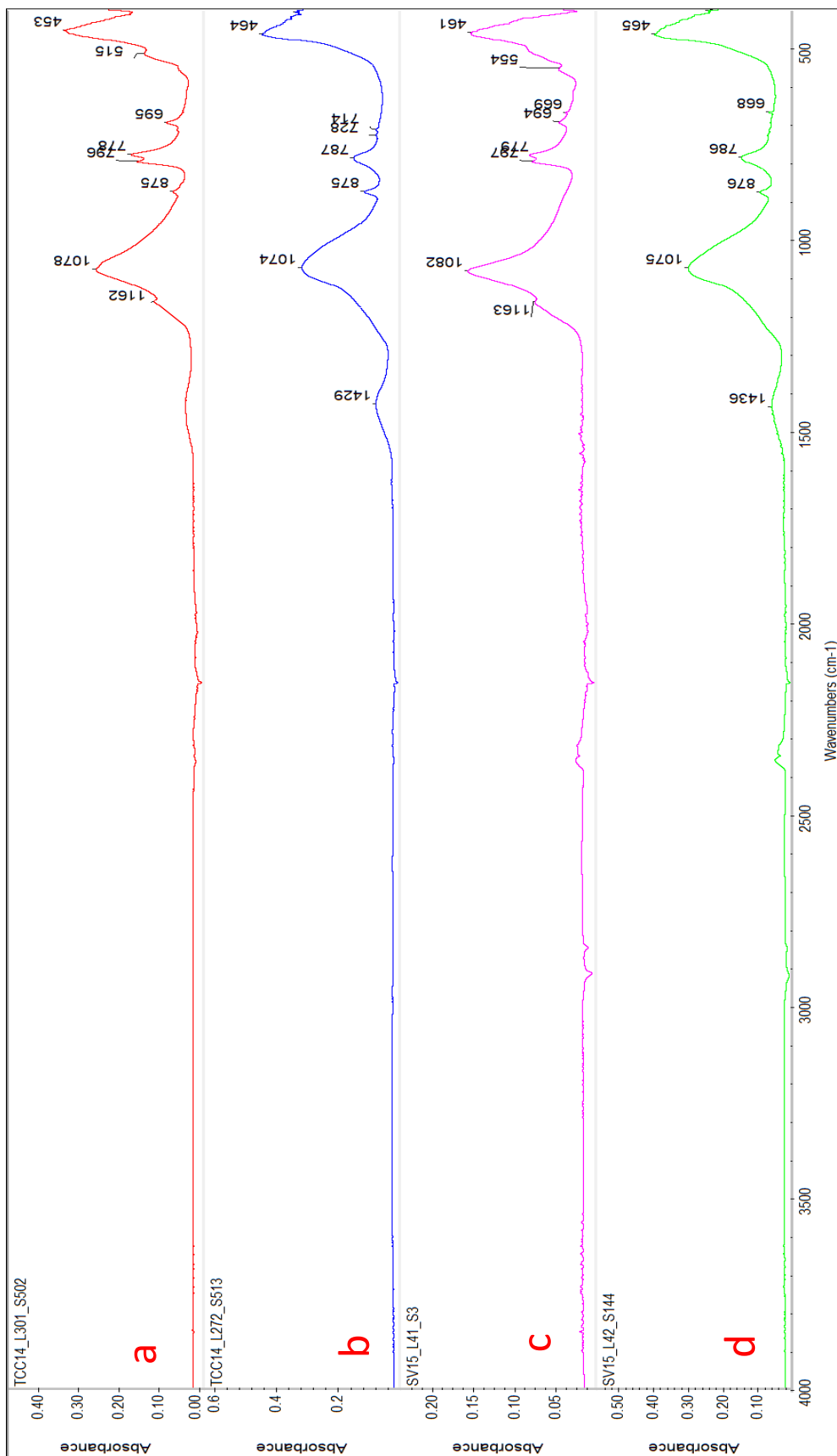


Figure 5-62: Representative ATR spectra of the artefact samples from Tač-Ćawla and Santa Verna. Quartz is represented in these spectra with peaks around 1080 and 694 cm^{-1} , between 778 and 780 cm^{-1} and between 795 and 799 cm^{-1} . Flint is represented in these spectra with peak around 1163, 555 and 462 cm^{-1} . Opal-A is represented in these spectra with peak around 1074 cm^{-1} , 788 cm^{-1} and 464 cm^{-1} . Calcite is represented in these spectra with peak around 1435, 874 and 714 cm^{-1} .

5.4.2.5. Ġgantija assemblage

Most of the samples from this assemblage present spectra with peaks within the absorbance bands of quartz. Moreover, they have a main peak with values close to 1080 cm^{-1} ($\pm 4\text{ cm}^{-1}$) which is characteristic of quartz minerals (Fig. 5.63a). Another characteristic feature of these spectra is the two neighbouring peaks that also supports the dominance of quartz. The one falls within the absorbance bands of 777 and 780 cm^{-1} , while the second is between 794 and 798 cm^{-1} (Fig. 5.63a). These samples also have peaks within the absorbance bands of flint (e.g. 1162 and 554 cm^{-1}). In addition, the main peak of some samples (e.g. GG15/S1/L1016) is related to the flint reference material, because of their similar values. The only exception is two samples (i.e. GG15/S1/L12 and GG15/S3/L1019) which present the main peak (e.g. 1070 cm^{-1}) and a minor (e.g. 461 cm^{-1}) within the restricted bands of the opal–A mineral (Fig. 5.63b). Furthermore, it presents a single peak (e.g. 788 cm^{-1}) in the area the quartz has two peaks (Fig. 5.63b) and is attributed to the presence of tridymite. Finally, the examination of the spectra has recorded few samples (e.g. GG15/S1/L12) with peaks (e.g. 1430 and 874 cm^{-1}) which fall within the absorbance bands of calcite (Fig. 5.63b).

5.4.2.6. Skorba assemblage

The samples from this assemblage present predominantly spectra with peaks within the absorbance bands of tridymite and calcite. They could be the dominant mineral of the samples, but they are mainly secondary minerals. Tridymite is identified with two characteristic peaks (e.g. 785 cm^{-1} and 668 cm^{-1}) and calcite with three (e.g. 1429 , 875 and 713 cm^{-1}). Some samples (e.g. SKB16/L6/S13) have the main peak with values close to 1080 cm^{-1} ($\pm 4\text{ cm}^{-1}$) which is characteristic for quartz (Fig. 5.63c). Another characteristic feature of these spectra is the two adjacent peaks that support the dominance of quartz. The one falls within the absorbance bands of 777 and 780 cm^{-1} , while the second is between 795 and 798 cm^{-1} (Fig. 5.63c). These samples also present peaks within absorbance bands of flint (e.g. 1163 and 557 cm^{-1}). Some other samples (e.g. SKB16/S3/L30) present their main peak (i.e. 1070 cm^{-1}) and a minor (i.e. 460 cm^{-1}) within the restricted bands of the opal–A mineral (Fig. 5.63d). Furthermore, it presents a single peak (e.g. 786 cm^{-1}) which has been attributed to tridymite (Fig. 5.63d). However, this assemblage also presents many samples (i.e. SKB16/S1/L20 and SKB16/S2/L12) with mixed results and made it difficult to conclude on their silicate minerals. Their main peak (e.g. 1074 cm^{-1}) is on the borderline between the opal–A and the tridymite minerals. Moreover, most of these samples (e.g. SKB16/S5/L13) present at least one of the characteristic peaks (i.e. 785 cm^{-1} and 668 cm^{-1}) related with the tridymite mineral. Therefore, it is possible that these samples consist of a blend of tridymite and opal–A minerals. Finally, there are some samples (e.g. SKB16/S5/L11) that have peaks (e.g. 1429 and 875 cm^{-1}) which fall within the absorbance bands of calcite (Fig. 5.63d).

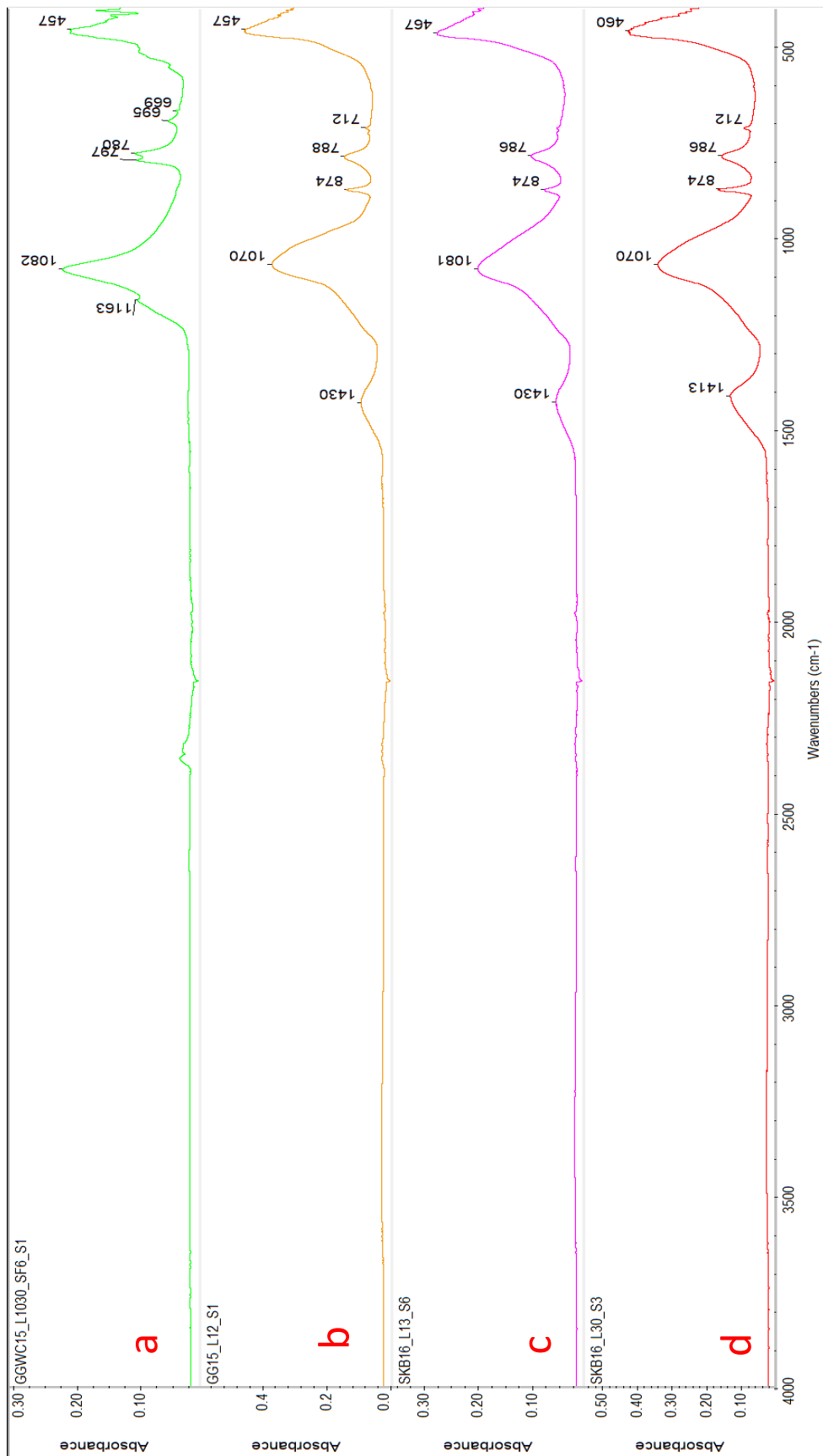


Figure 5-63: Representative ATR spectra of the artefact samples from Ġgantija and Skorba. Quartz is represented in these spectra with peaks around 1080 cm⁻¹, between 778 and 780 cm⁻¹ and between 795 and 799 cm⁻¹. Flint is represented in these spectra with peak around 1163 and 462 cm⁻¹. Opal-A is represented in these spectra with peak around 1070 cm⁻¹, 788 cm⁻¹ and 464 cm⁻¹. Calcite is represented in these spectra with peak around 1435, 874 and 712 cm⁻¹.

5.1.1. First remarks

The FTIR-ATR technique has provided some initial conclusions about the type of minerals reported in the investigated samples. The Maltese cherts are dominated by opal-A and contain calcite (n=21, 91%). There is one exception (F1S2) in which tridymite is the most common mineral, while no sample has quartz as the dominant mineral. On the contrary the Sicilian samples are dominated by quartz (n=16, 95%), while calcite is rarely reported in these samples.

Most of the samples of the examined assemblage have spectra dominated by quartz minerals. Nevertheless, there was a substantial amount of artefacts in all of the assemblages in which opal-A was the most common mineral. These artefacts also contained calcite which is a characteristic mineral reported also in the Maltese chert samples.

5.2. Portable X-ray Fluorescence (p-XRF)

p-XRF is an archaeometric methodology designed to identify the elementary composition of the examined samples (Shackley, 1998 and 1998a). It is used to record major elements as well as some trace elements, but is not suitable to distinguish between the minor and rare earth elements. This technique conducts the measurement on the surface of the sample, without causing any damage to the sample itself (Forster and Grave, 2012; Latham et al. 1992; Williams-Thorpe et al. 1999). The results are qualitative (it informs the user as to which elements are present in a sample, but does not contain information regarding how much of each element is present) and detect the chemical composition of the surface, which could differ from the composition of the inner part of the sample. Raw XRF data is excellent for analysis of samples where the question of interest is what is in the sample. The spectrum shows peaks where element-specific fluorescent energies were detected. The higher the peak, the more counts of that particular energy were detected. All the p-XRF spectra of the samples are found in the Appendix I (page 109).

5.2.1. Chert Formations

The chert samples of Malta present spectra which suggest that Calcium (henceforth Ca) has the most energy counts in comparison with the other elements (Fig. 5.64a). This is followed by silica (henceforth Si) and iron (henceforth Fe) and in most of the sample, they have a similar number of counts, which explains why their peaks are roughly on the same level. However, there are a few chert samples (e.g. M1S10) in which Fe has higher peaks than silica. Strontium (henceforth Sr) is also recorded in most of these chert samples, but present only a very small number of counts. Furthermore, nickel (henceforth Ni) and copper (henceforth Cu) are reported in the spectrum of some samples with very few counts (Fig. 5.64a).

The spectra of the chert samples from Gozo have demonstrated that the energy related to Ca has the most counts in the majority of these samples. This is followed by Si and Fe and in most of the sample, their peaks are on the same level. However, there are a few chert samples (e.g. F1S4) in which Fe has higher peaks than Si. Sr is also recorded in all of these chert samples, but it has only a few number of counts. The only exception is one sample (i.e. G2S6) which has different spectrum in comparison with all the other samples of the Maltese Islands. This sample has significantly higher peak related to silica, in comparison with other elements found. This is followed by Ca which is the second element in number of counts. Fe and Ni are other two elements recorded on the spectrum of this sample, but their number of energy counts is low. Finally, this sample has presented very small peaks of Cu and Sr.

The chert samples collected from Sicily present spectra which suggest that Si has the most energy counts in comparison with the other elements (Fig. 5.64b). Ca has the second highest peak in the Sicilian chert samples (e.g. S5), but in some samples (S13) the Fe is in this position. Moreover, the samples of the Radiolarian chert (i.e. S6) have not presented Ca in this analysis. Ni and Cu are reported in the spectra of all samples but with very small peaks (Fig. 5.64b). Sr is found only in few samples (e.g. S13), while in most of the samples it is below the detection limit. The only exception is one sample from West Sicily (i.e. S24) which has a completely different elementary composition in comparison with all the other samples of Sicily. The spectrum suggests that it consists only of the elements of Fe and Si. The Fe has the highest peak in the sample, while the silica presented a lower number of energy counts.

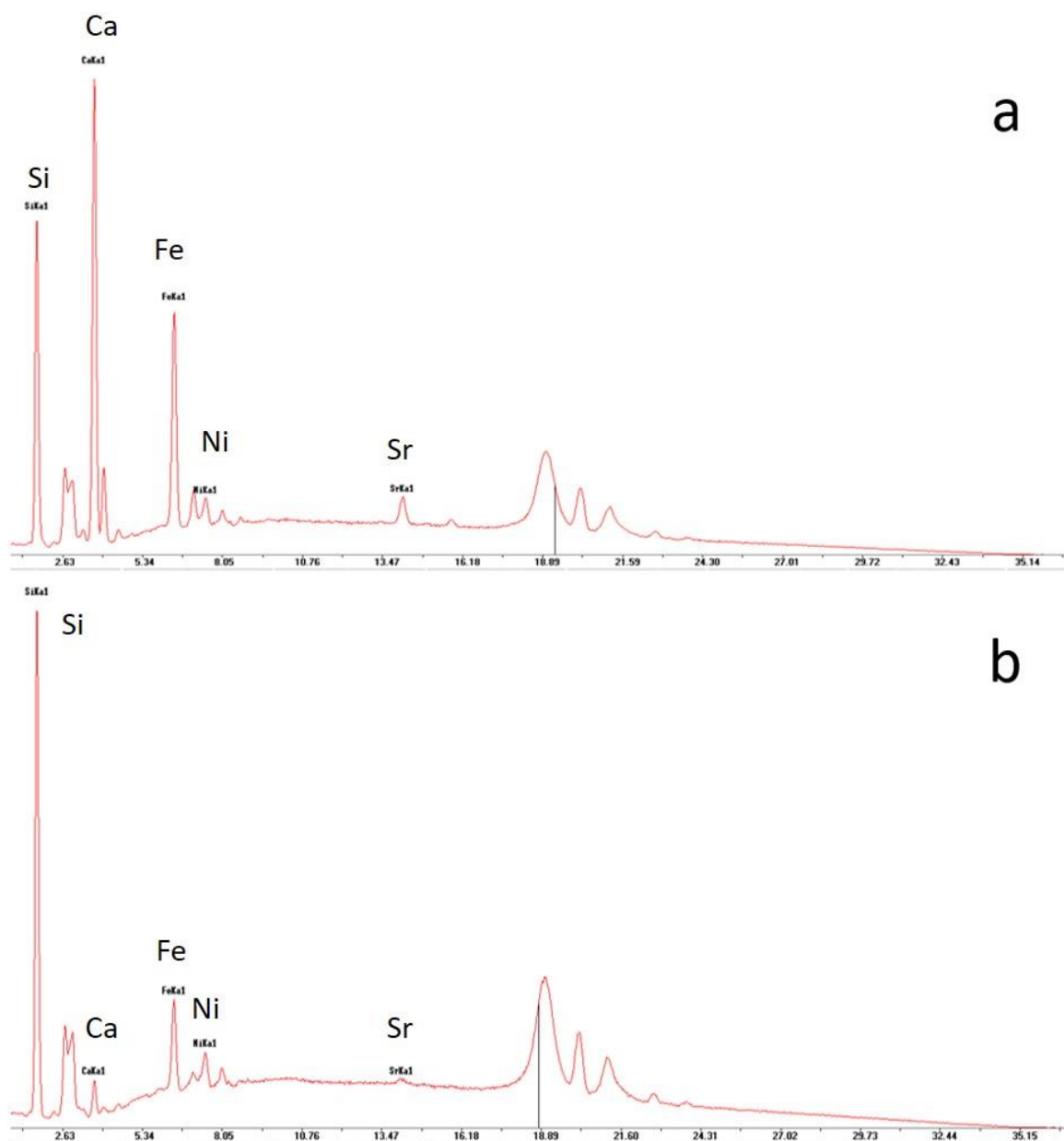


Figure 5-64: Representative p-XRF spectra of the rock samples from Malta (a) and Sicily (b).

5.2.2. Chert Assemblages

The samples of the Circle assemblage present spectra (Fig. 5.65) which are dominated by very high peaks of Si. This is followed by Ca and Fe which present high peaks, but lower than Si, in most of the samples. Ni and Cu are reported in all the samples, even though they have very small peaks. Sr is reported in some samples (e.g. BR91/S566/L662) with more energy counts than is the norm. However, there are a few artefacts (e.g. BR91/S566/L662) in which Ca present the highest peak in comparison with the other elements. These samples also present a variety of elements (e.g. titanium) and although they present small peaks, they are not found elsewhere.

Most of samples from the Kordin assemblage present spectra (Fig. 5.66) in which Si has the most energy counts. This is followed by Ca and Fe which alternate between the second and third element with the most counts in these samples. However, there are a few artefacts (e.g. KRD15/S69/L211) in which Ca present the highest peak among the recorded elements. Ni and Cu are found in most of the samples (e.g. KRD15/S27/L203) but with small peaks (Fig. 5.66). Some samples (e.g. KRD15/S98/L201) demonstrate the presence of Sr, titanium (henceforth Ti) and zirconium (henceforth Zr), even though they have very small peaks.

The samples of the Tač-Čawla assemblage mainly present spectra in which silica has the most energy counts (Fig. 5.67). Fe is the second in counts element (e.g. TCC14/S101/L85), but there are samples with Ca in that position (e.g. TCC14/S32A/L30). Furthermore, there are a few artefacts (e.g. TCC14/S37/L30) in which Ca has the highest peak among the recorded elements. The elements Ni and Cu are found in most of the samples (e.g. TCC14/S101/L85) but with small peaks. In addition, the spectrum of some samples (e.g. TCC14/S316B/L63) presents increased numbers of counts related to Sr, which have not been recorded in the sample artefacts of the previous assemblages. Furthermore, Ti and Zr are found in some spectra even though they have peaks close to the detection limit (Fig. 5.67).

Most of the samples selected from of the Santa Verna assemblage present spectra in which silica has the highest peak in comparison with the other elements (Fig. 5.68). Fe has the second higher peak (e.g. SV15/S2/L22), but there are samples in which Ca is in that position (e.g. SV15/S2/L22). Furthermore, there are few artefacts (e.g. SV15/S1/L4) in which Ca has the higher number of counts among the recorded elements. The elements of Ni and Cu are found in most of the samples but with small peaks. Moreover, the spectrum of some samples show increased numbers of counts related to Sr, which is also recorded in the Tač-Čawla assemblage. Additionally, Ti and Zr are found in some spectra even though they have peaks close to the detection limit.

The samples of the Ġgantija assemblage present predominantly spectra in which silica has the highest peak among all the recorded elements (Fig. 5.69). This is followed by Ca and Fe which alternate between the second and third element with the most energy counts. Sr is found in many samples (e.g. GGWC15/S26/L1019) and occasionally present a significant number of counts (Fig. 5.69). Ni and Cu are

reported in all the samples, but with relatively small number of counts. Nevertheless, there are a few artefacts (e.g. GGWC15/S1/L1012) in which Ca has the highest peak in comparison with the other elements. Additionally, many of these samples have Fe as the element with the second highest peak, which is followed by Si. This horizon has samples (e.g. GGWC15/S3/L1019) demonstrating Fe with high number of counts, which is a characteristic reported for the first time in the assemblages. Moreover, Ti and Zr are found in some of their spectra even though they have peaks close to the detection limit.

The Skorba assemblage includes many lithics for it is extremely difficult to identify their rock type (e.g. chert and limestone). The p-XRF has recorded their main elementary profile and allows the differentiation of the different chert or limestone material. This differentiation is successful to some extent, but there are many artefacts which cannot be related to a specific type of rock. The majority of samples from this assemblage present spectra in which Ca has the highest peak (Fig. 5.70). This is followed mainly by Fe which presents the second highest peak in most of these samples (e.g. SKB16/S2/L1). Silica has generally peaks lower than the ones of Ca and Fe, though not always (e.g. SKB16/S4/L23). Although this is the main order of the elements with the most energy counts, there are some samples that present a different order. There are samples (e.g. SKB16/S4/L11) in which Si has the most counts among the recorded elements, while others have Fe in this position (e.g. SKB16/S1/L5). Sr is reported in almost all the samples (e.g. SKB16/S2/L1 and SKB16/S5/L23) but present higher peaks when the peak of Fe is also high (Fig. 5.70). Ni and Cu are recorded in all the samples, but mainly with a small number of counts. Furthermore, Ti and Zr are found in some of the spectra even though they have peaks close to the detection limit. Lastly, there is one sample (i.e. SKB16/S5/L23) with a noticeable high peak related to Zinc (Zn), which is an element not found in any other sample.

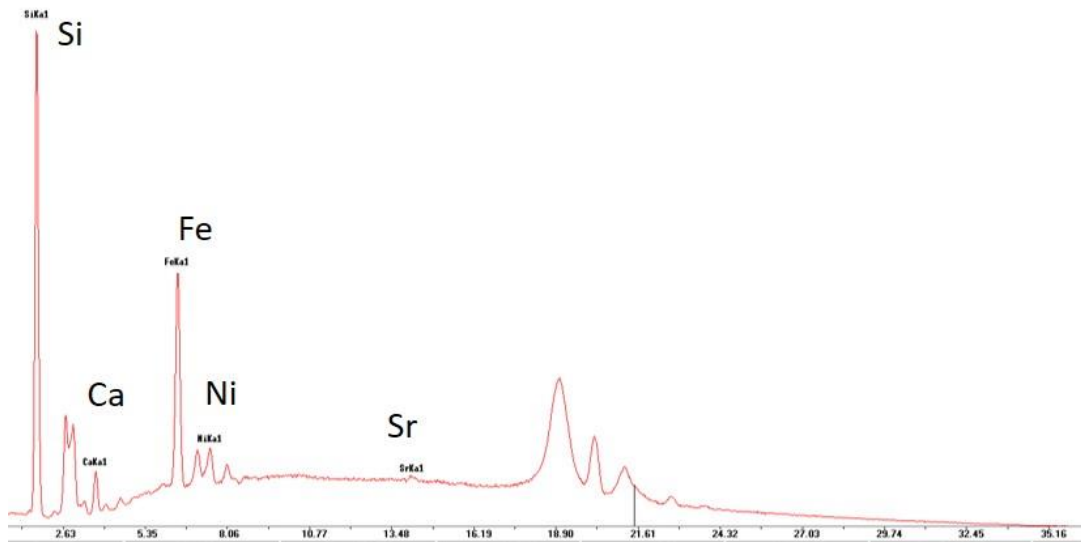


Figure 5-65: Representative p-XRF spectrum from the Circle.

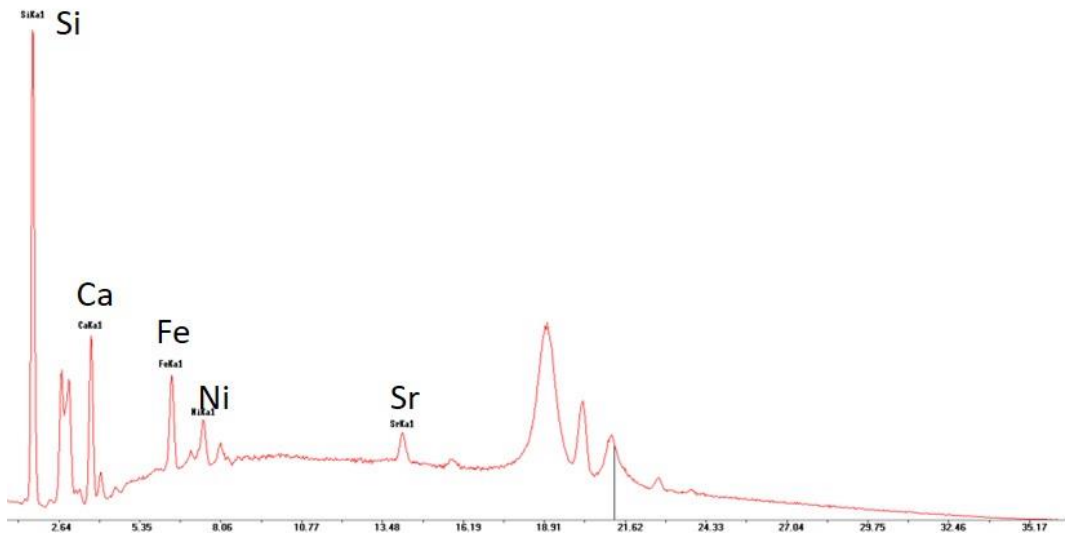


Figure 5-66: Representative p-XRF spectrum from Kordin.

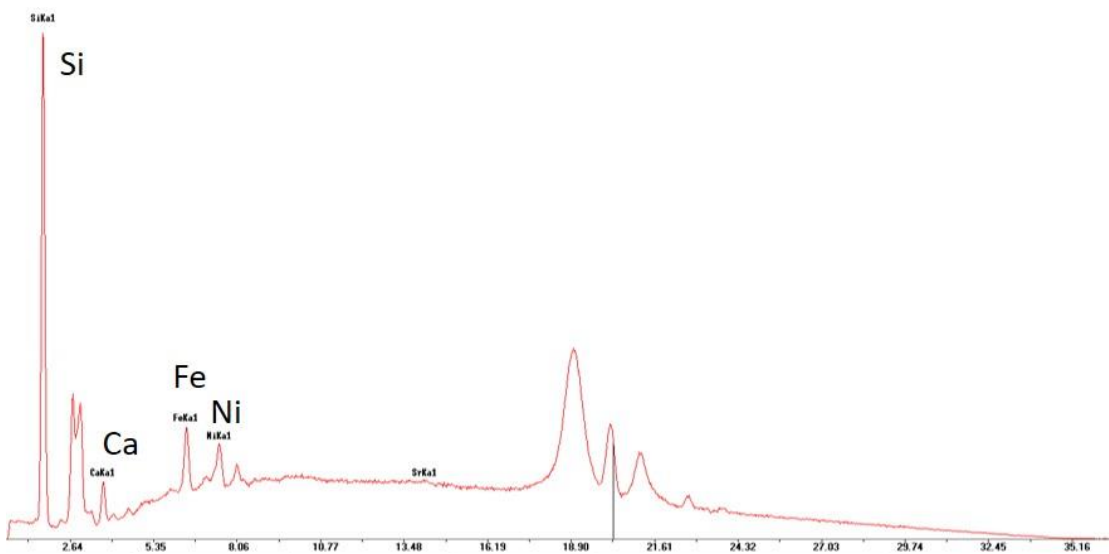


Figure 5-67: Representative p-XRF spectrum from Tač-Čawla.

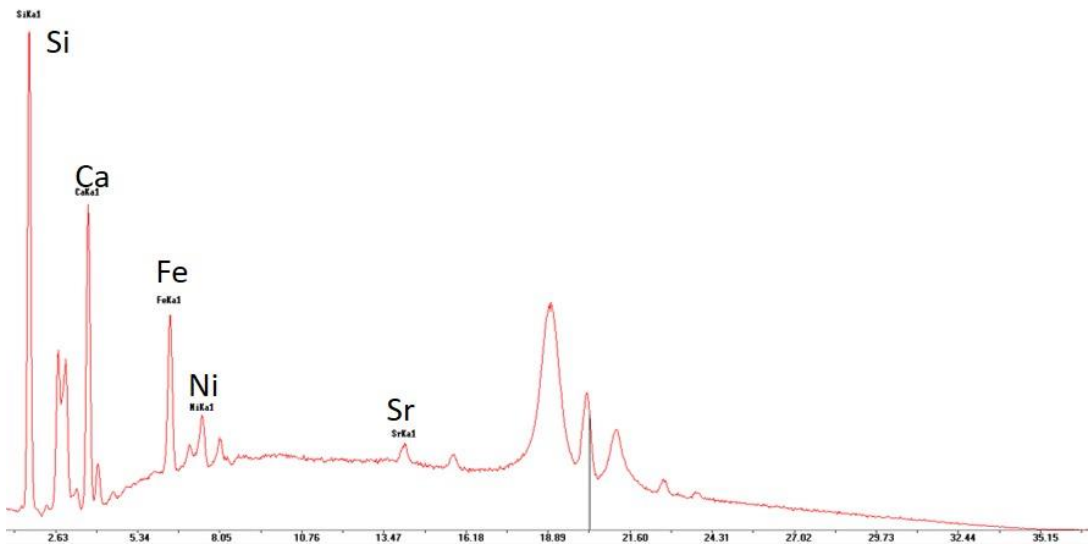


Figure 5-68: Representative p-XRF spectrum from Santa Verna.

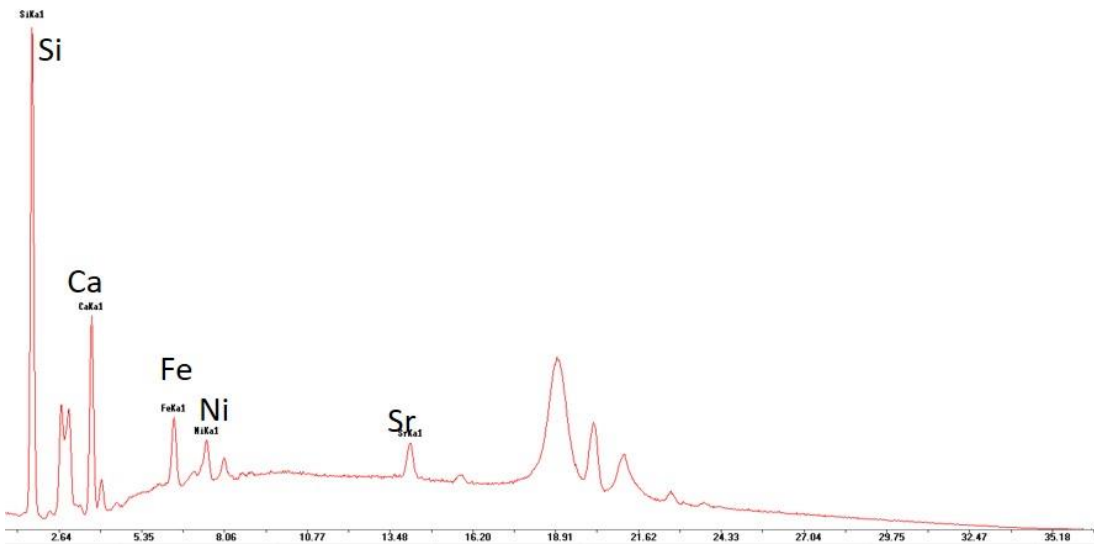


Figure 5-69: Representative p-XRF spectrum from Ġgantija.

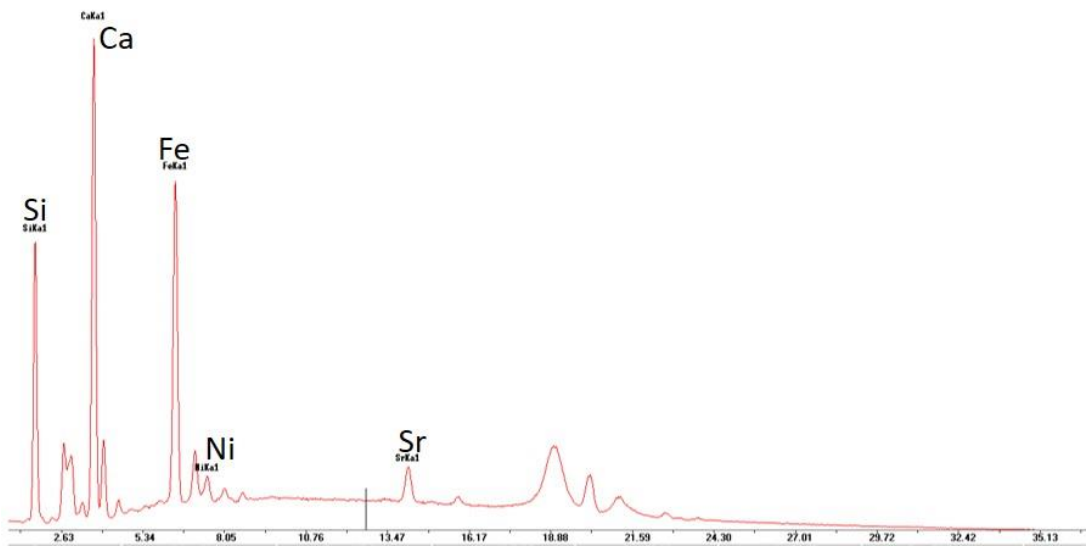


Figure 5-70: Representative p-XRF spectrum from Skorba

5.2.3. First remarks

The results have suggested that the Maltese cherts present spectra with the highest peak to be related to Ca (n=22, 96%) with Si and Fe as the elements with the next highest peaks. The only exception is the unique sample from Gozo (G2S6) which has the highest peak at Si. On the contrary, the Sicilian cherts are dominated with spectra presenting more energy counts related to Si (n=16, 84%), while Ca and Fe are only found with fewer number of counts. Sr, Ni and Cu are some elements found in both the Maltese and Sicilian samples but with very low readings. The peaks of these elements are higher in samples that have high peaks related to Fe and a connection between these elements is probable.

The artefact samples can be divided in two main groups based on the p-XRF results. The first consists of artefacts that have more energy counts related to Si and in the meantime lower peaks at Ca and Fe. The second group includes samples in which Ca has the highest peak, followed by the peaks of Si and Fe. Sr, Ni, Cu have been found within various samples but with small numbers of energy counts. The number of their counts increases when Fe present high peaks and they are possibly related.

5.3. Laser ablation - Inductively Coupled Plasma - Mass Spectrometry (LA-ICP-MS)

LA-ICP-MS is an excellent method used to identify the elementary composition of the examined samples (Speer, 2014; Neff, 2012). It is a quantitative technique which can record with great accuracy (parts per billion) the concentrations of the major, minor and trace elements of a sample. In addition, it has a low detection limit that further allows the recording of elements in ppm (part per million), such as the rare earth elements (REE). The ICP-MS is a destructive technique that requires powder samples of around 2–5 grams depending on the number of elements that need to be identified. The addition however of laser ablation (LA) equipment converts this technique to a non-destructive one without compromising the precision or accuracy of the measurements. Furthermore, it does not require any special treatment of the samples/artefacts which remain intact throughout the examination process.

Depending on the rock type and the focus of the research, the concentrations of specific elements are used to create models and patterns to find important information about the investigated rocks. The current research uses models and patterns to gather information about the environment, the inputs and conditions under which the investigated chert is formed. Although this seems outside the interest of the archaeological research, it is actually extremely important to sourcing lithics. The importance of this information lies on the baseline principle that it would be impossible or at least unlikely that different rock sources would have the same model and pattern results. There are geological theories (e.g. Murray et al, 1992; Murray, 1994) that show which elements should be selected to form the models and patterns, and subsequently identify the factors previously mentioned (e.g. type of environment). Moreover, the selection of these elements is made based on the extent that these factors influence their concentration and therefore place the examined rocks in specific categories. The tables with all the LA-ICP-MS analyses and ratios used in this chapter are found in the Appendix I (Table 10 to 23, p.163).

I have decided to explain the selection of elements and diagrams necessary to achieve my goals during the process of presenting the results in the following sub-chapter. I believe this should be more effective for the easy understanding of my selection criteria and also of the interpretations of results.

5.3.1. Chert Formations

Previous studies (e.g. Junguo et al, 2011) demonstrate that some major elements such as iron (henceforth Fe), aluminum (henceforth Al) and manganese (henceforth Mn) play a basic role in identifying the origin of chert. Additionally, the contents of Fe and Mn, in the rock formations, are associated with *hydrothermal sedimentation*¹⁹, while Al is related with terrigenous input²⁰. Therefore, this allows the identification of whether the examined rocks are related to *hydrothermal or biogenic*²¹ (i.e. organism) sedimentation. This is better understood with a ternary model (Junguo et al, 2011) which combines the concentrations of Fe, Al and Mn. Plotting this model with the rock samples of Malta and Sicily (Fig.5.71) demonstrates that all of the Maltese chert and most of the Sicilian (75%) are related to biogenic sedimentation. 10% (n=2) of the Sicilian samples are related to hydrothermal sedimentation, while one (S22p) has high extremely concentrations of Al and is placed outside the areas of the two types of sedimentation at the very top of the ternary diagram (Fig.5.71).

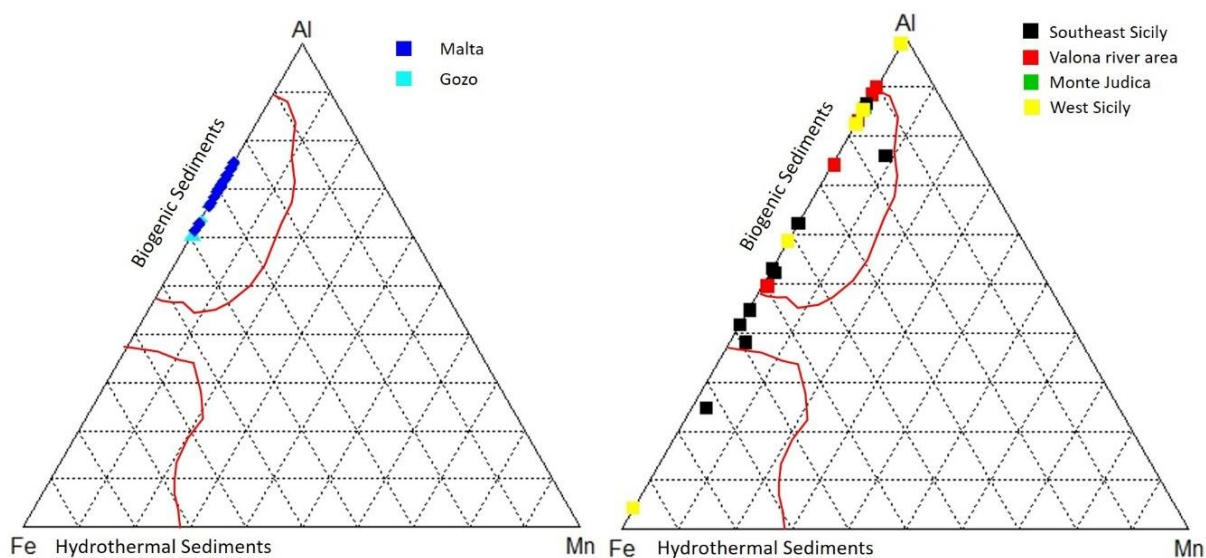


Figure 5-71: Ternary diagram examining the type of the sediments related to the Maltese rock samples (left) and the Sicilian chert samples (right). The line demarcations have followed the suggestion of Junguo et al. (2011).

¹⁹ Hydrothermal sedimentation refers to syngenetic sedimentation formed by underground hydrothermal fluids which are ejected through rock fractures or vent channels; they then flow into and mix with terrigenous clastics and the bottom water of a sea or lake. The sediments of this type are called hydrothermal sediments. (Daesslé and Cronan, 2001; He et al. 2016)

²⁰ Terrigenous inputs or sediments are the weathering products of rocks exposed at the Earth's surface. They are brought to the ocean by rivers, winds, and ice and may be redistributed in the ocean by currents. Accordingly, variations in composition, grain size, and flux of terrigenous marine sediments hold clues to important palaeoclimate variables such as wind speed and direction, aridity, glacial activity, and ocean current (Hemming, 2007).

²¹ Any pelagic sediment that contains more than 30% skeletal material (Boggs 2009). These sediments can be made up of either carbonate (or calcareous) ooze or siliceous ooze. The skeletal material in carbonate oozes is calcium carbonate, while in siliceous oozes are composed of opal (amorphous, hydrated silica). The most common contributors to the skeletal debris are such microorganisms as foraminifera and coccoliths (carbonate ooze), and diatoms, radiolarians and siliceous sponges (siliceous ooze).

The literature (e.g. Murray, 1994) further suggests that the concentrations of Fe, Al and titanium (henceforth Ti) can be chemical criteria for the depositional environment of sediments and therefore sedimentary rocks. Al and Ti are excellent indicators of terrigenous input, while Fe can be used as an indicator of hydrothermal input. There are other major elements suitable for reaching similar conclusions, but we focus on those elements (i.e. Al, Ti, Fe) because they are not affected by the lithology or age of the rock and they are relatively unaffected by diagenesis. This theory has created a model which uses the ratio Fe/Ti on the y-axis and the ratio Al/(Al+Fe) to distinguish between a hydrothermal²², pelagic²³ and continental margin²⁴ environment. Plotting the rock samples on this model (Fig.5.72) demonstrates that all of the Maltese cherts are located in a region related to a pelagic and continental margin environment. The Sicilian cherts are more widespread in the binary model than the Maltese chert sources. The Sicilian sources, therefore, can be related to all three environment types.

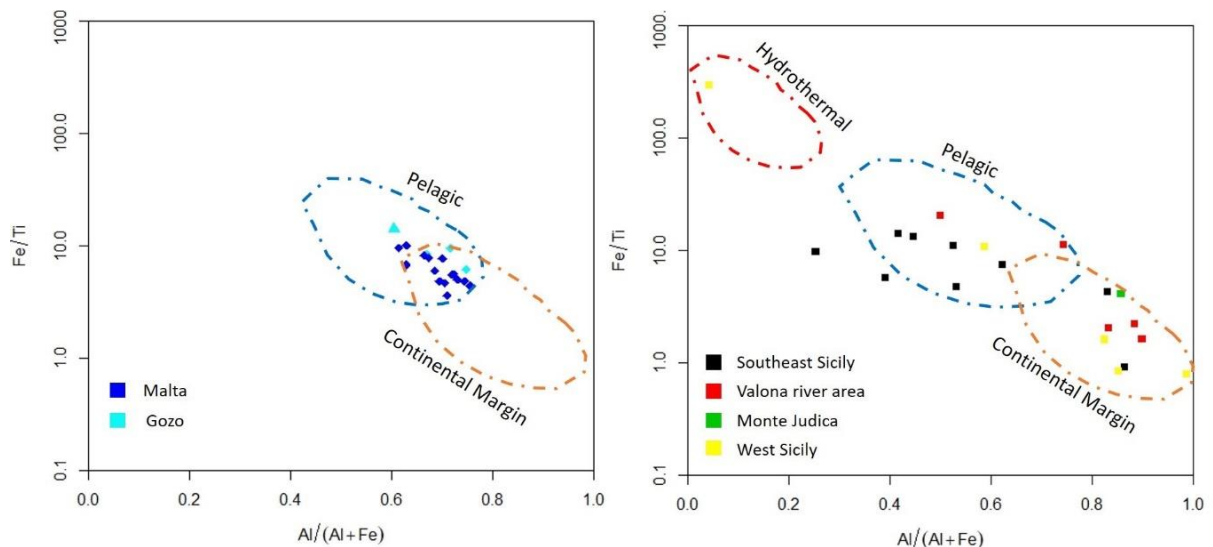


Figure 5-72: Binary diagram examining the type of depositional environment related to the Maltese chert samples (left) and the Sicilian chert samples (right). The line demarcations have followed the suggestion of Murray (1994).

²² A hydrothermal environment is a setting dominated by the circulation of hot, mainly aqueous fluids (He et al. 2016). In a mid-ocean ridge setting, seawater penetrates the crust, becomes heated, interacts with the crust so that its composition changes, then exits the crust at a hydrothermal vent on the ocean floor. The environment surrounding the vent sustains rich, anoxic chemotrophic ecology.

²³ A depositional environment between the hydrothermal and continental margin environment which mainly include open sea and deep ocean environments which are least affected from the other two types of depositional environments (Murray, 1994).

²⁴ A depositional environment found on the submarine edge of the continental crust distinguished by relatively light and isostatically high-floating material in comparison with the adjacent oceanic crust. It is the name for the collective area that encompasses the continental shelf, continental slope, and continental rise. The characteristics of the various continental margins are shaped by a number of factors. Chief among these are tectonics, fluctuations of sea level, the size of the rivers that empty onto a margin as determined by the amount of sediment they carry, and the energy conditions or strength of the ocean waves and currents along the margin (Hemming, 2007).

There have been studies (e.g. Garbán et al, 2017) that use the concentrations of trace elements to identify some of the conditions under which the rock formations were formed. They demonstrate that the concentrations of uranium (henceforth U), thorium (henceforth Th), vanadium (henceforth V) and nickel (henceforth Ni) can be useful indicators of the palaeo-oxygen level²⁵ of the depositional environments. The environments can be characterized as: a) anoxic (depleted in oxygen), b) dysoxic (low levels of oxygen) and c) oxic (enriched in oxygen). This theory has created a model which use the ratio $V/(V+Ni)$ on the y-axis and the ration U/Th to distinguish between and on which the examined samples are plotted. Most of the Maltese rock samples (75%) are gathered in a region which can be characterised as anoxic based of the concentration of U and Th and dysoxic (66%) based on the ratio of V and Ni (Fig.5.73). On the contrary, it is difficult to reach a certain conclusion on the Sicilian chert, due to the inconsistencies of the concentrations of V and Ni (Fig.5.73). The only safe interpretation is that they are enriched in U, especially in comparison with Th.

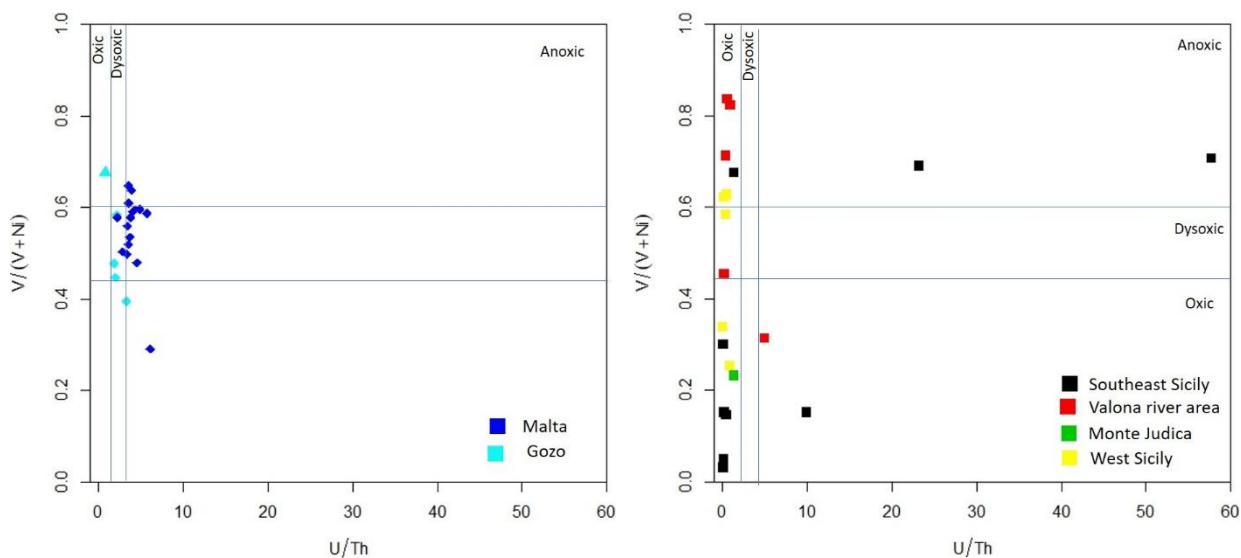


Figure 5-73: Binary diagram examining the oxygen level of the depositional environment of the Maltese chert samples (left) and the Sicilian chert samples (right). The line demarcations have followed the suggestion of Garbán et al (2017).

²⁵ The level of Oxygen in past climates, known as palaeoclimates. In geology this includes the climate and weather condition on a specific time in the geological scale (Danelian et al. 2004). The term palaeo-oxygen level in this investigation refers to the levels of oxygen during the deposition and formation process of different cherts.

The literature has demonstrated (e.g. Masuda 1977; Murray, 1994; Junguo et al, 2011) that the relative fractionations of the *rare earth elements (REEs)*²⁶ are a good geochemical tracer for studying the chert origin, palaeoenvironment as well as the oxidation and reduction conditions. In comparison with the major and trace elements, the REEs are not affected by the age of the rock or the tectonic history and are independent of diagenetic modification (Murray et al. 1992). These studies have provided normalised ratios (e.g. Ce/Ce*) and patterns which allow the identification of those features in the examined chert rocks. The values of the REEs are always normalised with suitable rock standards to avoid unnormal fluctuation of elemental abundances. The selected standard is always related to the type of rock formation that is under investigation. The rock types in the present analysis are sedimentary rocks and consist of cherts, limestone and silicified limestone. The World Average Shale standard (Piper, 1974), is the clear standard used in this analysis because amongst other shales, it also includes European shale material, and therefore provides the closest parallels with the Maltese and Sicilian samples within this study. The detailed table with the results of these ratios is found in the Appendix I (p.178; Table 22).

The values of Ce/Ce*, La_n/Ce_n and La_n/Lu_n ratios can provide a clear distinction between environmental regions and types of inputs of the examined samples. Most of the Maltese chert (n=14) has an average Ce/Ce* ratio of 0.77 which is an intermediate value between the readings expected for either a pelagic or continental margin environment. There are two exceptions (F1S2 and M1S1) that have values which are related to a ridge-proximal depositional regime. The values of La_n/Ce_n ratio show a stronger connection with a continental margin environment and influence of terrigenous inputs because it has readings closer to 1. The only exception is sample M1S1 which relates to a ridge-proximal depositional regime. Many of the Maltese chert samples (n=14) have a La_n/Lu_n ratio of around 1 which is related to a continental margin environment, but there are few samples (e.g. F1S21) connected with the other two types of environments. The values of these ratios amongst the Sicilian chert show great variability in comparison with the Maltese samples. Many of these samples (n=10) have the Ce/Ce* ratio around 0.58, which are values related to a pelagic environment. There are some (n=4) with ratios suggesting a connection with a continental margin environment, while a few (n=2) are related to a ridge-proximal depositional regime (S5, S16). The values of the La_n/Ce_n also support these findings with many Sicilian chert samples (n=10) presenting ratios between 2 and 3 which are characteristic of a pelagic environment. Moreover, it confirms that some samples are related to continental margin environment (e.g. S6, S7) and some (n=5) with a ridge-proximal depositional regime (e.g. S5, S16). The La_n/Lu_n ratio of the Sicilian chert samples presented similar results to the ones of the Maltese Islands. Many samples (n=12) have a ratio around 1 and which is related to a continental

²⁶ It is a group of 17 chemically similar metallic elements, including the 15 lanthanides, scandium and yttrium (Castor and Hedrick, 2006).

margin environment, but there are a few samples (S5, S16, S23) connected with a ridge regime, and a couple (S6b and S21) related to a pelagic environment.

The next step requires the examination of the normalised patterns of rare earth elements which can provide a holistic perspective of their concentration and the relationship between them. The patterns of the Maltese samples are almost identical to each other with only some minor differences (Fig.5.74a). These samples have low concentrations (10^{-1}) of these elements and present a noticeable depletion of terbium (henceforth Tb) and minor depletion of cerium (henceforth Ce) always in comparison with the neighbouring elements. The patterns of the Sicilian chert samples are significantly diverse (Fig.5.74b, c and d) and different from the Maltese samples. Most of these samples (n=18) have lower concentrations of REEs (10^{-2}) than the Maltese, while two chert samples (S6a and S19) are more enriched and show higher quantities of REE's (Fig.5.74b and c). They have comparable concentrations with the Maltese samples, but their patterns present greater fluctuation. The majority of the Sicilian samples (65%) present a significant depletion of Ce and minor depletion of Tb in contrast with the other RREs. The only exceptions are the chert samples (S6a and S7) from the Radiolarian formation (Fig.5.74c), which are relatively enriched in Ce. Finally, one sample from west Sicily (i.e. S24) presents an almost linear REE pattern (Fig.5.74d).

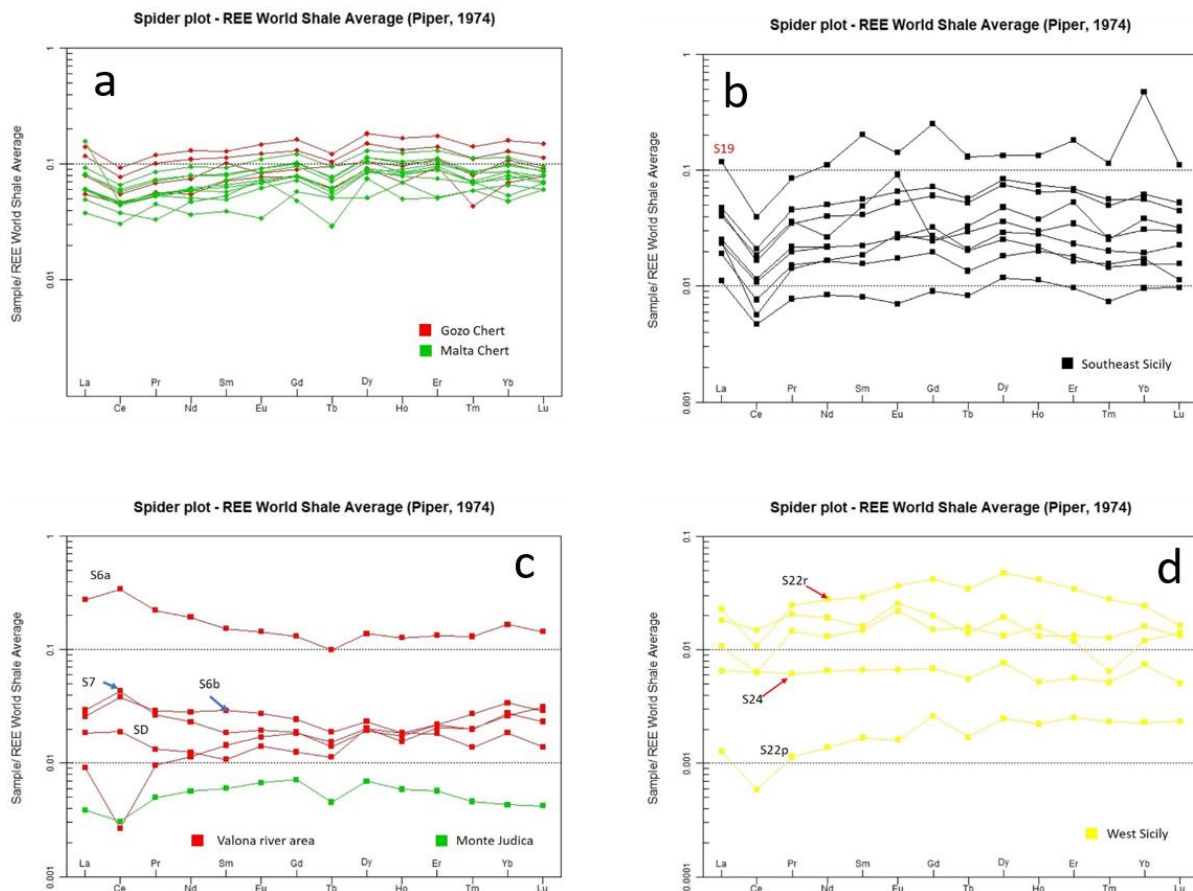


Figure 5-74: The normalised patterns of rare earth elements of the Maltese and the Sicilian chert samples.

5.3.2. Chert Assemblages

The theoretical background and the reasoning behind the adoption of the elements and models used have been explained in the previous sub-chapter. Here I have only included the visual depiction of the results and the explanation of the chert assemblages of this research. The samples have been allocated different colours based on common macroscopic features for the better understanding of the diagrams and illustrations, and not to suggest a common origin. Further interpretation and comparison with the chert sources are included in the discussion chapter.

The research on the chert artefacts starts from the triangle model which combines the concentrations of Fe, Al and Mn, to identify their type sedimentation (i.e. hydrothermal or biogenic). The majority of the examined artefacts of all the assemblages (n=111; 89%) are related to biogenic sedimentation (Fig.5.75 and 5.76). Nevertheless, there are some artefacts from the Circle (n=1), Tač-Čawla (n=1), Santa Verna (n=2) and Skorba (n=1) that fall within the hydrothermal sedimentation region. Moreover, there are a few artefacts from Kordin (n=1), Tač-Čawla (n=5), Ġgantija (n=1) and Skorba (n=2) that cannot be clearly correlated with either a biogenic or hydrothermal sedimentation.

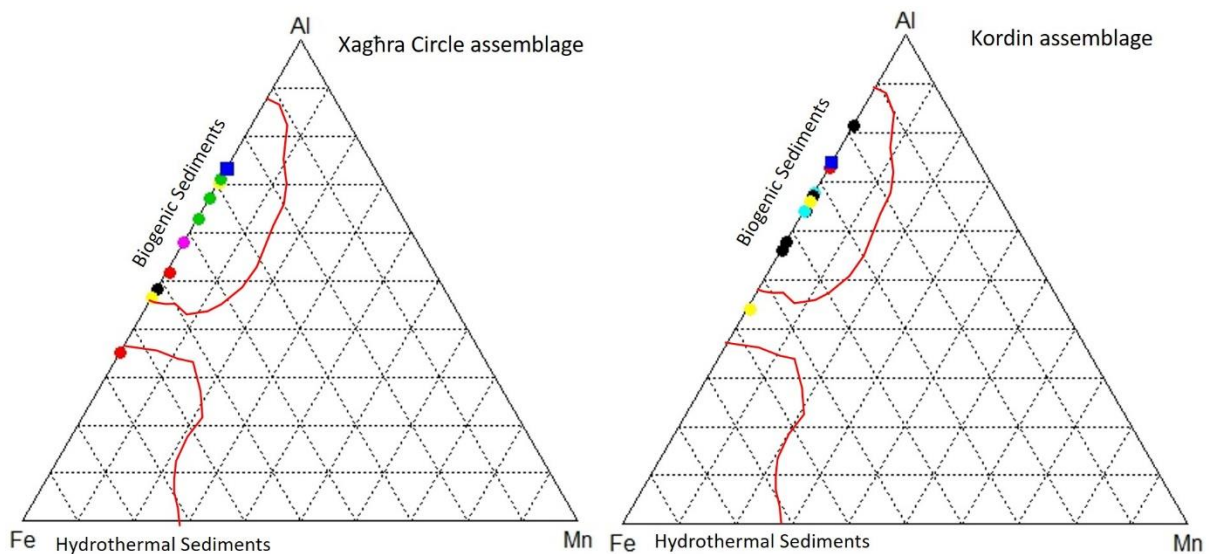


Figure 5-75: Ternary diagram examining the type of the sediments related to the Xaghra Circle artefact samples (left) and the Kordin artefact samples (right). The line demarcations have followed the suggestion of Junguo et al. (2011).

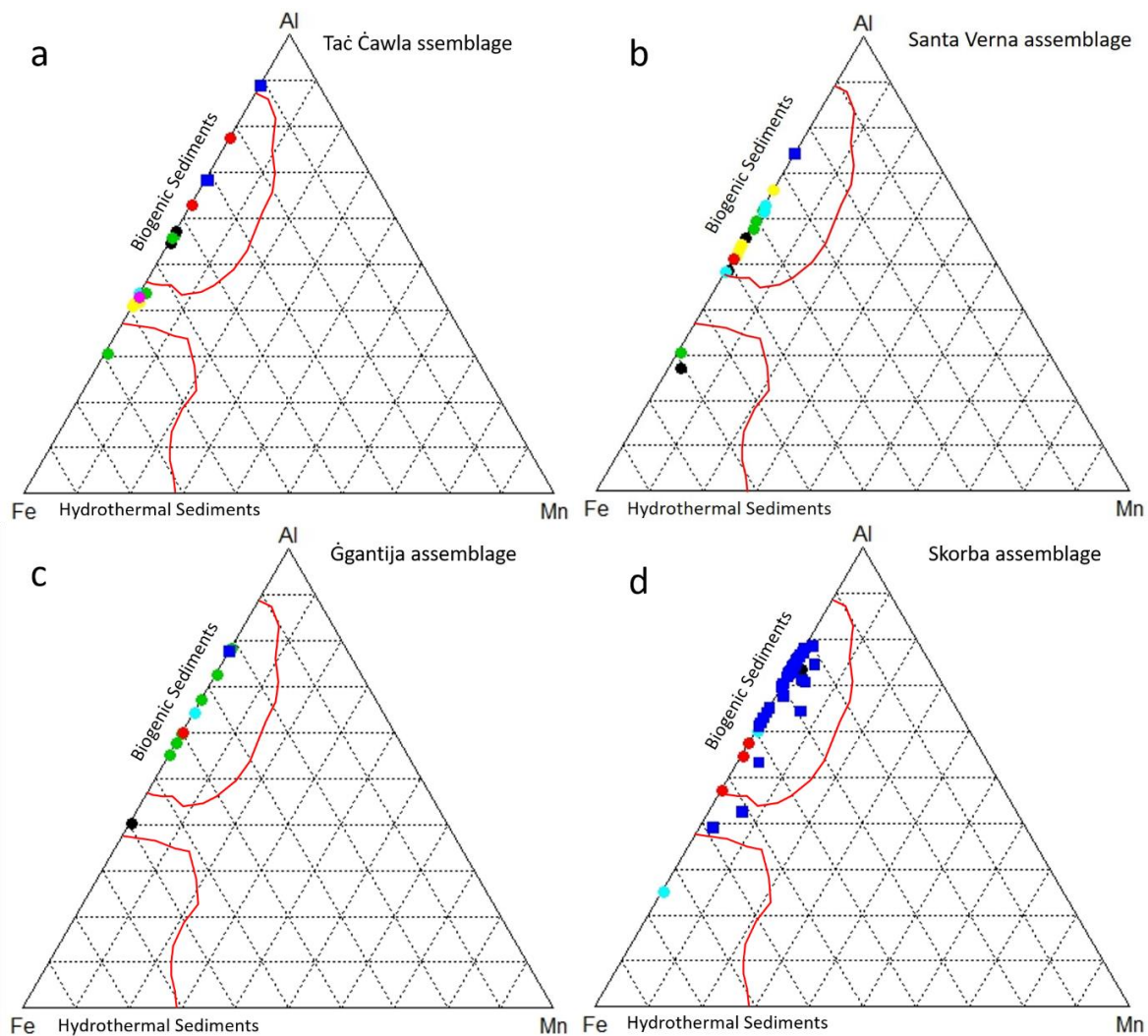


Figure 5-76: Ternary diagram examining the type of the sediments related to the artefact samples of a) Tač-Čawla, b) Santa Verna, c) Ġgantija and d) Skorba. The line demarcations have followed the suggestion of Junguo et al. (2011).

The second step is to use the concentrations of Fe, Al and Ti in a binary model and identify the depositional environment of the chert artefacts. The model demonstrates that most of the samples from the Circle (60%), Tač-Čawla (74%) and Santa Verna (75%) are in a region related to a pelagic environment (Fig.5.77a, c and d). On the contrary, the majority of the samples from Kordin (56%) and Skorba (52%) are in an intermediate region between a pelagic and continental margin environment (Fig.5.77b and f). There is only one sample in each of the assemblages of Tač-Čawla (TCC14/S577/L131) and Skorba (SKB16/S8/L2) that are clearly related to a continental margin environment. In addition, only at Skorba is there one sample (SKB16/S6/L12), which is very close to indicating a hydrothermal depositional environment. Nevertheless, there are some samples across the dataset (n=23) that fall outside the regions of these three types of environment. This is more common with the samples from Skorba where a substantial number of artefacts (n=18) fall outside the pelagic and continental margin environments (Fig.5.77f).

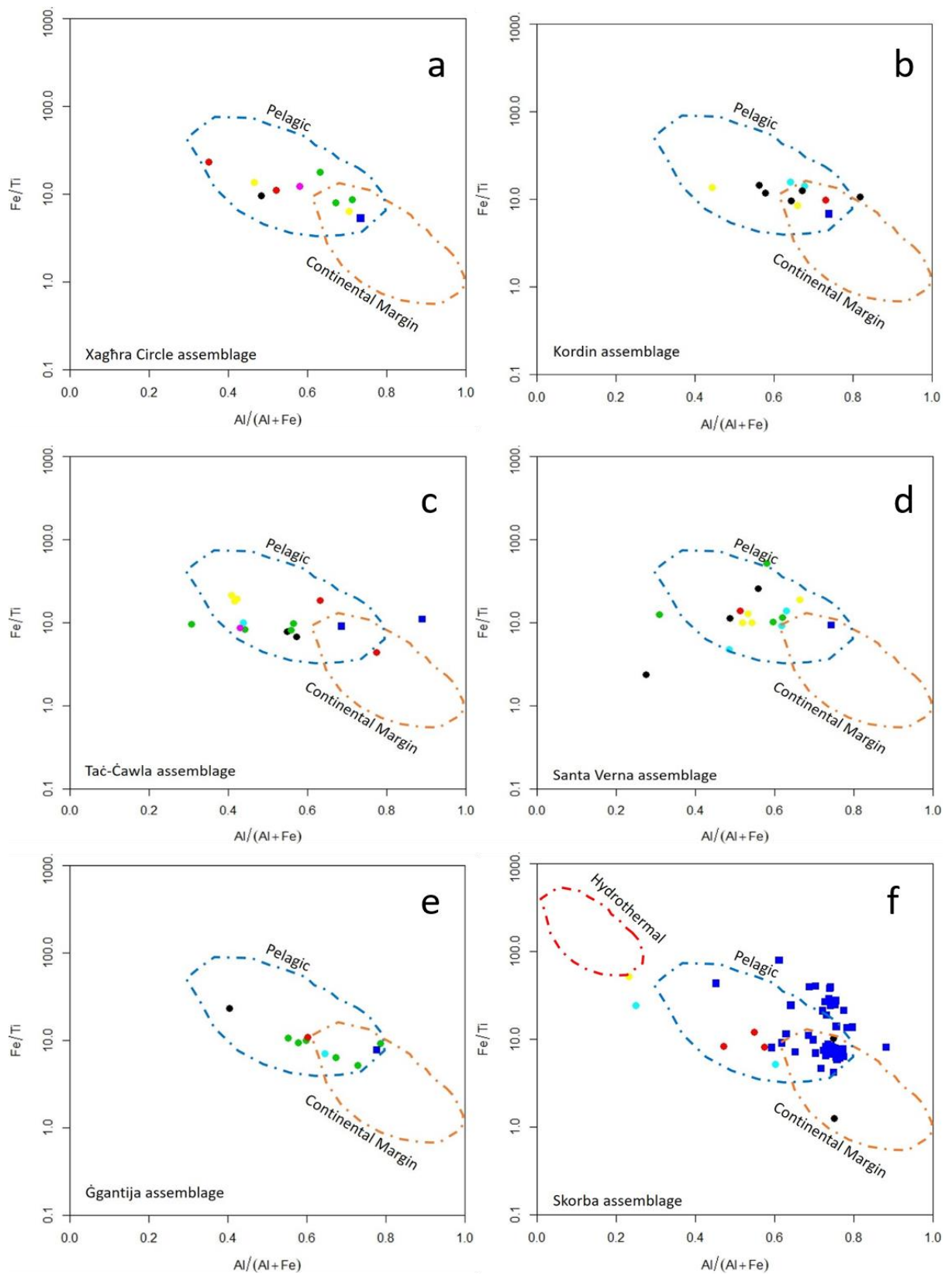


Figure 5-77: Binary diagram examining the type of depositional environment related to the artefact samples of a) the Circle, b) Kordin, c) Tač-Čawla, d) Santa Verna, e) Ġgantija and f) Skorba. The line demarcations have followed the suggestion of Murray (1994).

The next step in the analysis will look at the palaeo-oxygen levels of the depositional environments in which the chert is formed. The elements which show this factor of the depositional environment are U, Th, V and Ni and have been plotted against one-another below on a binary diagram (Fig.5.78 and 5.79). Unfortunately, the samples show little correlation and it is difficult to record specific and comparable information about their level of oxygen. Most of the samples (80%) have a $V/(V+Ni)$ ratio above 0.5 and they are found mainly in the upper part of the models which generally suggest low concentrations of oxygen during the deposition of sediments and the formation of the rocks (Garbán et al. 2017; Danelian et al. 2004). Furthermore, the models demonstrate that the samples are made from raw materials which have been formed under different levels of oxygen (e.g. anoxic and oxic). The only exception is the samples from the Skorba assemblage, the majority of which (75%) is gathered in the central of the graph (Fig.5.79b). They are mostly in a region characterised by anoxic conditions, but there are plenty (n=12) that fall in dysoxic conditions. Nevertheless, the samples show that they are made from materials which formed under similar palaeo-oxygen conditions.

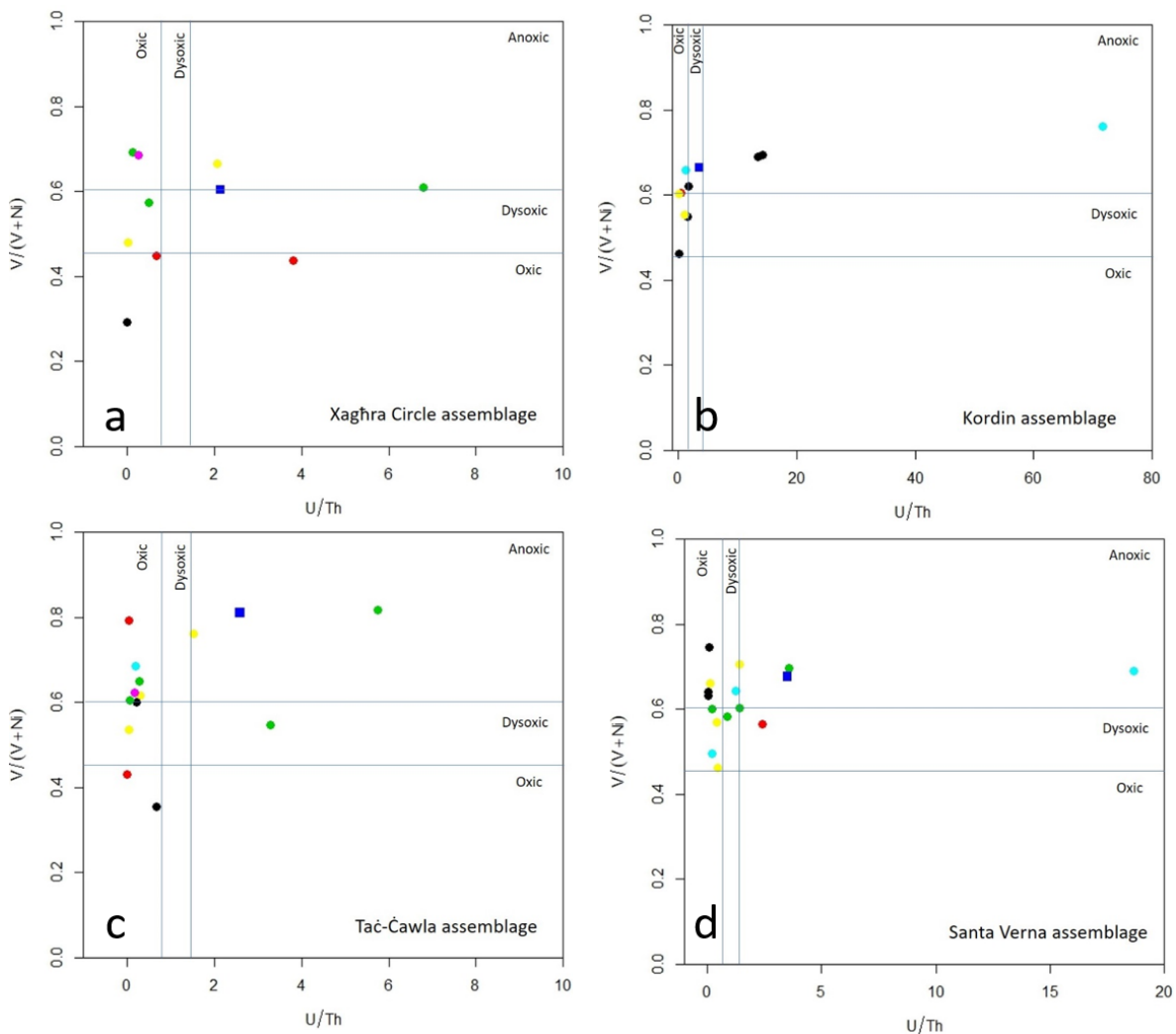


Figure 5-78: Binary diagram examining the oxygen level of the depositional environment related to the artefact samples of a) the Circle, b) Kordin, c) Tač-Ċawla and d) Santa Verna. The line demarcations have followed the suggestion of Junguo et al (2011).

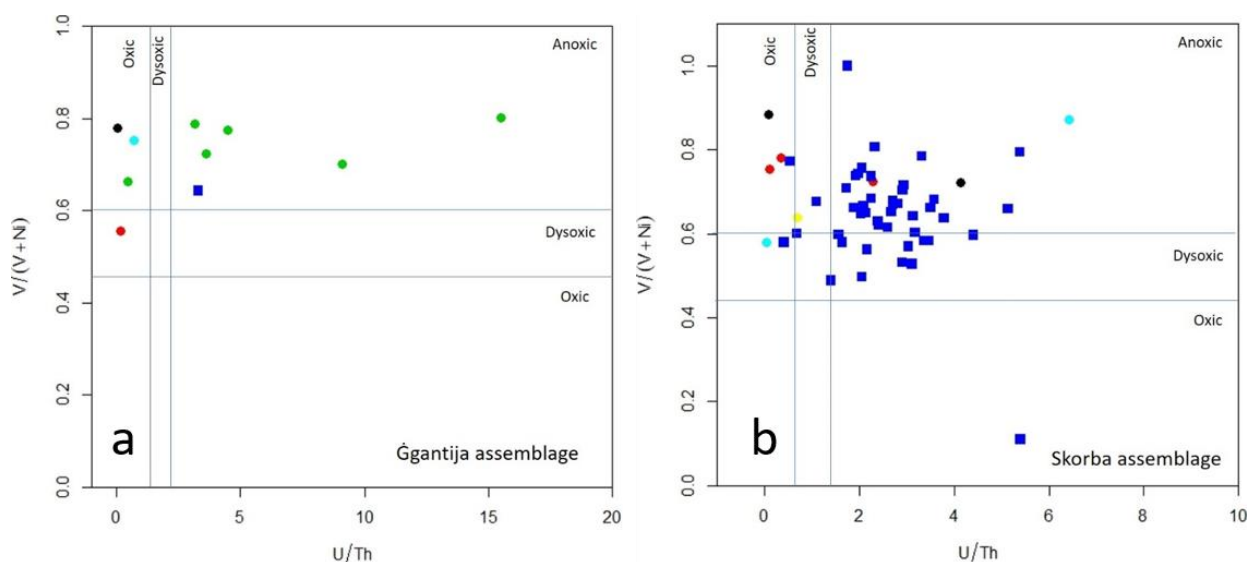


Figure 5-79: Binary diagram examining the oxygen level of the depositional environment related to the artefact samples of a) Ġgantija and f) Skorba. The line demarcations have followed the suggestion of Junguo et al. (2011).

The next step is to use the relative fluctuation of the rare earth elements (REEs) and collect further information about the origin of the investigated artefacts (e.g. sediments and palaeoenvironment). The REEs results of the artefacts are processed and investigated with the same method as the chert sources of Malta and Sicily outlined above in section 5.4.1. The Ce/Ce^* , La_n/Ce_n and La_n/Lu_n ratios (Masuda 1977; Murray, 1994; Junguo et al, 2011) can provide a clear distinction of environmental region and type of inputs of the examined samples (Appendix I, p. 179; Table 23).

Most of the Circle samples ($n=5$) have Ce/Ce^* ratios between 0.45 and 0.75, which are characteristic of a pelagic formational environment (e.g. BR93/S854/L897), but there are few ($n=3$) with values related to a proximal ridge environment (e.g. BR91/S611/L712) (Murray, 1994; Junguo et al, 2011). There is only one sample (BR91/ S566/S662) that relates to a continental margin environment, while one has an intermediate value between pelagic and continental margin environments. The La_n/Ce_n ratios indicate an intermediate stage between these two types of environment. The La_n/Lu_n ratios are mostly ($n=8$) between 0.8 to 1.3 which are related to a continental margin environment. In addition, there are two samples (BR89/S395/L449 and BR91/S564/L662) with values indicative of a proximal ridge environment. These findings, however, contradict the results of the previous ratios and they must be treated with caution.

Many of the Kordin samples ($n=6$) have a Ce/Ce^* ratio between 0.72 and 0.84, which are intermediate values between pelagic and continental margin environments. These samples (e.g. KRD15/S27/S203) have La_n/Ce_n ratio around 1 enhancing the possibility of a depositional environment with a strong continental input. Moreover, there are a few artefacts ($n=3$) with Ce/Ce^* ratio characteristic of a pelagic depositional environment. The La_n/Ce_n values do not correspond directly with either the pelagic and the continental margin environment and again present intermediate values

between the two. Furthermore, there is one sample (e.g. KRD15/L71) with a Ce/Ce* ratio characteristic of a proximal ridge environment, while with the La_n/Ce_n ratio is indicative of a pelagic formational environment. There is only one sample (KRD15/S1/L22) in the Kordin assemblage which has two ratios confirming the formation in a pelagic depositional environment. The third ratio investigated (La_n/Lu_n) overall supports the results of the other two ratios. However, a small number (n=3; 27%) of the samples from Kordin show readings which do not definitively support the findings of the other two ratios.

The samples of the Tač-Čawla assemblage have presented Ce/Ce*, La_n/Ce_n and La_n/Lu_n ratios that are related with all the different types of depositional environments. Some samples (n=4) have ratio values suggesting a continental margin environment, while others (n=4) present completely contradictory results (e.g. TCC14/S460/L273).

Many samples (n=6) of the Santa Verna assemblage (e.g. SV15/S2/L41 and SV15/S32/L5) have Ce/Ce* and La_n/Ce_n ratios which are representative of a continental margin environment (Murray et al, 1992). These results are supported by the La_n /Lu_n ratio, but this is not consistent and for many samples (n=9) it suggests a different formational environment (e.g. proximal ridge). Furthermore, there is one sample (e.g. SV15/S1/L80) with ratios related to a proximal ridge depositional environment. Some samples (n=6) have a La_n/Ce_n or La_n/Lu_n ratio suggesting a pelagic environment but this is not confirmed with the other ratios and they must be treated with caution (Masuda 1977; Murray et al, 1992; Junguo et al, 2011).

Many of the Ġgantija samples (n=5) have a Ce/Ce* ratio between 0.47 and 0.61 which is characteristic of a pelagic environment. The La_n/Ce_n ratio of these samples, however, has intermediate values between a pelagic and continental margin environment. This can be interpreted as the cherts have been formed in a pelagic environment with a terrigenous input (Murray et al, 1992). The only exception is one sample (i.e. GG15/S5/L1019) with both Ce/Ce* and La_n/Ce_n ratios characteristic of a pelagic environment. Moreover, there is one sample (i.e. GG15/S3/L1015) which both ratios points towards a continental margin environment (Murray et al, 1992; Junguo et al, 2011). There are other samples (n=2) with La_n/Ce_n ratios suggesting a continental margin environment but their Ce/Ce* ratio has intermediate values which suggest a pelagic input. There is finally one sample (i.e. GG15/S3/L1016) which presents different values than the rest of the examined artefacts. The Ce/Ce* is characteristic of a proximal ridge environment (Murray et al, 1992) while the La_n/Ce_n ration is suitable for a pelagic environment. This suggests that this artefact is made of a raw material that has been formed in a pelagic environment in close proximity to a hydrothermal ridge. The results of the La_n/Lu_n ratio support the findings from the other two rations (e.g. GG15/S6/L1019.), but in some samples, it has contradicting values (e.g. GG15/S3/L1016).

The majority of the Skorba samples (53%) have a Ce/Ce* ratio (around 1) and La_n/Ce_n ratio (around 1) that is characteristic of a continental margin environment (Murray et al, 1992; Junguo et al, 2011). The La_n/Lu_n ratio mostly support these findings (e.g. SKB16/S12/L10), but occasionally have values

which indicate a pelagic or proximal ridge environment of formation (e.g. SKB16/S1/L2). This suggests that these artefacts are made of raw materials that have been formed in a continental margin (Murray et al, 1992; Junguo et al, 2011), but with different types of inputs (e.g. pelagic). There are other samples with a Ce/Ce^* ratio between 0.50 and 0.66, which is characteristic of a pelagic environment. The La_n/Ce_n ratio also support these findings (e.g. SKB16/S3/L19), but occasionally some (n=13; 10%) have intermediate values between a pelagic and a continental margin environment. It is suggested that these cherts have been formed in a pelagic environment with terrigenous input. Furthermore, there are only a few samples (n=4) with Ce/Ce^* ratios characteristic of a proximal ridge environment (between 0.1 and 0.45). However, these results are not supported by the La_n/Ce_n and La_n/Lu_n ratios which present values related with a continental margin environment. The results from the other geochemical models are necessary to suggest the type of depositional environment of these samples. Lastly, there are a few samples (e.g. SKB16/S18/L10) with contradicting values and based on the current results, it is not possible to define their depositional environment.

The last step of the research involving the rare earth elements (REEs) is the examination of the normalised patterns of these elements which can provide an overall perspective on the fluctuation of the REEs and significantly contribute to connecting artefacts with sources. The samples from the Circle have low concentrations (<10ppm) of REEs and according to their pattern, they are divided into three groups (Fig.5.80). The first group includes one artefact (blue line) which has normalised REE concentrations at the same level, except the Tb element that presents a small depletion. The second group has lower normalised concentrations ($< 10^{-1}$ level) than the first and presents more fluctuating patterns. They have an important depletion of Ce and minor of Tb, and their patterns are very similar. Furthermore, they are enriched on gadolinium (henceforth Gb) and dysprosium (henceforth Dy), which are characteristic not reported to the groups. The third group has the lowest concentrations of REEs (10^{-2} level) and their patterns greatly fluctuate, which does not allow the recording of further characteristics.

The samples from Kordin have also low concentrations of REE's (<9ppm), but their patterns are not so clearly divided into groups as are the Circle samples. There is one sample (KRD15/S1/L22) that has higher normalised concentration (navy blue line) than the rest of the examined artefacts (Fig. 5.81). Compared to the rest of the Kordin assemblage this samples present completely different REE readings. Looking at the results and the original data from the LA-ICP-MS, the readings are not consistent and it is therefore possible that the internal heterogeneity of the lithic sample caused these fluctuating readings. The other samples have smoother patterns and most of them (n=10) have a noticeable depletion of Ce. Some of these have a minor depletion of Tb, while others (n=6) have a minor enrichment of Gb. The samples with the lowest normalised concentrations (10^{-2} level) are

depleted at the first group of elements of the diagram (Fig.5.81) which is known as light REE (LREE)²⁷ and enriched on the second group which is known as heavy REE (HREE).

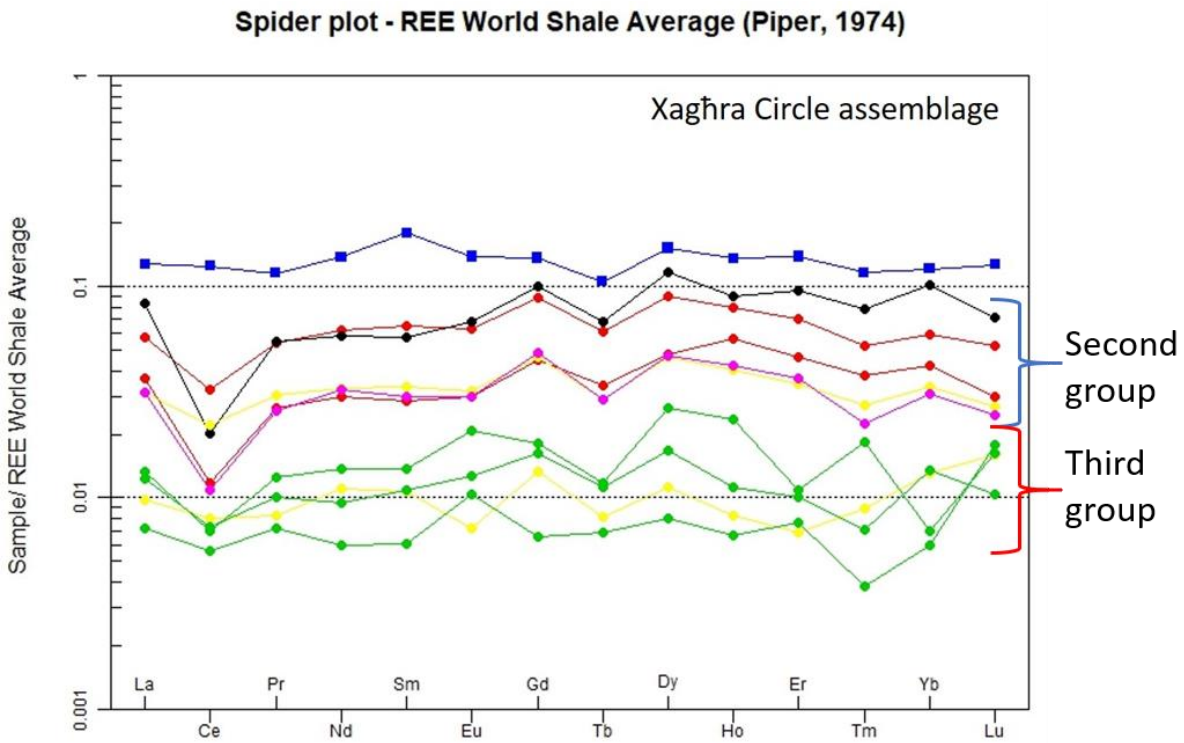


Figure 5-80: The normalised patterns of rare earth elements of the Circle artefact samples.

²⁷ The lanthanides (part of REEs explained in footnote 21) are divided into a) lower atomic weight elements from lanthanum (La) through to europium (Eu), referred to as light rare earth elements (LREE) and b) heavy atomic weight elements from gadolinium (Gd) through to lutetium (Lu) referred to a heavy rare earth elements (HREE).

Spider plot - REE World Shale Average (Piper, 1974)

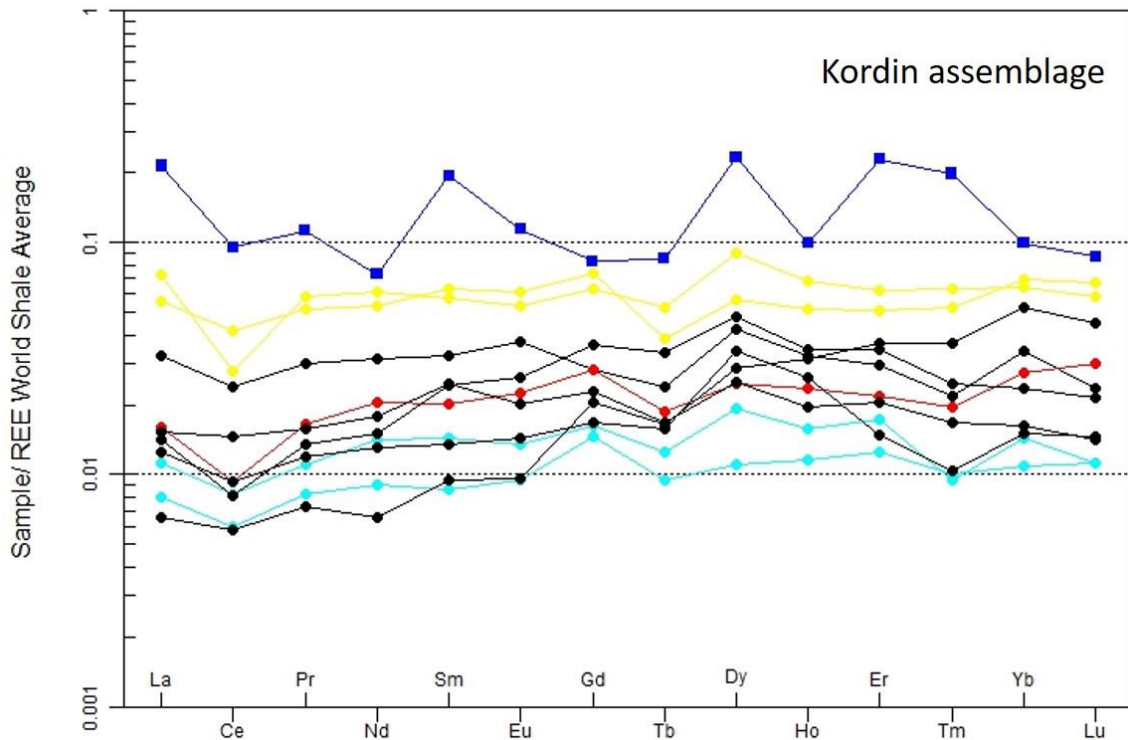


Figure 5-81: The normalised patterns of rare earth elements of the Kordin artefact samples.

The samples from Tač-Čawla have low concentrations (<4ppm), but in comparison with the previous assemblages, their patterns are less spread in the diagram (Fig.5.82). They all have a noticeable depletion of Ce, an enrichment of Gb and a minor depletion of Tb. The majority of the samples (54%) have a similar pattern, but deviations in different elements have been reported. However, there are two samples (TCC14/S193/L69 and TCCC14/S577/L131) with significantly fluctuating patterns (red line) that can be segregate from the other artefacts.

Most of the Santa Verna samples (n=16) also have low concentrations (<30ppm) and their pattern of accumulation are between 10^{-1} and 10^{-2} scale (Fig.5.83). They demonstrate a very similar pattern, which shows a characteristic depletion of Ce and a minor depletion of Tb. However, there is one sample (SV15/S1/L98) in this region of the diagram (red arrows) with distinct fluctuation which differs from the rest of the artefacts. The examination of the REE found two artefacts that are not in this region of the diagram. The first (black arrow) is the sample (SV15/S1/L52) with the highest quantity of REE's within the assemblages and has normalised concentrations around 1. The second (SV15/S1/L80) has the lowest quantity of REEs within the dataset (blue arrow), and some of its normalised concentrations are below 10^{-3} .

Spider plot - REE World Shale Average (Piper, 1974)

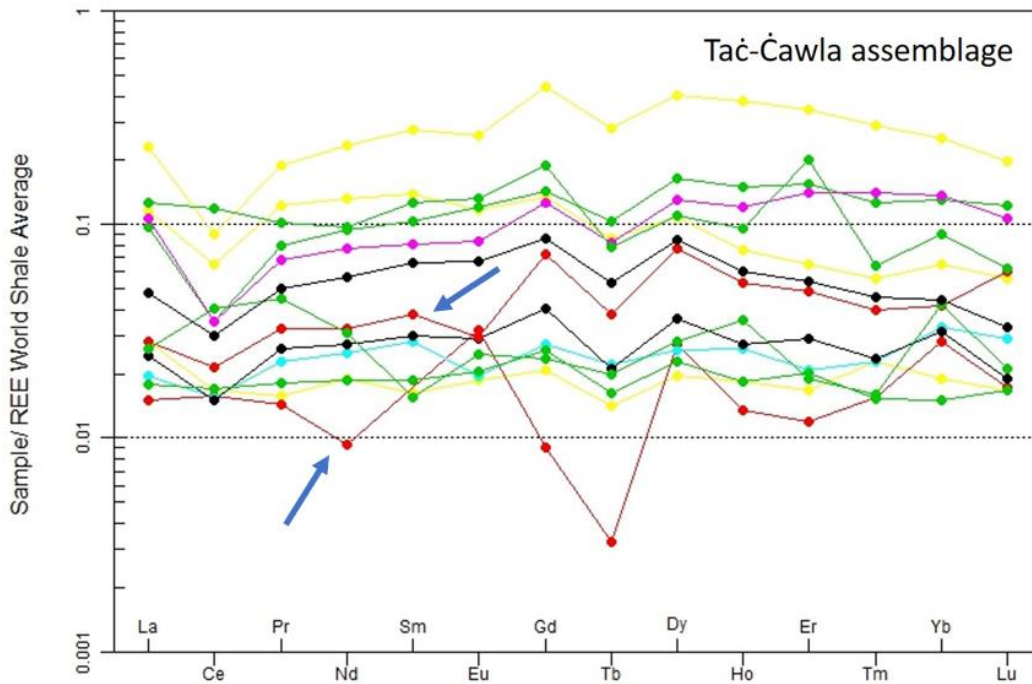


Figure 5-82: The normalised patterns of rare earth elements of the Tač-Čawla artefact samples. The blue arrows point on the two samples (TCC14/S193/L69 and TCC14/S577/L131) with the significantly fluctuating patterns.

Spider plot - REE World Shale Average (Piper, 1974)

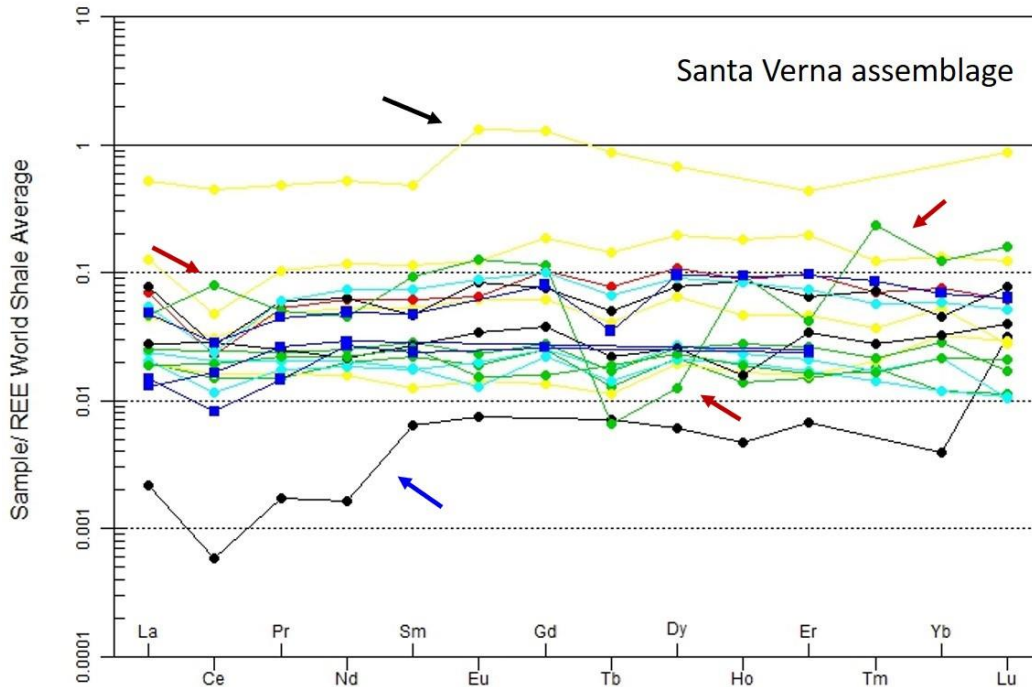


Figure 5-83: The normalised patterns of rare earth elements of the Santa Verna artefact samples. The red arrows point out the sample (SV15/S1/L98) with the distinct fluctuation. The black arrow points out the sample (SV15/S1/L52) with the highest quantity of REEs and the blue arrow points out the sample (SV15/S1/L80) with the lowest quantity of REEs.

The samples from Ġgantija have low concentrations (<9ppm) and according to their pattern, they are divided into three groups (Fig.5.84) similar to the samples from the Circle. The first group includes artefacts (GGWC15/S3/L1016 and GGWC15/S1/L12) with normalised concentrations slightly higher than 10^{-1} . They have low levels of Tb in comparison with the other measured REEs, while one (GGWC15/S3/L1016) has also a depletion of Ce (black arrow). The second group (GGWC15/S3/L1015 and GGWC15/S3/L1015) has lower concentrations than the first (< 10^{-1} level), but although they present similar normalised concentrations, their patterns exhibit differences. The only common characteristic reported in their pattern is the important depletion of Tb. The third group has the lowest concentrations of REEs (10^{-2} level) and despite their small differences, they have similar patterns. They are mainly characterised of an important depletion of Ce and minor of Tb.

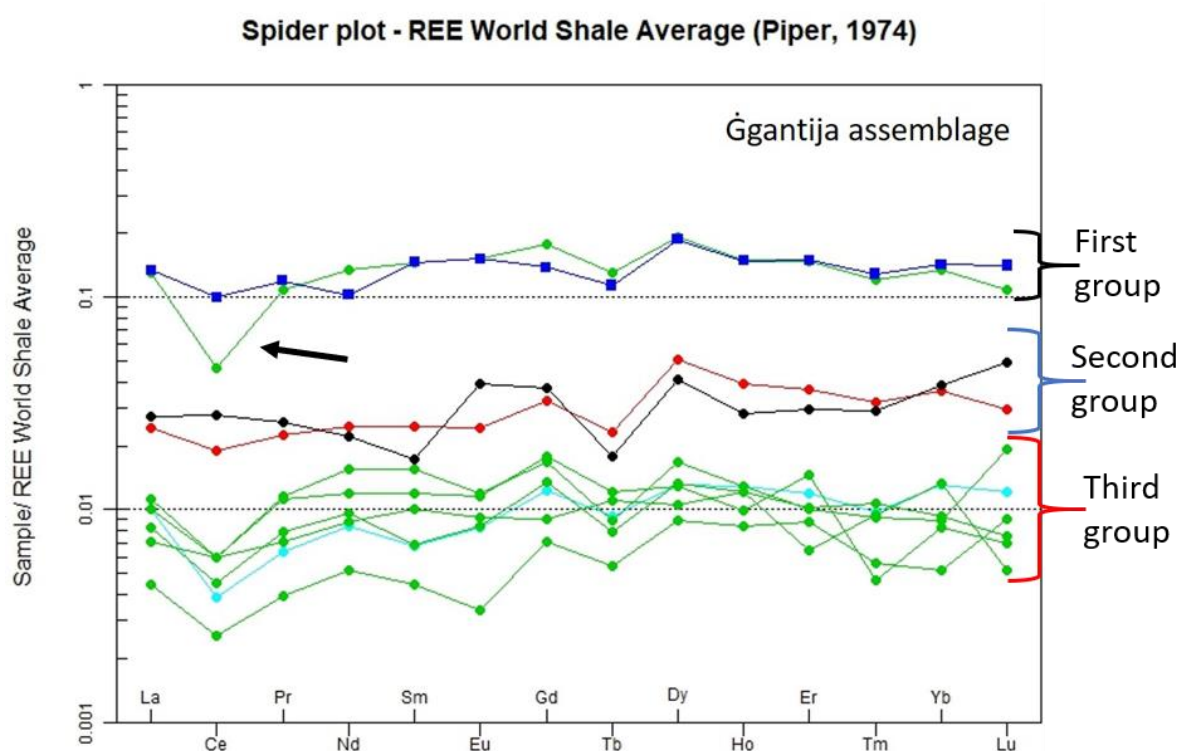


Figure 5-84: The normalised patterns of rare earth elements of the Ġgantija artefact samples. The black arrow points out the depletion of Ce at the sample GGWC15/S3/L1016.

The great number of artefacts found in Skorba has led to the selection and analysis of many samples from this assemblage (n=129). In order to avoid confusion and to be able to identify the differences between the examined artefacts, REEs pattern diagrams from each context of the excavation have been created (Appendix I, p182). These samples have low concentrations (<14ppm) and according to their pattern, they are divided into two groups. The first group includes the majority of the examined artefacts (n=45; 75%) which have normalised concentrations around 10^{-1} . Most of them (n=27; 60%) have relatively linear patterns which demonstrate a depletion of Ce and Tb. The second group has lower concentrations (< 10^{-2}) than the first and characterised by greatly fluctuating

patterns that do not allow the recording of further characteristics. Nevertheless, many of them (n=7; 47%) have an important depletion of Ce and minor of Tb and Tm.

5.3.3. First remarks

The Maltese cherts have originated from biogenic sediments which were deposited in an intermediate basin between pelagic and continental margin environments. Moreover, the deposition of these sediments was conducted under low levels of oxygen (anoxic to dysoxic conditions). The results on the Sicilian chert samples are more complex and suggest that the Island has different chert sources. Most of these cherts have originated from biogenic sediments, but some have been created from hydrothermal sediments. In addition, there were cherts which show a connection with both types of sediments. Some of these sediments have been deposited in a pelagic environment, while others were in a continental margin environment. The analyses of the Sicilian cherts indicate that Sicily is a place with multiple and diverse chert sources, especially in comparison with the Maltese Islands. Only one sample from western Sicily (S24) is consistent as it was formed by hydrothermal sediments which were deposited in a hydrothermal environment. The examination of the palaeo-oxygen level did not provide a better understanding of these cherts but again highlighted the diversity within the Sicilian cherts.

The results of the assemblages have provided a better understanding of their possible sources and formation processes involved in their origin. The vast majority of the samples originated from biogenic sediments which have been deposited in a pelagic environment. There are some samples, mainly from Skorba, which are formed from biogenic sediments deposited in an intermediate basin between pelagic and continental margin environments. These characteristics are similar to the Maltese cherts and their connection with the local sources is highly possible. There are a few artefacts that may be related with hydrothermal sediments and only one related with hydrothermal environments. Furthermore, there are some artefacts related to biogenic sediments that have been deposited in a continental margin environment. The palaeo-oxygen investigation enhances the findings of multiple sources and further confirms the usage of the local sources.

Understanding the formational processes and the conditions under which these occur is, in my opinion, the optimal means for defining the different rock sources. In pursuing this archaeometric analysis of the chert lithics in such detail, I argue that this approach allows for a completely holistic understanding of the *chaîne opératoire*. This will be developed further in chapter 6.

6 Discussion

6.1. The location and geological background of chert sources

It is established from the literature (Pedley et al. 1976, 2002) that the Maltese Islands have very simple geology and a mild tectonic state. It is also suggested (Cooke, 1893; Malone et al., 2009) that the chert formations are reported inside the middle layers of the Globigerina limestone (Miocene). The new geological fieldwork on the Maltese Islands during Spring 2016 and Spring 2017 has confirmed these claims and recorded that the chert outcrops are only found in specific locations in which the middle Globigerina Limestone is in bedded form. This was reported in the west and southwest parts of the Maltese Islands, where deep marine depositional conditions must have been present. This theory is suggested because the middle Globigerina Limestone was deposited in a shallow marine environment, which in normal conditions is not suitable for chert formations. It is not a coincidence that chert outcrops have been found at Fomm-IR-RiĦ bay in Malta, at the western end of the Victorian Lines (faults) and in an internal valley (Wied Pisklu) of Gozo, which is surrounded by collapsed karstic structures. The geotectonic status may explain why and how the chert outcrops are reported in these locations, but it is outside the scope of this research and it is reserved for future work, focused specifically on the matter. The hill south of Skorba is a possible location for chert outcrops, but the investigation has not provided any evidence. The middle Globigerina Limestone at the northeast part of Marsaxlokk bay in Malta has similarities with chert-bearing exposures, but again no indication of chert material was recorded. The exploitation (e.g. agriculture and industry) of these two locations has altered the landscape and it has proven impossible to define the existence of chert sources.

There is a commonly held belief that the island of Sicily is the origin of the foreign chert artefacts found on the Maltese Islands and part of my research was to test this theory. Although Sicily is geologically more complex than Malta and has a greater variety of formations, it has been more thoroughly investigated in the past. Therefore, the research focused on the most important chert outcrops of Sicily, collecting representative samples from all the different chert types available. The fieldwork survey (conducted by Chatzimpaloglou in 2017) on the island recorded the abundant resources of chert material in many areas of Sicily (Fig.17). The chert formations are mainly intercalated with limestones (e.g. Hyblean Plateau unit – Southeast Sicily), but they also form a distinct formation (Radiolarian – East Sicily). They are formed in marine, continental or volcanic environments and chronologically they ranged from the Triassic to the Pleistocene. This variety of environments and time is the first and clear difference between the Maltese and Sicilian chert sources. In contrast, the Maltese cherts are related only to a shallow marine environment and they are chronologically restricted in the Miocene (20 Ma).

Although this seems outside the frame of an archaeological research, it provides useful information about the sources of raw materials and can contribute significantly to sourcing stone artefacts. Understanding the geology of the area of interest and the conditions under which the formations were created, should contribute to the investigation of lithic sources. Therefore, by focusing on specific locations and by excluding areas that do not present the aforementioned appropriate characteristics, this enables our research strategy to be more effective. This is especially important for areas such as the Maltese Islands, the rock resources of which, have not been investigated to a level that is necessary for this type of research. The fieldwork conducted on the Maltese Islands also recorded chert outcrops on Gozo Island for the first time. These outcrops have never been mentioned previously in research and could change current beliefs regarding the availability of chert resources on the islands. Moreover, the geological investigations show that the important chert exposures are easily accessible on foot. These could not be found without the geological investigation of the island and this observation shows the contribution of geology in archaeological research. As a consequence, future research on the chert resources in the Maltese Islands should focus on the areas mentioned previously and/or in places with a similar status.

Furthermore, the fieldwork on Gozo and the discovery of the white and translucent outcrops are extremely important for geoarchaeological research, because current quarrying activities in the area are continuously altering the landscape. The last visit in 2017 also recorded the expansion of the road network, created especially for the quarries. More specifically, the path with the chert outcrops has become a road which has significantly damaged this exposure. The most unfortunate implication is that the road has completely buried this unique chert outcrop/source and no evidence of that can now be found. The current research has retrieved the only proof that such chert material exists on the Maltese Islands and these unique findings can be used in future sourcing and exchange network studies.

The fieldwork on Sicily also investigated which outcrops could be accessible and convenient sources for prehistoric artefact/tool manufacture. Additionally, it has investigated all the areas suggested by Vella (2008) as possible locations from where exotic material was imported to Malta. The province of Ragusa is the closest part of Sicily to Malta with important chert resources and evidence of prehistoric mining activity (Monte Tabuto). These features are used as arguments by scholars (Vella, 2008) to support their claim that Sicily is the origin of foreign chert material. The most interesting finds are reported from the area of Monterosso Almo, located in the northern part of the province. This research has recorded multiple and different types of chert outcrops, which were fine-grained, solid and dense. Their colour varied from greyish and black to dark orange and they were of suitable quality for tool crafting. The main advantages of this area are the extensive and widespread chert outcrops, their high level of accessibility and that chert material can be easily extracted from these exposures.

Furthermore, the presence of (possibly prehistoric) mining structures and the quarries verify the presence of human activity in this area for a long time, which increases the possibility that this area may be a source location of many artefacts found in Malta. On the contrary, the finds at Monte Tabuto are less promising and it is unlikely that chert material from there would have been exported to Malta. The chert outcrops today are small, limited, difficult to extract and with features of lower quality than other sources elsewhere in Sicily. However, it is possible that prehistoric/historic mining has depleted the chert source and the current exposures are the last remainder of an undefined chert exposure.

The province of Enna is in the central part of Sicily and is more remote from Malta, but the Radiolarian exposure demands further investigation. The first reason is the red colour shades, which are of a colour not reported on any other chert outcrop of Sicily and Malta. Moreover, the exposure of the Radiolarian formation is along the riverbeds of Valona river which was possibly active during prehistory. Erosion and river action enormously increase the range that this outcrop can reach and increase the probability of this material being found on Malta. This is enhanced by the fact that some artefacts (n=5) in the investigated assemblages are characterized by similar reddish colours. Although these are strong indicators, more research is needed on these artefacts and sources to absolutely establish a connection.

The province of Palermo and generally West Sicily have never been considered as a possible location of raw material. The greater distance from Malta, in comparison with other parts of the Island, and the absence of good evidence for prehistoric mining activity suggest the importation of material to Malta from this region as an unlikely event. Nonetheless, since this region presents a very interesting combination of chert outcrops, it was decided to pursue further research in this location.

6.2. Chert outcrops

The chert outcrops of the Maltese Islands were in bedded and nodular form, fine-grained and varying in size, shape and colour. The chert outcrops of Gozo were mainly of greyish colour, while the outcrops of Malta have olive-brown colours. The only distinctive exception is the one outcrop found in Gozo, which has been highlighted from the beginning in this work. During the whole period of fieldwork, no other chert outcrop was found to present similar characteristics (i.e. white and translucent) as these nodular cherts. In addition, some of the bedded outcrops showed features not compatible with chert formations, which could be silicified limestone or even silicified shales. They appear to be coarse-grained, relatively soft, have a rough texture and do not present a conchoidal fracture. Nevertheless, it can be suggested that all chert outcrops presented the appropriate macroscopic characteristics necessary to be considered as potential sources for chert tools/artefacts.

The chert outcrops of Sicily presented great diversity in their macroscopic characteristics but generally, they had better features in comparison to the Maltese cherts. They were fine-grained, semi-

translucent, in bedded and nodular form, while their size, shape and colour significantly differentiate. The black and translucent cherts were more common and were found in all the areas that have been investigated. There were some chert outcrops in East Sicily (province of Enna) that have similarities with outcrops in West Sicily. They were in small nodules and fragmented, with purple colour shade and inside a limestone of a similar age (Triassic). The only exception were some chert outcrops of West Sicily with an orange colour which is a feature not reported amongst those of the East. On the contrary, the Radiolarian outcrop was a unique formation with no equivalent in Sicily and Malta. The reddish colour, the extensive outcrop and old age (Triassic) are the main characteristics that separate them from the other chert sources. However, more information is necessary to make further remarks about these chert sources and the differences they display.

The combination of fieldwork and laboratory research could reveal the origin of the Silica (Si) component for the investigated chert sources. The geotectonic position of the Maltese Islands is at a substantial distance from any mid-ocean ridge and volcanic centre, which makes it unlikely for the Si to have a hydrothermal origin (hydrothermal sediments). The microscopic analysis demonstrated plenty of fossils such as radiolarian and sponge spicules were present, which could be the silica sources. Furthermore, the concentrations of the major elements (Fe, Al, Mn) suggest a biogenic origin of the Si (biogenic sediments). This becomes clear with the use of the ternary diagram (Fig. 6.1), which shows that all the chert formations of the Maltese Islands are gathered in the zone of the biogenic sediments. The situation in Sicily is more complex and caution is required when synthesizing the collected data from the different methods. Although it is mainly a sedimentary basin, the geotectonic position is close to volcanic centres, which could have possibly been an additional source of Si. This is supported by the geochemical findings of the ternary diagram (Junguo, 2011), which shows some chert samples (S24 and S19) to have hydrothermal sources (hydrothermal sediments). This might be an unexpected result for the Monterosso chert sample (S19), but it not for the chert sample (S24) from West Sicily because it is related to volcanic formations. Nonetheless, most of the Sicilian cherts (n=21) are placed in the regions that suggest a strong connection with biogenic sources. This is also confirmed from the microscopic examination, which recorded plenty of radiolaria (e.g. spoumelarian) and other Si related fossils (e.g. sponge spicules). Furthermore, it is clear that the Maltese samples are gathered on a specific area of the ternary model in comparison with the Sicilian. This suggests that the Maltese samples have inputs from more homogeneous Si sources than the Sicilian.

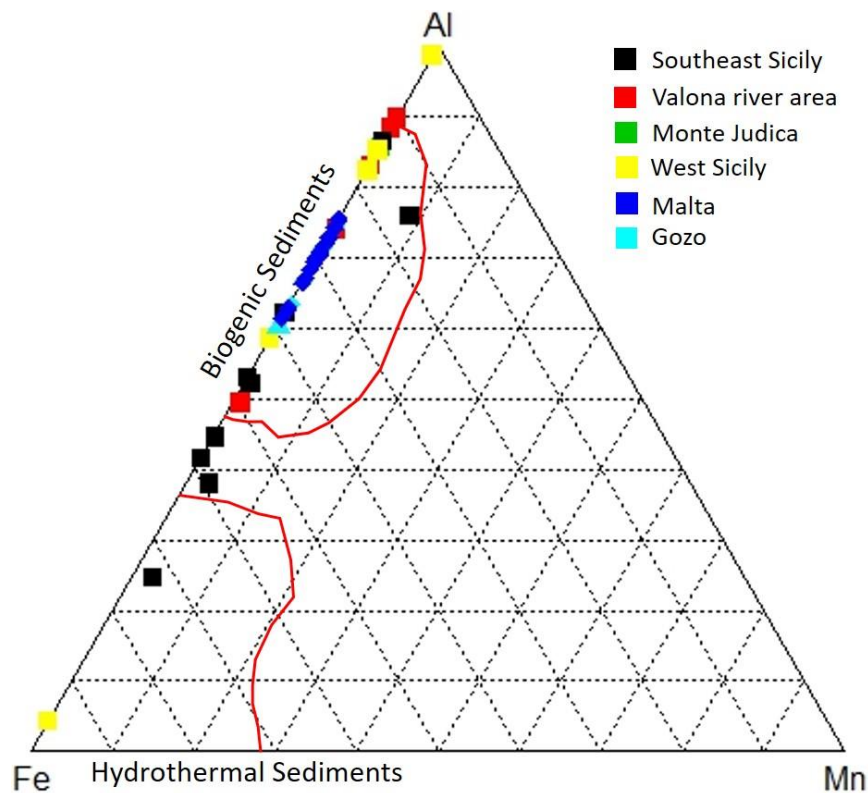


Figure 6-1: Ternary diagram examining the origin of the sediments of the investigated rock samples. The line demarcations have followed the suggestion of Junguo et al. (2011).

The major elements identified could also provide indications on the depositional environments of the different chert sources. The binary model suggested by Murray (1994) uses the concentrations of major elements (Fe, Ti, Al) and classifies the chert rocks of the Maltese Islands within an intermediate environment between a pelagic and continental margin environment (Fig. 6.2). On the contrary, the Sicilian cherts are more widespread in the model and the samples are categorized in different environments. Some of them relate to a pelagic environment (n=9), while others (n=9) related to a continental margin environment. There is only one sample (S24) found in the region that relates to a mid-ocean ridge (near or proximal) environment. This sample was collected from a chert formation related to volcanic activity and the geochemical data simply confirm this relationship. It is important that the geochemical results are treated with caution and the findings are always combined with the petrological features of the rocks examined. Nevertheless, when all the rock samples are inserted in the same model it is observed that the Maltese chert is restricted into a region within which no Sicilian chert has been found (Fig. 6.2). This is one additional difference between the two locations and this research claims that in terms of the type of sediments and the depositional environment, the two locations (i.e. Sicily and Malta) can be easily differentiated.

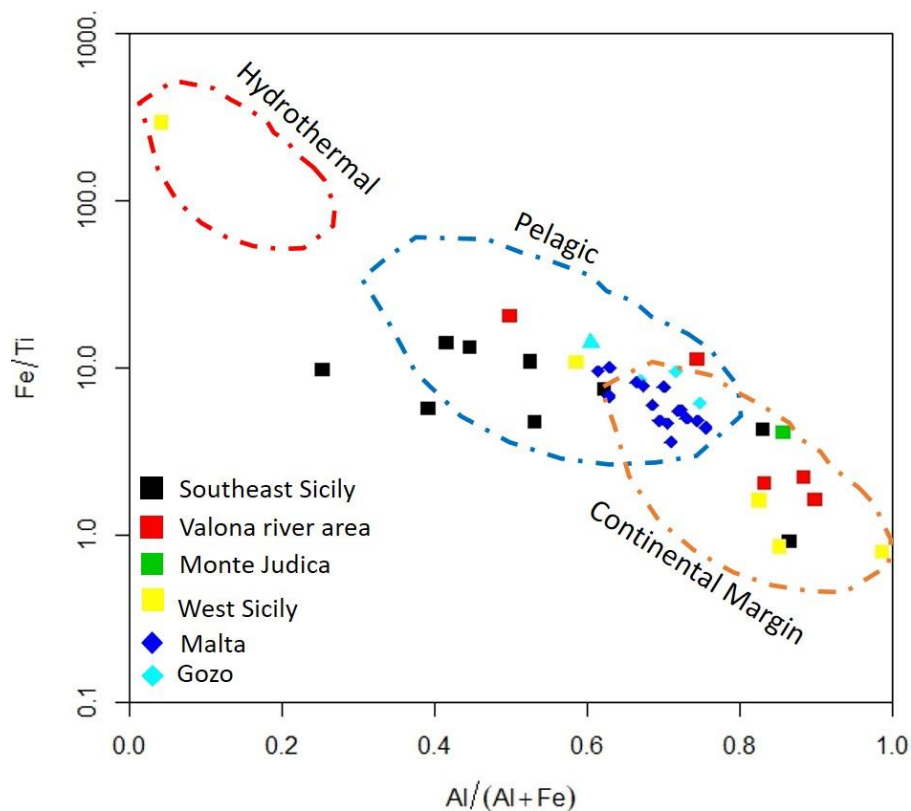


Figure 6-2: Binary diagram examining the depositional environment of the investigated rock samples. The line demarcations have followed the suggestion of Murray (1994).

The findings of the rare earth elements (REEs) generally confirmed the results about the nature of the depositional environment. The three used ratios (Ce/Ce^* , La_n/Ce_n and La_n/Lu_n) suggest that the Maltese chert rocks have been created in a continental margin environment with a strong pelagic input. Only a few samples produced values outside this status, which could be due to a random error or an unreliable result and do not imply a different type of environment. Since the Maltese samples come from one and the only formation, their respective results must be investigated as a group and not individually. The ratio results of the Sicilian samples are compatible with the findings of the depositional model (Fig. 6.2). The small number of ratio values that do not agree with the findings of the depositional model, should be treated with more consideration than those of the Maltese chert. The main reasons being: a) many of the samples are from different chert formations and b) the formations themselves span a timescale of hundred million years in which the depositional environment might have changed. Therefore, further investigation is necessary to identify the accuracy of these contradictory results. However, this type of investigation is more in the geological sphere of interest and not in the priorities of the research presented in this thesis. The findings of the full methodology suffice to draw safe conclusions on the connections between artefacts and sources, which is the research focus of this PhD research.

The REEs normalised patterns provide additional information about the investigated sources and show further differences (see 5.1.1 chapter). The Maltese samples have an almost identical and

smooth pattern with concentrations on the same level (10^{-1}). Moreover, all the samples present negative anomalies (depletion) on the elements of Cerium (Ce) and Terbium (henceforth Tb) which are indications of a pelagic influence. These confirm the results that they have been deposited in the same environment (continental margin) with similar conditions (pelagic input). In comparison, only a few Sicilian chert samples are in the same normalised concentration level (10^{-1}), but even they do not have the same smooth pattern. The normalised patterns of the Sicilian chert samples illustrate very clearly the differences between the regions. The chert samples from the same regions have similar patterns, but they are plotted on different normalised concentration levels. Moreover, their pattern does not fluctuate in the same manner from element to element, which indicates minor different inputs. The samples from Southeast Sicily (Fig.5.72b) have a strong negative anomaly (depletion) of Cerium (Ce) which suggests a deep pelagic environment. On the contrary, the samples from the Vallona river (see 5.1.1 chapter) present a positive anomaly (enrichment) of this element. They also show a general enrichment on the first group of REEs (LREE) in comparison with the second group (HREE). These two features on the patterns of the Vallona river samples indicate that their depositional environment has a strong hydrothermal input. The chert samples have a different normalised pattern which shows great variability in environment and inputs. This is also supported by the finding of the major element models which categorized them in different environments. The geology and fieldwork have shown from the beginning that the formations found in West Sicily are a combination of sedimentary and volcanic rocks of different age, which explain the contradictory geochemical results.

The next step is to investigate the different conditions, under which the examined rock sources have been deposited. An important condition is the level of oxygen during deposition because it can have a great effect on the final characteristics (e.g. macroscopic – colour) of the rock formation. The environments with high concentrations of oxygen are described as oxic, while the environments that are depleted in oxygen are anoxic. The concentrations of specific trace elements (i.e. U, Th, V and Ni) have been suggested (Garbán et al, 2017) as good indicators of the oxygen level and are used in a binary model to identify this factor in the examined samples (Fig. 6.3). It is demonstrated in this diagram that the Maltese samples are mainly gathered in the centre and away from the Sicilian samples. However, there are some (n=6) - and especially those from Gozo - that deviate and appear closer to the Sicilian samples. These samples have been deposited in an environment with a higher concentration of oxygen than the rest of the Maltese chert. All the samples from Malta (n=17) are related to anoxic environment in terms of the U/Th ratio, while the ratio $V/(V+Ni)$ is allocating them to more moderate levels (dysoxic).

The Gozo samples have similar $V/(V+Ni)$ values to the samples from Malta, but the U/Th values suggest that they have been deposited in an environment with higher concentrations of oxygen. On the contrary, the majority of the Sicilian samples (n=21) in terms of the U/Th ratio are related to oxic conditions. There are two (S18 and S3) with anoxic conditions, which also present increased values of

this ratio (enriched in U). The $V/(V+Ni)$ displayed diverse values, although results showed that the samples from the Valona river area have higher values in comparison with the ones from Southeast Sicily.

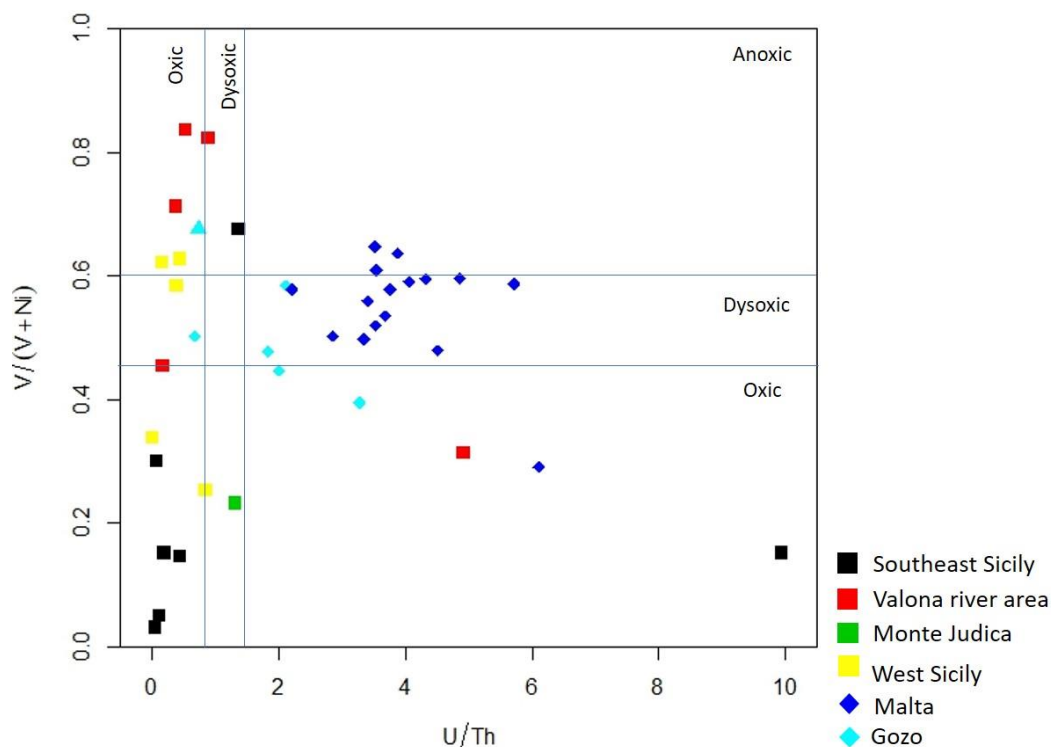


Figure 6-3: Binary diagram examining the oxygen level of the depositional environment of the investigated rock samples. The line demarcations have followed the suggestion of Garbán et al (2017).

The microscopic and mineralogical examination presented further differences between the two source locations of Malta and Sicily. The optical microscopy suggested that calcite minerals are the most common mineral in the Maltese chert outcrops, while quartz and chalcedony are mainly filling fossils, fragments and porous. This observation was also supported from p-XRF results that produce spectra in which Ca have the highest number of energy counts than those of Sicily. However, the FTIR results demonstrated that the dominant mineral is opal–A and also recorded the presence of tridymite. The dominance of silica (henceforth SiO_2) is also supported by the semi-quantitative data of the SEM examination of the thin sections. These contradictory results can be explained by the peculiar mineralogical structure of opal–A. This mineral is amorphous (not crystalline in structure) and it is difficult to distinguish it in a thin section, especially in those Maltese samples which have a very fine-grained matrix ($< 5\mu m$). In addition, the opal–A mineral has water (H_2O) in their chemical structure and this is possibly the reason why the p-XRF recorded Si with fewer number of counts than Ca. I have to remind, however, that the p-XRF provided qualitative results and the number of counts or the height of the peak should not be directly associated with the actual concentration of a recorded element.

The tridymite was only recorded in the FTIR by a small characteristic peak, while it is dominant only in one sample (F152). It is an intermediate mineral between opal–A and quartz, but it is an unstable

mineralogical form of SiO₂ and extremely difficult to identify under the microscope. A few other minerals were reported in these samples in minor concentrations and relate more to the host limestone than the chert outcrops. Dolomite is one of them and was recorded in the microscopic examination (Optical and SEM) and the FTIR analysis and mainly found in micro-crystals. The next mineral reported was feldspar, as mega-crystals or fragments inside the matrix of the chert samples. Feldspar and to a lesser extent pyrite and illite minerals are the sources of iron (Fe) which were reported in these samples. There were some samples (e.g. F1S4) with an abundance of carbonate minerals (i.e. calcite and dolomite) and iron concentrations higher than Si. These were most possibly not cherts, but more likely silicified limestone which macroscopically could not be distinguished from the actual chert rocks. The only exception was the unique, white and translucent sample from Gozo (G2S6) which consisted mainly of Si and crystalline silicate minerals (i.e. quartz and tridymite).

The results of the Sicilian chert samples were less complex, and they were dominated by quartz minerals and high concentrations of Si. Regardless of the area from which samples came, all of them had a microcrystalline matrix which consisted only of quartz. This was further verified by the data of FTIR, which recorded the presence of this mineral in all samples. The opal – A was found only in one sample with (e.g. S15) minor peaks. There were some calcite minerals in some of the samples (n=7), but they were related to the host limestone and not with the chert outcrops. The microscopic examination recorded hematite minerals in some samples (S13) and this explains the iron peak found in them (p-XRF). The S24 sample had a great number of energy counts related to Fe in the XRF spectrum and this feature is attributed to its connection with the volcanic activity of the West Sicily. The volcanic centres and ridge environments are known as abundant sources of iron. However, these findings were contradicted by the other methods, which demonstrated the predominance of quartz and subsequently of Si. The only exception was found in samples from Southeast Sicily (e.g. S4) in which opal – A or tridymite were the most common minerals. They also presented high concentrations of calcite which suggested that these samples were probably silicified limestones.

Some final comments can be made regarding the fossils reported in the examined rock samples, which enabled a deeper understanding of the type of sources. The Maltese samples presented radiolarian and sponge spicules which are the main source of Si. Some of the fossils retained the original structure and composition (opal – A) or even presented residues of organic matter, while others were fully replaced from quartz and chalcedony. Moreover, these chert samples were abundant in fossils of carbonated origin which are related to the host limestone. Most of them retain their original carbonate composition, although some were replaced with quartz minerals. The presence of so many fossils in their interior suggests that these rock formations have not undergone a long diagenetic transformation (from sediment to solid rock). This, in addition to the fact that they primarily consist of softer silicate minerals, suggests that they are considered of a low diagenetic level. This

means that they are relatively weaker and explains the “low-quality chert” term which is used by many archaeologists to describe them.

An interesting fact is that the intermediate examination (a scale between macro- and micro-examination) demonstrated that the white spots recorded on the majority of the Maltese chert are actually the carbonated fossils which retained their original composition. This is an excellent finding because it reveals that this feature (white spots) is not just a superficial feature but instead it is connected with the internal structure and is a strong representative characteristic of these chert outcrops/sources. The Sicilian chert presented radiolarian and other Si related fossils which should be the main source of Si. These were replaced with quartz and chalcedony minerals and did not have residues of organic matter. Moreover, they rarely presented fossils related to the host formation which are mainly replaced with quartz and/or chalcedony. This, in addition to the fact that they primarily consist of the strongest silicate mineral (quartz), suggests that they are considered of high diagenetic level. This means that they are relatively stronger and also explains the “good quality chert” term which is used from many archaeologists to describe them.

6.2.1. Chert source summary

The chert outcrops of the Maltese Islands were fine-grained, with greyish and olive-brown colours and had a distinctive spotted feature which relates to the remaining carbonated fossils. They were dominated by opal-A, but the carbonate minerals calcite and dolomite had a significant part in their internal structure. The only exception is one outcrop on Gozo (G2S6), which was characterized mainly by their white colour, high level of translucency and quartz minerals. Furthermore, the Maltese chert rocks were biogenic sediments which have been deposited in a continental margin basin with pelagic inputs and low concentrations of oxygen (anoxic to dysoxic).

The Sicilian chert had a greater diversity of colours, but the majority were fine-grained, shiny and with a high level of translucency (n=24). They were dominated by silicate minerals and especially quartz, while other types of minerals had a restricted presence. The majority of samples (n=21) were related to biogenic sediments, apart from two samples (S19 and S24) collected from the volcanic group of formations. This sample has also been deposited in a hydrothermal environment (ridge), which explains the high concentrations of Fe reported in this rock sample. The rest of the examined Sicilian outcrops have been deposited in pelagic or continental environments, but none of them has been formed in an environment similar to the one of the Maltese cherts. The results from the possible inputs of the environment were mixed and there could have been inputs from any of the three types (i.e. pelagic, continental and hydrothermal). The levels of oxygen were similar but were certainly different from the ones of Malta. The ratio of U/Th suggested that the majority of chert types are related to oxic conditions (n=21), but two show that they have been formed under anoxic conditions. The results were

not clear with the $V/(V+Ni)$ ratio, but it seemed that the chert samples from the different areas (e.g. Southeast Sicily) have been formed under similar levels of oxygen.

6.3. Chert artefacts

The archaeological research has revealed that the prehistoric communities of Malta showed enormous creativity. Between the first half of the 4th millennium and the middle of the 3rd millennium BC, they built large-scale monuments, known as the Stone Temples (Malone et al. 2009). This rare achievement might change our understanding of prehistoric Europe and therefore it is of great importance to understand the circumstances under which these monuments were built and who were their creators. Moreover, it is equally important to seek the degree of connectivity with the neighbouring communities and the influence of those communities on the Maltese society. Addressing these issues could provide an insight into the motivation and characteristics of the prehistoric people of Malta, who constructed these amazing monuments (Malone et al. 2009). One way to address these issues is by studying the material culture (e.g. pottery, artefacts) related to these monuments. That understanding can provide information on how sophisticated was the prehistoric society that settled on the Maltese Islands, as well as provide insights into the range of the resources they used. The latter will contribute towards the investigation of the degree of connectivity with neighbouring areas. The possible relation of the Maltese Islands with foreign areas may consequentially raise issues of trade routes and cultural exchange. Therefore, a proper investigation of the material culture of a prehistoric society can become a tool to address multiple and complex issues.

This research investigated the lithic assemblages of three temples, one funerary site, one settlement and one site which includes a temple beside/above a settlement. The original belief that these are all chert assemblages has been proven false, as this investigation has recorded a lot of non-chert material. Even the assemblage of Xagħra Circle which is the most advanced assemblages has samples of different materials. The biggest assemblage from these is the one from Skorba, as the examination for this thesis was conducted at the same time as the excavation and this allowed the opportunity to investigate the whole assemblages and its contexts. We can now establish that the majority of the artefacts in the assemblages is made from chert material, while fewer artefacts are made from obsidian. There are many lithics, especially in the Ġgantija and Skorba assemblages, which are patinated and their original macroscopic characteristics have been altered. The comparative examination between them and the Maltese chert exposures in the field has present evidence of their relationships. Moreover, the p-XRF results recorded high peaks of Ca and Fe and connected them with the silicified limestone found on the Maltese islands. It is unclear whether these pieces are debris of the manufacturing process or these resources have been also used for tool construction.

Before discussing the findings from the chert artefacts, it is important first to define briefly the main characteristics of a chert rock and highlight those that have been used in this research to separate them from the rest of the material. Cherts are generally fine-grained, dense, commonly very hard rocks, which break with a conchoidal fracture, often producing very sharp edges (Boggs, 2009; Tucker, 2001). They can be found on the field in a bedded or nodular form and predominantly inside host formations (e.g. limestone).

6.3.1. First group of artefacts (Brown chert artefacts)

Focusing on the chert artefacts the macroscopic investigation divided them into three big categories. The first group of artefacts was mainly characterized by brown colour shades (e.g. 10YR 4/2, 6/2) high homogeneity and density, while they can vary on the level of translucency, shine and grain size. They mainly have substantial size (L and W > 3cm), but small artefacts are also reported such as flake and flake scrapers which always have part of the cortex remaining (Fig. 6.4). Most of the finds in the Circle and Ġgantija assemblages are made from this type of chert material, while there are only a few of this artefact group in Santa Verna (<15%). This is very interesting and odd considering that these three sites are in Gozo and in very close proximity (walking distance) from each other (Fig. 6.5). Nonetheless, the key point which distinguishes and puts all these artefacts in the same group are the finds in the Ġgantija assemblages and especially those of the 1019 context. The artefacts of this context are made from the same core/nodule chert which allowed the recording of the full range of the macroscopic characteristics that this source can present. These finds have eliminated the possibility that the members of this group could derive from different sources. The only exceptions were two artefacts from the Circle (i.e. BR89/S395/L449 and BR91/S745/L845) that present distinctive characteristics (e.g. level of translucency) in comparison with the rest of the group members and it is possible that they were made from another source. It is essential to find these sources/outcrops in order to identify to what extent these two were made from the same or different sources.



Figure 6-4: Representative samples of the fist group of artefacts found in the context 1019 at Ġgantija.

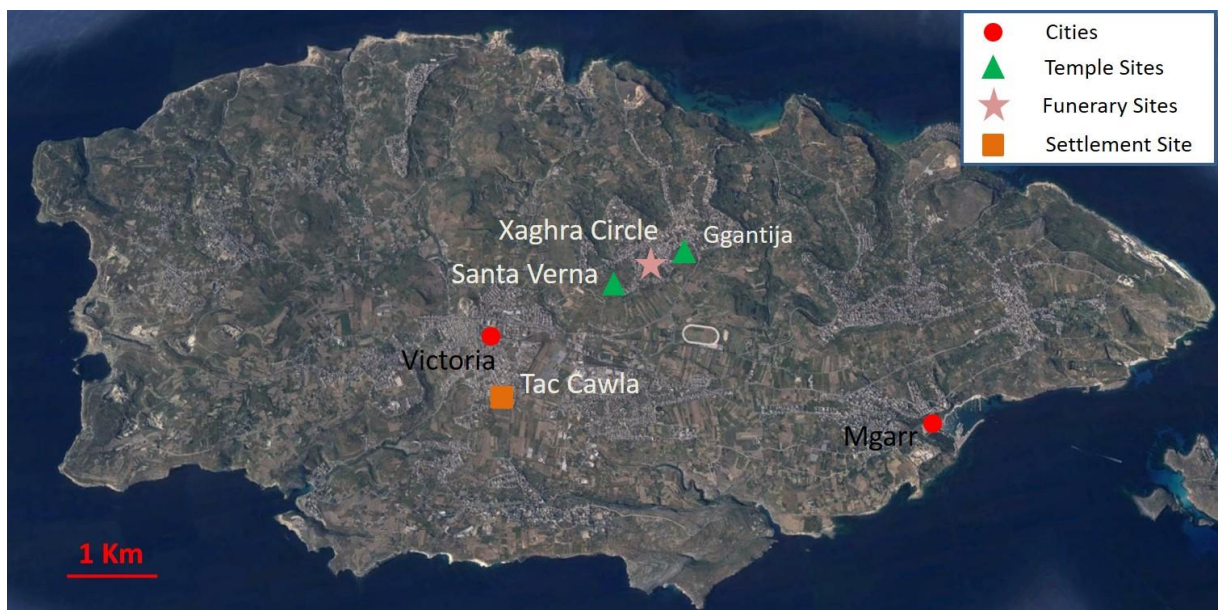


Figure 6-5: Satellite image with the investigated archaeological sites on Gozo Island (Maps Copyright @2018 Google).

It is important to clarify that the term "same source" does not mean "same outcrop" because a single rock formation (e.g. chert) can have more than one outcrop and exposures in different locations. A geological formation can be a few million years old (e.g. Maltese chert), but it can also be a few thousand million years old (e.g. Radiolarian formation in Sicily). It is impossible within such timescales to maintain the same characteristics, but it still remains the same formation. Although the raw materials can be collected from multiple outcrops which might have different macroscopic features, they still belong to the same formation hence the same source. This highlights the importance of using petrological methods because they allow examining the characteristics of sources which are least affected by time and location.

The results of the FTIR-ATR demonstrated that all the artefact samples consist mainly of quartz (Fig. 6.6). This was also supported by the p-XRF findings which showed that Si was the element that had the highest number of energy counts (Fig. 6.7). The results of these two techniques in addition to the macroscopic features made it clear that this group of artefacts is not related to the Maltese cherts. It is useful to remember here that this source predominantly consists of opal-A and has Ca as the element with the highest peak in the spectra. On the contrary, the Sicilian chert sources are dominated by quartz and Si which make them a suitable candidate as a source location. However, none of these sources has macroscopic characteristics similar to this group and this casts doubt on their compatibility. This problematic situation can be resolved with the geochemical data which can provide further information on actual sources of these artefacts and their connection with the Sicilian sources.

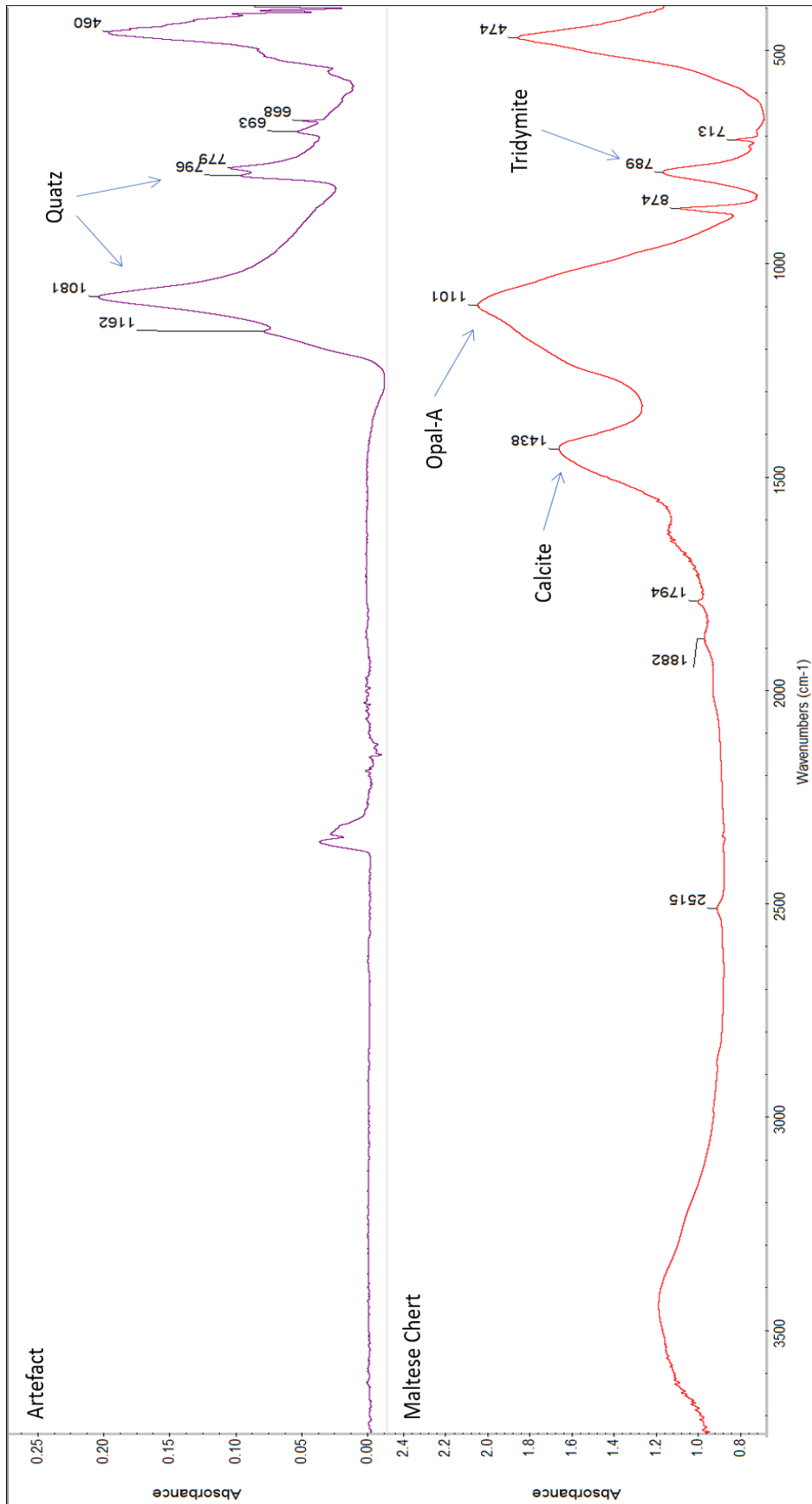


Figure 6-6: Comparison FTIR-ATR spectra between a representative artefact (GGWC15/L1019/S6sb) from the first group (above) and the chert sources (M1S3) of Malta (below).

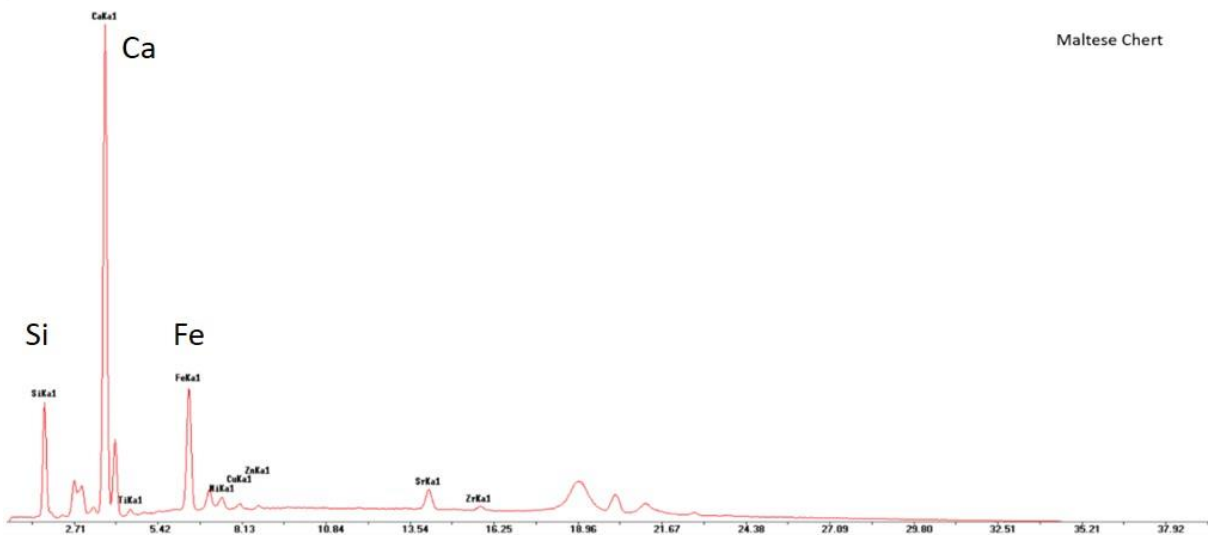
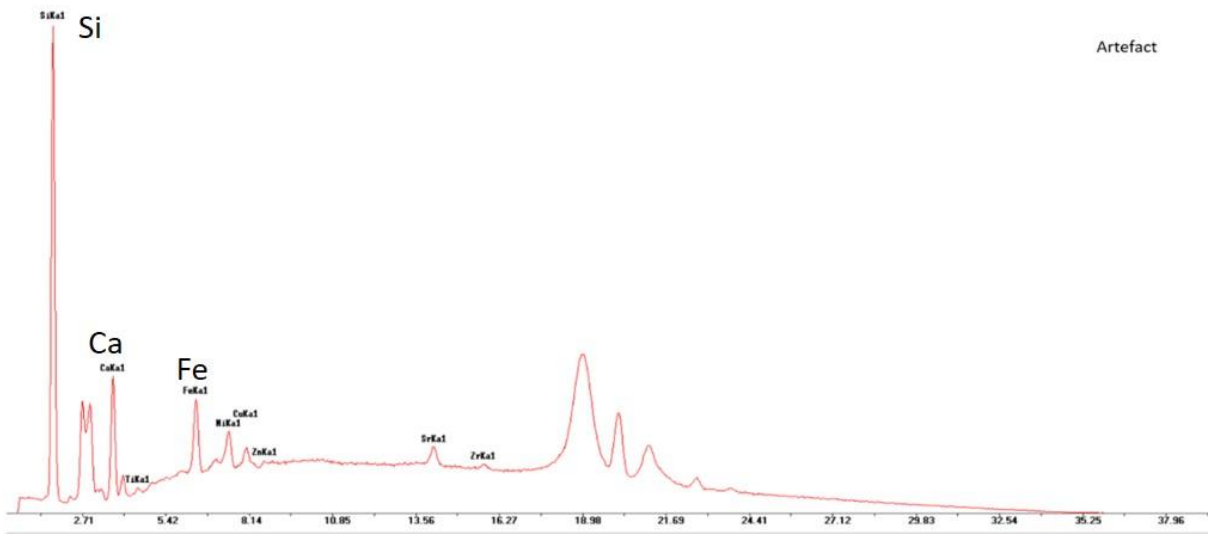


Figure 6-7: Comparable p-XRF spectra between a representative artefact (GGWC15/L1019/S6sb) from the first group (above) and the chert sources (M1S3) of Malta (below).

The samples of this group are plotted with the Sicilian chert samples in the ternary diagram, which identifies the type of sedimentation (i.e. hydrothermal or biogenic). Most of the artefacts (n=21) were related to biogenic sedimentation (Fig. 6.8) and were plotted in the same part of the model with some samples from Southeast and West Sicily (S17, S18 and S22r). There is only one sample from the Tač-Ĉawla assemblage (i.e. TCC14/S176/L100) that falls in the hydrothermal sedimentation area of the diagram and also close to one sample (S19) from Southeast Sicily (Fig. 6.8). Regarding the depositional environment, most of these samples (n=13) accumulated in the area of a pelagic environment (Fig. 6.9). Some samples deviated from the rest but since it is uncertain whether they all come from the same source, it is difficult to accurately interpret these results. However, this does not show a completely different environment, but it predominantly suggests an influence/input from a continental margin environment. These findings were also supported from the REEs ratios (i.e. Ce/Ce^* , La_n/Ce_n and La_n/Lu_n), which mainly indicated a pelagic environment with occasionally a continental margin input. Although these are uncertainties that require further research to be resolved, it is still certain that the source/s of this group has not been deposited in a hydrothermal or continental margin environment. Subsequently, the Sicilian chert sources related to these environments were excluded from the list of possible candidates. Moreover, these current findings support a connection between specific outcrops (S17, S18 and S22r) from Southeast and West Sicily and the majority of the artefact samples of this group (n=15). They also confirm a relationship between one sample from the Tač-Ĉawla assemblage (TCC14/S176/L100) and the outcrops from Southeast Sicily (S19).

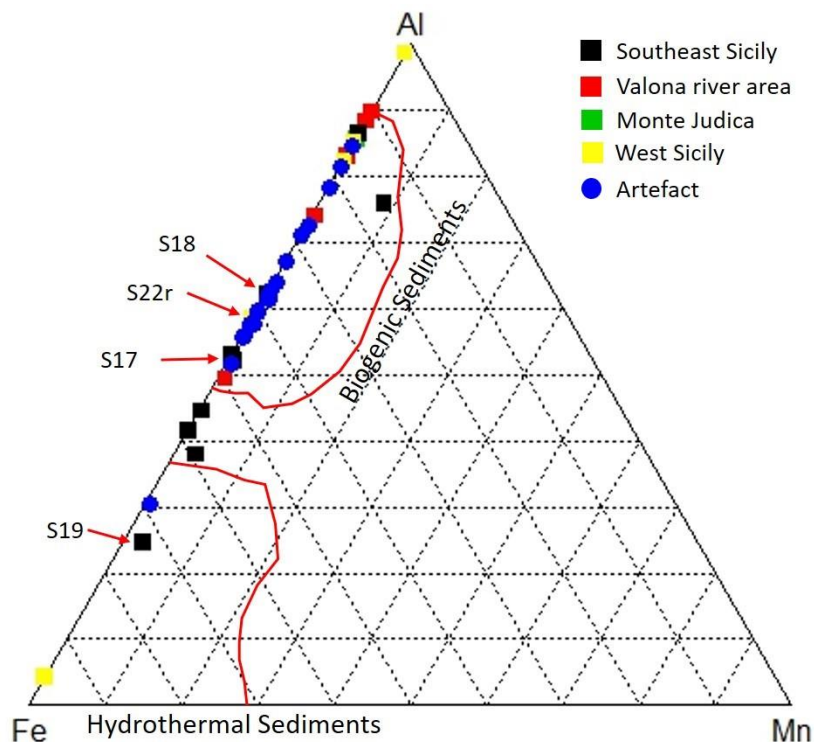


Figure 6-8: Ternary diagram cross-examining the Sicilian cherts and the artefacts of the first group regarding the type of sediment. The line demarcations have followed the suggestion of Junguo et al. (2011).

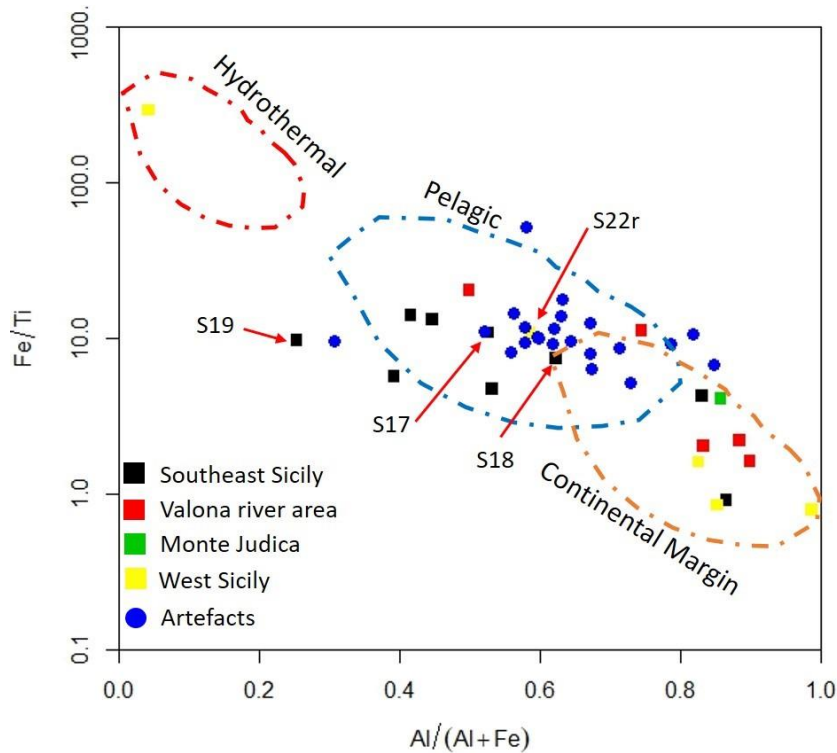


Figure 6-9: Binary diagram cross-examining the Sicilian cherts and the artefacts of the first group regarding the depositional environment. The line demarcations have followed the suggestion of Murray (1994).

The REEs normalised patterns of the artefact samples were plotted on the same level of concentrations (10^{-2}) and presented significant fluctuations on the second group of the REEs (HREEs). Moreover, they demonstrated higher concentrations on HREEs in comparison with LREEs and many of them ($n=17$; 77%) have a depletion on Tb and an additional smaller one on Ce. A closer examination of the patterns has even distinguished artefacts from the different assemblage (BR93/S854/L897, SV15/S1/L16, SKB15/S131/L211 and KRD15/S141/L150) that demonstrated a very similar REEs normalised pattern (Fig. 6.10). These results enhanced the previous findings and strongly suggest a common origin for this group of artefacts. The diversities and fluctuations reported are still features that need clarification, but until the actual source is identified these questions cannot be resolved. Furthermore, there are similarities between these artefacts and the Sicilian chert formations, but there are still differences which do not allow them to be regarded as their sources. This can be better illustrated with the REEs normalised patterns (Fig. 6.11) of the artefacts (e.g. SV15/S1/L16) and Sicilian chert (S17, S18 and S22r) that are linked in the previous models. Although the normalised concentrations are at the same level, the sharp fluctuations of the artefact patterns cast additional doubt on their compatibility.

This doubt is further enhanced from the results of the comparative study of the oxygen levels during deposition (Fig. 6.12). The majority of the artefact samples ($n=18$) demonstrated low concentration of oxygen (anoxic to dysoxic conditions) and are different from most of the Sicilian

samples. There were only few that suggested oxic conditions (enriched in oxygen) and their ratios were close to some of the West Sicily samples (e.g. S22r), even with those that were not compatible in previous models.

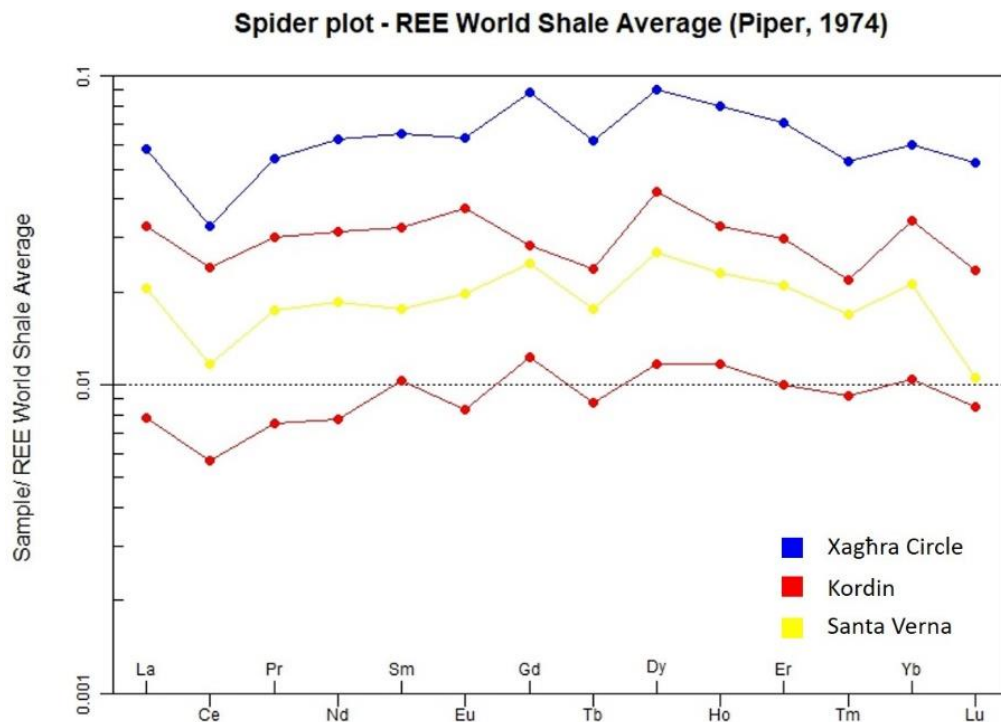


Figure 6-10: Spider plot with the REEs normalised concentrations of artefact samples from all the assemblages with the most similar pattern.

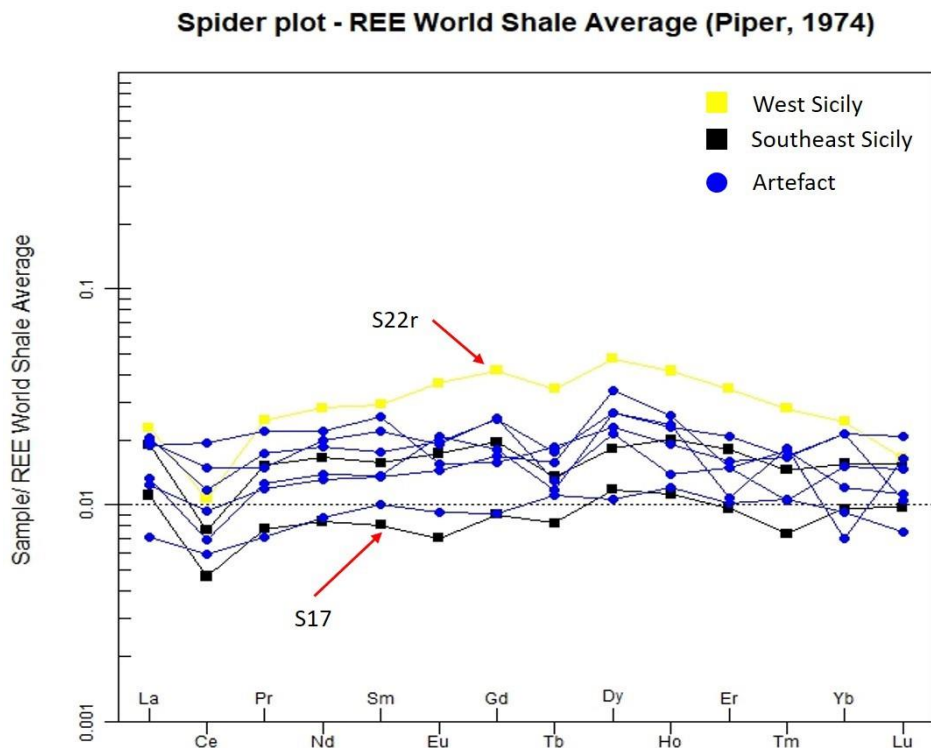


Figure 6-11: Comparable spider plot of the REEs concentrations between artefact samples of common origin and selective Sicilian chert outcrops.

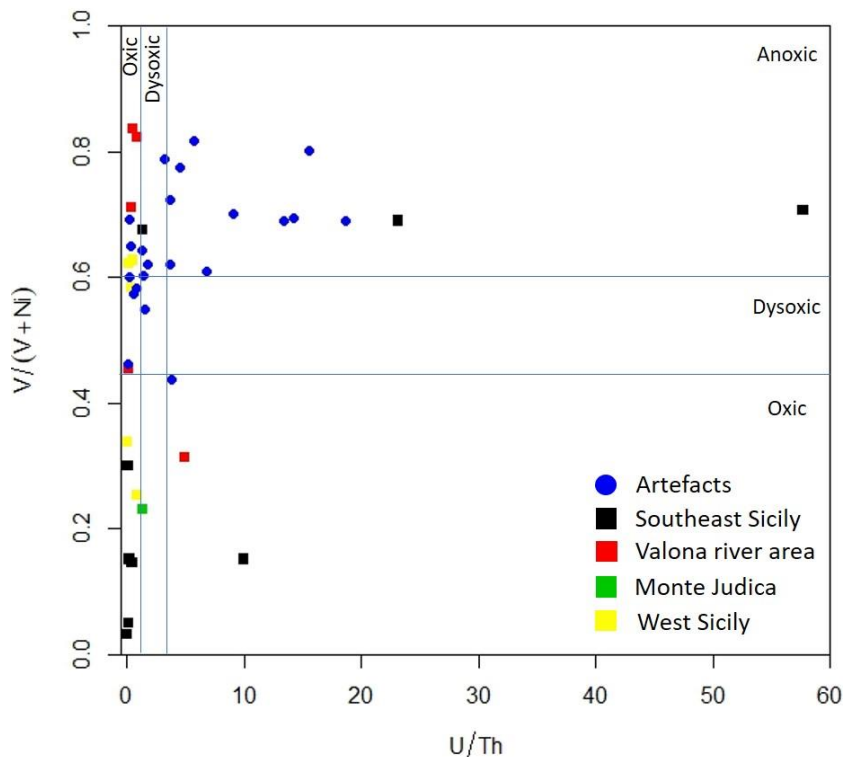


Figure 6-12: Binary diagram cross-examining the Sicilian cherts and the artefacts of the first group regarding the oxygen level of the depositional environment. The line demarcations have followed the suggestion of Garbán et al (2017).

Summarizing, this group of chert artefacts has the macroscopic, microscopic and chemical characteristics which strongly suggest a common source. Although their source has not yet been found, it is clear from the presented results (e.g. mineralogy) that they are not made from the Maltese chert sources. There are indications of a Sicilian origin, but the comparative study between them has not provided irrefutable data indicative of such a connection. Some geochemical results suggest a relationship with the chert sources from Monterosso Almo (Southeast Sicily) and Triona mountain (West Sicily) areas. However, these two sources geotectonically belong to completely different formations and it is impossible for both of them to be related to this group of the same time. An additional problem is that none of these sources presented the distinctive macroscopic features (e.g. colour) that grouped these artefacts together. While the origin of this group still remains unknown, some progress has been achieved. Proposing future research, a valid starting point would be an investigation of these two areas of Sicily and future research could seek chert sources that are macroscopically similar to this group. Although the Southeast Sicily has been extensively investigated, this has not been the case for West Sicily. It has chert sources/outcrops which have not been investigated through this work and maybe one of them could be the origin of these artefacts.

6.3.2. Second group of artefacts (local chert artefacts)

The second group of artefacts includes mainly opaque, dull and spotted findings which are macroscopically identical with the local chert sources. The latter feature (i.e. spotted) especially is the trademark of the Maltese chert formations because the examination has recorded that these irregular, white spots were actually the carbonated fossils found in these rocks (Fig. 6.13). They consistently appear on both the artefacts and the local chert sources and provide the key macroscopic evidence that connects these artefacts with the Maltese cherts. An additional common characteristic is their colour which varies between gray (e.g. 5Y 6/1) and brown shades (e.g. 10YR 6/6), while many of the members of this group have a semi-smooth texture. An important feature of the lithics from the Skorba assemblage is that in all the layers they were made from this type of chert rock (n=69; 49%). By contrast, in the Ġgantija and Taċ-Ċawla assemblages, the artefacts related to this chert source were limited in number and variety. Generally, the assemblages from the sites on Gozo island had fewer artefacts from this group in comparison with Skorba on Malta. The only exception is the Santa Verna assemblage, which had the highest number of artefacts. This must not be a coincidence, considering that this assemblage had the lowest representation of artefacts related to the brown group. This was either related to restricted access to raw materials or preference, but no further claim can be made at this stage. Furthermore, some assemblages presented artefacts similar only to outcrops found in Malta, while others do not show such a restriction. This research did not identify significant differences between the outcrops from these two locations and again the answer probably remains somewhere between preference and easier access.

It is worth highlighting that it was decided not to include artefacts in this second group that had similar features with the unique outcrop in Gozo (i.e. G2S6). Macroscopically they are completely different from the other local chert outcrops and therefore it is more appropriate for them to be included in the third and last group of artefacts. The reasons for this decision are well defined in the following sub-chapter which presents the findings for this group of artefacts.

The results of the FTIR-ATR demonstrated that most of the artefact samples (n=20; 67%) consisted mainly of opal-A (Fig. 6.14) and had a noticeable presence of tridymite. The p-XRF results have shown that Ca was the element with the highest peak, followed by Si and Fe with significantly lower peaks and therefore much less number of energy counts (Fig. 6.15). The results of these two techniques enhanced further the connection of this group with the local chert source and at the same time made it clear that they were not related to the Sicilian sources. The connection between this group and the local source will now be further examined using their geochemical results.



Figure 6-13: Representative samples of the second group of artefacts. The purple arrows point out the characteristic spots.

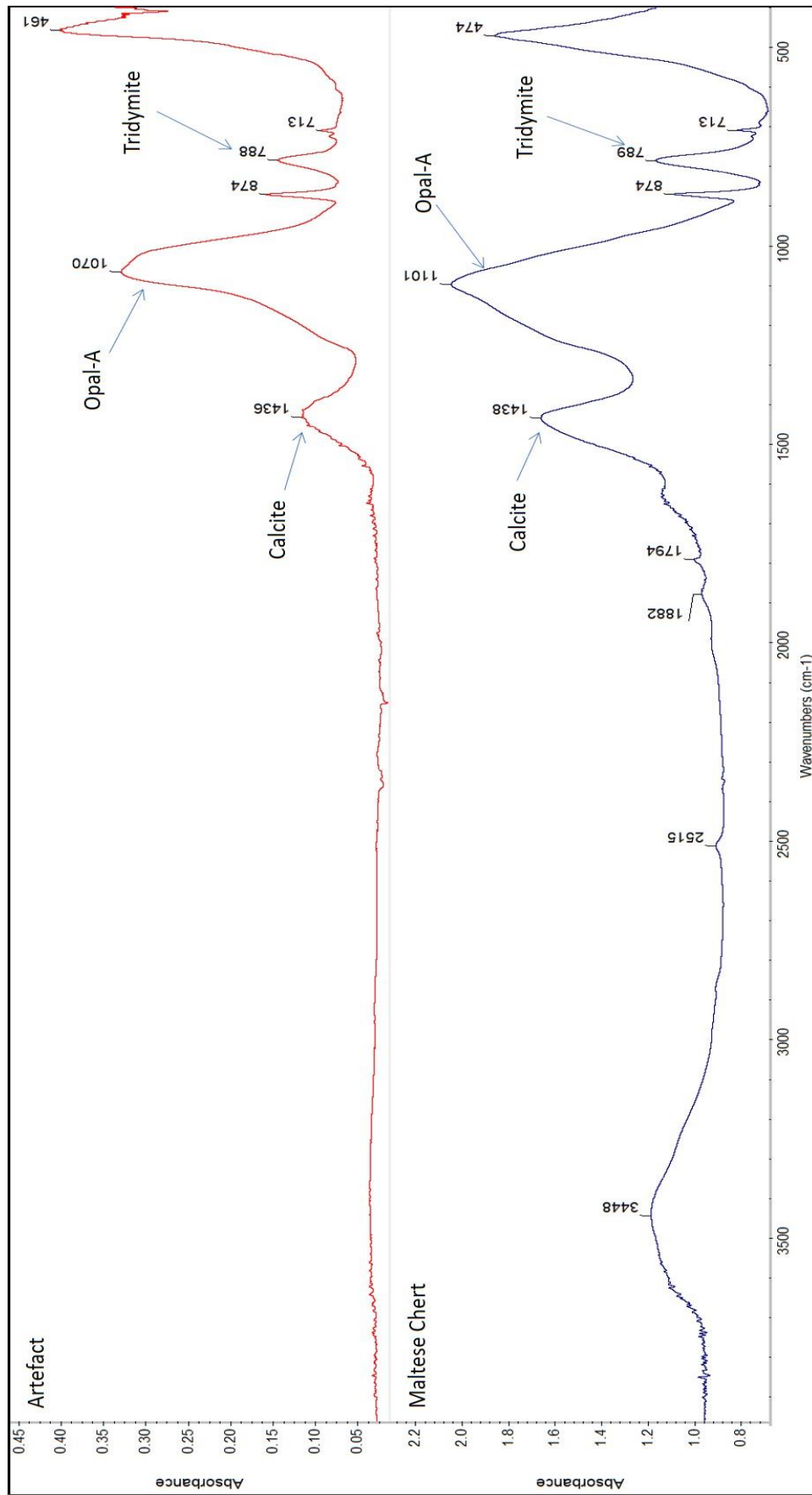
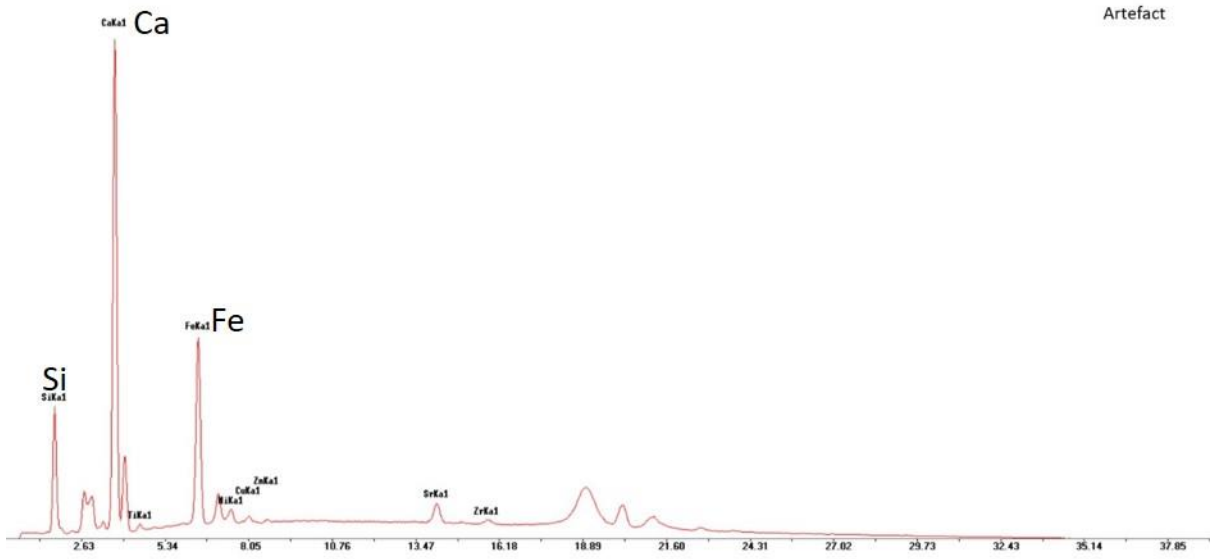
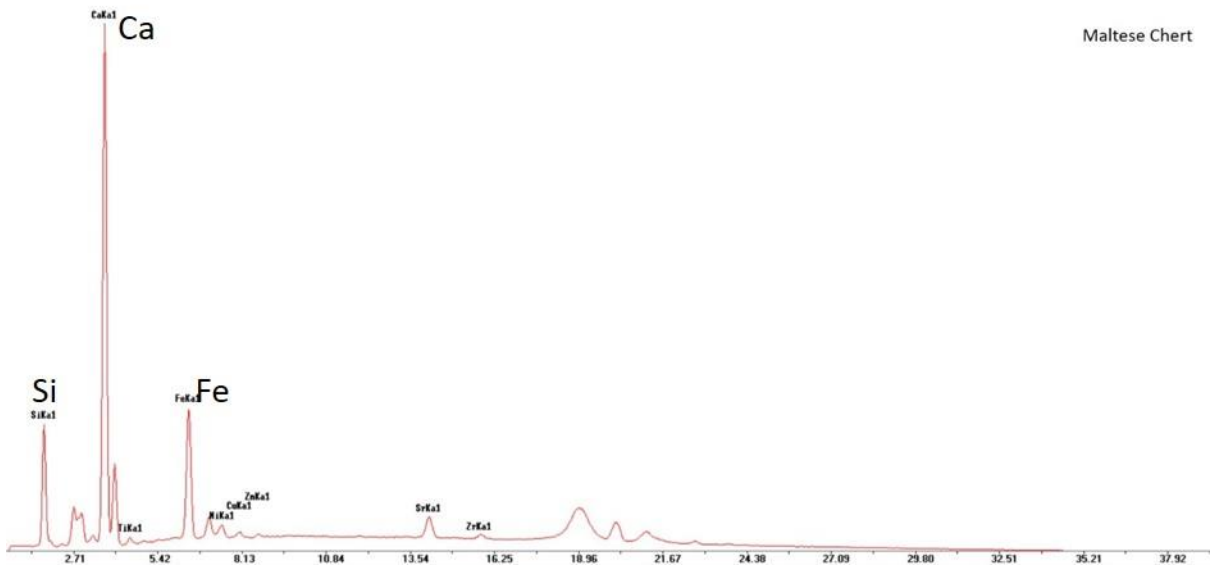


Figure 6-14: Comparison FTIR-ATR spectra between a representative artefact (BR91/S566/L622) from the second group (above) and the chert sources (M153) of Malta (below). The difference in the actual value of the main peak (opal-A) is because the artefact was analysed with ATR which have slightly values in silicate minerals.



Artefact



Maltese Chert

Figure 6-15: Comparable p-XRF spectra between a representative artefact (BR91/S566/L622) from the second group (above) and the chert sources (M1S3) of Malta (below).

In a manner similar to the process followed with the previous group, the samples of this group were plotted with the Maltese chert samples in the diagram which identified the type of sedimentation (i.e. hydrothermal or biogenic). The majority of the artefacts (n=58) were related to biogenic sedimentation (Fig. 6.16) and were plotted in exactly the same way as the model for the local samples. There were only two samples from Skorba assemblage (S3/L12b and S10/L13) that indicated a different type of sedimentation, however no further explanation can be provided with these results.

The artefacts from this group demonstrated some interesting findings regarding their concentrations of major elements. The model demonstrated that the artefact samples were divided mainly into sub-groups, which were in close proximity with each other (Fig. 6.17). The first group was placed in the exact same region as the Maltese chert samples which have been described as an intermediate between a pelagic and continental margin environment. This is additional evidence that the artefacts of this group are made from a chert source of the Maltese islands. The second sub-group is placed in an unspecified area of the model, but very close to the first sub-group. Checking their position in the diagram carefully, it is observed that the main difference is their higher concentration of Fe in comparison with Ti. Meanwhile, there is no change in the ratio of Al and Fe which suggests that this sub-group is actually made from an outcrop depleted in Titanium (henceforth Ti). It can be easily understood that if the concentrations of Ti were higher, these samples would have been in the same region as the rest of the samples (i.e. artefacts and rocks). The idea of a special outcrop is promoted, because there is still not enough evidence to suggest a different source. The validity of this interpretation is also supported from the REESs ratios (Ce/Ce^* , La_n/Ce_n and La_n/Lu_n) which are indicators of the depositional environment and presented greater stability in a formation especially in comparison with the major elements (e.g. Ti). The values of these ratios demonstrated that all the artefact samples have been deposited in a continental margin environment with a strong pelagic input, which is exactly the same environment as for the Maltese chert rocks. There were some deviations from the generally reported values, but they were in the range reported for the samples of the local source. Investigating these findings further, it has been recorded that they belong to samples from the Skorba assemblage (Appendix I, p173, Table 20 and 21), the majority of which has been found in context 10 of the 2016 excavation (n=10; 52%). This suggests that especially during that time of occupation/usage of the site, Maltese people had access to a chert outcrop with a lower than usual concentration of Ti.

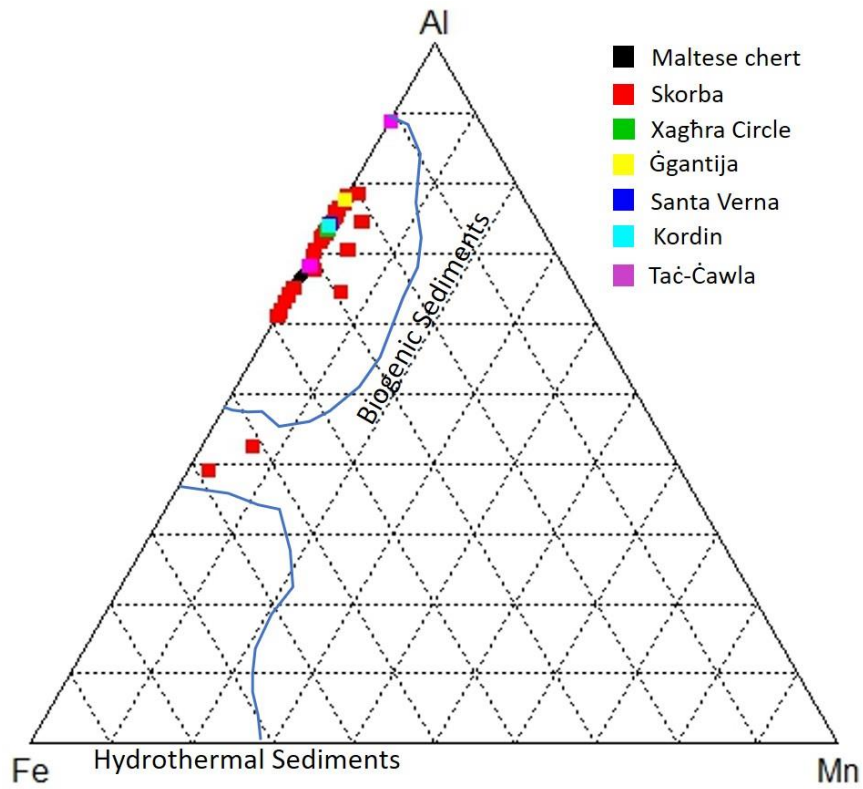


Figure 6-16: Ternary diagram cross-examining the Maltese cherts and the artefacts of the second group regarding the type of sediment. The line demarcations have followed the suggestion of Junguo et al. (2011).

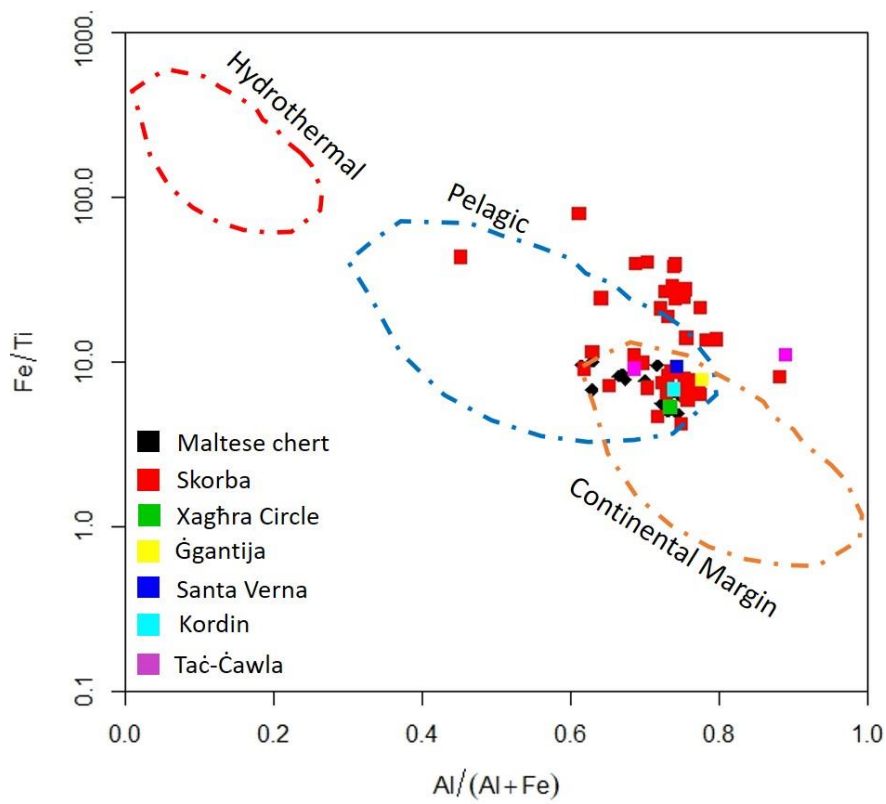


Figure 6-17: Binary diagram cross-examining the Sicilian cherts and the artefacts of the second group with respect to the depositional environment. The line demarcations have followed the suggestion of Murray (1994).

The REEs normalised patterns can provide further supportive results on the connection between this group of artefacts and the Maltese chert source. The pattern diagrams demonstrated (Chapter 5.4.2 and Appendix I, p.182) that the artefact samples were plotted on the same level of concentrations (close to 10^{-1}) and recorded a negative anomaly (depletion) on the Ce and Tb elements. They were also characterised from minimal fluctuation along the normalised concentrations of those elements (smooth pattern). Similar findings were found for samples from all the assemblages (Fig. 6.18), which were actually the same as the ones obtained from the Maltese chert source/outcrops (Chapter 5.4.1, Fig.5.72a). This is better illustrated at the comparable spider plots which include samples of the Maltese outcrops and the examined assemblages (Fig. 6.19). Furthermore, the compatibility of artefacts from the different contexts of Skorba suggest a consistent usage of the local source/outcrops throughout the occupation/activity of this archaeological site (Fig. 6.20). There are, of course, some artefact samples that present different patterns, but not outside the diversities reported for the local outcrops (Fig. 6.21).

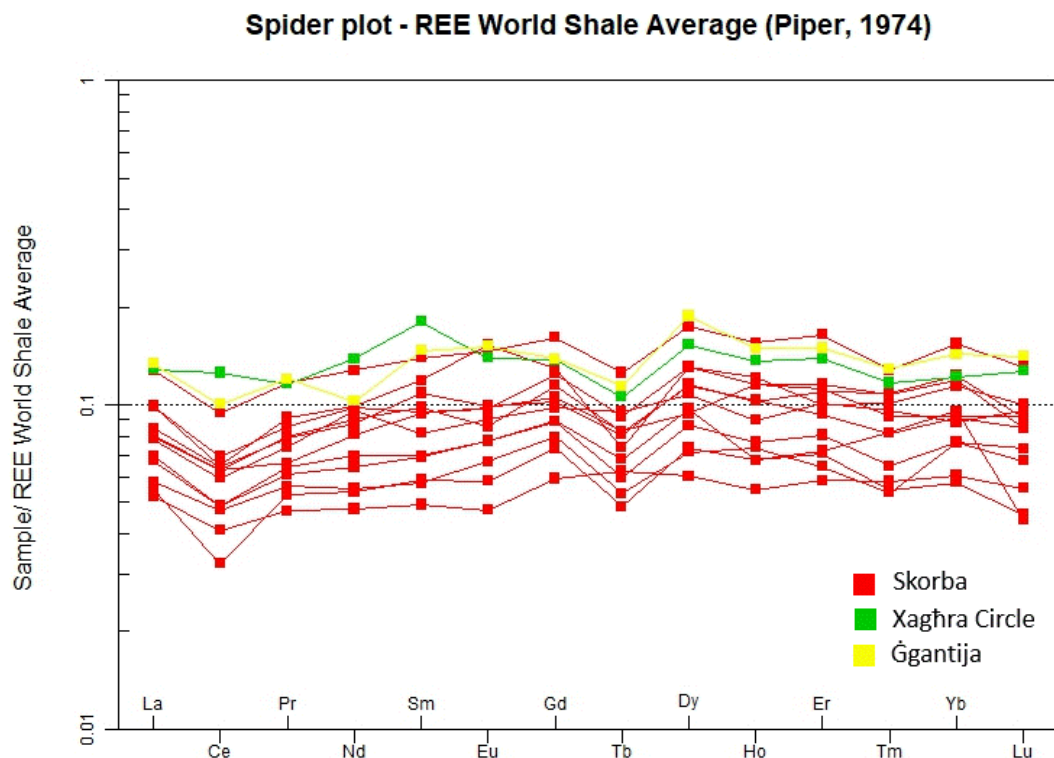


Figure 6-18: Comparable spider plot of the REE concentrations between representative artefact samples from all the examined assemblages which are considered of common local origin. The artefacts in this plot are: one from Xaghra Circle (BR91/S566/L662), one from Ġgantija (GGWC15/S1/L12) and eleven from Skorba (SKB16/S2/L5, S4/L5; SKB16/S2/L12b, S5/L12b; SKB16/S1/L16, S2/L16; SKB16/S1/L26, S6/L26, S7/L26; SKB16/S1/L30, S3/L30).

Spider plot - REE World Shale Average (Piper, 1974)

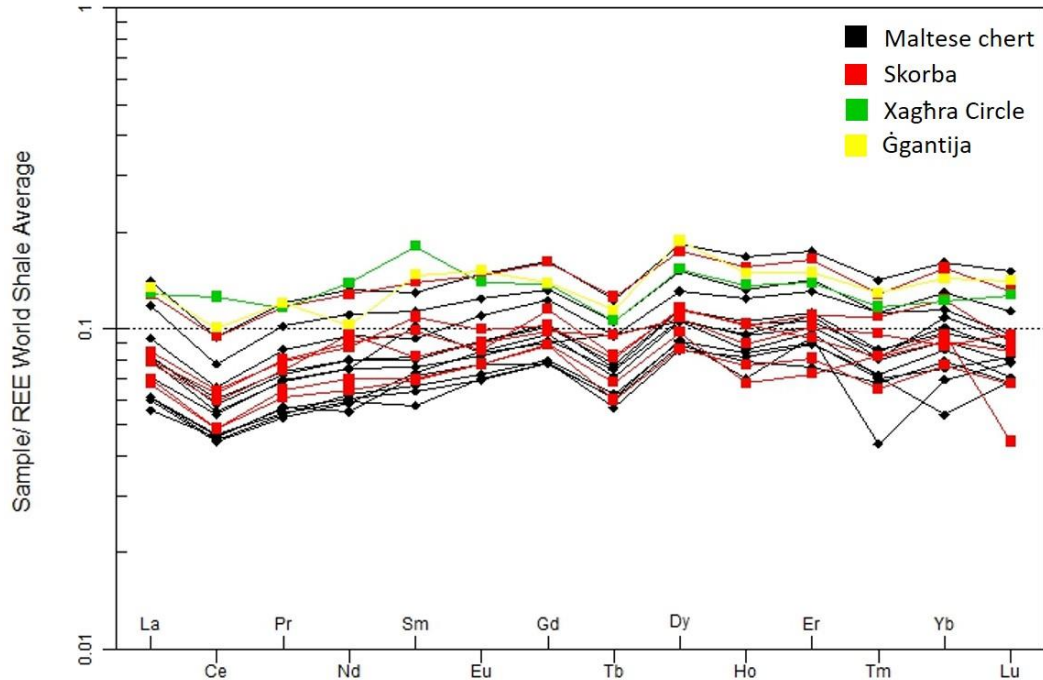


Figure 6-19: Comparable spider plot of the REE concentrations between representative Maltese chert samples (F1S4,G2S2,G2S1,G2S3,F1S3,M1S1b,M1S2,M1S3,M1S5,M1S4 and M1S10) and artefact samples of common local origin (BR91/S566/L662, GGWC15/S1/L12, SKB16/S2/L5, S4/L5; SKB16/S2/L12b, S5/L12b; SKB16/S1/L16, S2/L16; SKB16/S1/L26, S6/L26, S7/L26 and SKB16/S3/L30).

Spider plot - REE World Shale Average (Piper, 1974)

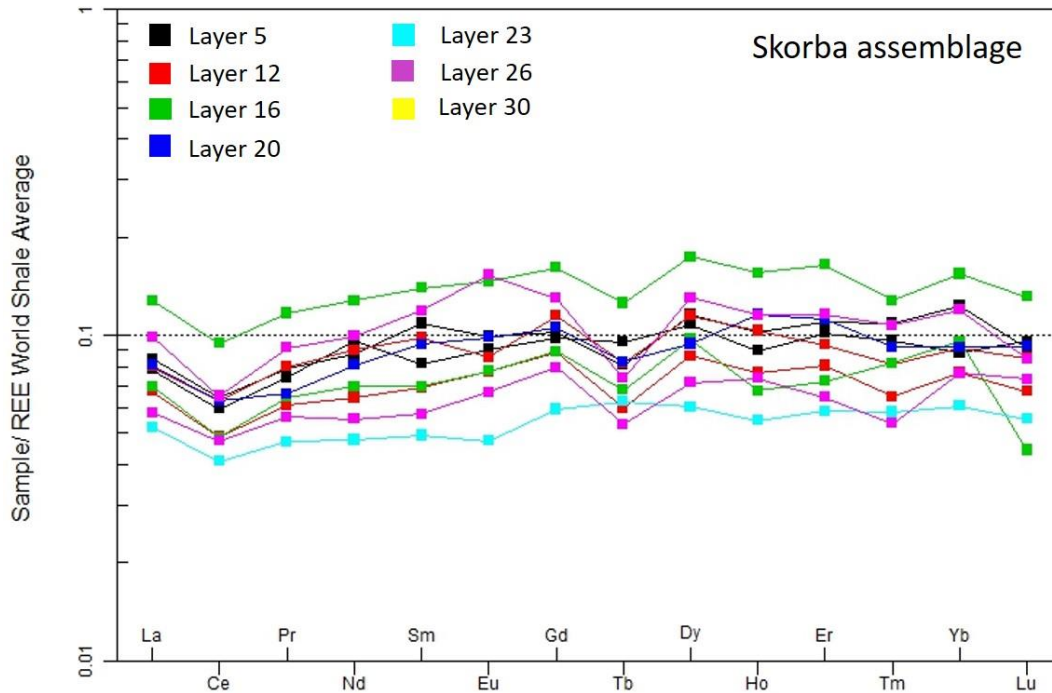


Figure 6-20: Comparable spider plot of the REE concentrations between representative artefact samples from the different layers of Skorba excavation (SKB16/S2/L5, S4/L5; SKB16/S2/L12b, S5/L12b; SKB16/S1/L16, S2/L16; SKB16/S2/L20; SKB16/S6/L26, S7/L26 and SKB16/S3/L30), which are considered of common local origin.

Spider plot - REE World Shale Average (Piper, 1974)

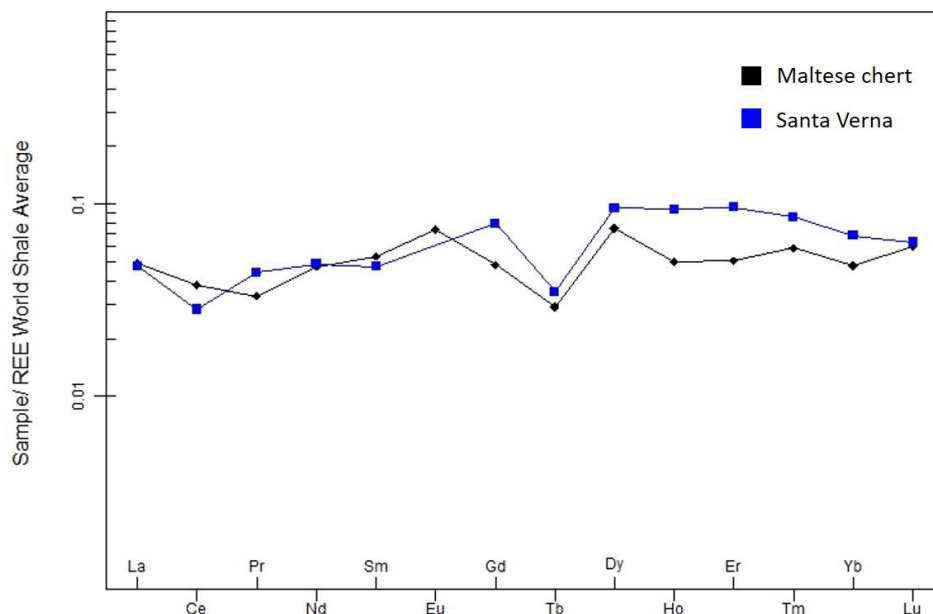


Figure 6-21: Comparable spider plot of the REE concentrations between an artefact sample from Santa Verna (SV15/S58/L134) that present a different pattern and a Maltese chert outcrop (sample M254).

Finally, the comparative study of the oxygen levels during deposition demonstrated (Fig. 6.22) that both artefacts and Maltese outcrops have been deposited under low concentrations of oxygen (anoxic to dysoxic conditions). Although the artefacts were more widespread and plotted higher in the model, the majority remains within the range set by the local chert outcrops (n=41; 67%).

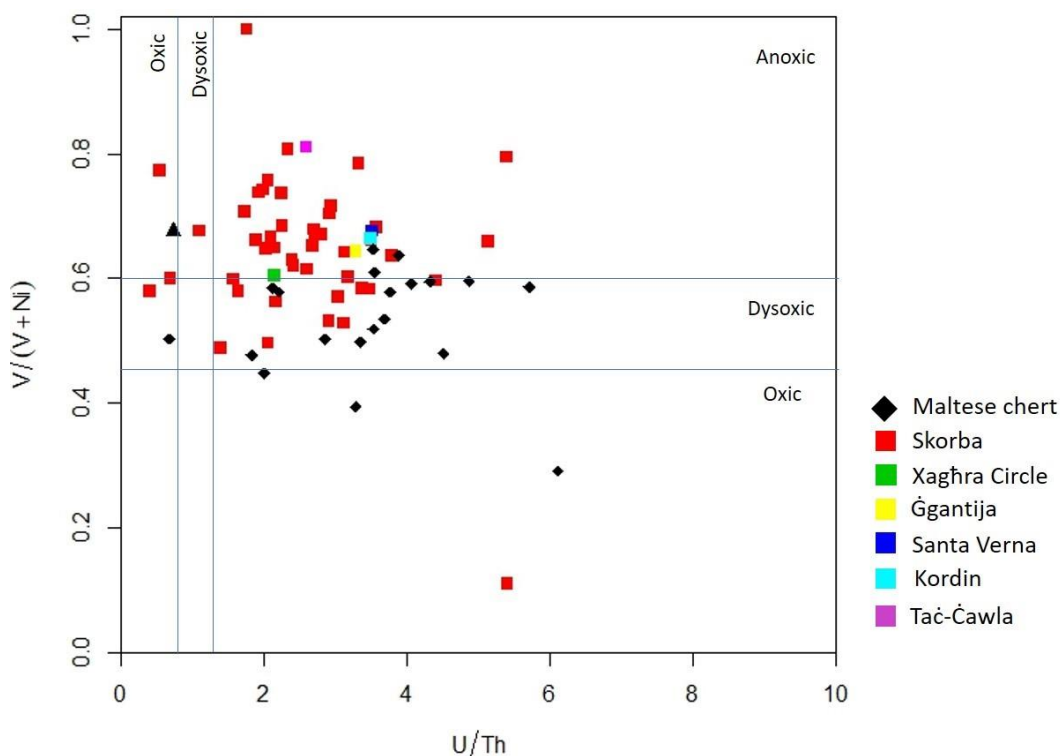


Figure 6-22: Binary diagram cross-examining the Maltese cherts and the artefacts of the second group with respect to the oxygen level of the depositional environment. The line demarcations have followed the suggestion of Garbán et al (2017).

Summarizing, this group of chert artefacts has the macroscopic, microscopic and geochemical evidence to strongly suggest that they have been made from Maltese chert rocks. This subsequently erases the possibility of them having been imported, and moreover even having been related to the Sicilian sources. In previous chapters, the differences between these two sources have already been presented and it is impossible for any artefact to be related to both of them at the same time. Even if there was a Sicilian source/outcrop similar to the Maltese one, it would be highly unlikely for such materials to be imported. Fieldwork has established that there would have been sufficient resources on the Maltese Islands to be used for artefacts and tools. Moreover, this Sicilian source is not of the highest standard for a typical chert formation, therefore it is considered highly unlikely that it was ever worth the effort to be imported.

Although it is difficult to know the exact locations of extraction, the current outcrops are easily accessible, and especially the one on Malta (Fomm-IR-Riġ bay), which is near with the Skorba Temple/settlement archaeological site. There is the possibility of outcrops which have not been found in this research, as the results from the Skorba findings support. Indeed, there is a period during the occupation/activity of the site (e.g. context 10), in which the Maltese people had access to an outcrop with lower concentrations in Ti than the rest of the local chert outcrop. The precise whereabouts of this outcrop is unknown, and could be part of future research, but it is possible that it has been already depleted, destroyed or obscured by later erosion processes.

6.3.3. Third group of artefacts (Imported chert artefacts)

The last group of chert artefacts includes predominantly small (L and W < 2.5cm), homogeneous, shiny, fine-grained and highly translucent material. However, the significant diversity of colours and the different level of translucency makes this group partly heterogeneous. Nevertheless, the members of this group do not have suitable features to be included in any of the other groups. Moreover, none of the sub-groups of artefacts described here has sufficient numbers to be an independent and distinctive group of chert artefacts. Indeed, the macroscopic examination has recorded many single artefacts with different characteristics from all the other members.

They are all under the umbrella of the four common characteristics stated above, but these are insufficient to consider these artefacts as having been made from the same chert source. Common macroscopic characteristics do not necessarily suggest a common source, but it is within the methodological structure of this research and strongly advisable to use such indications as a starting point for sourcing lithics. The petrological methodology should provide the necessary data with which to conclude on their origin and if possible, identify their sources. The results of the FTIR-ATR demonstrated that all the artefact samples consisted mainly of quartz. This was also supported by the p-XRF findings which showed, that Si has more energy counts. These findings in addition to the macroscopic features excluded the Maltese chert from the list of possible sources, and the focus then fell on a comparative study with the Sicilian sources. The connection between this group and the Sicilian sources will be further examined using their geochemical results. It has been decided to discuss first the findings from the main sub-groups and then continue with the results of the single artefact samples. This makes it easier to process and interpret the data of such a heterogeneous group and promote the consistency of the comparative study. In addition, the similarities between the members of the sub-groups are better explained and the possible connection with the Sicilian sources should be clearly outlined.

6.3.3.1. First sub-group (yellow artefacts)

The first sub-group includes yellow (e.g. 10YR 6/6, 10YR 5/4), homogeneous, shiny, semi-translucent and fine-grained artefacts (Fig). They have been reported in all assemblages with more than one representative, except for Ġgantija which had no artefacts with such characteristics. Furthermore, the Skorba assemblage had similar lithics in different layers/contexts along the sequence of the excavation and supported constant access to this type of chert rock or artefacts. However, they were restricted in number and size (L and W < 1.5 cm), especially in comparison with the other two groups and possibly their origin was from a distant location outside of the Islands. The combination of their characteristics has not been reported from any of the investigated sources and were possibly not

from Malta or Sicily at all. Additionally, the FTIR-ATR and p-XRF results (Fig. 6.23) of the artefacts demonstrated the dominance of quartz and silica and therefore the Maltese chert formations were certainly not their sources. The option of a Sicilian source is uncertain, and therefore the findings of the geochemical data were necessary to identify any possible connection.

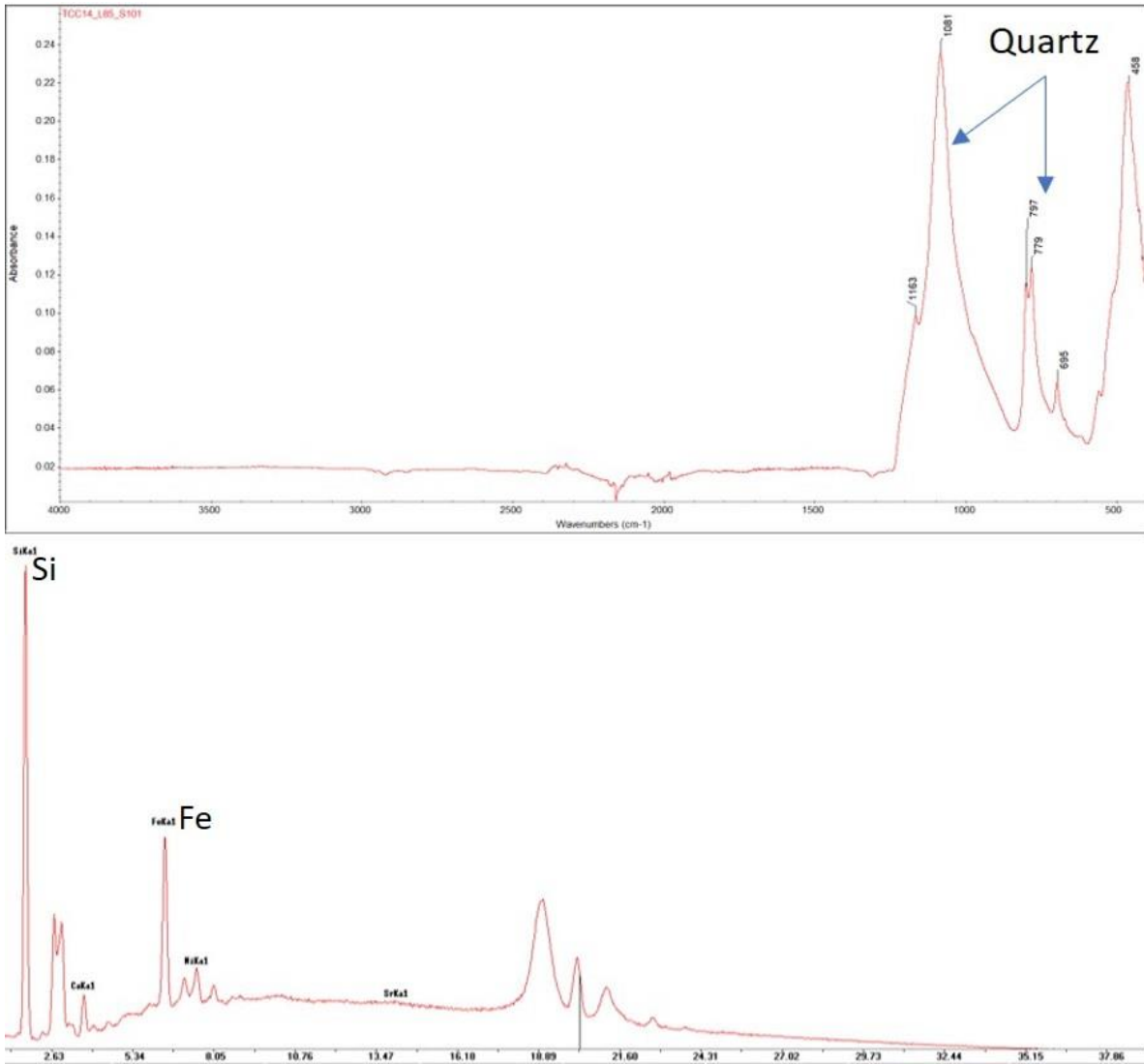


Figure 6-23: Representative FTIR-ATR and p-XRF spectra of the artefact (TCC14/S103/L85) included to this sub-group.

The samples of this sub-group were plotted with the Sicilian chert samples in the ternary diagram, but the findings were unclear (Fig. 6.24). Some of them are of biogenic sedimentation, but others are placed in an intermediate zone between biogenic and hydrothermal sedimentation. The distribution of the samples might imply different outcrops or sources, but nothing can be inferred at this point. This is also supported by the fact that they are plotted close to different sources from East Sicily (e.g. Monterosso and Valona river) which do not allow safe interpretations. The situation is the same for the depositional environment model, and it is difficult to have conclusive results either of their connection with the Sicilian sources or even of their common origin. Most of them (n=7; 70%) were plotted in the area of a pelagic environment (Fig. 6.25), but some samples deviated towards the other two types of environment. Moreover, the artefacts of a pelagic environment were divided into smaller groups and this increased the possibility of them being made from different outcrops. Although they were closer to the sources of Monterosso Almo, they were also placed close to other Sicilian sources and any interpretation would not be on a solid basis. The findings of these two models enhance the possibility that this sub-group includes artefacts from different sources. There were some similarities with the sources of Sicily, but they were not strong enough to draw a connection. The REE ratios (Ce/Ce^* , La_n/Ce_n and La_n/Lu_n) mainly indicated a pelagic environment with occasionally a continental margin input (Appendix I, Table 22), which generally supports the previous findings. Although this secured the reliability of the results of the previous models, it still did not provide any further information about their sources.

Having reached this stage without any probable candidate source, has nurtured the drive to continue analyzing and interpreting the data. This is a similar situation to the first group of artefacts, but the numbers of artefacts in the first group were much higher. Indeed, the research has examined more than 20 samples of the brown group, while this sub-group has in total 18 artefacts. Therefore, more data has been collected which allows better and more accurate interpretations to be made. The only possible solution, at the present moment, is to exclude some of the Sicilian sources. The data of the samples have shown no connection with hydrothermal or continental margin environments. Subsequently, most of the Sicilian chert sources from the Valona river, Monte Judica and West Sicily can be excluded from the list of possible candidates. Geochemically, the closer sources are those from Monterosso Almo, but they have many features which make them unsuitable and therefore more investigation is necessary. Hence the best option would be to conduct new research on Sicily for new and more suitable chert sources. If such sources are not found on this Island then, the research should move to other regions or Islands in this part of the Mediterranean area, perhaps even North Africa.

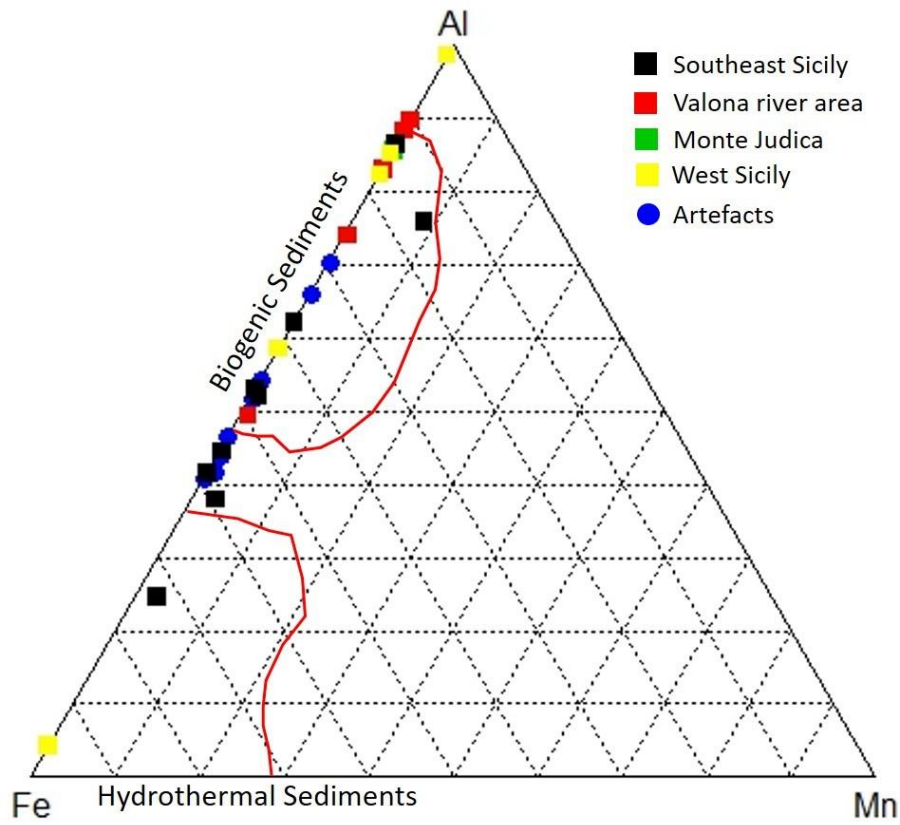


Figure 6-24: Ternary diagram cross-examining the Sicily cherts and the artefacts of this sub-group with respect to the type of sediment. The line demarcations have followed the suggestion of Junguo et al. (2011).

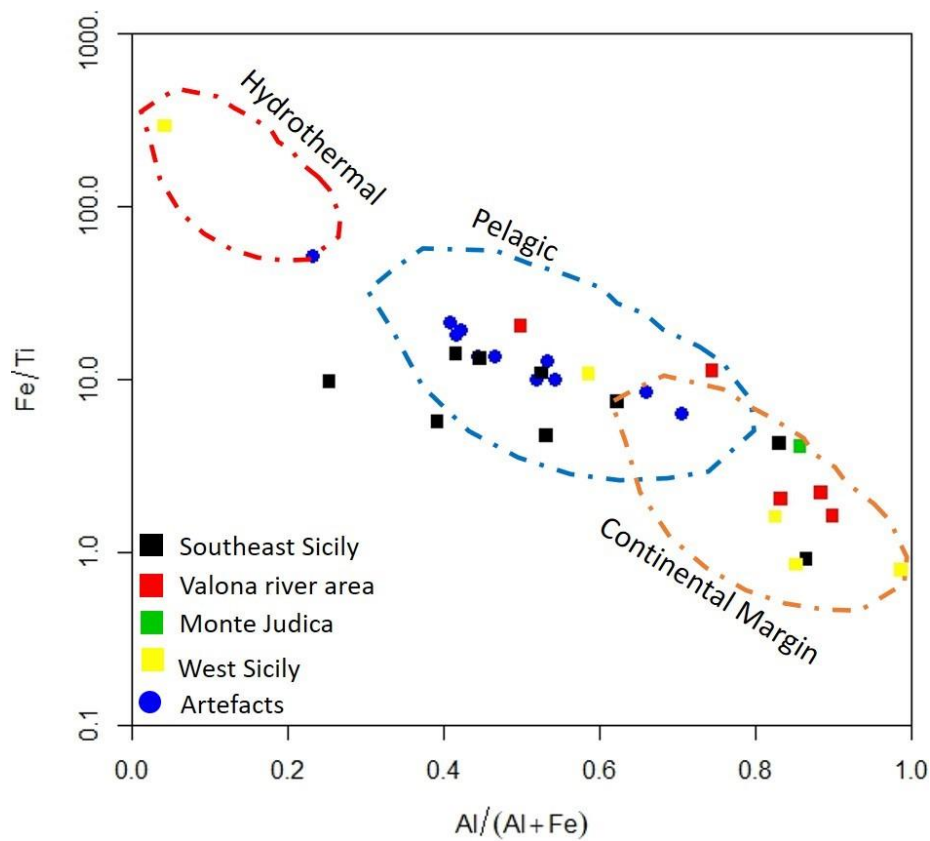


Figure 6-25: Binary diagram cross-examining the Sicilian cherts and the artefacts of this sub-group regarding the depositional environment. The line demarcations have followed the suggestion of Murray (1994).

6.3.3.2. Second sub-group (red artefacts)

The second sub-group includes five, red (5R 4/6 and 10R 3/4), homogeneous, shiny, semi-translucent or opaque (SKB16/S12/L13) and fine-grained artefacts (Fig. 6.26). They have been found only in the assemblages of Skorba (SKB16/S12/L13, SKB16/S7/L23, SKB16/S8/L23/S8), Ġgantija (GG15/S1/L008) and Santa Verna (SV15/S1/L68), but only the first had more than one artefact of this kind. Despite being smaller in number than the first sub-group, they have demonstrated very distinctive characteristics and could be easily distinguished from other artefacts. The combination of such features has only been reported from one specific chert formation of Sicily, while they are not related with the Maltese chert source. Indeed, only the Radiolarian formation found on the riverbed of the Valona river has very similar characteristics with these artefacts on which the research has focused. The FTIR-ATR and p-XRF results (Fig. 6.27) enhanced the connection with this formation and eliminated the possibilities of Maltese chert being a source candidate for these artefacts.



Figure 6-26: Representative samples of this lithic sub-group.

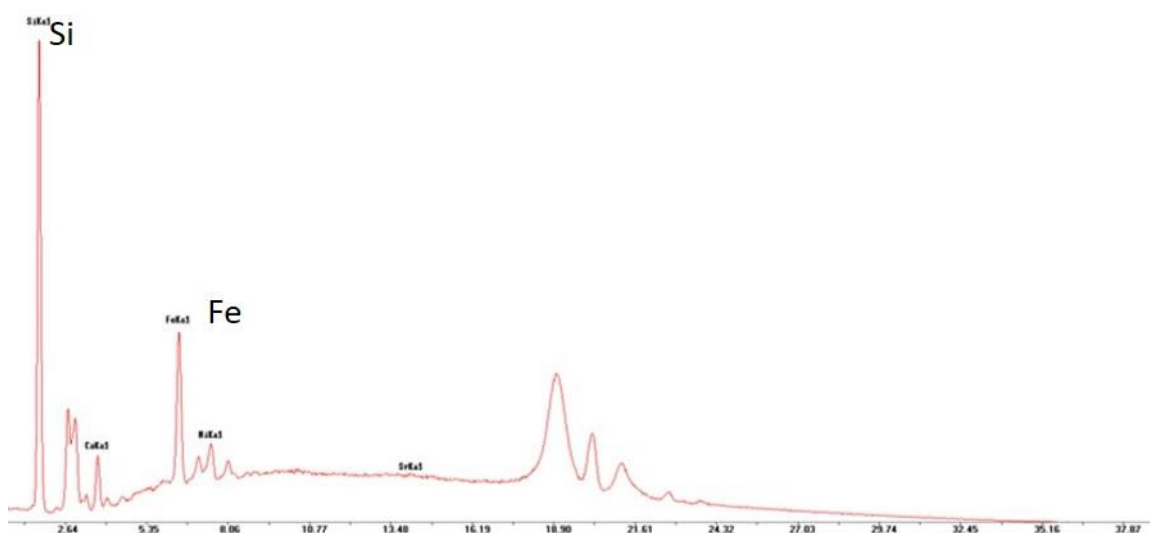
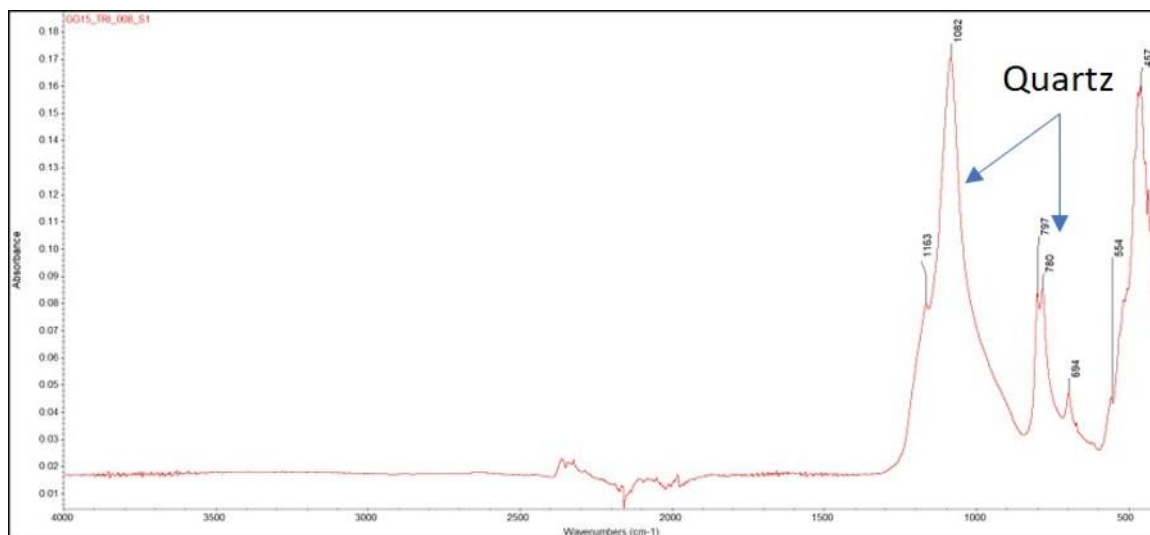


Figure 6-27: Representative FTIR-ATR and p-XRF spectra for the artefact (GG15/S1/L008) included to this sub-group.

Employing geochemical models, the samples of this sub-group were compared with those of the selected source. The samples in the ternary diagram were placed in the broader region related to biogenic sedimentation (Fig. 6.28), but only one of the radiolarian chert outcrops (S6b) was plotted in the same area with the artefacts. The rest of the rock samples appeared higher on the diagram and these findings cast doubt on the initial connection. Similar are the findings from the depositional environment model, where again only one of the radiolarian chert outcrops (S6b) was plotted in the same area as the artefacts. The difference between the rock and artefact samples was better defined in this diagram, as the artefacts were related with a pelagic environment, while the radiolarian outcrops were plotted inside the continental margin region (Fig. 6.29). This was also supported from the REE ratios (Appendix I, Table 22) and provides strong evidence against the possibility of these radiolarian outcrops being the source of the investigated artefacts.

The REE normalized patterns can further distinguish the differences between this sub-group of artefacts and the Radiolarian formation of Sicily. In fact, the comparative pattern diagram (Fig. 6.30)

makes it perfectly clear that this formation is not the source of these artefacts. The concentration levels of these artefacts were not consistent with those of the examined sources. Moreover, the artefacts presented generally lower concentrations of LREE in comparison with the source samples. This was highlighted by Ce, which was enriched in the source but depleted in the artefacts. Although some variation in concentrations can be accepted, such a significant difference in this element cannot be overlooked. Thus, it is highly unlikely that this sub-group of artefacts originated from the Radiolarian formation of Sicily. Sample S6b shows close proximity with the artefacts, but this was restricted to the major elements and contradicted the REEs findings which were considered more reliable and agreed with findings of the other samples from this formation. Although further geochemical analysis is required to clear up this uncertainty, it is probably because of the normal heterogeneous results found in these formations. Geological research never relies on the results of one sample and considers the overall findings from multiple samples to avoid misinterpretations.

Considering that there is no other similar formation reported on the island of Sicily, it is suggested that the source of this sub-group should be investigated at another location. This is the second group of artefacts which has not been connected with any of the investigated sources and locations. Adding to them the uncertainty of the first group, the research has presented possible evidence for the existence of at least one more area from where chert material has been imported. The holistic examination of these artefacts can possibly provide indications of the whereabouts of this unknown area. It is possible by combining the data from this research, to identify some characteristic of the source rocks of these artefacts. The next step is to investigate the geological structure of the neighbouring areas around Malta and locate which of them have or could have chert formations with similar characteristics to the unmatched artefacts. The final part will be to select the most suitable areas and employ a similar methodology to the research already undertaken in this thesis.

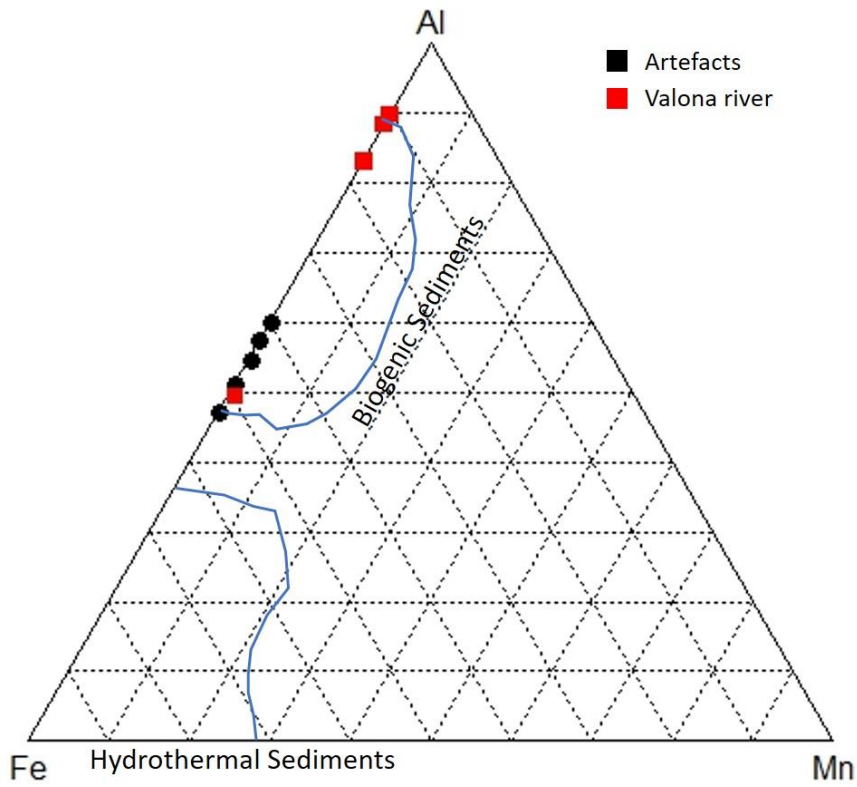


Figure 6-28: Ternary diagram cross-examining the Sicily cherts and the artefacts of this sub-group with respect to the type of sediment. The line demarcations have followed the suggestion of Junguo et al. (2011).

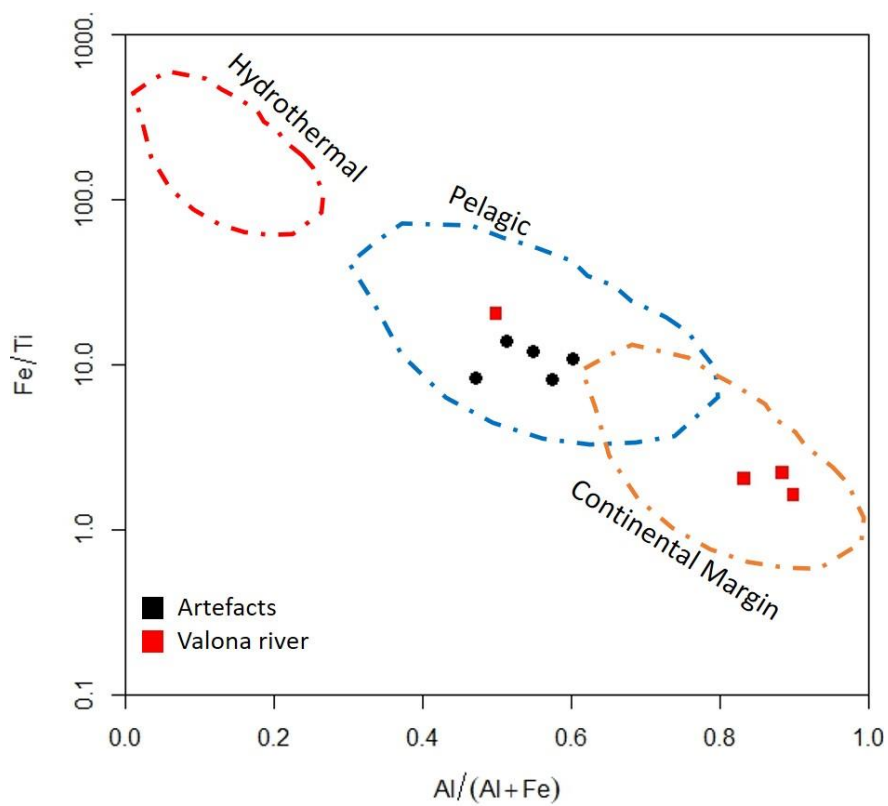


Figure 6-29: Binary diagram cross-examining the Sicilian cherts and the artefacts of this sub-group with respect to the depositional environment. The line demarcations have followed the suggestion of Murray (1994).

Spider plot - REE World Shale Average (Piper, 1974)

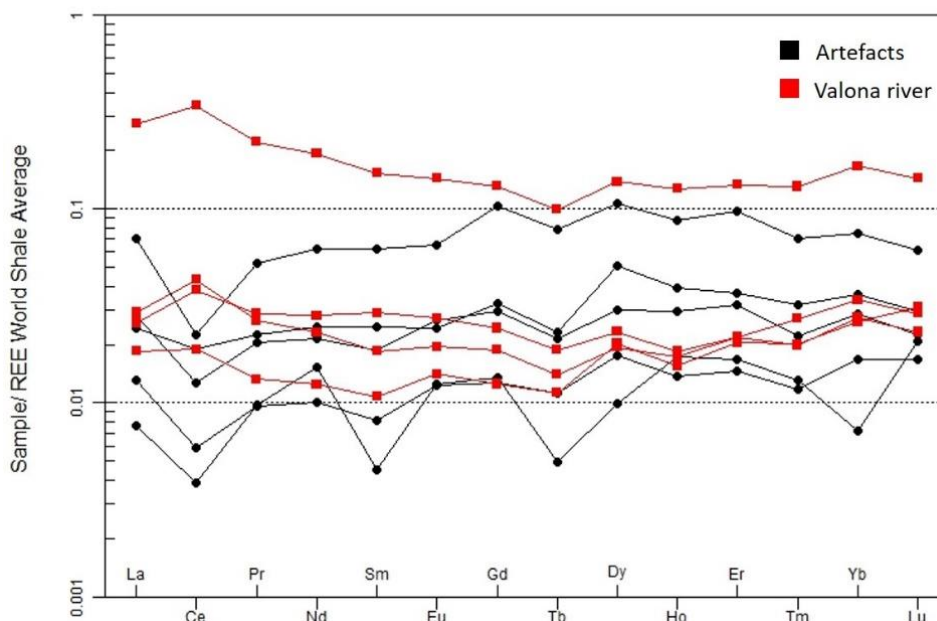


Figure 6-30: Comparable spider plot of the REE concentrations between the radiolarian samples artefact samples of this sub-group.

6.3.3.3. Third sub-group (white artefacts)

The third sub-group includes white, shiny (pearly), translucent fine-grained and mainly homogeneous artefacts (Fig. 6.31). Their characteristics are very similar to those from the unique chert outcrop found on Gozo (G2S6). Although they possibly relate to only one Maltese outcrop/source, they display no similarities with the main local chert sources and it has been decided to allocate them in this group. The outcrop on Gozo relates to a single, restricted exposure and only two samples have been collected, so the full spectrum of its properties is unknown. The only certainty is that this exposure is macroscopically completely different from all the other chert sources recorded on the Maltese Islands. Moreover, if these artefacts were not made from this outcrop then they would definitely be related to imported raw materials.

Artefacts of this sub-group have been reported in all assemblages, except of the Circle which is unexpected considering that this site is on the same island as this particular outcrop. To the contrary, the Skorba assemblage has such lithics in most of the contexts throughout the excavation sequence and suggests regular access to this type of chert rock. The p-XRF results (Fig. 6.32) showed that Si has the highest peak in both artefact and rock samples and the presence of Ca and Fe. However, the FTIR-ATR results (Fig. 6.33) have recorded the first important difference between these artefacts and the possible source. The samples of the sub-group are mainly consisted of quartz, while the rock samples presented opal-A and tridymite. These results cast some doubt on the connection between them, and these artefacts must be examined with great caution.



Figure 6-31: Representative samples of this sub-group.

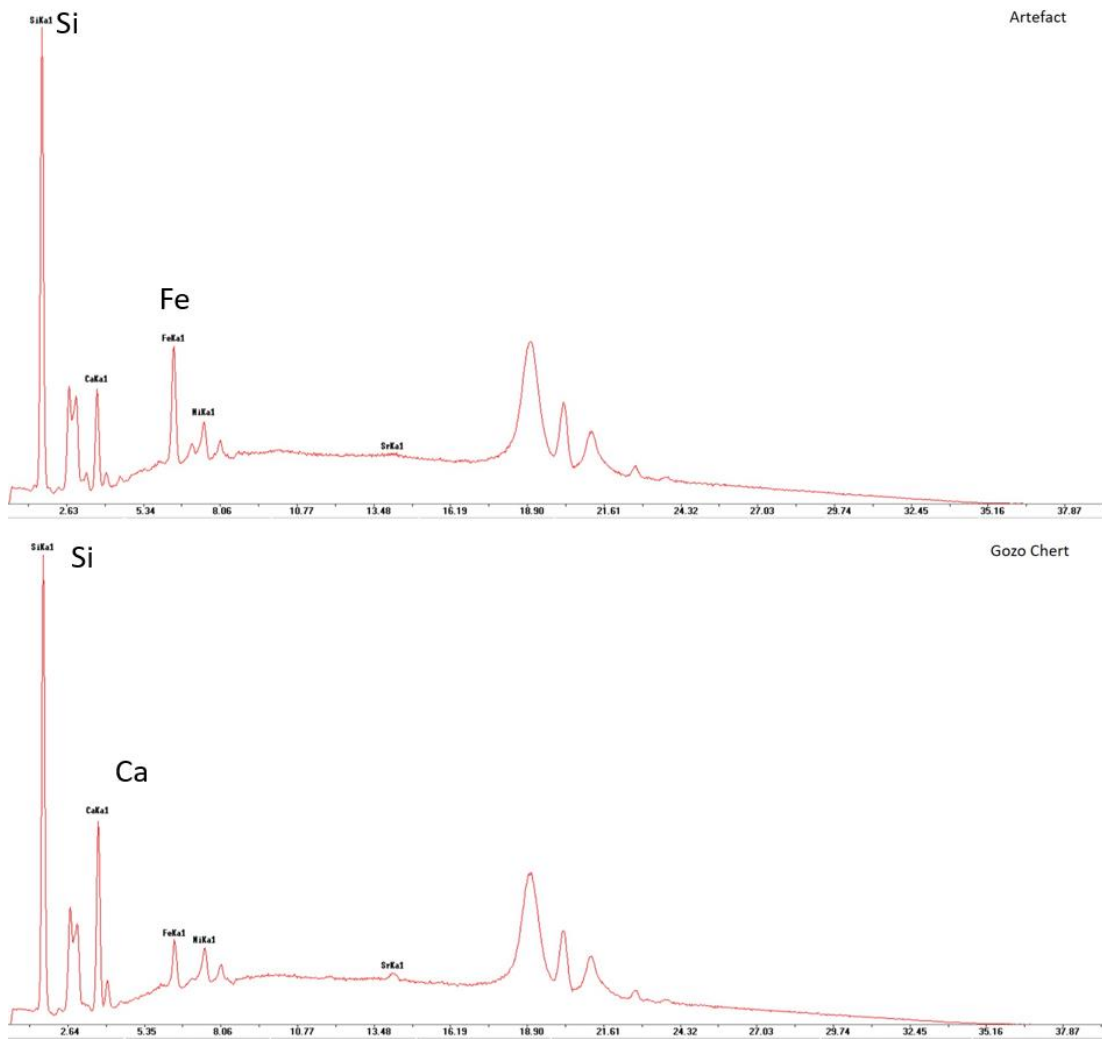


Figure 6-32: Representative p-XRF spectra of the artefacts included in this sub-group (GGWC15/1015/S3) (top) and the chert sources of Gozo (below).

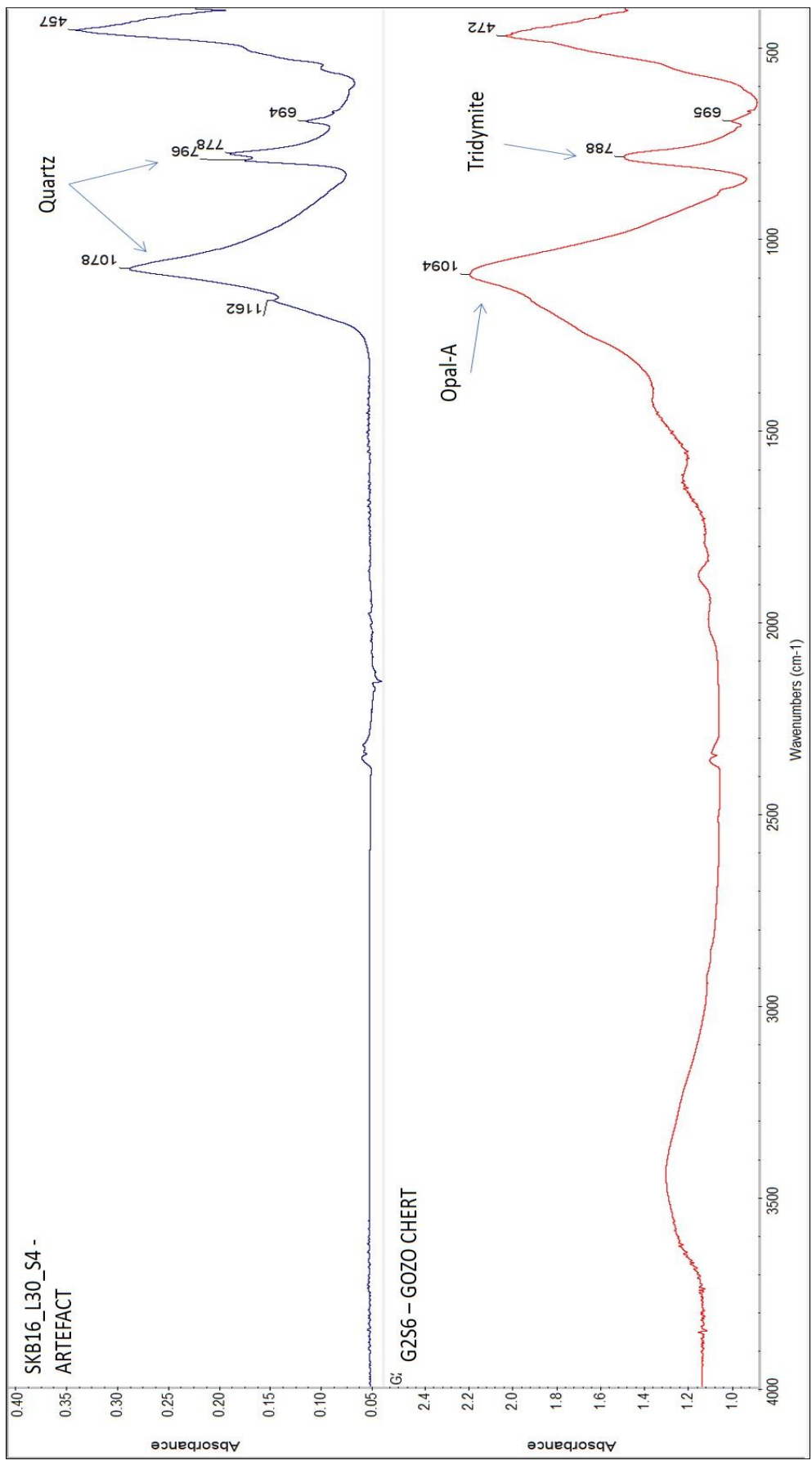


Figure 6-33: Comparative FTIR-ATR spectra between a representative artefact of this sub-group (above) and the chert sources of Gozo (below).

Continuing with the geochemical investigation, the samples of this sub-group were compared with those of the selected source (G2S6). The artefacts were mainly placed in the biogenic sedimentation region of the ternary model (Fig. 6.34), but two of them showed a connection with hydrothermal sediments. Moreover, the artefacts related to the first type of sediments were not gathered in the same area, which probably suggests a heterogenetic origin. Regarding the Gozo outcrop, only three artefacts (SKB16/S3/L16, SKB16/S8/L2 and KRD15/S42/L304) were placed close enough to support a connection with this source. This not only increases the doubts about the relationship of this sub-group with the local material, but also implies multiple sources. This hypothesis was further supported by the results from the depositional environment model (Fig.6.35) which demonstrates similar results. There were only two artefacts plotted close to the local outcrop (SKB16/S3/L16, KRD15/S42/L304), while most of the artefacts were placed in different environments (e.g. pelagic). These results were also supported by the REE ratios (Appendix I, Table 22 and 23) and highlighted the limited relationship of this sub-group with the specific outcrop on Gozo (G2S6). It is obvious that the initial assumption, based on the macroscopic similarities is false, and the artefacts of this sub-group exhibit great heterogeneity between its members. Although there are indications of a connection with the local outcrop, most of them (n=7; 78%) are likely related to multiple sources of exotic origin. The REE normalised patterns (Fig.6.36) confirmed the heterogeneous origin of these artefacts, which are with great certainty imported from elsewhere. The investigation in Sicily has not recorded any source with such features, so they must be imported from an alternative location. It is difficult to make any suggestions, but the results collected from this research can provide information about the source rocks. They must be formations with similar macroscopic features, with quartz as the most common mineral and be related to biogenic sediments which have been deposited in a pelagic environment. A future investigation should start by examining the geological status of the neighbouring areas and seek which of them are more likely to present rock formations with such characteristics. Additional information was provided from the oxygen-level model (Fig. 6.37), in which most of the artefacts (n=6; 67%) were related to high levels of oxygen during deposition (oxic).

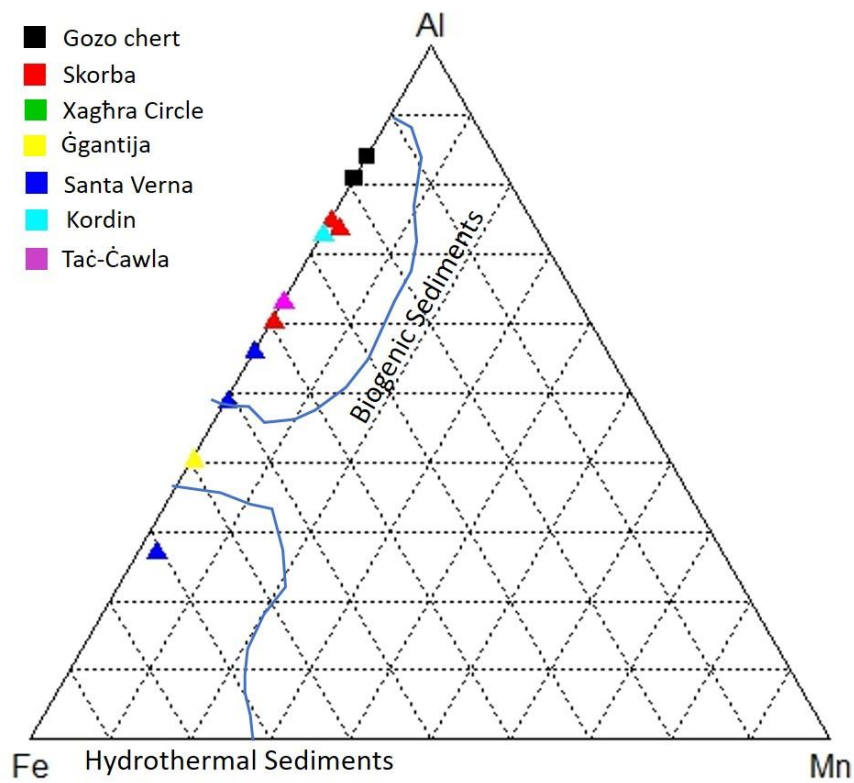


Figure 6-34: Ternary diagram cross-examining the Gozo chert outcrop (G2S6) and the artefacts of this sub-group with respect to the type of sediment. The line demarcations have followed the suggestion of Junguo et al. (2011).

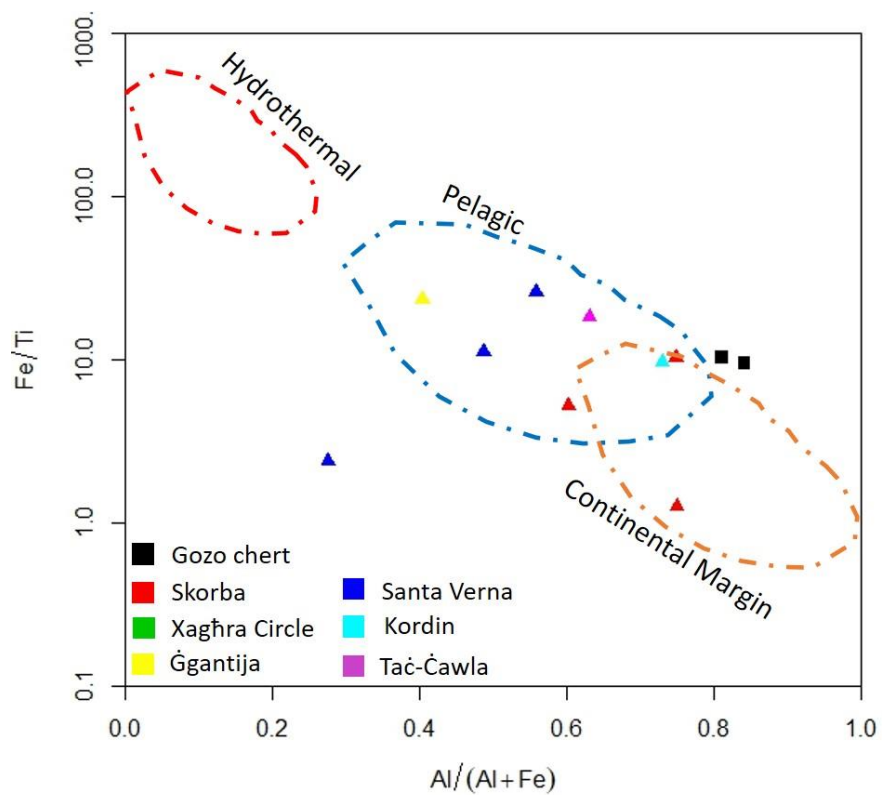


Figure 6-35: Binary diagram cross-examining the Gozo chert outcrop and the artefacts of this sub-group with respect to the depositional environment. The line demarcations have followed the suggestion of Murray (1994).

Spider plot - REE World Shale Average (Piper, 1974)

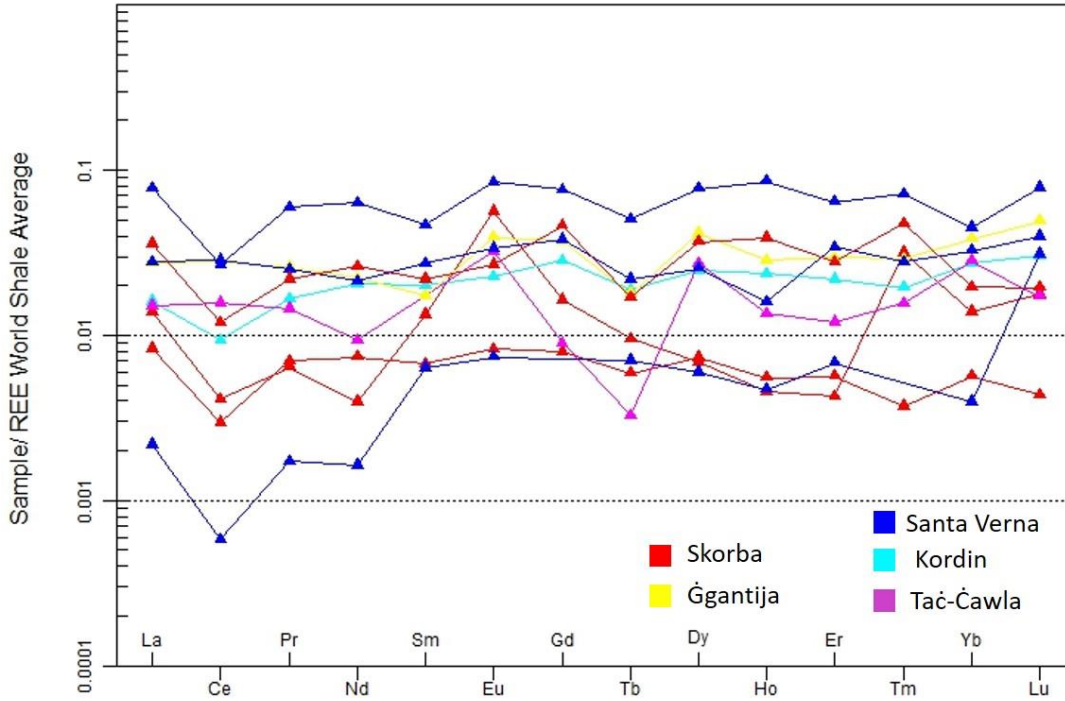


Figure 6-36: Comparable spider plot of the REE concentrations of the artefacts included in this sub-group.

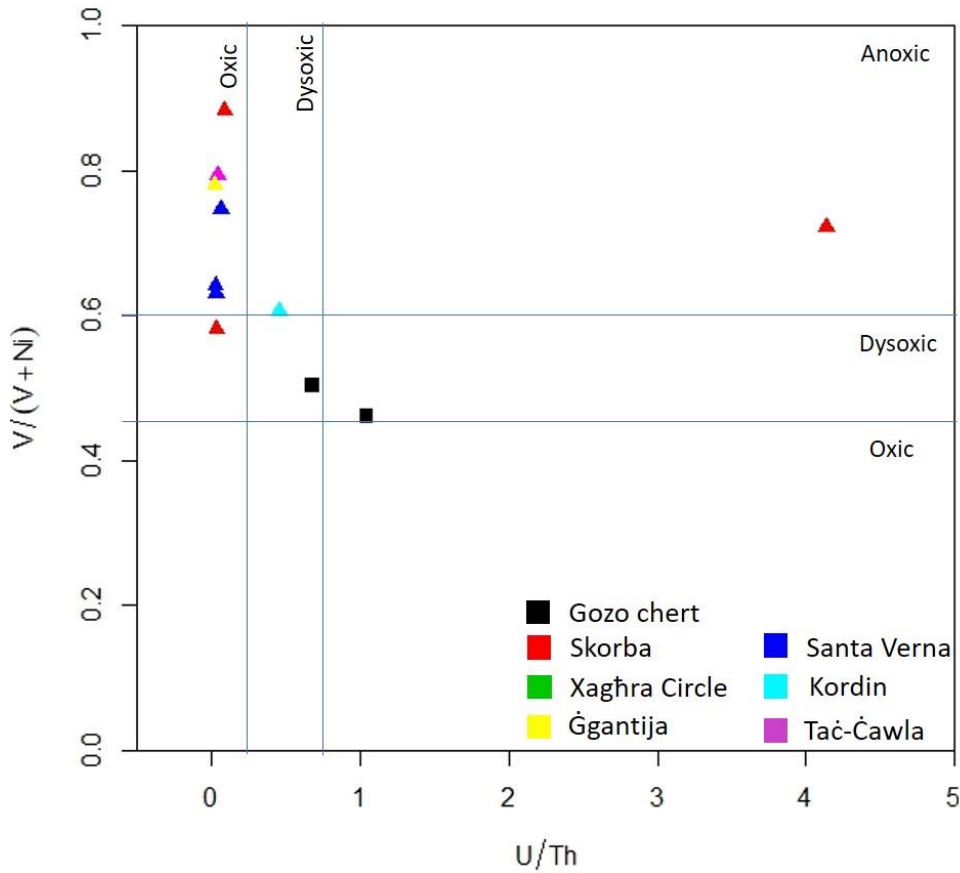


Figure 6-37: Binary diagram cross-examining the Gozo chert outcrop and the artefacts of this sub-group with respect to the oxygen level of the depositional environment. The line demarcations have followed the suggestion of Garbán et al (2017).

Nevertheless, the findings have shown the connection of a few members of this sub-group (SKB16/S3/L16, KRD15/S42/L304) with the local source. Although they might consist of different mineral types, they are in close proximity in all the geochemical models and present similar REE ratio values. In addition, isolating their REE normalised patterns (Fig. 6.38) and comparing them with the local outcrop, the connection between them can be further distinguished. Although there are differences between them, these artefacts are probably made from this local source. During the late Neolithic, there must have been a greater and better exposure of this outcrop, which has been exploited. The proposed location is more likely to have been the source material, but it is highly unlikely to be found in the current situation. The specific region is exploited for building materials and the expansion of the quarries is constantly changing the landscape. The samples from this source have been collected along a path, which in the last visit has been expanded to allow truck movements and unfortunately has concealed - if not destroyed - the chert exposures. The research has not found any indication of a similar chert material to be elsewhere on the Maltese Islands.

Spider plot - REE World Shale Average (Piper, 1974)

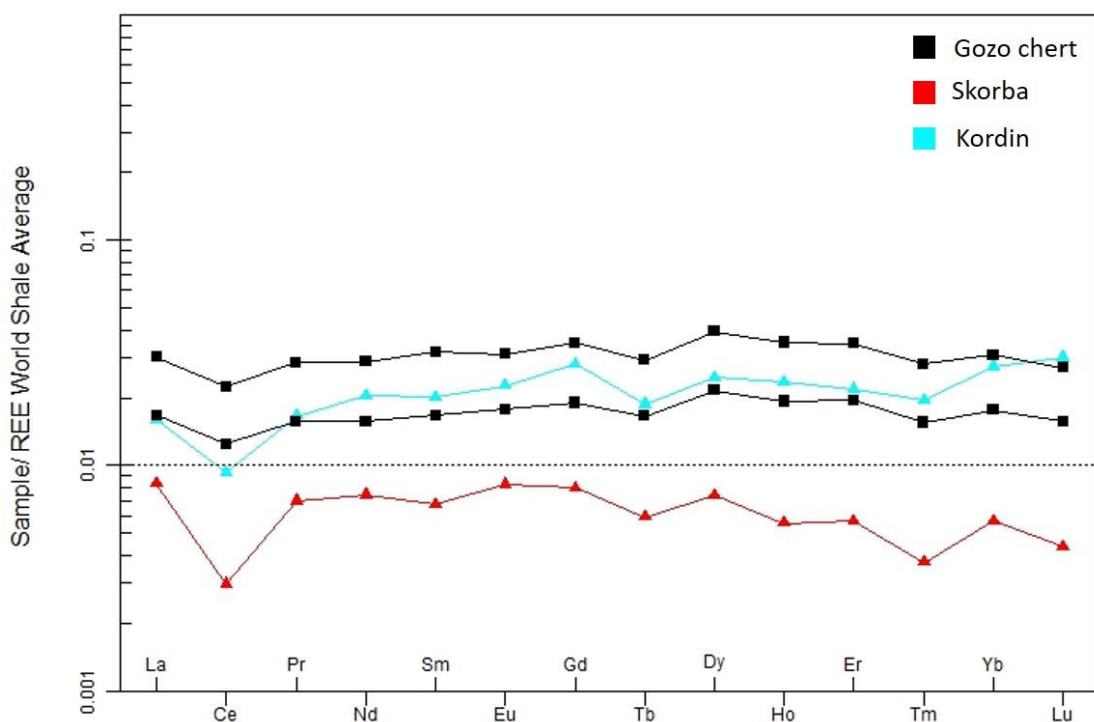


Figure 6-38: Comparable spider plot of the REE concentrations between representative rock and artefact samples (SKB16/S3/L16 and KRD15/S42/L304) of common local origin.

6.3.3.4. Fourth sub-group (black artefacts)

The fourth sub-group includes one artefact from the Tač-Ċawla (TCC14/S416/L178) and one from the Circle assemblages (BR91/S611/L712). They were heterogeneous, shiny (silky), semi-translucent, fine-grained and spotted artefacts, which had residues of a chalky cortex (Fig.6.39). They had a black colour (5YR 2/1) close to the cortex, but they were discoloured to lighter shades (e.g. brown – 10YR 5/4) towards the internal part of the artefacts. There was no other artefact in the examined assemblages with such distinctive characteristics. The importance of this sub-group lies in the great macroscopical resemblance of its members with specific chert outcrops recorded in Sicily (e.g. Monterosso Almo). The FTIR-ATR and p-XRF results (Appendix I) enhanced the connection with the chert sources of this region and eliminated any consideration of a Maltese origin.



Figure 6-39: The two members of this lithic sub-group.

Following the same sequence as the other sub-groups, the two artefacts were compared with the samples of the most suitable chert sources of Sicily. The artefacts were placed in the biogenic sedimentation region of the ternary model (Fig.6.40) and close to each other, with only two of the chert rocks demonstrated similar features. Similar were the findings from the binary model (Fig.6.41) which highlighted further the connection with Southeast Sicily. The sources from Monte Judica and West Sicily are excluded from possible sources because they have presented differences in terms of sediments and depositional environment. The same was also applied for a single chert outcrop from Monterosso Almo area (sample S19), which demonstrated characteristics completely incompatible with the investigated artefacts. These results were further supported from the REEs ratios (Appendix I, Table 22 and 23) and created solid foundations to claim that these artefacts were related to specific

chert sources from Monterosso Almo (samples S17 and S18) and the Modica area (i.e. sample S3). The connection of the artefacts with the specific outcrops is even better illustrated with the REE normalised patterns (Fig.6.42). The concentration levels and patterns between artefacts and outcrops are almost identical and probably these are the sources of this sub-group.

It is difficult to define which of the two places is the exact location from where the material was imported to Malta. Although there is a great distance between the two areas, the rock samples have been collected from a similar geological formation which explains their proximity in the models. It could be done with further investigation and with more techniques, but it would depend on the level of accuracy required. The fieldwork on Sicily is promoting the Monterosso Almo area, based on the better quality of materials, the greater resources and the easiest access to them. An additional factor that requires consideration is the proximity of these two areas to late Neolithic archaeological sites. However, this must be regarded with caution acknowledging the ability of the prehistoric people to travel great distances and engage in down the line exchange. Nevertheless, the research has provided solid evidence that these artefacts relate to the exploitation of specific chert outcrops/sources from Southeast Sicily. It is the second group of artefacts with strong evidence of their source (the first is the artefacts made from local chert) and the first showing a connection with foreign resources.

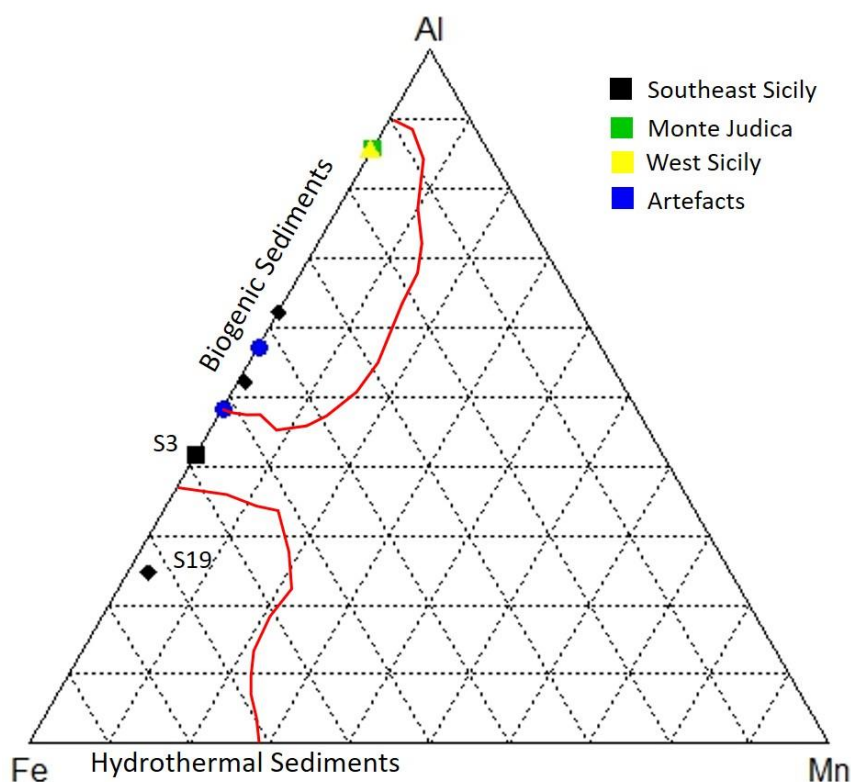


Figure 6-40: Ternary diagram cross-examining the Sicilian cherts and the artefacts of this sub-group with respect to the type of sediment. The line demarcations have followed the suggestion of Junguo et al. (2011).

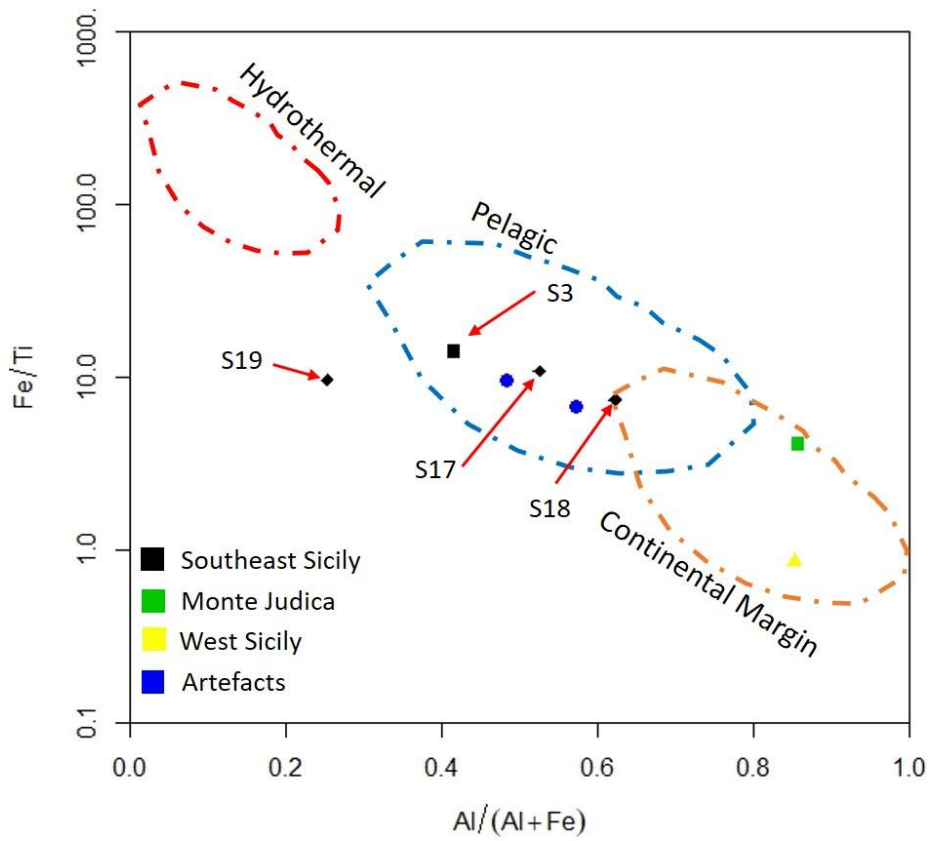


Figure 6-41: Binary diagram cross-examining the Sicilian cherts and the artefacts of this sub-group with respect to the depositional environment. The line demarcations have followed the suggestion of Murray (1994).

Spider plot - REE World Shale Average (Piper, 1974)

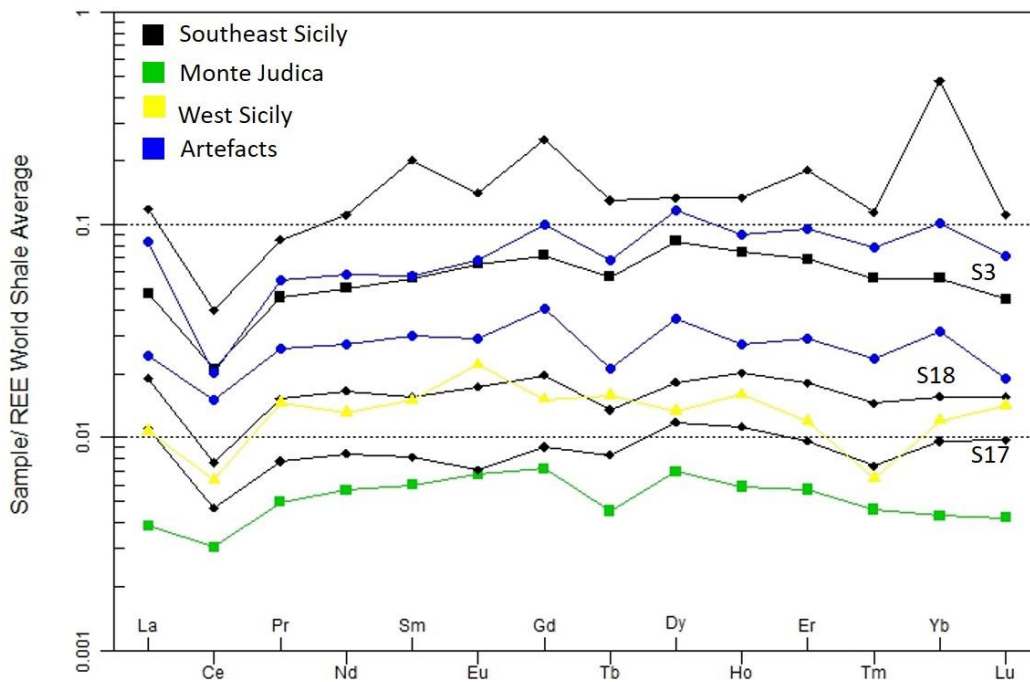


Figure 6-42: Comparable spider plot of the REE concentrations between representative rock and artefact samples of common local origin.

6.3.3.5. Fifth sub-group (artefacts from West Sicily)

The fifth sub-group includes again one artefact from the Taċ-Ċawla (i.e. TCC14/S460/L273) and one from the Circle assemblages (i.e. BR91/S564/L662). They were homogeneous, shiny (pearly), smooth, opaque and fine-grained artefacts, but they presented different colours (Fig.6.43). The sample from Taċ-Ċawla had an orange shade (i.e. 5YR 5/6), while the one from Xagħra Circle had a purple shade (i.e. 10R 6/2). The main reason that these two artefacts have been put in the same sub-group is their similarities with a source in West Sicily. The fieldwork on this part of the island examined a limestone formation (of Triassic age), which presented chert nodules of orange or purple shades, macroscopically similar with these artefacts. Moreover, it has been recorded that the orange outcrops had been fractured in the same manner as the artefact of Taċ-Ċawla, additional evidence of their connection. The FTIR-ATR and p-XRF results (Appendix I) provided further common characteristics between the artefacts and the chert source of West Sicily, and in the meantime, they erase any remaining consideration of a Maltese origin.



Figure 6-43: The two members of this lithic sub-group.

It relies on the geochemical evaluation to secure the connection of this sub-group with a specific source in West Sicily. The artefacts were placed in the biogenic sedimentation region of the ternary model (Fig.6.44) and close to each other, while only one of the chert rocks demonstrated similar features. This was the sample from the orange outcrop (S22r) which was interestingly plotted exactly on the same spot as the purple artefact (i.e. BR91/S564/L662). The sample from the purple outcrop (S22p) was on the top of the ternary, probably because of the very low Iron concentration. Similar were the findings from the binary model (Fig.6.45), which enhanced the connection with the West

Sicilian source. The artefacts were of the same environment (i.e. pelagic) and again the orange outcrop was placed in exactly the same position as the artefact from the Circle assemblage. The purple outcrop was placed again at a distance from the other three samples, which was also attributed to the very low Iron concentration. It is uncertain to what extent this lack of Fe relates to the source material or is just restricted to this specific outcrop. Unfortunately, only one sample of this outcrop has been collected and it has proven to be impossible to explain this situation. Nevertheless, this can be addressed by investigating the concentrations of rare earth elements (REEs) and their ratio values (i.e. Ce/Ce^* , La_n/Ce_n). Indeed, their results (Appendix I, Table 22) suggest a pelagic environment with possible influence from a ridge environment for both the artefact and source samples. Furthermore, the link between them can be even better illustrated with the diagram of the REE normalised patterns (Fig.6.46). The patterns of all the investigated samples were almost identical which provided more evidence of the connection between the West Sicilian chert formation and this sub-group. However, the REE normalised pattern of the purple chert outcrop was placed in much lower concentration levels than the other samples and raised again some concerns. It is evident that more samples and analysis is required from this outcrop to address the uncertainties and draw safe conclusions. Nonetheless, the relationship of this sub-group with West Sicily has been established and this region is certainly a location from where chert material was imported to the Maltese Island.

These findings in addition to those of the previous sub-group (i.e. fourth) suggest a special connection of the Xagħra Circle and Taċ-Ċawla with Sicily. These archaeological sites are located on Gozo which is closer to Sicily than Malta and therefore it is possible that imported material from Sicily would arrive first on this island. Ramlia Bay is very close to these sites and one of the few beaches of the island which provides easy access to the mainland and shelter to ships/boats. Therefore, it could have been a convenient place for those sailing from Sicily to make a stop there and unload their goods. It cannot be said that this is the first or the only stop of the sailor to the Maltese Islands, but it certainly fulfills the requirements of a landing point of arrival.

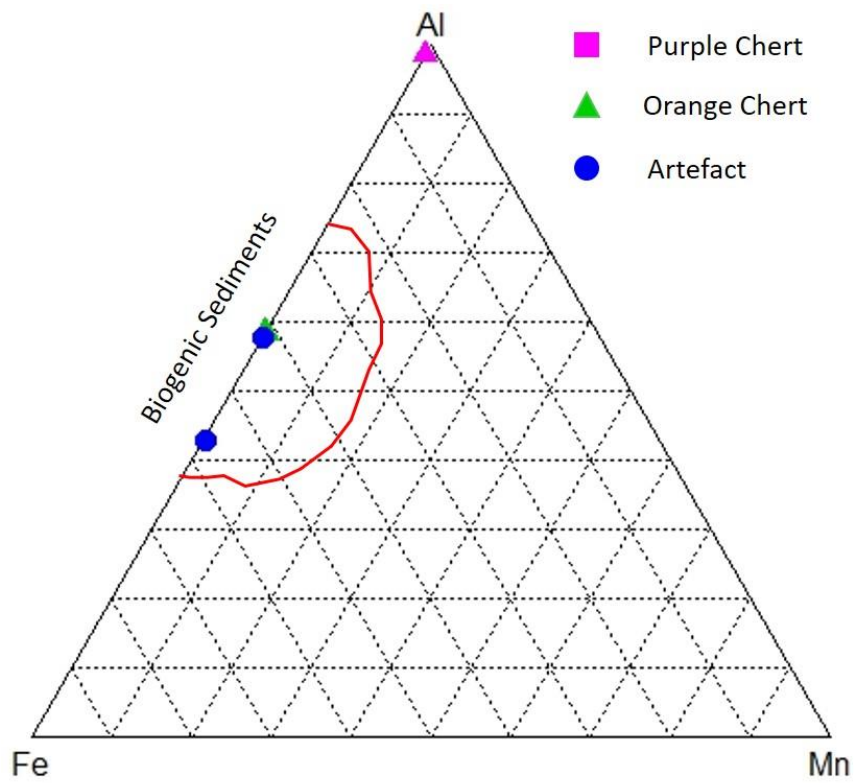


Figure 6-44: Ternary diagram cross-examining the Sicilian cherts and the artefacts of this sub-group with respect to the type of sediment. The line demarcations have followed the suggestion of Junguo et al. (2011).

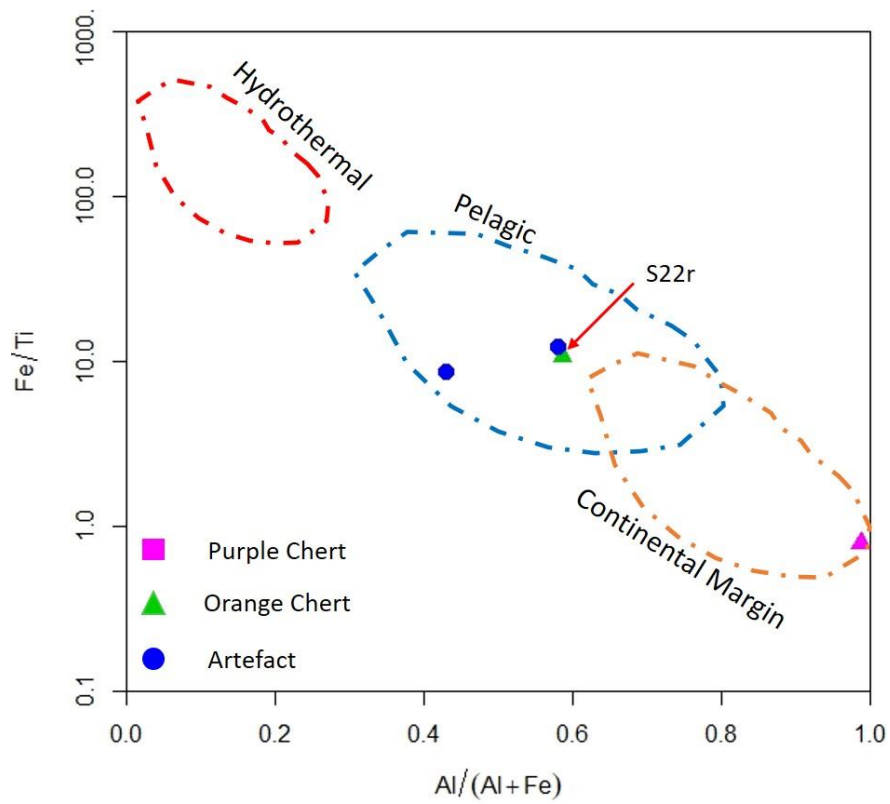


Figure 6-45: Binary diagram cross-examining the Sicilian cherts and the artefacts of this sub-group with respect to the depositional environment. The line demarcations have followed the suggestion of Murray (1994).

Spider plot - REE World Shale Average (Piper, 1974)

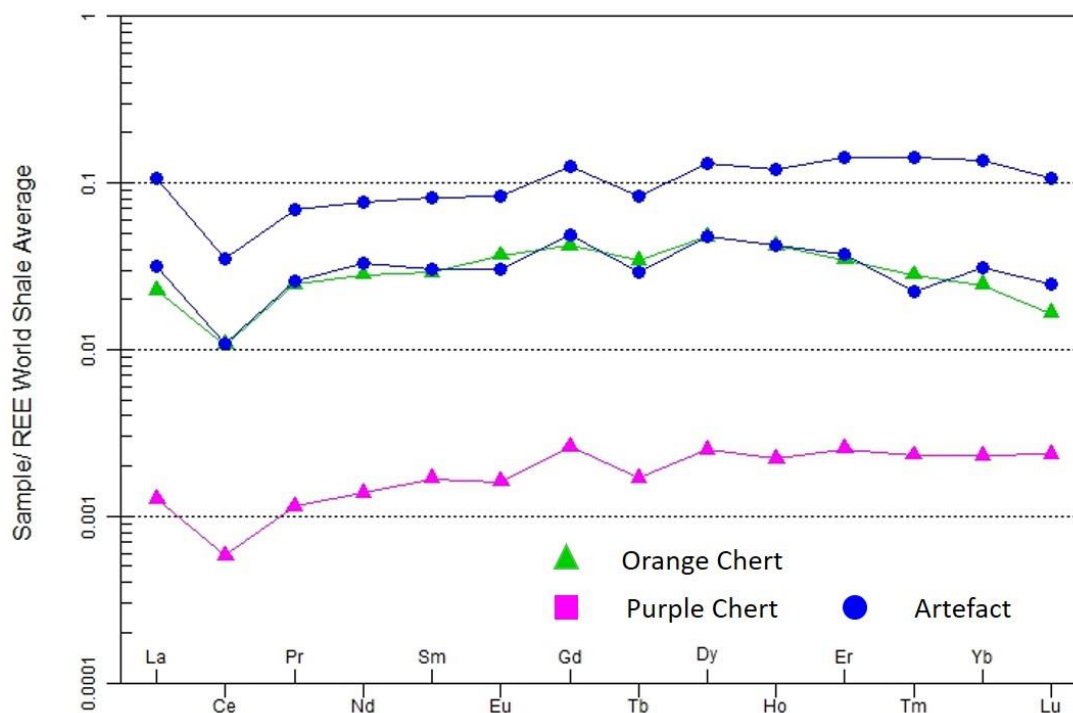


Figure 6-46: Comparable spider plot of the REE concentrations between representative rock and artefact samples of common local origin.

6.3.3.6. Sixth sub-group (artefacts of unknown origin)

The final sub-group includes all the single artefacts recorded in the assemblages which could not be related to the other sub-groups or the two previous groups. Additionally, they have presented macroscopic characteristics unrelated to the chert sources of Sicily. The problem with these artefacts is their small size which prevents recording of their features with sufficient accuracy. However, there is one sample from Santa Verna (SV15/S2/L22) and one from Kordin (KRD15/S156/L306) which have similar characteristics possibly suggesting a common origin. They were smooth, opaque, fine-grained and spotted samples with a distinctive variegate colour feature (from red to gray). Similar is the situation of one sample from the Circle (BR93/S854/L897) and one from Ġgantija (GG15/S3/L1016) and they again possibly had a common origin. Nevertheless, none of the investigated sources has these characteristics and these samples have been allocated to this group. It is difficult to make interpretations of results from a heterogeneous group and especially when there is an absence of a probable source. Therefore, the general findings will be discussed to provide some indications/characteristics of their sources and examine the possibility that these macroscopically similar artefacts have a common origin.

Macroscopically, none of the members of this sub-group can be related to local chert sources and most likely they have been made from imported material. The FTIR-ATR and p-XRF results (Fig.6.47) of

these artefacts demonstrated the dominance by quartz and silica which supported the previous findings and eliminates any suggestion of a Maltese origin. The investigation continued to the geochemical models which further illustrated the different origins of these artefacts. The samples were plotted in the ternary model (Fig.6.47) and demonstrated a relationship with a variety of sediments. Similar were the findings from the binary model (Fig.6.48), which showed the artefacts to be deposited in different environments. Most of the samples (n=12; 70%) were from cherts of biogenic sediments which have been deposited in a pelagic environment, but they present significant heterogeneity in these broader regions, which eliminates any suggestion of common source. This can be easily understood from the smaller groups in which the samples were gathered, within the regions of the two diagrams. Furthermore, some other artefacts were plotted outside these regions, which implied a different type of sedimentation and environment. These results were generally supported by the REE ratios (Ce/Ce^* , La_n/Ce_n), but some values (Appendix I, Table 23) contradicted the findings of the models. The diversity of this sub-group does not allow any to reach safe conclusions to be reached, and the results must be treated with caution. It is therefore preferable to collect and treat this information as general suggestions about the types of chert formation, on which future research should focus. It is established that this material, regardless of their features, has been imported and is possibly not only from Sicily. Moreover, any suggestion of a foreign location must include the geological information collected from this sub-group. The place of interest should mainly have chert formations related to biogenic sediments and pelagic environments. The option of hydrothermal sedimentation and/or ridge environment should not be neglected, but it is of little importance because only a few samples have presented such characteristics. However, this feature could be crucial when prospecting for a source region/location that presents a combination of such geological formations.

It has been outside of the scope of this research to investigate other regions except for Malta and Sicily, and therefore no suggestions outside this framework can be provided. Considering all the information collected from the areas of interest, the only possibly suitable area to present such resources is West Sicily. It is known from the literature (Catalano & D'Argenio, 1978) that this region mainly consists of pelagic formations and occasionally offer multiple chert outcrops. The current research has not been able to investigate the full spectrum of chert sources there and it is highly possible that some chert formations yet to have been recorded. Therefore, a new and more extensive reconnaissance survey for chert sources on West Sicily in the future looks very promising. Additionally, there are chert sources on this part of the island that relate to hydrothermal/volcanic activity. It has not been possible for the full extent of these to be investigated, and it could be the case that they are potential sources of some of the artefacts reported in this sub-group and others.

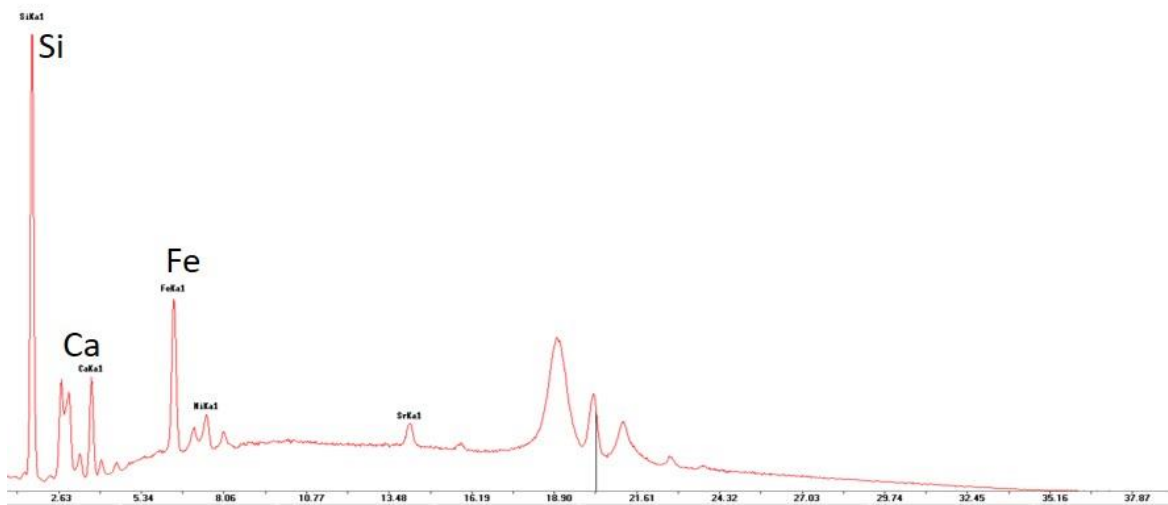
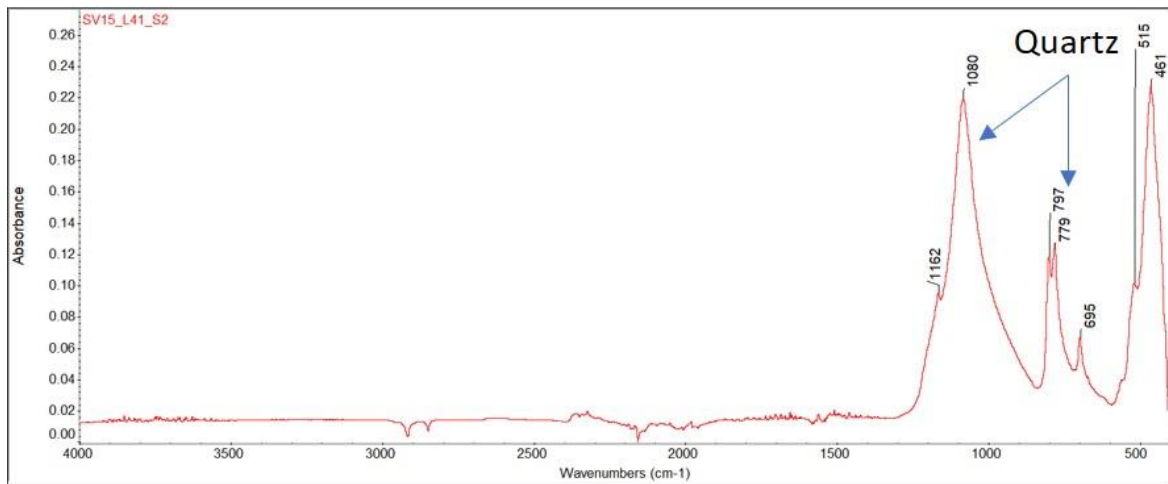


Figure 6-47: FTIR-ATR (above) and p-XRF (below) spectra of a representative artefact of this sub-group (SV15/S2/L41).

Returning to the current findings, at the beginning of this sub-chapter common macroscopic features were reported between one sample from the Circle (i.e. BR93/S854/L897) and one from Ġgantija (i.e. GG15/S3/L1016). By cross-examining their results with the other methods (e.g. FTIR-ATR) and especially with the geological models, it is been clear that they are from a common source. They are both related to biogenic sediments (Fig.6.47) and a pelagic environment (Fig.6.48), and most importantly they are placed very close to each other (arrows on diagrams). The common origin and most likely the common source of these two artefacts is further supported from the REE normalised patterns (Fig.6.49) which are almost identical in terms of pattern and concentration levels. Although their source remains unknown, it is certain that they were made from the same chert material.

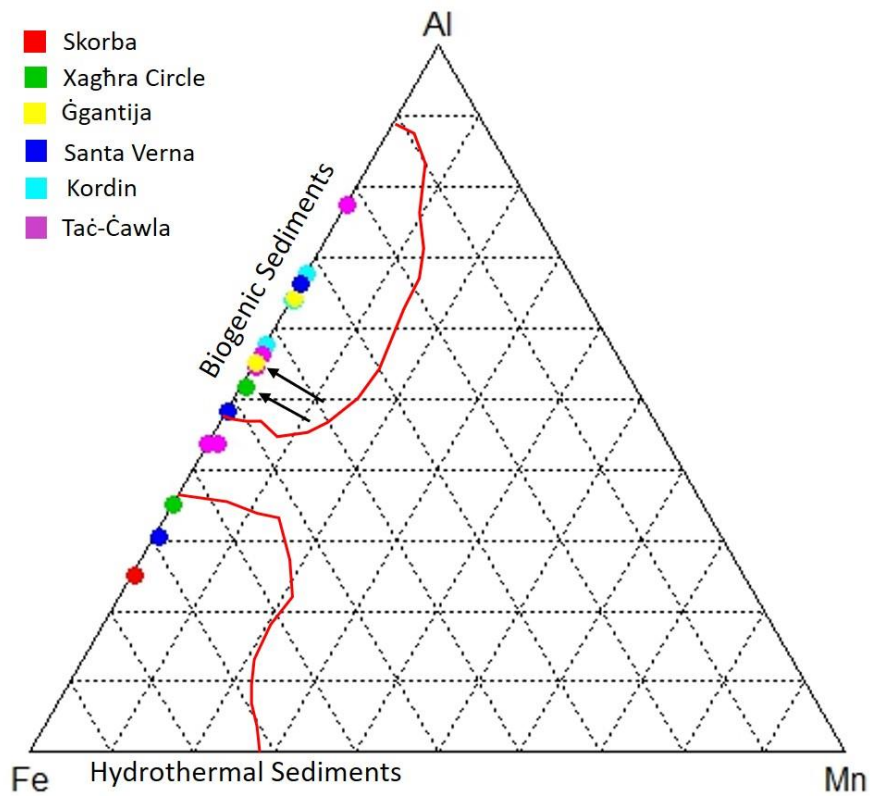


Figure 6-48: Ternary diagram examining the artefacts of this sub-group with respect to the type of sediment. The black arrows show the two macroscopically similar artefacts of this group. The line demarcations have followed the suggestion of Junguo et al. (2011).

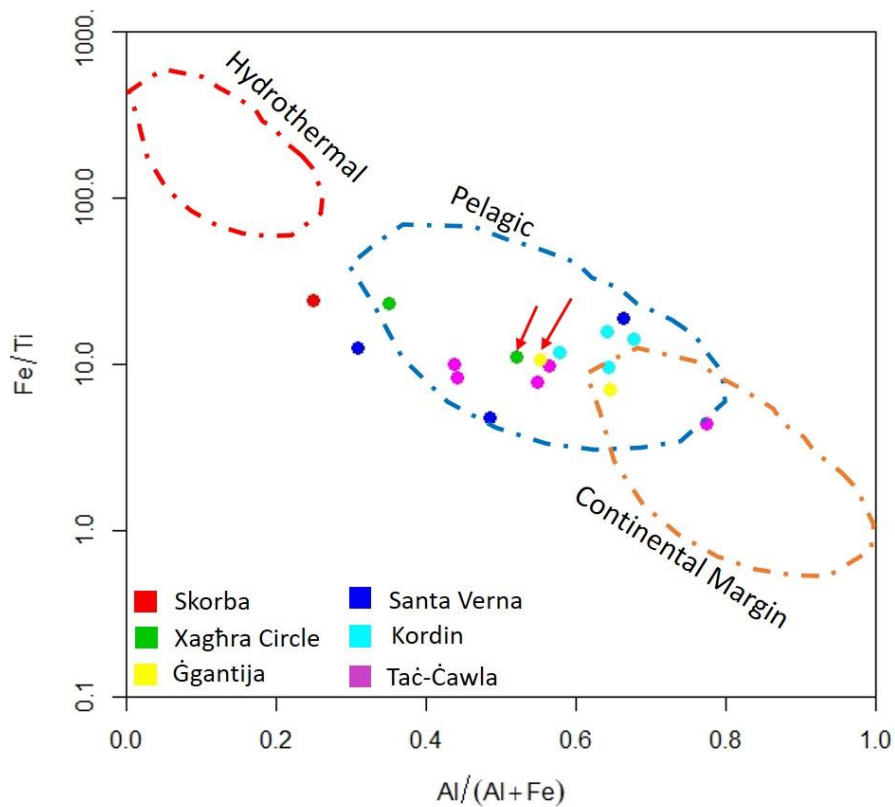


Figure 6-49: Binary diagram examining the artefacts of this sub-group with respect to the depositional environment. The red arrows show the two macroscopically similar artefacts of this group. The line demarcations have followed the suggestion of Murray (1994).

Spider plot - REE World Shale Average (Piper, 1974)

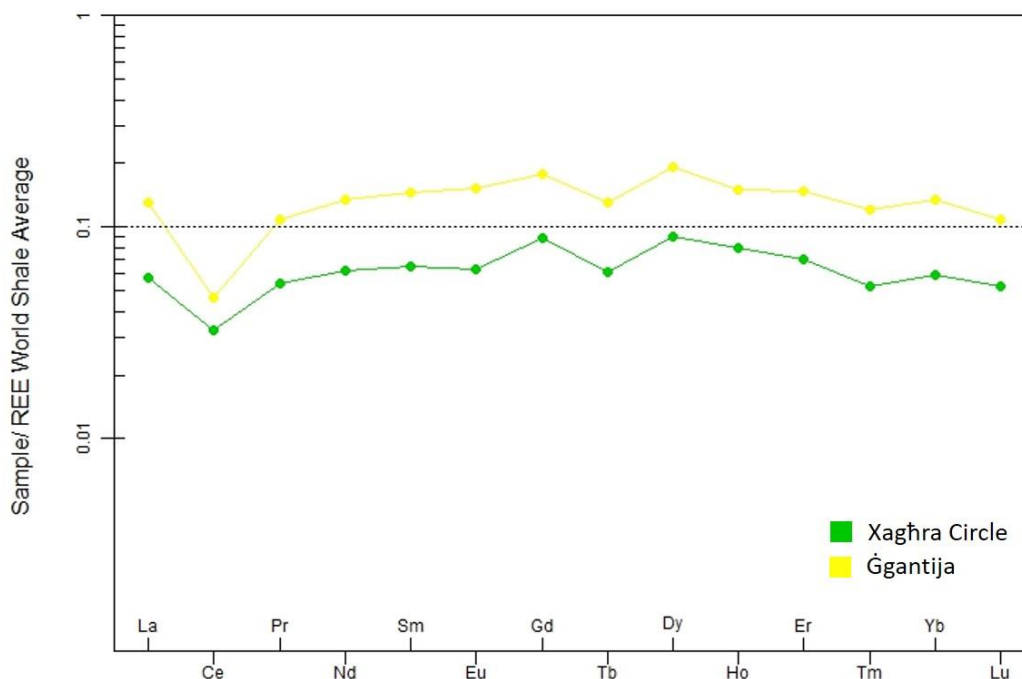


Figure 6-50: Spider plot of the REE concentrations of the two macroscopically similar artefacts.

6.3.4. Artefacts summary

The macroscopic investigation has divided the chert artefacts into three main groups which have been reported in all the examined assemblages. The FTIR-ATR and p-XRF results have shown that the members of the first and third group predominantly consisted of quartz and Si, while the second included artefacts mainly with opal-A and high concentrations of Ca. The combination of these methodologies provides strong indications of a non-local origin for the artefacts of the first group. The majority share common macroscopic characteristics and they were probably made from the same source. The employment of geochemical method strengthens this argument but also suggests the presence of secondary sources with similar characteristics. The cross-examination with the Sicilian sources revealed a possible connection, but no suitable source has yet been found. It seems that the closest sources are those of West Sicily, but the actual source has not been found there. The main issue is the lack of a source with similar macroscopic characteristics.

The results of macroscopy, FTIR-ATR and p-XRF have provided strong indications that the second group was connected with the chert sources of the Maltese Islands. Furthermore, the cross-examination with the geochemical results between these artefacts and the local chert sources has provided strong and undoubted evidence towards their Maltese origin. It has been even possible to find a perfect match between artefact and specific outcrops from Malta and Gozo islands.

The third group of artefacts was not related to the local chert sources based on the macroscopic, mineralogical and elemental characteristics. However, it did not have the uniformity of the first group and presented a variety of macroscopic features. The members of this group are far smaller in size compared with the other two groups and could be divided into several sub-groups. In addition, it had fewer members in each of the examined assemblages which were dominated by the other two groups. The geochemical investigation has identified two sub-groups which appear to be related to specific Sicilian sources. The first (i.e. black sub-group) was strongly related to the sources from Southeast Sicily and most probably with outcrops found in Monterosso Almo area. The second has been connected with a specific source located in West Sicily, which until now has never been considered as a possibility. This revealed a new location from where materials may have been imported to Malta, and therefore expands the horizons in which the Maltese people may have been interacting with other populations.

Furthermore, the research has not managed to connect some sub-groups with any of the reported Sicilian cherts and therefore their sources remain unknown. The second sub-group is an excellent example of this situation and although a similar chert formation has been found on Sicily (i.e. Radiolarian), the geochemical investigation has proven that they were made from a completely different type of chert rock. West Sicily is a region which has not been fully explored and possibly many of its resources are still unknown, but other possible locations should be considered. This research has provided useful information on the characteristics of the actual sources of the artefacts with unknown origin. These allow future research to have a starting point and cross-examine these data with the geological status of new candidate regions. Regardless of the specific research objectives, this research has the potential to slowly unfold the full extent of the exchange/trade network in which the Maltese islands may have been acting and reveal the possible cultural and traditional interactions the late Neolithic Maltese people had with their neighbouring islands.

6.4. Chaîne opératoire

This is a supplementary part of the research conducted during this research study on the Neolithic chert assemblages of the Maltese islands and was included in a later stage of the original research plan for this thesis. The manufacturing techniques and technologies associated with the production of chert artefacts have been observed and assessed in order to identify the crafts and traditions used by the Neolithic population of Malta. This, alongside with the sourcing of raw material, can provide indications of the social dynamics of this community and their possible relationships with neighbouring areas in the Mediterranean Sea. Moreover, this combination can provide strong indications on the level of access that this Neolithic society has on external resources and the transmission and movements of raw materials in the central Mediterranean area.

Furthermore, these findings merge smoothly and form the *chaîne opératoire* of Neolithic chert artefacts of Malta. This could further address questions regarding the technological choices made during production, and how the choice of raw material affects the techniques used. Employing a single technique on different material would suggest great skills and expertise, while multiple techniques would imply an understanding of the different properties of the materials and the ability of the craftsman to adapt to the changing conditions. Creating a variety of tools from a similar material shows how people mastered new skills, while creating specific tools from only one chert material suggests possible craft traditions and also optimization of the available resources.

The examination of the assemblages has made it clear that the first technique of the manufacturing process is percussion flaking. It has been employed on the raw material (objective piece) to create suitable detached pieces, which were mainly flakes. In addition, many chips and shatters have been reported in the assemblages (n=22), but they were possibly by-products of the process. The assemblages of Skorba and Ġgantija have a significant amount of debitage pieces which lack any modification. Similar pieces have been recorded in the other assemblages but not to the same extent as on these two sites. Moreover, these are only related to the brown and local categories of raw material and not the third. Although this is expected for the local resources, it is not expected to be the case for the first group which is considered to be imported material. The numbers and the variety of pieces related to this material are similar to the local chert, which either suggests easy and constant access to this chert source or the importation of this raw material to the Maltese Islands. Furthermore, these are strong indications of crafting artefacts/tools from this type of chert made *in-situ* at these sites. This is supported by the many decortication flakes reported in the assemblages which are extracted to increase or create a striking platform surface. The most compelling evidence, however, is the finds of the recent Ġgantija excavations and especially those in the context 1019. This layer included all the possible rock pieces produced during a manufacturing process from the beginning (e.g. raw material) to the end (e.g. blades). The discovery of this complete *chaîne opératoire* not only

confirms that the crafts have been conducted locally but also allows the recording of all the steps of a local manufacturing procedure. The research does not suggest that this has been the only craft tradition on the Maltese Islands, but has contributed significantly to resolve many uncertainties for the lithic assemblages.

Focusing on the flake pieces, most of them (n=73; 86%) presented indications of additional/secondary percussion, which can either aim to extract more flakes from this piece or give the desired form to the artefacts. The feature “arris” is caused by these actions and can be described as a borderline between surfaces from which material has been extracted. Many of the flakes (n=44; 45%) had evidence of modification on their dorsal surface, while the ventral surface was untouched. The artefacts presenting this pattern are described as unimarginal (Andrefsky, 2005), which are the predominant type of flakes and flake tools in the examined assemblages. Nevertheless, there are few bimarginal artefacts with evidence of modification to both surfaces. These artefacts are mostly related to the third group of chert sources, while no artefact of the local chert presents such features.

Some artefacts do not have evidence of percussion further than the one that detached them from the original core. On the contrary, they have features related to pressure flaking (Inizan et. al., 1999), a technique which focuses on enhancing the utility of the artefacts/tool. This type of flaking is particularly consistent with the members of the first group of chert artefacts and has a strong connection with scrapers and flake scrapers. The edges of these tools have been modified with this technique, with the evidence found on the dorsal surface (Fig. 6.4). There are some flat flakes of this material that retain part of the cortex and they are considered decortication flakes (Inizan et. al., 1999). The edges of these are often modified using the pressure flaking technique and may have been used as a scraper. These findings can be considered evidence of retouch and demonstrate the ability of the local population to optimize their available resources. Although the artefacts of this material are produced on the Maltese Islands, this technique has never been recorded on artefacts related to the local chert sources. This feature requires further investigation and most likely relates to the properties of the chert material. Moreover, it must not be coincidence that there are no scraper type tools made from the local chert.

The discussion until now has been focused on the two main categories of chert material mainly because they are believed to be manufactured locally. This material can provide important information on the craft techniques and traditions used or exploited from the local population, and most likely give an insight into the social dynamics of this society. Moreover, the variety of lithics, as well as the size of many of them, have allowed the recording with great accuracy of the general *chaîne opératoire* of this Neolithic craft, and allowed comparison with similar situations in the broader neighbouring areas. Although a holistic investigation is necessary to assess further the level of skills present on Malta, some initial remarks can be drawn.

The manufacturing process included only a few steps and the techniques recorded lack of complexity but sufficed to produce artefacts and tools. Many of them (n=42; 49%) are different types of flakes (e.g. prismatic flakes, blades) and scrapers, but they are very simple and lack decoration and features that suggest skilful craftsmanship. The only exceptions are the lithics from the Circle and Ġgantija, which indicate far higher manufacture techniques than those reported for the other assemblages. The first assemblage includes a scraper (e.g. BR91/S745/L845), which most likely been has been created with the Levallois technique (Andrefsky, 2005). There are certainly simple versions in comparison with the Levallois technique which suggests that there may have been influence and change to the local craft traditions. Unfortunately, nothing further can be inferred until more is known about the context in which these artefacts have been found. The assemblage from Ġgantija does not include such artefacts and does not record similar techniques but reports noticeable variations in the artefacts. The centre of interest is again context 1019 where the focus falls on one specific blade (i.e. GG15/S14/L1019) with special features (e.g. basal border, tang). Indeed, such features have not been reported anywhere else and highlight the significance of that period (context 1019), not just in the Ġgantija temples, but within the whole Neolithic context of the Maltese Islands. Accurate interpretations about the significance of these findings can only be drawn when more information is available about this period in the Temples. Nevertheless, the Circle and Ġgantija temples are the latest in comparison with the other investigated sites and this possibly shows the evolving craft traditions used by the Neolithic population of Malta to higher levels. This possibly demonstrates a shift in the social dynamics of this community and may suggest influences from neighbouring areas.

The situation with the artefacts from the third group is more difficult and complex, and consequently they were treated independently from the other two groups. The research has found strong evidence of their exotic origin, but their size and numbers make it impossible to understand the *chaîne opératoire* from which they emerge. They all have evidence of the final techniques employed on them, but there are no indications of the initial actions. It is possible for some of the features of the initial flaking to be present, but the restricted examination surfaces do not allow them to be recognised. Pressure flaking is the most common technique reported, while evidence of percussion has been also found. The first is used to retouch the artefacts (e.g. SV15/S1/L80) and increase their utility span, while the second has provided part of their final form. These, of course, are general remarks and of low accuracy, but they are the best outcome under the current conditions.

The small size has resulted from multiple retouch actions, which possibly suggests their great value to the Maltese people and also limited access to fresh material. Some have extensive modifications on every surface which indicate constant efforts to maximize their utility until they reached depletion. There are strong indications supporting the previous statement and most likely the artefacts have been imported to Malta in an already complete form. This is supported by the total absence of any objective piece macroscopically similar to these artefacts. Nevertheless, the final retouch actions may have been

conducted by Maltese people for the reasons previously described. Moreover, many of the finds are actually fragments/parts of bigger artefacts, and are therefore probably the broken tools of the craftsman involved. This can further explain their great value to the local population and also the constant retouch they undergo.

Comparing these findings with those of the also exotic chert of the first group, it is highly unlikely that they have a common origin. Although the possibility of Sicily still remains as an option, the difficulty of accessing such raw material is undeniable and other possibilities must be considered. This is supported from artefacts (e.g. GG15/S3/L1016) with unique features (e.g. serration) which are indicators of different techniques and skills. Moreover, special consideration must also be given to one artefact from Taċ-Ċawla (i.e. TCC14/S103/L85) on the ventral surface of which there is evidence of polishing. It is the only artefact that presented such a technique and its appearance on a specific type of chert (i.e. first sub-group of the third group) may not be a coincidence. It is clear that these are interpretations of the current findings, and a holistic and wider consideration of all the Neolithic sites is necessary. Furthermore, many uncertainties are going to be resolved when the interpretations of the context of the investigated archaeological sites have been fully completed.

6.5. Integrating with FRAGSUS

Many of the findings from the different research strands of the FRAGSUS project are still under analysis, and only until their full publication, we will have a clearer picture of at least some aspects of the Maltese Neolithic. Nevertheless, it seems appropriate to try and merge some of the project's initial wider findings with the results of this research.

Currently, the best line of corroborative evidence comes from the re-analysed pottery assemblages, which contain sherds indicative of pottery that have been imported from Sicily (Malone, pers. comms.). In addition, there is also one confirmed case of a site in Sicily (Licata Caduta) where Maltese pottery was found to be imported (Barone et al 2011). Presumably, the pottery contained what was being traded/exchanged, rather than being a commodity in itself. These initial remarks on ceramics align with the findings of this research that Maltese chert artefacts are originated from Sicilian sources. However, the radiocarbon-dating results are necessary to clarify if the connection between the two islands was a regular occurrence or a single movement. It would also be useful to learn if the Sicilian pottery originated from areas close to Monterosso Almo and West Sicily chert sources identified in this research.

Furthermore, the work on pottery has shown that there is a strong connection between the ceramic traditions of Sicily and Malta. It will be interesting to establish how extensive was this connection and if it expands to other craft routines (e.g. lithics). Additionally, it would be beneficial to compare the *chaîne opératoire* observed in the Maltese chert assemblages with that from the assemblage found within the Licata Caduta site.

Regardless of the connections between the two islands, the evidence of seafaring on Malta is scant and it is possible that this activity was not so important to their subsistence economy. This, however, does not agree with the findings of this research. The first group of chert raw material is not local and has been found in all the investigated assemblages. Moreover, it is abundant and consistently present throughout the occupation of these sites. This provides strong indirect evidence of constant seafaring activity that was connecting the Neolithic population of Malta with other nearby regions such as Sicily. Therefore, ships or another type of sailing vessels were arriving regularly to the Maltese islands and unloading chert raw materials and artefacts.

The constant importation of this chert might also be related to the obsidian artefacts found on Malta. Initial work on the obsidian of Xagħra Circle (Malone, 2009) suggests an origin from both Lipari and Pantelleria. Previous research on Mediterranean obsidian (Williams-Thorpe, 1995; Cann and Renfrew, 1964) has revealed the extensive transfer-network, during the Neolithic, and it is likely that through that network this particular chert was arriving in Malta. However, such investigation attempts can be fruitless because obsidian and chert formations rarely coexist in the same location. It would be

more efficient to identify the places that obsidian was exported and investigate their resources. It could be through these indirect routes that chert material arrived in Malta.

The outcome of the bioarchaeological research could provide new insight into the matter of the chert network and guide a future provenancing investigation. Evidence of the recent DNA analyses and diet (isotope analyses) of the Neolithic Maltese population could provide indications of their possible connections with other areas such as Sicily. Indeed, there are indications of connections with Europe in the palaeo-anthropological studies of the Neolithic human burials from Brochtorff Circle on Gozo (Powers, R. and Thompson, J. pers. comms.). Future detailed information about the population origins of Maltese early farmers and where they received their food supplies from could directly corroborate this research on external chert sources.

6.6. Methodological remarks

The methodology employed is based on geological and petrological techniques suitable for identifying different aspects of a rock formation. Although these are not related to conventional archaeological research, they are more suitably used to source lithic materials. The techniques used in this research have found strong and solid evidence about the sources of some artefacts and provided useful information about the possible origin of other members of the assemblages. It has also provided the opportunity to test these techniques in a different research area and explore the advantages and disadvantages of each technique. The gained experience from this research will benefit future research in selecting the most suitable methodologies to achieve the proposed goals and aims on sourcing lithic assemblages.

The main characteristic of this methodology is the usage of geochemical tracers and REE patterns for the identification of sources. Although their composition and association are evaluated by ratios and statistical models, the results produced are examined and interpreted based on specific geochemical and geological theories (Luedtke, 1992; Murray, 1994). For example, the ratio of La and Ce has been used to distinguish the chert rocks based on their depositional environment. Previous geochemical research (e.g. Murray, 1994) employing this ratio has provided the theoretical background, shown its significance and the expected range of values.

Nonetheless, many provenancing studies use multivariable statistical analysis without connecting them with the necessary geological background. They do not explain the geochemical theory that led to the selection of the measured elements nor do they provide a geochemical/geological justification of their statistical results. However, a merely statistical association of elements is not sufficiently reliable for identifying the characteristics of chert sources, let alone connecting them with individual chert artefacts. The main reason is that without the appropriate explanation, a statistical connection between elements can easily be a coincident or even an error. Hence this can lead to false assumptions or confusion, and even more importantly make it impossible to pin-point the actual source, with all the implication this can have.

An important element in sourcing lithics is the requirement for a reference source to compare with the lithic artefacts being investigated. Suitable methodologies are costly, time-consuming and require great effort from the researcher to interpret the data. The results of the lithics analyses provide information about the original source rock, but without comparison, the conclusion of the research cannot go much further than simple suggestions. Therefore, potential sources to compare with are essential in order to reach strong and solid conclusions, even if the selected source does not match the lithic artefacts. Providing evidence and excluding a rock formation from the list of possible sources creates a forward momentum towards the answer of the actual source. Furthermore, it provides an internal standard of the methodology which secures the accuracy and consistency of the results. The

majority of the geological formations have been previously investigated and their characteristics are already known in the literature. Hence, unexpected results or values can be identified, and the necessary modifications can be made to minimize errors. In addition, it avoids any possible misinterpretations on findings that otherwise can be confusing and may lead to the wrong conclusions being made.

The next subject of discussion and always a debatable issue in such investigations, is the selection of the best techniques to use in source provenancing investigations. There is no right answer to this, as there are always going to be issues of availability and funding, which cannot be under-estimated. The main concern must be to select a group of techniques that provides the necessary types of results to reach the goals of the research. The types of results that every researcher needs to investigate are the macroscopic, mineralogical and elementary contexts of the lithic samples. The first should follow the baseline provided from previous researchers (Crandell, 2006; Luedtke 1992) on provenancing lithics to minimize the subjective element that it is always present in such investigations. Systematic macroscopic investigation allows the scientific grouping of the artefacts and minimizes the effort required for selecting representative samples. Nonetheless, it is a subjective technique and lack the validation to connect lithics with their sources alone.

The mineralogy of rocks is indicative of their formation process and can provide evidence of the different type of rock material. There are rock materials such as chert which are considered homogenous and dominated by one single mineral. However, this research has revealed the significant mineralogical differences between the chert of Malta and Sicily, and highlights the importance of assessing this factor. There are many techniques which can provide this information, but in this research microscopy and FTIR-ATR spectroscopy were used. There are no restrictions (no permission needed) for the examination of the raw material samples gathered from the field, and this allowed all of these techniques (Optical and SEM-EDS microscopy, FTIR-ATR spectroscopy, XRF and LA-ICP-MS) to be employed on them. Maltese chert has never been studied in the past and nothing is known about its properties. Microscopy helped to established important information about the sources and record the differences with the Sicilian sources. However, as it is a destructive technique it is highly unlikely to be employed on the artefacts recovered from secure contexts on archaeological sites.

FTIR-ATR spectroscopy is the best and the less invasive method (less than 10 μ gr sample is require) to record with great accuracy the mineralogical context of the samples. It does not give information about the fossils or the internal structure of the source, but rarely is such information necessary for sourcing lithics. Similar results can be obtained by using the XRD technique and it is more accurate than the FTIR-ATR. The disadvantage of this techniques is the requirement of powder samples of 2gr and more in size, which is a significant quantity when removed from archaeological artefact materials. In addition, the time of analyzing each sample is greater (around an hour) and this has an important impact on the overall cost of the research. It is true that FTIR-ATR is a new technique and minerals with

minor presence cannot be recorded, but again this level of precision is not necessarily required in such an investigation. Nevertheless, the comparative study of the rock sources using microscopy and FTIR-ATR has allowed the minimizing of any uncertainties or errors in this research. It is actually to the benefit of any research to include such internal comparative studies to increase the precision and accuracy of interpretation of data. The last but perhaps the most crucial point in sourcing lithic artefacts is the investigation of their elemental composition.

Although the aforementioned techniques can provide good indications on the origin of these artefacts, it is the geochemical investigation which is capable of identifying the most probable source. Geochemistry had been greatly studied in the past and many suitable techniques have been created to measure the elemental composition of many types of soil, rock or sediment (De Bruin, 1972; Murray et al. 1992; Sánchez de la Torre, 2017). The current research has chosen to use XRF and LA-ICP-MS techniques to examine the samples. XRF is a fast and non-destructive technique, yet a qualitative method with limited applications (Kempe, 1983; Luedtke, 1992). It is very useful in the field for a quick separation of materials and when the access is limited, but it is not suitable for homogeneous material, such as chert rocks. Moreover, the analysis is conducted on the surface of the samples, which as has been shown in this research, produces results that can be easily misinterpreted and lead to the wrong conclusions. Additionally, it is considered unreliable when the research is focusing on light elements such Si. In comparison, the LA-ICP-MS is highly accurate and provides the quantitative elementary profile of the samples (Speer, 2014). The concentrations of the elements are used in well-explored models to identify important aspects of the rock samples. Although such information is strictly geological, it is suggested that only materials from the same source can present similar results on specific categories (Murray et al. 1992; Murray, 1994).

Many geological research and provenancing studies have used the neutron activation analysis (NAA) as an alternative method to record the geochemical composition of samples. However, this requires a Neutron Activation reactor which is something not commonly found in research laboratories. On the contrary, most of the earth science laboratories and departments have an ICP-MS (or equivalent) that solves paperwork and administration problems. In addition, the neutron activation analysis (NAA) is much more costly and time consuming than the ICP-MS technique. Moreover, the recent addition of laser ablation (LA) has minimized the effect on the samples (powder samples are needed for ICP-MS) and actually to a lesser extent than FTIR-ATR. Furthermore, it allows the analysis of many samples within a "one run" process, which has significantly reduced the cost of using this technique.

This though has an impact on the accuracy on the collected results in comparison with the traditional bulk ICP-MS analyses. The powder samples can provide more reliable results on the actual concentration of each element than the spot analyses. Although the accuracy of a LA-ICP-MS has been exhaustively tested, it is advisable to use ratios between elements and not their actual values. The ratios between elements is not affected by the analytical technique used and through this the

possible errors on the calculated values are eliminated. Moreover, the bulk results are more representative as they are the outcome of analysing part of the sample while the spot measurements are projecting the composition of the spot-location on the sample. To minimize this uncertainty, multiple-spot analysis is performed on each sample and the final elementary composition is the average of all the spot measurements. Some investigations (Gale, 1981; Delage, 2003) have used isotope analyses as a way to source chert finds and particularly Sr isotopic analyses. This research has an initial plan to include Sr isotopes but due to laboratory difficulties this technique was abandoned. Nevertheless, this can be a supplementary technique to the ICP-MS method and cannot solely provide strong evidence on the origin of chert artefacts. The disadvantage of this technique is the requirement of powder samples (except if is equipped with a laser) and has a substantial cost. Overall, I strongly suggest that future provencing research of lithics should at a minimum include macroscopic examination, FTIR-ATR and LA-ICP-MS analyses as the prime methodological suite.

7 Conclusion

This PhD research has successfully re-examined the chert/flint assemblages found by the Cambridge Gozo project of the 1987-94 and more recently by the FRAGSUS project from the late Neolithic archaeological sites of Xagħra Circle, Ġgantija, Taċ-Ċawla, Santa Verna, Kordin and Skorba in Malta and Gozo. The selected methodological suite of techniques has identified the petrological characteristics of chert artefacts from these sites and their probable sources from the local Maltese chert formation, as well as the main possible chert sources in Sicily.

The Maltese Islands have chert outcrops on both Malta and Gozo which can sustain a robust local production of chert artefacts. The examined assemblages have a substantial number of artefacts (i.e. second group) with macroscopic similarities to the local chert sources. The laboratory investigation has shown that they are petrologically identical and has scientifically confirmed their connection. Furthermore, it has highlighted the significant differences between the Maltese and Sicilian chert sources and made clear that these two locations provide different types of chert rocks.

The petrological investigation has further confirmed the existence of a similar number of artefacts related to non-local chert sources. Moreover, it provides strong evidence for the connection between some of these artefacts and specific Sicilian sources. Indeed, artefacts from the assemblages of the Xagħra Circle and Taċ-Ċawla (i.e. third group/fourth sub-group) are shown scientifically to be connected with the chert sources of Southeast Sicily, most likely from the area of Monterosso Almo. In addition, there is strong evidence suggesting that two other artefacts (i.e. third group/fifth sub-group) from the same two sites have petrological similarities to a specific chert formation of West Sicily.

However, the success of this research is not restricted to relating artefacts with sources, but also shows the potential to disassociate artefacts scientifically from possible sources. There are artefacts from Skorba, Santa Verna and Ġgantija (i.e. third group/second subgroup) which, macroscopically, are similar to those from one formation in East Sicily. However, the geochemical data strongly suggests that they derive from a completely different source and indicates that their origin should be sought elsewhere.

The possibility of an additional source is supported by other artefacts from these same assemblages (e.g. third group/first sub-group) which do not relate on any level with the Sicilian or Maltese sources. In addition, there are a substantial number of artefacts (i.e. first group) with characteristics unfamiliar to these sources. They are found in similar proportions to the artefacts of local origin (i.e. second group) and their sources must have been easily accessible to the local population. Although a Sicilian origin is possible, the current petrological evidence has not provided a suitable source candidate. Therefore, it is highly likely that at least one more location exists, from which chert material has also been imported to Malta.

The type of tools and manufacturing techniques observed, provide further understanding of the conditions under which these assemblages have been formed. The local material includes a variety of flakes, debitage, debris and pieces of cortex which indicate a local manufacture. The chert material related to the first group presents a variety, in shape and size, of objective pieces, debitage and also rejuvenation flakes, confirming that raw materials from both chert types reached the investigated Neolithic sites. Moreover, this evidence provides proof that the beginning of the manufacturing *chaîne opératoire* related to these materials, was placed at or near these sites. Although this is expected for the local material, it is certainly a surprise for the other type of chert which is imported to the Maltese Islands and further confirms the convenient access the Maltese people must have had to this type of chert.

Furthermore, the *chaîne opératoire* recorded on both these chert materials is similar (i.e. techniques and products) which is additional evidence of their exploitation by Maltese craftsmen. There are techniques (e.g. pressure flaking) and types of artefacts/tools (e.g. scrapers) related only with the foreign material, but it is not clear if this is related to the different properties of the chert rock or a cultural choice. There are other techniques (e.g. Levallois technique) recorded on both materials, but on the local chert these are in the simplest form and not as elaborate as on the imported chert. Although similar *chaîne opératoire* has been reported in the assemblages of all the sites, Ġgantija and the Xagħra Circle have presented techniques and special artefact features not recorded elsewhere. There must be a connection between these findings and their position in the Neolithic timeframe of the Maltese Islands, but further investigation is necessary on this matter. Nevertheless, the findings from these two groups of chert material confirm the existence of a locally employed *chaîne opératoire* which is recorded at all the investigated Neolithic sites of the Maltese Islands.

The situation is completely different regarding the third group of chert material reported from these sites. It includes a very small proportion of the assemblages and consists mainly of small artefacts or fragments of them. There is a total absence of objective pieces (pre-prepared) and this makes it highly unlikely that such raw material was imported to these islands in this form. This strongly suggests a restriction of access to these chert sources and that they were possibly of great value. The importance of these artefacts is highlighted from the evidence of constant retouching, which amongst other reasons may have been intended to extend their utility. Their small size, and the absence of objective pieces, are strong indications that they arrived in the form of finished tools/artefacts. This further confirms the interaction with a neighbouring society and/or possibly cultural influences through a different *chaîne opératoire*. However, the small size of these finds does not allow a thorough investigation of the techniques employed and the extent of influence and interaction are difficult to define.

Nevertheless, the artefacts of the third group have been used by the local population and most likely they have been the instruments of the local craftsmen used to create other tools/artefacts. This

is explained by the many artefact fragments of this group which may have resulted during the manufacturing procedure. Use as tools to employ their local techniques confirms the ability of local people able to understand and assess the rock 'quality' of the different chert materials available. Furthermore, this present strong evidence that the Neolithic Maltese communities had been deliberately sourcing raw stone material for specific purposes.

Finally, this research has used a scientific methodology suite for sourcing lithic artefacts which can provide conclusive evidence of exploitation sources. The multiple applied techniques are suitable for producing reliable results for sourcing chert assemblages as each method approaches a different, yet related, quality of the rock. Together, they provide detailed information on the macroscopic, microscopic and geochemical characteristics of the chert sources and lithic artefacts. Having been assessed in tandem, these provide evidence to robustly match chert artefacts with their original sources. Although destructive analysis techniques are more accurate and reliable, these are best employed on the non-archaeological material (i.e. source samples), in the role of an internal standard for the methodology. The many non-destructive and accurate techniques available can be used to minimize the impact on the archaeological artefacts themselves. This research strongly supports the inclusion in any future lithic sourcing research of the macroscopic, FTIRS and LA-ICP-MS techniques. A possible addition to these would be the Strontium Isotopic analyses (Gale, 1981; Delage, 2003) which in combination with the REE results can provide a strong indicator of what is called "fingerprint" of the chert source. The procedure I would advise future researchers to follow would be to start with the macroscopic examination of the potential source and the chert finds. It gives a first contact with the material under investigation and the possible sub-categories present. This should be followed by the FTIRS analyses to identify possible mineralogical differences, and then focus on the elementary profile with the contribution of the LA-ICP-MS and Sr isotopic analyses. They will provide with great accuracy which potential sources were exploited or not, and match chert artefacts with their original sources.

This was the first comprehensive, and on a substantial scale, attempt to source chert artefacts from the late Neolithic period of Malta. The results will certainly contribute to a better understanding of these communities on many levels, but there is an important work still to be done that goes beyond the frame of this PhD research. The next step will be to investigate the proportions of the three main chert groups across time and space. Having defined these groups, it will be useful to return to these assemblages and investigate the ratio of these materials found at each site and the variation between the investigated sites. This could not be done during this investigation, because it was first necessary to identify conclusively these three groups of cherts. It will be equally important and interesting to examine how the proportions and the type of material change over time within the sites. This chronological cross-examination will be possible through collaboration with the excavators. The recent work at Skorba, for instance, has been conducted in such a way that the finds are stratigraphically correlated and therefore chronologically secure in archaeological terms although some residuality of

chert from earlier periods cannot be completely excluded. The radiocarbon and OSL data from the contexts will provide a highly reliable chronological sequence and make it possible for future research to cover this gap in my research. Further insight into provenancing of the lithic assemblages from late Neolithic Malta will be a cross-examination between the material of current investigated sites with other Neolithic sites on the Maltese Islands. This, however, will be a time-consuming study and considering the number of sites and finds, possibly a task for many research projects. In addition, the investigation on the *chaîne opératoire* related to these assemblages would be another extensive but significant task. The current research has only 'scratched the surface' of the potential information potentially available and a more elaborate study is necessary to fully identify the series of actions followed within the manufacturing process. After the interesting initial findings of this thesis, future full-scale research will certainly provide a better understanding of the craft traditions employed on Maltese Islands during the late Neolithic.

8 Bibliography

- Adachi, M. Yamamoto, K. and Sugisakih R. 1986. Hydrothermal chert and associated siliceous rocks from the northern pacific: Their geological significance as indication of ocean ridge activity. *Sedimentary Geology*, 47, pp. 125-148.
- Abela, G., F. 1647. Della Descrittione di Malta. Isola nel Mare Siciliano, con le sue Antichità ed altre notizie. Malta: P. Bonacota.
- Alexander, D. 1988. A review of the physical geography of Malta and its significance for tectonic geomorphology. *Quaternary Science Reviews* 7, 41-53.
- Ammerman, A., Cesana, A., Polglase, C. & Terrani, M. 1990. Neutron activation analysis of obsidian from two neolithic sites in Italy. *Journal of Archaeological Science* 17, 209–220.
- Ammerman, A. & Polglase, C. 1993. The exchange of obsidian at Neolithic sites in Italy. In (F. Healy & C. Scarre, Eds) *Trade and Exchange in European Prehistory*. Oxford: Oxbow, Monograph 33, pp. 101–107.
- Ammerman, A. & Polglase, C. 1997. Analyses and descriptions of the obsidian collections from Arene Candide. *Quaternaria Nova*, in press.
- Amodio Morelli, L., G. Bonardi, V. Colonna, D. Dietrich, G. Giunta, F. Ippolito, V. Liguori, S. Lorenzoni, A. Paglionico, V. Perrone, G. Piccarreta, M. Russo, P. Scandone, Zanettin Lorenzoni and A. Zuppetta 1976. L'arco Calabro-Peloritano nell'orogene Appenninico-Maghrebide. *Mem. Soc. Geol. It.*, v. 17, p. 1–60.
- Andreeva, P., Stefanova, E., Gurova, M., 2014. Chert raw materials and artefacts from NE Bulgaria: A combined petrographic and LA-ICP-MS study. *Journal of Lithic Studies* vol.1, n. 2, p. 25-45.
- Andrefsky, W., Jr. 2005. *Lithics: Macroscopic Approaches to Analysis*. Second Edition. Cambridge: Cambridge University Press.
- Apel, J. 2001. *Daggers, Knowledge and Power. The Social Aspects of FlintDagger Technology in Scandinavia 2350–1500 cal BC*. Uppsala.
- Ashby, T., Bradley, R. N., Peet, T. E. & Tagliaferro, N. 1913. Excavations in 1908-11 in various megalithic buildings in Malta and Gozo. *Papers of the British School at Rome* 6 (1): 1-126.
- Ashby, T. & Zammit, T. 1916. Excavations in Malta in 1914. *Man* 16: 1-6.
- Attard-Montalto, N., Shortland, A., Rogers, K. 2012. The Provenancing of Ochres from the Neolithic Temple Period in Malta. *Journal of Archaeological Science* 39(4), pp. 1094-1102.
- Attard Tabone, J. 1999. The Gozo circle rediscovered. In Mifsud, A. & Savona Ventura, C. (eds.) *Facets of Maltese prehistory*. Malta: Prehistoric Society, 169-81.
- Ballin, T. B. 2000. Classification and Description of lithic artefacts: A discussion of the Basic lithic terminology. *Lithics* 21, 9-15.
- Bates, R., L., Jackson, J., A. (ed.). 1980. *Glossary of geology*. 2nd edn. American Geological Institute, Falls Church, Va.
- Bar-Yosef, Ofer and Philip Van Peer. 2009. The Chaine Operatoire Approach in Middle Paleolithic archaeology. *Current Anthropology* 50(1): 103-131.

- Barone, G. Gulli, D. Mazzoleni, P. Raneri, S. Tanasi, D. 2011. Archaeometric identification of Maltese imports in prehistoric Sicily: Żebbuġ phase pottery from Licata Caduta (Agrigento). *Malta Archaeological Review*, v. 10, p. 23-30
- Becker, C. J. 1952. Die nordschwedischen Flintdepots. *Acta Archaeologica* XXIII, pp. 65–79.
- Bianchi, F., Carbone, S., Grasso, M., Invernizzi, G., Lentini, F., Longaretti, G., Merlini, S. & Mostardini, F. 1989. Sicilia orientale: pro. lo geologico Nebrodi-Iblei. — *Mem. Soc. Geol. It.* 38: 429-458.
- Bigazzi, G., Meloni, S., Oddone, M., G. Radi, G. 1986. Provenance Studies of Obsidian Artifacts: Trace Elements Analysis and Data Reduction. *Journal of Radioanalytical and Nuclear Chemistry, Articles* 98/2, 353-363.
- Biró, K. 1986. Sources of raw materials used for the manufacture of chipped stone implements in Hungary. In: Sieveking and Hart ed.: *The Scientific Study of Flint and Chert*. Cambridge, 121-133.
- Biró, K. 1992. Lithotheca - an effective help for provenance studies. *Acta Archaeologica Carpathica* 31, 179-184.
- Biró, K., Dobosi, K-T., V. 1991. LITOTHECA- Comparative Raw Material Collection of the Hungarian National Museum. Budapest.
- Blades, B., Adams, B. 2009. *Lithic Materials and Paleolithic Societies*, 1st edition. Blackwell Publishing.
- Bleed, Peter 2001. Trees or chains, links or branches: Conceptual alternatives for consideration of stone tool production and other sequential activities. *Journal of Archaeological Method and Theory* 8(1): 101-127.
- Boggs, S., 2009. *Petrology of Sedimentary Rocks*, Second Edition. Cambridge University Press, 612p.
- Briois, F. 2005. Les industries de pierre taillée néolithiques en Languedoc Occidental. Vol. 20, *Monographies d'Archéologie Méditerranéenne*. Lattes.
- Brothwell, D., Higgs, E. 1969. *Science in Archaeology: A Survey of Progress and Research*. Second Edition, Thames and Hudson.
- Brothwell, D., Higgs, E. (ed.). 1963. *Science and archaeology*. Thames and Hudson, London.
- Bruggencate, Rachel E., Milne, S. B., Fayek, M., Park, R. W., Stenton, D. R., Hamilton, A. C. 2016. "Characterizing southern Baffin Island chert: A cautionary tale for provenance research." *Journal of Archaeological Science: Reports*.
- Bruker AXS, Inc, 2010. *Tracer Series User Guide*. USA. Website: www.bruker.com
- Bustillo, M. A. et al., 2009. Is the Macroscopic Classification of Flint Useful? A Petroarchaeological Analysis and Characterization of Flint raw material from the Iberian Neolithic mine of Casa Montero. *Archaeometry* 51, Vol. 2 pp 175–196.
- Cann, J.R., Renfrew, C. 1964. The characterization of obsidian and its application to the Mediterranean Region. *Proceedings of the Prehistoric Society*, XXXX: 111.
- Carbone, S., S. Catalano, M. Grasso, F. Lentini and C. Monaco 1990. *Carta geologica della Sicilia centro-orientale*. Scala 1:50.000. S.El.Ca., Firenze.
- Carbone, S., M. Grasso and F. Lentini 1986. *Carta Geologica del settore Nord-Orientale Ibleo*, scala 1:50.000, S.El.Ca., Firenze.

- Carbone, S., M. Grasso and F. Lentini 1984. Carta Geologica della Sicilia Sud-Orientale, scala 1:100.000, S. El. Ca, Firenze.
- Catalano, R. 2004. Geology of Sicily: an introduction. Bocconeia 17. Palermo, Italy.
- Catalano, R. & D'Argenio, B. 1978. An essay of palinspastic restoration across the western Sicily. *Geol. Romana* 17, pp. 145-159.
- Catalano, R., D'Argenio, B. 1982. Schema geologico della Sicilia. In: R. Catalano & B. D'Argenio (Eds.), Guida alla geologia della Sicilia occidentale. Soc. Geol. It., Palermo.
- Catalano, R., A. Franchino, S. Merlini and A. Sulli 2000. Central western Sicily structural setting interpreted from seismic reflection profiles. *Mem. Soc. Geol. It.*, v. 55, p. 5–16.
- Catalano, R., Torelli, L. 1989. From Sardinia Channel to Sicily Strait. A geologic section based on seismic and eld data. In: *The Lithosphere in Italy*. Acc. Naz. Lincei, Atti Convegni Lince 80, pp. 109-127.
- Catling, H. W. 1963. Minoan and Mycenaean pottery: composition and provenance. *Archaeometry* 6, p. 1-9.
- Caspar, J.-P. (1984). Matériaux lithiques de la préhistoire. In D. Cahen & P. Haesaerts (Eds.), *Peuples chasseurs de la Belgique préhistorique dans leur cadre naturel* (pp. 107–114). Brussels: Patrimoine de l'Institut royal des Sciences naturelles de Belgique.
- Cazzella, A. and Moscoloni, M. 2005. Gli sviluppi culturali del III e II millennio a.C. a Tas-Silg. *Scienze dell' Antichità* 12, p. 15-32.
- Clough, T., H. and Cummins W., A. 1979, Stone axe studies: Archaeological, petrological, experimental and ethnographic. Research report No 23. Council for British Archaeology.
- C.N.R. 1991. Structural model of Italy, sheet n. 6, scale 1:500.000. Publ. P.F. Geodinamica, Dir. F. Barberi, S. El. Ca, Firenze.
- He, C. Ji, L. Wu, Y. Su, A. and Zhang, M. 2016. Characteristics of hydrothermal sedimentation process in the Yanchang Formation, south Ordos Basin, China: Evidence from element geochemistry. *Sedimentary Geology* 345, p33–41.
- Cooke, J. H. 1891. Notes on the 'Pleistocene Beds' of Gozo. *Geol. Mag.* n.28, pp.348-55.
- Cooke, J. H. 1893a. The marls and clays of the Maltese Islands. *Q. Jl geol. Soc. Lond.* n. 49, pp.117-28.
- Cooke, J. H. 1893b. On the occurrence of concretionary masses of flint and chert in the Maltese limestones. *Geo/Mag.*, n.30, pp.157-60.
- Cooke, J. H. 1896a. Notes on the Globigerina Limestone of the Maltese Islands. *Geo. Mag.* n.33, pp.502-11.
- Cooke, J. H. 1896b. Notes on the 'Pleistocene Beds' of the Maltese Islands. *Geo. Mag.* n.32, pp. 201-10.
- Cooke, J. H. 1896. Contributions to the stratigraphy and palaeontology of the Globigerina Limestones of the Maltese Islands. *Q. Jl geol. Soc. Lond.* n. 52, pp.461-2.
- Cooney, G., and Mandai, S. (1998). The Irish Stone Axe Project, Monograph 7, Wordwell Bay.
- Costopoulos, A. 2003. Prehistoric flint provenance in Finland: reanalysis of Southern data and initial results for the North. *Fennoscandia archaeologica* XX, pp. 41–54.

- Cotterell, B., Kamminga, J., 1987. The formation of flakes. *American Antiquity* 52, p. 675-708.
- Crandell, O. 2006. "Macroscopic and Microscopic Analysis of Chert; A Proposal for Standardization of Methodology and Terminology", B.C.S.S., vol 12, Alba Iulia, Romania.
- Cresswell, R. 1983. Transfers de techniques et chaînes opératoires. *Techniques et Cultures* 2, 143–163.
- Cresswell, R. 1993. Tendances et faits, logique et histoire. *Techniques et Culture* 21, 37–59.
- Crew, H. 1975. An evaluation of the relationship between the Mousterian complexes of the eastern Mediterranean: A technological approach. In *Problems in prehistory: North Africa and the Levant*, ed. F. Wendorf and A. E. Marks, 427–437. Dallas: SMU Press.
- Daesslé, L. W. and Cronan D.S. 2001. Hydrothermal input in recent sediments proximal to the Eastern Lau Spreading Centre, Lau Basin, SW Pacific. *Ciencias Marinas*, 27(1), pp. 635–659.
- Danelian T., Tsikos H., Gardin S., Baudin F., Bellier J. P. and Emmanuel L. 2004. Global and regional palaeoceanographic changes as recorded in the mid-Cretaceous (Aptian–Albian) sequence of the Ionian Zone (northwestern Greece). *Journal of the Geological Society*, 161/4, 703-709.
- Dart, C. J. Bosence, D. W. J. and K. R. McClay, K. R. 1993. Stratigraphy and structure of the Maltese graben system. *Journal of the Geological Society*, 150, 1153-1166.
- Delage, C. 2003. *Siliceous Rocks and Prehistory: Bibliography on Geo-Archaeological Approaches to Chert Sourcing and Prehistoric Exploitation*. Oxford: John and Erica Hedges. (BAR International Series, 1168).
- Delage, C. 2007. *Chert availability and prehistoric exploitation in the Near East: An Introduction*. Oxford: John and Erica Hedges.
- Del Ben, A. and P. Guarnieri 2000. Neogene Transpression in the Cefalù Basin (Southern Tyrrhenian): comparison between land and marine data. *Mem. Soc. Geol. It.*, v. 55, p. 27–33.
- De Bruin, M., Korthoven, P., J., M., Bakels, C., C., Groen, F., C., A. 1972. The use of non – destructive activation analysis and pattern recognition in the study of Flint artefacts.
- Di Stefano, P. Vitale, F. 1992. *Carta Geologica dei Monti Sicani Occidentali*. University of Palermo. IGMI.
- Di Stefano, P. et al. 2013. *Carta Geologica D' Italia*. Sabta Margherita di Belice, Foglio 619. IGMI.
- Dixon, J. E. (1976). Obsidian characterization studies in the Mediterranean and Near East. In (R. E. Taylor, Ed.) *Advances in Obsidian Glass Studies*. Park Ridge, NJ: Noyes Press, pp. 288-333.
- Dugdale, W. 1656. *The antiquities of Warwickshire*. Thomas Warren, London.
- Ekshtain, R., Malinsky-Buller, A., Ilani, S., Segal, I., Hovers, E. 2014. "Raw material exploitation around the Middle Paleolithic site of 'Ein Qashish." *Quaternary International* 331:248–66.
- Ellenberg, L. 1983. Die kusten von Gozo. *Essener Geographische Arbeiten* 6, 129-160.
- English Heritage. 2004. *Geoarchaeology. Using Earth Sciences to Understand the Archaeological Record*.ard
- Evans, J., D. 1953. The prehistoric Culture–Sequence in the Maltese Archipelago. *Proceedings of the Prehistoric Society*, pp.41 – 95. Malta.
- Evans, J., D. 1959. *Malta*. Thames and Hudson publications. London.

- Evans, J., D. 1971. *The Prehistoric Antiquities of the Maltese Islands: a Survey*. The Athlone Press, University of London.
- Farell et al. in press. Holocene vegetation history of the Maltese Islands
- Felix, R. 1973. Oligo-Miocene stratigraphy of Malta and Gozo. Doctoral thesis University of Utrecht, pp. 104.
- Fenech, K. 2007. Human-induced changes in the environment and landscape of the Maltese Islands from the Neolithic to the 15th century AD as inferred from a scientific study of sediments from Marsa, Malta. *British Archaeological Reports, International Series 1692*. Oxford: Archaeopress.
- Finetti, I., R., et al. 2005. Geological Outline of Sicily and Lithospheric Tectono-Dynamics of its Tyrrhenian Margin from New CROP Seismic Data. CROP PROJECT: Deep Seismic Exploration of the Central Mediterranean and Italy. Ch. 15, pp. 319.
- Finetti, I.R., F. Lentini, S. Carbone, S. Catalano and A. Del Ben. 1996. Il Sistema Appennino Meridionale–Arco Calabro–Sicilia nel Mediterraneo centrale: studio geologico-geofisico. *Boll. Soc. Geol. It.*, v. 115, p. 529–559.
- Fish, P. 1979. The interpretive potential of Mousterian debitage. *Anthropological Research Papers 16*. Tempe: Arizona State University.
- Foglini, F., Prampolini, M., Micallef, A., Angeletti, L., Vanfdelli, L., Deidum, A. & Taviani, M. 2016. Late Quaternary coastal landscape morphology and evolution of the Maltese Islands (Mediterranean Sea) reconstructed from high-resolution seafloor data, in Harff, J., Bailey, G. & Luth, F. (eds.) *Geology and archaeology: Submerged landscapes of the continental shelf*, pp.77-95. London: Geological Society Special Publication 411.
- Forster, N., Grave, P. 2012. Non-destructive pXRF analysis of museum-curated obsidian from the Near East. *Journal of Archaeological Science* 39, p. 728-736.
- Foucher, P. 2004. “Les industries lithiques du complexe Gravettien-Solutréen dans les Pyrénées.” Université de Toulouse.
- Francaviglia, V. 1984. Characterization of Mediterranean obsidian sources by classical petrochemical methods. *Preistoria Alpina - Museo Tridentino di Scienze Naturali*, Vol. 20, p. 311-332.
- Freller, T. 2013. *The Observing Eye. The French artist Jean Houel in Malta*. Malta: Midsea Books.
- Furlani, S., Antonioli, F., Biolchi, S., Gambin, T., Gauci, R., Lo Priesti, V., Anzidei, M., Devoto, S., Palombo, M. & Sulli, A. 2013. Holocene sea level change in Malta. *Quaternary International* 288, 146-157.
- Gabel, C. 1965. *Stone Age hunters of the Kafue. The Gwisho a site*. Boston University Press.
- Gale, N.H., 1981. Mediterranean Obsidian Source Characterisation by Strontium isotope analysis, *Archaeometry*, 23, 1,41-51.
- Galea, P. 2019. Central Mediterranean Tectonics – A Key player in the geomorphology of the Maltese Islands. pp.19-30. In: R. Gauci and J. A. Schembri (eds.) *Landscapes and Landforms of the Maltese Islands [World Geomorphological Landscapes]*. Springer Nature, Switzerland.
- Galea, P. 2007. Seismic history of the Maltese Islands and considerations on seismic risk. *Annals of Geophysics* 50(6): 725–740.

- Garbán, G. Martínez, M. Márquez, G. Rey, O. Escobar M. Esquinas, N. 2017. Geochemical signatures of bedded cherts of the upper La Luna Formation in Táchira State, western Venezuela: Assessing material provenance and paleodepositional setting. *Sedimentary Geology* 347, 130-147.
- Gardiner, W., Grasso, M. & Sedgeley, D. 1995. Plio-Pleistocene fault movement as evidence for mega-block kinematics within the Hyblean-Malta Plateau, central Mediterranean. *Journal of Geodynamics* 19, 35-51.
- Geneste, J.-M. 1985. Analyse lithique d'industries Mouste'riennes du Pe'rigord: Une approche technologique du comportement des groupes humaines au Pale'olithique Moyen. PhD diss., Universite' de Bordeaux.
- Ghisetti, F. and L. Vezzani 1984. Thin-skinned deformations of the western Sicily thrust belt and relationships with crustal shortening: Mesostructural data on the Mt. Kumeta-Alcantara Fault Zone and related structures. *Boll. Soc. Geol. It.*, v. 103, p. 129–157.
- Gijn A.L. van. 2010. *Flint in Focus: Lithic Biographies in the Neolithic and Bronze Age*. Leiden, Sidestone Press.
- Giunta, G. and V. Liguori 1973. Evoluzione paleotettonica della Sicilia. *Boll. Soc. Geol. It.*, v. 92, p. 903–924.
- Gonzalez, J., L. et al., 2014. Characteristics and Genesis of el Sauz chert, an important prehistoric lithic resource in south Texas. *Lithic Technology*, Vol. 39 No. 3, pp. 151 – 161.
- Goodyear, Albert C. 1979. A Hypothesis for the Use of Cryptocrystalline Raw Materials Among Paleo-Indian Groups of North America. Research Manuscript Series. Book 127.
- Grégoire, S. 2000. "Origine des matières premières des industries lithiques du Paléolithique pyrénéen et méditerranéen. Contribution à la connaissance des aires de circulations humaines." Université de Perpignan.
- Grasso M. and F. Lentini 1982. Sedimentary and tectonic evolution of the Eastern Hyblean Plateau (South-eastern Sicily) during Late Cretaceous to Quaternary time. *Palaeog. Palaeocl. Palaeoecol.*, v. 39, p. 261–280.
- Grima, R. 2004. *The Archaeological Drawings of Charles Fredrick de Brocktorff*. Malta: Midsea Books Ltd and Heritage Malta.
- Guarnieri, P., S. Carbone and A. Di Stefano 2002. The Sicilian orogenic belt: a critical tapered wedge?. *Boll. Soc. Geol. It.*, v. 121, p. 221–230.
- Guilcher, A. & Paskoff, R. 1975. Remarques sur la geomorphologie littorale de l'archipel maltais. *Bulletin de l'Association Geographique de France* 427, 225-231.
- Guiliano, M. Asia, L. Onoratini, G. Mille, G. 2007. Applications of diamond crystal ATR FTIR spectroscopy to the characterization of ambers. *Spectrochimica Acta Part A*, 67, pp. 1407–1411.
- Gurova, M., Andreeva, P., Stefanova, E., Stefanov, Y., Kočić, M., Borić, D. 2016. "Flint raw material transfers in the prehistoric Lower Danube Basin: An integrated analytical approach." *Journal of Archaeological Science: Reports* 5:422–41.
- Hall, E. T. (1960) X-ray fluorescent analysis applied to archaeology. *Archaeometry* 3, 29-35.
- Harbottle, G. (1970). Neutron activation analysis of potsherds from Knossos and Mycenae. *Archaeometry* 12, 23-34.

- Harff, J., Bailey, G. & Luth, F. (eds.) 2016. *Geology and archaeology: Submerged landscapes of the continental shelf*. London: Geological Society Special Publications.
- Hassler, Emily R., George H. Swihart, David H. Dye, and Ying Sing Li. 2013. "Non-destructive provenance study of chert using infrared reflectance microspectroscopy." *Journal of Archaeological Science* 40 (4):2001–6.
- Hawkins, A. L., E. Tourigny, D. G. F. Long, P. J. Julig, and J. Bursley. 2008. "Fourier Transform Infrared Spectroscopy of Geological and Archaeological Chert from southern Ontario." *North American Archaeologist* 29 (3–4):203–24.
- Hermes, O. D., and Ritchie, D. (1997a). Application of pétrographie and geochemical methods to sourcing felsitic archaeological materials in southeastern New England. *Geoarchaeology* 12: 1- 30.
- Hess, C., H. 1996. Chert Provenance Analysis at the Mack Canyon Site, Sherman County, Oregon: An Evaluative Study. *Geoarchaeology: An International Journal*, Vol. 11, No. 1, p. 51-81.
- Higashimura, T., Warashina, T. 1975. Sourcing of Sanukite Stone Implements by X-ray Fluorescence Analysis. *Journal of Archaeological Science* 2, 169-178.
- Hobbs, W. H. 1914. *The Maltese Islands: a tectonic-topographic study*. Scott. Geogr. Mag. n.30, pp. 1-13.
- Hofman, J. L., Todd, L. W, and Collins, M. B. 1991. Identification of central Texas Edwards chert at the Folsom and Lindenmeier sites. *Plains Anthropologist* 36, p. 297-308.
- Högberg, A. 2002. Production Sites on the Beach Ridge of Järavallen. *Aspects of Tool Preforms, Action, Technology, Ritual and the Continuity of Place*. *Current Swedish Archaeology* 10(2002), pp. 137–162.
- Hogberg, A., D. Olausson, and R. Hughes. 2012. "Many Different Types of Scandinavian Flint – Visual Classification and Energy Dispersive X-ray Fluorescence." *Fornvannen-Journal of Swedish Antiquarian Research* 107 (4): 225–40.
- Houel, J. P. L. L. 1782-87. *Voyage pittoresque des isles de Sicile : de Malte et de Lipari, où l'on traite des antiquités qui s'y trouvent encore; des principaux phénomènes que la nature y offre; du costume des habitans, & de quelques usages*. Paris: Imprimerie de Monsieur.
- Hughes, R., E., Högberg, A., Olausson, D. 2010. Sourcing flint from Sweden and Denmark, A pilot study employing non-destructive energy dispersive X-ray fluorescence spectrometry. *Journal of Nordic Archaeological Science* 17, pp. 15–25.
- Hunt, C.O. 1997. Quaternary deposits in Maltese Islands: A microcosm of environmental change in Mediterranean lands. *Geo-Journal* 41 (2), 101-109.
- Hyde, H.P.T. 1955. *Geology of the Maltese Islands*. Malta.
- Inizan M.-L., M. Reduron-Ballinger, G. Roche, and J. Tixier. 1999. *Pré-histoire de la Pierre Taille'e*. Vol. 4. *Technologie de la Pierre Taille'e*. Meudon: CREP.
- Jelinek, A. J. 1991. Observations on reduction patterns and raw materials in some Middle Paleolithic industries in the Perigord. In *Raw material economies among prehistoric hunter-gatherers*, ed. A. Montet-White and S. Holen, 7–32. *Publications in Anthropology* 19. Lawrence: University of Kansas Press.

- Joyce, A., Elam, M., J., Glascock, M., D., Neff, H. and Winter, M. 1995. Exchange Implications of Obsidian Source Analysis from the Lower Rio Verde Valley, Oaxaca, Mexico. *Latin American Antiquity*, Vol. 6, No. 1, pp. 3-15.
- Junguo, H., Yongzhang Z., Hongzhong, Li. 2011. Study on Geochemical Characteristics and Depositional Environment of Pengcuolin Chert, Southern Tibet. *Journal of Geography and Geology*. Vol. 3, No. 1
- Kelly, R. L. (1985). Hunter-Gatherer Mobility and Sedentism: A Great Basin Study, Ph.D. Dissertation, Department of Anthropology, University of Michigan, USA.
- Kempe, D.R.C., & Harvey, A., P. 1983. *The petrology of Archaeological artefacts*. Clarendon press, Oxford.
- Kerry, K. W., and D. O. Henry. 2000. Conceptual domains, competence, and chaîne opératoire in the Levantine Mousterian. In *The archaeology of Jordan and beyond: Essays in honor of James A. Sauer*, ed. L. E. Stager, J. A. Greene, and M. D. Coogan, 238–254. Winona Lake, IN: Eisenbrauns.
- KeyMaster Technologies, Inc. 2001. *pXRF Spectrum Analysis Tools for the TRACER*. USA
- Knutsson, K. 1988. Making and using stone tools. AUN 11. Uppsala.
- Kowta, M. 1980. *Recognizing Artifacts*. California Department of Forestry and Fire Protection. USA.
- Koztowski, J., K. 1973. The Origin of Lithic Raw Materials Used in the Palaeolithic of the Carpathian Countries. *Acta Archaeologica Carpatha*, p. 135-19.
- Lanning, E. 1970. Pleistocene Man in South America. *World Archaeology*, Vol. 2, No. 1, pp. 90-111.
- Larson, M. L. (1994). Toward a holistic analysis of chipped stone assemblages. In Carr, P. (ed.), *The Organization of North American Prehistoric Chipped Stone Technologies*, International Monographs in Prehistory, Ann Arbor, MI, pp. 57-67.
- Latham, T. S., Sutton, P. A., and Verosub, K. L. 1992. Non-destructive XRF characterization of basaltic artifacts from Truckee, California. *Geoarchaeology* 7, p.81-101.
- Lentini F. 2000. *Carta Geologica della Provincia di Messina, scala 1:50.000, 3 fogli*. S.El.Ca., Firenze.
- Lentini, F. 1984. *Carta Geologica della Sicilia Sub-orientale. Dai tipi dell'istituto Geografico Militare*. Istituto di scienze della terra. University of Catania, Sicily, Italy.
- Lentini, F., Carbone, S., & Catalano, S. 1994. Main structural domains of the central mediterranean region and their Neogene tectonic evolution. *Bollettino di Geofisica Teorica e Applicata*, 36, 141-144.
- Lentini, F., Carbone, S., Catalano, S. 1995. Main structural domains of the central Mediterranean region and their Neogene tectonic evolution. *Boll. Geofis. Teor. Appl.* 36, n. 141-144.
- Lentini, F., S. Carbone, S. Catalano and M. Grasso 1996a. Elementi per la ricostruzione del quadro strutturale della Sicilia Orientale. *Mem. Soc. Geol. It.*, v. 51, p. 179–195, 1 carta geol.
- Lentini, F., S. Catalano and S. Carbone 1996b. The External Thrust System in Southern Italy: a target for petroleum exploration. *Petrol. Geosci.*, v. 2, p. 333–342.
- Leroi-Gourhan, A. 1964. *Le geste et la parole: Technique et langage*. Paris: Éditions Albin Michel.
- Lickorish, H., M. Grasso, R.W.H. Butler, A. Argnani and R. Maniscalco 1999. Structural styles and regional tectonic setting of the “Gela Nappe” and frontal part of the Maghrebian thrust belt in Sicily. *Tectonics*, v. 18, p. 655–668.

- Luedtke, B. 1978. Chert Sources and Trace-Element Analysis. *American Antiquity*, Vol. 43, No. 3, pp. 413-423.
- Luedtke, B. 1979. The Identification of Sources of Chert Artifacts. *American Antiquity*, Vol. 44, No. 4, pp. 744-757.
- Luedtke, B. 1992. An archaeologist's guide to chert and flint. *Archaeological Research Tools 7*, Los Angeles: Institute of Archaeology, University of California.
- Maliva, R.G. Knoll, A. H. Simonson, B. M. 2005. Secular change in the Precambrian silica cycle: Insights from chert petrology. *Geol. Soc. Am. Bull.*, 117, pp. 835-845.
- Malone, C., Stoddart, S., Bonanno, A., Trump, D., with Gouder, T. and Pace A. (editors). 2009. Mortuary customs in prehistoric Malta. Excavations at the Brochtorff Circle at Xagħra (1987-1994), McDonald Institute, Cambridge.
- Malyk-Selivanova, N., Ashley, G., M., Gal, R., Glascock, M., D. and Neff, H. 1998. Geological–Geochemical Approach to “Sourcing” of Prehistoric Chert Artifacts, Northwestern Alaska. *Geoarchaeology: An International Journal*, Vol. 13, No. 7, p. 673–708.
- Masuda, H., S., A. 1977. Cerium in chert as an indication of marine environment of its formation. *Nature* Vol. 266, pp. 346.
- Matiskainen, H., Vuorinen, A. & Burman, O. 1989. The Provenance of Prehistoric Flint in Finland. In Y. Maniatis (ed.): *Archaeometry: Proceedings of the 25th International Symposium*, pp. 625–643. Amsterdam.
- Mayr, A. 1901. Die vorgeschichtlichen Denkmäler von Malta. *Abhandlungen der k. bayer. Akademie der Wissenschaft, I Cl., XXI Bd. III Abth.*
- McDonnell, R. D., Kars, H., and Jansen, J. B. H. (1997). Petrography and geochemistry of flint from six Neolithic sources in southern Limburg (The Netherlands) and northern Belgium. In Ramos- Millan, A., and Bustillo, M. A. (eds.), *Siliceous Rocks and Culture*, Editorial Universidad de Granada, Granada, Spain, pp. 37.
- Meignen, L. 1995. Levallois lithic production systems in the Middle Paleolithic of the Near East: The case of the unidirectional method. In *The definition and interpretation of Levallois technology*, ed. H. Dibble and O. Bar-Yosef, 361–380. *Monographs in World Archaeology 23*. Madison, WI: Prehistory Press.
- Merrick, H., V., Brown, F., H. 1984. Obsidian sources and patterns of source utilization in Kenya and northern Tanzania: some initial findings. *African Archaeological Review*, Volume 2, Issue 1, pp 129–152.
- Micallef, A., Foglini, F., Bas, L., Angeletti, L., Maselli, V., Pasuto, A. & Taviani, M. 2013. The submerged paleo-landscape of the Maltese Islands: Morphology evolution and relation to Quaternary environment change. *Marine Geology* 335, 129-147.
- Milne, S. B., Hamilton, A., Fayek, M. 2009. “Combining Visual and Geochemical Analyses to Source Chert on Southern Baffin Island, Arctic Canada.” *Geoarchaeology International Journal* 24 (4): 429–49.
- Moholy-Nagy, H., and Nelson, F., W. 1990. New data on sources of obsidian artifacts from Tikal, Guatemala. *Ancient Mesoamerica* 1, p. 71-80.

- Moroni, B., Petrelli, M. 2005. Geochemical Characterization of flint artifacts by Inductively Couple Plasma Mass Spectrometry with Laser sampling (LA – ICM – MS): Results and Prospects. *Mediterranean Archaeology and Archaeometry*, Vol. 5, No 2, pp. 49 – 62.
- Moscoloni, M. & Vella C., 2012. The Tas-Silġ Lithic Assemblage: Preliminary Observations on Lithic Typology and Technological Choices from the 2003-2010 SEASONS. Sapienza Università di Roma.
- Müller, C.M. Molinelli, A. Karlowatz, Aleksandrov, A. Orland, T. Mizaikoff, B. 2012. Infrared Attenuated Total Reflectance Spectroscopy of Quartz and Silica Micro and Nanoparticulate Films. *J. Physical Chemistry*, 116, 37-43.
- Müller, C.M. Pejčić, B. Esteban, L. Piane, C.D. Raven, M. Mizaikoff, B. 2014. Infrared Attenuated Total Reflectance Spectroscopy: An Innovative Strategy for Analyzing Mineral Components in Energy Relevant Systems. *Scientific Reports* 4: 6764.
- Munsell, 2014. *Munsell rock Colour book*. Revised on 2009. Michigan, USA.
- Morris, T. O. 1952. *The Water Resources of Malta*. Government Printing Office, Malta.
- Munday, F. C. 1976. Intersite variability in the Mousterian of the central Negev. In *Prehistory and palaeoenvironments in the central Negev*, vol. 2, The Avdat/Aqev area, part 2, and the Har Harif, ed. A. E. Marks, 113–140. Dallas: SMU Press.
- Murray, J. 1890. The Maltese Islands, with special reference to their geological structure." *Scot. Geog. Mag.*, n. 6, pp. 449-88.
- Murray, M. A., Caton Thompson, G. 1923a. *Excavation in Malta part I*. Bernard Quaritch. London.
- Murray, M. A. 1925. *Excavation in Malta part 2*. Bernard Quaritch. London.
- Murray, M. A., Ainsworth Mitchell, C., Ward, T., J. 1929. *Excavation in Malta part I*. Bernard Quaritch. London.
- Murray, M., A. 1923–29. *Excavations in Malta*. Vols 3. London: B. Quaritch.
- Murray, R.W., Buchholtzen Brink, M. R., Gerlach, D., C., Price Russ III, G. and Jones, D., J. 1992. Rare earth, major, and trace element composition of Monterey and DSDP chert and associated host sediment: Assessing the influence of chemical fractionation during diagenesis. *Geochimica et Cosmochimica Acta* Vol. 56, pp. 2657-2671.
- Murray, R. W., 1994. Chemical criteria to identify the depositional environment of chert: general principles and applications. *Sedimentary Geology* 90, pp. 213-232.
- Nazaroff A., J., Baysal, A., Çiftçi, Y. and Prufer K. 2015. Resilience and Redundance: Resource Networks and the Neolithic Chert Economy at Çatalhöyük, Turkey. *European Journal of Archaeology* 18 (3), 402-428.
- Neff, H. 2012. Laser ablation ICP-MS in archaeology. In Lee, M.S. (ed), *Mass Spectrometry Handbook*. Hoboken: Wiley, pp. 829-843.
- Negash, A., Shackley, M., S. 2006. Geochemical Provenance of Obsidian Artefacts from the MSA Site of PORC EPIC, Ethiopia. *Archaeometry* 48, 1, p,1–12.
- Newbery, J. 1968. The perched water table in the Upper Limestone aquifer of Malta. *J. Instn Wat. Engrs.* n,22, pp.551-70.

- Odell, G., H. 2000. Stone Tool Research at the End of the Millennium: Procurement and Technology Journal of Archaeological Research, Vol. 8, No. 4. America.
- Ogniben, L. 1960: Nota illustrativa dello schema geologico della Sicilia nord-orientale. — Riv. Min. Sic. 64-65: 183-222.
- Oil Exploration Directorate. 1993. Geological Map of the Maltese Islands. Sheet 1 – Malta – Scale 1:25,000. Malta: Office of the Prime Minister.
- Olivares, M., Tarrino, A., Murelaga, X., Baceta, J.I., Castro, K., Etxebarria, N. 2009. Non-destructive spectrometry methods to study the distribution of archaeological and geological chert samples. Spectrochimica Acta Part A 73.
- Olofsson, A., Rodushkin, I. 2011. Provenancing flint artefacts with ICP–MS using REE signatures and Pb isotopes as discriminants: Preliminary results of a case study from northern Sweden. Archaeometry 53.
- Ortega, D. 2002. “Mobilitat i desplaçaments dels grups caçadors-recol·lectors a inicis del Paleolític superio a la regió pirinenca oriental.” Cypsela 14:11–26.
- Parish, R., M., Swihart, G., H., Li, Y., S. 2013. Evaluating Fourier Transform Infrared Spectroscopy as a Non-Destructive Chert Sourcing Technique. Geoarchaeology: An International Journal 28, p 289–307.
- Pawlik, A. F. 2009. Is the functional approach helpful to overcome the typology dilemma of lithic archaeology in Southeast Asia? IPPA BULLETIN 29, pp. 6-14.
- Pecoraino, M. (ed.) 1989. La Sicilia di Jean Houel all'Ermitage. Palermo: Sicilcassa.
- Pedley, M.H. 1993. Geological maps of the Maltese Islands. Scale, 1: 25,000, 2 sheets. In: Oil exploration directorate, 1993. Sheet 1 (Malta); Sheet 2 (Gozo and Comino) British Geological Survey, Keyworth.
- Pedley, H. M. 1978. A new lithostratigraphical and palaeoenvironmental interpretation for the coralline limestone formations (Miocene) of the Maltese Islands. Overseas geology and mineral Resources 54, 1-17.
- Pedley, H. M. 1975. The Oligo-Miocene Sediments of the Maltese Islands. Unpublished Ph.D. thesis, University of Hull.
- Pedley, H. M. 1974. Miocene seafloor subsidence and later subaerial solution subsidence structures in the Maltese Islands. Proc. Geol. Ass. n.85, pp. 533-47.
- Pedley, H.M. House, M.R. and Waugh, B. 1976. The Geology of Malta and Gozo. Proceedings of the Geologists' Association 87(3): 325-341.
- Pedley, M.H. Clarke and Galea, P. 2002. Limestone isles in a crystal sea: the geology of the Maltese Islands. Enterprises Group, Malta.
- Pelegrin, J. 1990. Prehistoric lithic technology: Some aspects of research. Archaeological Review from Cambridge 9, 116–125.
- Perlès, C. 1989. Les industries lithiques taillées de Franchthi (Argolide, Grèce), tome 1: Présentation générale et industries Paléolithique. Indiana University Press, Bloomington.
- Pessina, A. & Vella, N. 2005. Un archeologo italiano a Malta. Luigi Maria Ugolini. An italian archaeologist in Malta. Sta Venera (Malta): Midsea Books - Heritage Malta.

- Pétrequin, P., Errera, M., Cassen, S., Guathier, E., Hovorka, D., Klassen, L. & Sherridan, A. 2011. From Mont Viso to Slovakia: the two axe heads of Alpine jade from Golianovo. *Acta Archaeologica Academiae Scientiarum Hungaricae* 62: 243-68.
- Pettitt, P., Rockman, M., Chenery, S., 2012. The British Final Magdalenian: Society, settlement and raw material movements revealed through LA-ICP-MS trace element analysis of diagnostic artefacts. *Quaternary International* vol. 272-273, pp. 275 – 287.
- Pigeot, N. 1990. Technical and social actors: Flint knapping specialist at Magdalenian Etoilles. *Archaeological Review from Cambridge* 9:126–141.
- Pollard, A. M. (ed.) 1999. *Geoarchaeology: exploration, environments, resources*. Geological Society, London, Special Publications, 165, pp.7-14.
- Piper, D. Z. 1974. Rare earth elements in Sedimentary Cycle: A Summary. *Chemical Geology*, 14, 285-304.
- Prampolini, M., Fogliani, F., Biolchi, S., Devoto, S., Angelini, S. & Soldati, M. 2017. Geomorphological mapping of terrestrial and marine areas, northern Malta and Comino (central Mediterranean Sea). *Journal of Maps* 13, 457-469.
- Puglisi, D. 2014. Tectonic evolution of the Sicilian Maghrebian Chain inferred from stratigraphic and petrographic evidences of Lower Cretaceous and Oligocene flysch. *GEOLOGICA CARPATHICA*, 65, 4, pp. 293—305.
- Rapp, G. 1977. The archaeological field staff: the geologist. *Journal of Field Archaeology* 2, pp. 229-237.
- Renfrew, A. C. 1986a. The prehistoric Maltese achievement and its interpretation, in *Archaeology and Fertility Cult in the Ancient Mediterranean*. ed. Bonanno, A. Gruner Publishing, pp. 118–30. Amsterdam.
- Renfrew, A. C. 1973. *Before civilization*. Jonathan Cape. London.
- Reuther, C.D. 1984. Tectonics of the Maltese Islands. *Centro (Malta)* 1, 1-16.
- Reuther, C. D. and Eisbacher, G. H. 1985. Pantelleria Rift - crustal extension in a convergent intraplate setting. *Geologische Rundschau* 74(3), 585–597.
- Ricq-de Bouard, M., Fedele, F., G. 1993. Neolithic rock resources across the Western Alps: circulation data and models. *Geoarchaeology: An International Journal*, Vol. 8, No. 1, 1-22.
- Rizzo, C. 1932. *Geology of the Maltese Islands*. Malta: Government Printing Office.
- Rosenfeld, A. 1965. *The inorganic raw materials of Antiquity*. Weidenfeld and Nicolson. London.
- Roure, F., Howell, D.G., Muller, C. & Moretti, I. 1990: Late Cenozoic subduction complex of Sicily. *Journ. Struct. Geology* 12(2): 259-266.
- Ruffell, A., Hunt, C., Grima, R., McLaughlin, R., Malone, C., Schembri, P.J., French, C. & Stoddart, S. 2018. Water and cosmology in the prehistoric Maltese World: Fault control on the hydrogeology of Ggantija. *Journal of Archaeological Science. Reports* 20, 183-191.
- Sagona, C. 2015. *The archaeology of Malta*. University of Melbourne. Cambridge University Press.
- Sánchez de la Torre, M., Le Bourdonnec, F.-X., Dubernet, S., Gratuze, B., Mangado, X., Fullola, J., M. 2017. The geochemical characterization of two long distance chert tracers by ED-XRF and LA-ICP-MS.

- Implications for Magdalenian human mobility in the Pyrenees (SW Europe). *STAR: Science & Technology of Archaeological Research*, Vol. 3, No. 2, 15–27.
- Sant Cassia, P. 1993. The discovery of Malta. Nature, culture and ethnicity in 19th century painting (review article). *Journal of Mediterranean Studies* 3: 354-77.
- Sayre, E., V., Dodson, R., W. 1957. Neutron activation study of Mediterranean potsherds. *American Journal of Archaeology* 61, 35-41.
- Schembri, P.J. Hunt, C. Pedley, M. Malone, C. Stoddart, S. 2009. The environment of the Maltese Islands [pp.17-39]; Malone, C.; Bonnanno, A.; Trump, D.; Dixon, J.; Leighton, R.; Pedley, M.; Stoddart, S. & Schembri, P.J. (2009) Material culture [pp.219-313]. In: Malone, C.; Stoddart, S.; Bonnanno, A.; Trump, D.; Gouder, T. & Pace, A. (eds) *Mortuary customs in prehistoric Malta: excavations at the Brochtorff Circle at Xaghra, Gozo (1987-94)* [McDonald Institute Monograph]. Cambridge, U.K.: McDonald Institute for Archaeological Research; xxx + 521pp.
- Schembri, P.J. & Lanfranco, E. 1993. Development and the natural environment in the Maltese Islands, in Lockhart, D.G., Drakakis-Smith, D. & Schembri, P.J. (eds.) *The development process in small island states*, pp. 247-266. London & New York: Routledge.
- Schembri, P.J. 1997. The Maltese Islands: climate, vegetation and landscape. *GeoJournal* 41, 1-11.
- Schembri, P.J. 1994. Malta's natural heritage. In Frenzo, H. & Friggeeri, O. (eds.) *Malta culture and identity*, pp. 105-124. Valletta: Ministry of Youth and the Arts.
- Schembri, P.J. 1993. Physical geography and ecology of the Maltese Islands: a brief overview. In: Busuttil, S.; Lerin, F. & Mizzi, L. (eds) *Malta: food, agriculture, fisheries and the environment*. pp.27-39; Paris, France: CIHEAM; 192pp.
- S´eronie-Vivien, M., & S´eronie-Vivien, M.-R. (1987). *Les Silex du M'esozo'ique nord-aquitain. Approche g'eologique de l'´etude des silex pour servir `a la recherche pr´ehistorique*. Bordeaux: Soci´et´e Linn´eenne de Bordeaux.
- Sellet, F. 1993. *Chaˆıne op´eratoire*; The concept and its applications. *Lithic Technology*, Vol. 18, no. 1 & 2.
- Schlanger, N. 1996. Understanding Levallois: Lithic technology and cognitive archaeology. *Cambridge Archaeological Journal* 6: 231–254.
- Shackley, M. S. 1998. Gamma rays, X-rays and stone tools: Some recent advances in archaeological chemistry. *Journal of Archaeological Science* 25: 259-270.
- Shackley, M. S. 1998a. *Archaeological Obsidian Studies*. Plenum Press.
- Shea, J. J. 2017. *Stone tools in human evolution. Behavioral differences among technological primates*. Cambridge University Press. USA.
- Shelley, P., H. 1993. A Geoarchaeological Approach to the Analysis of Secondary Lithic Deposits. *Geoarchaeology: An International Journal*, Vol. 8, No. 1, p. 59-72.
- Shen, B. et al. 2018. Hydrothermal origin of syndepositional chert bands and nodules in the Mesoproterozoic Wumishan Formation: Implications for the evolution of Mesoproterozoic cratonic basin, North China. *Precambrian Research*, vol. 310, pp. 213-228.
- Shockey, D. 1994. Fluorescence and heat treatment of three lithic materials found in Oklahoma. *Bulletin of the Oklahoma Anthropological Society* 43: 86-100.

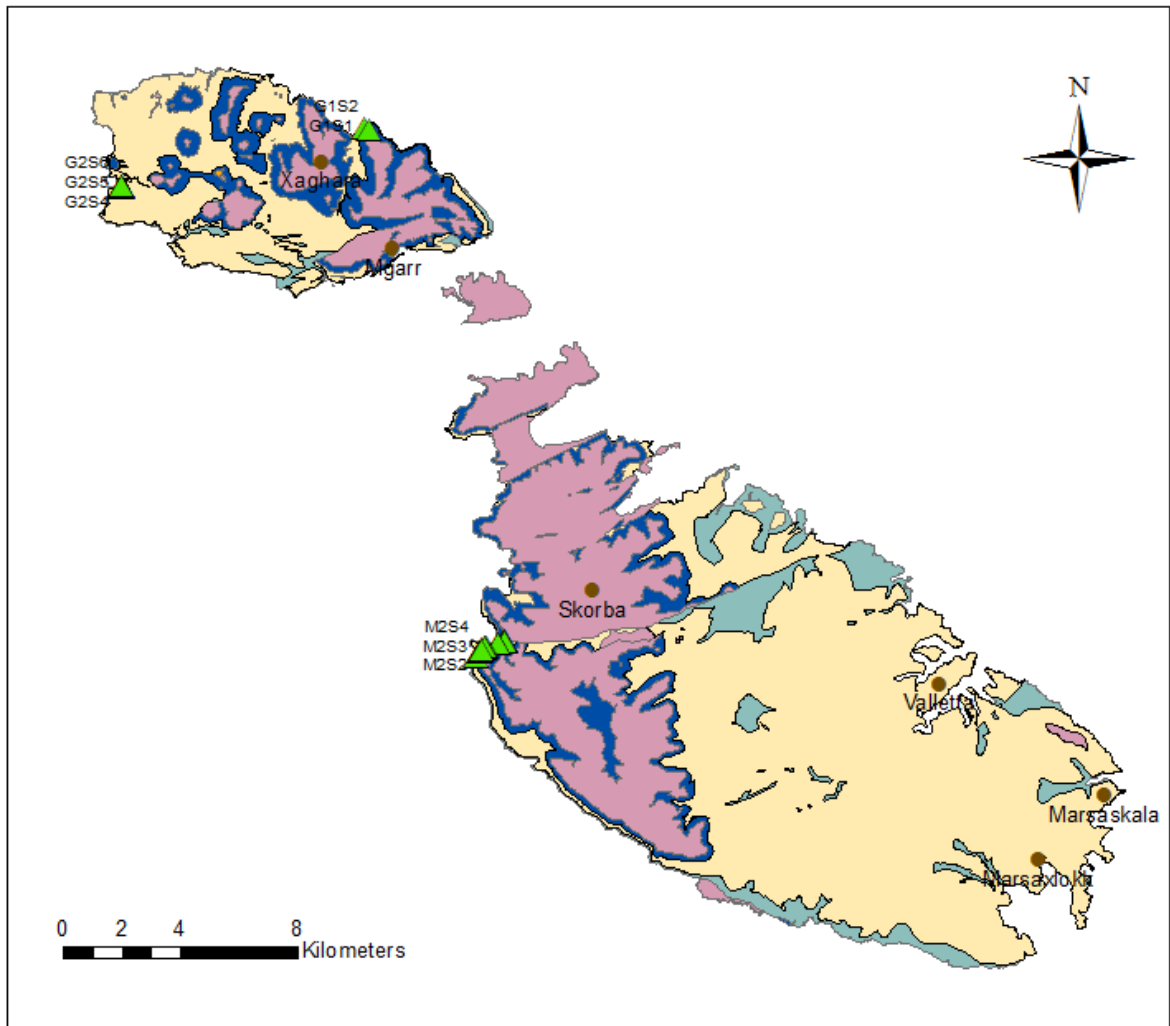
- Shockey, D. 1995. Some observations of polarization and fluorescence in primary and secondary source lithic materials. *Bulletin of the Oklahoma Anthropological Society* 44: 91-115.
- Shotton, F., W., Hendry, G., L. 1979. The Developing Field of Petrology in Archaeology. *Journal of Archaeological Science* 6,75-84.
- Shott, Michael J. 2003. *Chaîne Opératoire* and Reduction Sequence. *Lithic Technology* 28(2): 95–105.
- Sieveking, G., G., Craddock, P., T., Hughes, M., J., Bush, P., Ferguson, J. 1970. Characterization of Prehistoric flint mine products. *Nature* vol. 228, 251.
- Sieveking, G., DE G., Newcomer, M. H. 1987. The human uses of flint and chert. Proceedings of the fourth international flint symposium held at Brighton Polytechnic 10-15 April 1983.
- Smith, B. C. 2011. *Fundamentals of Fourier Transform Infrared Spectroscopy*, 2nd edn. Boca Raton, FL: CRC Press.
- Smith, I. F. 1965. *Windmill Hill and Avebury: excavations by Alexander Keiller 1925-1939*. Clarendon Press, Oxford.
- Smith, I., F., Simpson D., D., A. 1966. Excavations of a round barrow on Overton Hill, North Wiltshire. *Proceeding of the Prehistoric society* 32, 122-55.
- Smith, G., D., Clark, R., J.H. 2004. Raman microscopy in archaeological science. *Journal of Archaeological Science* 31, p.1137–1160.
- Soressi, M., Geneste, J-M. 2011. The history and efficacy of the *chaîne opératoire* approach to lithic Analysis: Studying Techniques to Reveal Past Societies in an Evolutionary Perspective. *Paleo Anthropology*, 334–350.
- Speer, C., A., 2014. Experimental sourcing of Edwards Plateau chert using LA-ICP-MS. *Quaternary International* 342, pp. 199 – 213.
- Speer, C., A. 2016. “A comparison of instrumental techniques at differentiating outcrops of Edwards Plateau chert at the local scale.” *Journal of Archaeological Science: Reports* 7:389–93.
- Spratt, T. A. B. 1843. On the geology of the Maltese Islands. *Proc. geol. Soc.* 4, 225-32.
- Spratt, T. A. B. 1854. *The Geology of Malta and Gozo*. p.7, Malta.Strand, E. A. 2012. The textile *chaîne opératoire*: Using a multidisciplinary approach to textile archaeology with a focus on the Ancient Near East. *Paleorient*, 38.1-2, pp. 21-40.
- Stoddart, S. K. F. 1999. Mortuary customs in prehistoric Malta. In Mifsud, A. & Savona-Ventura, C. (eds.), *Facets of Maltese Prehistory*. Mosta: Prehistoric Society of Malta, 183-90.
- Terradas, X. 2001. “La gestión de los recursos minerales en las sociedades cazadoras-recolectoras.” *Treballs d’Etnoarqueologia* 4, p. 176.
- Tixier, J., M.-L. Inizan, and H. Roche. 1980. *Pre´histoire de la Pierre Taille´e*. Vol. 1. Terminologie et technologie. Antibes: CREP.
- Tostevin, G. B. 2011. Levels of Theory and Social Practice in the Reduction Sequence and *Chaîne Opératoire* Methods of Lithic Analysis. *PaleoAnthropology*, 351–375.
- Trechmann, C. T. 1938. Quaternary conditions in Malta. *Geological magazine*, 75 (1), p. 1-27.

- Trombold et al. 1993. Chemical characteristics of obsidian from archaeological sites in western Mexico and the Tequila source area: Implications for regional and pan-regional interaction within the northern Mesoamerican periphery. *Ancient Mesoamerica* 4, p. 255-270.
- Trump, D. 1961a. Skorba, Malta and Mediterranean. *Antiquity* 35, pp. 300–303.
- Trump, D. 1961b. The late prehistory of Malta. *Proceedings of the Prehistoric Society* 27, pp.253–62. Skorba. Oxford University Press, London.
- Trump, D. 1966. Skorba: Excavations carried out on behalf of the National Museum of Malta, 1961–3. Research reports of the Society Antiquity of London 22. London.
- Trump, D. 2002. Malta: Prehistory and Temples. Midsea Books Ltd, Malta.
- Trump, D. 2015. Skorba, 1961–63 Excavations. Mgarr Local Council/ Heritage Malta, Malta.
- Tucker, M.E. 2001. Sedimentary Petrology. Black Scientific Pub.
- Turq, A. 2005. Réflexions méthodologiques sur les études de matières premières lithiques: 1 - des lithothèques au matériel archéologique. *Paléo*, 17, 111–132.
- Tykot, R., H. 2004. Scientific methods and applications to archaeological provenance studies. *Proceedings of the International School of Physics “Enrico Fermi” Course CLIV*, M. Martini, M. Milazzo and M. Piacentini (Eds.) IOS Press, Amsterdam.
- Tykot, R. H. 1991. Survey and analysis of the Monte Arci (Sardinia) obsidian sources. *Old World Archaeology Newsletter* 14, 23–27.
- Tykot, R. H. 1992. The sources and distribution of Sardinian obsidian. In (R. H. Tykot & T. K. Andrews, Eds) *Sardinia in the Mediterranean: A Footprint in the Sea. Studies in Sardinian Archaeology Presented to Miriam S. Balmuth*. Sheffield: Sheffield Academic Press, pp. 57–70.
- Tykot, R. H. 1995. Prehistoric trade in the Western Mediterranean: the sources and distribution of Sardinian Obsidian. Ph.D. Thesis, Harvard University, Ann Arbor, MI, U.S.A. (University Microfilms).
- Tykot, R. H. 1996. Obsidian procurement and distribution in the central and western Mediterranean. *Journal of Mediterranean Archaeology* 9, 39–82.
- Tykot, R. H. 1997. Mediterranean islands and multiple flows: the sources and exploitation of Sardinian obsidian. In (M. S. Shackley, Ed.) *Method and Theory in Archaeological Volcanic Glass Studies. Advances in Archaeological and Museum Science Series*. New York: Plenum.
- Tykot, R., H. & Ammerman, A., J. 1997. New Directions in Central Mediterranean Obsidian Studies. *Antiquity* 71(274), p. 1000-1006.
- Ugolini, L., M. 2012. Malta: Origini della Civiltà Mediterranea (reprinted text of the 1934 edition with English translation and additions by A. Pessina and N. C. Vella). Valletta, Malta. Midsea Books.
- Van Peer, P. 1992. The Levallois reduction strategy. *Monographs in World Archaeology* 13. Madison, WI: Prehistory Press.
- Vance, J. G. 1842. Description of an ancient temple near Crendi, Malta. *Archaeologia* 29: 227-40.
- Vella, C. 2008a. Report on the lithic tools of Sicilian origin from the prehistoric site of Skorba, Malta. In *Malta and Sicily: Miscellaneous Research Projects*, edited by A. Bonanno. *Officina di Studi Medioevale*, University of Malta, Palermo.

- Vella, C. 2008b. Distribution patterns of imported lithic tools in Early Neolithic Skorba. *Heritage Malta, Malta*. in M.E. Zammit - J. Mallia (eds.), *Ta Hagraat and Skorba: Ancient Monuments in a Modern World*, Valletta 2008, pp. 75-86.
- Vella, C. 2009. The lithic toolkit of Late Neolithic Ta' Hagraat, Malta. *Origini* 31, pp. 85-102.
- Vella, C. 2010. The Lithic Assemblage of the Promontory site at Ras IL-Pellegrin. *Traces in Time* n.1, pp. 6-26.
- Vella, C. 2011. The lithics, in D. Tanasi - N.C. Vella (eds.), *Site, Artifacts and Landscape - Prehistoric Borg in-Nadur, Malta*, pp. 173-194.
- Vossmerbäumer, H. 1972. Malta, ein Beitrag zur Geologie und Geomorphologie des Zentralmediterranen Raumes. *Wurzburger Geographische Arbeiten* 38, 1-213.
- Ward, G., K., Smith, I., E. 1974. Characterization of Chert Sources as an Aid to the Identification of Patterns of Trade, Southeast Solomon Islands: A Preliminary Investigation *Mankind* 9, pp. 281-6.
- Williams-Thorpe, O., Warren, S. E. & Barfield, L. H. 1979. The sources and distribution of archaeological obsidian in northern Italy. *Preistoria Alpina* 15, 73-92.
- Williams-Thorpe, O., Warren, S. E. & Courtin, J. (1984). The distribution and sources of archaeological obsidian from southern France. *Journal of Archaeological Science* 11, 135-146.
- Williams-Thorpe, O. (1995). Review article. Obsidian in the Mediterranean and the Near East: a provenancing success story. *Archaeometry* 37, 217-248.
- Williams-Thorpe, O., Potts, P. J., and Webb, P. C. 1999. Field-portable non-destructive analysis of lithic archaeological samples by X-ray fluorescence instrumentation using a mercury iodide detector: Comparison with wavelength-dispersive XRF and a case study in British stone axe provenancing. *Journal of Archaeological Science* 26: 215-237.
- Yellin-Dror, A., Grasso, M., Ben-Avraham, Z. & Tibor, G. 1997. The subsidence history of the northern Hyblean plateau margin, southeastern Sicily. *Tectonophysics* 282, 277-289.
- Zammit, T. 1910. The Hal Saflieni Prehistoric Hypogeum at Casal Paula, Malta. *First Report*. Malta.
- Zammit, T. 1915-16. The Hal-Tarxien Neolithic Temple, Malta. *Archaeologia* 67: 127-44.

APPENDIX I

Geological Map Of The Maltese Islands



Legend

Geological Formations

- Upper Coralline Limestone Formation
- Greensand Formation
- Blue Clay Formation
- Globigerina Limestone Formation
- Lower Coralline Limestone Formation

- Towns
- Sample_locations

Figure .1: The geological map of Maltese Islands presenting the sample locations.

Table 1: Description of the geological samples from the Maltese Islands, their location and coordinates.

Sample	Type	Form	Area	Latitude	Longitude
G1S1	Limestone	N/A	Ir-Ramla bay	36° 3'48.66"N	14°17'15.59"E
G1S2	Calcite	Vein	Ir-Ramla bay	36° 3'47.96"N	14°17'21.78"E
G1S3	Calcite	Lens	Ir-Ramla bay	36° 2'41.00"N	14°11'43.78"E
G2S1	Chert	Nodular	Dwejra Point	36° 2' 41,03"N	14° 11' 4378"E
G2S2	Chert	Nodular	Dwejra Point	36° 2'41.10"N	14°11'43.80"E
G2S3	Chert	Bedded	Dwejra Point	36° 2'41.60"N	14°11'43.68"E
G2S4	Chert	Bedded	Dwejra Point	36° 2'42.00"N	14°11'43.49"E
G2S5	Chert	Bedded	Dwejra Point	36° 2'43.00"N	14°11'43.10"E
G2S6	Chert	Nodular	Dwejra Point	36° 3'48.66"N	14°17'15.59"E
F1S4	Chert	Bedded	Dwejra Point	36° 2'42.08"N	14°11'43.50"E
M1S1	Chert	Nodular	Fomm-IR-RIĦ bay	35°54'20.32"N	14°20'32.00"E
M1S2	Chert	Nodular	Fomm-IR-RIĦ bay	35°54'20.33"N	14°20'31.92"E
M1S3	Chert	Bedded	Fomm-IR-RIĦ bay	35°54'22.47"N	14°20'31.50"E
M1S4	Chert	Bedded	Fomm-IR-RIĦ bay	35°54'22.28"N	14°20'31.30"E
M1S5	Chert	Bedded	Fomm-IR-RIĦ bay	35°54'20.65"N	14°20'29.94"E
M1S6	Chert	Nodular	Fomm-IR-RIĦ bay	35°54'18.64"N	14°20'21.03"E
M1S7	Chert	Nodular	Fomm-IR-RIĦ bay	35°54'18.64"N	14°20'21.03"E

M1S8	Chert	Bedded	Fomm-IR-RI# bay	35°54'14.72"N	14°20'5.08"E
M1S9	Chert	Nodular	Fomm-IR-RI# bay	35°54'14.55"N	14°20'4.52"E
M1S10	Chert	Nodular	Fomm-IR-RI# bay	35°54'13.84"N	14°20'4.35"E
M1S11	Chert	Nodular	Fomm-IR-RI# bay	35°54'14.79"N	14°20'4.85"E
F1S2	Chert	Bedded	Fomm-IR-RI# bay	35°54'20.69"N	14°20'29.51"E
F1S3	Chert	Bedded	Fomm-IR-RI# bay	35°54'13.60"N	14°20'0.02"E
M2S1	Chert	N/A	Fomm-IR-RI# bay	35°54'4.10"N	14°19'53.67"E
M2S2	Chert	Nodular	Fomm-IR-RI# bay	35°54'9.16"E	14°19'57.58"E
M2M3	Chert	Nodular	Fomm-IR-RI# bay	35°54'9.10"N	14°19'56.58"E
M2S4	Chert	Bedded	Fomm-IR-RI# bay	35°54'12.22"N	14°19'59.73"E

Table 2: Description of the geological samples from Sicily, including their origin, age, location and coordinates.

Sample	Type	Geological Group	Age	Area	Latitude	Longitude
S1	Chert	Hyblean Plateau	Miocene	Monte Tabuto	N 36 58.052	E14 38.825
S2	Silicified limestone	Hyblean Plateau	Miocene	Modica	N 36 49.465	E14 43.464
S3	Chert	Hyblean Plateau	Miocene	Modica	N 36 49.459	E14 43.453
S4	Chert	European group – Monte Judica unit	Triassic	Contrada la vina	N 37 30.643	E14 40.582
S5	Chert	European group – Monte Judica unit	Triassic	Contrada la vina	N 37 30.645	E14 40.580
S6	Chert	European group – Monte Judica unit	Jurassic – Cretaceous	Valona River	N 37 30.645	E14 40.462
S7	Chert	European group – Monte Judica unit	Jurassic – Cretaceous	Valona River	N 37 30.645	E14 40.462
S8	Chert	European group – Monte Judica unit	Jurassic – Cretaceous	Valona River	N 37 30.645	E14 40.462

S9	Chert	European group – Monte Judica unit	Triassic	Monte Santo	N 37 29.626	E 14 40.565
S10	Chert	European group – Monte Judica unit	Triassic	Monte Santo	N 37 29.626	E 14 40.565
S11	Chert	European group – Monte Judica unit	Triassic	Monte Santo	N 37 29.626	E 14 40.565
S12	Silicified limestone	Hyblean Plateau	Oligocene – Miocene	Monterosso Almo	N37 05.794	E14 46.024
S13	Chert	Hyblean Plateau	Cretaceous	Monterosso Almo	N 37 05.804	E14 45.692
S14	Chert	Hyblean Plateau	Cretaceous	Monterosso Almo	N37 05.843	E14 45.685
S15	Chert	Hyblean Plateau	Cretaceous	Monterosso Almo	N 37 05.828	E14 45.673
S16	Chert	Hyblean Plateau	N/A*	Monterosso Almo	N 37 05.828	E14 45.673
S17	Chert	Hyblean Plateau	Cretaceous	Monterosso Almo	N 37 05.804	E14 45.692
S18	Chert	Hyblean Plateau	Eocene	Monterosso Almo	N 37 05.801	E14 45.523
S19	Chert	Hyblean Plateau	Pliocene?	Monterosso Almo	N 37 05.797	E14 45.584
S20	Chert	Hyblean Plateau	Eocene	Monterosso Almo	N 37 05.949	E14 45.201
S21	Chert	Hyblean Plateau	Eocene	Monterosso Almo	N37 05.962	E14 45.145
S22	Chert	European group – Del Bacino Sicano unit	Upper Triassic	Triona mountain	N37 43.134	E13 15.818
S23	Chert	European group – Del Bacino Sicano unit	Lower – Middle Jurassic	Genuardo Mountain	N37 42.709	E013 12.238
S24	Chert	Volcanic formation	Jurassic*	Genuardo Mountain	N 37 42.499	E 13 10.984
S25	Chert	European group – Del Bacino Sicano unit	Middle – Upper Jurassic	Genuardo Mountain	N37 42.672	E013 10.983

Table 3: Macroscopic description of the chert samples collected from Malta. The colours were determined based on the Munsell rock Colour book (Munsell, 2014).

Sample	Type	Area	Colour	Fabric	Lustre	Translucency	Feel	Grain	Pattern	Cortex
G1S1	Limestone	Gozo	Yellowish Gray (5Y 8/1)	Heterogenous	Dull	Opaque	Semi-smooth	Course	N/A	N/A
G1S2	Calcite		Dark Yellowish Orange (10YR 6/6)	Homogenous	Pearly Shine	Translucent	Smooth	Fine	N/A	N/A
G1S3			Dark Yellowish Orange (10YR 6/6)	Homogenous	Pearly Shine	Translucent	Smooth	Fine	N/A	N/A
G2S1	Chert		Dusky Brown (5YR 2/2)	Homogenous	Greasy Shine	Opaque	Semi-smooth	Fine	Lamellae	Limestone
G2S2			Light Greenish Gray (5GY 8/1) to Greyish Blue (5PB 5/2)	Homogenous	Greasy Shine	Opaque	Semi-smooth	Medium-coarse	Core, Intermediate zone and external zone	Limestone
G2S3			Olive Gray (5Y 3/2)	Homogenous	Dull	Opaque	Rough	Medium	N/A	Limestone
G2S4			Olive Gray (5Y 3/2)	Heterogenous	Dull	Opaque	Rough	Course	Laminated Spotched	N/A
G2S5			Dusky Yellow (5Y 6/4)	Heterogenous	Dull	Opaque	Rough	Course	Broad mottling	Limestone
G2S6			White (N9)	Homogenous	Pearly Shine	Translucent	Smooth	Fine	N/A	Limestone
F1S4			Dusky Yellow (5Y 6/4)	Heterogenous	Dull	Opaque	Rough	Course	Broad mottling	Limestone
M1S1		Chert	Malta	Pale Greenish Yellow (10Y 8/2)	Heterogenous	Dull	Opaque	Smooth	Fine	Finely Laminated
M1S2	Moderate Olive Brown (5Y 4/4)			Homogenous	Dull	Opaque	Smooth	Fine	Spotched	Limestone
M1S3	Moderate Greenish Yellow (10Y 7/4)			Homogenous	Dull	Opaque	Smooth	Fine	Laminated	Limestone
M1S4	Moderate Yellow Green (5GY 7/4) to Moderate Olive Brown (5Y 4/4)			Homogenous	Dull	Opaque	Semi-smooth	Fine	Laminated Spotted	Limestone

M1S5			Moderate Olive Brown (5Y 4/4)	Homogenous	Dull	Opaque	Smooth	Fine	Finely Laminated	N/A
M1S6	Chert	Malta	Moderate Olive Brown (5Y 4/4) to Grayish Yellow Green (5GY 7/2)	Homogenous	Dull	Opaque	Semi-smooth	Fine	Finely Laminated	Limestone
M1S7			Light Olive Brown (5Y 5/6)	Homogenous	Dull	Opaque	Smooth	Fine	Laminated	N/A
M1S8			Moderate Olive Brown (5Y 4/4) to Dark Greenish Yellow (10Y 6/6)	Homogenous	Dull	Opaque	Semi-smooth	Fine	1) White, Streaking 2) Dark Laminated	N/A
M1S9			Moderate Yellow (5Y 7/6) to Moderate Olive Brown (5Y 4/4)	Homogenous	Dull	Opaque	Rough	Medium	1) White Bands 2) Dark Laminated Spotted	N/A
M1S10			Dark Yellowish Brown (10 YR 4/2)	Homogenous	Dull	Opaque	Semi-smooth	Fine	Finely Laminated Spotted	N/A
M1S11			Light Olive Brown (5Y 5/6)	Homogenous	Dull	Opaque	Smooth	Fine	Finely Laminated	N/A
F1S2			Dusky Yellow (5Y 6/4)	Homogenous	Dull	Opaque	Smooth	Fine	Finely Laminated	Limestone
F1S3			Yellowish Gray (5Y 7/2)	Homogenous	Dull	Opaque	Semi-smooth	Fine	Laminated	Limestone
M2S1			Grayish Brown (5Y 3/2)	Homogenous	Dull	Opaque	Semi-smooth	Fine	N/A	N/A
M2S2			Dark Yellowish Brown (10 YR 4/2)	Homogenous	Medium	Opaque	Smooth	Fine	1) White Streaking to Laminated 2) Dark Finely Laminated	N/A
M2S3			Light Olive (10Y 5/4)	Homogenous	Dull	Opaque	Semi-smooth	Medium	Lines -> Finely Laminated	N/A
M2S4			Moderate Olive Brown (5Y 4/4)	Homogenous	Dull	Opaque	Smooth	Fine	N/A	N/A

Table 4: Macroscopic description of the chert samples collected from Sicily. The colours were determined based on the Munsell rock Colour book (Munsell, 2014).

Sample	Type	Colour	Fabric	Lustre	Translucency	Feel	Grain	Pattern	Cortex
S1	Chert	Pale yellowish brown (10YR 6/2)	Homogenous	Dull	Opaque	Semi-smooth	Medium – grain	N/A	N/A
S2	Silicified limestone	Very pale orange (10YR 8/2)	Homogenous	Dull	Opaque	Semi-smooth	Medium – grain	Spotted	N/A
S3	Chert	Brownish black (5YR 2/1)	Homogenous	Pearly shine	Opaque	Smooth	Fine – grain	N/A	Silicified limestone
S4	Chert	Light gray (N7)	Heterogenous	Pearly shine	Semi – translucent	Rough	Fine – grain	N/A	N/A
S5	Chert	Grayish black (N2)	Homogenous	Dull	Opaque	Rough	Fine – grain	N/A	N/A
S6a	Chert – Radiolarian	3 layers with different colours (from top): Moderate red (5R 5/4) Pale olive (10Y 6/2) Grayish red (5R 4/2)	Homogenous	Pearly shine	Opaque	Semi-smooth	Fine – grain	N/A	N/A
S6b	Chert – Radiolarian	3 layers (from top): Greenish gray (5G 6/1) Dark greenish gray (5G 4/1) Blackish red (5R 2/2)	Homogenous	Dull	Opaque	Semi-smooth	Fine – grain	N/A	N/A
S7	Chert – Radiolarian	4 layers (from top): Moderate red (5R 5/4) Pale olive (10Y 6/2) Grayish red (5R 4/2) Light olive gray (5Y 6/1)	Homogenous	Pearly shine	Opaque	Semi-smooth	Fine – grain	N/A	N/A
S8	Chert – Radiolarian with a middle of limestone	5 layers (from top): Grayish green (10GY 5/2) Pale red (5R 6/2) Grayish orange pink (5YR 7/2) Grayish red (5R 4/2) Light greenish gray (5GY 8/1)	Homogenous	Dull	Opaque	Semi-smooth	Fine – grain	N/A	N/A

S9	Chert	Brownish black (5YR 2/1)	Homogenous	Dull	Opaque	Semi-smooth	Fine – grain	N/A	N/A
S10	Chert	Medium dark gray (N4)	Homogenous	Pearly shine	Opaque	Semi-smooth	Fine – grain	N/A	N/A
S11	Chert	Brownish black (5YR 2/1)	Heterogenous	Pearly shine	Opaque	Semi-smooth	Fine – grain	N/A	N/A
S12	Silicified limestone	Grayish orange (10YR 7/4)	Homogenous	Dull	Opaque	Semi-smooth	Medium – grain	N/A	N/A
S13	Chert	Medium light gray (N6)	Heterogenous	Silky shine	Opaque	Semi-smooth	Medium to rough grain	N/A	Silicified limestone
S14	Chert	2 layers (from top): Light olive gray (N7) Dusky Brown (5YR 2/2)	Heterogenous	Silky shine	Opaque	Semi-smooth	Fine to medium grain	N/A	N/A
S15	Chert	Medium light gray (N6)	Heterogenous	Silky shine	Opaque	Smooth	Fine – grain	Spots -> carbonate residues	N/A
S16	Chert	2 layers (from top): Dusky yellowish brown (10YR 2/2) Light brownish gray (5YR 6/1)	Homogenous	Waxy shine	Semi – translucent	Semi-smooth	Fine – grain	Spotted	N/A
S17	Chert	Olive black (5Y 2/1)	Heterogenous	Silky shine	Opaque	Semi-smooth	Fine – grain	Spots -> carbonate residues	N/A
S18	Chert	Moderate brown (5Y 3/4) and Grayish black (N2)	Homogenous	Pearly shine	Translucent	Smooth	Fine – grain	Spots -> carbonate residues	Chalky limestone
S19	Chert	Moderate yellowish brown (10YR 5/4) and Grayish brown (5YR 3/2)	Homogenous	Pearly shine	Semi – translucent	Smooth	Fine – grain	Spots -> carbonate residues	Chalky limestone
S20	Chert	Moderate yellowish brown (10YR 5/4)	Homogenous	Pearly shine	Semi – translucent	Smooth	Fine – grain	Spots	Limestone ?
S21	Chert	Grayish red (10R 4/2)	Homogenous	Pearly shine	Semi – translucent	Smooth	Fine – grain	Spots	N/A
S22r	Chert	Moderate reddish brown (10R 4/6)	Homogenous	Pearly shine	Opaque	Semi-smooth	Fine – grain	N/A	N/A
S22p	Chert	Pale brown (5YR 5/2)	Homogenous	Dull	Semi – translucent	Smooth	Fine – grain	N/A	N/A

S23	Chert	Dusky yellowish brown (10YR 2/2)	Homogenous	Dull	Opaque	Semi-smooth	Fine – grain	N/A	N/A
S24	Chert	Dusky yellowish orange (10YR 5/4) to Moderate yellowish brown (10YR 4/2)	Homogenous	Dull	Opaque	Semi-smooth	Fine – grain	N/A	N/A
S25	Chert	Medium dark gray (N4)	Heterogenous	Pearly shine	Semi – translucent	Semi-smooth	Fine – grain	Spots	N/A

Table 5: The lithic assemblages of the archaeological sites investigated, and the main types of rock identified.

Archaeological Site	Location of assemblage	Total number of artefacts	Chert artefacts	Obsidian artefacts	“Other” artefacts	Number of samples
Ġgantija	University of Malta	170	85	10	75	21
Santa Verna	University of Malta	723	284	67	372	21
	University of Malta	180	51	70	59	
Kordin	University of Malta	215	152	23	40	14
Taċ-Ċawla	Museum of Archaeology	693	457	111	125	21
Xagħra Circle	Museum of Archaeology	225	198	0	27	11
Skorba	University of Malta	<1200	N/A	N/A	N/A	61

Table 6: Explanatory table of the coding system employed on the assemblages of the Neolithic Maltese site under the FRAGSUS project.

Sample Code	Archaeological Site	Year of excavation	Context number (L)	Sample number (S)
BR89/S395/L449	Brochtorff Xagħra Circle (BR)	1989	449	395
KRD15/S69/L211	Kordin (KDR)	2015	211	69
TCC14/S193/L69	Taċ-Ċawla (TCC)	2014	69	193
SV15/S3/L41	Santa Verna (SV)	2015	41	3
GG15/S6/L1019	Ġgantija (GG)	2015	1019	6
SKB16/L2/S4	Skorba (SKB)	2016	2	4

Table 7: The macroscopic description of the chert artefacts investigated from all the assemblages except Skorba. The N/A indication means that this information was not available (sample code) or present (cortex and pattern). The number in brackets reported in the sample column indicate the number of finds included in the sample bags, because occasionally there were more than one finds inside them.

Number	Sample	Layer	Location	Colour*	Fabric	Lustre	Translucency	Texture	Grain	Cortex	Pattern
1	N/A (1)	1019	Ġgantija	chert cortex							
2	N/A (15)	1019	Ġgantija	silicified limestone							
3	N/A (3)	1019	Ġgantija	10YR 4/2	Homogeneous	Dull	sub-translucent	Semi smooth	Medium	N/A	N/A
4	9915	002/TRI	Ġgantija	Patinated							
5	N/A (1)	008/TRI	Ġgantija	10R 3/4	Homogeneous	Pearly shine	translucent	Smooth	Fine	N/A	N/A
6	N/A (1)	008/TRI	Ġgantija	Patinated							
7	N/A (1)	1015	Ġgantija	10YR 5/4	Homogeneous	Pearly shine	translucent	Smooth	Fine	N/A	N/A
8	N/A (2)	1016	Ġgantija	10YR 4/2	Homogeneous	Silky shine	sub-translucent	Semi smooth	Medium	N/A	N/A
9	N/A (4)	[1042]	Ġgantija	10YR 4/2	Homogeneous	Silky shine	sub-translucent	Semi smooth	Medium	N/A	N/A
10	N/A (2)	[1004]	Ġgantija	10YR 4/2	Homogeneous	Silky shine	sub-translucent	Semi smooth	Medium	N/A	N/A
11	N/A (2)	1016	Ġgantija	10YR 4/2	Homogeneous	Silky shine	sub-translucent	Semi smooth	Medium	N/A	N/A
12	N/A	[1030] SF4	Ġgantija	Patinated							
13	N/A	[1030] SF3	Ġgantija	chert cortex							
14	N/A	[1030] SF8	Ġgantija	Patinated							
15	N/A	[1030] SF9	Ġgantija	silicified limestone							
16	N/A	[005] TRI	Ġgantija	chert cortex							
17	N/A (1)	1015	Ġgantija	10YR 4/2	Homogeneous	Pearly shine	translucent	Smooth	Fine	N/A	N/A
18	N/A (1)	1015	Ġgantija	5Y 3/2	Homogeneous	Silky shine	sub-translucent	Semi smooth	Fine	N/A	N/A
19	N/A (1)	[1012]	Ġgantija	10YR 6/2	Homogeneous	Dull	Sub – translucent	Semi smooth	Medium	N/A	N/A
20	N/A (2)	[1012]	Ġgantija	Patinated							

21	N/A (1)	[1012]	Ġgantija	chert but too small to describe							
22	N/A (1)	[1012]	Ġgantija	5Y 4/1	Homogeneous	Dull	Opaque	rough	Medium	N/A	N/A
23	N/A	[1030] SF6	Ġgantija	10YR 4/2	Homogeneous	Pearly shine	translucent	Smooth	Fine	N/A	N/A
24	N/A	1040	Ġgantija	10YR 6/2	Homogeneous	Dull	Opaque	Semi smooth	Medium	Limestone N/A	N/A
25	N/A (1)	12	Ġgantija	10YR 6/2	Heterogenous	Dull	Opaque	Semi smooth	Medium	N/A	Spotted fossils
26	N/A (1)	12	Ġgantija	5Y 2/1	Homogeneous	Dull	Opaque	Semi smooth	Medium	N/A	N/A
27	N/A	[1021] SF10	Ġgantija	10YR 5/4	Homogeneous	Pearly shine	translucent	Semi smooth	Fine	N/A	N/A
28	N/A	[1021]	Ġgantija	Patinated							
29	N/A	[1030] SF2	Ġgantija	Patinated							
30	N/A (2)	[1040]	Ġgantija	10YR 4/2	Homogeneous	Dull	Opaque	Smooth	Fine	N/A	N/A
31	N/A (1)	[1016]	Ġgantija	5YR 3/2	Homogeneous	Silky shine	sub-translucent	Smooth	Fine	N/A	N/A
32	N/A (1)	[1016]	Ġgantija	5YR 3/2	Homogeneous	Pearly shine	translucent	Smooth	Fine	N/A	N/A
33	N/A (5)	[1019]	Ġgantija	chert cortex and patinated pieces							
34	N/A (26)	[1019]	Ġgantija	10YR 7/4 to 6/2 and 4/2	Homogeneous	Dull	Opaque	Semi smooth	Medium	N/A	N/A
35	96	42	Santa Verna	10YR 6/2	Homogeneous	Dull	Opaque	Smooth	Fine	N/A	N/A
36	92	42	Santa Verna	N/A	Heterogenous	Dull	Opaque	rough	Medium	Yes, brow soil	N/A
37	78	20	Santa Verna	N2	Homogeneous	Silky shine	Sub-trans	Semi smooth	Fine	Yes, brown soil	N/A
38	73	20	Santa Verna	10R 5/4	Homogeneous	Pearly shine	Opaque	Smooth	Fine	N/A	N/A
39	75	20	Santa Verna	10R 2/2	Homogeneous	Dull	Opaque	Smooth	Fine	N/A	N/A
40	4	4	Santa Verna	N7	Homogeneous	Pearly shine	Sub-trans	Smooth	Fine	N/A	N/A
41	7	3	Santa Verna	5Y 6/4	Heterogenous	Dull	Opaque	Semi smooth	Fine	N/A	Carbonated fossils spotted
42	3	4	Santa Verna	5Y 7/2	Homogeneous	Dull	Opaque	Semi smooth	Fine	limestone	N/A

43	144	42	Santa Verna	5Y 2/1	Heterogenous	Silky shine	Opaque	Smooth	Fine	N/A	Lines carboned
44	147	63	Santa Verna	5YR 4/1	Homogeneous	Pearly shine	Sub-trans	Semi smooth	Medium	N/A	N/A
45	N/A	46TRC	Santa Verna	5Y 7/2	Heterogenous	Dull	Opaque	Semi smooth	Medium	N/A	Lines laminas
46	103	62 [65]	Santa Verna	5YR 3/2	Heterogenous	Pearly shine	Translucent	Smooth	Fine	N/A	Spotted carbonated
47	102	62 [65]	Santa Verna	Completely patinated							
48	106	65	Santa Verna	5Y 7/2	Heterogenous	Dull	Opaque	Smooth	Fine	N/A	Spots & Lines
49	N/A	19	Santa Verna	10YR 6/2 to 10YR 7/4	Homogeneous	Dull	Opaque	Semi smooth	Fine	N/A	N/A
50	50	11	Santa Verna	N/A Covered almost totally with soil							
51	58	12	Santa Verna	5Y 2/1	Heterogenous	Pearly shine	Opaque	Semi smooth	Fine	N/A	Lines carboned
52	N/A	5	Santa Verna	5Y 6/1	Heterogenous	Dull	Opaque	rough	coarse	N/A	Fossils carbonate residues
53	80	34	Santa Verna	10YR 7/4	Homogeneous	Dull	Opaque	Semi smooth	Fine	N/A	N/A
54	89	42	Santa Verna	10Y 7/4	Homogeneous	Dull	Opaque	Smooth	Fine	limestone	N/A
55	Sample 1	13	Santa Verna	10YR 6/2	Homogeneous	Pearly shine	Opaque	Smooth	Fine	N/A	Spots fossils
56	N/A	19	Santa Verna	5Y 7/2	Homogeneous	Dull	Opaque	Smooth	Fine	Yes lime	Spots lines
57	155	121	Santa Verna	5Y 7/2	Homogeneous	Dull	Opaque	Semi smooth	Fine	Yes, brown soil	N/A
58	88	42	Santa Verna	5Y 7/6	Heterogenous	Dull	Opaque	Semi smooth	Medium	limestone	laminas
59	N/A	1	Santa Verna	5Y 7/2	Homogeneous	Dull	Opaque	Smooth	Medium	N/A	Spotted fossils
60	95	19	Santa Verna	5Y 7/2	Homogeneous	Dull	Opaque	Semi smooth	Medium	Silicate lime	N/A
61	N/A	20 TRC	Santa Verna	10YR 6/2	Heterogenous	Dull	Opaque	Semi smooth	Medium	N/A	Spotted fossils

62	134	58	Santa Verna	10YR 5/4	Heterogenous	Dull	Opaque	Smooth	Medium	N/A	Spotted fossils
63	999	N/A	Santa Verna	5YR 5/2	Homogeneous	Silky shine	Opaque	Smooth	Medium	N/A	N/A
64	N/A	16	Santa Verna	10YR 6/2	Homogeneous	Dull	Opaque	Semi smooth	Medium	N/A	N/A
65	110	65	Santa Verna	Patinated							
66	113 (1)	75	Santa Verna	5Y 2/1	Homogeneous	Pearly shine	Opaque	Smooth	Medium	N/A	N/A
67	113 (1)	75	Santa Verna	5Y 7/2	Heterogenous	Dull	Opaque	Semi smooth	Medium	N/A	Spotted fossils
68	115 (1)	75	Santa Verna	10YR 6/2	Homogeneous	Dull	Opaque	Smooth	Medium	N/A	Patina covered
69	115 (1)	75	Santa Verna	Limestone							
70	28	7	Santa Verna	5Y 7/2	Heterogenous	Dull	Opaque	Semi smooth	Medium	N/A	Spotted fossils
71	26	3 TrA	Santa Verna	5Y 6/4	Homogeneous	Dull	Opaque	Smooth	Fine	limestone	Spotted fossils
72	27	7(8N/A)	Santa Verna	5Y 7/2	Heterogenous	Dull	Opaque	Semi smooth	Medium	N/A	Spotted fossils
73	29	1	Santa Verna	5Y 7/2	Homogeneous	Dull	Opaque	Semi smooth	Medium	N/A	Spotted fossils
74	156	119	Santa Verna	10YR 6/2	Homogeneous	Pearly shine	Sub-trans	Smooth	Fine	N/A	spots
75	158	119	Santa Verna	10YR 6/2	non-homogeneous	Dull	Opaque	rough	coarse	N/A	N/A
76	33	6	Santa Verna	5Y 7/2	Heterogenous	Dull	Opaque	rough	Medium	N/A	Spotted fossils
77	34	6	Santa Verna	5YR 3/2	Homogeneous	Pearly shine	Sub-trans	Smooth	Fine	N/A	N/A
78	32	5	Santa Verna	5YR 2/1	Homogeneous	Dull	Opaque	Smooth	Fine	N/A	N/A
79	38	8	Santa Verna	10YR 5/4	Homogeneous	Pearly shine	Translucent	Smooth	Fine	N/A	spots
80	17	6	Santa Verna	10YR 6/2	Homogeneous	Pearly shine	Translucent	Smooth	Fine	N/A	N/A
81	13	3	Santa Verna	5Y 6/4	Heterogenous	Dull	Opaque	rough	coarse	N/A	spots
82	10	3	Santa Verna	5Y 6/4	Heterogenous	Dull	Opaque	Semi smooth	Medium	N/A	Spotted fossils

83	24(3)	Trench D	Santa Verna	10 YR 8/2 to 10YR 6/2	Homogeneous	Dull	Opaque	Smooth	Fine	N/A	N/A
84	107	TR D	Santa Verna	10YR 6/2	Homogeneous	Dull	Sub-trans	Semi smooth	Medium	N/A	N/A
85	107	TR D	Santa Verna	10YR 8/2	Homogeneous	Dull	Opaque	Smooth	Medium	N/A	N/A
86	107	TR D	Santa Verna	5Y 7/2	Homogeneous	Dull	Opaque	Smooth	Medium	N/A	N/A
87	N/A (3)	62/TR E	Santa Verna	10 YR 8/2 to 5Y 7/2	Homogeneous	Dull	Opaque	Smooth	Fine	limestone	spots
88	97	N/A	Santa Verna	10YR 6/6	Homogeneous	Pearly shine	Sub-trans	Smooth	Fine	N/A	N/A
89	97 (2)	N/A	Santa Verna	10YR 6/2	Homogeneous	Dull	Opaque	Semi smooth	Medium	N/A	Spotted fossils
90	29(2)	32	Santa Verna	5Y 7/2	Homogeneous	Dull	Opaque	Smooth	Fine	N/A	laminas
91	121	N/A	Santa Verna	5B 5/1 to 5YR 2/1	Homogeneous	Pearly shine	Opaque	Smooth	Fine	N/A	N/A
92	85(1)	14	Santa Verna	10YR 7/4	Homogeneous	Silky shine	Opaque	Smooth	Fine	N/A	N/A
93	85(2)	14	Santa Verna	10YR 6/2	Heterogenous	Dull	Opaque	Semi smooth	Medium	N/A	Spotted fossils
94	85(3,4)	14	Santa Verna	5Y 7/2	Homogeneous	Dull	Opaque	Semi smooth	Medium	N/A	N/A
95	85(5)	14	Santa Verna	10YR 4/2	Homogeneous	Dull	Opaque	Semi smooth	Medium	N/A	Spotted fossils
96	N/A (9)	20	Santa Verna	5Y 8/1	Homogeneous	Dull	Opaque	Semi smooth	Medium	N/A	Spotted fossils
97	N/A (2)	20	Santa Verna	10YR 6/2	Heterogenous	Dull	Opaque	rough	Medium	N/A	Spotted fossils
98	N/A (1)	20	Santa Verna	5Y 7/2	Homogeneous	Dull	Opaque	Semi smooth	Medium	N/A	N/A
99	N/A (1)	20	Santa Verna	10YR 2/2	Heterogenous	Silky shine	Opaque	Semi smooth	Medium	N/A	Spotted fossils
100	N/A	98	Santa Verna	10YR 4/2	Homogeneous	Silky shine	Sub-trans	Semi smooth	Medium	N/A	N/A
101	99	21	Santa Verna	5G 4/1	Heterogenous	Silky shine	Opaque	Smooth	Medium	N/A	Spotted fossils
102	N/A	98	Santa Verna	5YR 3/2	Homogeneous	Pearly shine	Sub-trans	Smooth	Fine	N/A	N/A

103	N/A (3)	95	Santa Verna	10YR 8/2	Homogeneous	Dull	Opaque	Semi smooth	Medium	N/A	Spotted fossils
104	N/A (1)	95	Santa Verna	10YR 6/2	Homogeneous	Dull	Opaque	Semi smooth	Medium	N/A	spots
105	N/A (1)	95	Santa Verna	10YR 6/2	Homogeneous	Dull	Sub-translucent	Smooth	Medium	N/A	N/A
106	N/A (3)	52	Santa Verna	5Y 7/2	Homogeneous	Dull	Opaque	Semi smooth	Medium	N/A	Spotted fossils
107	N/A (1)	52	Santa Verna	10YR 5/4	Homogeneous	Pearly shine	Opaque	Smooth	Fine	N/A	N/A
108	N/A (8)	52 (bottle)	Santa Verna	5Y 8/4	Homogeneous	Dull	Opaque	Semi smooth	Medium	N/A	spots
109	N/A	61	Santa Verna	10YR 4/2	Homogeneous	Pearly shine	Translucent	Smooth	Fine	N/A	N/A
110	N/A	65	Santa Verna	5Y 7/2	Heterogenous	Dull	Opaque	Semi smooth	Medium	N/A	Spotted fossils
111	N/A (7)	68	Santa Verna	5Y 7/2	Homogeneous	Dull	Opaque	Semi smooth	Medium	N/A	Spotted fossils
112	6(1)	65	Santa Verna	5YR 5/6	Homogeneous	Pearly shine	Sub-trans	Smooth	Fine	N/A	N/A
113	6(2)	65	Santa Verna	10YR 6/6	Homogeneous	Pearly shine	Translucent	Smooth	Fine	N/A	N/A
114	6(3)	65	Santa Verna	10YR 6/2	Homogeneous	Dull	Opaque	Semi smooth	Medium	N/A	spots
115	67	34	Santa Verna	10YR 4/2	Homogeneous	Dull	Opaque	Semi smooth	Medium	N/A	N/A
116	N/A	75	Santa Verna	10YR 6/2	Heterogenous	Dull	Opaque	Semi smooth	Medium	N/A	Spotted fossils
117	8(1)	75	Santa Verna	5Y 7/2	Heterogenous	Dull	Opaque	rough	Medium	N/A	Spotted fossils
118	8(2)	75	Santa Verna	10YR 4/2	Heterogenous	Dull	Opaque	rough	Medium	N/A	Spotted fossils
119	N/A (2)	73	Santa Verna	5Y 7/2	Homogeneous	Dull	Opaque	Semi smooth	Medium	N/A	laminas
120	N/A (1)	74	Santa Verna	5YR 5/6	Homogeneous	Pearly shine	Translucent	Smooth	Fine	N/A	N/A
121	N/A (2)	73	Santa Verna	5Y 7/2	Heterogenous	Dull	Opaque	Semi smooth	Medium	N/A	laminas
122	N/A (6)	13 Trench F	Santa Verna	Chert Cortex							

123	N/A (6)	13 Trench F	Santa Verna	Patinated								
124	N/A (5)	13 Trench F	Santa Verna	5Y 7/2	Heterogenous	Dull	Opaque	Semi smooth	Medium	N/A	Spotted fossils	
125	N/A	13 Trench F	Santa Verna	10YR 6/2	Homogeneous	Dull	Sub-trans	Smooth	Fine	N/A	N/A-core and external zone	
126	N/A (11)	78 ss9	Santa Verna	Small fragments unable to describe								
127	N/A (1)	78 ss9	Santa Verna	5R 5/4	Homogeneous	Pearly shine	Sub-trans	Smooth	Fine	N/A	N/A	
128	N/A	3 Tra	Santa Verna	Chert Cortex								
129	N/A	5	Santa Verna	Patinated								
130	N/A (4)	41	Santa Verna	Patinated								
131	N/A (2)	41	Santa Verna	5Y 7/2	Homogeneous	Dull	Opaque	Smooth	Medium	N/A	N/A	
132	N/A (1)	41	Santa Verna	10YR 6/2	Homogeneous	Dull	Opaque	Semi smooth	Medium	N/A	Spotted fossils	
133	N/A (1)	41	Santa Verna	10YR 4/2	Homogeneous	waxy shine	Sub-trans	Semi smooth	Medium	N/A	N/A	
134	N/A (1)	41	Santa Verna	10YR 5/4	Homogeneous	Pearly shine	Translucent	Smooth	Fine	N/A	N/A	
135	N/A (1)	41	Santa Verna	10YR 6/2	Homogeneous	Silky shine	Translucent	Smooth	Fine	N/A	N/A	
136	N/A (6)	46	Santa Verna	Chert Cortex								
137	N/A (5)	42	Santa Verna	5Y 7/2	Heterogenous	Dull	Opaque	Semi smooth	Medium	N/A	Spotted fossils	
138	N/A (2)	42	Santa Verna	5Y 2/1 to 5Y 6/1	Heterogenous	Dull	Opaque	Semi smooth	Medium	N/A	Spotted fossils	
139	N/A (1)	42	Santa Verna	10YR 6/6	Homogeneous	Pearly shine	Opaque	Smooth	Fine	N/A	N/A	
140	N/A (1)	48 SS12	Santa Verna	10YR 5/4	Heterogenous	Dull	Opaque	Smooth	Medium	N/A	Spotted fossils	
141	N/A (4)	48 ss12	Santa Verna	Patinated								
142	N/A	36	Santa Verna	5Y 7/2	Homogeneous	Pearly shine	highly Translucent	Smooth	Fine	N/A	N/A	
143	N/A	33	Santa Verna	10YR 4/2	Homogeneous	Pearly shine	Translucent	Smooth	Fine	N/A	N/A	
144	N/A (3)	38	Santa Verna	Patinated								

145	N/A (2)	38	Santa Verna	10YR 7/4	Homogeneous	Dull	Opaque	Semi smooth	Medium	N/A	Spots fossils
146	N/A (1)	38	Santa Verna	N5	Heterogenous	Dull	Opaque	Semi smooth	Medium	N/A	Spotted fossils
147	N/A (11)	34	Santa Verna	Patinated							
148	N/A (1)	34	Santa Verna	Small fragment unable to describe							
149	N/A (2)	34	Santa Verna	5YR 5/2	Homogeneous	Dull	Opaque	Semi smooth	Medium	N/A	N/A
150	N/A (6)	34	Santa Verna	Patinated							
151	N/A (1)	32	Santa Verna	10YR 6/2	Homogeneous	Dull	Opaque	Semi smooth	Medium	N/A	Spotted fossils
152	N/A (1)	32	Santa Verna	Chert Cortex							
153	N/A (1)	17	Santa Verna	10YR 6/2	Homogeneous	Dull	Opaque	Semi smooth	Medium	N/A	spotted fossils
154	N/A (1)	19W	Santa Verna	Patinated							
155	N/A (1)	19w	Santa Verna	5Y 4/1	Homogeneous	Dull	Opaque	Smooth	Medium	N/A	N/A
156	N/A (1)	16	Santa Verna	10YR 4/2	Homogeneous	waxy shine	Opaque	Semi smooth	Medium	N/A	N/A
157	N/A	19 TRD	Santa Verna	10YR 4/2	Homogeneous	Pearly shine	Opaque	Smooth	Fine	N/A	N/A
158	N/A (4)	g	Santa Verna	Chert Cortex and 3 patinated pieces							
159	N/A	107	Santa Verna	10YR 7/4	Homogeneous	Pearly shine	Opaque	Smooth	Fine	N/A	N/A
160	N/A (7)	104D	Santa Verna	Small fragment unable to describe one is 10R3/4							
161	N/A (2)	38 TRC	Santa Verna	10YR 6/2	Homogeneous	Dull	Opaque	Semi smooth	Medium	N/A	laminas
162	N/A (1)	60	Santa Verna	5YR 6/4	Homogeneous	Dull	Opaque	Semi smooth	Medium	N/A	N/A
163	N/A (12)	20 Trench C	Santa Verna	Patinated							
164	N/A	65	Santa Verna	10YR 2/2	Homogeneous	Dull	Opaque	Smooth	Fine	N/A	N/A
165	N/A (4)	32	Santa Verna	patinated cortex							
166	N/A (1)	20 TRC	Santa Verna	patinated cortex							
167	N/A (13)	20 TRC	Santa Verna	Patinated							

168	N/A (2)	22	Santa Verna	10YR 6/2	Homogeneous	Dull	Opaque	Semi smooth	Medium	N/A	N/A
169	N/A (1)	22	Santa Verna	10R 4/6	Homogeneous	Pearly shine	Opaque	Smooth	Fine	N/A	N/A
170	N/A (1)	39	Santa Verna	5YR 3/2	Homogeneous	Pearly shine	Opaque	Smooth	Fine	N/A	N/A
171	N/A (1)	98	Santa Verna	Chert Cortex							
172	N/A (2)	46	Santa Verna	Chert Cortex							
173	N/A (4)	52	Santa Verna	Chert Cortex							
174	N/A (1)	52	Santa Verna	Not chert but really interesting							
175	N/A (1)	52	Santa Verna	5Y 7/2	Heterogenous	Silky shine	Sub-trans	Semi smooth	Fine	N/A	N/A
176	N/A	68	Santa Verna	Chert Cortex							
177	N/A (1)	16	Santa Verna	5Y 4/1	Homogeneous	Dull	Opaque	Smooth	Fine	N/A	N/A
178	N/A (1)	16	Santa Verna	10YR 7/4	Homogeneous	Dull	Opaque	Semi smooth	Medium	N/A	N/A
179	N/A (8)	17 TRC	Santa Verna	Chert Cortex and patinated pieces							
180	N/A (3)	17 TRC	Santa Verna	5Y 7/2	Homogeneous	Dull	Opaque	Semi smooth	Medium	N/A	Spotted fossils
181	N/A (1)		Santa Verna	5Y 3/2	Homogeneous	Pearly shine	Opaque	Smooth	Fine	N/A	N/A
182	N/A (21)	68 TRG	Santa Verna	Chert Cortex and silicified limestone							
183	N/A (1)	68 TRG	Santa Verna	10R 4/6	Homogeneous	Pearly shine	Sub-trans	Smooth	Fine	N/A	N/A
184	N/A (1)	68 TRG	Santa Verna	N6	PATINAN/A	Pearly shine	Opaque	Smooth	Fine	N/A	N/A
185	N/A (1)	68 TRG	Santa Verna	10YR 5/4	Homogeneous	Pearly shine	Sub-trans	Smooth	Fine	N/A	N/A
186	N/A (1)	68 TRG	Santa Verna	10R 7/4	PATINAN/A	Pearly shine	Opaque	Smooth	Fine	N/A	N/A
187	117	75	Santa Verna	Too small to tell even if it is not chert							
188	N/A	35	Santa Verna	10YR 5/4	Homogeneous	Dull	Opaque	Semi smooth	Medium	N/A	N/A
189	N/A	69	Santa Verna	10YR 6/2	Homogeneous	Dull	Opaque	Semi smooth	Medium	N/A	N/A
190	27	201N/A	Kordin	5Y 2/1	Homogeneous	Silky shine	Opaque	Smooth	Fine	N/A	N/A
191	201	102	Kordin	10YR 6/2	Heterogenous	Dull	Opaque	Semi smooth	Medium	N/A	N/A

192	137(1)	312	Kordin	10YR 5/4	Homogeneous	Dull	Opaque	Semi smooth	Medium	N/A	N/A
193	137(1)	312	Kordin	Patinated							
194	26	201	Kordin	Patinated							
195	N/A (1)	71	Kordin	Chert cortex							
196	N/A (1)	71	Kordin	10YR 7/4	Heterogenous	Dull	Opaque	Semi smooth	Fine	N/A	Spotted fossils
197	103	211	Kordin	10YR 4/2	Homogeneous	Dull	sub-translucent	Semi smooth	Fine	N/A	N/A
198	N/A (1)	71/W	Kordin	Chert cortex							
199	N/A (1)	71/W	Kordin	10YR 6/2	Heterogenous	Dull	Opaque	Semi smooth	Medium	N/A	Spotted fossils
200	123	210	Kordin	10YR 4/2	Homogeneous	Dull	sub-translucent	Semi smooth	Medium	N/A	N/A
201	N/A	77/TrIA	Kordin	Patinated							
202	148	147N/A/IIB	Kordin	Patinated							
203	144	306	Kordin	10YR 6/6	Homogeneous	Pearly shine	Opaque	Smooth	Fine	N/A	N/A
204	156	306/TRIVB/sieve	Kordin	5YR 3/2 to N4	Homogeneous	Pearly shine	Opaque	Smooth	Fine	N/A	N/A
205	121	211	Kordin	10YR 4/2	Homogeneous	Dull	sub-translucent	Smooth	Fine	N/A	N/A
206	120	211/Tr iii	Kordin	chert but too small to describe							
207	100	211	Kordin	10YR 4/2	Homogeneous	Dull	sub-translucent	Smooth	Fine	N/A	N/A
208	137	211	Kordin	10YR 6/2	Homogeneous	Dull	sub-translucent	Semi smooth	Medium	N/A	N/A
209	207	207	Kordin	Patinated, but must be same as 121 and 137							
210	135	209	Kordin	5G 4/1	Homogeneous	Waxy shine	Opaque	Smooth	Fine	N/A	N/A
211	N/A	56(IA)	Kordin	10YR 4/2	Heterogenous	Dull	Opaque	Semi smooth	Medium	N/A	Spotted fossils
212	137	210	Kordin	Patinated							
213	N/A	201	Kordin	Patinated							

214	N/A	57	Kordin	Chert cortex							
215	N/A	<139> (150)	Kordin	10YR 4/2	OTHERWISE chert but too small to describe						
216	9	201	Kordin	10YR 6/2	Homogeneous	Pearly shine	sub-translucent	Smooth	Fine	N/A	N/A
217	N/A (1)	22	Kordin	10YR 6/6	Heterogenous	Dull	Opaque	Semi smooth	Medium	N/A	Spotted fossils
218	N/A (1)	22	Kordin	Chert cortex							
219	107	210	Kordin	chert but too small to describe							
220	62	109N/A	Kordin	10YR 7/4	Homogeneous	Dull	sub-translucent	Smooth	Fine	N/A	N/A
221	133	211	Kordin	10YR 4/2	Homogeneous	Pearly shine	sub-translucent	Smooth	Fine	N/A	N/A
222	109	31/TR I	Kordin	Patinated							
223	N/A	71	Kordin	10YR 7/4 to 5YR 4/4	Homogeneous	Pearly shine	Translucent	Smooth	Fine	N/A	N/A
224	30	207	Kordin	5YR 3/2	Homogeneous	Pearly shine	Translucent	Smooth	Fine	N/A	N/A
225	161	210	Kordin	Patinated							
226	N/A	<2> 1	Kordin	Patinated							
227	153	306	Kordin	Patinated Cortex							
228	N/A	57	Kordin	Chert cortex							
229	61(1)	306	Kordin	Patinated							
230	61(1)	306	Kordin	10YR 4/2	Homogeneous	Pearly shine	sub-translucent	Smooth	Fine	N/A	N/A
231	N/A	57/TRIA	Kordin	5Y 6/4	Heterogenous	Dull	Opaque	rough	Medium	N/A	N/A
232	18	201	Kordin	10YR 4/2	Homogeneous	Pearly shine	sub-translucent	Smooth	Fine	N/A	N/A
233	12	201	Kordin	Patinated							
234	104	210	Kordin	10YR 6/2	Homogeneous	Dull	sub-translucent	Semi smooth	Medium	N/A	N/A
235	147	147 IIB	Kordin	Chert cortex							
236	17	201	Kordin	Patinated							

237	N/A (2)	75/TRIA	Kordin	5Y 6/4	Heterogenous	Dull	Opaque	rough	Medium	N/A	Spotted fossils
238	N/A (1)	75/TRIA	Kordin	Chert cortex							
239	N/A	304	Kordin	Silicified limestone							
240	42	304	Kordin	5YR 8/1	Homogeneous	Pearly shine	Translucent	Smooth	Fine	N/A	N/A
241	27	203	Kordin	10YR 4/2	Homogeneous	Silky shine	sub-translucent	Semi smooth	Fine	N/A	N/A
242	64	211N/A	Kordin	10YR 4/2	Homogeneous	Silky shine	sub-translucent	Semi smooth	Fine	N/A	N/A
243	124	211	Kordin	10YR 6/2	Heterogenous	Dull	Opaque	Semi smooth	Medium	N/A	Spotted fossils
244	34	207	Kordin	10YR 4/2	Homogeneous	Pearly shine	sub-translucent	Smooth	Fine	N/A	N/A
245	86	201	Kordin	10YR 6/2	Homogeneous	Dull	Opaque	Semi smooth	Medium	N/A	N/A
246	80	210	Kordin	10YR 6/2	Homogeneous	Dull	Opaque	Semi smooth	Medium	N/A	N/A
247	69	211	Kordin	10YR 6/2	Homogeneous	Dull	Opaque	Semi smooth	Medium	N/A	N/A
248	78	210	Kordin	10YR 4/2	Homogeneous	Pearly shine	sub-translucent	Smooth	Fine	N/A	N/A
249	16	211	Kordin	10YR 4/2	Homogeneous	Pearly shine	sub-translucent	Smooth	Fine	N/A	N/A
250	46	201	Kordin	Patinated							
251	128	210	Kordin	5YR 5/2	Homogeneous	Dull	sub-translucent	Semi smooth	Medium	N/A	N/A
252	28	207	Kordin	10YR 6/2 4/2	Homogeneous	Dull	Opaque	rough	Medium	N/A	N/A
253	126	210	Kordin	Patinated, white							
254	14	201	Kordin	Patinated, white							
255	82	210	Kordin	10YR 6/2	Homogeneous	Dull	Opaque	Semi smooth	Medium	N/A	N/A
256	94	201	Kordin	10YR 6/2	Homogeneous	Dull	sub-translucent	Semi smooth	Medium	N/A	N/A

257	48	201	Kordin	10YR 4/2	Homogeneous	Dull	sub-translucent	Semi smooth	Medium	N/A	Patinated
258	65	210	Kordin	10YR 6/2	Homogeneous	Dull	Opaque	Semi smooth	Medium	N/A	N/A
259	33	201	Kordin	10YR 4/2	Homogeneous	Dull	Opaque	Semi smooth	Medium	N/A	N/A
260	37	210	Kordin	10YR 4/2	Homogeneous	Dull	sub-translucent	Semi smooth	Medium	N/A	Patinated
261	20	201	Kordin	10YR 4/2	Homogeneous	Dull	sub-translucent	Semi smooth	Medium	N/A	N/A
262	711	210	Kordin	10YR 6/2	Homogeneous	Dull	Opaque	Semi smooth	Medium	N/A	Patinated
263	42	207	Kordin	Patinated							
264	38	201	Kordin	chert but too small to describe							
265	125	210	Kordin	10YR 6/2	Homogeneous	Dull	sub-translucent	rough	Medium	N/A	N/A
266	36	201	Kordin	Patinated							
267	45	201	Kordin	chert but too small to describe							
268	43	207	Kordin	Patinated, looks similar to S33 and S125							
269	134	211	Kordin	10YR 6/2	Homogeneous	Dull	sub-translucent	Semi smooth	Medium	N/A	N/A
270	N/A (1)	1	Kordin	Silicified limestone							
271	N/A (1)	1	Kordin	5YR 2/1	Heterogenous	Dull	Opaque	Semi smooth	Medium	N/A	Spotted fossils
272	127	210	Kordin	Patinated							
273	83	201	Kordin	Patinated, looks similar to S33							
274	115	57	Kordin	10YR 7/4	Homogeneous	Dull	Opaque	Semi smooth	Fine	N/A	Spotted fossils
275	53	201	Kordin	Patinated							
276	47	210	Kordin	10YR 4/2	Homogeneous	Dull	sub-translucent	Semi smooth	Medium	N/A	Patinated
277	47	211	Kordin	10YR 6/2	Homogeneous	Dull	Opaque	Semi smooth	Medium	N/A	N/A

278	16	201	Kordin	10YR 4/2	Homogeneous	Pearly shine	Translucent	Smooth	Fine	N/A	N/A
279	23	207	Kordin	Similar with S16/201							
280	77	201	Kordin	10YR 4/2	Homogeneous	Pearly shine	Translucent	Smooth	Fine	N/A	N/A
281	31	201	Kordin	10YR 6/2	Homogeneous	Silky shine	sub-translucent	Smooth	Fine	N/A	N/A
282	88	208	Kordin	Patinated							
283	52	N/A Tr iii	Kordin	10YR 4/2	Homogeneous	Silky shine	Opaque	Smooth	Fine	N/A	N/A
284	N/A (5)	5 TRIC	Kordin	Patinated							
285	N/A (1)	5 TRIC	Kordin	small lamina of chert not able to describe, most of the sample is limestone							
286	N/A (1)	5 TRIC	Kordin	10YR 7/4	Heterogenous	Dull	Opaque	rough	Medium	N/A	Spotted fossils
287	11	201	Kordin	Patinated							
288	22	201	Kordin	10YR 6/2	Homogeneous	Dull	sub-translucent	Smooth	Fine	N/A	N/A
289	8	301	Kordin	Patinated							
290	21	201	Kordin	5Y 2/1	Heterogenous	Pearly shine	sub-translucent	Semi smooth	Fine	N/A	spotted
291	129	210	Kordin	10YR 6/2	Homogeneous	Dull	sub-translucent	Semi smooth	Medium	N/A	N/A
292	50	211	Kordin	10YR 4/2	Homogeneous	Pearly shine	Translucent	Smooth	Fine	N/A	N/A
293	51	211	Kordin	10YR 6/2	Heterogenous	Dull	Opaque	Semi smooth	Medium	N/A	Spotted fossils
294	73	210	Kordin	10YR 4/2	Homogeneous	Dull	Opaque	Semi smooth	Medium	N/A	N/A
295	77?	Tr iii	Kordin	10YR 6/2	Homogeneous	Silky shine	Translucent	Smooth	Fine	N/A	N/A
296	163	215	Kordin	10YR 6/2	Homogeneous	Dull	Opaque	Semi smooth	Medium	N/A	N/A
297	98	201	Kordin	10YR 4/2	Homogeneous	Pearly shine	Opaque	Smooth	Fine	N/A	N/A
298	10	201	Kordin	10YR 6/2	Homogeneous	Pearly shine	sub-translucent	Semi smooth	Fine	N/A	N/A
299	25	201	Kordin	10YR 6/2	Homogeneous	Dull	Opaque	Semi smooth	Medium	N/A	N/A

300	142	209	Kordin	Patinated							
301	70	211	Kordin	10YR 6/2	Homogeneous	Dull	Opaque	rough	Medium	N/A	N/A
302	145	212	Kordin	Silicified limestone							
303	99	201	Kordin	10YR 6/2	Homogeneous	Pearly shine	sub-translucent	Semi smooth	Medium	N/A	N/A
304	35	207	Kordin	10YR 4/2	Homogeneous	Pearly shine	sub-translucent	Smooth	Medium	N/A	N/A
305	41	201	Kordin	Patinated							
306	68	210	Kordin	10YR 4/2	Homogeneous	Silky shine	Translucent	Semi smooth	Medium	N/A	N/A
307	54	211	Kordin	Patinated							
308	49	201	Kordin	Patinated							
309	N/A	210	Kordin	10YR 4/2	Homogeneous	Pearly shine	Translucent	Semi smooth	Fine	N/A	N/A
310	141	150N/A TRIIB	Kordin	5Y 3/2	Homogeneous	Pearly shine	Opaque	Semi smooth	Fine	N/A	N/A
311	97	210	Kordin	10YR 4/2	Homogeneous	Silky shine	sub-translucent	Semi smooth	Fine	N/A	N/A
312	6(1)	304	Kordin	5YR 7/2	Homogeneous	Pearly shine	Highly translucent	Smooth	Fine	N/A	N/A
313	6(1)	304	Kordin	5YR 6/4	Chert too small to describe						
314	105	N/A Tr iii	Kordin	10YR 4/2	Homogeneous	Silky shine	sub-translucent	Semi smooth	Fine	N/A	N/A
315	121	306	Kordin	Patinated							
316	87	201	Kordin	too small to describe							
317	32	207	Kordin	10YR 6/2	Homogeneous	Dull	Opaque	Semi smooth	Medium	N/A	N/A
318	124	306	Kordin	Patinated							
319	N/A	211	Kordin	10YR 6/2	Homogeneous	Pearly shine	Opaque	Semi smooth	Fine	N/A	N/A
320	128	312	Kordin	N6	Homogeneous	Pearly shine	Opaque	Semi smooth	Fine	N/A	N/A
321	147	N/A	Kordin	too small to describe							

322	157	306	Kordin	10YR 6/6	Homogeneous	Pearly shine	Opaque	Smooth	Fine	N/A	N/A
323	163	306	Kordin	Chert cortex or coralline limestone							
324	130	211	Kordin	Chert cortex							
325	105	211	Kordin	10YR 6/2	Homogeneous	Dull	Opaque	Semi smooth	Medium	N/A	N/A
326	147	215	Kordin	5YR 8/1	Homogeneous	Pearly shine	Translucent	Smooth	Fine	N/A	N/A
327	151	306	Kordin	Silicified limestone							
328	40	207	Kordin	Patinated							
329	164	306	Kordin	Chert cortex or coralline limestone							
330	101	211	Kordin	too small to describe							
331	13	201	Kordin	Patinated							
332	89	209	Kordin	10YR 4/2	Homogeneous	Pearly shine	sub-translucent	Semi smooth	Fine	N/A	N/A
333	5	304	Kordin	N4	too small to describe further						
334	63	116	Kordin	Patinated							
335	N/Aiii	201	Kordin	Patinated							
336	57	100	Tac Cawla	10YR 4/2	Homogeneous	Dull	Opaque	Semi smooth	Fine	N/A	N/A
337	265	157	Tac Cawla	10YR 7/4	Heterogenous	Dull	Opaque	Semi smooth	Medium	N/A	N/A
338	109	119	Tac Cawla	Patinated							
339	101	85	Tac Cawla	5Y 2/1	Homogeneous	Pearly shine	Opaque	Smooth	Fine	N/A	N/A
340	63	91	Tac Cawla	10YR 6/6	Homogeneous	Pearly shine	sub-translucent	Smooth	Fine	N/A	N/A
341	103	85	Tac Cawla	10YR 6/6	Homogeneous	Pearly shine	sub-translucent	Smooth	Fine	N/A	N/A
342	87	77	Tac Cawla	Patinated							
343	188	178/191	Tac Cawla	10YR 4/2	Homogeneous	Dull	Opaque	Semi smooth	Fine	N/A	N/A
344	66	74	Tac Cawla	10YR 4/2	Homogeneous	Dull	Opaque	Semi smooth	Medium	N/A	N/A

345	49	63	Tac Cawla	10YR 4/2	Homogeneous	Dull	Opaque	Semi smooth	Fine	Yes	N/A
346	66	74	Tac Cawla	10YR 6/2	Homogeneous	Dull	Opaque	Semi smooth	Medium	N/A	N/A
347	1	1	Tac Cawla	too eroded to describe							
348	110	Tr I	Tac Cawla	Patinated							
349	160	N/A	Tac Cawla	10YR 4/2 to 10YR 6/2	Homogeneous	Pearly shine	Opaque	Smooth	Medium	N/A	N/A
350	344	164	Tac Cawla	N9	Patinated if it is chert, very rare to be so white						
351	361	244	Tac Cawla	10YR 7/4	Homogeneous	Dull	Opaque	Semi smooth	Medium	Globo limestone	Spotted fossils
352	342	211	Tac Cawla	5Y 5/2	Homogeneous	Silky shine	Opaque	Smooth	Fine	N/A	N/A
353	449	273	Tac Cawla	Possibly patinated, it's difficult to describe							
354	491	301	Tac Cawla	10YR 6/2	Homogeneous	Silky shine	Opaque	Semi smooth	Medium	N/A	N/A
355	480	286	Tac Cawla	10YR 4/2	Homogeneous	Pearly shine	Opaque	Smooth	Fine	N/A	N/A
356	484	272	Tac Cawla	10YR 6/2	Homogeneous	Dull	Opaque	Semi smooth	Medium	N/A	N/A
357	376	243	Tac Cawla	too eroded to describe							
358	369	246	Tac Cawla	N3	Homogeneous	Silky shine	Opaque	Smooth	Fine	N/A	N/A
359	362	243	Tac Cawla	chert cortex							
360	368	233	Tac Cawla	chert cortex							
361	360	N/A	Tac Cawla	too small to describe							
362	366	244	Tac Cawla	10YR 7/4 to 10YR 4/2	Homogeneous	Pearly shine	Opaque	Semi smooth	Fine	N/A	Spotted fossils
363	379	244	Tac Cawla	too small to describe							
364	378	244	Tac Cawla	5Y 7/2	Homogeneous	Pearly shine	Opaque	Smooth	Fine	N/A	Spotted fossils
365	367	233	Tac Cawla	5Y 5/2	Homogeneous	Dull	Opaque	Semi smooth	Medium	N/A	Spotted fossils
366	365	244	Tac Cawla	10YR 6/2	Homogeneous	Dull	Opaque	Semi smooth	Medium	N/A	Spotted fossils

367	363		Tac Cawla	10YR 6/2	Homogeneous	Dull	Opaque	Semi smooth	Medium	N/A	N/A
368	375	251	Tac Cawla	N2	otherwise too small describe						
369	371	243	Tac Cawla	too eroded to describe							
370	377	244	Tac Cawla	too small to describe							
371	309	206/233N/A	Tac Cawla	5YR 5/6	Homogeneous	Pearly shine	translucent	Smooth	Fine	N/A	N/A
372	315	139	Tac Cawla	5Y 4/1	Homogeneous	Pearly shine	Opaque	Smooth	Fine	N/A	N/A
373	305	136	Tac Cawla	Patinated							
374	311	233	Tac Cawla	Patinated							
375	319	208	Tac Cawla	too small to describe							
376	314	N/A	Tac Cawla	5YR 2/2	Heterogenous	Pearly shine	translucent	Semi smooth	Fine	N/A	N/A
377	316	139	Tac Cawla	10YR 5/4	Homogeneous	Pearly shine	sub-translucent	Smooth	Fine	N/A	N/A
378	316b	63	Tac Cawla	N3	Homogeneous	Pearly shine	Opaque	Smooth	Fine	N/A	N/A
379	312	233	Tac Cawla	too eroded to describe, might be silicified limestone							
380	317	208	Tac Cawla	chert cortex							
381	313	136	Tac Cawla	10YR 7/4	Homogeneous	Dull	Opaque	Semi smooth	Medium	N/A	Spotted fossils
382	302	208	Tac Cawla	Patinated							
383	301	208	Tac Cawla	too eroded to describe							
384	300	136	Tac Cawla	Patinated							
385	N/A	185	Tac Cawla	too small to describe							
386	602	276 ss 153	Tac Cawla	10YR 4/2	too small to describe OTHERWISE						
387	604	206	Tac Cawla	too small to describe							
388	N/A	148	Tac Cawla	10YR 6/2	Homogeneous	Dull	Opaque	rough	Medium	N/A	Spotted fossils
389	563	93 ss93	Tac Cawla	10YR 7/4	Homogeneous	Dull	Opaque	rough	Medium	N/A	N/A
390	570 (3)	139	Tac Cawla	10YR 6/2 to 5Y 7/2	Homogeneous	Dull	Opaque	Semi smooth	Medium	N/A	spots

391	559	178N/A Ss103	Tac Cawla	10R 4/6	Homogeneous	Pearly shine	translucent	Smooth	Fine	N/A	N/A
392	558	286 ss64	Tac Cawla	too small to describe							
393	N/A	233	Tac Cawla	Patinated							
394	566	280 ss161	Tac Cawla	chert cortex or silicified limestone, with 4 pieces in the bag							
395	557	233	Tac Cawla	too small to describe							
396	568	120 ss169	Tac Cawla	5R 7/4							
397	543	208 ss120	Tac Cawla	too small to describe							
398	561	129	Tac Cawla	5Y 4/1	Homogeneous	Silky shine	Opaque	Smooth	Fine	N/A	N/A
399	576	261	Tac Cawla	too small to describe							
400	585	206	Tac Cawla	5Y 7/2	Heterogenous	Dull	Opaque	Semi smooth	Medium	N/A	spots
401	590	261	Tac Cawla	unable to describe							
402	591	268	Tac Cawla	chert cortex or silicified limestone							
403	588	139	Tac Cawla	5Y 7/2	Homogeneous	Dull	Opaque	Smooth	Fine	N/A	Spotted fossils
404	587	136N/A	Tac Cawla	chert cortex							
405	577	131	Tac Cawla	5R 6/2	Homogeneous	Pearly shine	translucent	Smooth	Fine	N/A	N/A
406	553	139 ssS62	Tac Cawla	10R 4/2	Heterogenous	Pearly shine	sub-translucent	Smooth	Fine	N/A	spots
407	592	268	Tac Cawla	chert cortex or silicified limestone							
408	N/A	168 ss137	Tac Cawla	chert cortex or silicified limestone							
409	559	85 ss50	Tac Cawla	5Y 4/1	Heterogenous	Silky shine	Opaque	Semi smooth	Medium	N/A	Spotted fossils
410	584	178	Tac Cawla	chert cortex							
411	556	206 ss 74	Tac Cawla	too small to describe							
412	554 (2)	261 ss139	Tac Cawla	chert cortex or silicified limestone							
413	554 (1)	261 ss139	Tac Cawla	10R 4/2	Homogeneous	Dull	Opaque	Semi smooth	Fine	N/A	spots
414	582	233/243	Tac Cawla	Patinated							

415	574	301	Tac Cawla	10YR 7/4	Homogeneous	Dull	Opaque	Semi smooth	Medium	N/A	N/A
416	583	261	Tac Cawla	chert cortex							
417	564 (1)	205	Tac Cawla	Patinated							
418	564 (1)	205	Tac Cawla	5Y 4/1 to 5Y 2/1	Heterogenous	Pearly shine	Opaque	Smooth	Fine	N/A	N/A
419	569	268 ss154	Tac Cawla	chert cortex							
420	572	268 ss143	Tac Cawla	5Y 7/2	Homogeneous	Silky shine	Opaque	Semi smooth	Medium	N/A	Spotted fossils
421	481	272	Tac Cawla	too small to describe							
422	481	272	Tac Cawla	10R 4/6	Homogeneous	Pearly shine	translucent	Smooth	Fine	N/A	N/A
423	494	301	Tac Cawla	10YR 6/2	Homogeneous	Silky shine	Opaque	Semi smooth	Fine	Yes	N/A
424	492	301	Tac Cawla	10YR 6/2	Homogeneous	Dull	Opaque	Semi smooth	Medium	N/A	N/A
425	497	301	Tac Cawla	10YR 6/2	Homogeneous	Dull	Opaque	Semi smooth	Medium	N/A	N/A
426	493	301	Tac Cawla	10YR 6/2	Homogeneous	Dull	Opaque	Semi smooth	Medium	N/A	N/A
427	485	272	Tac Cawla	10YR 6/2	Homogeneous	Dull	Opaque	Semi smooth	Medium	N/A	N/A
428	482	272	Tac Cawla	10YR 6/2	Homogeneous	Dull	Opaque	Semi smooth	Medium	Yes	N/A
429	489	292	Tac Cawla	10YR 6/2	Homogeneous	Dull	Opaque	Semi smooth	Medium	N/A	N/A
430	499	301	Tac Cawla	10YR 6/2	Homogeneous	Dull	Opaque	Semi smooth	Medium	N/A	N/A
431	495	301	Tac Cawla	too eroded to describe, possibly chert cortex							
432	483	N/A	Tac Cawla	Patinated and too small to describe							
433	498	301	Tac Cawla	N3	Heterogenous	Dull	Opaque	Semi smooth	Medium	N/A	Spotted fossils
434	487	292	Tac Cawla	5YR 7/2	Homogeneous	Dull	Opaque	Semi smooth	Medium	N/A	Spotted fossils
435	486	272	Tac Cawla	chert cortex							

436	490	292	Tac Cawla	chert cortex or silicified limestone								
437	357	243	Tac Cawla	N3	Heterogenous	Dull	Opaque	Semi smooth	Medium	N/A	Spotted fossils	
438	343	205	Tac Cawla	N3	Heterogenous	Dull	Opaque	Semi smooth	Medium	N/A	Spotted fossils	
439	358	243	Tac Cawla	chert cortex								
440	340	205	Tac Cawla	chert cortex								
441	355	244	Tac Cawla	10YR 7/4	Homogeneous	Dull	Opaque	Semi smooth	Medium	N/A	spots	
442	354	243	Tac Cawla	too small to describe								
443	356	243	Tac Cawla	too small to describe, but possibly chert cortex								
444	352	247	Tac Cawla	10R 4/6	Homogeneous	Pearly shine	translucent	Smooth	Fine	N/A	N/A	
445	sf511	286	Tac Cawla	10YR 6/2	Homogeneous	Dull	Opaque	Semi smooth	Medium	Yes	N/A	
446	517	269	Tac Cawla	10YR 6/2	Homogeneous	Dull	Opaque	rough	Medium	Yes	N/A	
447	508	272	Tac Cawla	chert cortex								
448	505 (1)	261	Tac Cawla	too eroded to describe								
449	505 (3)	261	Tac Cawla	too small to describe								
450	501	301	Tac Cawla	10YR 7/4	Homogeneous	Dull	Opaque	rough	Medium	N/A	N/A	
451	503	301	Tac Cawla	10YR 6/2	Homogeneous	Dull	Opaque	rough	Medium	N/A	N/A	
452	504	261	Tac Cawla	too small to describe								
453	513	272	Tac Cawla	10YR 6/2	Heterogenous	Dull	Opaque	Semi smooth	Medium	N/A	Spotted fossils	
454	516	268	Tac Cawla	chert cortex								
455	512	N/A	Tac Cawla	too small to describe								
456	sf509?	272	Tac Cawla	chert cortex								
457	320	205	Tac Cawla	N3	Homogeneous	Dull	Opaque	Semi smooth	Medium	N/A	Spotted fossils	
458	sf338	244	Tac Cawla	Patinated								
459	322	205	Tac Cawla	too small to describe								

460	337	245	Tac Cawla	5Y 3/2	Homogeneous	Pearly shine	sub-translucent	Smooth	Fine	N/A	N/A	
461	334 (1)	233	Tac Cawla	Patinated								
462	334 (1)	233	Tac Cawla	10YR 7/4	Homogeneous	Dull	Opaque	Semi smooth	Medium	N/A	Spotted fossils	
463	334 (1)	233	Tac Cawla	10YR 6/2	Heterogenous	Dull	Opaque	rough	Medium	N/A	N/A	
464	324	139	Tac Cawla	Patinated								
465	321	233	Tac Cawla	too small to describe								
466	330	211	Tac Cawla	chert cortex	or silicified limestone							
467	328	139	Tac Cawla	chert cortex	or silicified limestone							
468	325 (1)	139	Tac Cawla	10YR 7/4	Heterogenous	Dull	Opaque	Semi smooth	Medium	N/A	Spotted fossils	
469	325 (2)	139	Tac Cawla	10YR 6/2	Heterogenous	Dull	Opaque	Semi smooth	Medium	N/A	Spotted fossils	
470	325 (1)	139	Tac Cawla	5YR 5/6	Homogeneous	Pearly shine	translucent	Smooth	Fine	N/A	N/A	
471	323	233	Tac Cawla	chert cortex or external part of chert								
472	324	211	Tac Cawla	too eroded to describe								
473	sf439N/A	262	Tac Cawla	10YR 5/4	Homogeneous	Silky shine	sub-translucent	Smooth	Fine	N/A	N/A	
474	427	179	Tac Cawla	5YR 6/4	Homogeneous	Dull	Opaque	Semi smooth	Medium	N/A	N/A	
475	437	N/A	Tac Cawla	too small to describe								
476	420	63	Tac Cawla	10YR 6/2	Homogeneous	Dull	Opaque	Semi smooth	Medium	N/A	N/A	
477	426	126	Tac Cawla	Patinated								
478	428	136	Tac Cawla	10YR 6/2	Heterogenous	Dull	Opaque	Semi smooth	Medium	N/A	Spotted fossils	
479	416	178	Tac Cawla	5YR 2/1	Homogeneous	Pearly shine	translucent	Smooth	Fine	N/A	spots	
480	401	209	Tac Cawla	10R 4/6	Homogeneous	Pearly shine	Opaque	Smooth	Fine	N/A	N/A	
481	419 (1)	178	Tac Cawla	10YR 6/2	Homogeneous	Dull	Opaque	Semi smooth	Medium	N/A	N/A	
482	419 (1)	178	Tac Cawla	10YR 4/2	Homogeneous	Silky shine	sub-translucent	Smooth	Fine	N/A	N/A	

483	403	261	Tac Cawla	10YR 6/2	Homogeneous	Pearly shine	sub-translucent	Smooth	Fine	N/A	N/A
484	405	266	Tac Cawla	10YR 7/4	Homogeneous	Pearly shine	sub-translucent	Smooth	Fine	N/A	N/A
485	411	214	Tac Cawla	5Y 5/2	Homogeneous	Dull	Opaque	Smooth	Medium	N/A	N/A
486	418	999	Tac Cawla	Patinated							
487	413	233	Tac Cawla	5Y 7/2	Homogeneous	Dull	Opaque	Semi smooth	Medium	N/A	Spotted fossils
488	410 (1)	261	Tac Cawla	5Y 7/2	Heterogenous	Dull	Opaque	Semi smooth	Medium	N/A	Spotted fossils
489	410 (1)	261	Tac Cawla	chert cortex							
490	415	206	Tac Cawla	too small to describe							
491	408	261	Tac Cawla	Patinated							
492	407	261	Tac Cawla	10YR 6/2	Homogeneous	Dull	Opaque	Semi smooth	Medium	N/A	Spotted fossils
493	403	261	Tac Cawla	chert cortex							
494	406	261	Tac Cawla	5Y 7/2	Heterogenous	Dull	Opaque	Semi smooth	Medium	N/A	Spotted fossils
495	404 (1)	261	Tac Cawla	Patinated							
496	404 (1)	261	Tac Cawla	too small to describe							
497	400 (1)	261	Tac Cawla	Patinated							
498	400 (2)	261	Tac Cawla	too eroded to describe							
499	390	261	Tac Cawla	too small to describe							
500	385	261	Tac Cawla	too small to describe							
501	384 (1)	244	Tac Cawla	10YR 7/4	Heterogenous	Dull	Opaque	Smooth	Medium	N/A	Spotted fossils
502	384 (1)	244	Tac Cawla	5Y 7/2	Homogeneous	Dull	Opaque	Smooth	Medium	N/A	N/A
503	384 (4)	244	Tac Cawla	chert cortex							
504	386 (1)	168	Tac Cawla	10YR 6/6	Homogeneous	Pearly shine	sub-translucent	Smooth	Fine	N/A	N/A
505	396 (1)	243	Tac Cawla	too small to describe							

506	389 (1)	261	Tac Cawla	Patinated								
507	381	235	Tac Cawla	10YR 6/2	Homogeneous	Dull	Opaque	Semi smooth	Medium	N/A	N/A	
508	383	235	Tac Cawla	10YR 6/2	Homogeneous	Dull	Opaque	Semi smooth	Medium	N/A	N/A	
509	380	243	Tac Cawla	chert cortex								
510	388	261	Tac Cawla	10YR 6/2	Heterogenous	Dull	Opaque	Semi smooth	Medium	N/A	N/A	
511	398	262	Tac Cawla	Patinated								
512	393	261	Tac Cawla	too small to describe								
513	465	271?	Tac Cawla	10 YR 6/2 to 10YR 4/2	Homogeneous	Dull	Opaque	Semi smooth	Medium	Yes	N/A	
514	460	273	Tac Cawla	5YR 5/6	Homogeneous	Pearly shine	Opaque	Smooth	Fine	N/A	N/A	
515	462	273	Tac Cawla	too small to describe								
516	478	272	Tac Cawla	N3	Heterogenous	Dull	Opaque	Semi smooth	Medium	N/A	Spotted fossils	
517	477	272	Tac Cawla	too small to describe								
518	469	272	Tac Cawla	Patinated								
519	467	272	Tac Cawla	too small to describe								
520	476	245	Tac Cawla	5Y 3/2	Homogeneous	Pearly shine	Opaque	Semi smooth	Medium	Yes	N/A	
521	479 (1)	272	Tac Cawla	too eroded to describe								
522	479 (1)	272	Tac Cawla	too small to describe								
523	461	272	Tac Cawla	too small to describe								
524	456	268	Tac Cawla	too small to describe								
525	455	273	Tac Cawla	too small to describe								
526	458	273	Tac Cawla	too small to describe								
527	452	273	Tac Cawla	too small to describe								
528	444	271	Tac Cawla	Patinated								
529	459 (1)	273	Tac Cawla	10YR 6/2	Homogeneous	Dull	Opaque	Smooth	Medium	N/A	spots	

530	459 (1)	273	Tac Cawla	chert cortex								
531	457	272	Tac Cawla	10YR 6/2	Homogeneous	Dull	Opaque	Semi smooth	Medium	N/A	N/A	
532	440	TAF	Tac Cawla	10YR 6/2	Homogeneous	Dull	Opaque	Semi smooth	Medium	N/A	N/A	
533	454	261	Tac Cawla	chert cortex								
534	445	155	Tac Cawla	N6	Homogeneous	Pearly shine	translucent	Smooth	Fine	N/A	N/A	
535	sf536	136	Tac Cawla	10YR 8/2	Homogeneous	Silky shine	translucent	Semi smooth	Fine	N/A	N/A	
536	526	261	Tac Cawla	chert cortex								
537	528	261	Tac Cawla	too eroded to describe								
538	sf542 (1)	228	Tac Cawla	5Y 7/2	Homogeneous	Dull	Opaque	Semi smooth	Medium	N/A	spots	
539	sf542 (2)	228	Tac Cawla	chert cortex								
540	sf521	243	Tac Cawla	10YR 4/2	Homogeneous	Dull	Opaque	Semi smooth	Fine	N/A	N/A	
541	547	243 ss138	Tac Cawla	too small to describe								
542	525	261	Tac Cawla	5Y 7/2	Homogeneous	Dull	Opaque	Semi smooth	Medium	N/A	N/A	
543	sf533	74	Tac Cawla	10YR 4/2	Homogeneous	Dull	Opaque	Semi smooth	Medium	Yes	N/A	
544	sf540	259	Tac Cawla	unable to describe								
545	532	301	Tac Cawla	Patinated								
546	544 (2)	206	Tac Cawla	10YR 6/2	Homogeneous	Dull	Opaque	Semi smooth	Medium	N/A	spots	
547	524	130	Tac Cawla	chert cortex								
548	538	103	Tac Cawla	unable to describe								
549	522 (2)	136	Tac Cawla	5Y 7/2	Homogeneous	Dull	Opaque	Semi smooth	Medium	N/A	spots	
550	539	261	Tac Cawla	chert cortex								
551	500	301	Tac Cawla	10YR 4/2	Homogeneous	Pearly shine	Opaque	Smooth	Fine	Yes	N/A	

552	502	301	Tac Cawla	10YR 6/2	Homogeneous	Dull	Opaque	Semi smooth	Medium	Yes	N/A
553	sf515	281	Tac Cawla	10YR 6/2	Homogeneous	Dull	Opaque	Semi smooth	Medium	Yes	N/A
554	589	58	Tac Cawla	N3	Heterogenous	Dull	Opaque	Smooth	Medium	N/A	N/A
555	545	206	Tac Cawla	N7	Homogeneous	Pearly shine	highly translucent	Smooth	Fine	Yes	N/A
556	578	273	Tac Cawla	chert cortex or silicified limestone							
557	595	81	Tac Cawla	5YR 4/1 or 10R 4/2	Heterogenous	Silky shine	sub-translucent	Smooth	Fine	N/A	N/A
558	558	286	Tac Cawla	Patinated							
559	600	261	Tac Cawla	too small to describe							
560	16	cxt71	Tac Cawla	10YR 6/2	Homogeneous	Dull	Opaque	rough	Medium	Yes	N/A
561	sf12	cxt55	Tac Cawla	too eroded to describe							
562	14	34	Tac Cawla	Patinated							
563	sf13	trench I	Tac Cawla	chert cortex							
564	17	69	Tac Cawla	10YR 6/2	Homogeneous	Silky shine	sub-translucent	Smooth	Fine	N/A	N/A
565	8 (2)	TRZ top soil	Tac Cawla	chert cortex							
566	10? (1)	1 TR I	Tac Cawla	chert cortex							
567	3 (2)	27	Tac Cawla	5Y 7/2	Homogeneous	Dull	Opaque	Smooth	Medium	Yes	
568	sf18 (1)	cxt69 TRI	Tac Cawla	too small to describe							
569	200	178	Tac Cawla	5R 5/4	Homogeneous	Pearly shine	Opaque	Smooth	Fine	N/A	N/A
570	218	178	Tac Cawla	N6	too small to describe further						
571	201	178	Tac Cawla	chert cortex							
572	206	178	Tac Cawla	Patinated							
573	215	174	Tac Cawla	5Y 7/2	Homogeneous	Dull	Opaque	Semi smooth	Medium	N/A	spots
574	217	178	Tac Cawla	5Y 7/2	Homogeneous	Dull	Opaque	Semi smooth	Medium	N/A	spots

575	203	63	Tac Cawla	10YR 4/2	Homogeneous	Silky shine	sub-translucent	Semi smooth	Fine	Yes	N/A	
576	219	161	Tac Cawla	10YR 4/2	Homogeneous	Pearly shine	sub-translucent	Semi smooth	Fine	N/A	N/A	
577	205	69	Tac Cawla	chert cortex or silicified limestone								
578	131	144	Tac Cawla	10YR 6/2	Homogeneous	Dull	Opaque	rough	Medium	N/A	N/A	
579	120	130	Tac Cawla	5YR 2/1	Homogeneous	Pearly shine	translucent	Smooth	Fine	N/A	spots	
580	135	71	Tac Cawla	chert cortex								
581	138	26	Tac Cawla	Patinated								
582	122	130	Tac Cawla	Patinated								
583	127	134	Tac Cawla	Patinated								
584	139	26	Tac Cawla	10YR 6/2	Homogeneous	Dull	Opaque	Semi smooth	Medium	N/A	N/A	
585	129	144	Tac Cawla	too small to describe								
586	124	71	Tac Cawla	Patinated or silicified limestone								
587	133	126	Tac Cawla	Patinated							Yes	
588	136	26	Tac Cawla	too small to describe								
589	126	73	Tac Cawla	chert cortex								
590	132	126	Tac Cawla	chert cortex								
591	128	134	Tac Cawla	10YR 6/6	Homogeneous	Pearly shine	Opaque	Smooth	Fine	N/A	N/A	
592	102	85	Tac Cawla	10YR 4/2	Homogeneous	Pearly shine	sub-translucent	Smooth	Fine	Yes	N/A	
593	112	85	Tac Cawla	5YR 2/2	Homogeneous	Pearly shine	translucent	Smooth	Fine	N/A	N/A	
594	114	81	Tac Cawla	10YR 6/6	Homogeneous	Pearly shine	Opaque	Smooth	Fine	N/A	N/A	
595	118	134	Tac Cawla	chert cortex								
596	107	120	Tac Cawla	chert cortex eroded								
597	115 (1)	130	Tac Cawla	10YR 6/2	Heterogenous	Dull	Opaque	Semi smooth	Medium	N/A	N/A	
598	115 (1)	130	Tac Cawla	Patinated								
599	25 (2)	1 TR I	Tac Cawla	too small to describe								

600	23 (2)	63	Tac Cawla	chert cortex or silicified limestone								
601	28	ctx69	Tac Cawla	5Y 7/2	Homogeneous	Dull	Opaque	Semi smooth	Medium	N/A	spots	
602	21	64	Tac Cawla	chert cortex								
603	sf27	ctx69	Tac Cawla	chert cortex or silicified limestone								
604	22 (2)	69	Tac Cawla	chert cortex								
605	22 (1)	69	Tac Cawla	too small to describe								
606	97 (1)	80	Tac Cawla	10YR 7/4	Homogeneous	Dull	Opaque	Semi smooth	Medium	N/A	N/A	
607	95	N/A	Tac Cawla	10YR 6/2	Homogeneous	Dull	Opaque	Semi smooth	Medium	N/A	N/A	
608	96	71	Tac Cawla	10YR 7/4	Homogeneous	Dull	Opaque	rough	Medium	N/A	N/A	
609	81	74	Tac Cawla	10YR 4/2	Homogeneous	Silky shine	translucent	Smooth	Fine	N/A	N/A	
610	80	71	Tac Cawla	chert cortex or silicified limestone								
611	89	85	Tac Cawla	too small to describe								
612	86 (1)	30	Tac Cawla	Patinated								
613	86 (1)	30	Tac Cawla	5Y 3/2	Homogeneous	Silky shine	Opaque	Semi smooth	Medium	N/A	N/A	
614	99 (1)	80	Tac Cawla	Patinated if it is chert, very rare to be so white								
615	82 (3)	77	Tac Cawla	Patinated								
616	98	71	Tac Cawla	10YR 6/2	Homogeneous	Dull	Opaque	Semi smooth	Medium	N/A	N/A	
617	92 (1)	70	Tac Cawla	Patinated								
618	92 (1)	70	Tac Cawla	10YR 4/2	Homogeneous	Silky shine	sub-translucent	Semi smooth	Medium	N/A	N/A	
619	92 (2)	70	Tac Cawla	too small to describe								
620	197	178	Tac Cawla	10YR 8/2	Homogeneous	Dull	Opaque	Smooth	Fine	N/A	spots	
621	183	136	Tac Cawla	5Y 7/2	Homogeneous	Dull	Opaque	Semi smooth	Medium	N/A	spots	
622	194	69	Tac Cawla	If it is chert, patinated								
623	191	26	Tac Cawla	chert cortex or silicified limestone								

624	214	178	Tac Cawla	too small to describe							
625	193	69	Tac Cawla	10YR 5/4	Homogeneous	Pearly shine	translucent	Smooth	Fine	N/A	N/A
626	190	179	Tac Cawla	10YR 4/2	Homogeneous	Dull	Opaque	Smooth	Fine	Yes	N/A
627	187	191	Tac Cawla	10YR 4/2	Homogeneous	Silky shine	sub-translucent	Semi smooth	Fine	N/A	N/A
628	SF185	185Trl	Tac Cawla	10YR 4/2	Homogeneous	Silky shine	sub-translucent	Semi smooth	Fine	N/A	N/A
629	213	195	Tac Cawla	too small to describe							
630	192	69	Tac Cawla	5GY 4/1	Homogeneous	Pearly shine	Opaque	Semi smooth	Fine	N/A	N/A
631	198 (2)	178	Tac Cawla	too small to describe							
632	51 (2)	89	Tac Cawla	10YR 6/2	Heterogenous	Dull	Opaque	Semi smooth	Medium	N/A	N/A
633	51 (1)	89	Tac Cawla	10YR 4/2	Homogeneous	Silky shine	Opaque	Semi smooth	Fine	N/A	N/A
634	51 (1)	89	Tac Cawla	5Y 7/2	Homogeneous	Dull	Opaque	Smooth	Fine	N/A	spots
635	59	77	Tac Cawla	If it is chert, patinated							
636	60 (1)	93	Tac Cawla	Patinated							
637	53	83	Tac Cawla	too small to describe							
638	64 (2)	91	Tac Cawla	10YR 4/2	Homogeneous	Silky shine	Opaque	rough	Medium	N/A	N/A
639	64 (1)	91	Tac Cawla	too small to describe							
640	58	100	Tac Cawla	10YR 6/2	Homogeneous	Dull	Opaque	rough	Medium	N/A	N/A
641	65	74	Tac Cawla	10YR 6/2	Homogeneous	Dull	Opaque	Semi smooth	Medium	Yes	N/A
642	55	91	Tac Cawla	too small to describe							
643	50	100	Tac Cawla	10YR 6/2	Homogeneous	Dull	Opaque	Semi smooth	Medium	N/A	N/A
644	56	100	Tac Cawla	chert cortex							
645	62	91	Tac Cawla	Patinated							
646	67? (1)	83	Tac Cawla	Patinated							
647	67? (1)	83	Tac Cawla	chert cortex							

648	67? (1)	83	Tac Cawla	10YR 6/2	Homogeneous	Dull	Opaque	rough	Medium	N/A	N/A
649	68	91	Tac Cawla	If it is chert, patinated							
650	144	N/A	Tac Cawla	5Y 4/4	Homogeneous	Pearly shine	Opaque	Smooth	Fine	N/A	N/A
651	156	154	Tac Cawla	10YR 6/2 to 5Y 7/2	Homogeneous	Pearly shine	translucent	Smooth	Fine	N/A	spots
652	141	21	Tac Cawla	If it is chert, patinated							
653	153	162	Tac Cawla	too small to describe							
654	155	154	Tac Cawla	chert cortex or silicified limestone							
655	152	162	Tac Cawla	chert cortex or patinated							
656	143	N/A	Tac Cawla	chert cortex or silicified limestone							
657	140	26	Tac Cawla	chert cortex							
658	157	154	Tac Cawla	chert cortex or silicified limestone							
659	151	83	Tac Cawla	too small to describe							
660	35	69	Tac Cawla	10YR 6/2	Homogeneous	Dull	Opaque	Semi smooth	Medium	N/A	N/A
661	37	30	Tac Cawla	10YR 4/2 to 10YR 2/2	Homogeneous	Dull	Opaque	Semi smooth	Medium	N/A	N/A
662	36	77	Tac Cawla	Patinated							
663	45 (1)	86	Tac Cawla	chert cortex or silicified limestone							
664	45 (1)	86	Tac Cawla	chert cortex							
665	45 (1)	86	Tac Cawla	10YR 6/2	Homogeneous	Silky shine	translucent	Semi smooth	Fine	N/A	N/A
666	33	77	Tac Cawla	too small to describe							
667	SF30	ctx69	Tac Cawla	chert cortex or silicified limestone							
668	38	80	Tac Cawla	10YR 6/2 to 10YR 4/2	Homogeneous	Pearly shine	Opaque	Semi smooth	Medium	N/A	N/A
669	40	43	Tac Cawla	5Y 7/2	Homogeneous	Dull	Opaque	Smooth	Medium	N/A	spots
670	47 (1)	95	Tac Cawla	10YR 6/2	Homogeneous	Dull	sub- translucent	Semi smooth	Medium	N/A	N/A
671	47 (1)	95	Tac Cawla	too small to describe							

672	32 (2)	30	Tac Cawla	10YR 4/2	Homogeneous	shine pearly to silky	Opaque	Semi smooth	Medium	Yes	N/A
673	32 (1)	30	Tac Cawla	too eroded to describe							
674	43	86	Tac Cawla	10YR 6/2 to 10YR 4/2	Homogeneous	Pearly shine	sub-translucent	Smooth	Fine	N/A	N/A
675	176	100	Tac Cawla	10YR 4/2 to 10YR 2/2	Homogeneous	Silky shine	Opaque	Smooth	Fine	Yes	N/A
676	162	155	Tac Cawla	5YR 3/2	Homogeneous	Pearly shine	Opaque	Smooth	Fine	N/A	N/A
677	196	69	Tac Cawla	10YR 6/2	Homogeneous	Pearly shine	sub-translucent	Semi smooth	Fine	N/A	N/A
678	167	157	Tac Cawla	chert cortex, eroded							
679	173	74	Tac Cawla	chert cortex							
680	170	100	Tac Cawla	10YR 4/2	Homogeneous	Dull	Opaque	rough	Medium	N/A	N/A
681	168	159	Tac Cawla	5YR 5/2	Homogeneous	Pearly shine	translucent	Smooth	Fine	N/A	N/A
682	172	157	Tac Cawla	too small to describe							
683	163	26	Tac Cawla	chert cortex or silicified limestone							
684	178 (1)	163	Tac Cawla	10YR 6/2	Homogeneous	Silky shine	sub-translucent	Semi smooth	Medium	N/A	N/A
685	252	179	Tac Cawla	5Y 5/6	Homogeneous	Dull	Opaque	Smooth	Fine	N/A	N/A
686	259	179	Tac Cawla	10YR 4/2	Homogeneous	Pearly shine	sub-translucent	Smooth	Fine	N/A	N/A
687	241	196	Tac Cawla	chert cortex or silicified limestone							
688	246	197	Tac Cawla	5Y 7/2	Heterogenous	Dull	Opaque	Semi smooth	Medium	N/A	spots
689	249	197	Tac Cawla	5Y 7/2	Homogeneous	Dull	Opaque	Smooth	Medium	N/A	spots
690	257	205	Tac Cawla	5Y 7/2	Heterogenous	Dull	Opaque	Semi smooth	Medium	N/A	Spotted fossils
691	244 (2)	197	Tac Cawla	Patinated							
692	240	196	Tac Cawla	Patinated and cortex							
693	243	200	Tac Cawla	too small to describe							
694	258	206	Tac Cawla	too small to describe							

695	247	200	Tac Cawla	too eroded to describe								
696	254	206	Tac Cawla	too small to describe								
697	222	178	Tac Cawla	5Y 7/2	Patinated	cortex						
698	239	178	Tac Cawla	chert cortex								
699	235 (1)	196	Tac Cawla	5Y 7/2	Heterogenous	Dull	Opaque	Semi smooth	Medium	N/A	Spotted fossils	
700	227 (3)	178	Tac Cawla	too small to describe and the big is patinated								
701	237	200	Tac Cawla	too eroded to describe								
702	232	178	Tac Cawla	10YR 7/4 to 10YR 6/2	Heterogenous	Silky shine	sub-translucent	Semi smooth	Fine	N/A	laminated	
703	228	196	Tac Cawla	5R 4/2	Homogeneous	Pearly shine	translucent	Smooth	Fine	N/A	N/A	
704	275	208	Tac Cawla	10YR 5/4	Homogeneous	Pearly shine	Opaque	Smooth	Fine	N/A	N/A	
705	267	206	Tac Cawla	5YR 5/6	Homogeneous	Pearly shine	Opaque	Smooth	Fine	N/A	N/A	
706	264	203	Tac Cawla	10YR 4/2	Homogeneous	Silky shine	sub-translucent	Semi smooth	Medium	N/A	N/A	
707	272	148	Tac Cawla	chert cortex or silicified limestone								
708	278	208	Tac Cawla	silicified limestone								
709	279	209	Tac Cawla	too small to describe								
710	274	208	Tac Cawla	10YR 6/2	Heterogenous	Dull	Opaque	Smooth	Medium	N/A	spots and laminas	
711	273 (2)	148	Tac Cawla	Patinated and 1 too small to describe								
712	275	148	Tac Cawla	5Y 7/2	Homogeneous	Dull	Opaque	rough	Medium	N/A	Spotted fossils	
713	274 or 294	211	Tac Cawla	Patinated cortex								
714	266	206	Tac Cawla	too eroded to describe, might be cortex								
715	263 (2)	178	Tac Cawla	1 too eroded to describe and 1 too small possibly limestone								
716	260	179?	Tac Cawla	N5	Heterogenous	Pearly shine	Opaque	Smooth	Medium	N/A	Spotted fossils	
717	261	179	Tac Cawla	too eroded to describe								

718	264	206	Tac Cawla	unable to describe								
719	268	203	Tac Cawla	chert cortex								
720	283	134	Tac Cawla	too small to describe								
721	293 (1)	211	Tac Cawla	Patinated								
722	293 (1)	211	Tac Cawla	10YR 7/4	Homogeneous	Dull	Opaque	Semi smooth	Medium	N/A	N/A	
723	288	214	Tac Cawla	10YR 4/2	Homogeneous	Silky shine	Opaque	Smooth	Fine	N/A	N/A	
724	297	210	Tac Cawla	Patinated								
725	285 (1)	179+63	Tac Cawla	10YR 6/2	Homogeneous	Dull	Opaque	Semi smooth	Medium	N/A	N/A	
726	298	206	Tac Cawla	Patinated								
727	280	203	Tac Cawla	chert cortex								
728	296 (1)	227	Tac Cawla	Patinated								
729	281	203	Tac Cawla	unable to describe								
730	75	ctx69	Tac Cawla	10R 6/6	Homogeneous	Silky shine	Opaque	Semi smooth	Medium	N/A	N/A	
731	71 (1)	30	Tac Cawla	10R 6/6	Homogeneous	Silky shine	Opaque	Semi smooth	Medium	N/A	N/A	
732	71 (1)	30	Tac Cawla	chert cortex or silicified limestone								
733	73	107	Tac Cawla	10YR 6/2 to 10YR 7/4	Homogeneous	Silky shine	Opaque	Semi smooth	Medium	N/A	N/A	
734	74	1	Tac Cawla	10YR 6/2	Homogeneous	Silky shine	Opaque	Smooth	Medium	N/A	N/A	
735	77	7	Tac Cawla	10YR 4/2 to 10YR 2/2	Homogeneous	Pearly shine	Opaque	Smooth	Fine	N/A	N/A	
736	72	15	Tac Cawla	10YR 8/2	Homogeneous	Dull	Opaque	Semi smooth	Medium	N/A	Spotted fossils	
737	79	74	Tac Cawla	Patinated								
738	76N/A	1	Tac Cawla	N8	Homogeneous	Pearly shine	highly translucent	Smooth	Fine	N/A	N/A	
739	70 (2)	100	Tac Cawla	too small to describe								
740	555	85 ss[50]	Tac Cawla	N5	Heterogenous	Dull	Opaque	Semi smooth	Fine	N/A	Spotted fossils	

741	745	845	Xaghra Circle	10YR 4/2	Homogeneous	Pearly shine	Opaque	Smooth	Fine	N/A	N/A
742	566	662	Xaghra Circle	5Y 6/1	Heterogenous	Dull	Opaque	Semi smooth	Medium	N/A	Spotted fossils
743	843	4	Xaghra Circle	10YR 6/6	Homogeneous	Pearly shine	Translucent	Smooth	Fine	N/A	Spotted carbonate
744	564	662	Xaghra Circle	10R 6/2	Homogeneous	Pearly shine	Semi-Translucent	Smooth	Fine	N/A	Spots carbonate
745	611	712	Xaghra Circle	10YR 5/4	Heterogenous	Silky shine	Translucent	Semi smooth	Fine	Yes	Spotted carbonate
746	291	334	Xaghra Circle	10YR 6/6	Homogeneous	Pearly shine	Opaque	Smooth	Fine	N/A	N/A
747	854	897	Xaghra Circle	5YR 3/4	Homogeneous	Pearly shine	Translucent	Smooth	Fine	N/A	N/A
748	1142	1279	Xaghra Circle	10YR 4/2	Homogeneous	Silky shine	Opaque	Smooth	Fine	Yes	N/A
749	395	449	Xaghra Circle	5YR 3/2	Homogeneous	Pearly shine	Translucent	Smooth	Fine	Yes	N/A
750	110	274	Xaghra Circle	5YR 3/2	Homogeneous	Pearly shine	Opaque	Smooth	Fine	N/A	N/A
751	767	783	Xaghra Circle	10YR 6/2	Homogeneous	Dull	Opaque	Semi-Smooth	Medium	N/A	N/A

*The colours were determined based on the Munsell rock Colour book, 2014.

Table 8: The macroscopic description of the chert artefacts from Skorba assemblage.

Sample	Layer	Location	Colour*	Fabric	Luster	Translucency	Texture	Grain	Cortex	Pattern	Notes for sampling
1	1	Skorba	N1 to 5YR 2/1 and 5Y 4/1	Heterogenous	Dull	Opaque	Semi-smooth	Fine	N/A	spotted fossils	
2	1	Skorba	5Y 7/2	Homogenous	Dull	Opaque	Smooth	Fine	N/A	spotted fossils	Patinated
3	1	Skorba	10YR 6/2	Heterogenous	Silky shine	Opaque	Smooth	Fine	N/A	spotted fossils	Local
4	1	Skorba	5Y 7/2	Homogenous	Dull	Opaque	Smooth	Fine	N/A	N/A	Patinated
5	1	Skorba	N1 to 5YR 2/1 and 5Y 4/1	Heterogenous	Dull	Opaque	Semi-smooth	Fine	N/A	spotted fossils	
6	1	Skorba	5Y 7/2	Homogenous	Dull	Opaque	Smooth	Fine	N/A	N/A	Patinated
7	1	Skorba	10YR 7/4	Homogenous	Dull	Opaque	Semi-smooth	Medium	N/A	N/A	Limestone
8	1	Skorba	5Y 7/2	Heterogenous	Dull	Opaque	Smooth	Fine	N/A	spotted fossils	Local
9	1	Skorba	N1 to 5Y 4/1	Heterogenous	Dull	Opaque	Semi-smooth	Fine	N/A	spotted fossils	
10	1	Skorba	5R 4/2	Homogenous	Pearly shine	Opaque	Smooth	Fine	N/A	N/A	
11	1	Skorba	10 YR 6/6	Homogenous	Pearly shine	Translucent	Smooth	Fine	N/A	N/A	Foreign
12	1	Skorba	N6	Homogenous	Pearly shine	Opaque	Smooth	Fine	N/A	N/A	Foreign
13	1	Skorba	10 YR 5/4	Homogenous	Pearly shine	Translucent	Smooth	Fine	N/A	N/A	Foreign
14	1	Skorba	10 YR 7/4	Homogenous	Dull	Opaque	Smooth	Fine	N/A	N/A	Patinated
15	1	Skorba	10 YR 7/4	Homogenous	Dull	Opaque	Smooth	Fine	N/A	N/A	Patinated
16	1	Skorba	10YR 6/2	Heterogenous	Dull	Opaque	Smooth	Fine	N/A	spotted fossils	Local
1	2	Skorba	5Y 8/4	Homogenous	Dull	Opaque	Smooth	Fine	N/A	Spotted	Patinated
2	2	Skorba	5Y 8/4	Heterogenous	Dull	Opaque	Smooth	Fine	N/A	Fine laminated	Patinated
3	2	Skorba	5YR 4/1	Homogenous	Dull	Opaque	Smooth	Medium	N/A	N/A	Not chert
4	2	Skorba	5Y 8/4	Homogenous	Dull	Opaque	Smooth	Fine	N/A	Laminated	Patinated
5	2	Skorba	5Y 4/1	Homogenous	Dull	Opaque	Smooth	Fine	N/A	N/A	Not chert
6	2	Skorba	5Y 4/1	Homogenous	Dull	Opaque	Smooth	Fine	N/A	Spotted	Local material
7	2	Skorba	N1	Homogenous	Dull	Opaque	Semi-smooth	Medium	N/A	N/A	Not chert
8	2	Skorba	N9	Heterogenous	Pearly shine	Translucent	Smooth	Fine	N/A	Spots	Similar with G2S6

1	3	Skorba	10 YR 7/4	N/A	N/A	N/A	N/A	N/A	N/A	N/A	Patinated
2	3	Skorba	10 YR 7/4	Homogenous	Silky shine	Opaque	Smooth	Medium	N/A	N/A	Foreign?
3	3	Skorba	5Y 8/4	Homogenous	Dull	Opaque	Smooth	Medium	N/A	Spotted	Local
4	3	Skorba	N1	Homogenous	Dull	Opaque	Semi-smooth	Medium	N/A	N/A	Patinated
1	5	Skorba	10Y 8/2	Homogenous	Dull	Opaque	Smooth	Fine	N/A	spots	Patinated
2	5	Skorba	5YR 4/1	Heterogenous	Dull	Opaque	Semi-smooth	Fine	N/A	spots	Local
3	5	Skorba	N1	Homogenous	Silky shine	Opaque	Smooth	Fine	N/A	spots	not chert
4	5	Skorba	10Y 8/2	Homogenous	Dull	Opaque	Smooth	Fine	N/A	spots	Patinated
5	5	Skorba	10Y 8/2	Homogenous	Dull	Opaque	Smooth	Fine	N/A	spots	Patinated
6	5	Skorba	10Y 8/2	Homogenous	Dull	Opaque	Smooth	Fine	N/A	spots	Patinated
1	10	Skorba	N1	Homogenous	Silky shine	Opaque	Semi-smooth	Fine	N/A	N/A	not chert
2	10	Skorba	N1	Homogenous	Silky shine	Opaque	Semi-smooth	Fine	N/A	N/A	not chert
3	10	Skorba	5YR 7/2	Heterogenous	Silky shine	Opaque	Smooth	Fine	N/A	spotted	Local
4	10	Skorba	5YR 7/2	Heterogenous	Pearly shine	Opaque	Smooth	Fine	N/A	spotted	Local
5	10	Skorba	N/A	N/A	N/A	N/A	N/A	N/A	N/A	N/A	Patinated
6	10	Skorba	5Y 4/1	Heterogenous	Dull	Opaque	Semi-smooth	Fine	N/A	spotted	Local, not chert
7	10	Skorba	N/A	N/A	N/A	N/A	N/A	N/A	N/A	N/A	Patinated
8	10	Skorba	10Y 7/4	Homogenous	Dull	Opaque	Smooth	Fine	N/A	spotted	
9	10	Skorba	10YR 4/2	Heterogenous	Dull	Opaque	Rough	Fine	N/A	spotted	Local
10	10	Skorba	N1	Homogenous	Silky shine	Opaque	Semi-smooth	Fine	N/A	N/A	not chert
11	10	Skorba	10YR 6/2	Heterogenous	Dull	Opaque	Smooth	Fine	N/A	spotted	Local
12	10	Skorba	5YR 4/1	Homogenous	Dull	Opaque	Semi-smooth	Fine	N/A	N/A	
13	10	Skorba	N1	Homogenous	Silky shine	Opaque	Semi-smooth	Fine	N/A	N/A	not chert
14	10	Skorba	5YR 2/1	Homogenous	Pearly shine	Opaque	Smooth	Fine	N/A	spots	Local
15	10	Skorba	10YR 8/6	Homogenous	Dull	Opaque	Rough	Medium	N/A	N/A	Limestone
16	10	Skorba	10Y 7/4	Homogenous	Dull	Opaque	Smooth	Fine	N/A	spotted	
17	10	Skorba	N1	Homogenous	Silky shine	Opaque	Semi-smooth	Fine	N/A	N/A	not chert
18	10	Skorba	10R 4/6	Homogenous	Dull	Opaque	Rough	Medium	N/A	N/A	Limestone
19	10	Skorba	5YR 2/2	Homogenous	Pearly shine	Sub-translucent	Smooth	Fine	Chalky lime?	N/A	Foreign
21	10	Skorba	10YR 6/2	Homogenous	Silky shine	Opaque	Smooth	Fine	N/A	lines	Foreign?

1	11	Skorba	10YR 8/2	Homogenous	N/A	N/A	N/A	N/A	N/A	N/A	Patinated, 2 more samples
2	11	Skorba	5Y 5/2	Homogenous	Dull	Opaque	Smooth	Fine	N/A	spotted	Local, 3 more samples
3	11	Skorba	10YR 6/2	Homogenous	Dull	Opaque	Semi-Smooth	Fine	N/A	spotted	Local
4	11	Skorba	10YR 4/2	Homogenous	Pearly shine	Sub- translucent	Smooth	Fine	N/A	N/A	Foreign
5	11	Skorba	N4	Homogenous	Dull	Opaque	Semi-Smooth	Fine	N/A	N/A	not chert
6	11	Skorba	N1	Homogenous	Dull	Opaque	Semi-Smooth	Medium	N/A	N/A	not chert, 5 more samples
7	11	Skorba	Chert cortex								
1	12	Skorba	N5	Heterogenous	Dull	Opaque	Smooth	Fine	N/A	spotted	Local, not chert
2	12	Skorba	10YR 6/2	Heterogenous	Dull	Opaque	Smooth	Fine	N/A	spotted	Local
3	12	Skorba	5Y 7/2	Heterogenous	Silky shine	Opaque	Smooth	Fine	N/A	spotted	Local
4	12	Skorba	5YR 5/6	Heterogenous	Dull	Opaque	Rough	Medium	N/A	N/A	Limestone, +5 similar pieces
5	12	Skorba	10YR 4/2	Heterogenous	Dull	Opaque	Smooth	Fine	Limestone	spotted	Local
6	12	Skorba	10YR 6/2	Heterogenous	Dull	Opaque	Smooth	Fine	N/A	spotted	Local
7	12	Skorba	N3	Heterogenous	Dull	Opaque	Rough	Medium	N/A	spotted	Not chert
8	12	Skorba	5YR 2/1 to N1	Homogenous	Dull	Opaque	Semi-smooth	Fine	N/A	N/A	not chert, +9 similar pieces
9	12	Skorba	10YR 6/2	Homogenous	Dull	Opaque	Semi-smooth	Fine	N/A	spotted	Local, partly patinated
10	12	Skorba	N/A	N/A	N/A	N/A	N/A	N/A	N/A	N/A	Obsidian
11	12	Skorba	13 pieces in bag	There were artefacts and debitage made from rock if partly from local chert and partly from limestone (cortex), all had a level of patination							Local
1	12b	Skorba	N1	Homogenous	Dull	Opaque	Semi-smooth	Fine	N/A	N/A	Arrowhead
2	12b	Skorba	10YR 5/4	Heterogenous	Dull	Opaque	Semi-smooth	Fine	N/A	spotted	Local
3	12b	Skorba	10YR 8/6	Heterogenous	Dull	Opaque	Semi-smooth	Medium	N/A	spotted	Local
4	12b	Skorba	10YR 5/4	Heterogenous	Dull	Opaque	Semi-smooth	Fine	N/A	Dark small lines	Local
5	12b	Skorba	N3	Homogenous	Dull	Opaque	Semi-smooth	Fine	N/A	N/A	
6	12b	Skorba	10YR 6/6	Homogenous	Pearly shine	Translucent	Smooth	Fine	N/A	N/A	Foreign
1	12c	Skorba	10YR 4/2	Homogenous	Silky shine	Opaque	Smooth	Fine	N/A	N/A	Local

2	12c	Skorba	10YR 6/2 to 5YR 4/4	Heterogenous	Dull	Opaque	Smooth	Fine	N/A	spotted	Local?
3	12c	Skorba	5YR 2/1	Homogenous	Dull	Opaque	Smooth	Fine	N/A	N/A	
4	12c	Skorba	5YR 4/1	Heterogenous	Dull	Opaque	Semi- smooth	Fine	N/A	spotted	Local
5	12c	Skorba	N1	Homogenous	Dull	Opaque	Smooth	Fine	N/A	N/A	
1	13	Skorba	5Y 8/4	N/A	N/A	N/A	N/A	N/A	N/A	N/A	PATINATED, LOCAL MATERIAL
2	13	Skorba	10YR 6/2	Heterogenous	Dull	Opaque	Smooth	Fine	N/A	spotted	Local
3	13	Skorba	5YR 7/2	N/A	N/A	N/A	N/A	N/A	Limestone	N/A	Local
4	13	Skorba	N1 to 10YR 4/2	Heterogenous	Dull	Opaque	Smooth	Fine	N/A	spotted	Local
5	13	Skorba	5YR 7/2	Heterogenous	Dull	Opaque	Semi- smooth	Fine	Limestone	spotted	Local
6	13	Skorba	N1 to N2	Heterogenous	Dull	Opaque	Semi- smooth	Fine	N/A	spotted	Local?
7	13	Skorba	N3 to 10YR 6/2	Homogenous	Dull	Opaque	Smooth	Fine	N/A	N/A	Not chert
8	13	Skorba	N1	Homogenous	Dull	Opaque	Semi- smooth	Fine	N/A	N/A	Not chert
9	13	Skorba	10R 4/6	Non- Homogenous	Dull	Opaque	Rough	Coarse	N/A	N/A	Limestone
10	13	Skorba	10YR 8/6	Homogenous	Dull	Opaque	Semi- smooth	Medium	N/A	spots	Limestone
11	13	Skorba	10YR 6/2	Homogenous	Dull	Opaque	Semi- smooth	Medium	N/A	N/A	
12	13	Skorba	10R 3/4	Homogenous	Pearly shine	Opaque	Smooth	Fine	N/A	N/A	Foreign
13	13	Skorba	10YR 7/4	Homogenous	Dull	Opaque	Semi- smooth	Medium	N/A	N/A	Foreign
1	16	Skorba	5Y 7/2 to 10Y 8/2	Heterogenous	Dull	Opaque	Semi- smooth	Fine	N/A	spotted	
2	16	Skorba	10Y 8/2	Heterogenous	Dull	Opaque	Semi- smooth	Fine	Limestone	spotted fossils	
3	16	Skorba	5Y 7/6	Heterogenous	Silky shine	Sub- translucent	Rough	Coarse	N/A	spots	
1	19	Skorba	10YR 4/2	Heterogenous	Silky shine	Sub- translucent	Rough	Coarse	N/A	broad mottling	Foreign
2	19	Skorba	5Y 7/2	Heterogenous	Dull	Opaque	Semi- smooth	Fine	N/A	spotted	Local
3	19	Skorba	5Y 7/2	Heterogenous	Dull	Opaque	Semi- smooth	Fine	N/A	spotted	Local

4	19	Skorba	5YR 7/2 to 10YR 4/2	Heterogenous	Dull	Opaque	Semi- smooth	Fine	N/A	spotted	Local
5	19	Skorba	N1 to N2	Homogenous	waxy shine	Opaque	Semi- smooth	Medium	N/A	N/A	Not chert, same with S6
6	19	Skorba	N1 to N2	Homogenous	waxy shine	Opaque	Semi- smooth	Medium	N/A	N/A	Not chert, same with S5
1	20	Skorba	N1	Homogenous	Silky shine	Opaque	Semi- smooth	Fine	N/A	N/A	not chert
2	20	Skorba	N1	Homogenous	Silky shine	Opaque	Semi- smooth	Fine	N/A	N/A	not chert
3	20	Skorba	10YR 5/4	Heterogenous	Silky shine	Sub- translucent	Smooth	Medium	N/A	N/A	Local
4	20	Skorba	5Y 7/2	Homogenous	Dull	Opaque	Smooth	Fine	N/A	spotted	Local
5	20	Skorba	N1	N/A	N/A	N/A	N/A	N/A	N/A	N/A	This is missing, mixed with other pieces?
1	23	Skorba	5YR 2/1	Homogenous	Dull	Opaque	Smooth	Fine	N/A	laminas	not chert
2	23	Skorba	5Y 5/2	Homogenous	Dull	Opaque	Semi- smooth	Medium	N/A	spotted, laminas	Local
3	23	Skorba	5Y 5/2	Homogenous	Dull	Opaque	Semi- smooth	Medium	N/A	spotted	Local
4	23	Skorba	5Y 7/2	Homogenous	Dull	Opaque	Smooth	Fine	N/A	spotted	Local
5	23	Skorba	5Y 7/2	Homogenous	Dull	Opaque	Smooth	Fine	N/A	spotted	Local
6	23	Skorba	10YR 8/2	Patinated							Local
7	23	Skorba	5R 4/6	Homogenous	Pearly shine	Translucent	Smooth	Fine	N/A	N/A	not local, Sicily?
8	23	Skorba	10R 5/4	Homogenous	Pearly shine	Translucent	Smooth	Fine	N/A	N/A	not local, Sicily?
9	23	Skorba	5YR 2/1	Homogenous	Dull	Opaque	Smooth	Fine	N/A	N/A	not chert
10	23	Skorba	5YR 2/1	Homogenous	Dull	Opaque	Smooth	Fine	N/A	N/A	not chert, convened with soil
11	23	Skorba	5YR 2/1	Homogenous	Dull	Opaque	Smooth	Fine	N/A	N/A	not chert, covered with soil
12	23	Skorba	N1	Homogenous	Dull	Opaque	Smooth	Medium	N/A	N/A	not chert
1	26	Skorba	10YR 6/2	Homogenous	Dull	Opaque	Semi- smooth	Fine	N/A	spotted	Local
2	26	Skorba	10YR 4/2	Homogenous	Dull	Opaque	Semi- smooth	Fine	Limestone	N/A	Local
3	26	Skorba	10YR 7/4	Patinated							Local

4	26	Skorba	N3	Homogenous	Dull	Opaque	Semi-smooth	Fine	N/A	spotted	not chert
5	26	Skorba	N3	Homogenous	Silky shine	Opaque	Semi-smooth	Medium	N/A	spotted	not chert
6	26	Skorba	5Y 7/2	Homogenous	Dull	Opaque	Smooth	Fine	N/A	spots	Local
7	26	Skorba	5Y 7/2 to 10YR 6/2	Homogenous	Dull	Opaque	Smooth	Medium	N/A	N/A	Local
8	26	Skorba	10YR 6/2	Homogenous	Dull	Opaque	Semi-smooth	Medium	N/A	spotted	Local
9	26	Skorba	10YR 5/4	Homogenous	Pearly shine	sub- translucent	Smooth	Fine	N/A	N/A	not local
10	26	Skorba	10R 5/4	Homogenous	Pearly shine	Opaque	Smooth	Fine	N/A	N/A	not local
11	26	Skorba	10R 6/2	PATINATED	N/A	N/A	N/A	N/A	N/A	N/A	not local
12	26	Skorba	N2	Homogenous	Dull	Opaque	Semi-smooth	Medium	N/A	N/A	not chert
13	26	Skorba	N2	Homogenous	Dull	Opaque	Semi-smooth	Medium	N/A	N/A	not chert, covered with soil
1	30	Skorba	5Y 7/2	Heterogenous	Dull	Opaque	Semi-smooth	Fine	N/A	spotted	Local
2	30	Skorba	N6	Heterogenous	Dull	Opaque	Smooth	Fine	N/A	spotted	Limestone
3	30	Skorba	N3	Homogenous	Dull	Opaque	Smooth	Fine	N/A	spots	Limestone
4	30	Skorba	10YR 5/4	Homogenous	Pearly shine	Translucent	Smooth	Fine	N/A	N/A	Foreign
131	211	Skorba	10YR 4/2	Homogeneous	Pearly shine	sub-translucent	Smooth	Fine	N/A	N/A	It's similar with GG[1019]

*The colours were determined based on the Munsell rock Colour book, 2014.

Table 9: Typology and Craft techniques. The table records the site, the content and the year of the excavation, and the type of raw material of the each find. These are followed by the typological features of each find. When a feature is not defined the initials NIF (Not Identified Feature) is imported.

Sample	Content	Site	Year	Raw Material	Piece	Type	Category	Name	Flaking method	Features
1	[1019]	Ggantija	2015	Chert	Detached piece	Debitage (GD=2.9cm/SD=1.9cm)	Flake debitage	Proximal flake	Percussion	Ventral surface raised hump, ripple marks/ dorsal surface, proximal edge
2	[1019]	Ggantija	2015	Chert	Detached piece	Flake (GD=2.5cm/SD=1.1cm)	Prismatic flake/ Unimarginal flake tool	Blade	Percussion	Ventral surface raised hump/ dorsal surface, arris triangle shape, weathering cuts
3	[1019]	Ggantija	2015	Chert	Detached piece	Debitage (GD=3.1cm/SD=2.1cm)	Flake debitage	Proximal flake	primary and secondary percussion, secondary pressure for retouch	Ventral and dorsal surface proximal edge
4	[1019]	Ggantija	2015	Chert	Detached piece	Flake (GD=1.7cm/SD=1.3cm)	Bending flake	unimarginal flake tool	Percussion	Ventral and dorsal surface, flake extracted for retouch
5	[1019]	Ggantija	2015	Chert	Detached piece	Debitage (GD=2.9cm/SD=1.9cm)	Flake debitage	Proximal flake	Percussion	Ventral surface raised hump/ dorsal surface, proximal edge
6	[1019]	Ggantija	2015	Chert	Detached piece	Flake (GD=2.7cm/SD=2.2cm)	Decortication Flake	Flake scraper?	Percussion, secondary flaking retouch edge	Ventral and dorsal surface, edge retouch, cortex
7	[1019]	Ggantija	2015	Chert	Detached piece	Flake (GD=2.7cm/SD=2.2cm)	Decortication Flake/ Unimarginal flake tool	Flake scraper?	Primary Percussion, secondary pressure, retouch edge	Ventral and dorsal surface, edge retouch, cortex
8	[1019]	Ggantija	2015	Chert	Detached piece	Flake (GD=2.9cm/SD=0.8cm)	Prismatic flake	Micro-Blade (W<8mm)	Primary and secondary percussion/ secondary pressure for sharpness and retouch edges	Ventral surface, raised hump, ripple marks/ dorsal surface arris, edge retouch, unmodified shoulders, subconcave base
9	[1019]	Ggantija	2015	Chert	Detached piece	Flake (GD=3.8cm/SD=2.0cm)	Prismatic flake/ Unimargianl flake tool	NIF	Primary and secondary Percussion	Ventral and dorsal surface, arris from flake removed, triangle shape

10	[1019]	Ggantija	2015	Chert	Detached piece	Flake (GD=2.0cm/SD=1.5cm)	Flake debitage	Proximal flake debitage	Primary and secondary percussion	Ventral and dorsal surface, proximal end, erailure flake scar
11	[1019]	Ggantija	2015	Chert cortex	Detached piece	Debitage (GD=2.8cm/SD=2.5cm)	Debitage shatter	NIF	Primary Percussion	NIF
12	[1019]	Ggantija	2015	Chert	Detached piece	Flake (GD=1.45cm/SD=1.0cm)	Flake shatter	Flake debris	Primary Percussion?	Ventral and dorsal surface
13	[1019]	Ggantija	2015	Chert	Detached piece	Flake (GD=1.6cm/SD=1.2cm)	Flake debitage	Proximal flake	Primary and secondary Percussion	Ventral surface, raised hump and erailure flake scar/ dorsal surface, flakes removed
14	[1019]	Ggantija	2015	Chert	Detached piece	Flake (GD=2.7cm/SD=1.0cm)	Prismatic flake	Blade	Percussion	Ventral and dorsal surface/ basal border, notch?, tang?
15	[1019]	Ggantija	2015	Chert	Detached piece	Flake (GD=1.45cm/SD=1.0cm)	Bending flake	Flake tool	Percussion	Ventral surface, raised hump, erailure flake scar/ dorsal surface central flake extracted, arris, edges retouch?
16	[1019]	Ggantija	2015	Chert cortex	Detached piece	Flake (GD=2.5cm/SD=1.55cm)	flake tool	Flake tool shatter	Percussion and secondary pressure	Ventral and dorsal surface/ arris on dorsal flake removal, edge retouch
17	[1019]	Ggantija	2015	Chert	Detached piece	Flake (GD=2.35cm/SD=1.7cm)	Flake debitage	Flake shatter	Primary Percussion?	Ventral and dorsal surface/ flake removed from dorsal surface
18	[1019]	Ggantija	2015	Chert	Detached piece	Flake (GD=2.5cm/SD=1.4cm)	Flake tool	Unimarginal flake tool	Primary and secondary Percussion	Ventral surface, ripple marks/ dorsal surface arris flake removed, weathered edges
19	[1019]	Ggantija	2015	Chert cortex	Detached piece	Debitage (GD=2.6cm/SD=1.1cm)	Debris	Debitage Shatter	Primary Percussion?	NIF
20	[1019]	Ggantija	2015	Chert cortex	Detached piece	Debitage (GD=2.8cm/SD=1.9cm)	Debris	Flake shatter	Primary and secondary Percussion	Ventral surface, raised hump and erailure flake scar/ dorsal surface, flakes removed

21a	[1019]	Ggantija	2015	Chert	Detached piece	Flake (GD=2.15cm/SD=1.6cm)	Flake tool	Blade	Primary Percussion	Ventral surface, raised hump/ dorsal surface, edge weathered from use?
21b	[1019]	Ggantija	2015	Chert	Detached piece	Flake (GD=1.7cm/SD=1.55cm)				
22	[1019]	Ggantija	2015	Chert	Detached piece	Flake (GD=2.4cm/SD=1.4cm)	Prismatic flake	Unimarginal flake tool	Primary and secondary Percussion	Ventral surface, raised hump/ dorsal surface, arris flakes removed, edge retouched
23	[1019]	Ggantija	2015	Chert	Detached piece	Debitage (GD=1.6cm/SD=1.2cm)	Flake debris	Proximal flake debitage	Primary Percussion	Ventral surface, raised hump/ proximal end/ dorsal surface
24	[1019]	Ggantija	2015	Chert	Detached piece	Flake (GD=2.7cm/SD=2.4cm)	Flake tool	Unimarginal flake tool	Primary and secondary Percussion	Ventral surface, raised hump/proximal end/ dorsal surface, flakes removed, edge weathered from use
25	[1019]	Ggantija	2015	Chert	Detached piece	Flake (GD=1.5cm/SD=1.0cm)	Flake chip	Unimarginal flake tool	Primary and secondary Percussion	Ventral surface, raised hump, ripple marks and erailure flake scar/ dorsal surface, flakes removed edge retouch
26	[1019]	Ggantija	2015	Chert	Detached piece	Flake (GD=3.2cm/SD=2.2cm)	Flake tool	Flake scraper?	Primary and secondary Percussion	Ventral surface, erailure flake scar/ dorsal surface, arris flake reshape distal end retouch
27	[1019]	Ggantija	2015	Chert	Objective piece	Core (GD=5.8cm/SD=3.3cm)	Unidirectional core	NIF	Primary and secondary Percussion	Flakes removed from one surface
28	[1019]	Ggantija	2015	Chert	Detached piece	Flake (GD=3.2cm/SD=2.9cm)	Bending flake	Unimarginal flake tool	Primary and secondary Percussion	Ventral surface, raised hump/ dorsal surface, arris flake removed to shape end edges retouch
29	[1019]	Ggantija	2015	Chert cortex	Detached piece	Flake (GD=2.5cm/SD=1.8cm)	Flake tool	unimarginal flake tool	Primary and secondary Percussion	Ventral surface, erailure flake scar/proximal end/ dorsal surface, arris flake removal for shape

30	[1019]	Ggantija	2015	Chert	Detached piece	Flake (GD=3.0cm/SD=2.85cm)	Bending flake	Unimarginal flake tool	Primary and secondary Percussion	Ventral surface, raised hump, erailure flake scar/proximal end/ dorsal surface, arris flake removal shape and retouch
5/sb	[1019]	Ggantija	2015	Chert	Detached piece	Flake (GD=1.4cm/SD=0.5cm)	Flake chip	Blade tip	NIF	Ventral and dorsal surface
6/sb	[1019]	Ggantija	2015	Chert	Detached piece	Debitage (GD=1.6cm/SD=1.25cm)	Flake debris	Flake shatter	Primary Percussion and secondary pressure	Ventral and dorsal surface/ bimarginal flake removed with pressure
7/sb	[1019]	Ggantija	2015	Chert	Detached piece	Debitage (GD=1.5cm/SD=0.7cm)	Flakedebitage	Proximal flake	Primary Percussion	Ventral surface, raised hump/ dorsal surface/ proximal end
8/sb	[1019]	Ggantija	2015	Chert	Detached piece	Flake (GD=2.9cm/SD=2.1cm)	Bending flake	Unimarginal flake tool	Primary and secondary Percussion, secondary pressure	Ventral surface/ dorsal surface, arris, flake removed for shapineg
1	[1030] SF6	Ggantija	2015	Chert	Detached piece	Flake (GD=2.9cm/SD=2.0cm)	Decortication/ rejuvenation Flake	NIF	Primary percussion	Ventral surface, erailure flake scar/ dorsal surfaces with cortex
1	008/TRI	Ggantija	2015	Chert	Detached piece	Flake (GD=1.6cm/SD=1.4cm)	Bimarginal flake tool	Flake fragment?	Percussion, retouched edges	Ventral and dorsal surface/ 2 arris for flake removal for retouch. Fragment and not many features are clear
1	12	Ggantija	2015	Chert	Detached piece	Flake (GD=4.8cm/SD=3.2cm)	Unimarginal Flake tool	NIF	Primary and secondary percussion, secondary for retouch edges/ indication of levallois technique	Ventral surface / dorsal surfaces with retouched edges
1	[1012]	Ggantija	2015	Chert	Detached piece	Debitage (GD=1.9cm/SD=1.4cm)	Debitage flake	Flake Shatter	NIF	Ventral and dorsal surface
2	[1012]	Ggantija	2015	Chert	Detached piece	Flake (GD=2.4cm/SD=2.3cm)	Bimarginal flake tool	Flake scraper	Primary and secondary percussion, secondary for retouch/ pressure for retouch the edges	Ventral surface, flake removed; pressure? / dorsal surfaces with arris, flake revoned for retouch and edge retouched for sharpening the scrapper

N/A	1040	Ggantija	2015	Chert	Objective Piece	Core (GD=4.0cm/SD=2.5cm)	Multidirectional cores	Bipolar core?	Percussion and pressure	Many surfaces, flakes extracted from all surfaces
1	1015	Ggantija	2015	Chert	Detached piece	Flake (GD=2.5cm/SD=1.1cm)	Prismatic flake/ Bimargianl flake tool	Blade	Percussion/ secondary pressure flaking for retouch	Ventral surface retouch/ dorsal surfaces with arris for retouch and resharpen/ feather edge
2	1015	Ggantija	2015	Chert	Detached piece	Flake (GD=3.2cm/SD=1.35cm)	Decortication flakes	Scraper planes?	Percussion, secondary for retouch/ pressure for retouch the edges	Ventral and dorsal surfaces/ steep angled scraping edge and use wear evidence on one face
3	1015	Ggantija	2015	Chert	Detached piece	Flake (GD=1.55cm/SD=1.0cm)	NIF	Unimargianl flake tool	Primary percussion, secondary pressure for retouch the edges	Ventral surface ripple marks/ dorsal surfaces with arris pressure flake removed, retouched edge
2	[1016]	Ggantija	2015	Chert	Detached piece	Flake (GD=1.6cm/SD=1.4cm)	Flake debris	Spall	Primary percussion and secondary? pressure	Ventral surface, ripple marks/ dorsal surfaces, ripple marks of flake removal, pressure?
3	[1016]	Ggantija	2015	Chert	Detached piece	Flake (GD=3.0cm/SD=1.4cm)	Prismatic flake/ Unimargianl flake tool	Blade	Percussion and secondary pressure/ retouch the edges method uncertain	Ventral surface ripple marks/ dorsal surfaces with arris, flake removal for retouch and edge retouched serration
1	[1016]	Ggantija	2015	Chert	Detached piece	Debitage (GD=1.3cm/SD=0.85cm)	Flake debris	Flake shatter	Primary percussion	Ventral and dorsal surface
1	[1004]	Ggantija	2014	Chert	Detached piece	Flake (GD=2.5cm/SD=1.7cm)	Prismatic flake/ Unimargianl flake tool	Flake tool	Primary and secondary percussion, secondary pressure for retouch	Ventral surface / dorsal surfaces with arris, flake removal for retouch, sharpening the surface
2	[1004]	Ggantija	2014	Chert	Detached piece	Flake (GD=2.3cm/SD=1.5cm)	Decortication flake	Rejuvenation Flake/ flake scraper?	Primary percussion, secondary pressure for retouch one edge	Ventral surface / dorsal surfaces with cortex and retouched edge
1	22	Santa Verna	2015	Chert	Detached piece	Debitage (GD=3.9cm/SD=3.5cm)	Flake	Proximal Flake	Primary percussion	Ventral surface, ripple marks and stick point/ dorsal surface

2	22	Santa Verna	2015	Chert	Detached piece	Flake (GD=1.5cm/SD=1.3cm)	Unimarginal flake	Unimarginal flake tool	Secondary percussion	Ventral surface/ dorsal surface, double arris serration
1	34	Santa Verna	2015	Chert	Detached piece	Flake (GD=2.8cm/SD=1.65cm)	Bending flake	Unimarginal flake tool/ blade?	Primary and secondary percussion	Ventral surface, raised hump, ripple marks/ dorsal, arris, sticking point of second stick/ haft element - tang
67	34	Santa Verna	2015	Chert	Detached piece	Flake (GD=3.2cm/SD=2.1cm) or Debitage	Conchoidal flake or Debitage flake	Flake tool/ Proximal flake	Primary percussion	ventral surface, raised hump, erailure scar/ dorsal surface
1	41	Santa Verna	2015	Chert	Detached piece	Flake (GD=2.0cm/SD=1.1cm)	Flake tool	Unimarginal flake tool	Primary percussion and secondary pressure	ventral surface, raised hump?/ dorsal surface flake extraction, multi-directions
2	41	Santa Verna	2015	Chert	Detached piece	Flake (GD=2.0cm/SD=1.4cm)	Flake tool	Unimarginal flake tool	Primary percussion and secondary pressure	ventral surface/ dorsal surface, arris centre, edge retouch and pressure flakes removed from arris top
3	41	Santa Verna	2015	Chert	Detached piece	Flake (GD=2.0cm/SD=1.2cm)	Flake tool	bimarginal flake tool/ blade?	Primary and secondary percussion, secondary pressure	ventral and dorsal surface, arris from different stages of retouch, pressure flakes removed from many parts for resharp, edge retouch and serration, tang?
38	8	Santa Verna	2015	Chert	Detached piece	Flake (GD=2.3cm/SD=1.0cm)	Prismatic flake	Blade/ unimarginal flake tool	Primary and secondary percussion, secondary pressure	Ventral surface, raised hump, ripple marks, two sticking points/ dorsal arris, pressure flakes removed, on side has flake removed possibly not with pressure
1	61	Santa Verna	2015	Chert	Detached piece	Flake (GD=2.8cm/SD=1.3cm)	Conchoidal/ Prismatic flake	Blade/ unimarginal flake tool	Primary percussion? secondary pressure	ventral surface, raised hump, erailure scar/ dorsal surface, arris, flake removed with struck prior to this flake and pressure flakes removed for retouch especially the top and one side

1	33	Santa Verna	2015	Chert	Detached piece	Flake (GD=4.1cm/SD=1.4cm)	Prismatic flake	Blade?/ rejuvenation flake	Primary and secondary percussion	ventral surface, raised hump? Ripple marks/ dorsal surface, arris
134	58	Santa Verna	2015	Chert	Detached piece	Flake (GD=3.3cm/SD=2.2cm)	Conchoidal flake	Unimarginal flake tool	Primary percussion, secondary flaking	Dorsal surface, arris flake extraction, edge retouch -> serration
1	98	Santa Verna	2015	Chert	Detached piece	Flake (GD=5.1cm/SD=3.5cm)	NIF	Unimarginal flake tool	Primary and secondary percussion/ pressure	ventral surface, raised hump, 2 erailure flake scar/ dorsal surface, multiple flake extracted
1	17 (TRC)	Santa Verna	2015	Chert	Detached piece	Debitage (GD=2.2cm/SD=0.9cm)	Flake debitage	Flake shatter/ Decortication flakes?	NIF	ventral surface/ dorsal surface with cortex
1	52	Santa Verna	2015	Chert	Detached piece	Flake (GD=2.1cm/SD=1.4cm)	Flake tool/ Decortication flake	Unimarginal flake tool	Percussion	Ventral surface, ripple marks, raised hump?/ dorsal surface, arris for flake removal, cortex?
1	36	Santa Verna	2015	Chert	Detached piece	Chip (GD=1.05cm/SD=1.0cm)	Flake tool	Unimarginal flake tool	Percussion/ secondary pressure	Ventral surface/ dorsal, arris
144	42	Santa Verna	2015	Chert	Detached piece	Flake (GD=2.3cm/SD=2.0cm)	Flake	NIF	Percussion?	Ventral and dorsal surface/ polished on both surfaces! No rough surfaces left
32	5	Santa Verna	2015	Chert	Detached piece	Flake (GD=2.6cm/SD=2.4cm)	decortication flakes/ flake tool	Scraper	Primary percussion, secondary pressure	ventral surface, raised hump, erailure flake scar/ dorsal surface, cortex, full edges retouch
1	16	Santa Verna	2015	Chert	Detached piece	Flake (GD=3.7cm/SD=1.8cm)	Prismatic Flake	Blade	Percussion/ percussion for flake extraction	Ventral surface/ dorsal surface, arris flake extraction
1	80	Santa Verna	2015	Chert	Detached piece	Flake (GD=2.5cm/SD=1.6cm)	Prismatic Flake	Unimarginal flake tool/ Blade?	Primary Percussion/ secondary pressure	Ventral surface, raise hump, erailure flake scar/ dorsal surface, retouch, multi-arris flake extraction, edge retouched, serration
1	4	Santa Verna	2015	Chert	Detached piece	Flake (GD=2.4cm/SD=0.6cm)	Prismatic Flake	Blade	Percussion/ percussion for flake extraction	Ventral surface/ dorsal surface, arris flake extraction, retouch for sharpening

1	4	Santa Verna	2015	NIF	Detached piece	Flake (GD=1.5cm/SD=0.56cm)	Prismatic Flake	Micro-Blade	Percussion/ pressure for retouch	Ventral surface/ dorsal surface, arris utility, extensive retouch of edges for sharpness?, serration
156	306/TRI VB/sieve	Kordin	2015	Chert	Detached piece	Debitage (GD=1.8/SD=0.8cm)	Flake debitage	Proximal flake	Percussion possibly	Raised hump and ripple marks on ventral surface
42	304	Kordin	2015	chert	Detached piece	Flake (GD=1.2/SD=1.1cm)	Flake tool	Unimarginal flake tool	NIF/Percussion?	Ventral and dorsal surface, arris on dorsal and ripple marks on the ventral
?	71	Kordin	2015	flint	Detached piece	Debitage (GD=1.8/SD=1.1cm)	Flake debitage	Proximal flake/rejuvenation flake?	Percussion	Ventral and dorsal, ripple marks, discernible point of applied force/striking platform, the strike was with an angle?
98	201	Kordin	2015	chert	Detached piece	Flake (GD=3.7/SD=1.9cm)	Prismatic flake	Burin	Percussion, burin blow	ventral and dorsal surface, raised hump, feather edge at distal end, step flaking for sharpening
141	150? TRIIB	Kordin	2015	chert	Detached piece	Flake (GD=2.8/SD=1.5cm)	Prismatic flake	Unimarginal flake tool	Percussion, secondary percussion flaking,	ventral and dorsal surface, raised hump, ripple marks, from secondary flaking erailure scar, unimarginal retouch
?(1)	22	Kordin	2015	chert	Detached piece	Flake (GD=5.5/SD=3cm)	flake tool	Unimarginal flake tool	Percussion	ventral surface with raised mark and erailre flake scar, dorsal surface with secondary flaking for producing more flakes
34	207	Kordin	2015	chert	Detached piece	Flake (GD=5.5/SD=3.2cm)	Decortication flakes	Flake scraper	Percussion and secondary percussion, pressure for retouch	Ventral surface raised hump more than one, ripple marks of different direction, flake scars
195	209	Kordin	2015	chert	Detached piece	Debitage (GD=2.1/SD=1.3cm)	Debitage Flake	flake shatter	NIF	ventral and dorsal surface, no sticking platform

69	211	Kordin	2015	chert	Detached piece	Flake (GD=3.7/ SD=3.5cm)	Conchoidal Flake	Scraper	Percussion and secondary percussion, pressure for retouch	ventral surface, raised hump, flake scar, dorsal surface axis for flake extraction, secondary unimarginal edge modification with pressure
144	306	Kordin	2015	chert	Detached piece	Debitage (GD=1.4/ SD=0.8cm)	Flakedebitage	Flake shatter	percussion? NIT	ventral and dorsal surface, with arris, ripple marks on both surfaces
27	207	Kordin	2015	chert	Detached piece	Debitage (GD=2.1/ SD=1.6cm)	Flakedebitage	Proximal flake	Percussion	ventral surface, raised marks and dorsal surface with arris, similar with S42/L304
27	203	Kordin	2015	chert	Detached piece	Flake (GD=3.1/ SD=2.1cm)	Non-bifacial	Flake scraper	Percussion and secondary pressure flaking	ventral surface, raised hump, dorsal cortex, unimarginal edge modification
9	201	Kordin	2015	Chert	Detached piece	Flake (GD=2/ SD=1.5cm)	Flake tool	Unimarginal flake tool	Percussion, secondary flaking ventral surface	ventral surface, raised hump, flake scar, secondary flaking modification, arris, dorsal surface. First tool where ventral surface was modified
133	211	Kordin	2015	Chert	Detached piece	Flake (GD=3.3/ SD=3cm)	Conchoidal Flake/ decortication flake	Scraper	Percussion and secondary pressure for retouch	ventral surface, raised hump, dorsal surface cortex, secondary unimarginal edge modification
513	272	Tac Cawla	2014	Chert	Detached piece	Flake (GD=3/ SD=1.6cm)	Flake tool	Unimarginal Flake	Percussion	Ventral and dorsal surface. Arris on one of the surface/ fragment of a bigger flake
37	30	Tac Cawla	2014	Chert	Detached/ Objective piece	Flake (GD=3cm/ SD=1.5cm)	Prismatic Flake/ Tool	Unhafted bifaces tool	Percussion	Ventral surface with flake removed, striking point recorded on one side and arris from flake removal/ Dorsal surface with flakes removed and arris / sticking platform on the other side

103	85	Tac Cawla	2014	Chert	Detached piece	Flake (GD=2.1cm/SD=0.5cm)	Prismatic/ Bending flake	Blade, Unhafted bifacse tool	Percussion/ First and secondary flaking	Ventral surface retouched with arris, dorsal surface with girding and polishing close to point tip FIRST TIME FOUND
252	179	Tac Cawla	2014	Chert	Detached piece	Flake (GD=2.2cm/SD=1.6cm)	Conchoidal Flake	Unimarginal flake scraper	Percussion/ First and secondary flaking, pressure for retouch	Ventral surface, erailure scar, raised hump/ dorsal surface, retouch and arris, unimarginal edge modification
275	208	Tac Cawla	2014	Chert	Detached piece	Flake (GD=2.2cm/SD=1.6cm)	Biface tool/ flake tool	Unhafted biface tool/ Bimarginal flake tool	Primary percussion, secondary pressure for retouch	Ventral and dorsal surfaces, arris from flake removal with pressure for retouch or sharpening
577	131	Tac Cawla	2014	Chert	Detached piece	Flake (GD=2.5cm/SD=1.4cm)	Conchoidal Flake	Unimargianl flake tool	Primary and secondary percussion, secondary for retouch extracting more flakes	Ventral surface with ripple marks and erailure flake scar and/ dorsal surfaces, arris from flake removal from a different sticking platform and arris
193	69	Tac Cawla	2014	Chert	Detached piece	Flake (GD=1.7cm/SD=1.5cm)	Flake tool	Unimargianl flake tool	Percussion, secondary for retouch or extracting more flakes	Ventral surface / dorsal surfaces with arris possible for retouch
595	81	Tac Cawla	2014	Chert	Detached piece	Flake (GD=2.6cm/SD=1.0cm)	Prismatic flake/ Unimargianl flake tool	Blade	Primary and secondary percussion, secondary for retouch/ pressure for retouch the edges	Ventral surface / dorsal surfaces with arris possible for retouch and edge retouched for sharpening the blade, feather edge
460	273	Tac Cawla	2014	Chert	Detached piece	Debitage (GD=1.6cm/SD=1.1cm)	Shatter	Flake Shatter	NIF	Ventral surface and dorsal surfaces with surface of flake extraction
502	301	Tac Cawla	2014	Chert	Detached piece	Flake (GD=3.95cm/SD=2.2cm)	Flake tool	Bimarginal flake tool/ Blade?	Primary percussion, and secondary pressure	ventral surface, ripple marks and edge retouch/ dorsal surface, flake removal, arris and serration, something NOT reported before
176	100	Tac Cawla	2014	Chert	Detached piece	Flake (GD=2.7cm/SD=2.6cm)	Decortication flakes	Flake Shatter	Percussion	Ventral surface, ripple marks and erailure scar/ dorsal with cortex/ no retouch

32A	30	Tac Cawla	2014	Chert	Detached piece	Debitage (GD=3.8cm/SD=3.5cm)	Flake	Flake shatter/Decortication flake?	Percussion	ventral surface, raised hump/dorsal surface
32B	30	Tac Cawla	2014	Chert	Detached piece	Flake (GD=2.7cm/SD=2.0cm)	Flake tool	Unimarginal flake tool	Primary Percussion, secondary percussion flake extraction	Ventral surface, raised hump/dorsal with retouch and arris
567	206	Tac Cawla	2014	Secondary Calcite	Detached piece	Debitage (GD=2.6cm/SD=1.8cm)	Non-flake	Angular Shatter	NIF	NIF
144	?	Tac Cawla	2014	Chert	Detached piece	Flake (GD=1.7cm/SD=1.1cm)	Flake tool	Unimarginal flake tool	NIF/ Secondary pressure	ventral surface/ dorsal surface retouched, flake extracted
416	178	Tac Cawla	2014	Chert	Detached piece	Flake (GD=2.5cm/SD=1.8cm)	Conchoidal Flake	Unimarginal flake tool	Primary and secondary percussion/ secondary pressure retouch	Ventral surface, raised hump, ripple marks and erailure scar/ dorsal arris flake extraction, edge retouch and serration
101	85	Tac Cawla	2014	Chert	Detached piece	Flake (GD=1.5cm/SD=1.3cm)	Flake too	Unimarginal flake tool	NIF/secondary percussion and pressure	ventral/ dorsal arris edge retouch and further edge retouch
162	155	Tac Cawla	2014	Chert	Detached piece	Debitage/debris (GD=1.5cm/SD=1.2cm)	Flake	Flake shatter	NIF	ventral with curve/ dorsal retouch with flake removal arris but not certain
316b	63	Tac Cawla	2014	Chert	Detached piece	Flake (GD=2.2cm/SD=2.2cm)	Flake tool	Unimarginal flake tool	NIF/ secondary pressure	ventral surface/ dorsal retouch flake extraction, polished?
745	845	Xaghra Circle	1991	Chert	Detached piece	Flake	Conchoidal Flake	Scraper (GD=4cm)	Percussion and pressure for retouch	raised hump on ventral surface, bulb of force, erailure flake scar, dorsal with secondary flaking, unimarginal
566	662	Xaghra Circle	1991	chert	Detached piece	Flake	Prismatic flake	blade (L=4/W=2cm)	Percussion and pressure for retouch	raised hump on ventral surface, dorsal with secondary flaking and arris, unimarginal

843	4	Xaghra Circle	1993	Flint	Detached piece	Debri (GD= 1,8 cm)	Flake Debitage	Proximal Flake/ Erailure flake	Percussion	Ventral surface, bulb of force, dorsal surface
564	662	Xaghra Circle	1991	Flint	Detached piece	Flake (L=1,1/W=1,6)	Flake tool	Unimarginal flake tool	Percussion	Ventral surface with ripple marks, dorsal surface with secondary flaking, unimarginal
611	712	Xaghra Circle	1991	Flint	Detached piece	Flake	Prismatic flake	blade (L=2,2/W=1cm)	Percussion	Ventral and dorsal surface with secondary flaking and arris, unimarginal
291	334	Xaghra Circle	1989	Flint	Detached piece	Flake	Prismatic flake	microblade (L=1,5/W=0,8cm)/ no scraper	Percussion and pressure for retouch	proximal end, ventral surface, bulb of force, dorsal with secondary flaking and arris, unimarginal retouched edges
854	897	Xaghra Circle	1993	Chert	Detached piece	Flake	Prismatic flake	blade (L=1,8/W=0,9cm)	Percussion and pressure for retouch	Ventral surface, ripple marks, dorsal with secondary flaking, unimarginal retouched edges
1142	1279	Xaghra Circle	1994	Chert	Detached piece	Flake	decortication flakes	Flake Scraper (GD=2,6cm)	Percussion and pressure for retouch	Ventral surface, bulb of force, proximal end, unimarginal edge modification
395	449	Xaghra Circle	1989	Flint scraper	Detached piece	Flake	decortication/side struck flakes	Flake Scraper (GD=3cm)	Percussion and pressure for retouch	Ventral surface, bulb of force, proximal end, erailure flake scar, dorsal unimarginal edge modification
110	274	Xaghra Circle	1988	Flint	Detached piece	Flake	Prismatic flake	NIF (L=2,1/W=1,4cm), bending flake?	Percussion and pressure for retouch (Levallois)	Ventral surface, ripple marks, distal end, dorsal unimarginal modification, flakes removal indications with percussion
767	783	Xaghra Circle	1991	Chert	Detached piece	Flake	Conchoidal flake	Flake Scraper (GD=5cm/SD=3,4cm)	Percussion and pressure for retouch	raised hump on ventral surface, bulb of force, erailure flake scar, dorsal surface with ripple marks and with secondary flaking, unimarginal

Top-soil and Upper strata of excavation

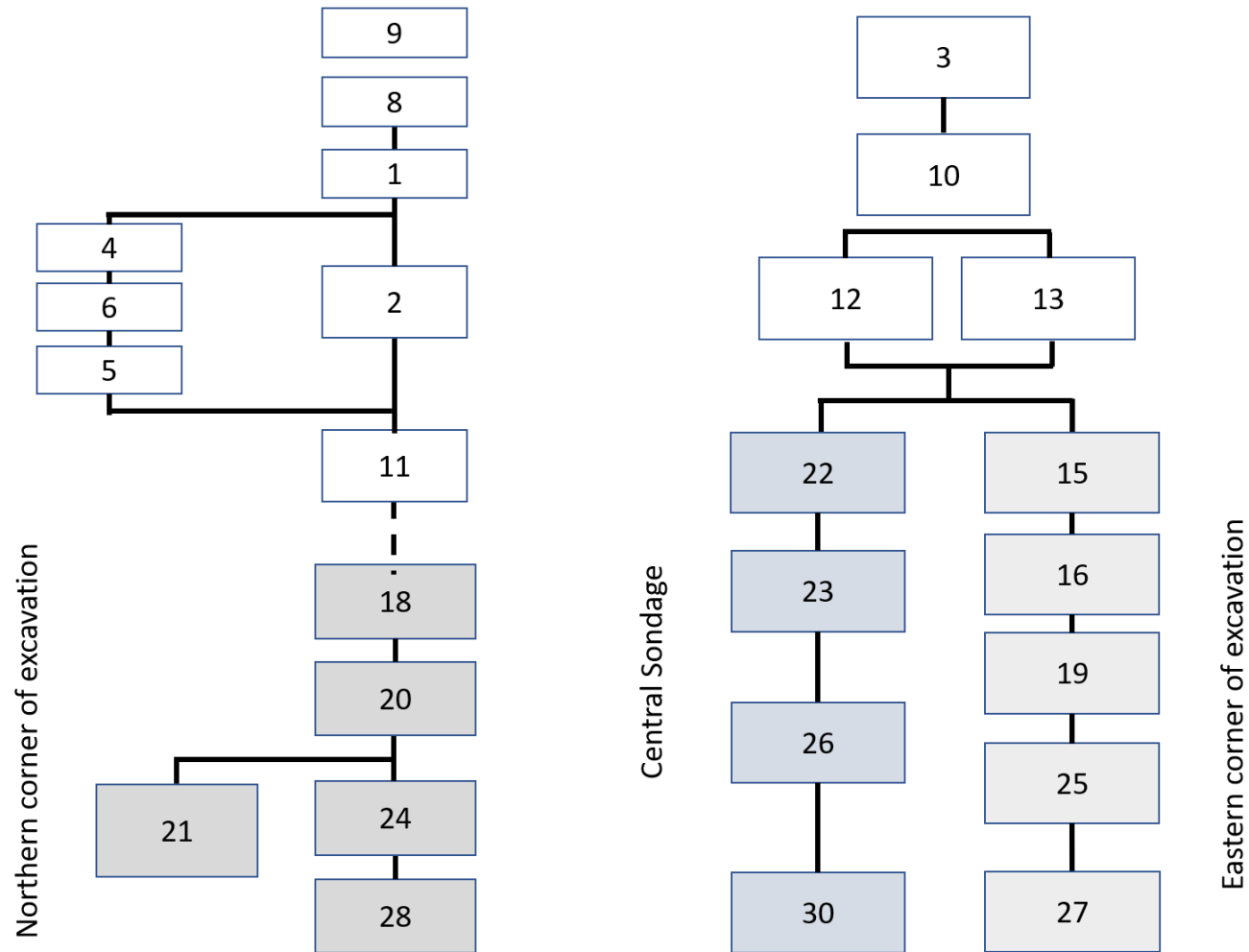


Figure 2: The Harris Matrix of 2016 Skorba excavation. The white boxes show the top-soil and the Upper strata of the trenches. The dark grey boxes the northern corner, the blue the central sondage and light grey the eastern corner of the excavation.

Images of the spectra collected with the FTIR – ATR method.

Rock Samples

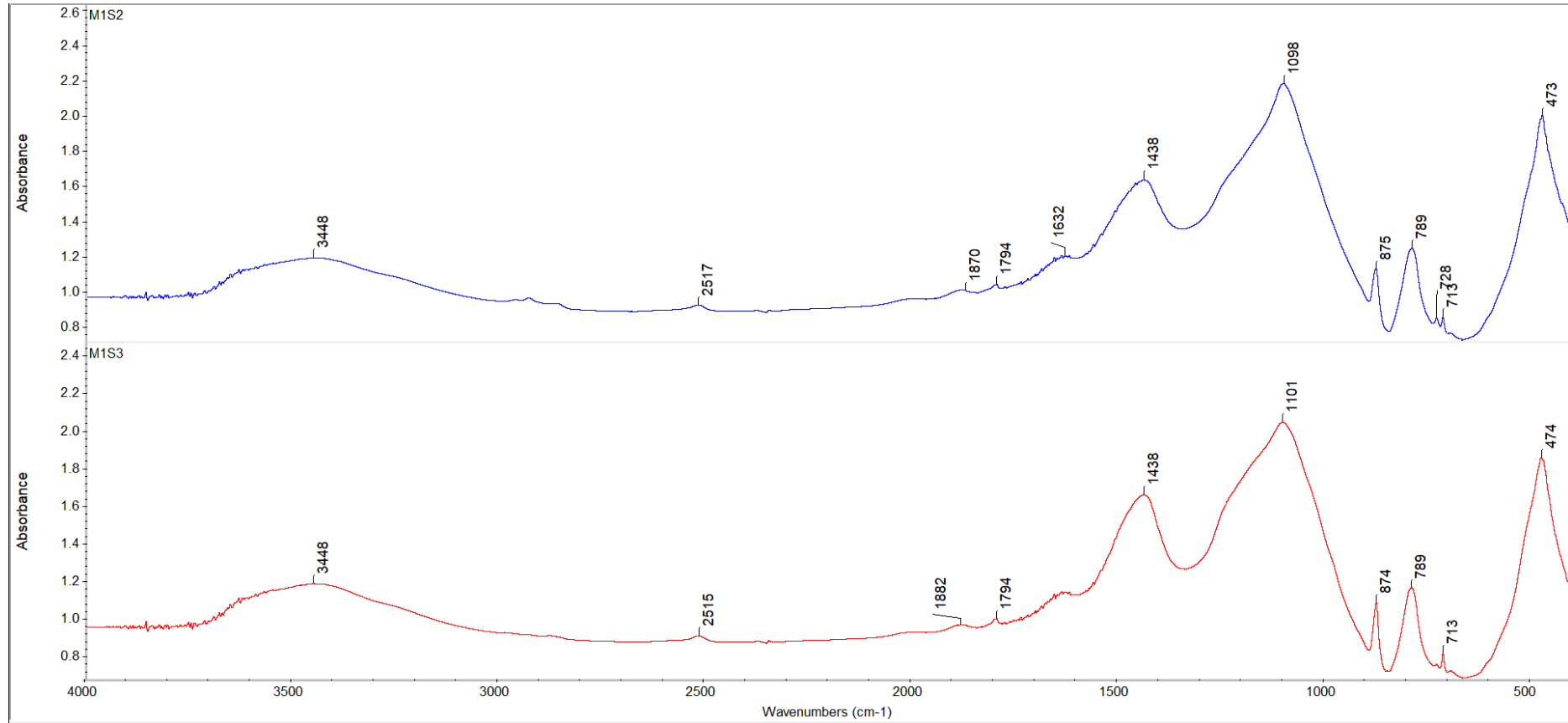


Figure.3: FTIR spectra of the samples from Malta.

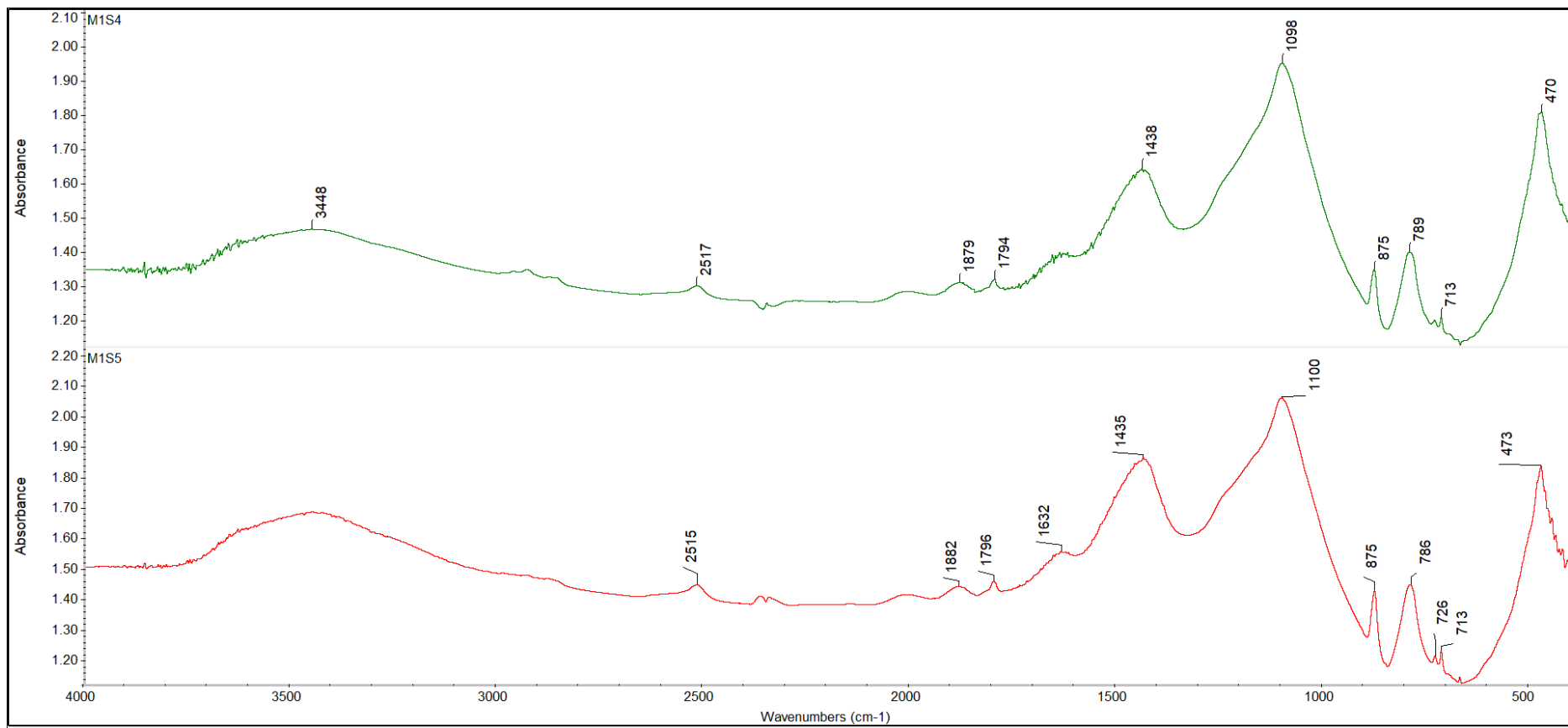


Figure 4: FTIR spectra of the samples from Malta.

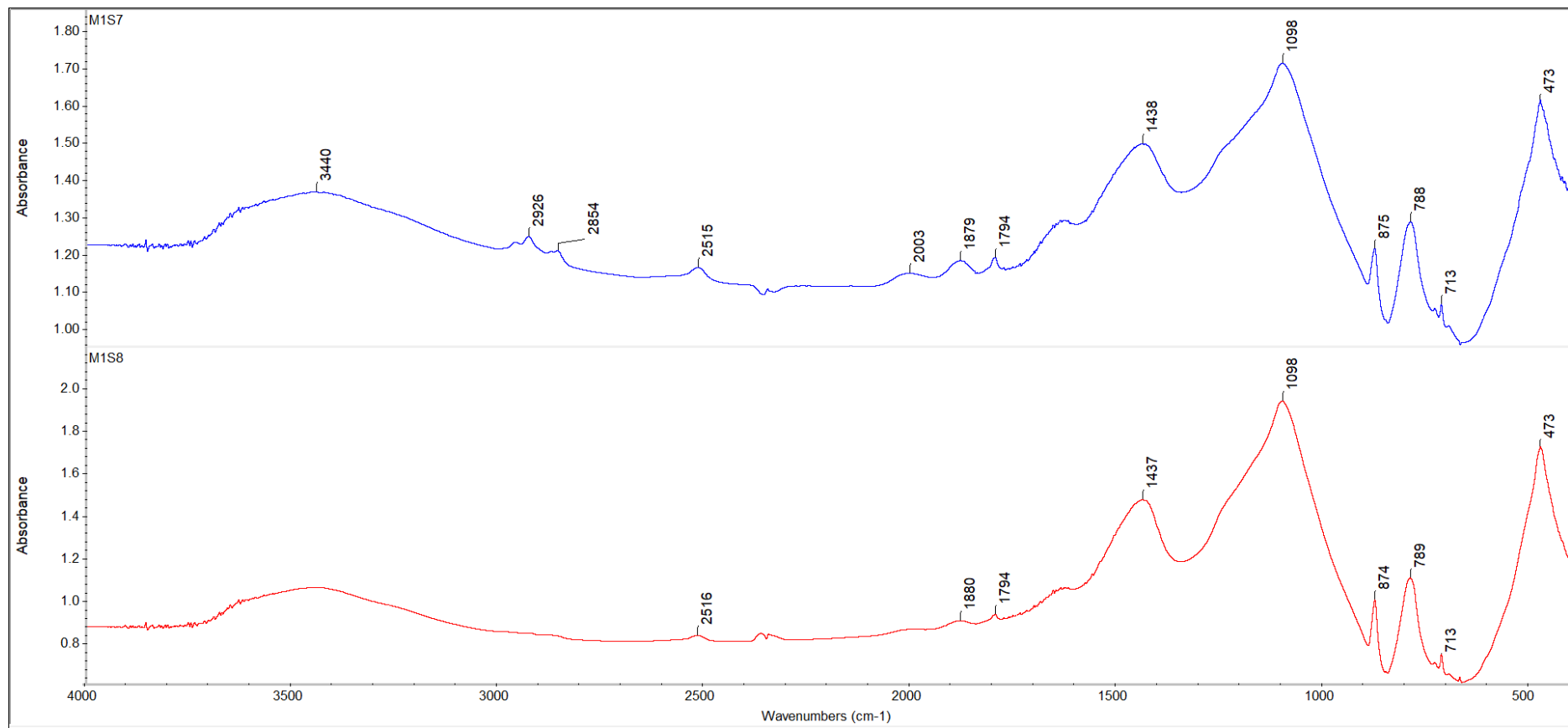


Figure 5: FTIR spectra of the samples from Malta.

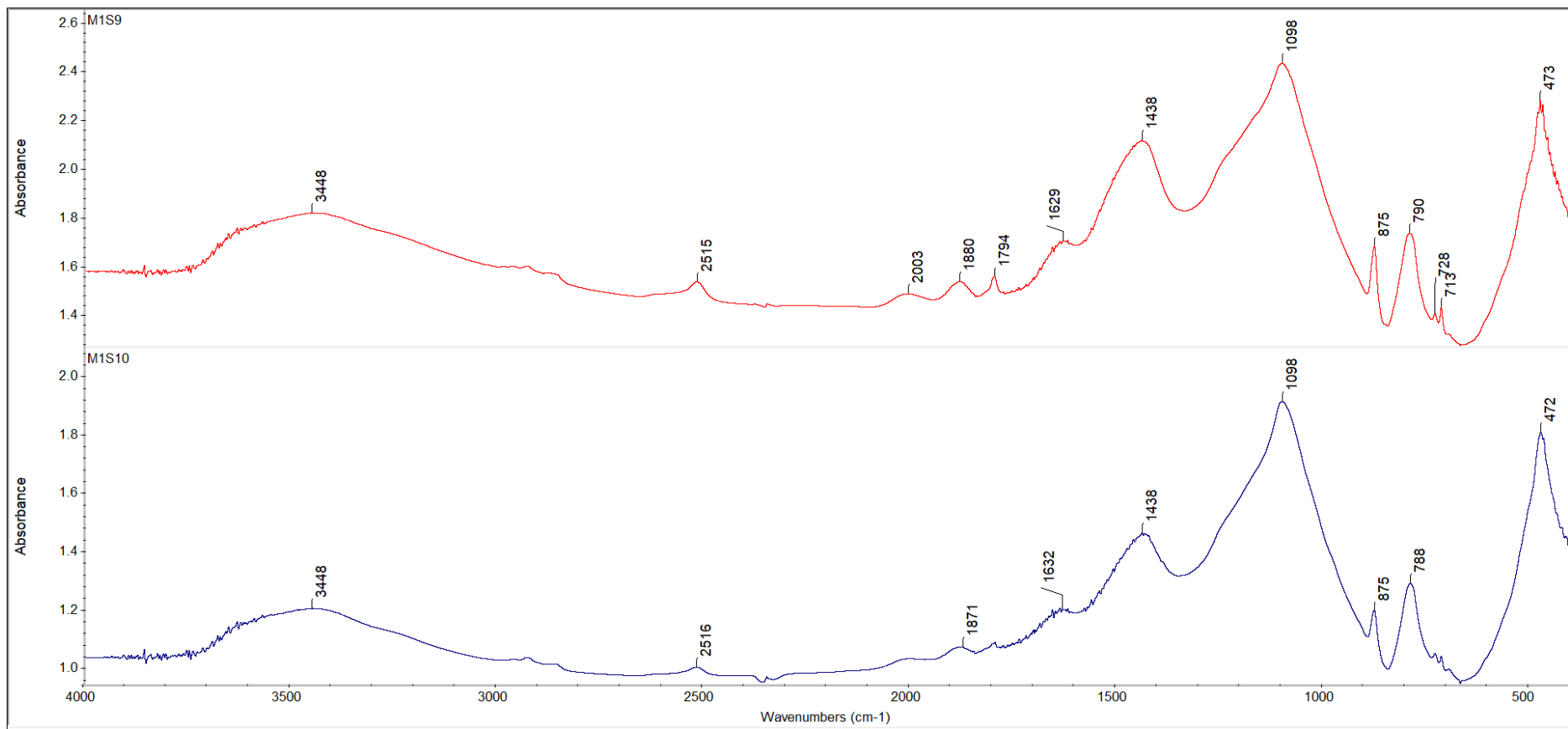


Figure 6: FTIR spectra of the samples from Malta.

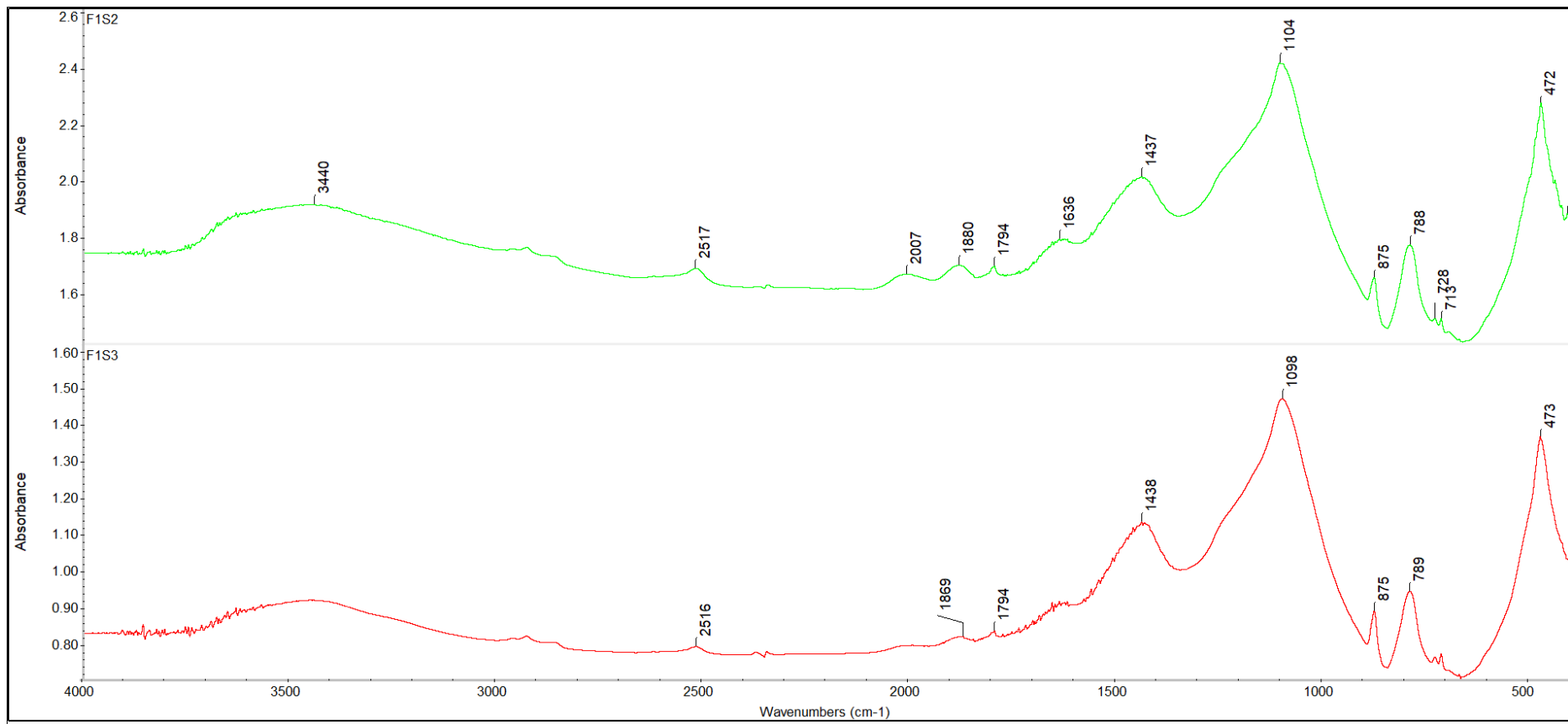


Figure 7: FTIR spectra of the samples from Malta.

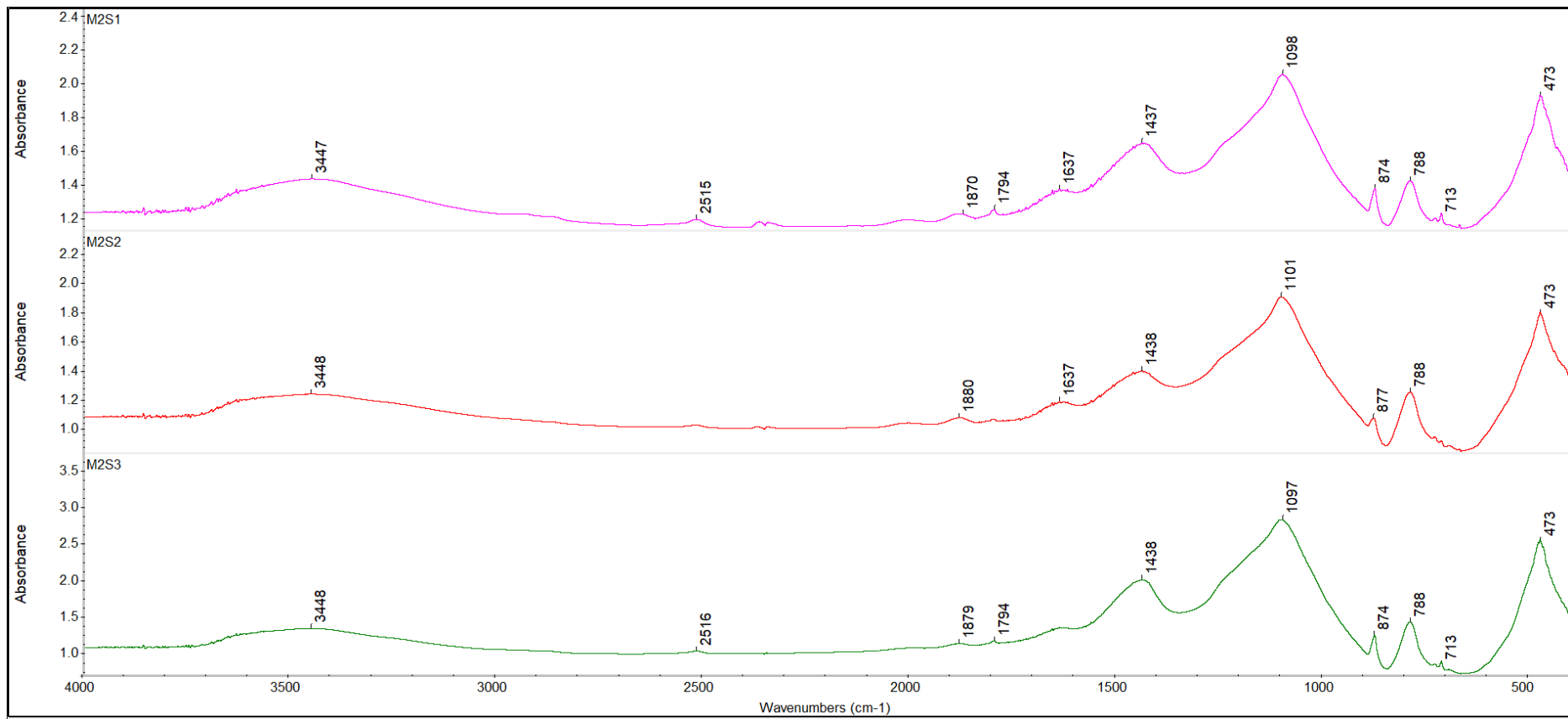


Figure 8: FTIR spectra of the samples from Malta.

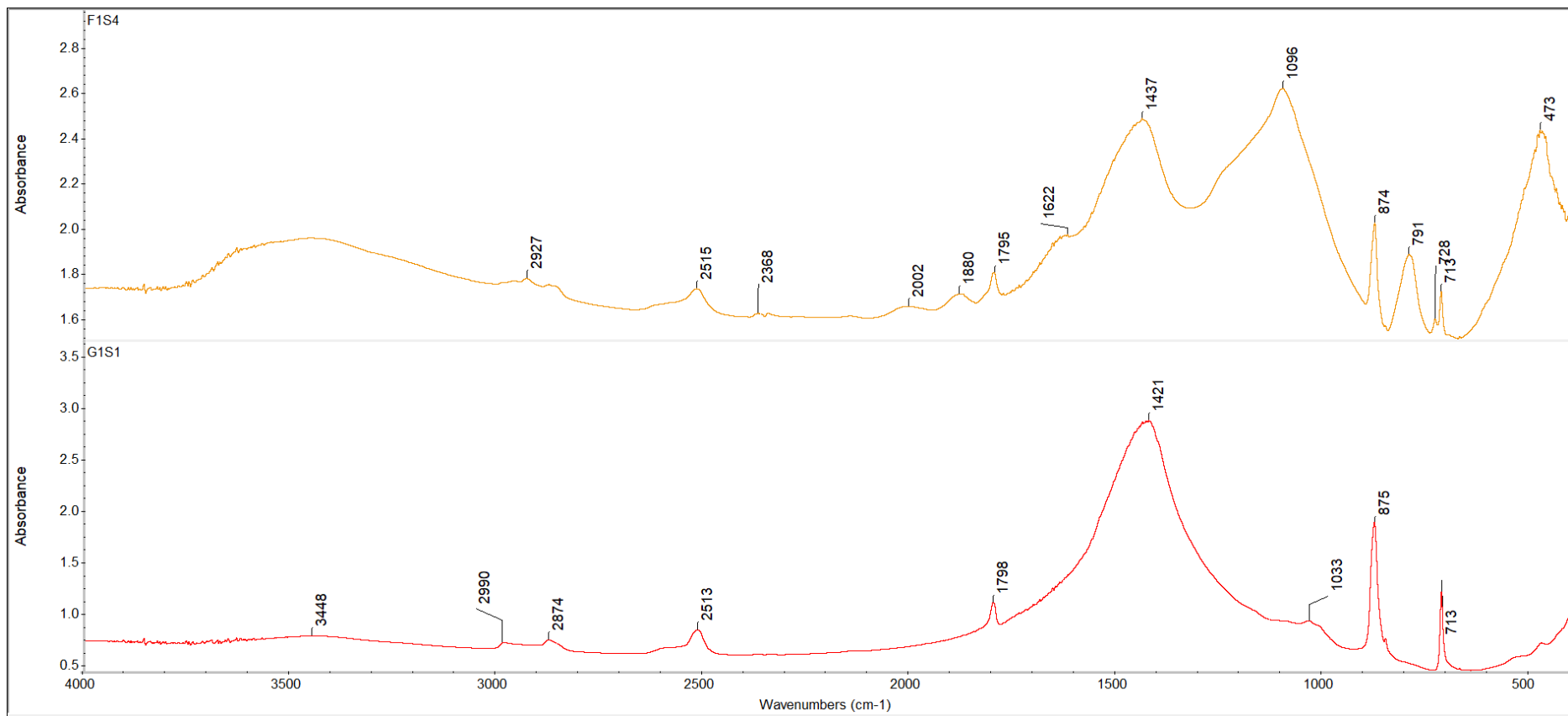


Figure 9: FTIR spectra of the samples from Gozo.

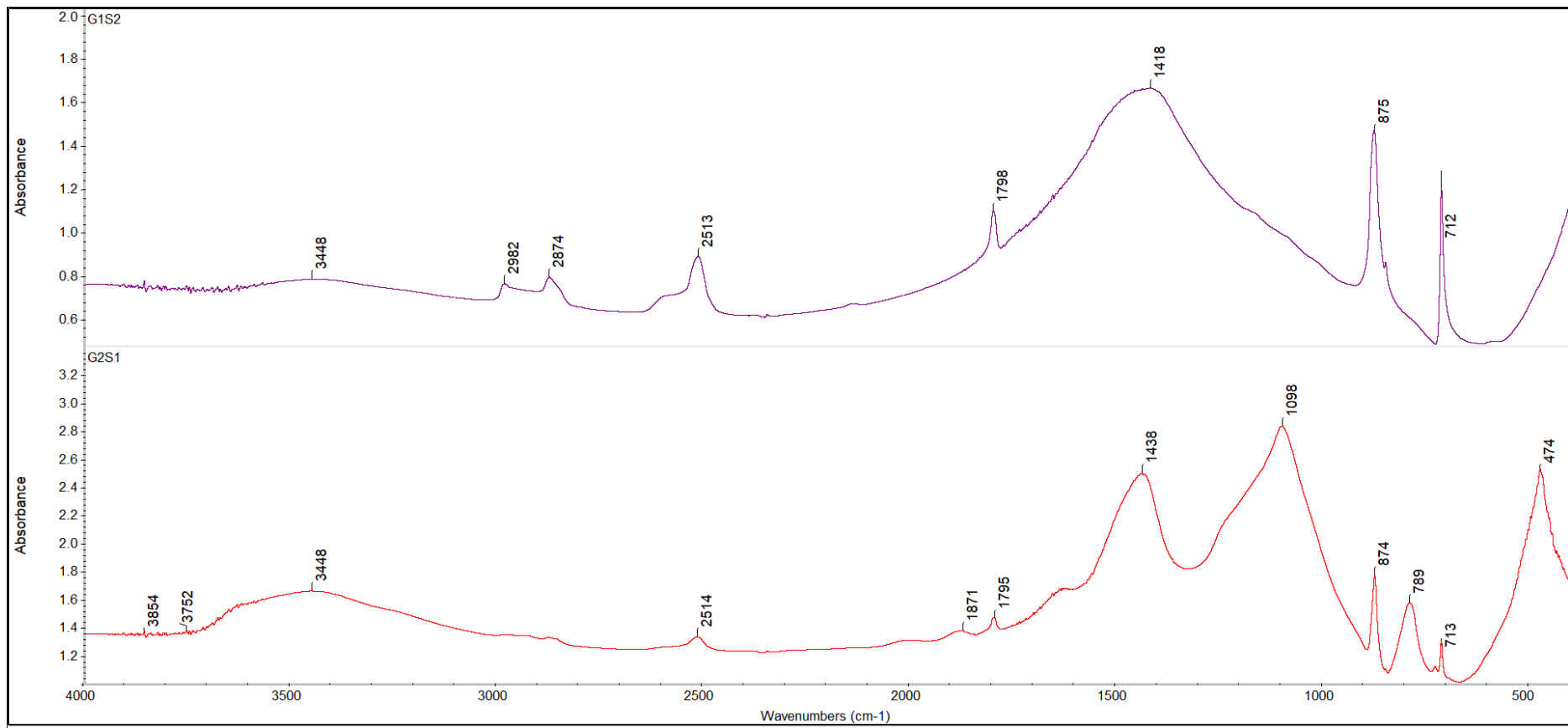


Figure 10: FTIR spectra of the samples from Gozo.

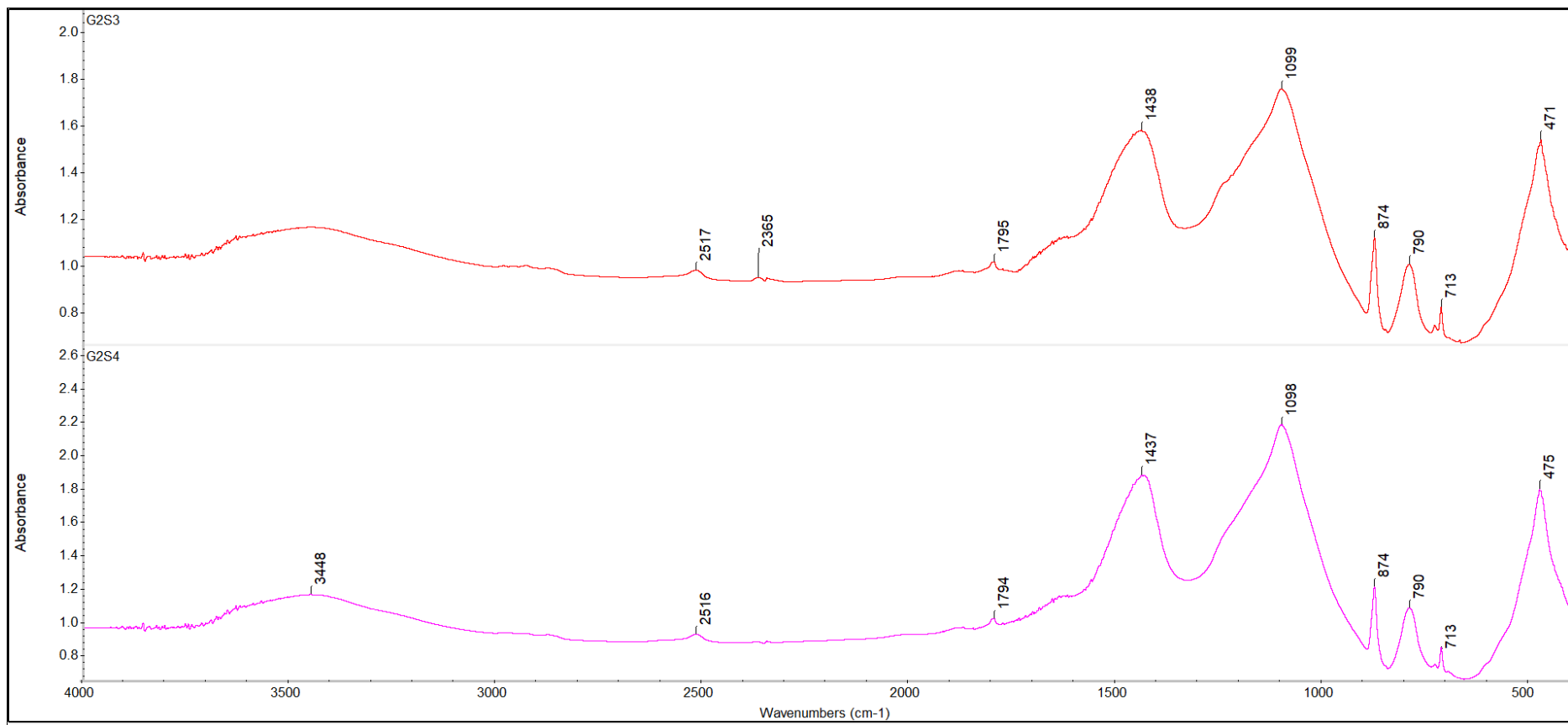


Figure 11: FTIR spectra of the samples from Gozo.

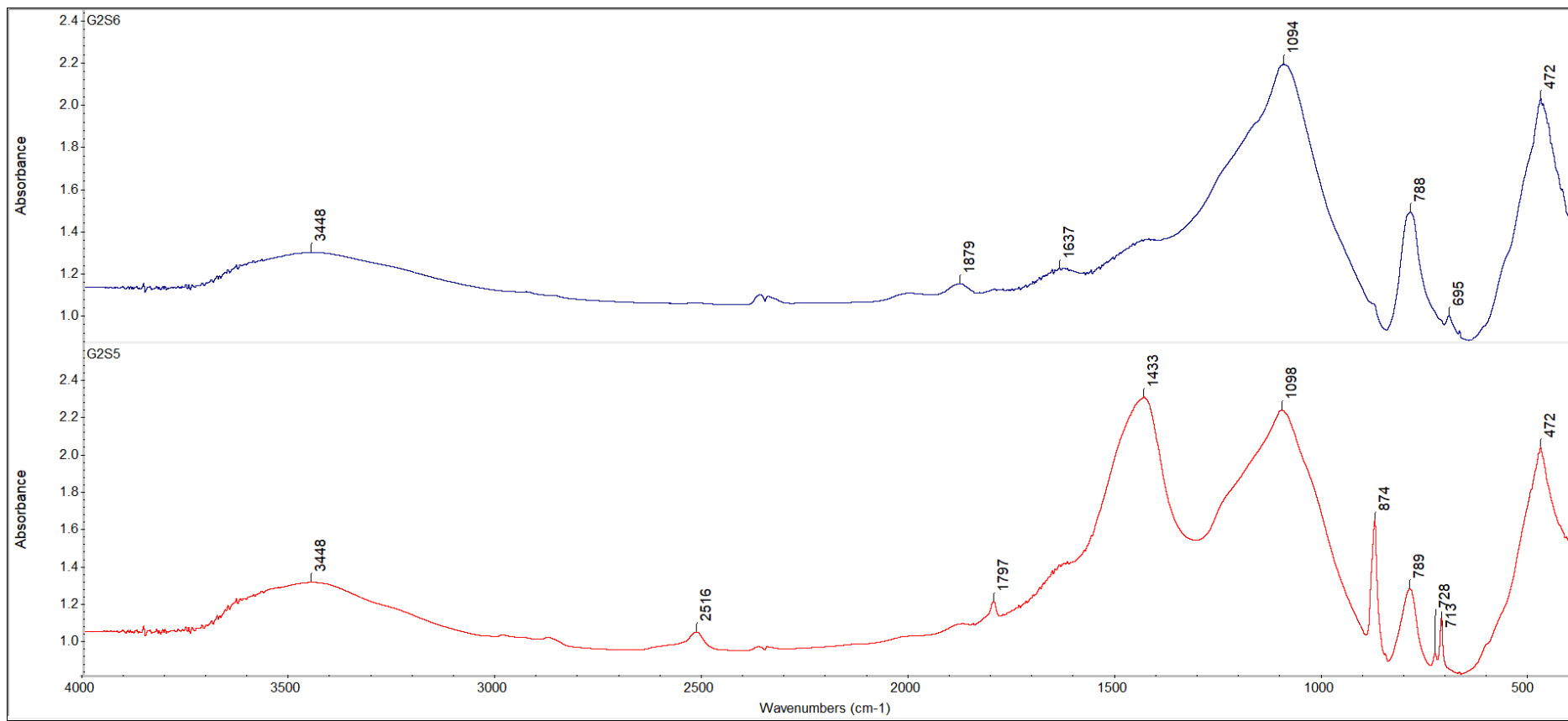


Figure 12: FTIR spectra of the samples from Gozo.

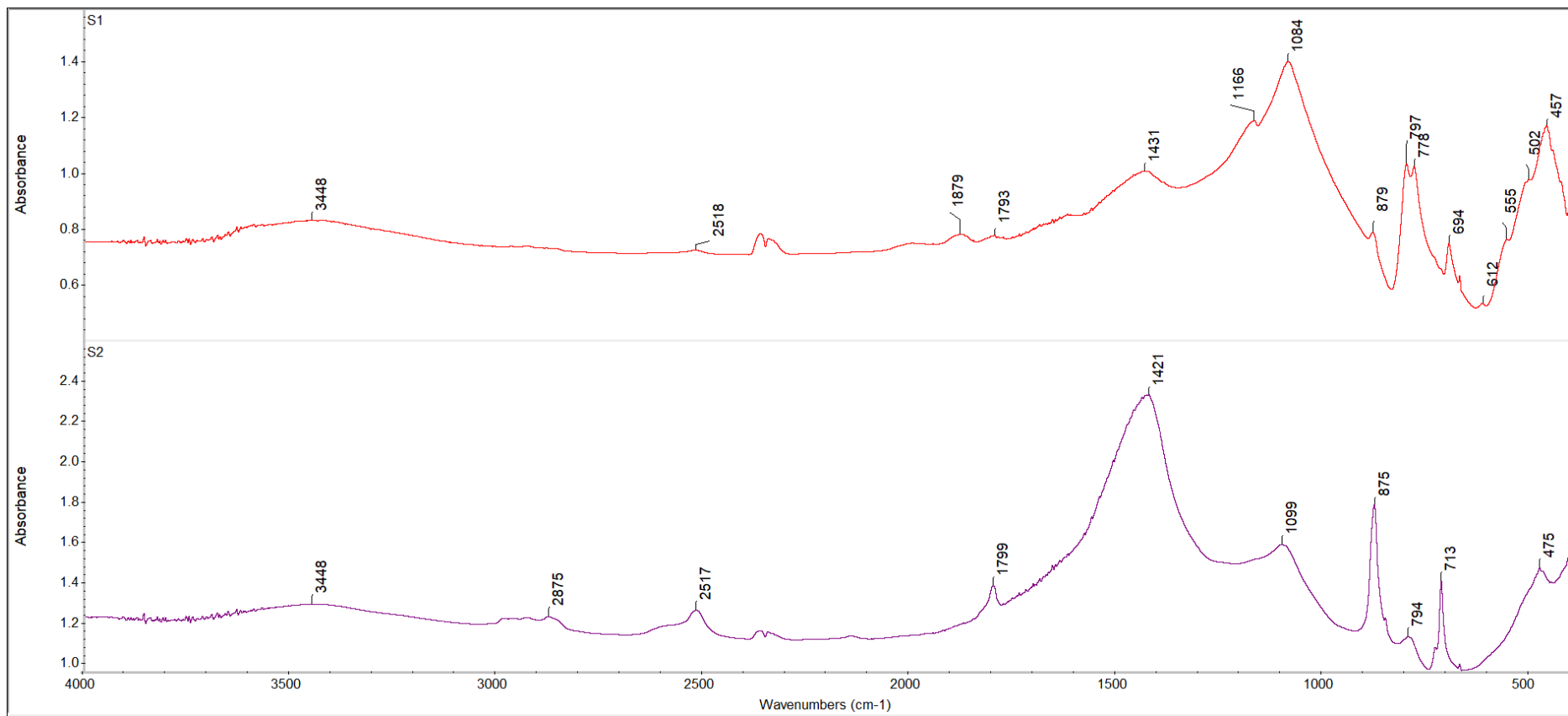


Figure 13: FTIR spectra of the samples from Sicily.

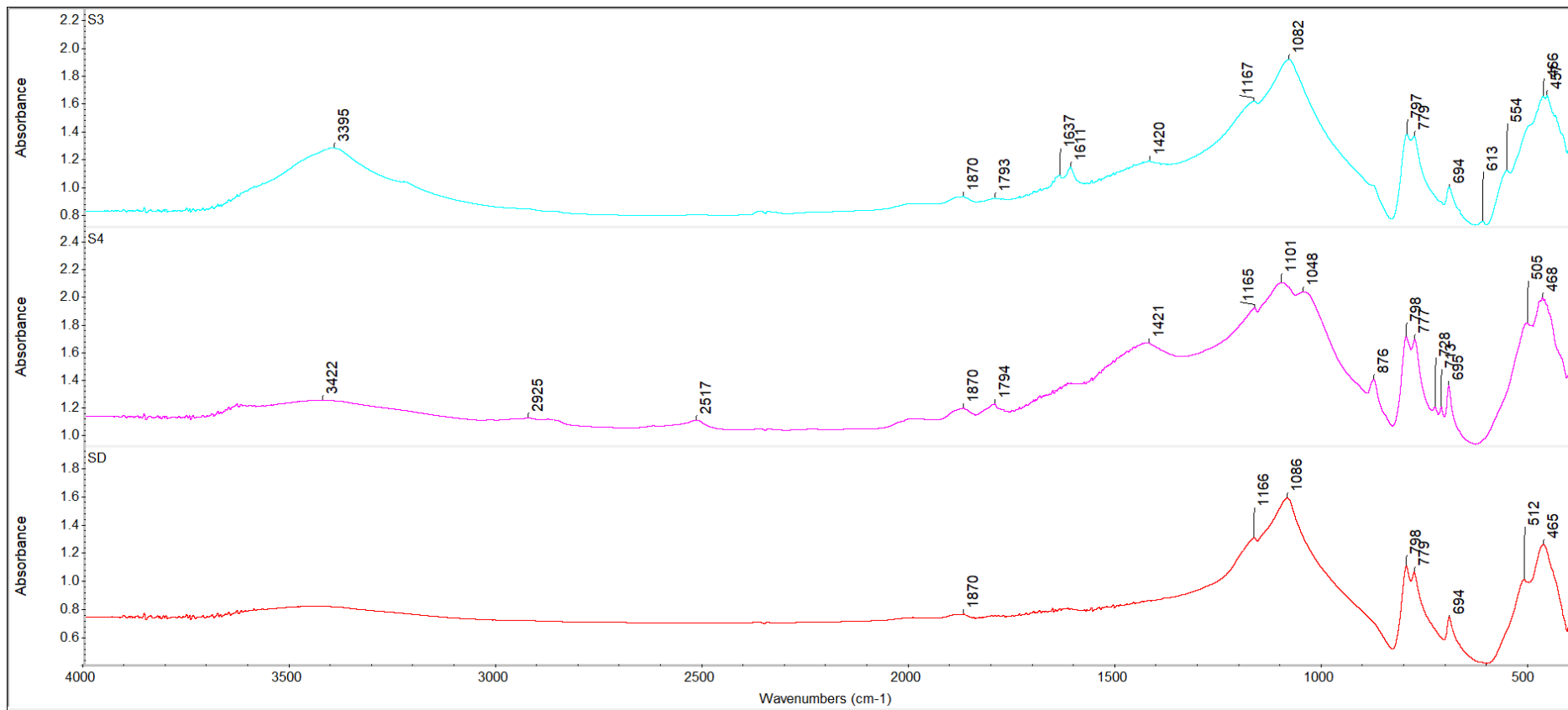


Figure 14: FTIR spectra of the samples from Sicily.

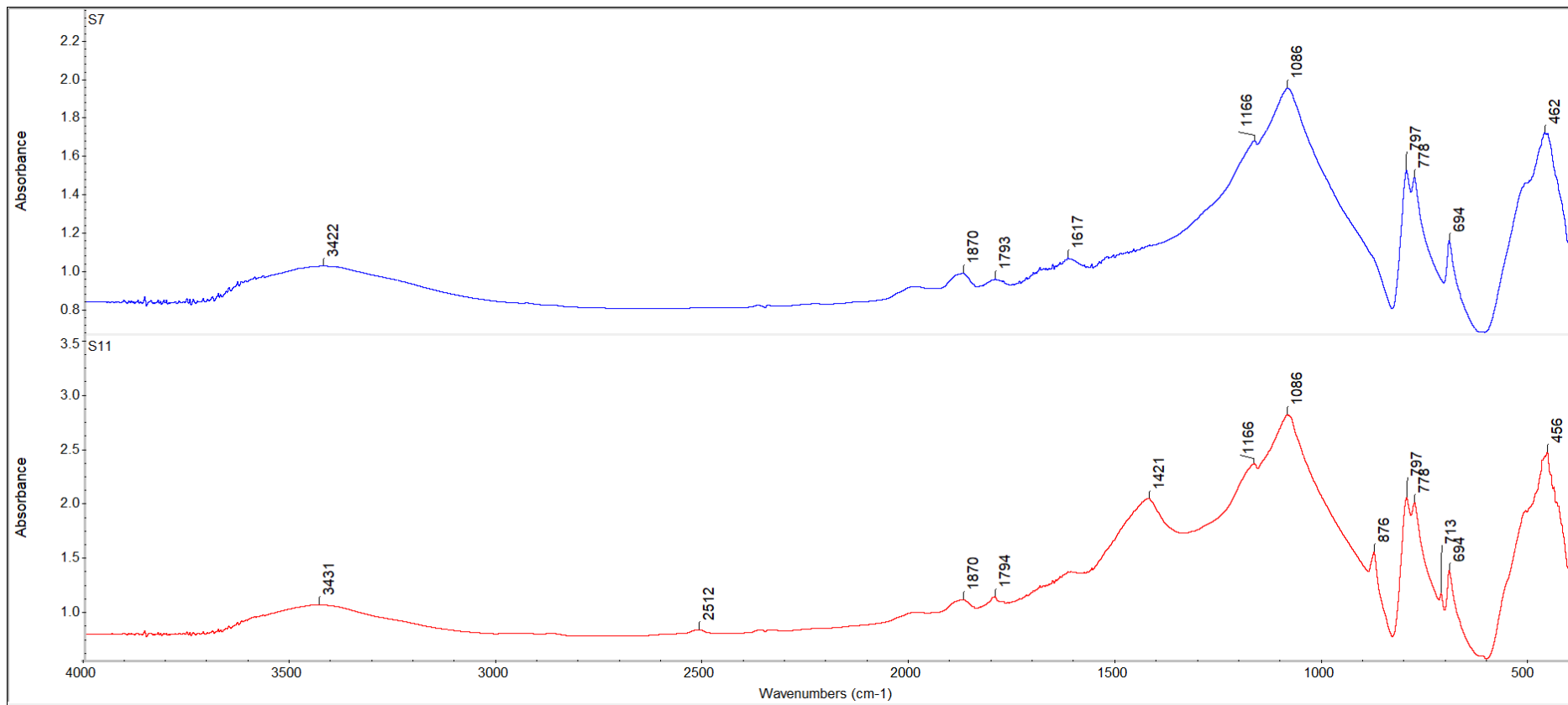


Figure 15: FTIR spectra of the samples from Sicily.

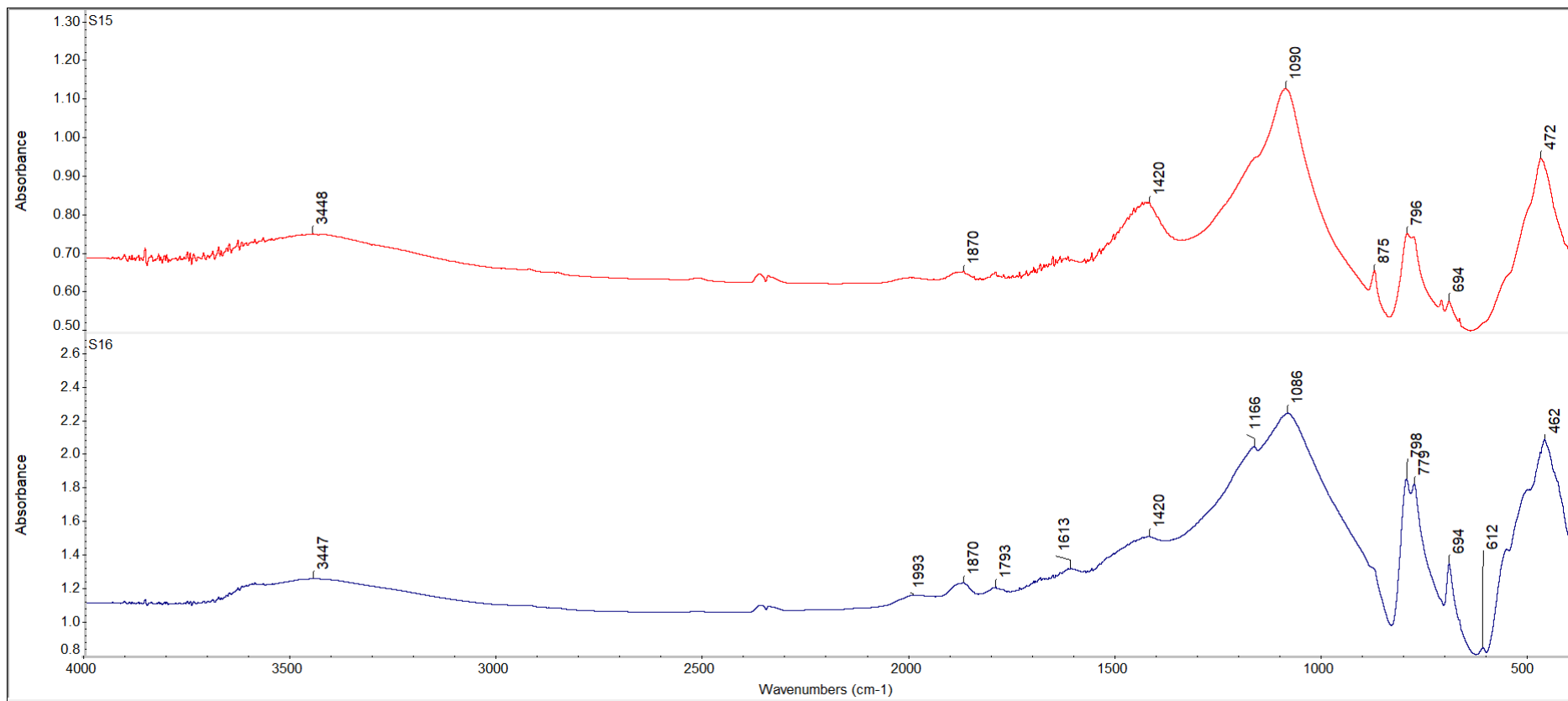


Figure 16: FTIR spectra of the samples from Sicily.

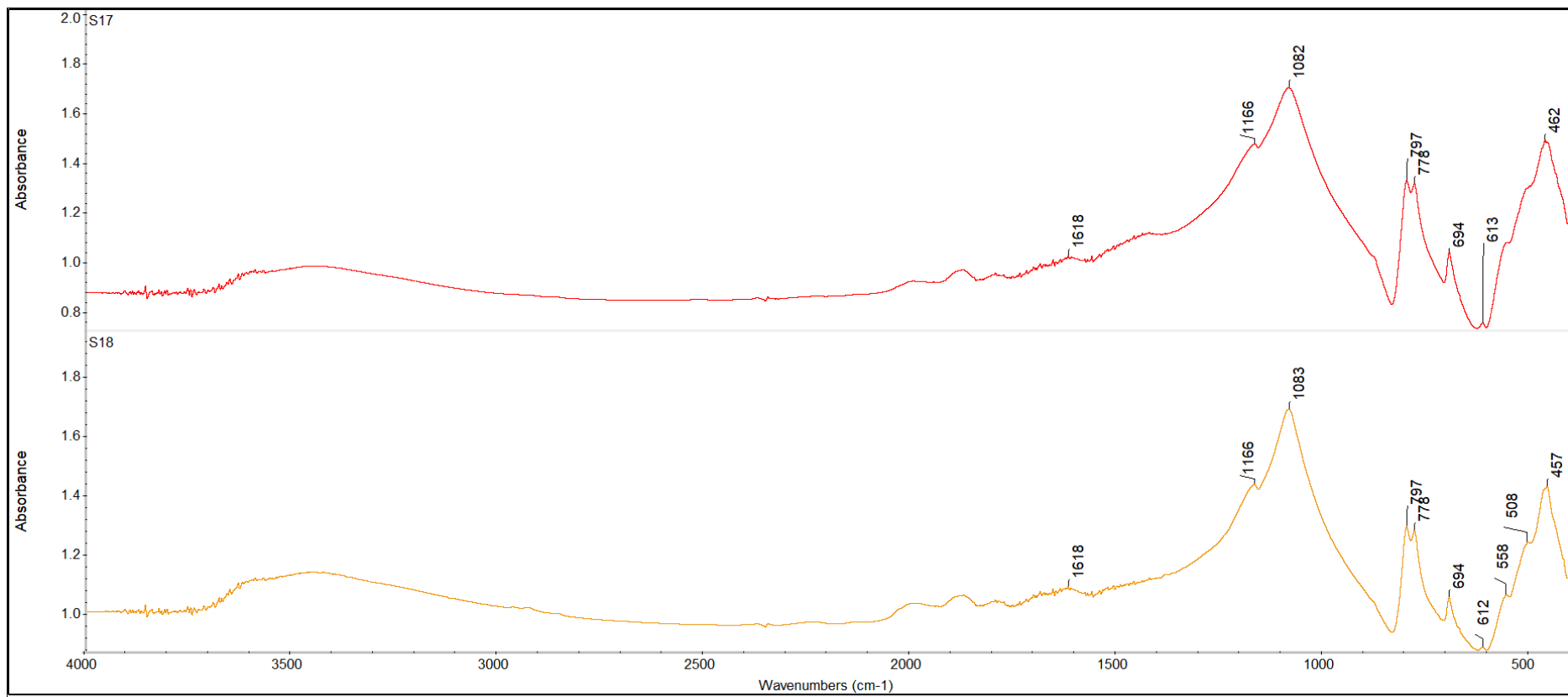


Figure 17: FTIR spectra of the samples from Sicily.

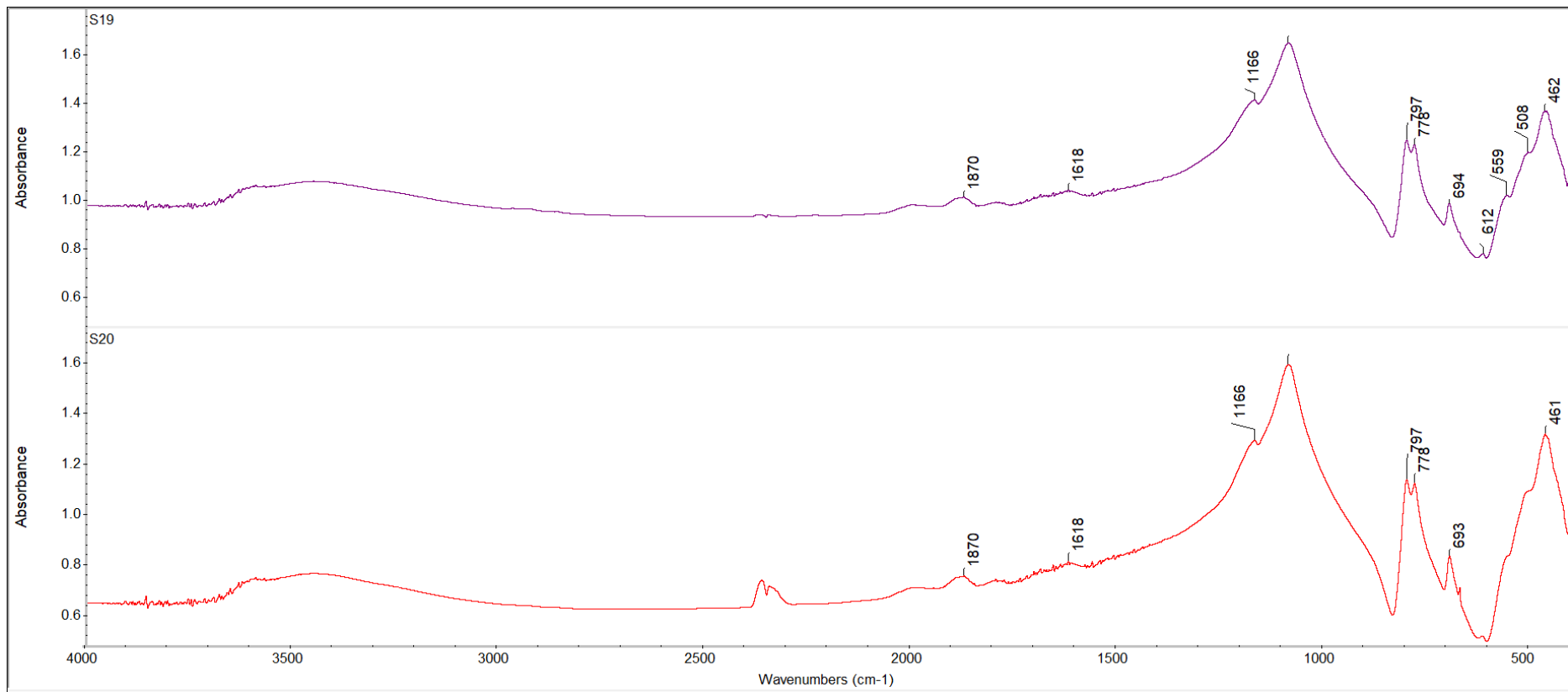


Figure 18: FTIR spectra of the samples from Sicily.

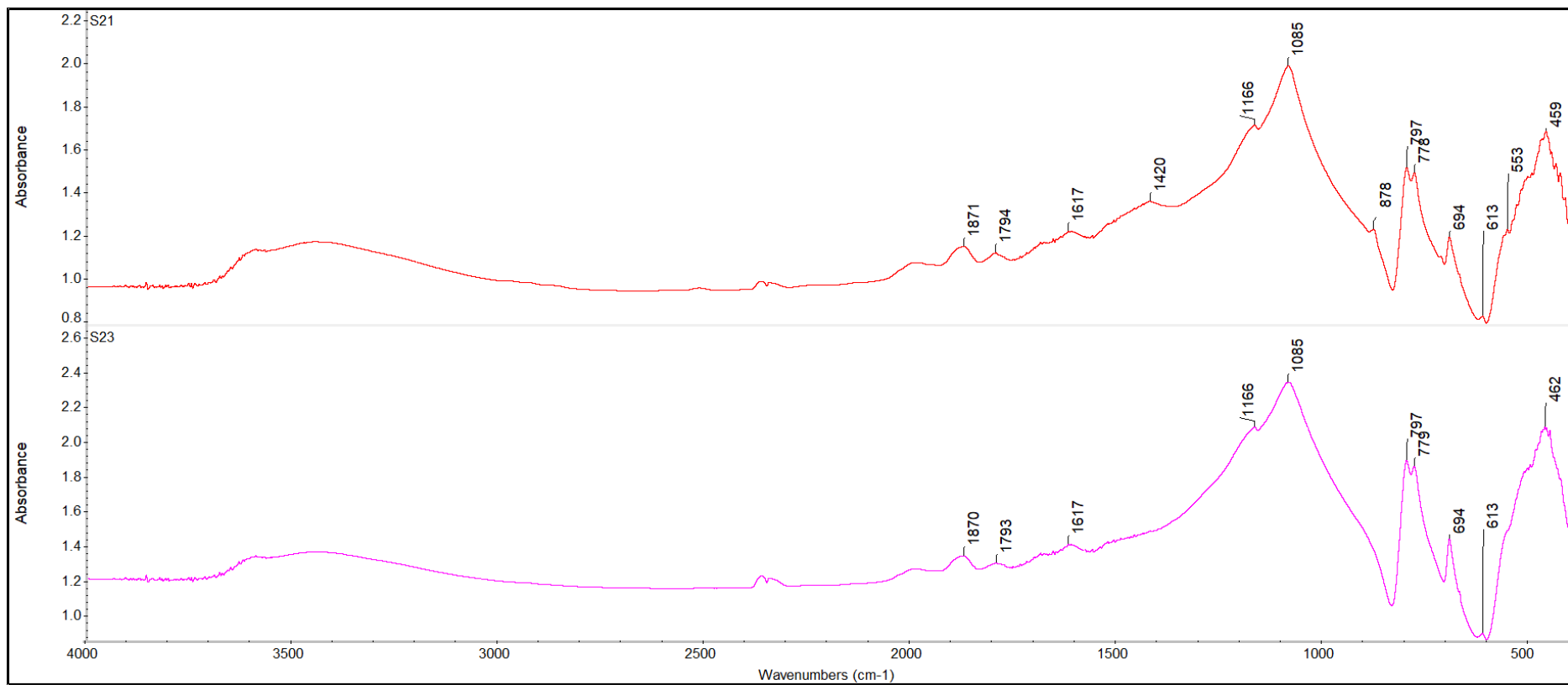


Figure 19: FTIR spectra of the samples from Sicily.

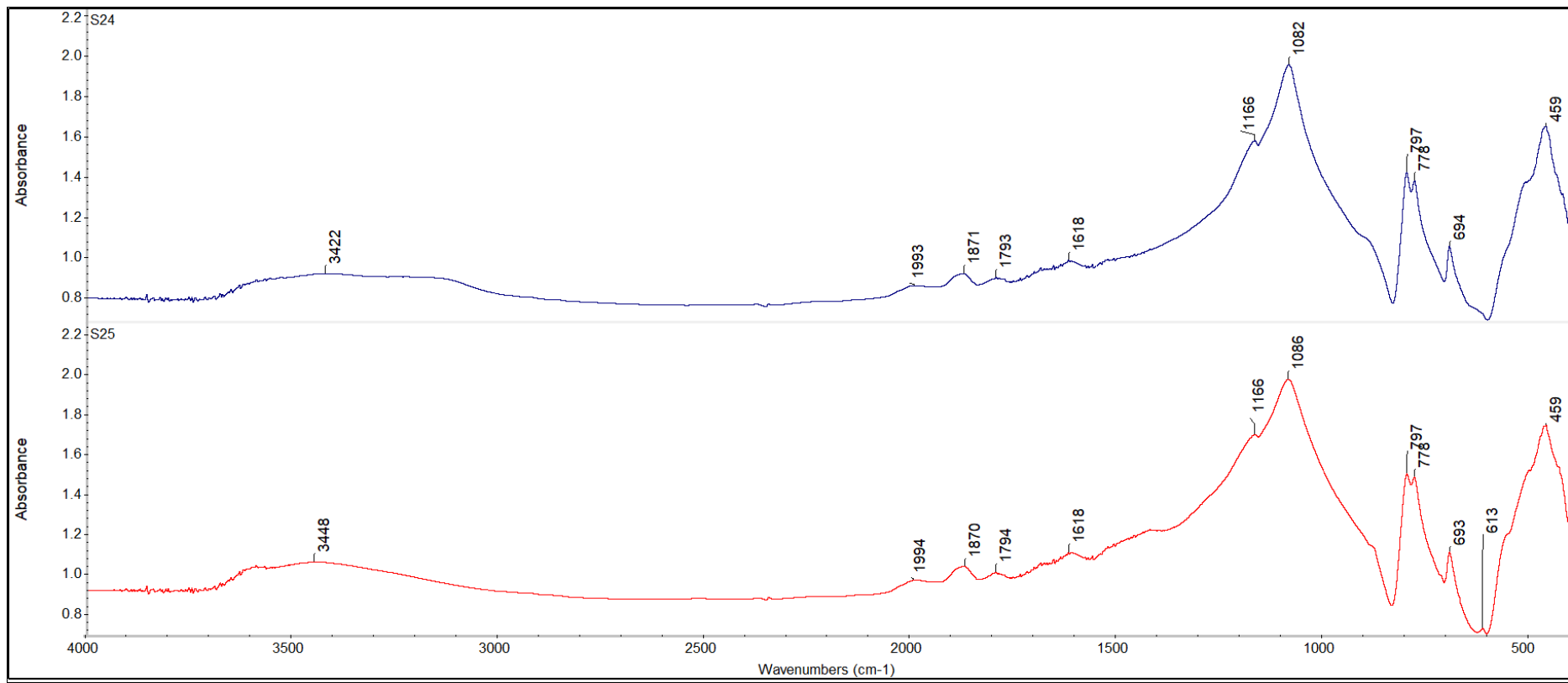


Figure 20: FTIR spectra of the samples from Sicily.

Artefact Samples

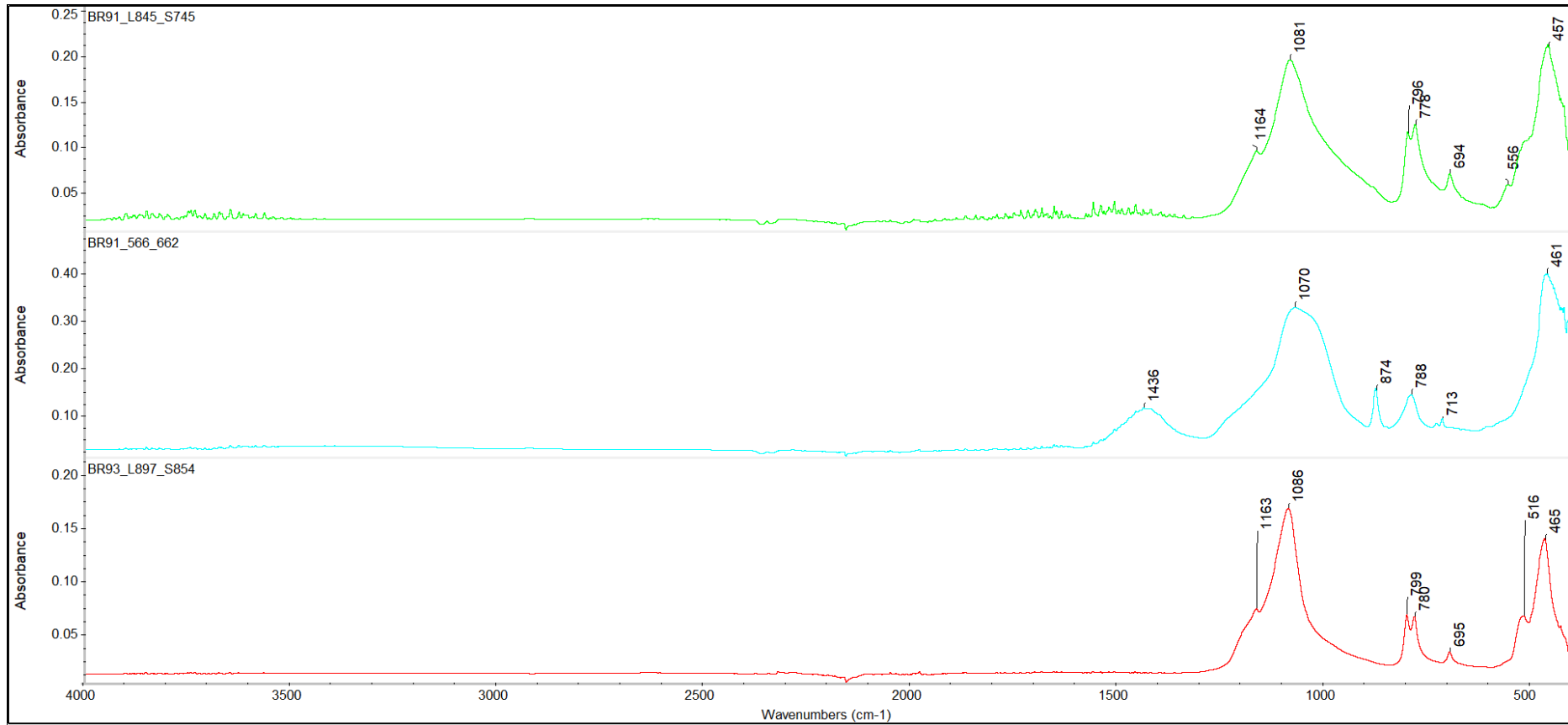


Figure 21: ATR spectra of the samples from Xagħra Circle.

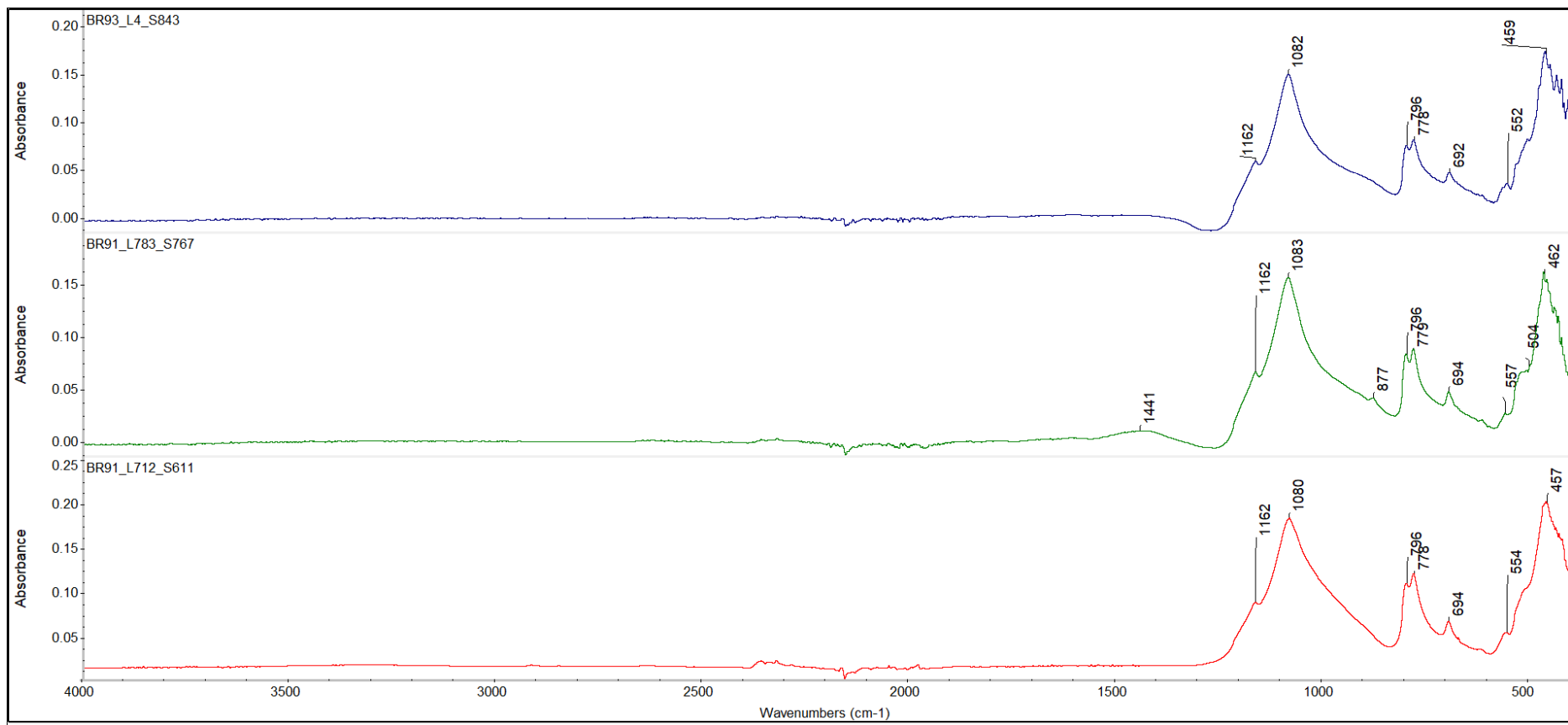


Figure 22: ATR spectra of the samples from Xaghra Circle.

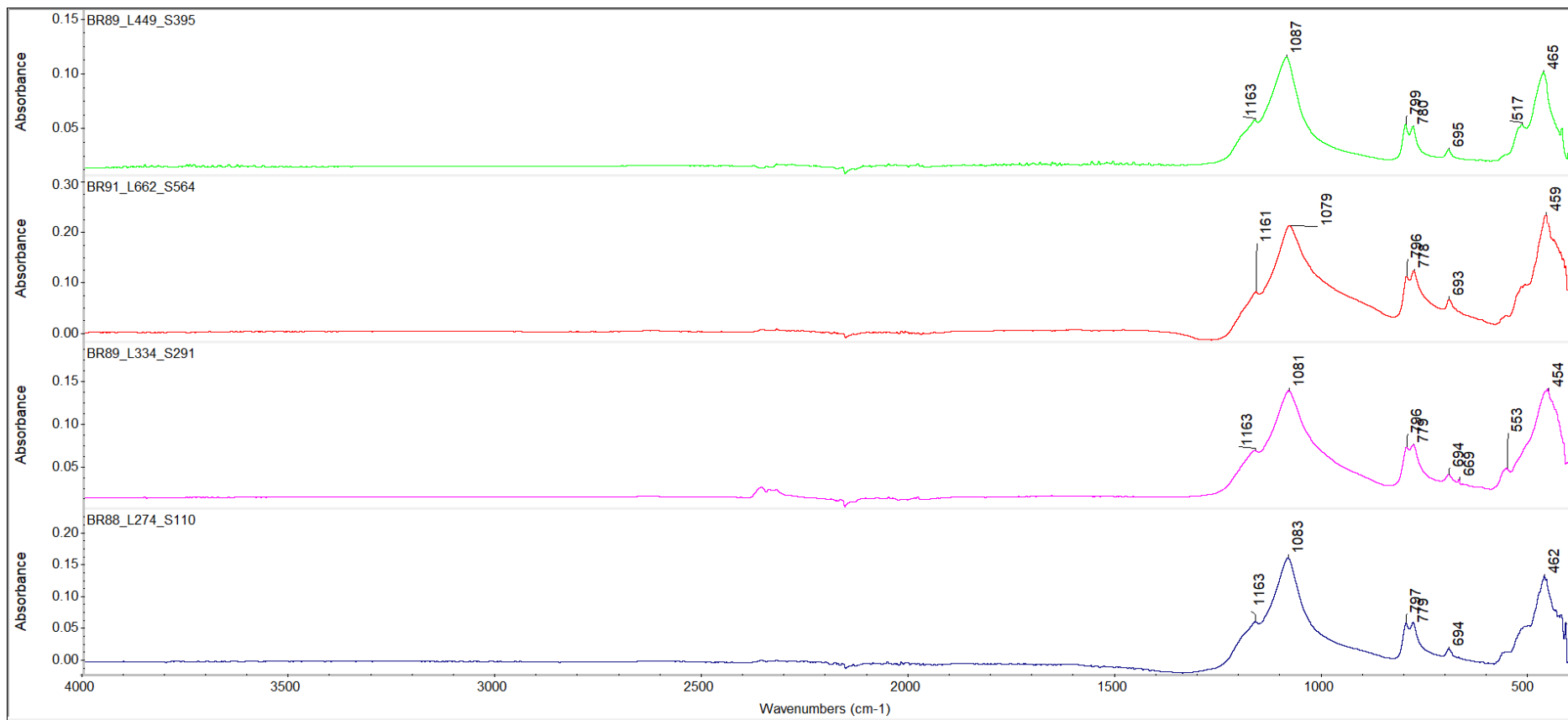


Figure 23: ATR spectra of the samples from Xaqhra Circle.

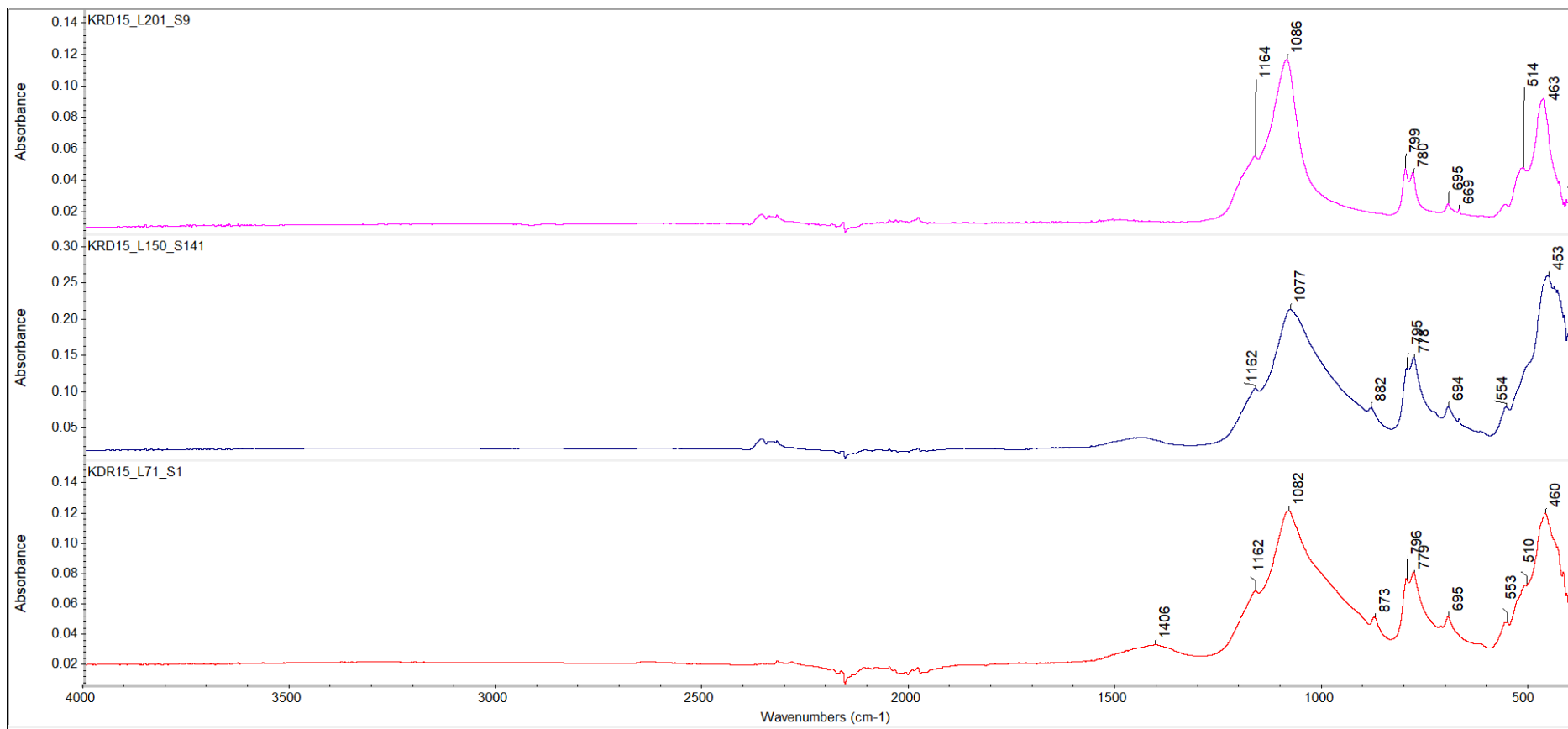


Figure 24: ATR spectra of the samples from Kordin.

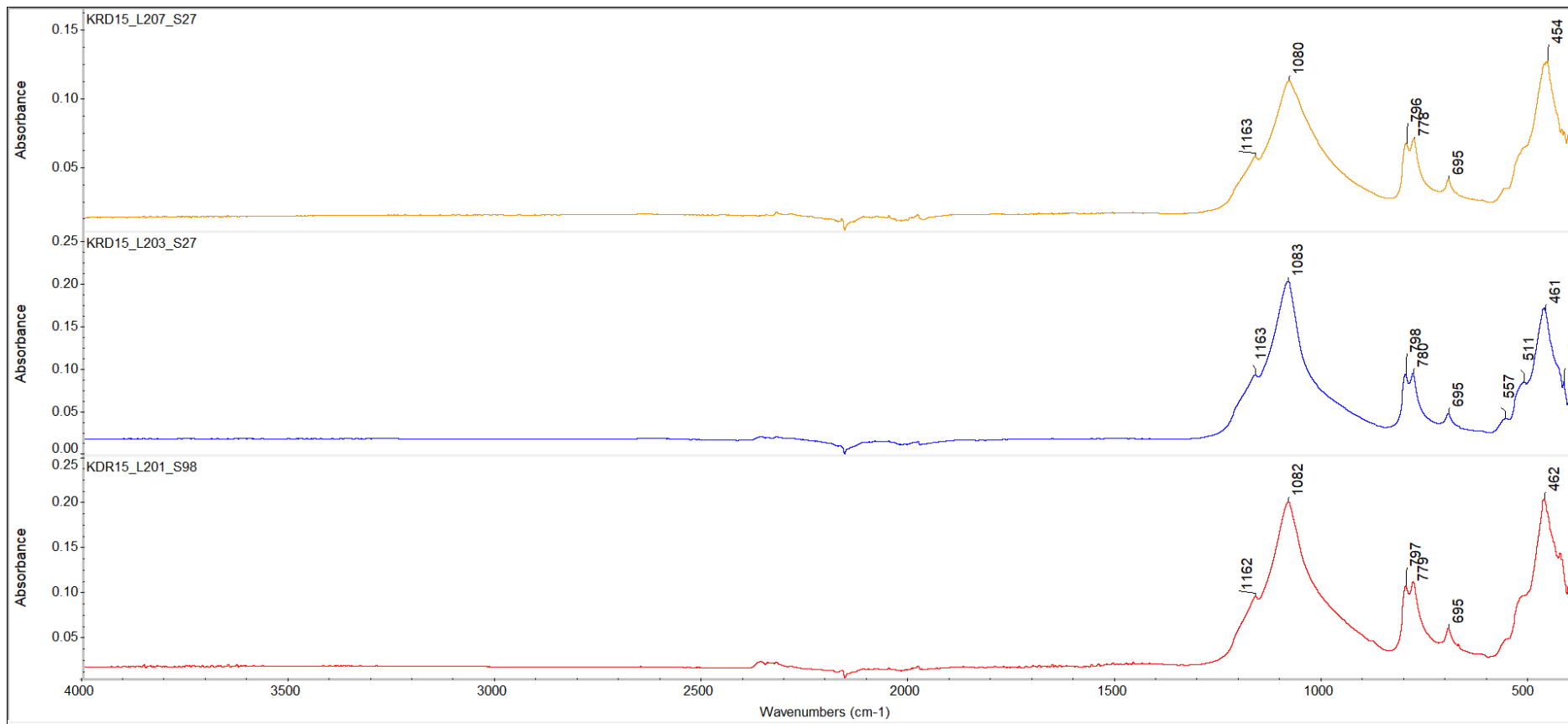


Figure 25:ATR spectra of the samples from Kordin.

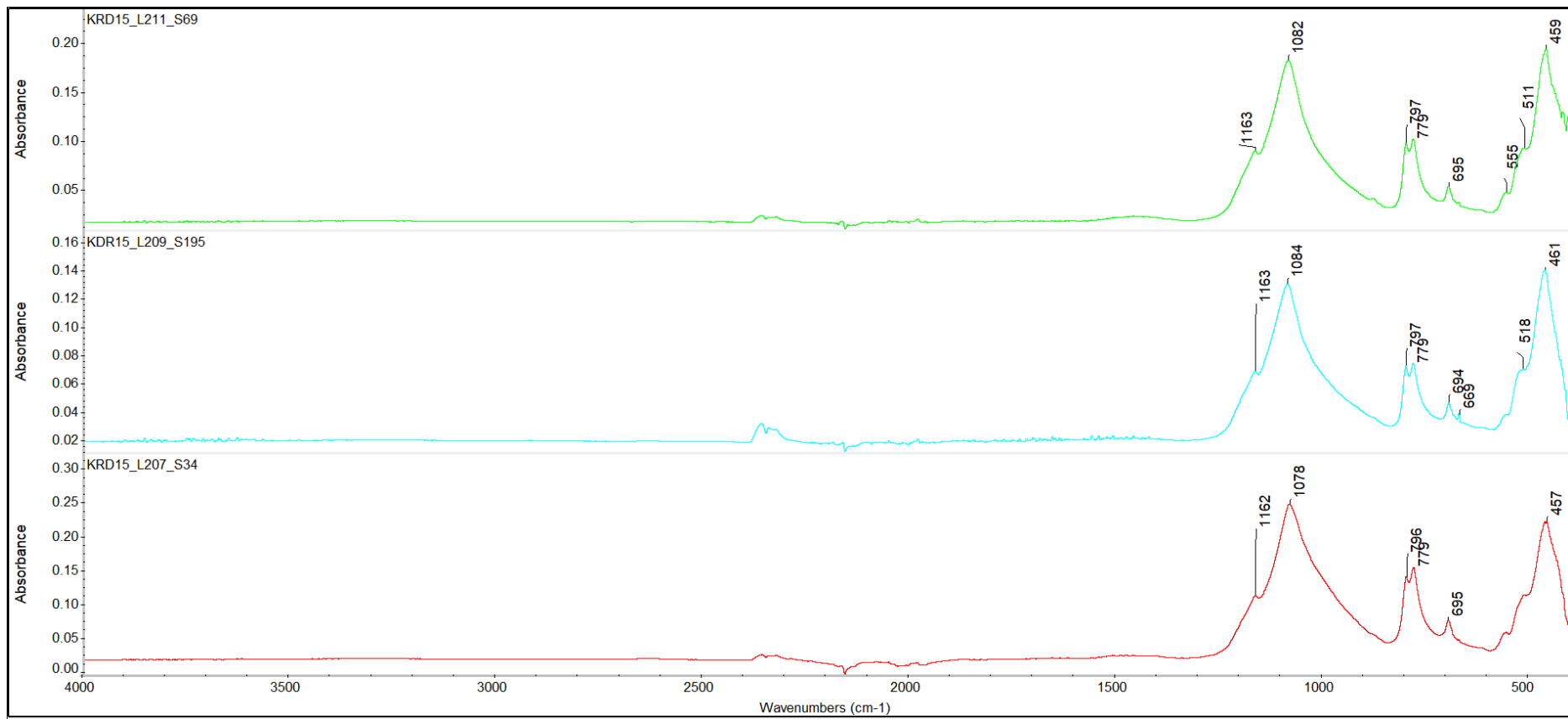


Figure 26: ATR spectra of the samples from Kordin.

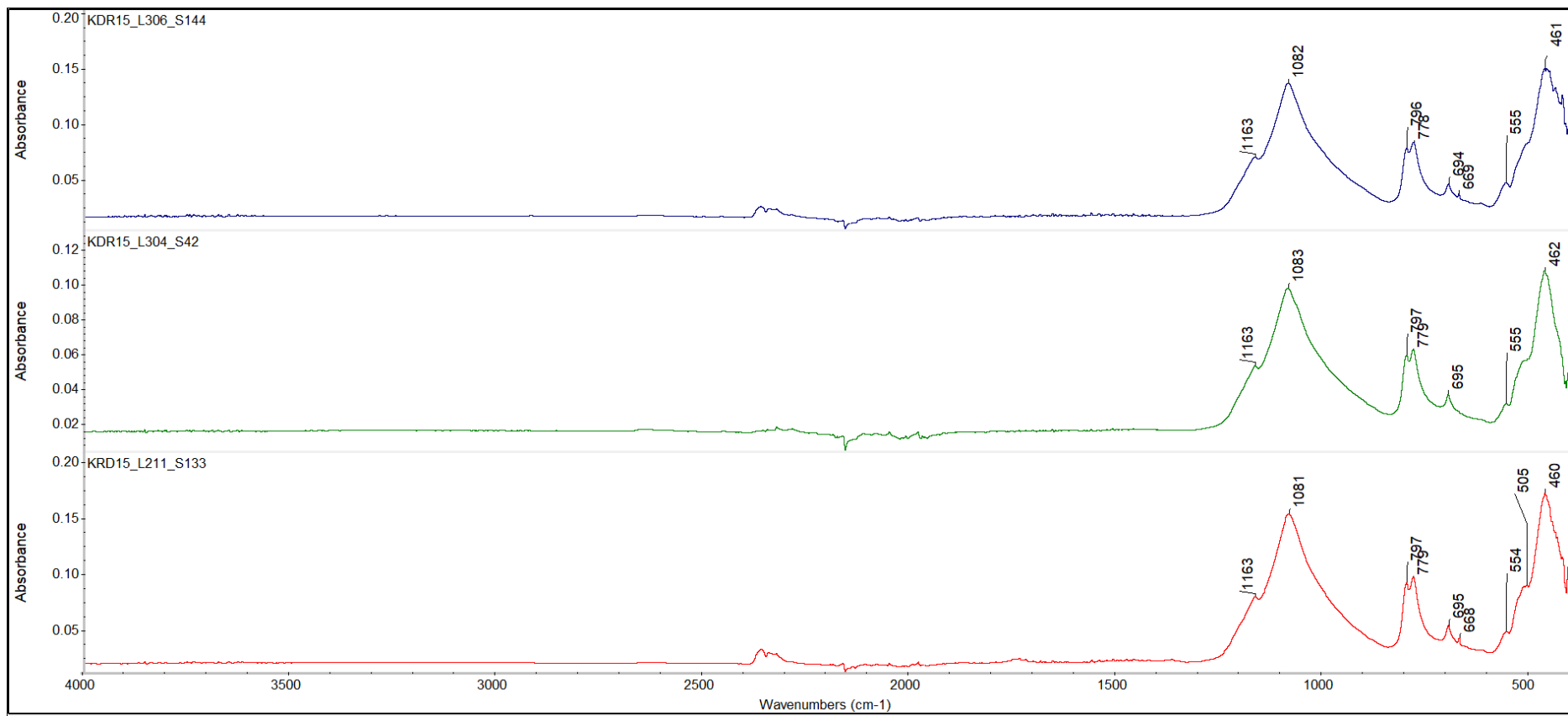


Figure 27: ATR spectra of the samples from Kordin.

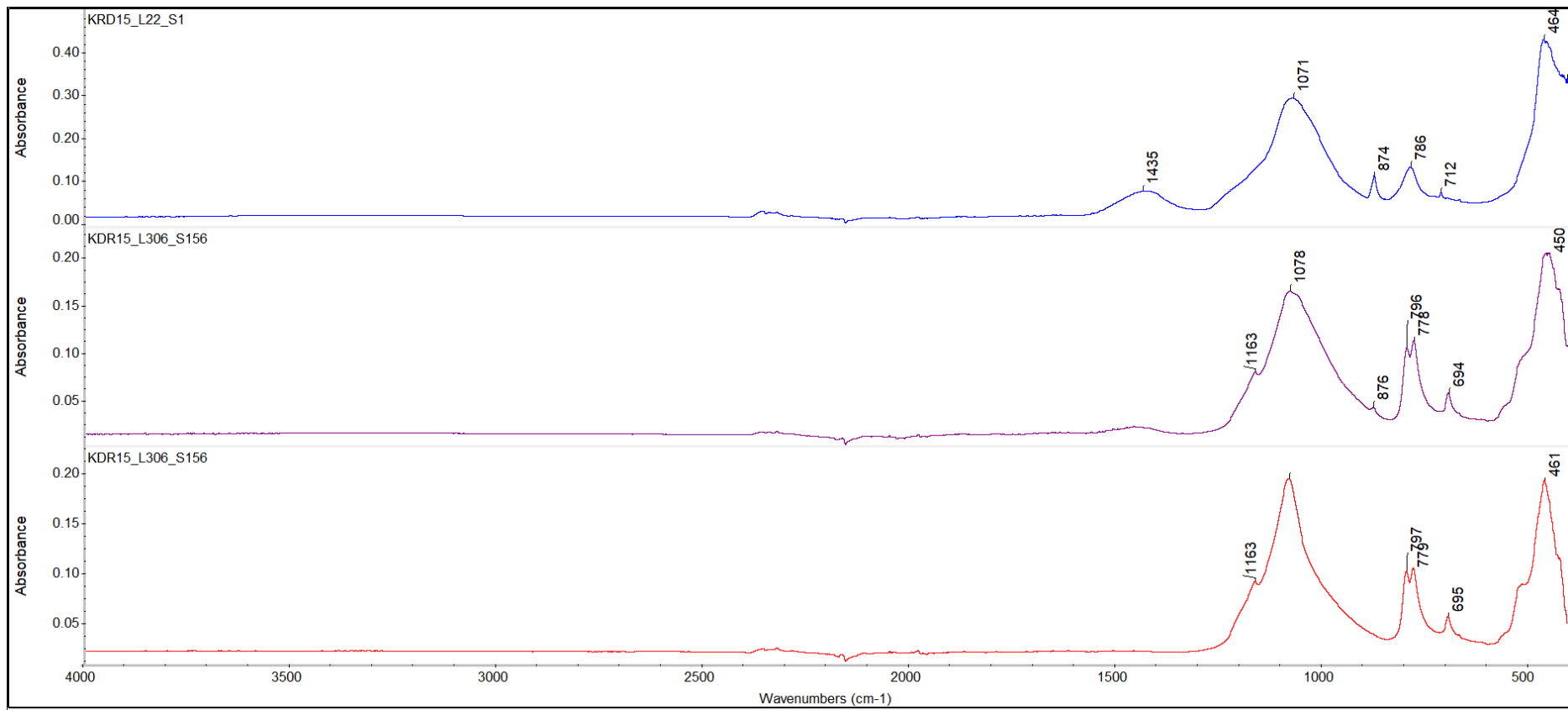


Figure 28: ATR spectra of the samples from Kordin.

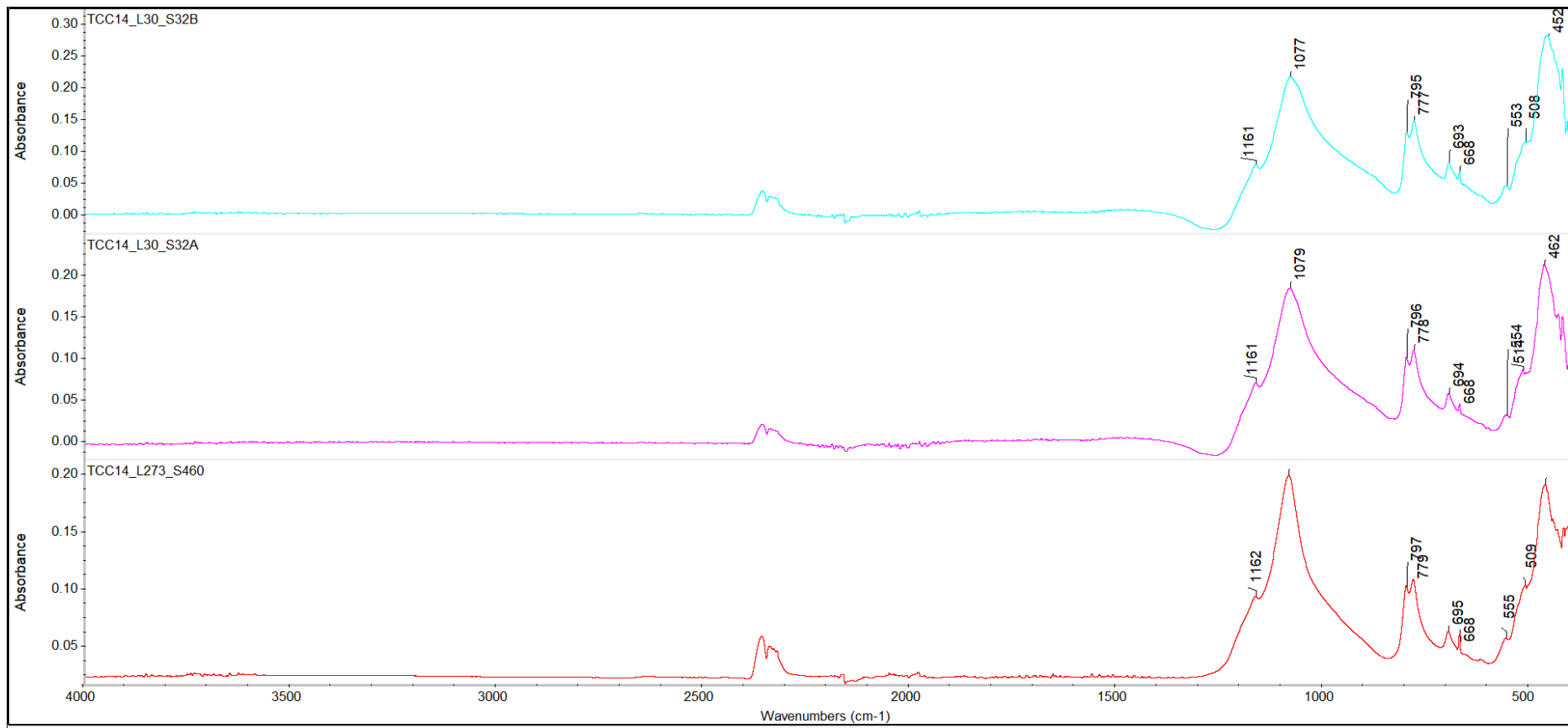


Figure 29: ATR spectra of the samples from Tač-Čawla.

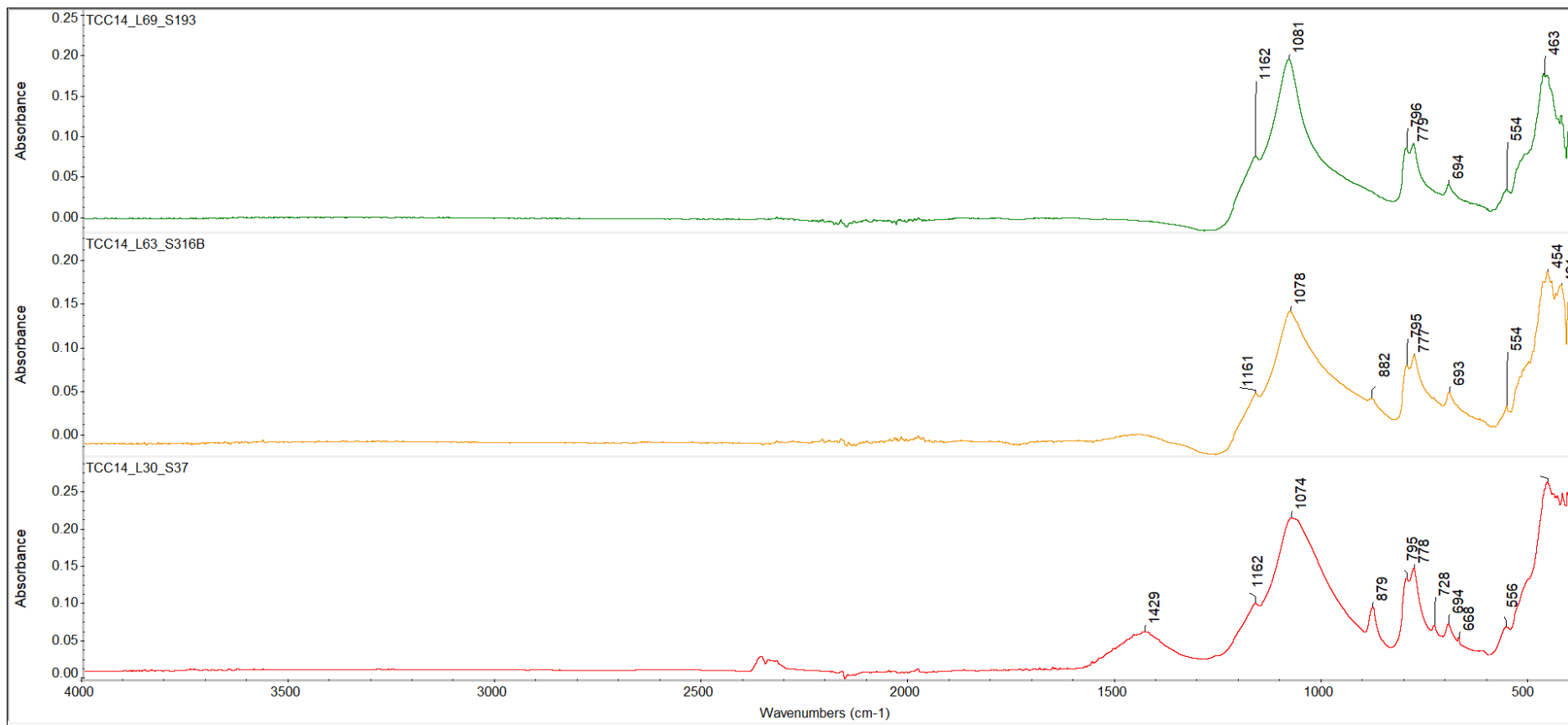


Figure 30: ATR spectra of the samples from Tač-Ćawla.

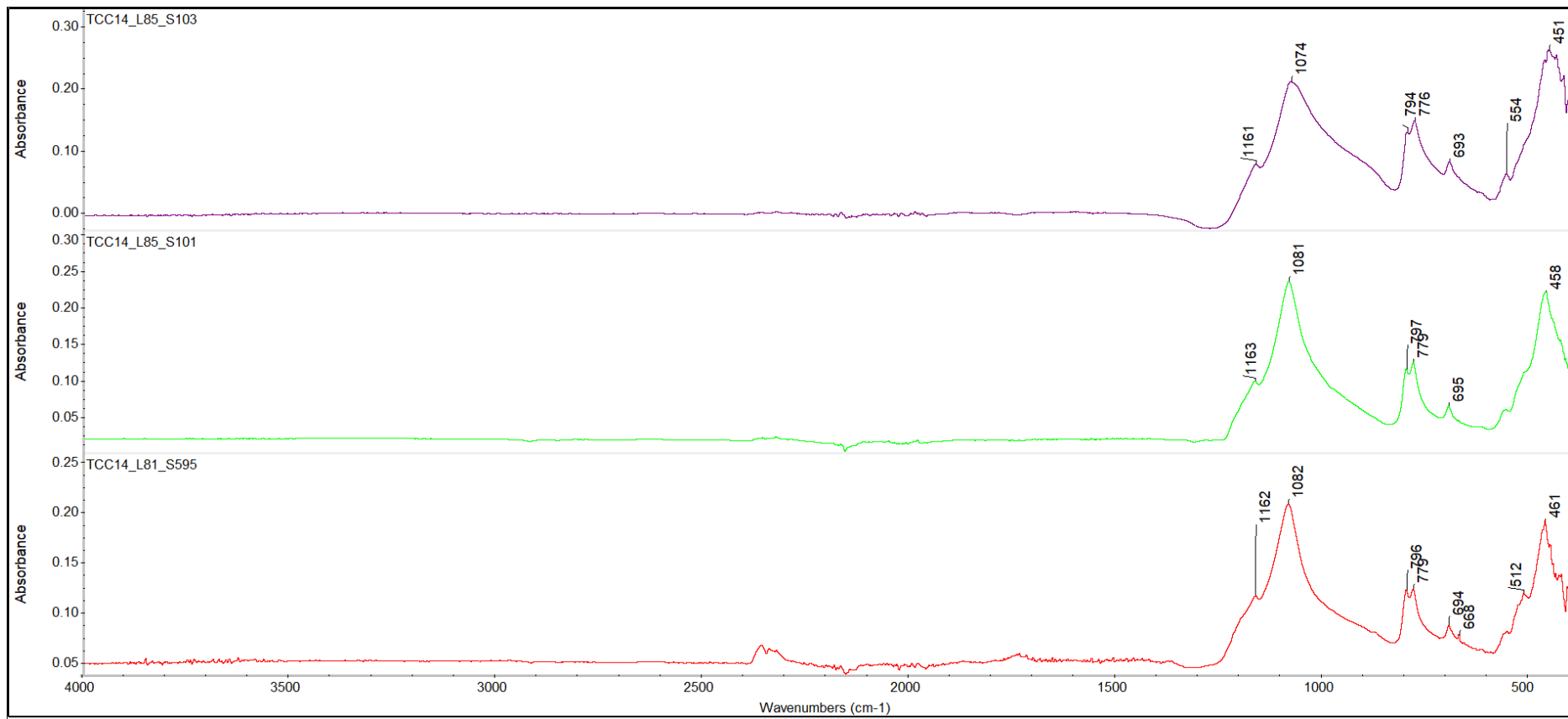


Figure 31: ATR spectra of the samples from Tač-Čawla.

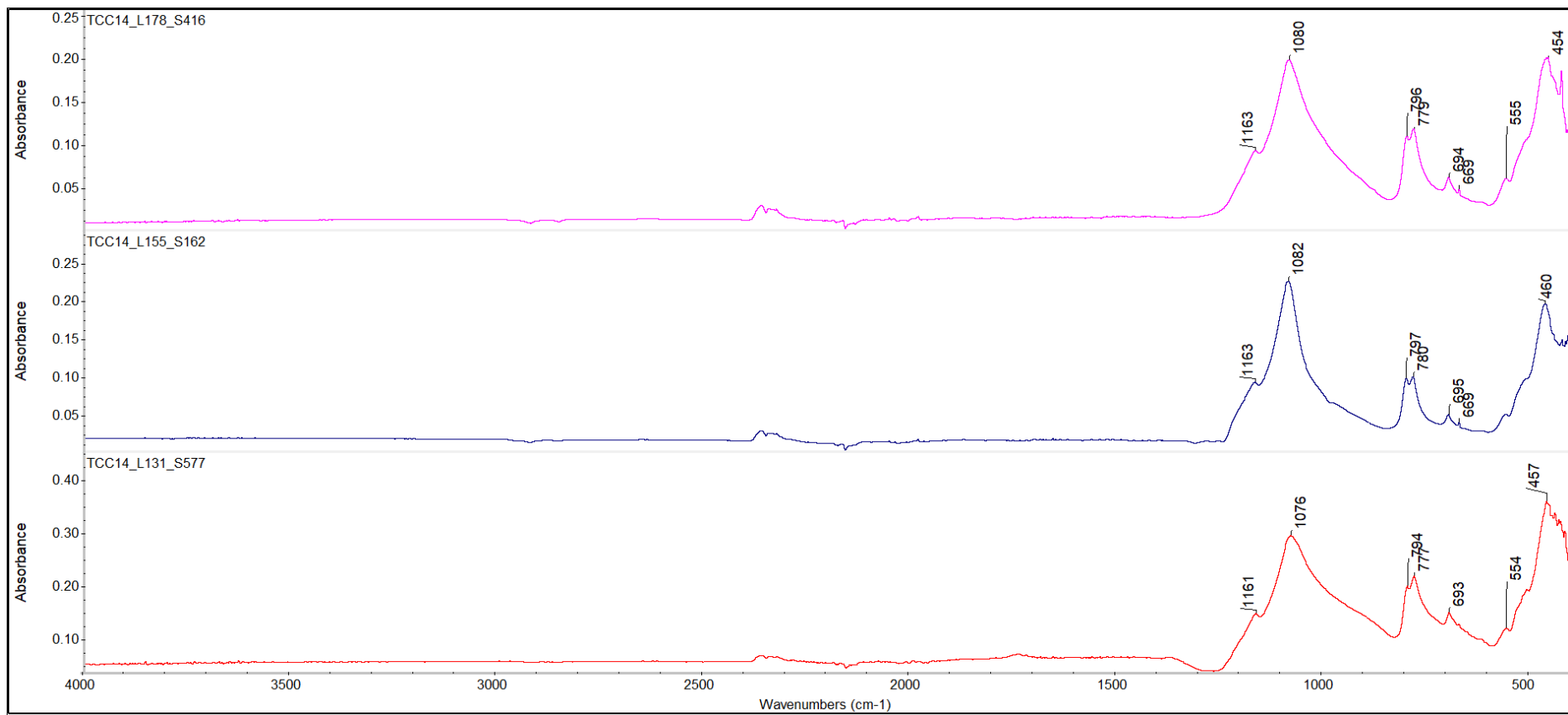


Figure 32: ATR spectra of the samples from Tač-Čawla.

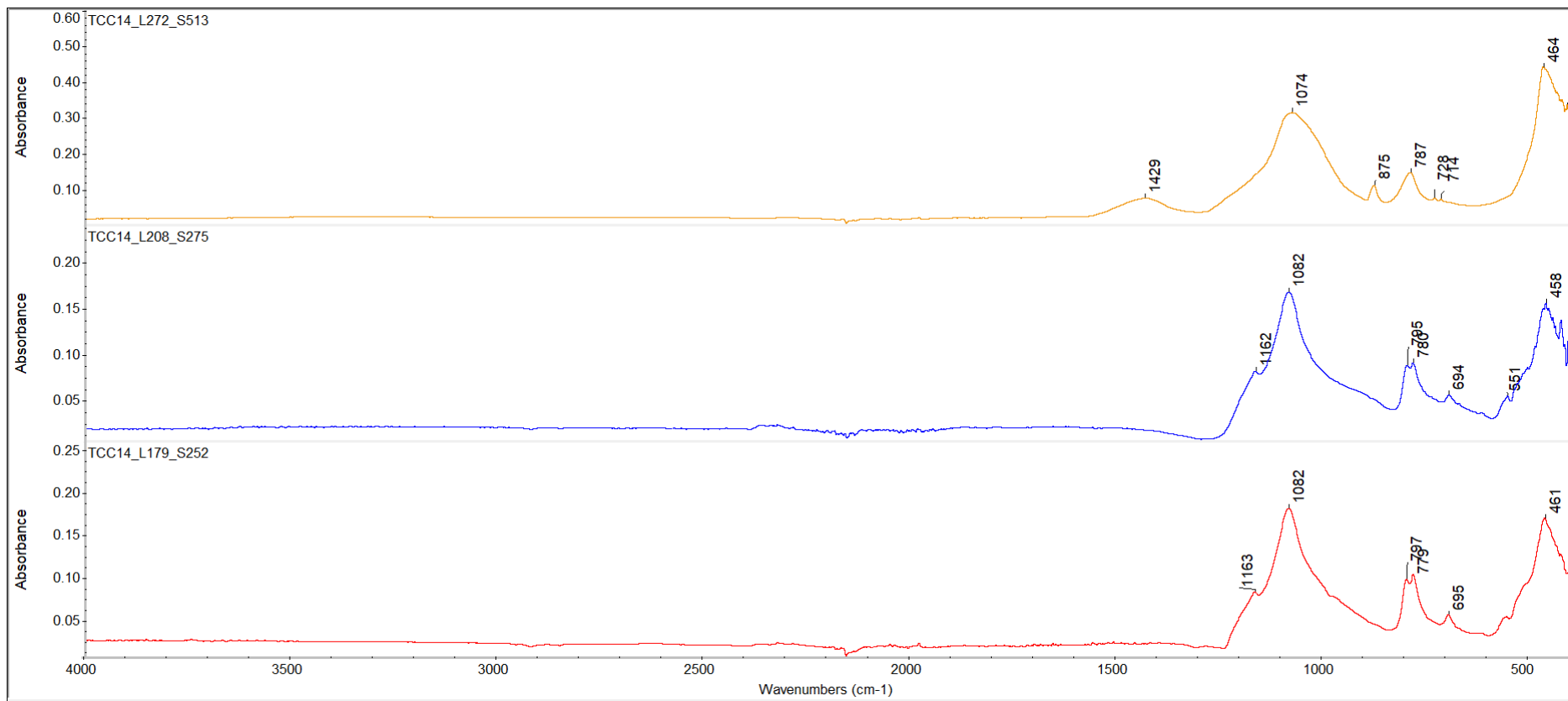


Figure 33: ATR spectra of the samples from Tač-Čawla.

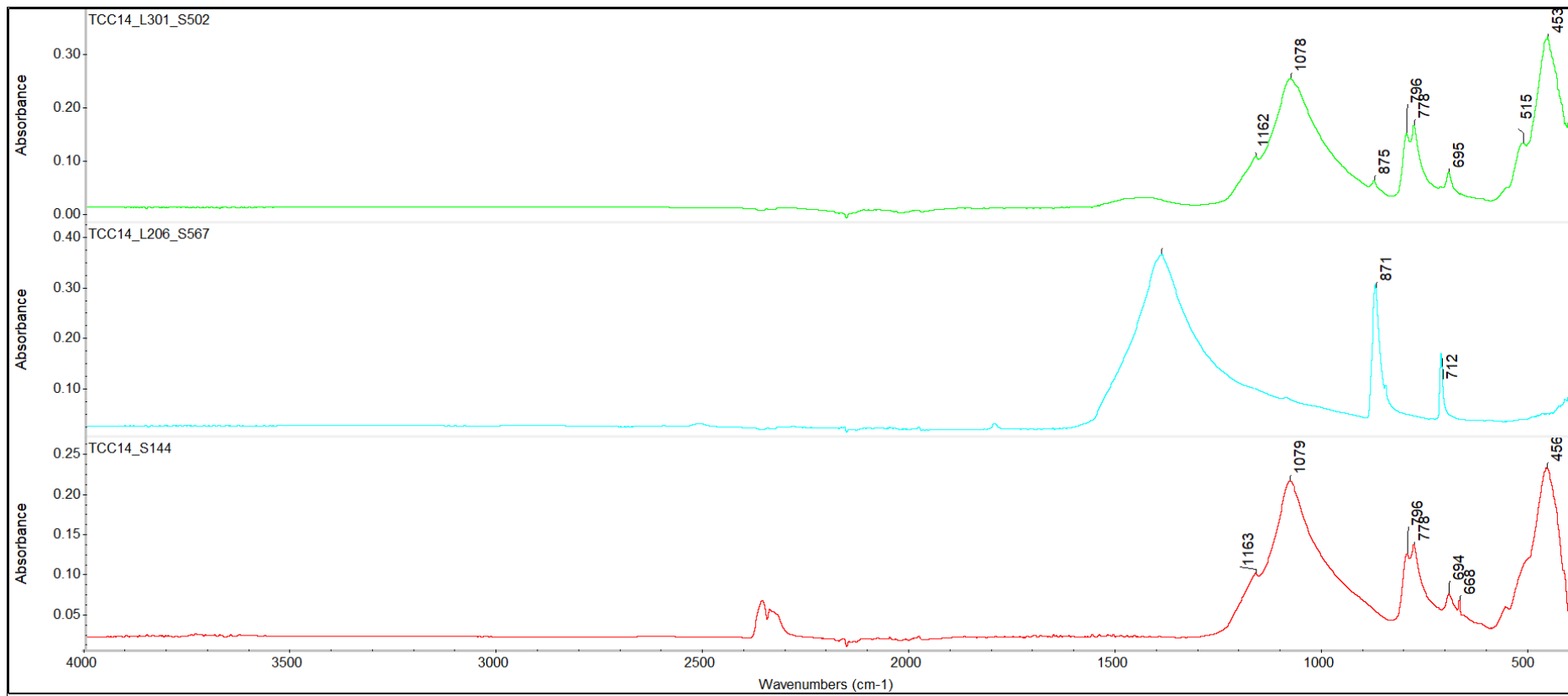


Figure 34: ATR spectra of the samples from Tač-Ćawla.

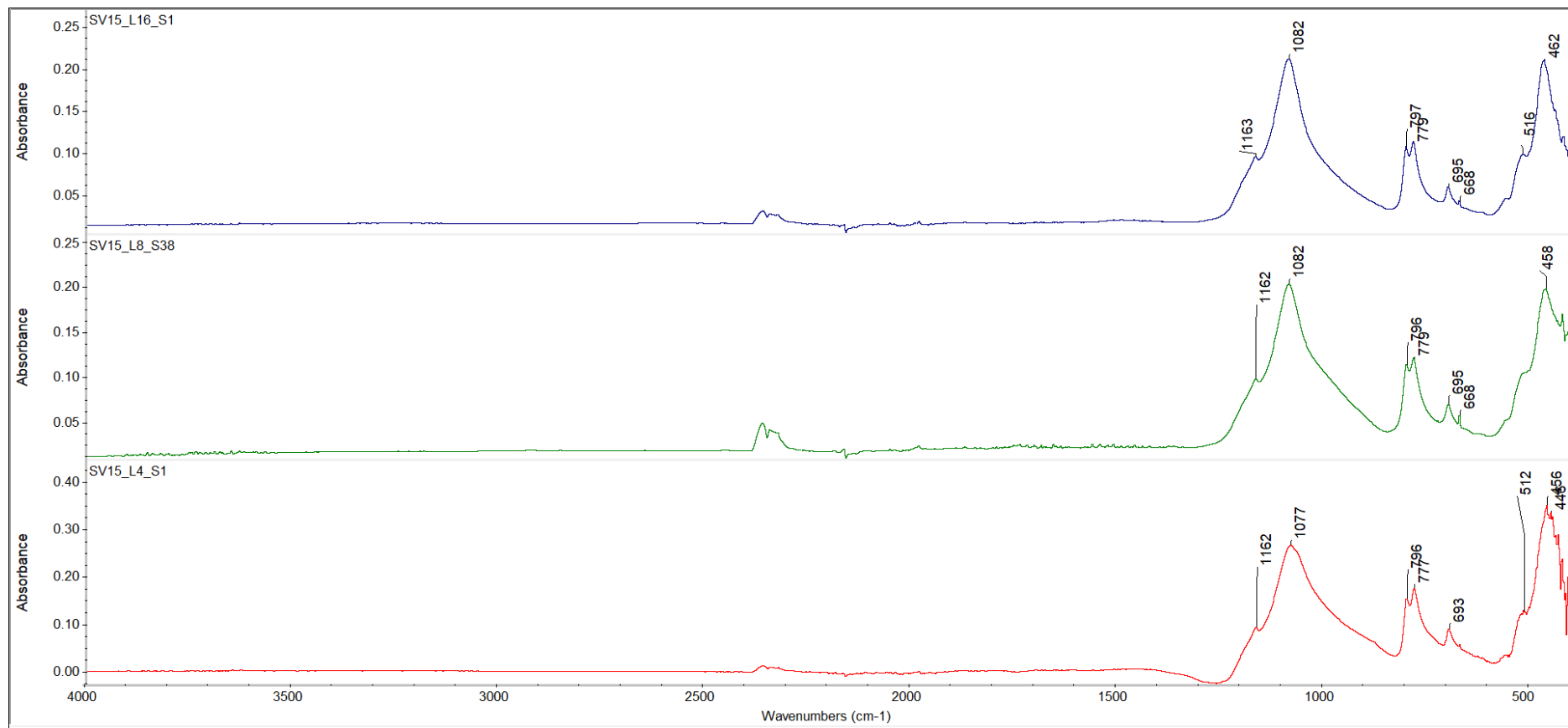


Figure 35: ATR spectra of the samples from Santa Verna.

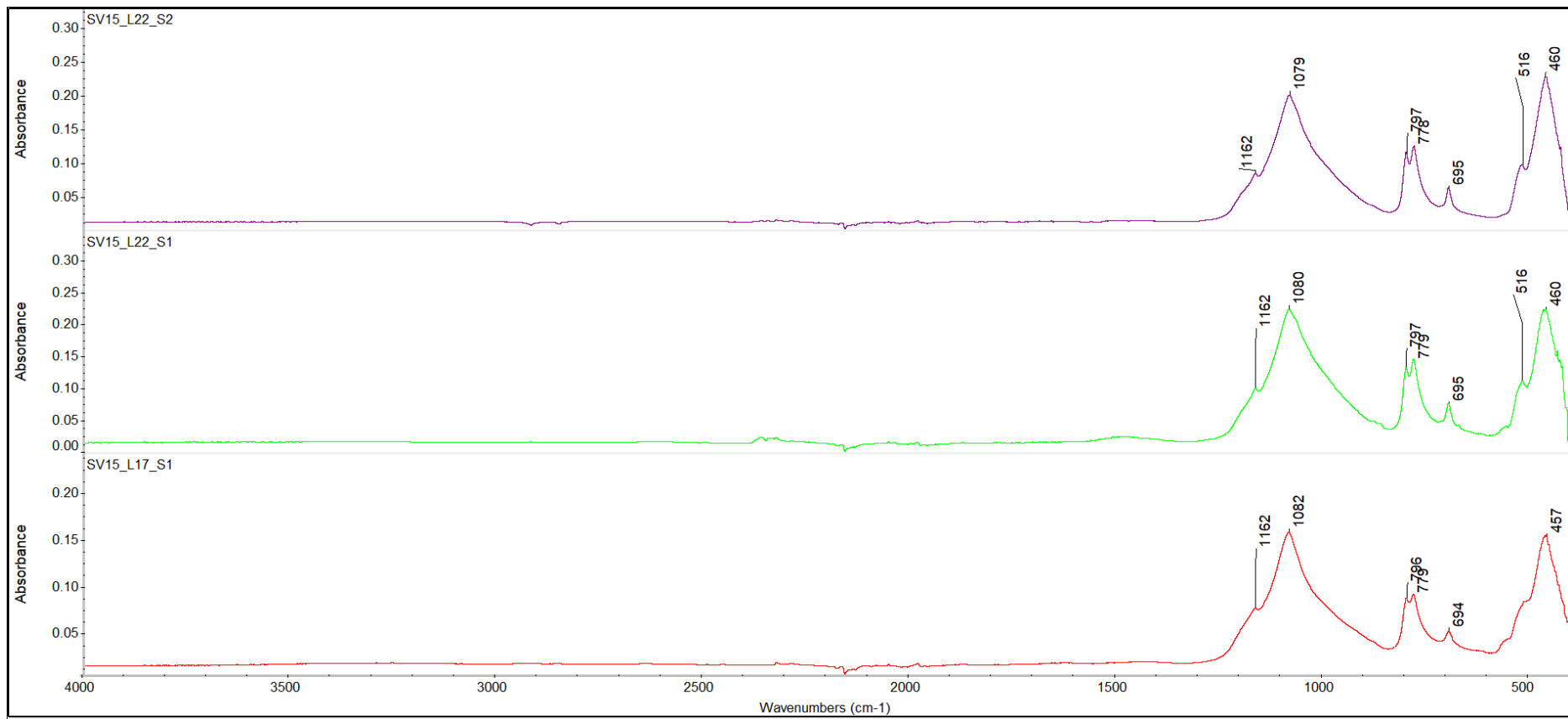


Figure 36: ATR spectra of the samples from Santa Verna.

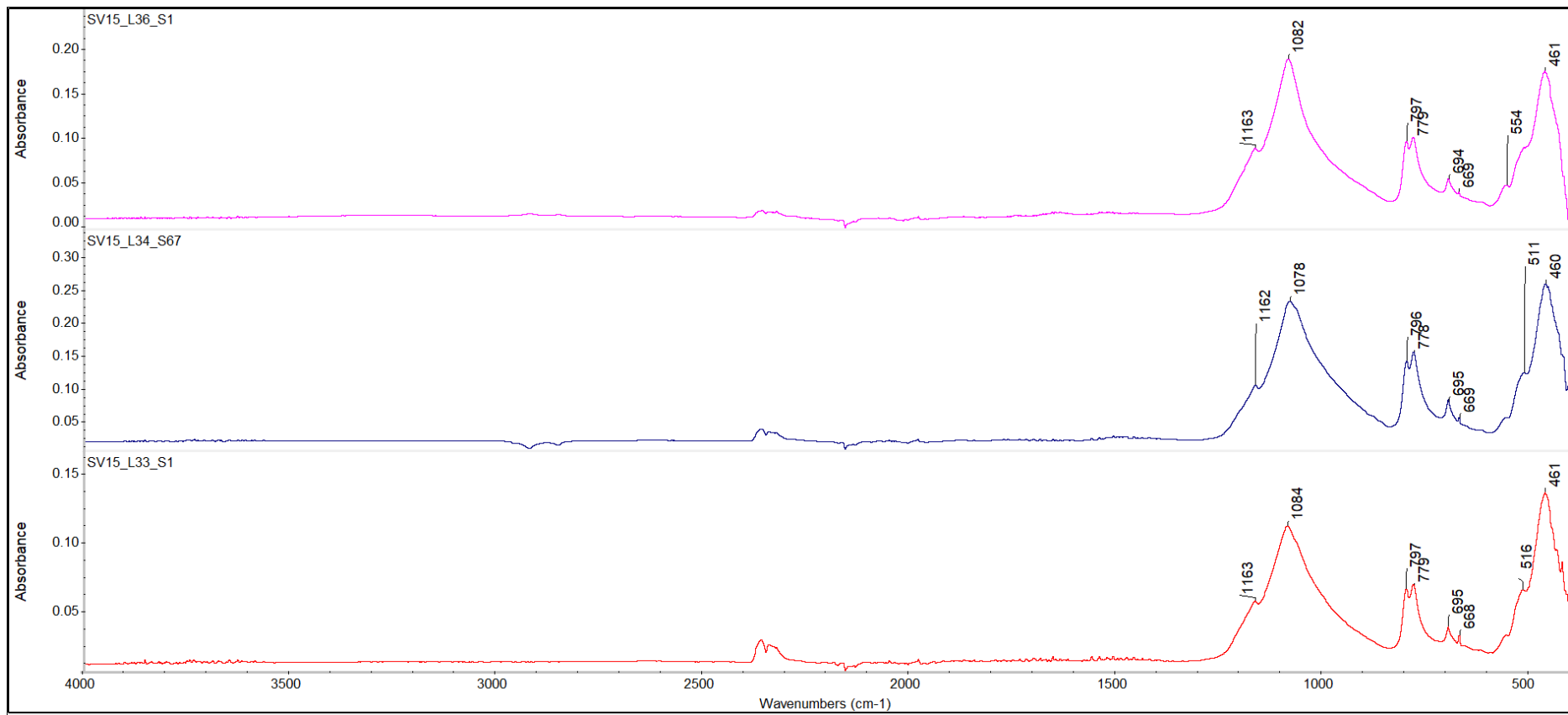


Figure 37: ATR spectra of the samples from Santa Verna.

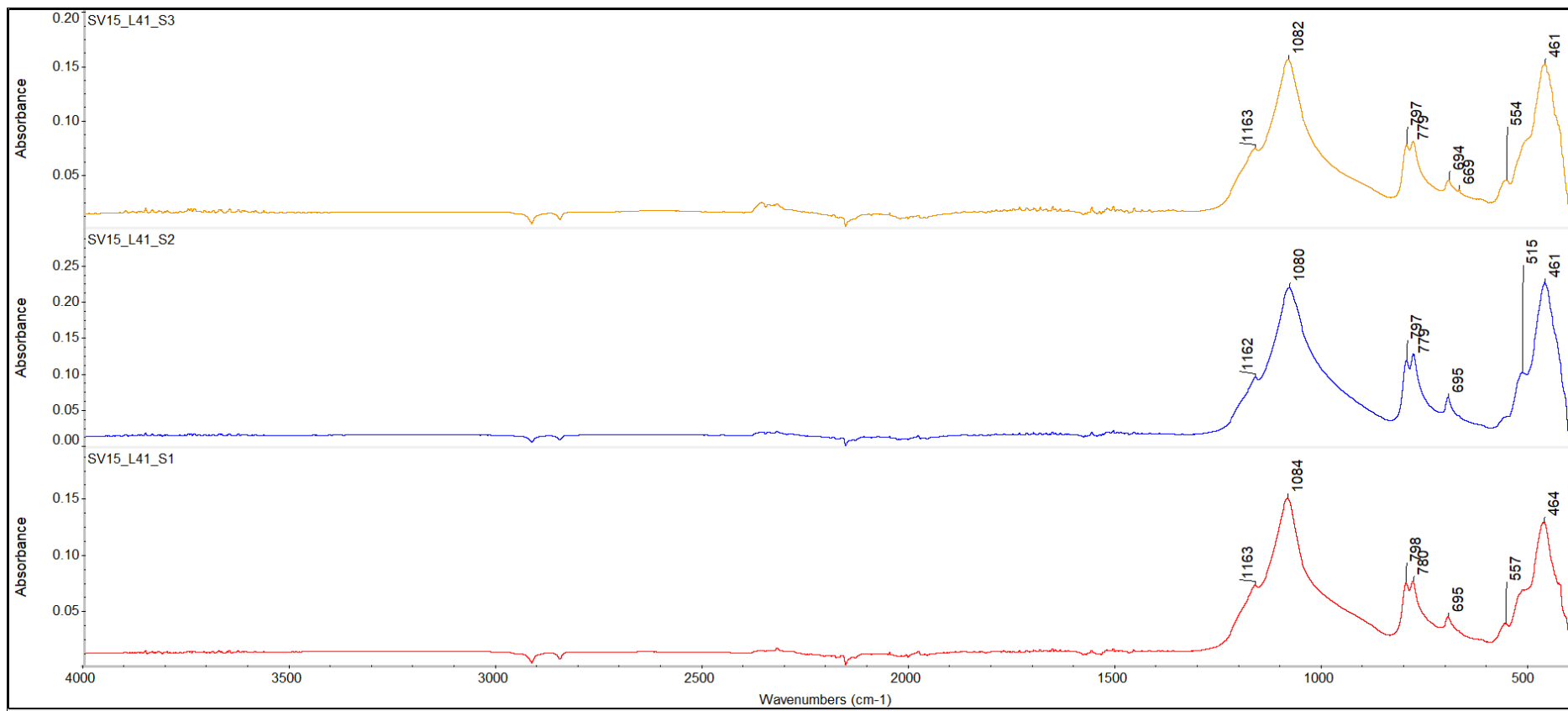


Figure 38: ATR spectra of the samples from Santa Verna.

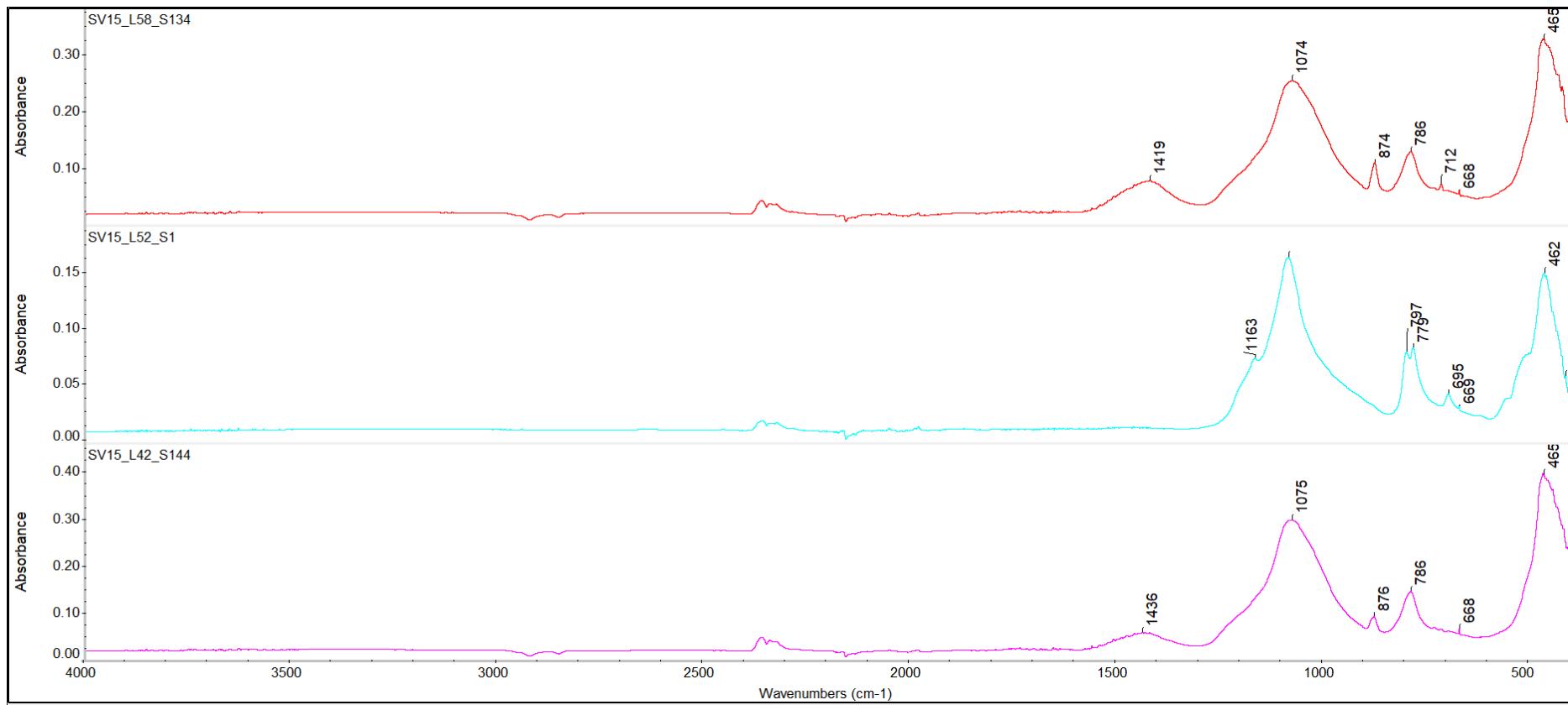


Figure 39: ATR spectra of the samples from Santa Verna.

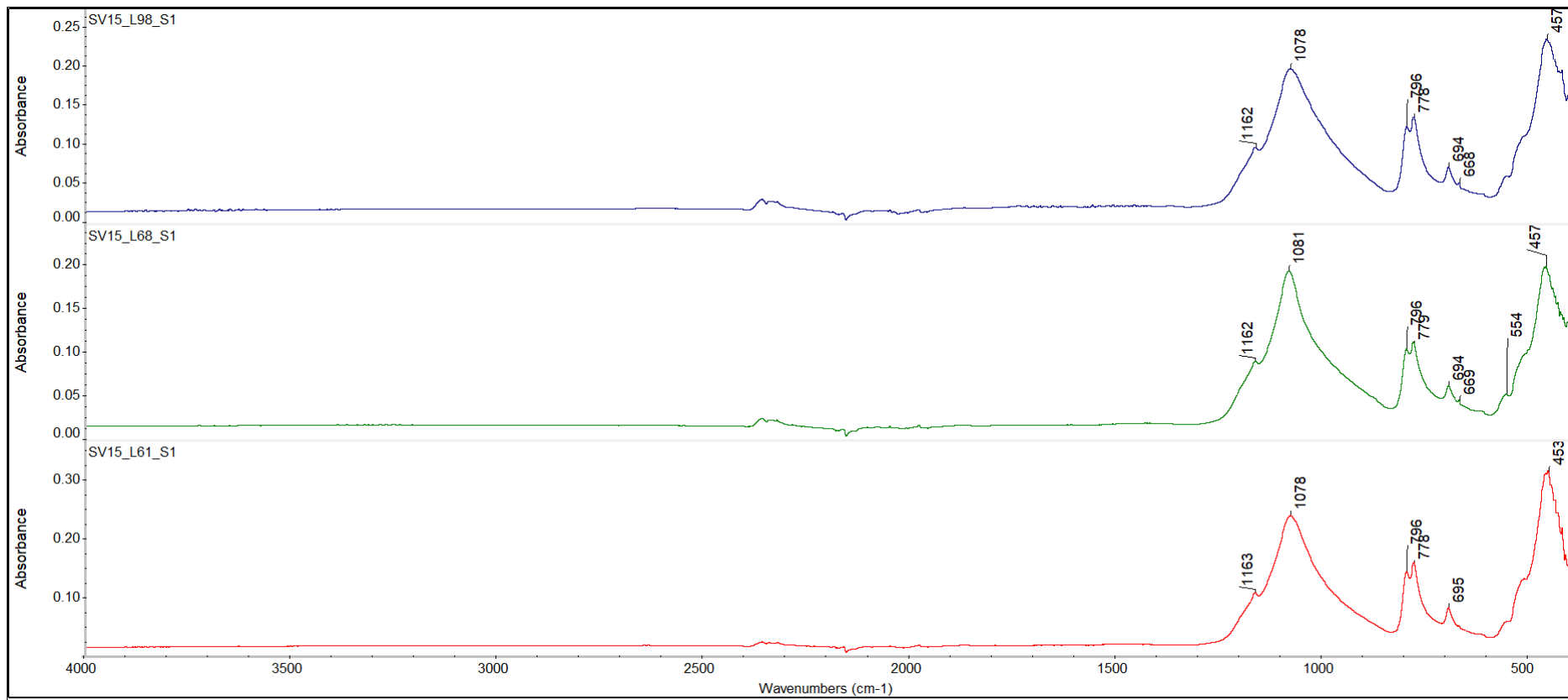


Figure 40: ATR spectra of the samples from Santa Verna.

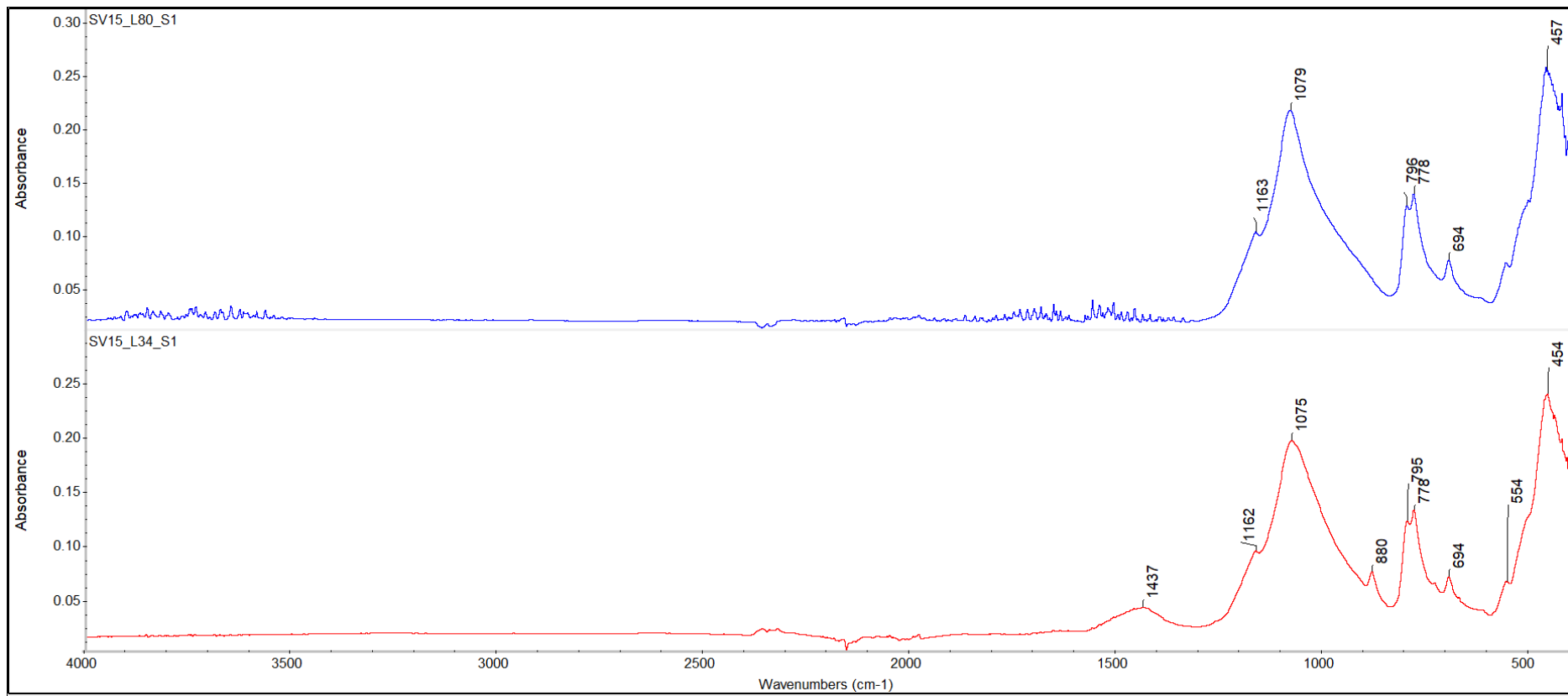


Figure 41: ATR spectra of the samples from Santa Verna.

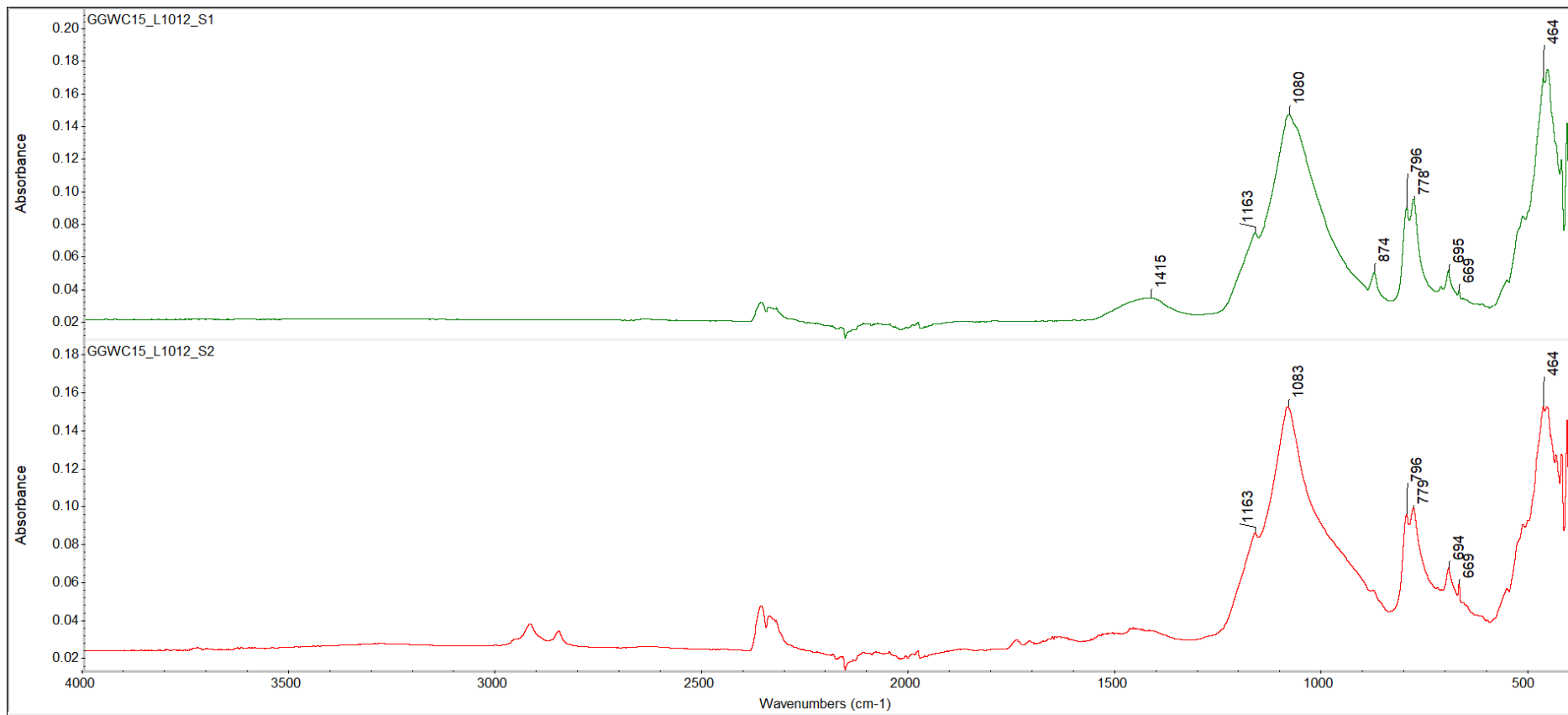


Figure 42: ATR spectra of the samples from *Ggantija* context 1012.

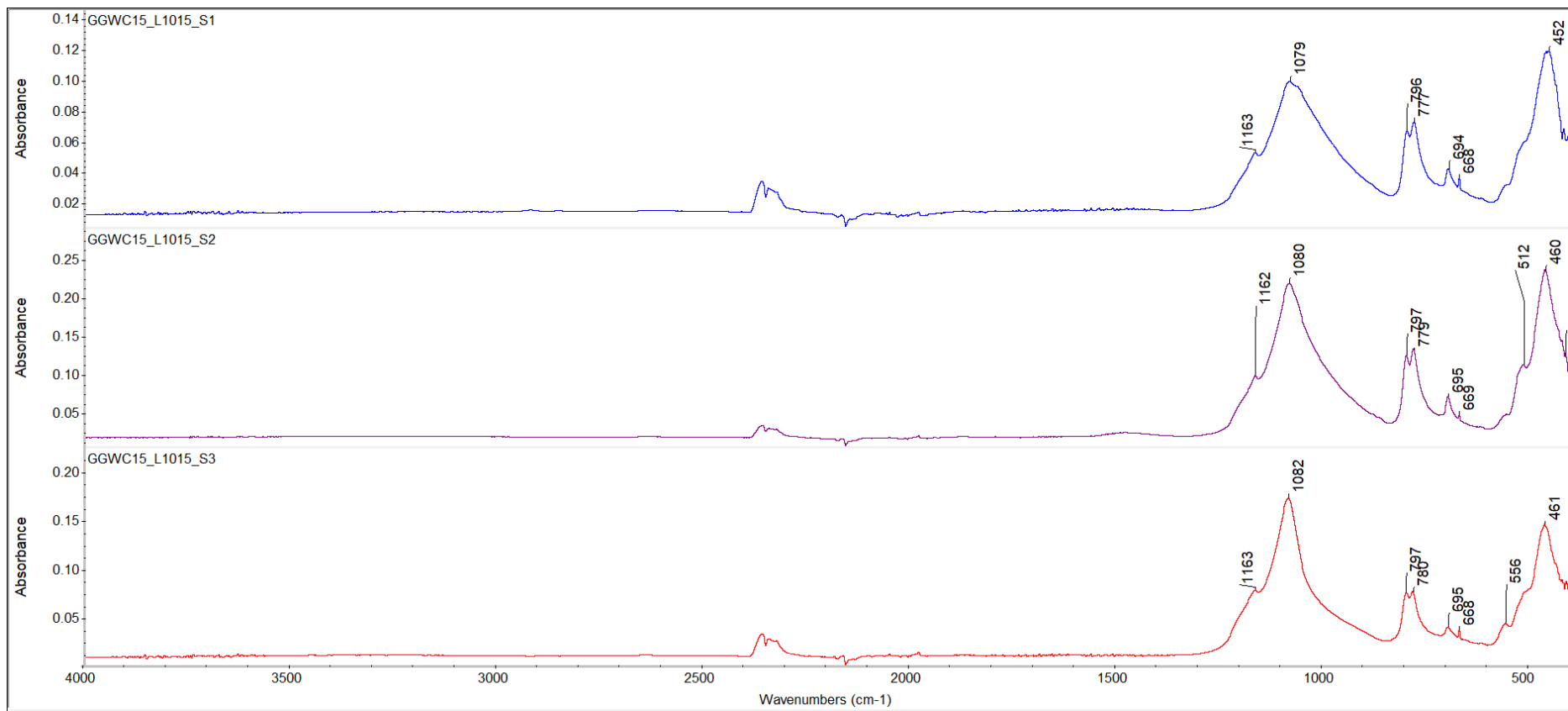


Figure 43: ATR spectra of the samples from *Ggantija* context 1015.

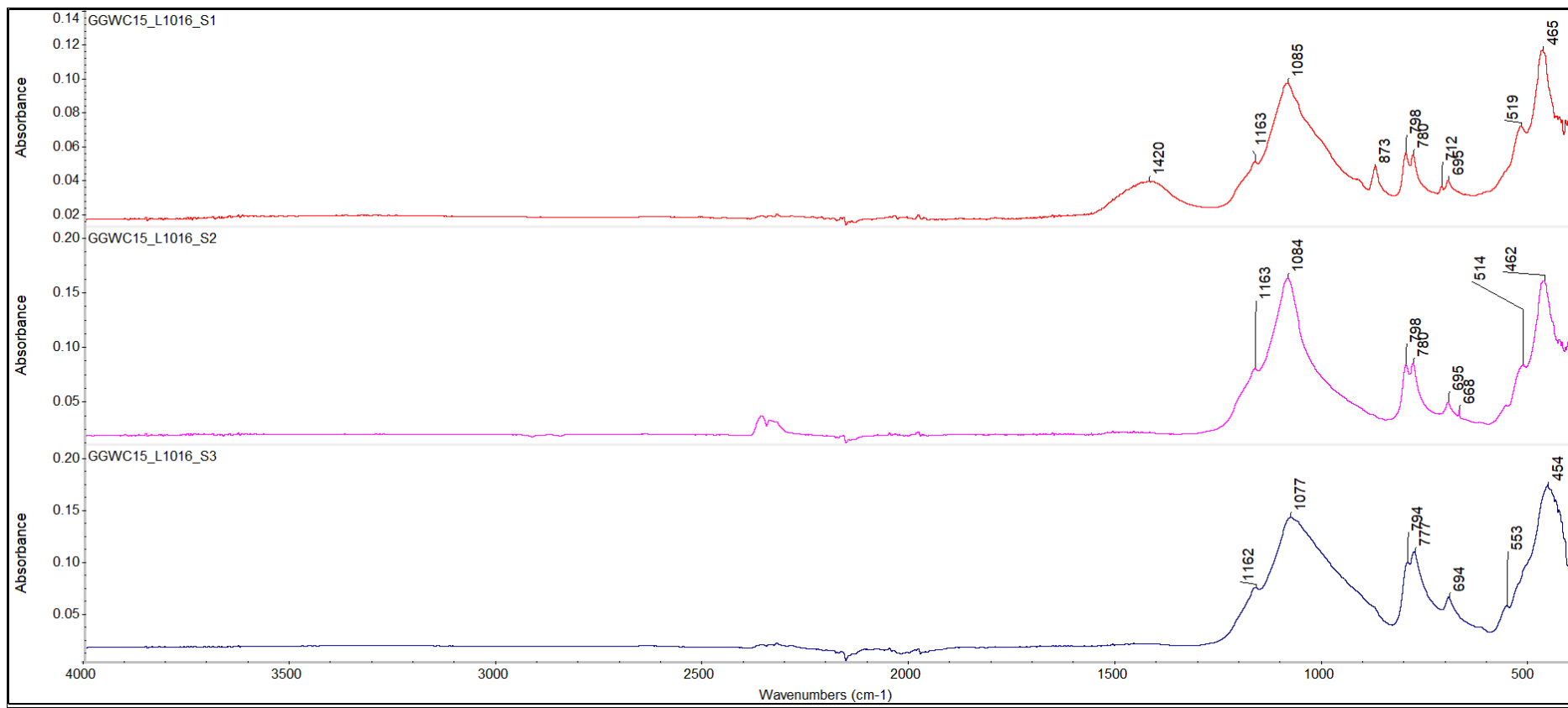


Figure 44: ATR spectra of the samples from *Ggantija* context 1016.

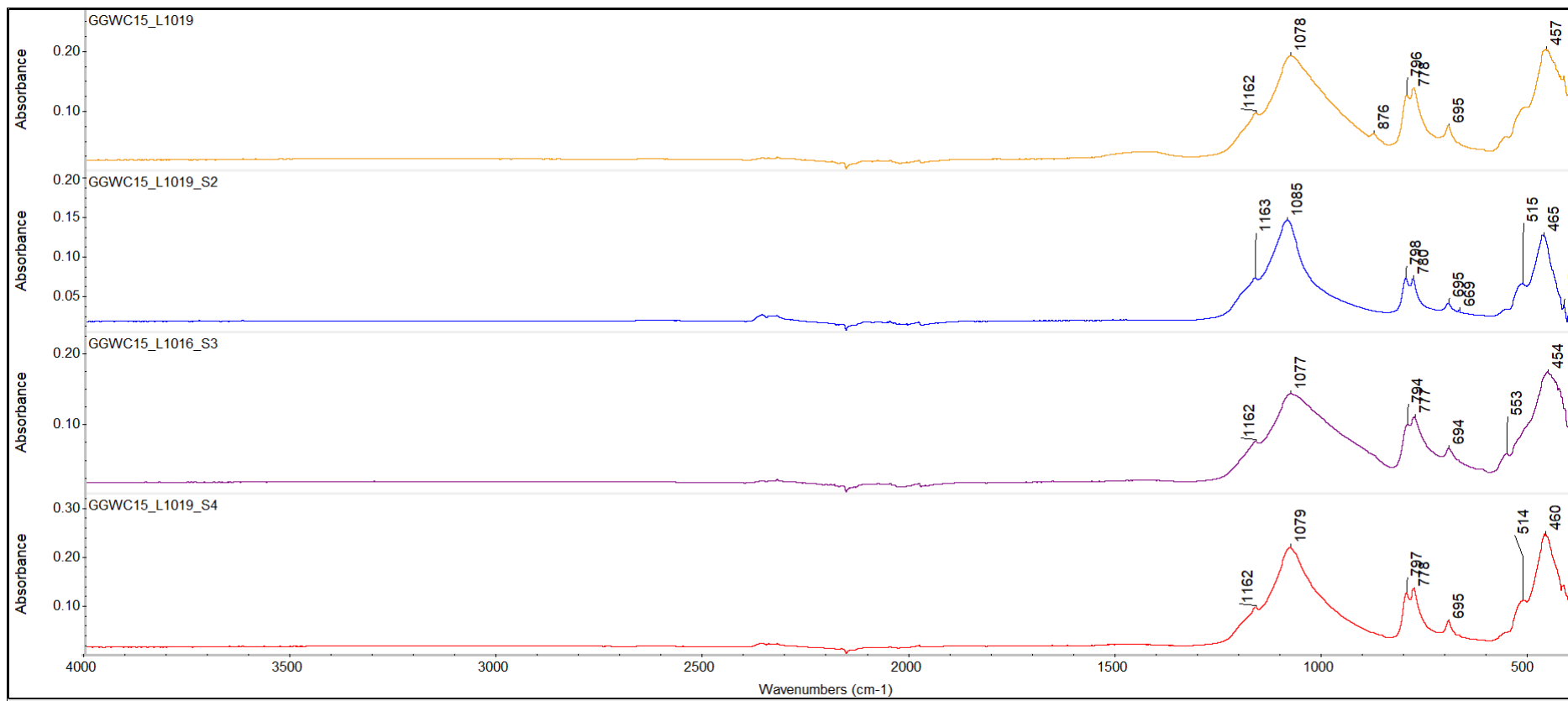


Figure 45:ATR spectra of the samples from *Ggantija* context 1019.

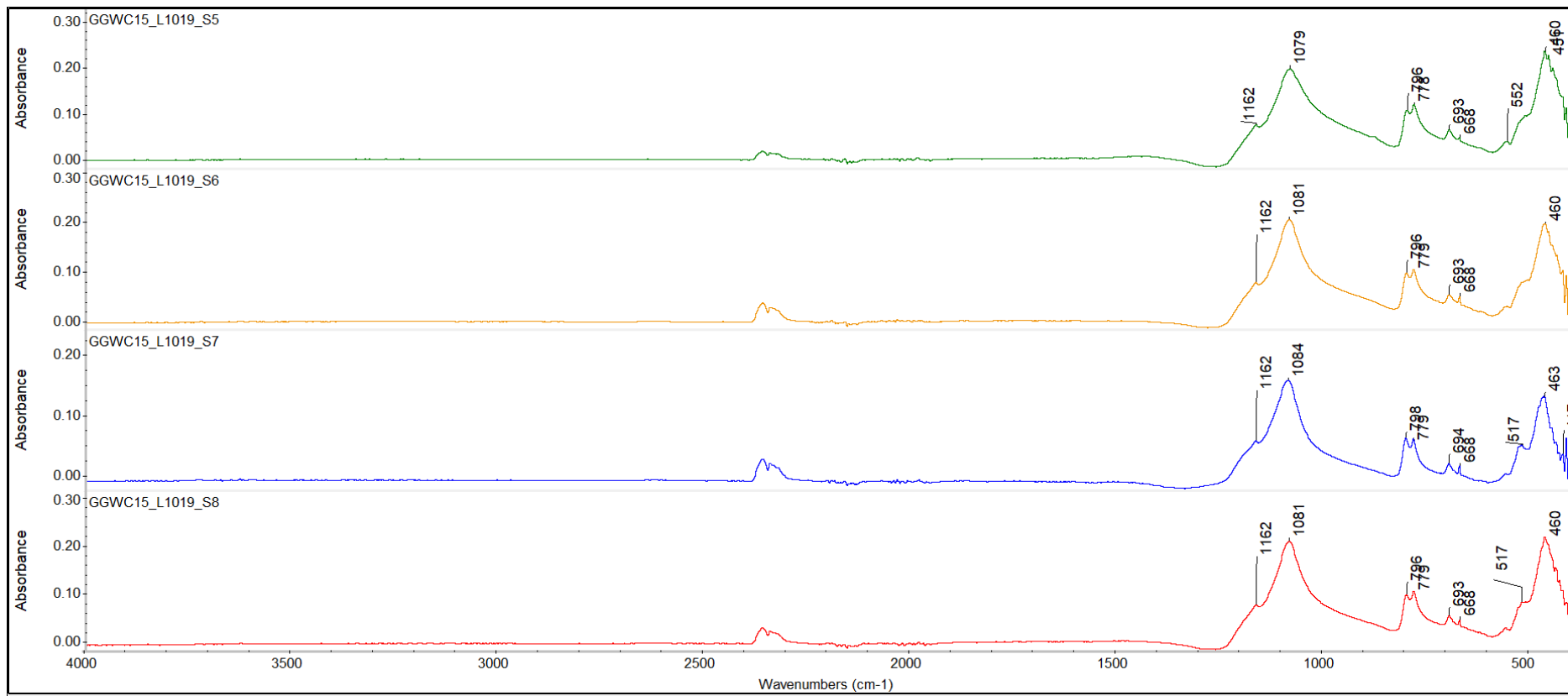


Figure 46: ATR spectra of the samples from Ġgantija context 1019.

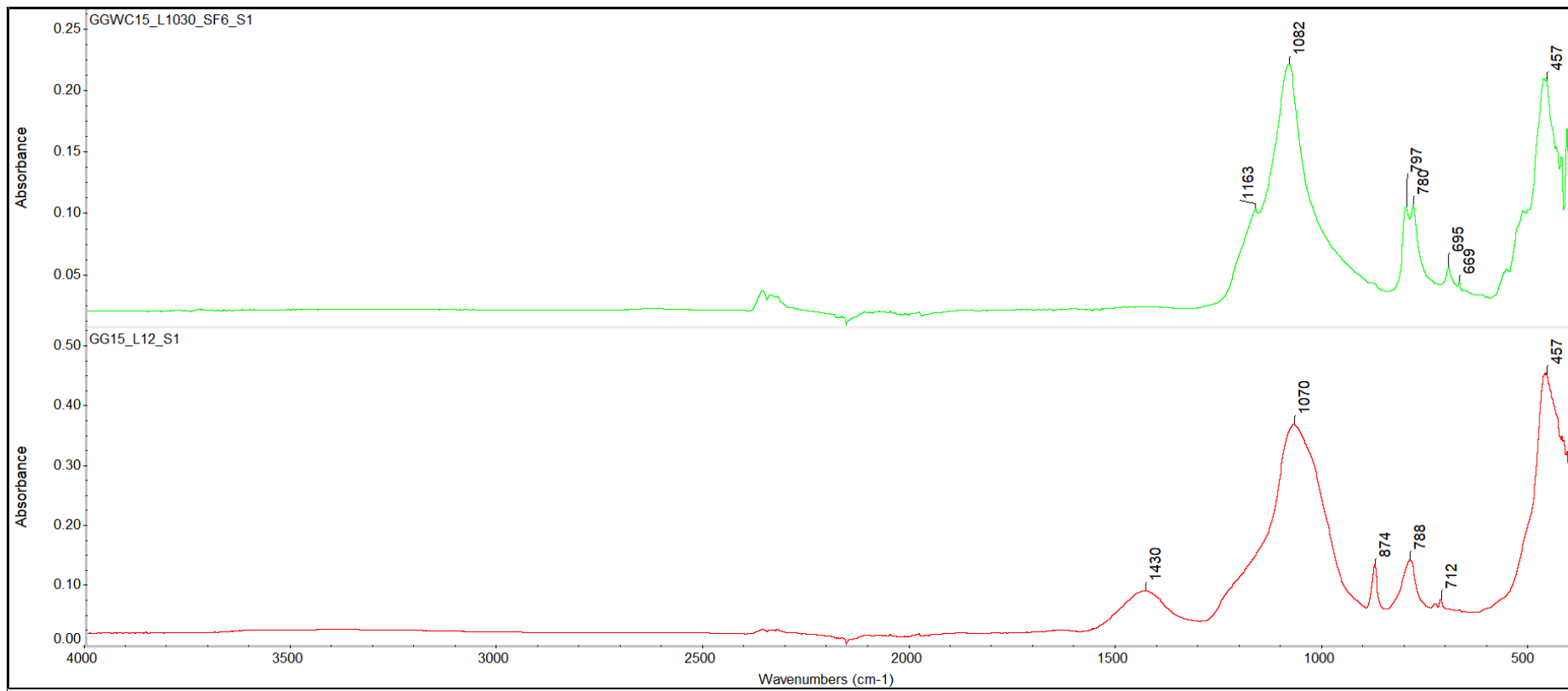


Figure 47: ATR spectra of the samples from Ggantija context 1030 and 12.

Images of the spectra collected with the portable XRF method.

Rock Samples

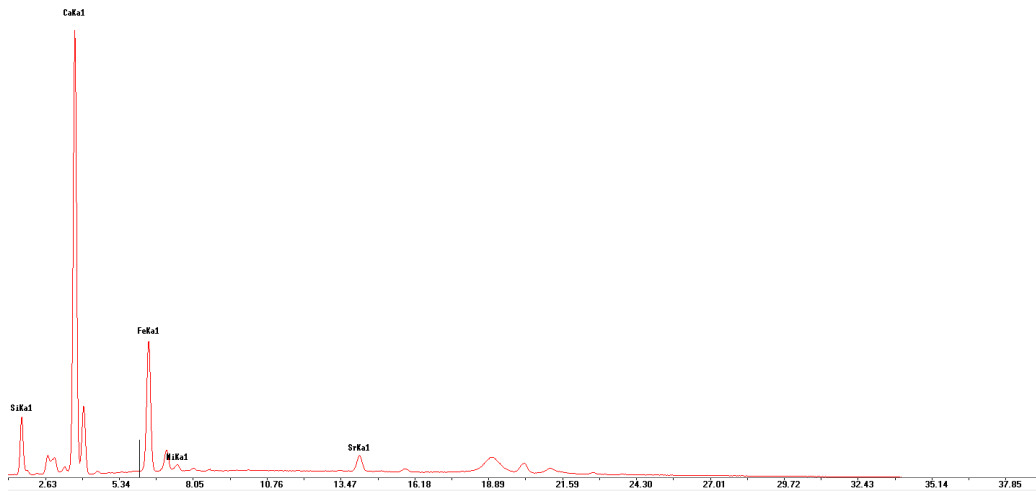


Figure 48: p-XRF spectrum of sample F1S2.



Figure 49: p-XRF spectrum of sample G1S1.



Figure 50: p-XRF spectrum of sample G1S2.

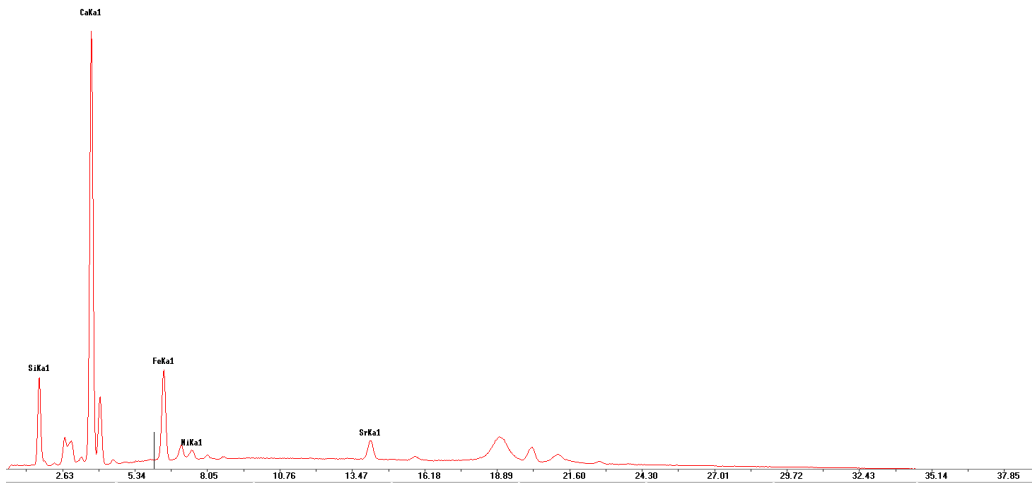


Figure 51: p-XRF spectrum of sample G2S1.

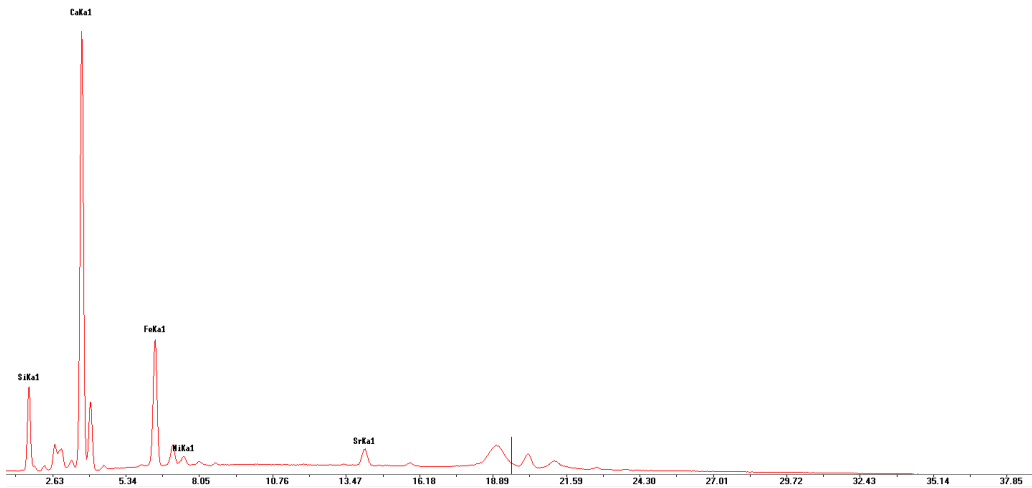


Figure 52: p-XRF spectrum of sample G2S2.

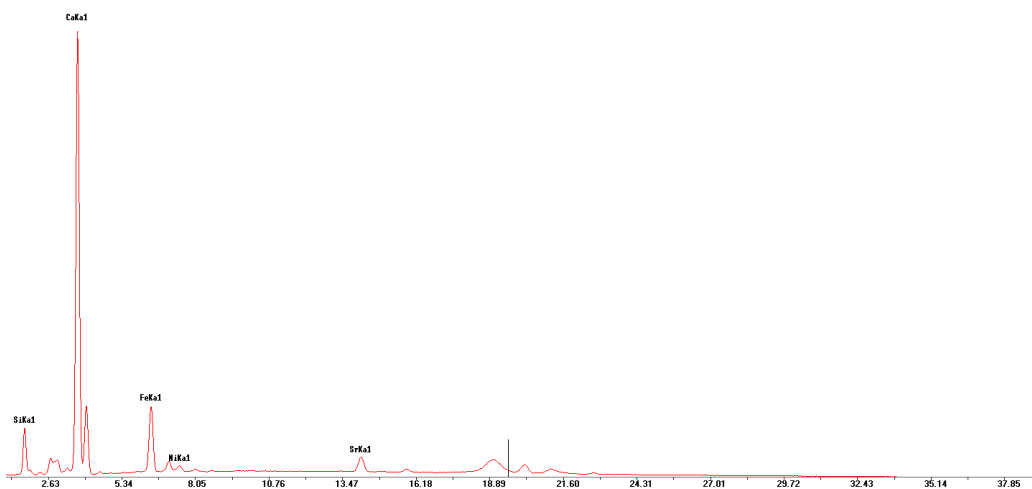


Figure 53: p-XRF spectrum of sample G2S3.

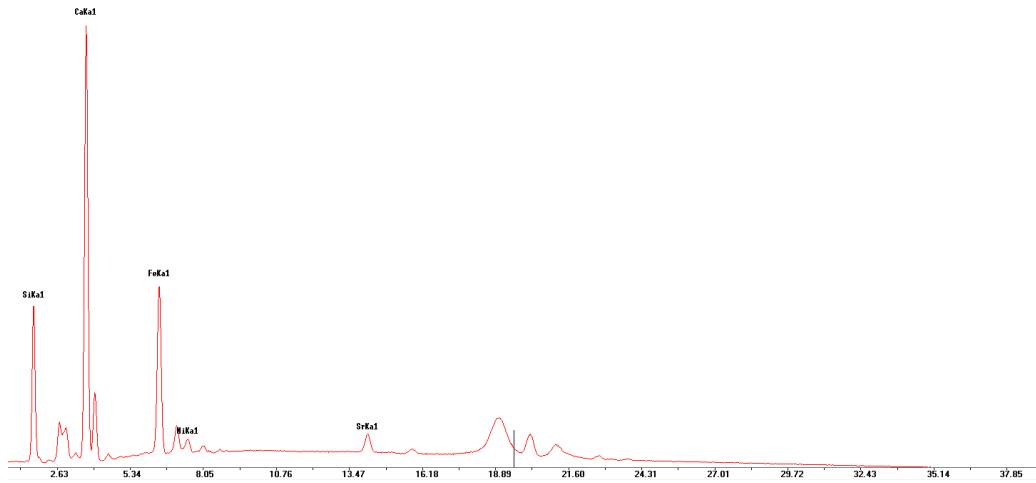


Figure 54: p-XRF spectrum of sample G2S4.

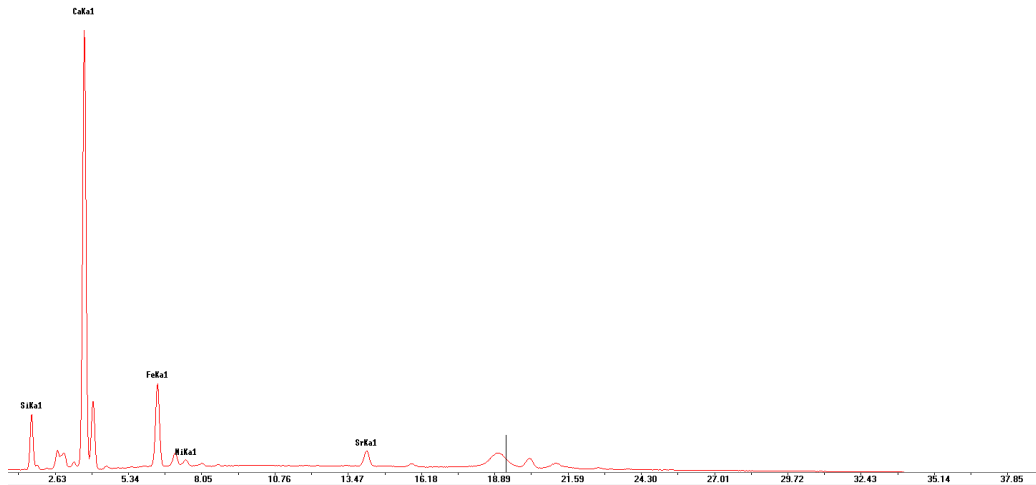


Figure 55: p-XRF spectrum of sample G2S5.

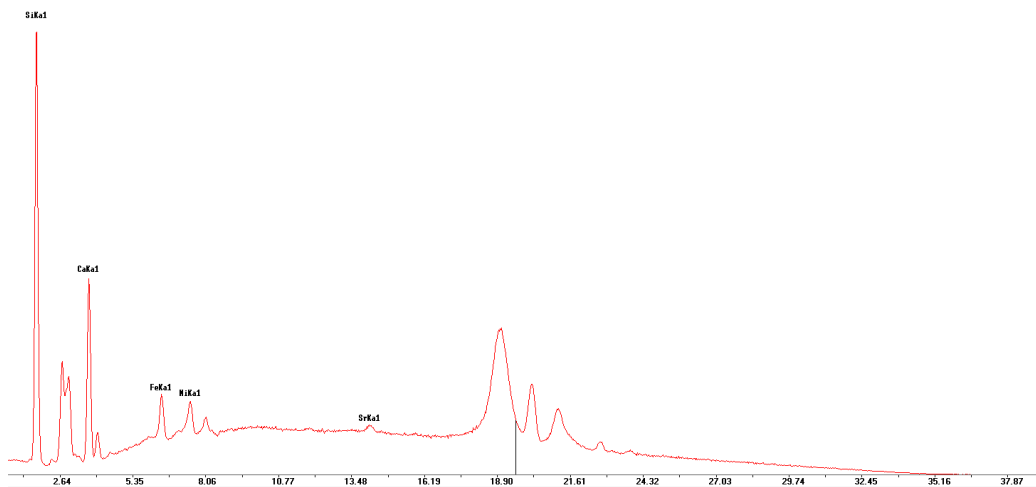


Figure 56: p-XRF spectrum of sample G2S6.

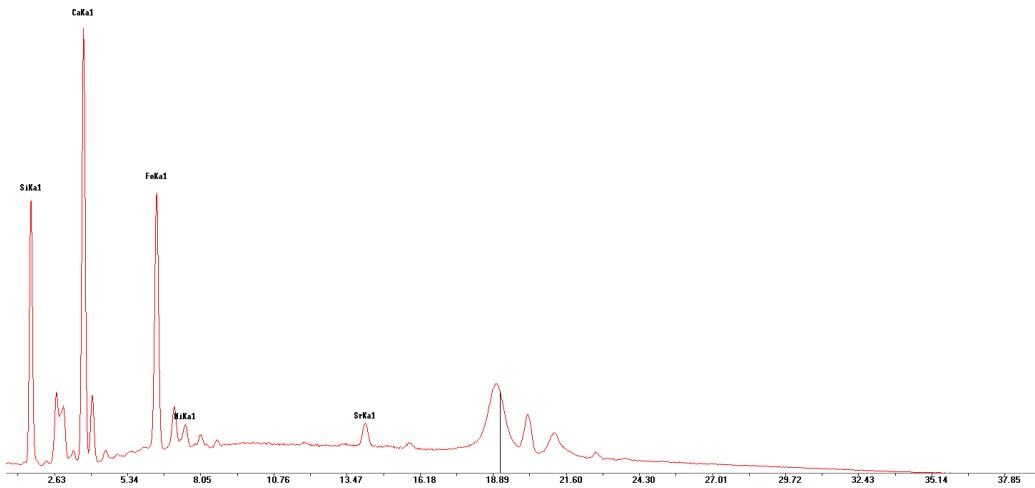


Figure 57: p-XRF spectrum of sample M1S1.

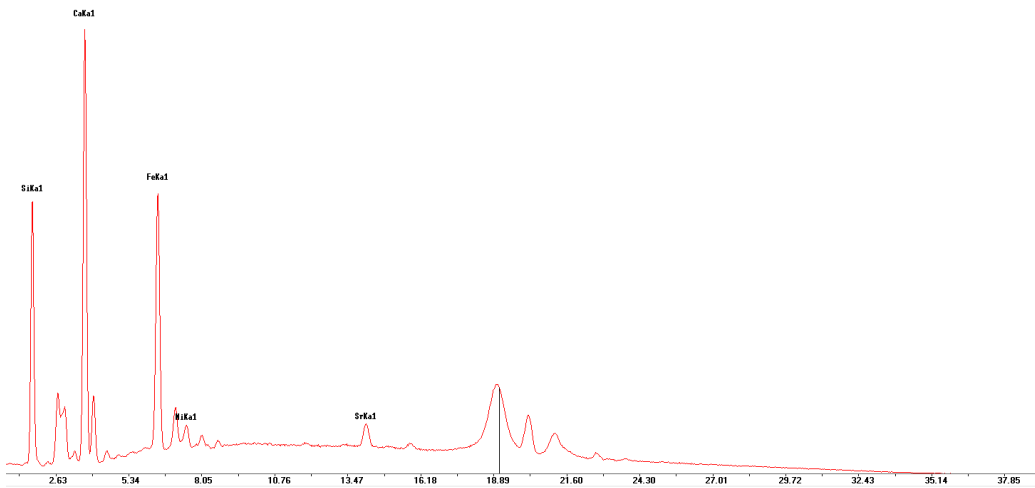


Figure 58: p-XRF spectrum of sample M1S2.

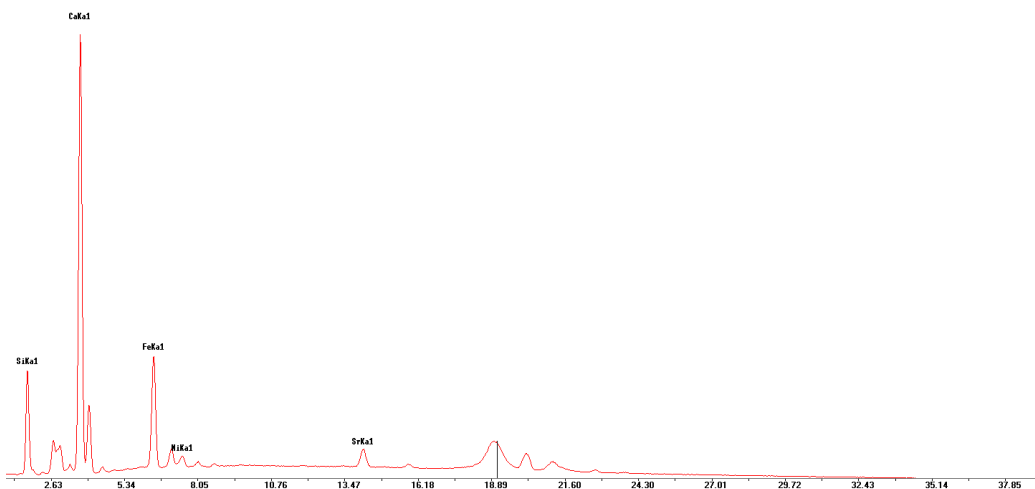


Figure 59: p-XRF spectrum of sample M1S3.

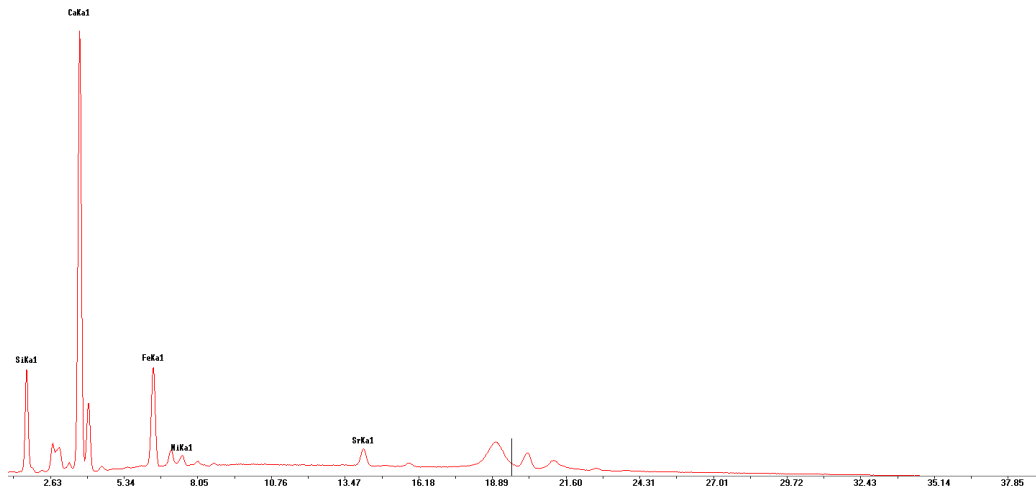


Figure 60: p-XRF spectrum of sample M1S5.

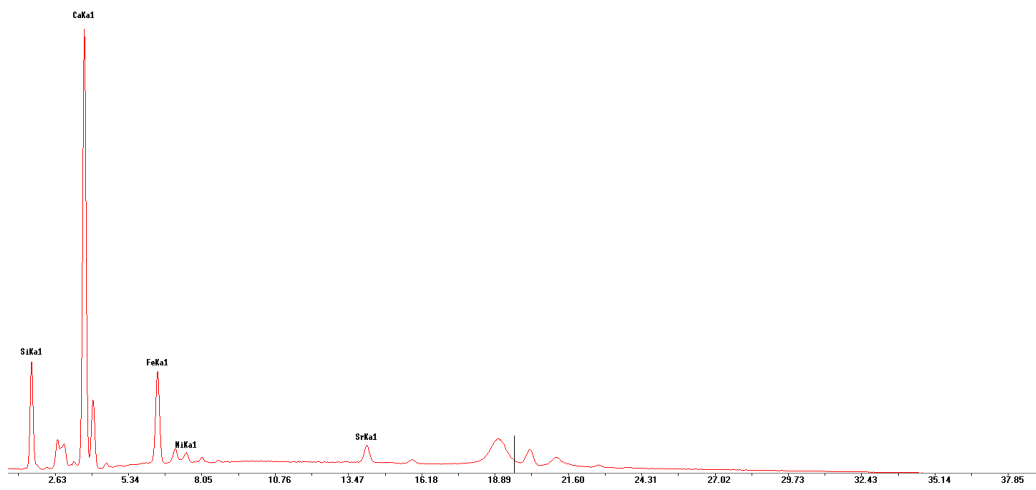


Figure 61: p-XRF spectrum of sample M1S6.

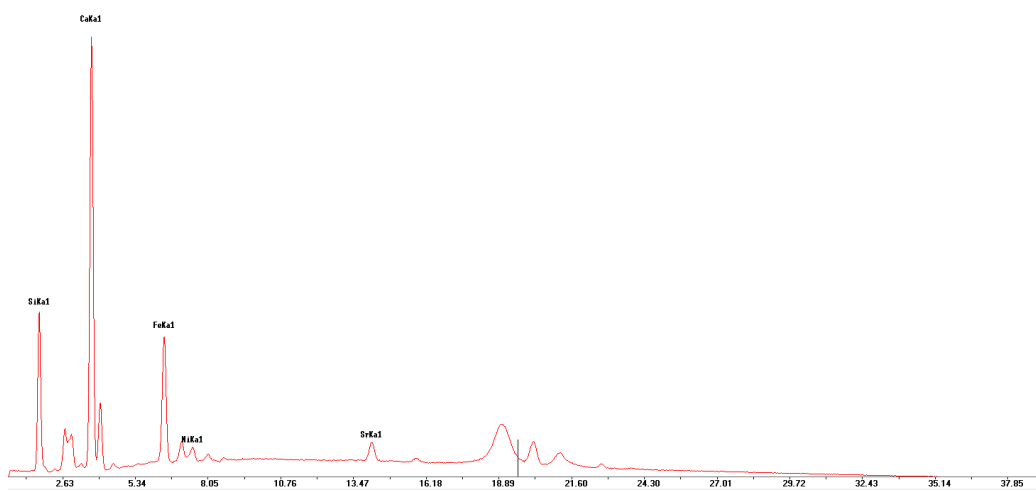


Figure 62: p-XRF spectrum of sample M1S7.

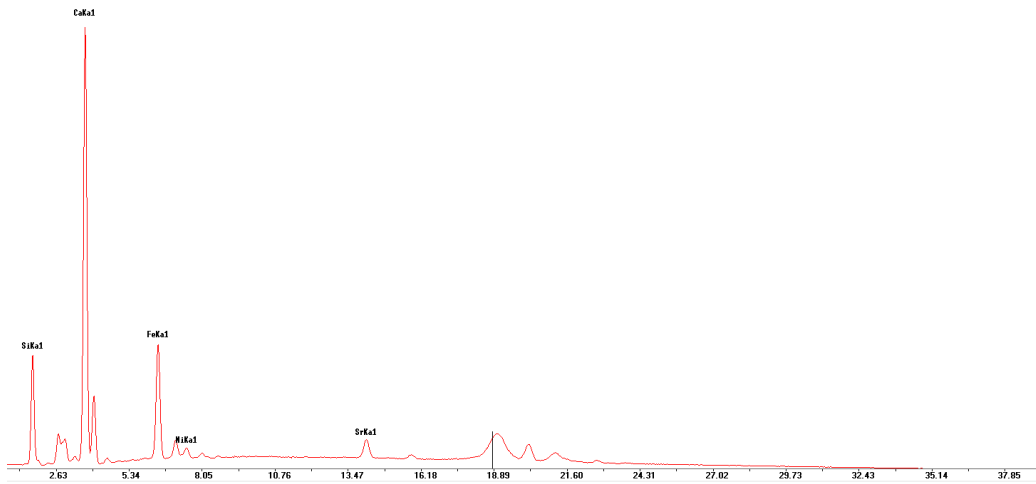


Figure 63: p-XRF spectrum of sample M1S8.

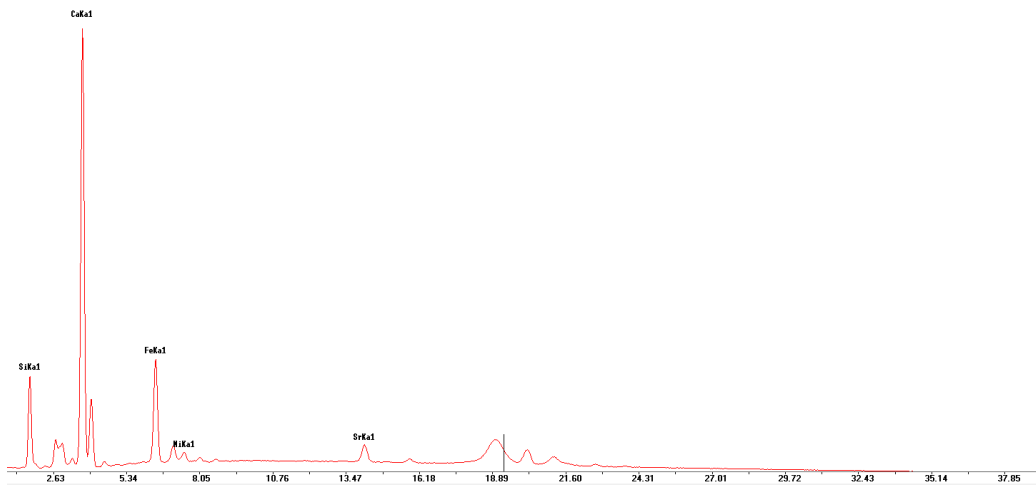


Figure 64: p-XRF spectrum of sample M1S9.

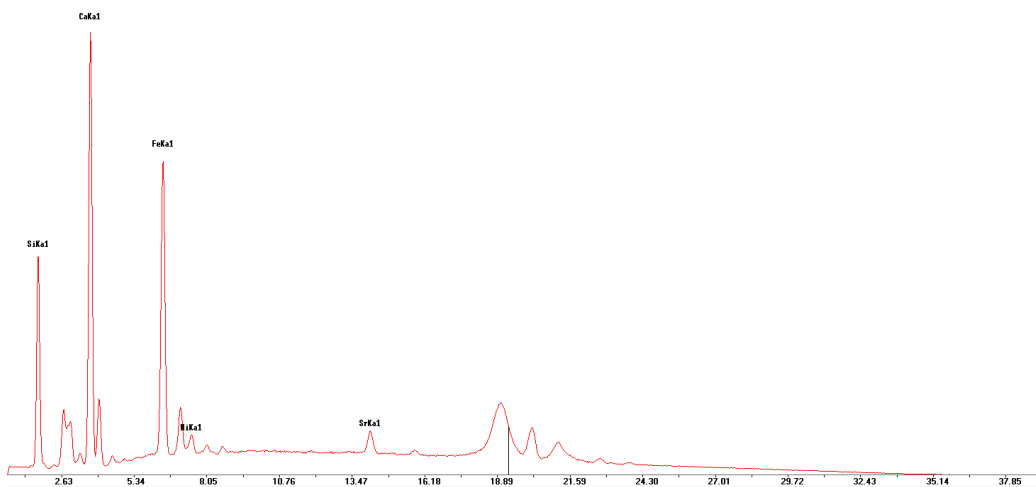


Figure 65: p-XRF spectrum of sample M1S10.

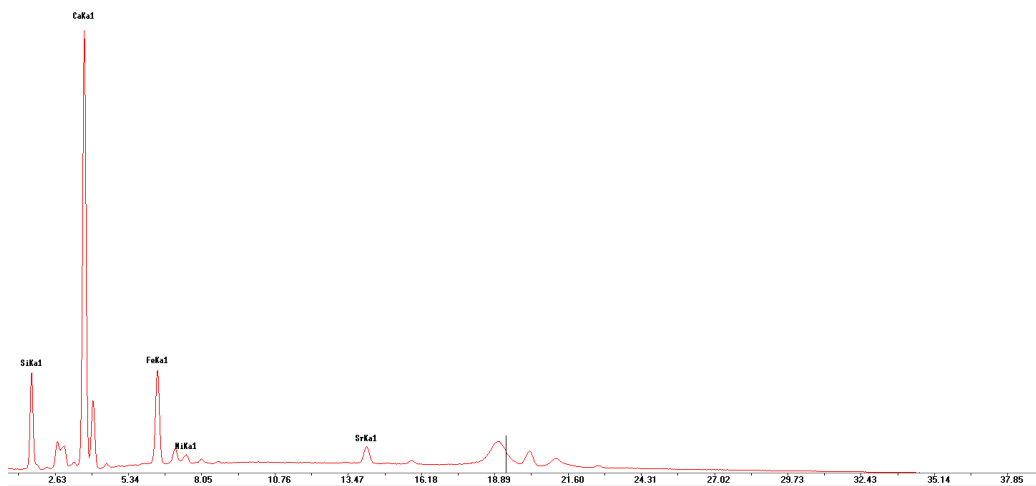


Figure 66: p-XRF spectrum of sample M1S11.

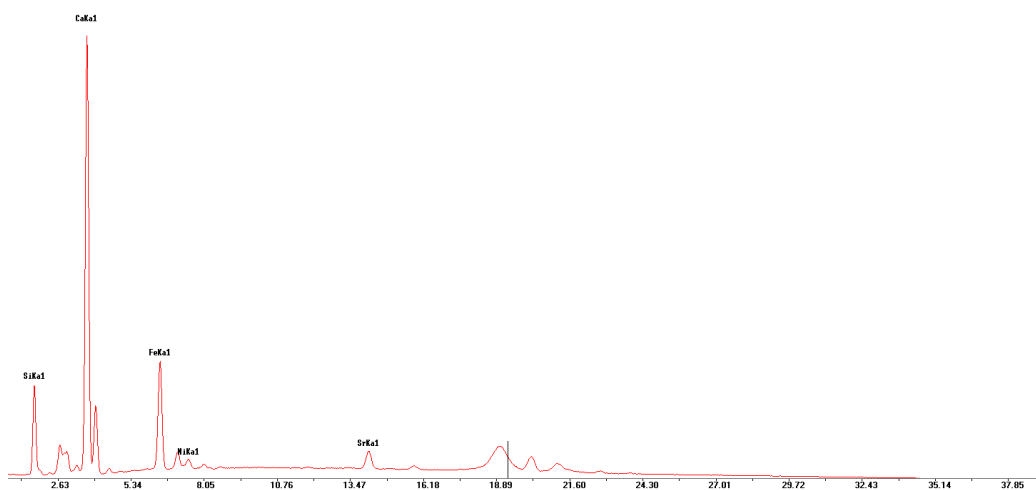


Figure 67: p-XRF spectrum of sample M2S1.

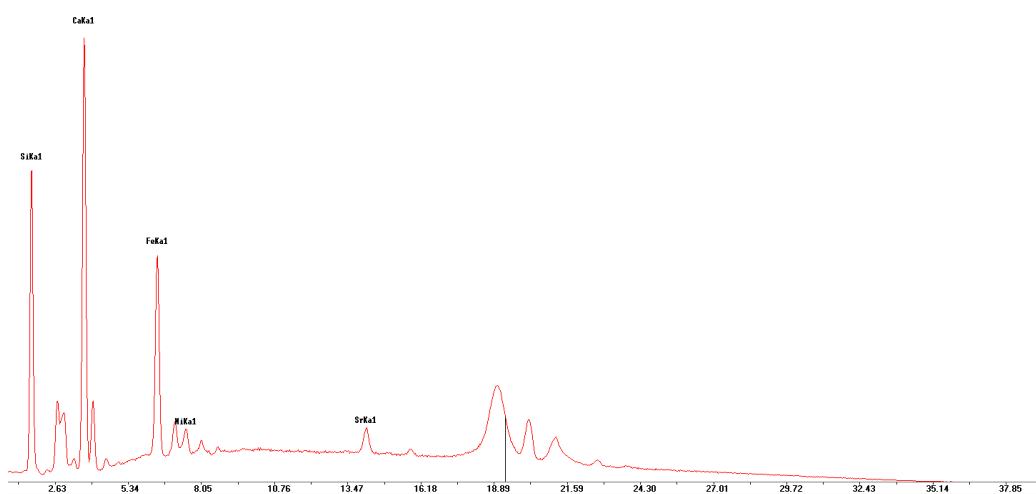


Figure 68: p-XRF spectrum of sample M2S2.

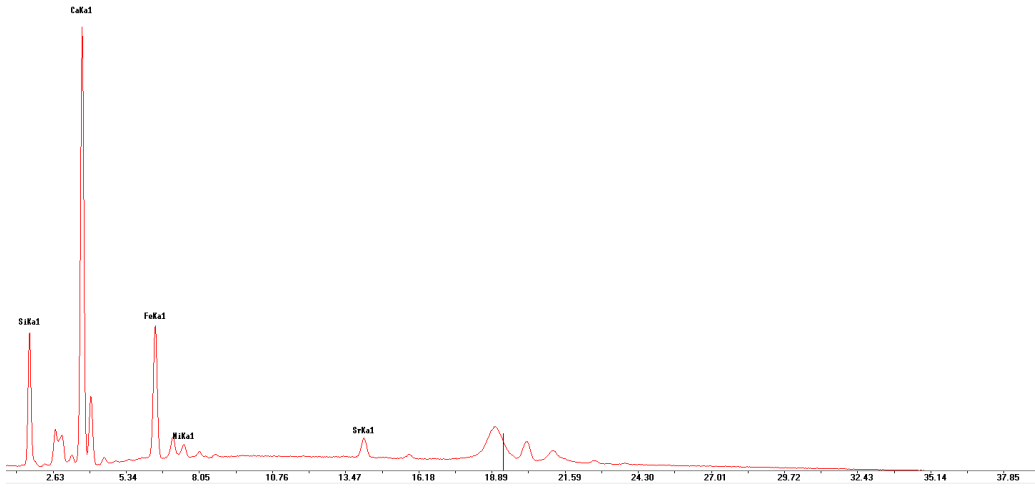


Figure 69: p-XRF spectrum of sample M2S3.

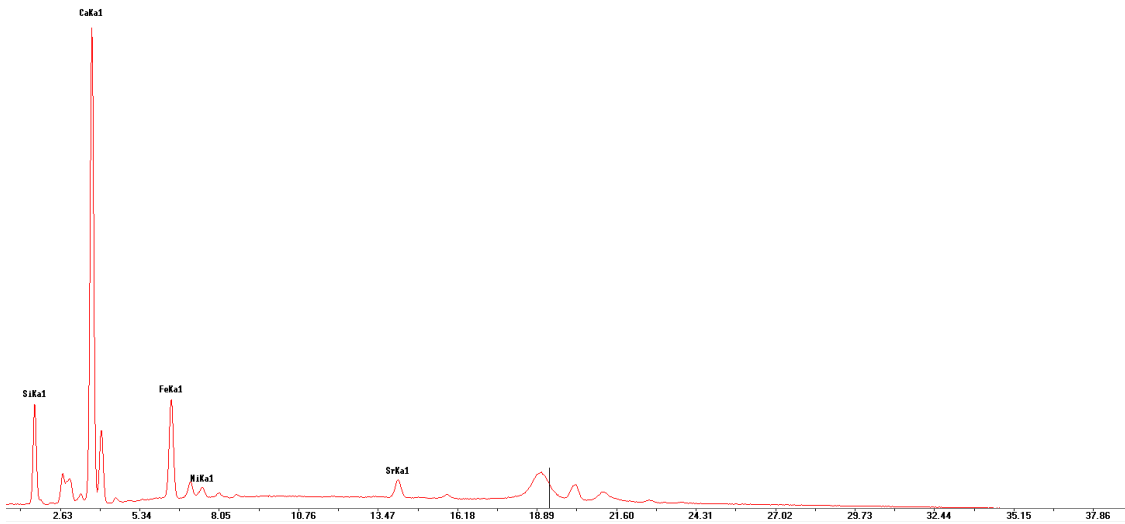


Figure 70: p-XRF spectrum of sample M2S4.

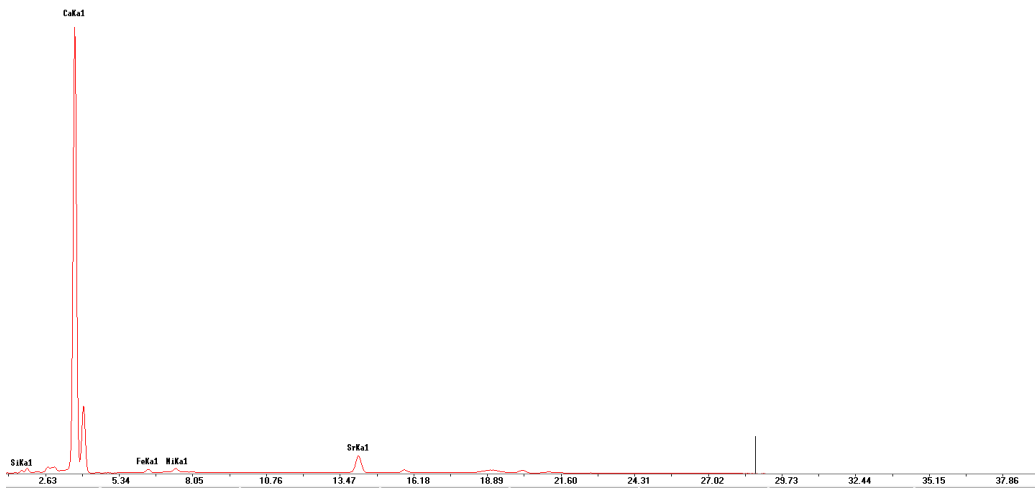


Figure 71: p-XRF spectrum of sample S2.

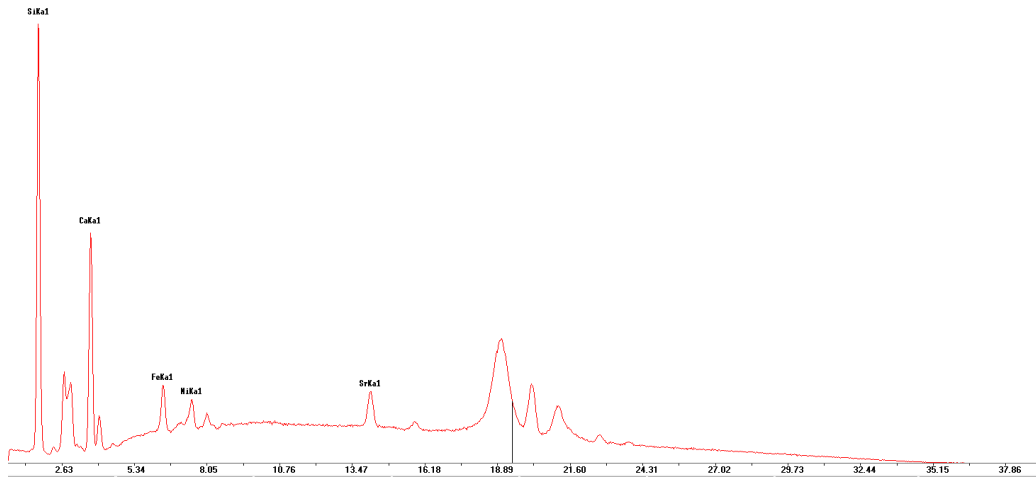


Figure 72: p-XRF spectrum of sample S3

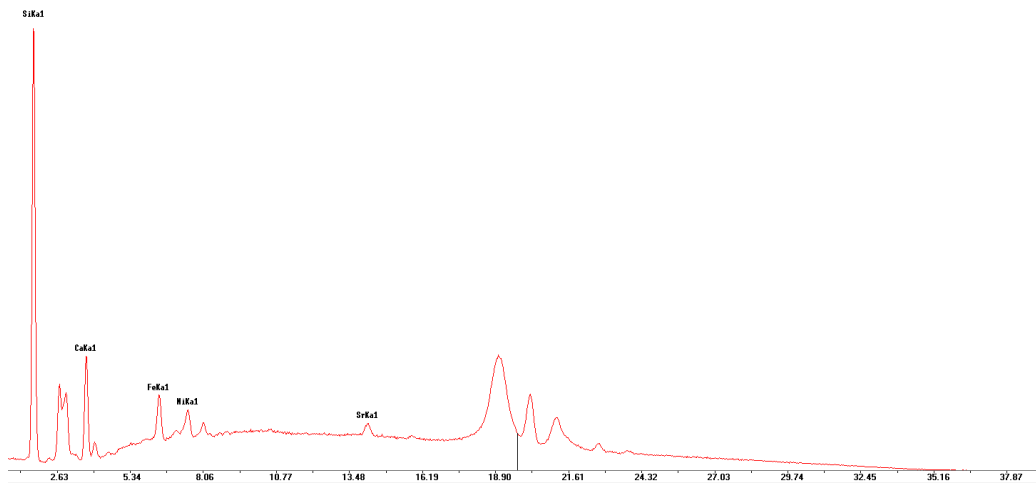


Figure 73: p-XRF spectrum of sample S5.

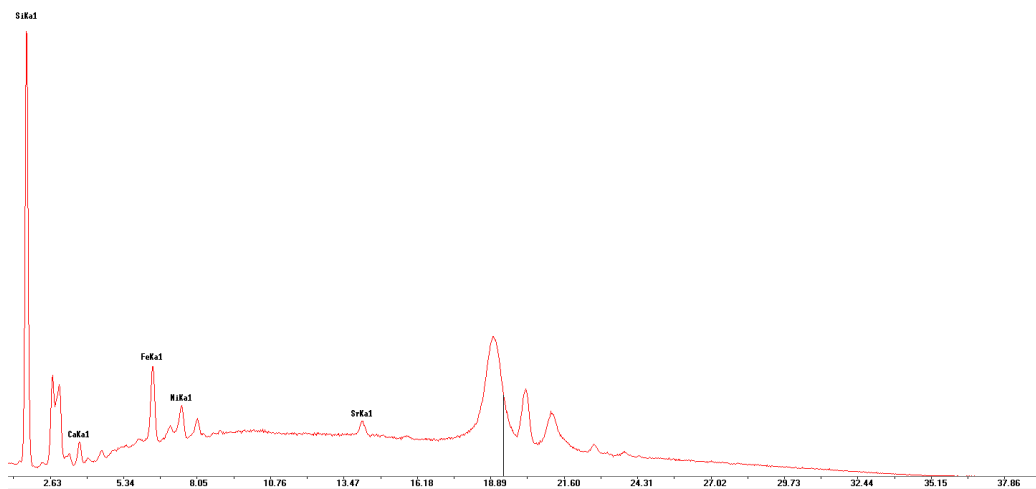


Figure 74: p-XRF spectrum of sample S6.

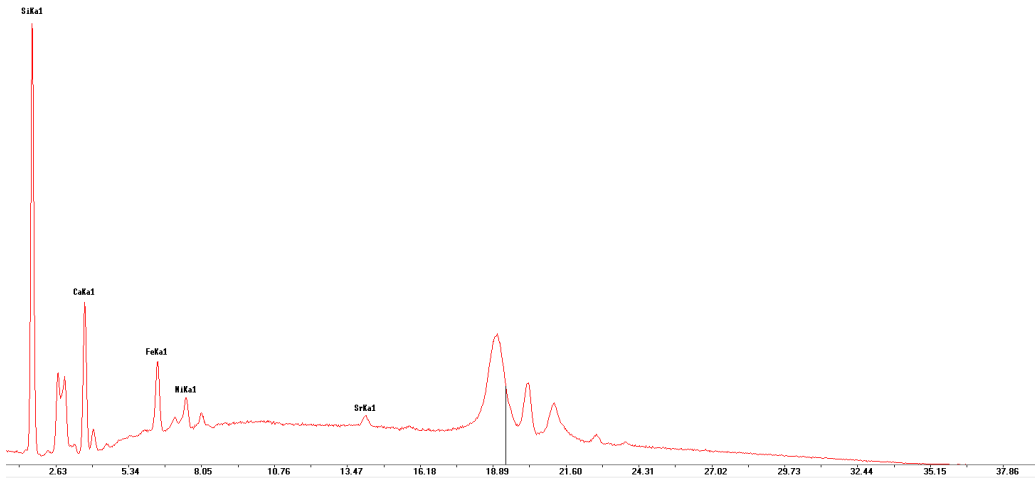


Figure 75: p-XRF spectrum of sample S10.

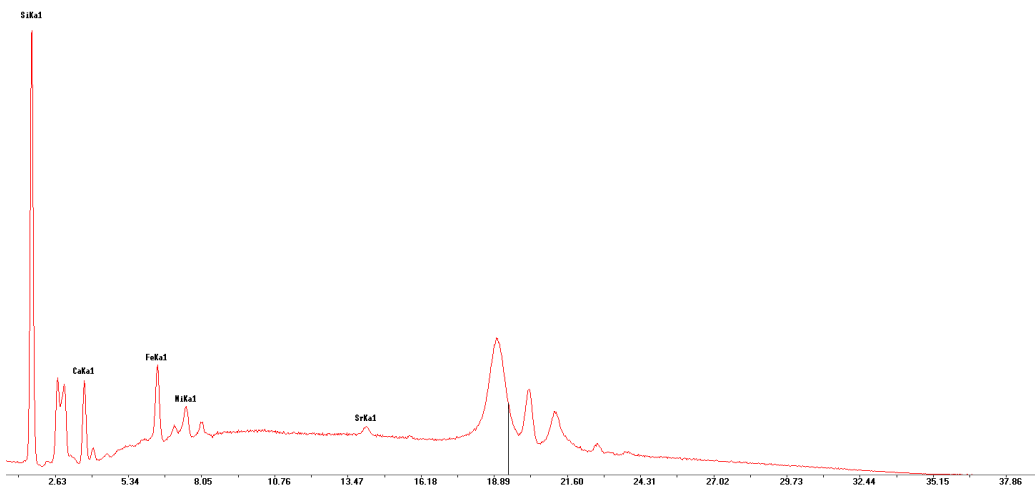


Figure 76: p-XRF spectrum of sample S11.

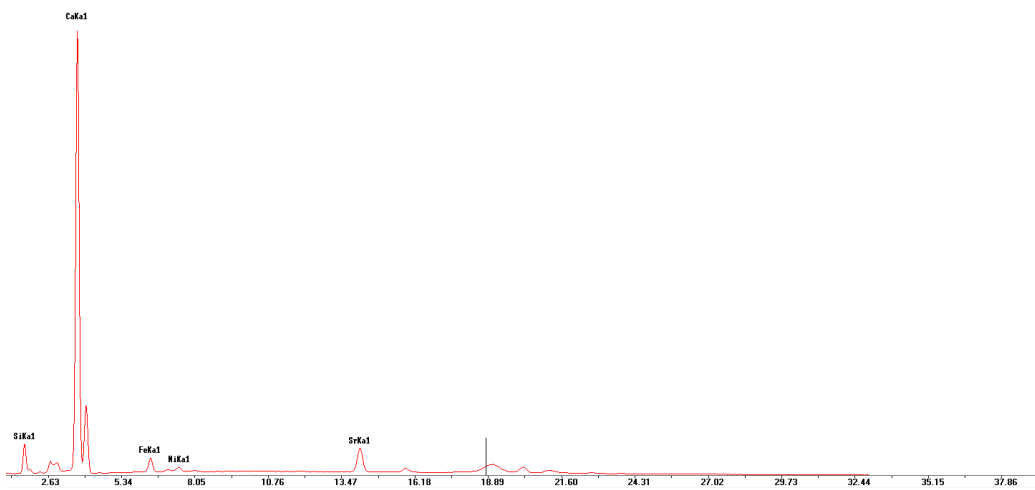


Figure 77: p-XRF spectrum of sample S12.

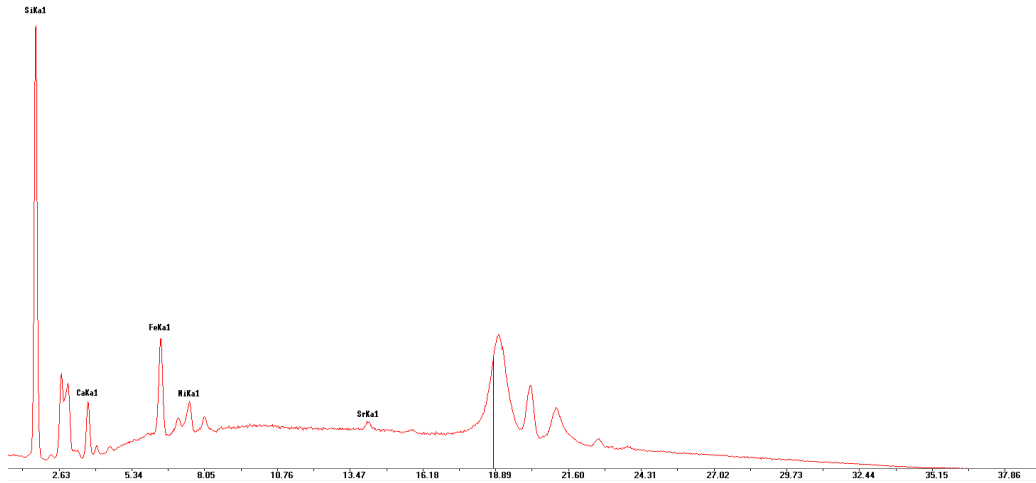


Figure 78: p-XRF spectrum of sample S13.

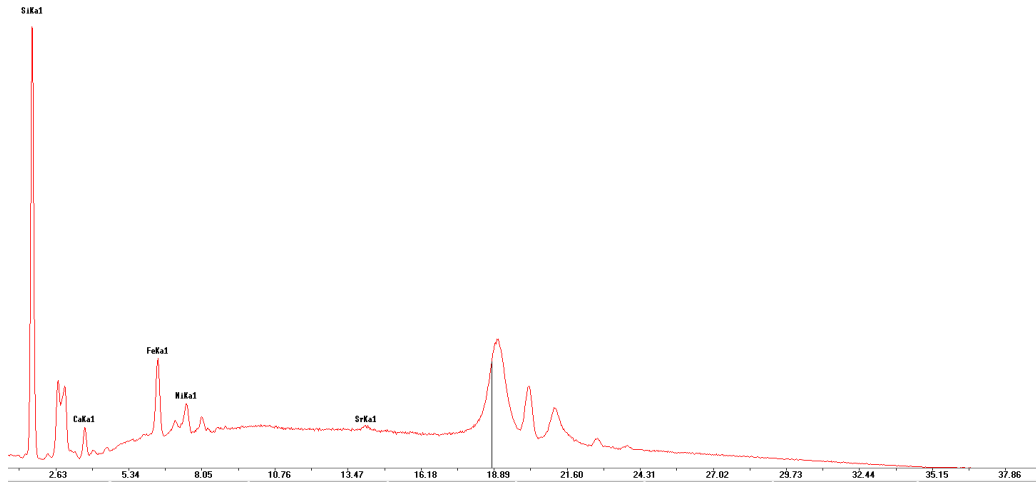


Figure 79: p-XRF spectrum of sample S14.

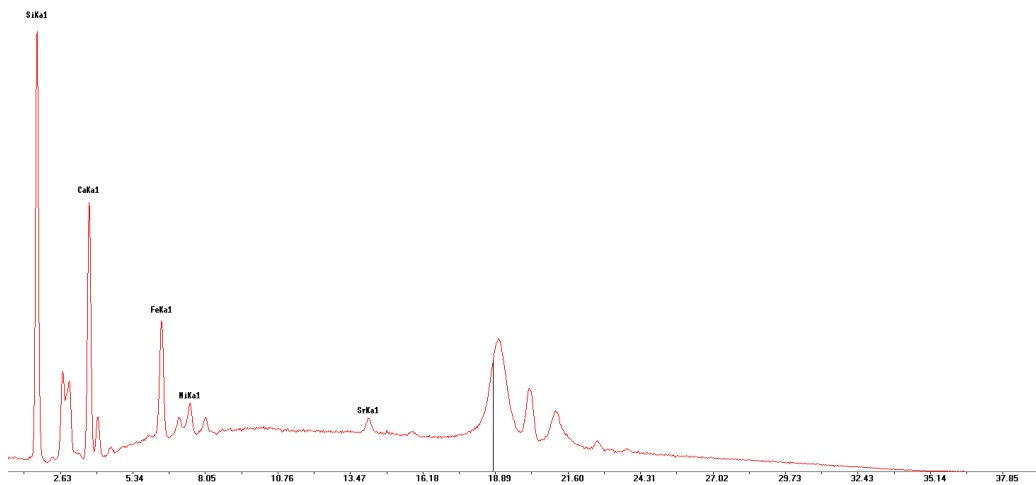


Figure 80: p-XRF spectrum of sample S15.

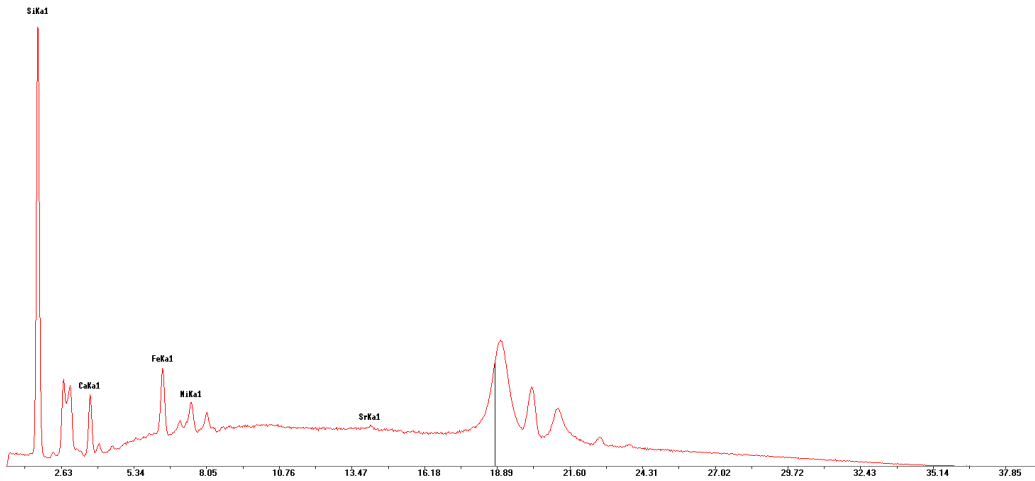


Figure 81: p-XRF spectrum of sample S18.

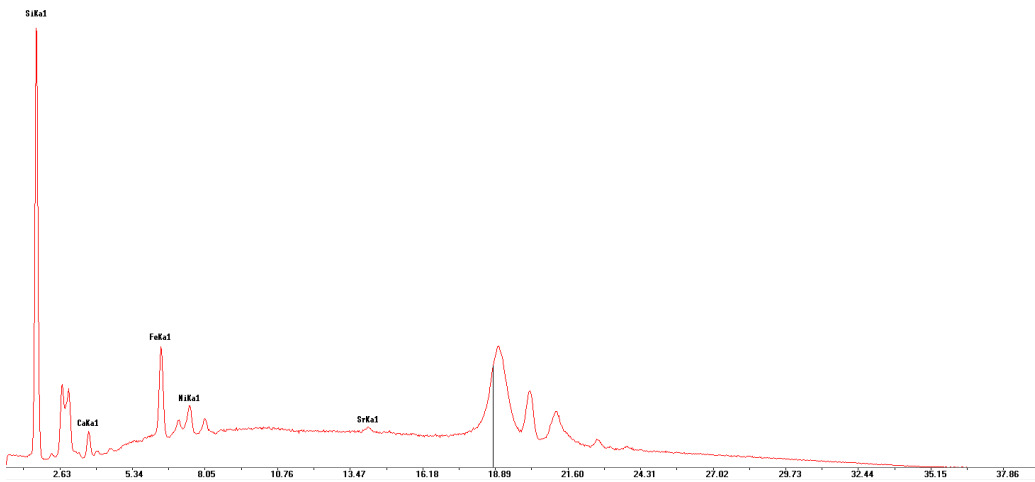


Figure 82: p-XRF spectrum of sample S19.

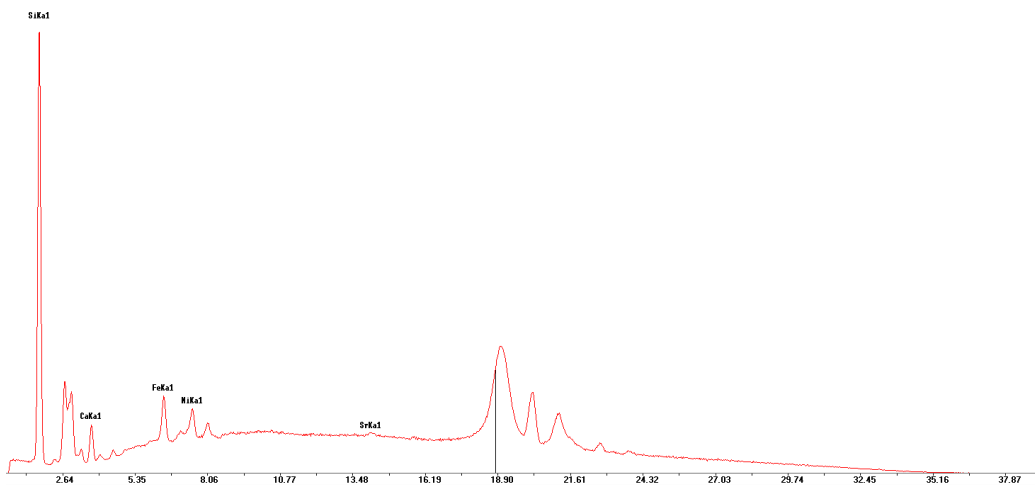


Figure 83: p-XRF spectrum of sample S20.

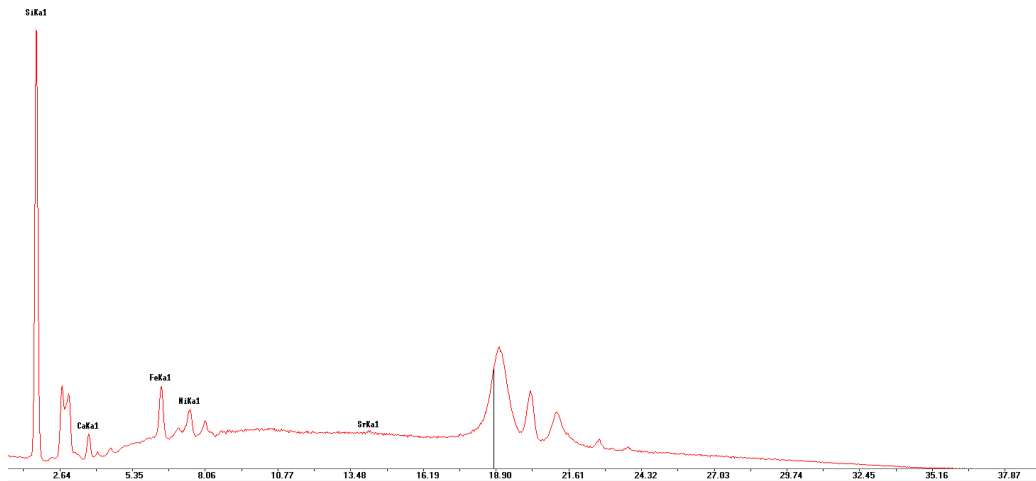


Figure 84: p-XRF spectrum of sample S21.

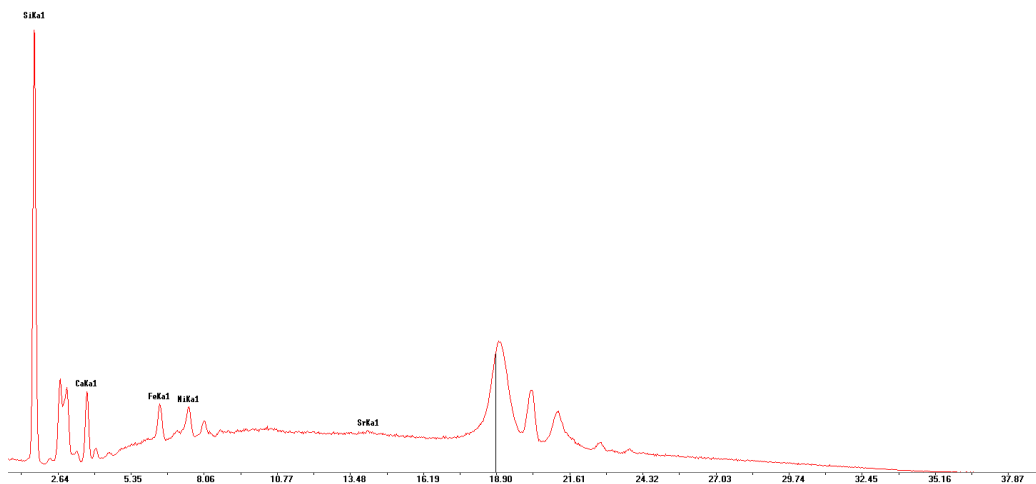


Figure 85: p-XRF spectrum of sample S22r.

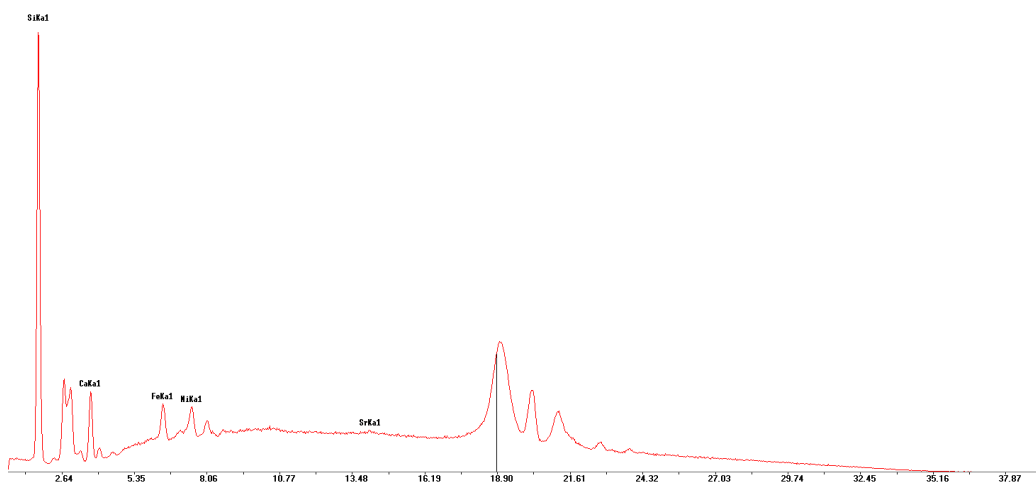


Figure 86: p-XRF spectrum of sample S22p.

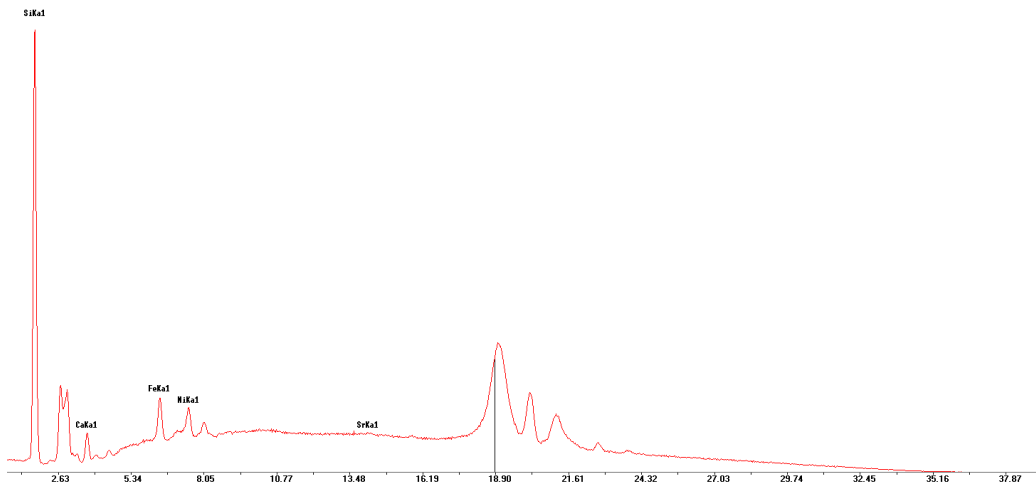


Figure 87: p-XRF spectrum of sample S23.

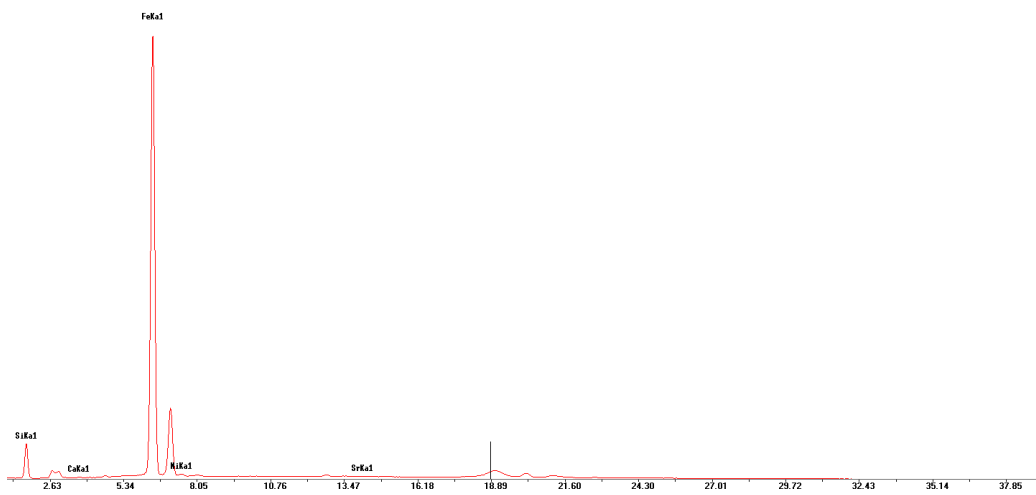


Figure 88: p-XRF spectrum of sample S24.

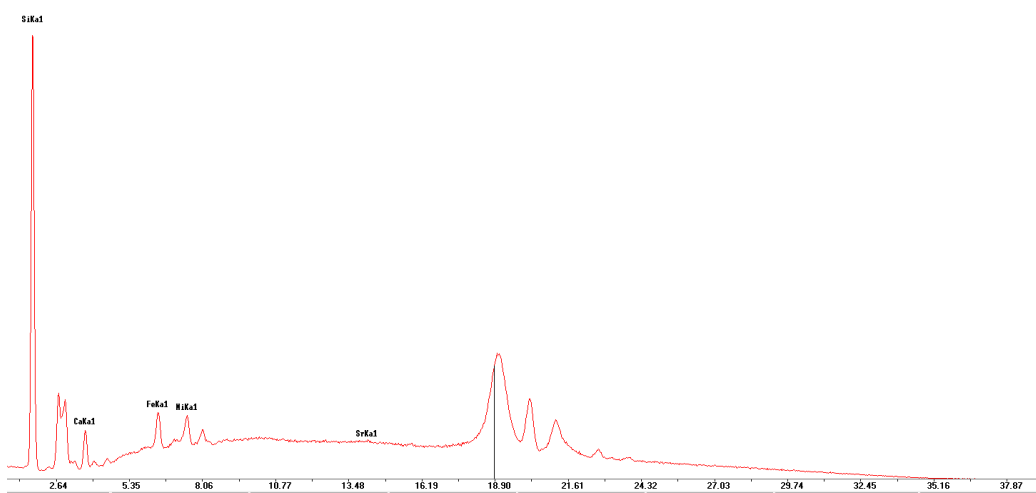


Figure 89: p-XRF spectrum of sample S25.

Artefact Samples

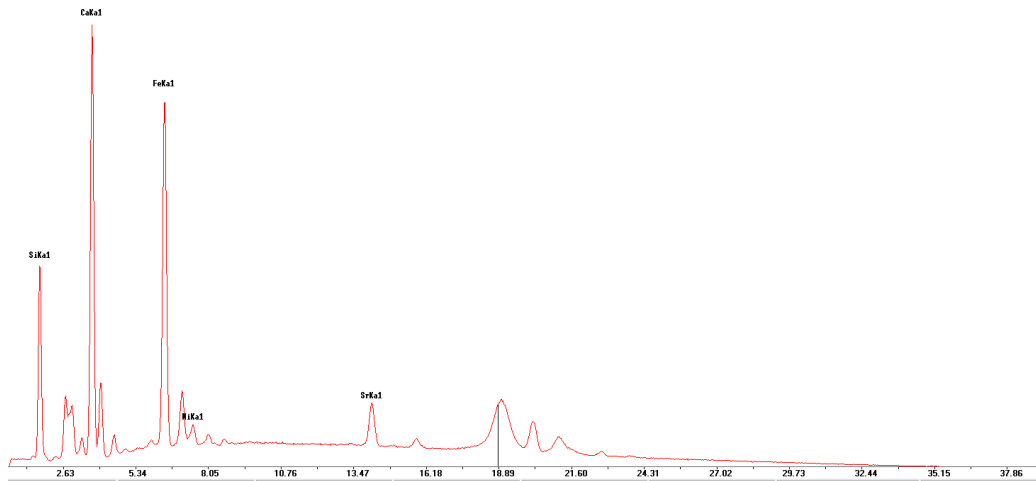


Figure 90: p-XRF spectrum of sample BR91/S564/L662 from Xagħra Circle.

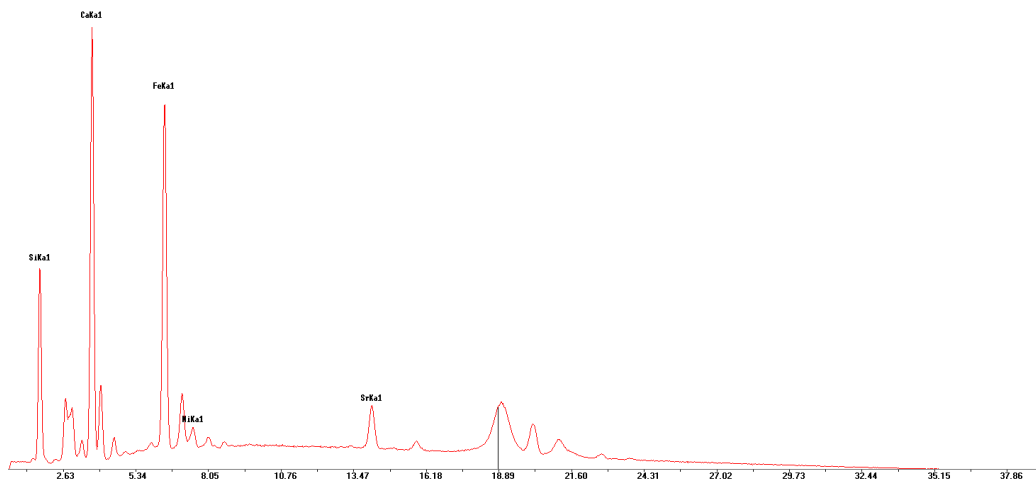


Figure 91: p-XRF spectrum of sample BR91/S566/L662 from Xagħra Circle.

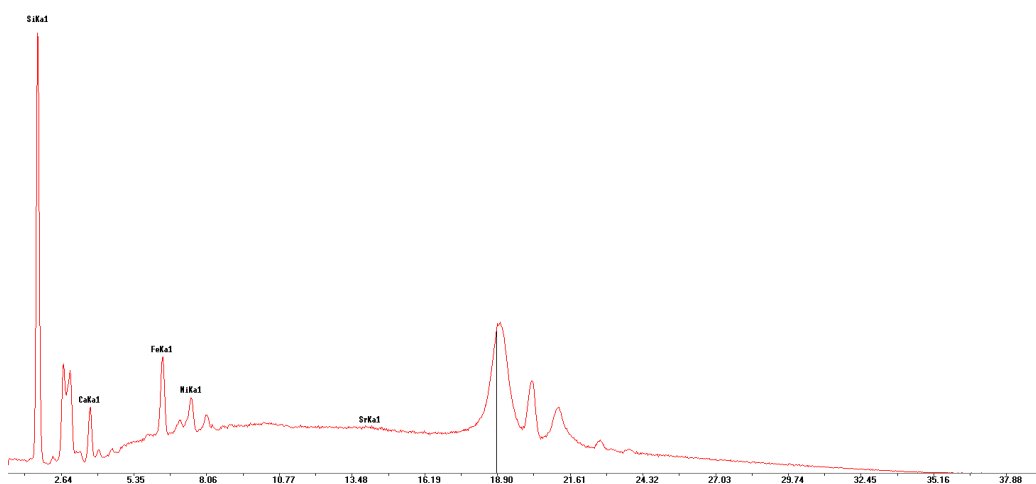


Figure 92: p-XRF spectrum of sample BR93/S843/L4 from Xagħra Circle.

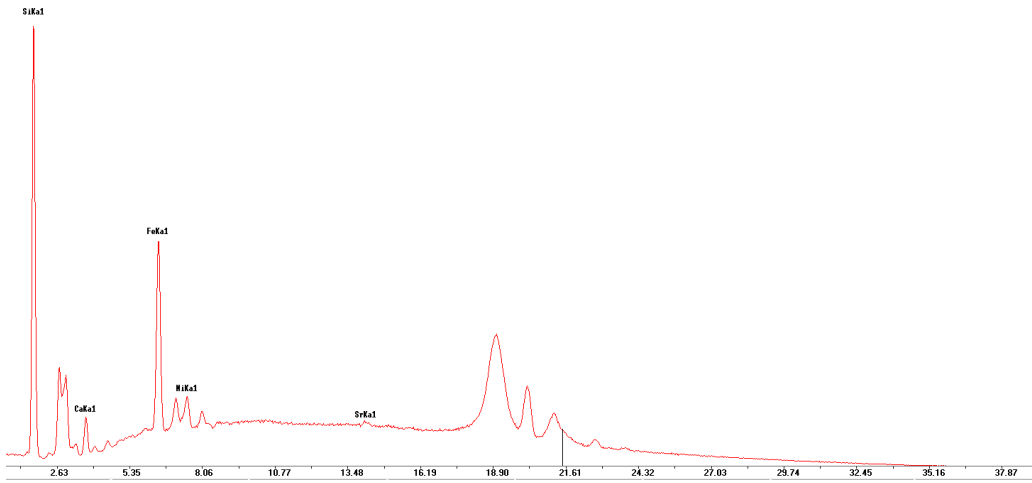


Figure 93: p-XRF spectrum of sample BR94/S1142/L1279 from Xagħra Circle.

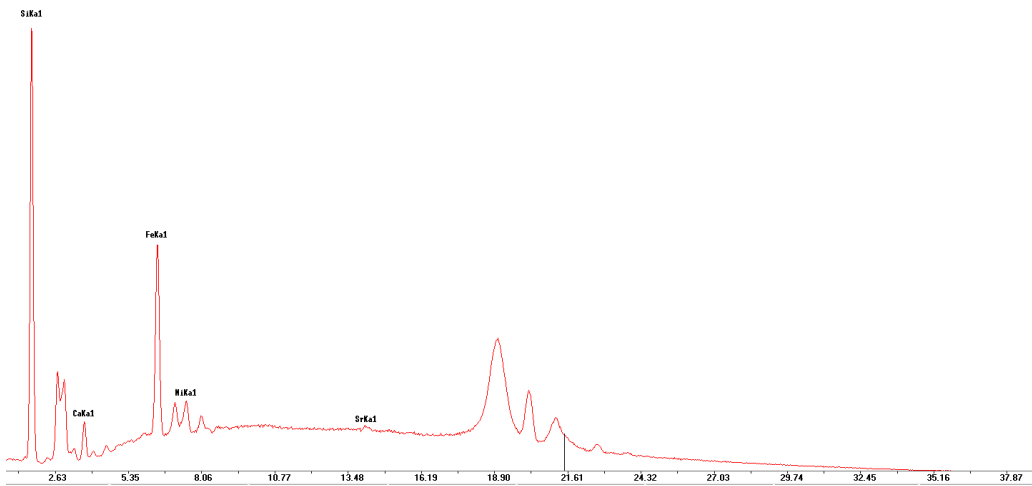


Figure 94: p-XRF spectrum of sample BR93/S854/L897 from Xagħra Circle.

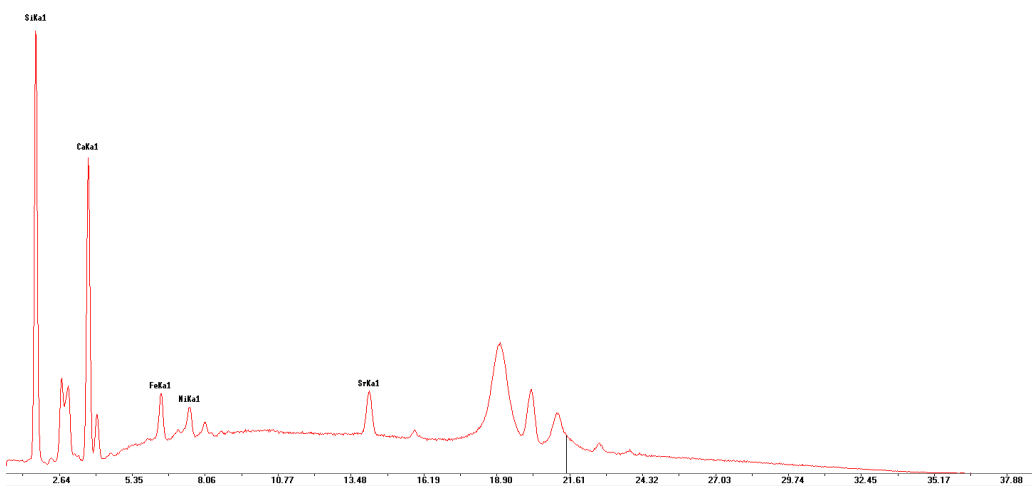


Figure 95: p-XRF spectrum of sample BR93/S767/L783 from Xagħra Circle.

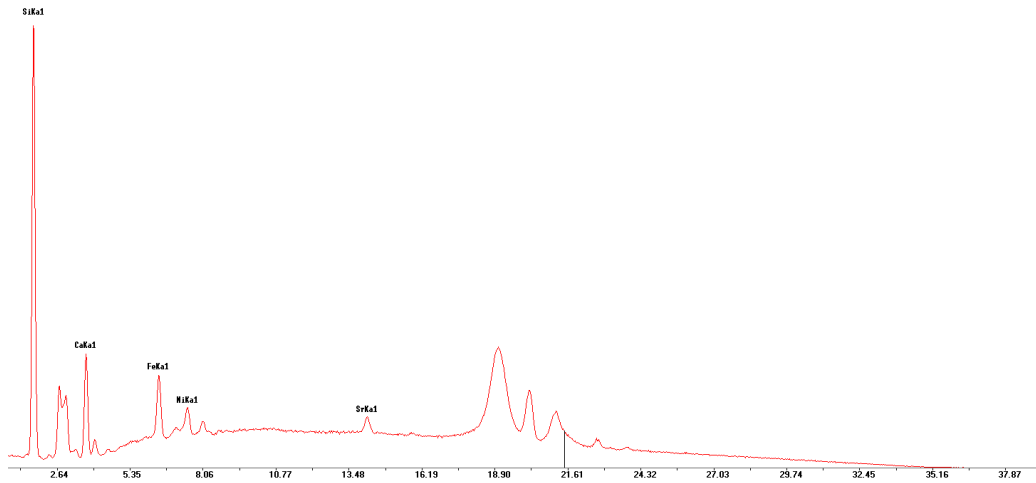


Figure 96: p-XRF spectrum of sample BR91/S745/L845 from Xagħra Circle.

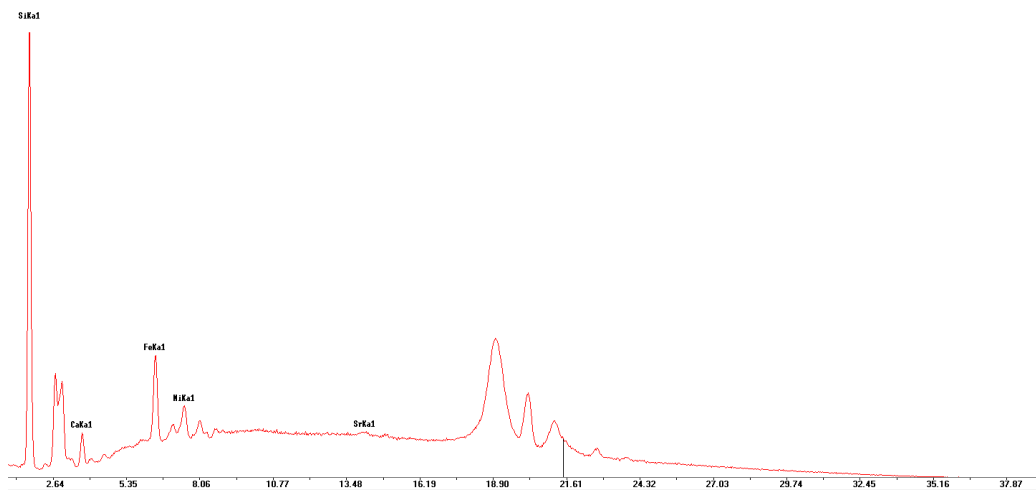


Figure 97: p-XRF spectrum of sample BR91/S611/L712 from Xagħra Circle.

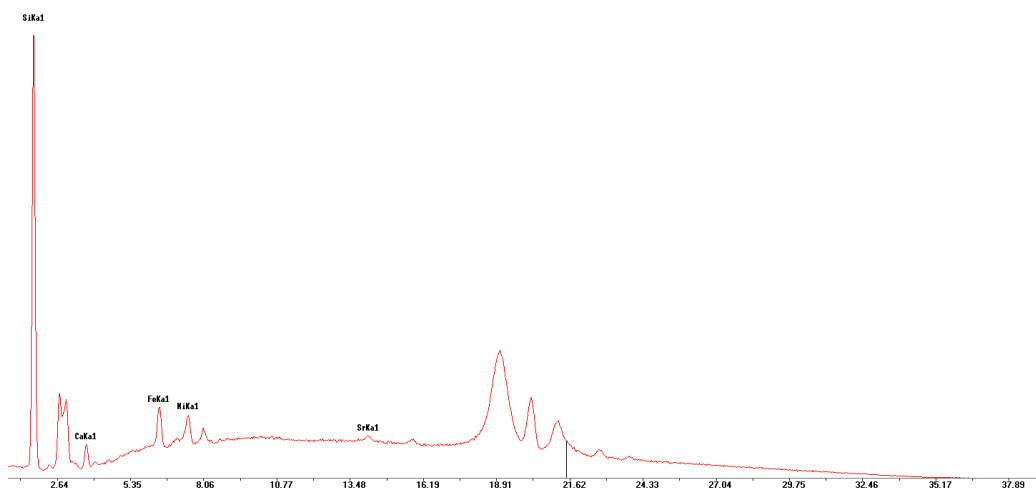


Figure 98: p-XRF spectrum of sample BR89/S395/L449 from Xagħra Circle.

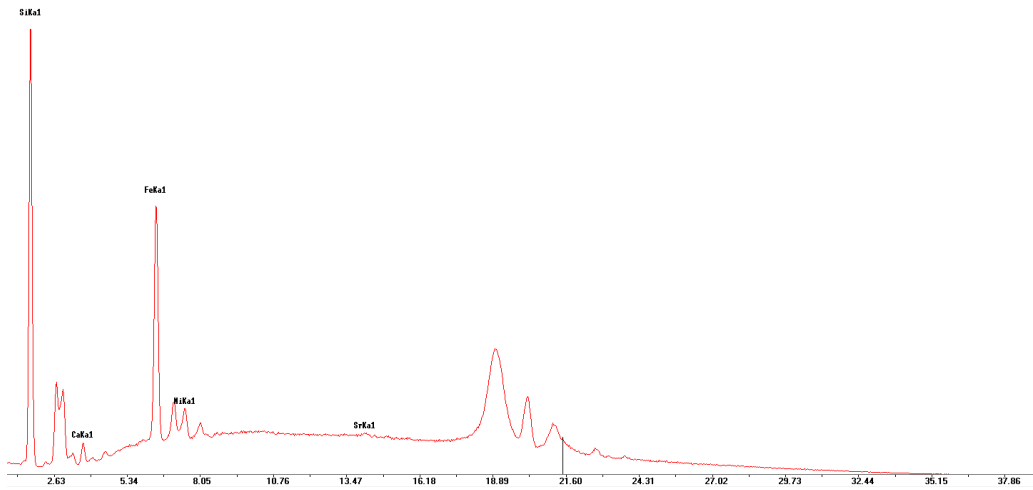


Figure 99: p-XRF spectrum of sample BR89/S291/L334 from Xagħra Circle.

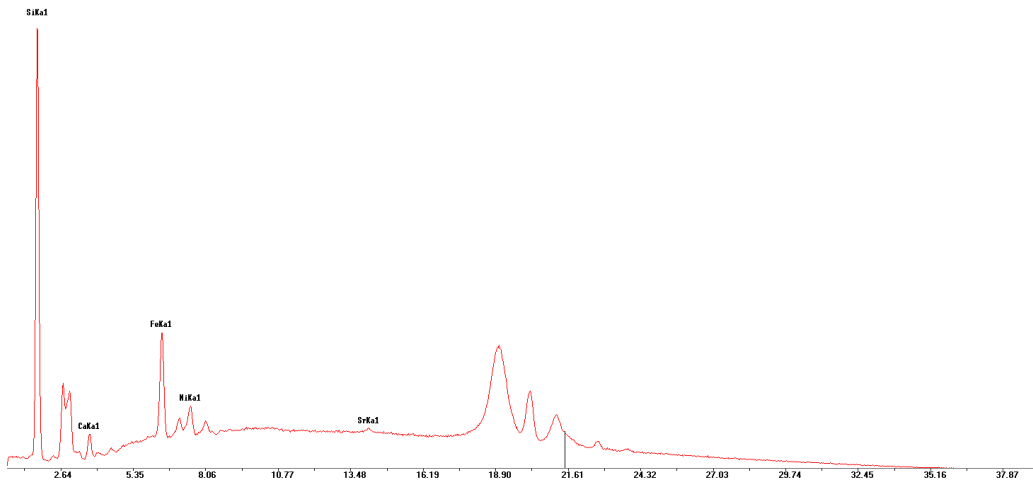


Figure 100: p-XRF spectrum of sample BR88/S110/L274 from Xagħra Circle.

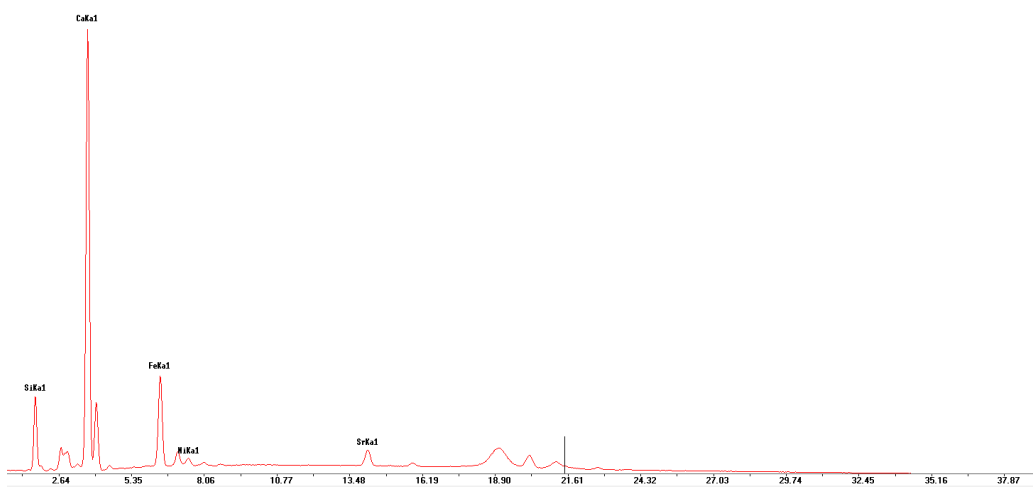


Figure 101: p-XRF spectrum of sample KRD15/L22/S1/TRIA from Kordin.

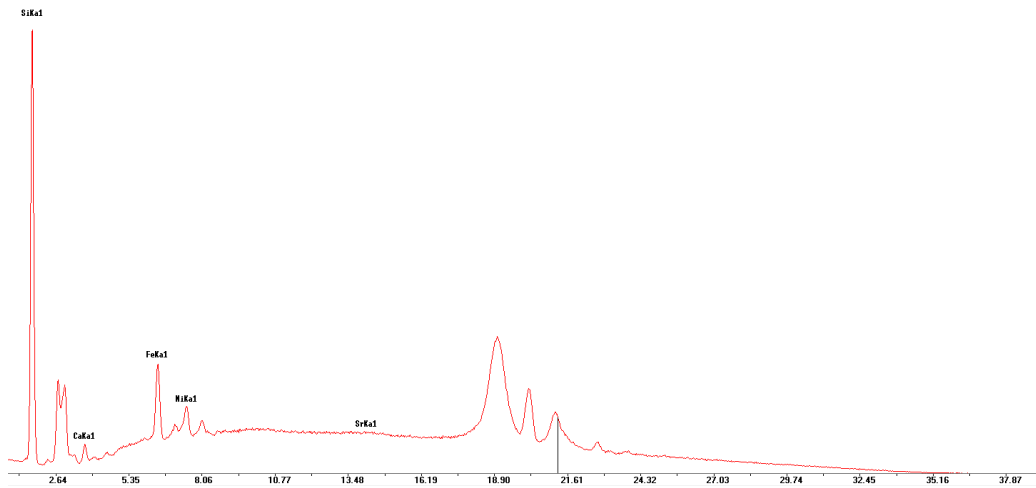


Figure 102: p-XRF spectrum of sample KRD15/L71/S1/TRIA from Kordin.

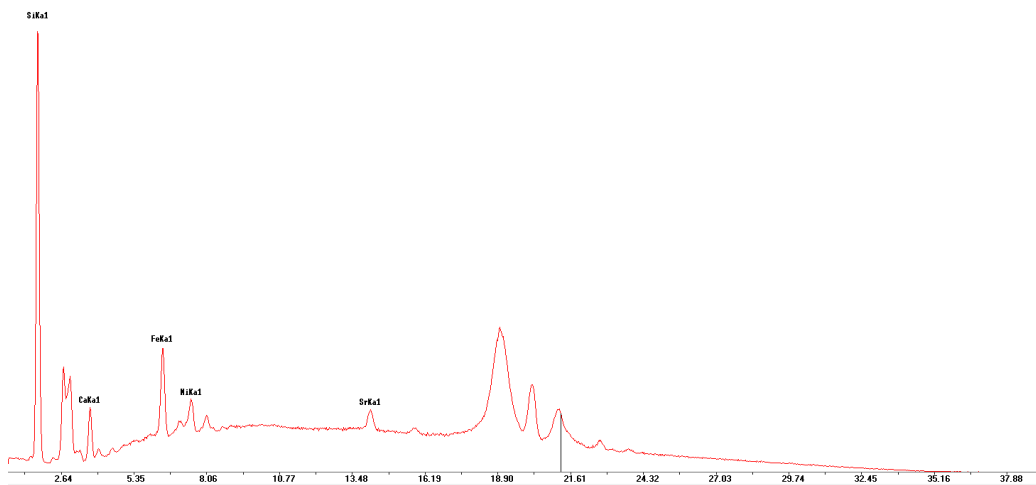


Figure 103: p-XRF spectrum of sample KRD15/L201/S9 from Kordin.

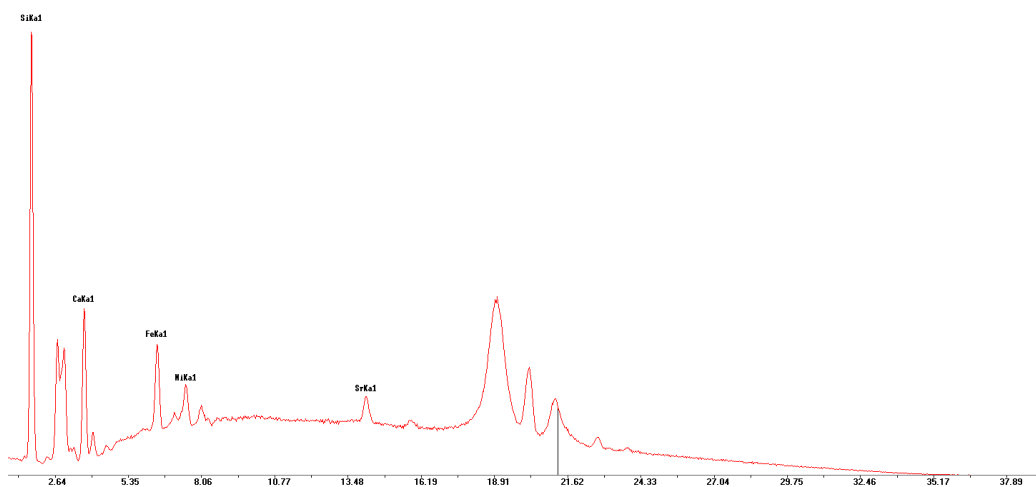


Figure 104: p-XRF spectrum of sample KRD15/S27/L203 from Kordin.

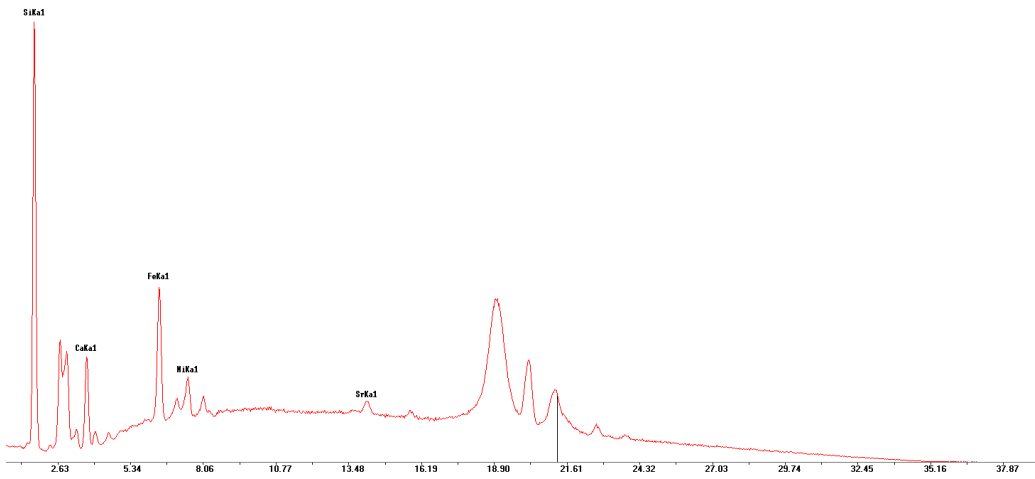


Figure 105: p-XRF spectrum of sample KRD15/S27/L207 from Kordin.

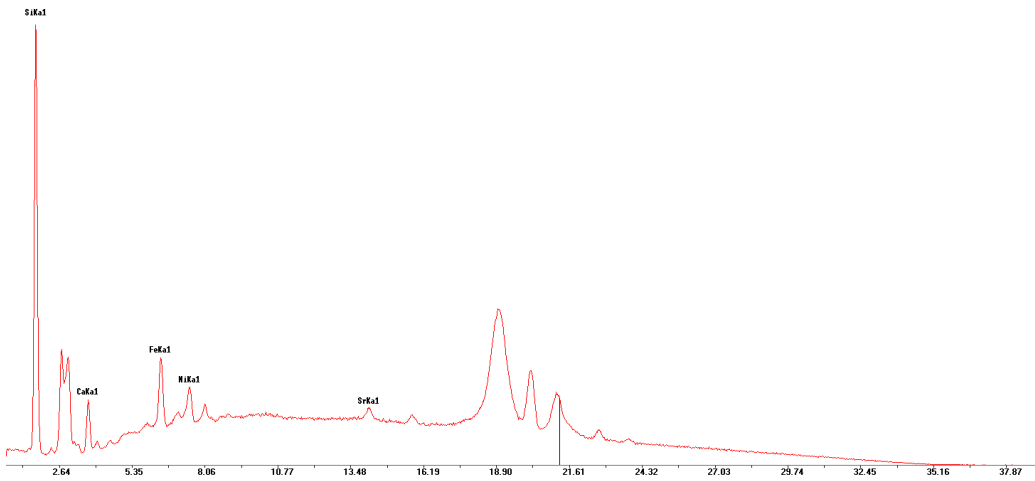


Figure 106: p-XRF spectrum of sample KRD15/S34/L207 from Kordin.

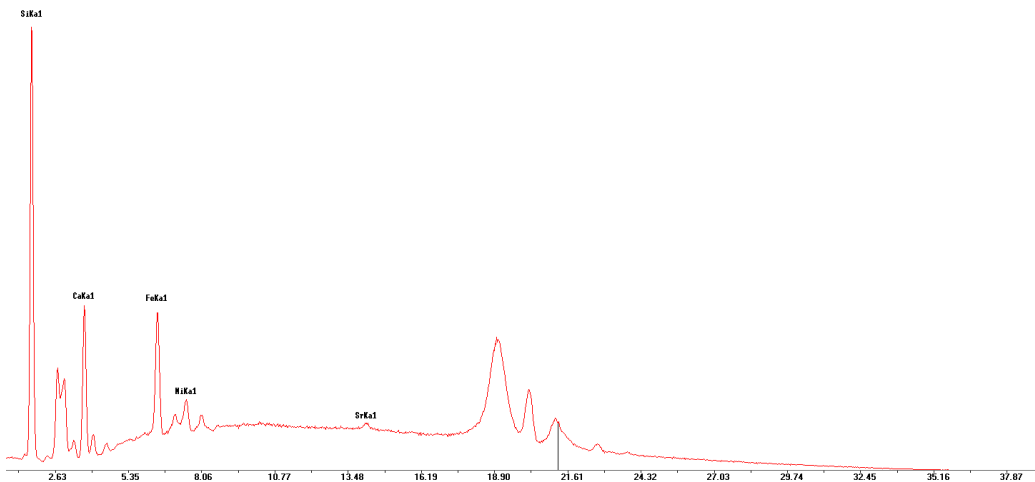


Figure 107: p-XRF spectrum of sample KRD15/S42/L304 from Kordin.

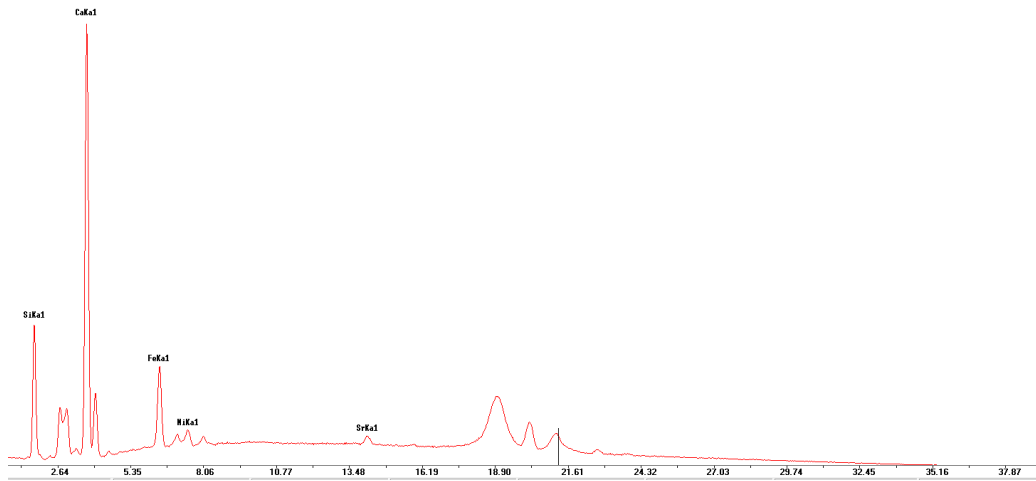


Figure 108: p-XRF spectrum of sample KRD15/S69/L211 from Kordin.

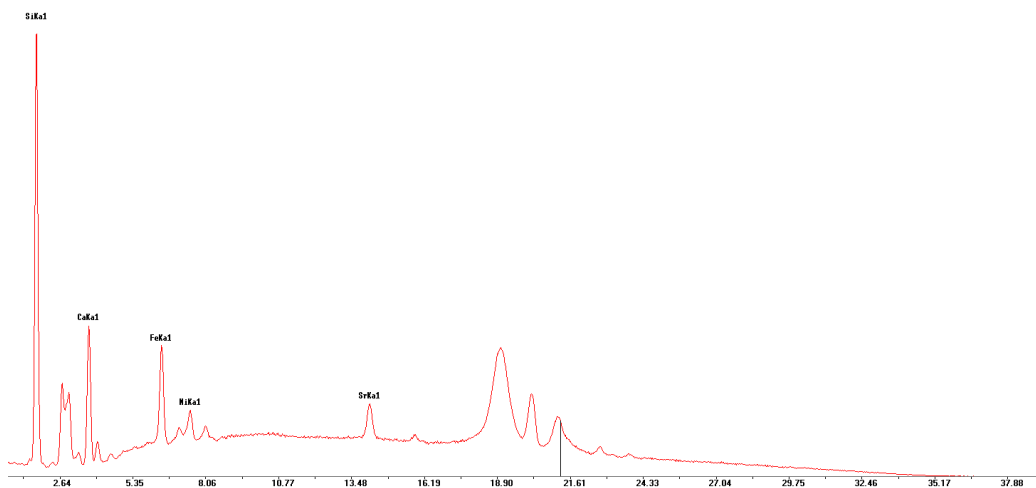


Figure 109: p-XRF spectrum of sample KRD15/S98/L201 from Kordin.

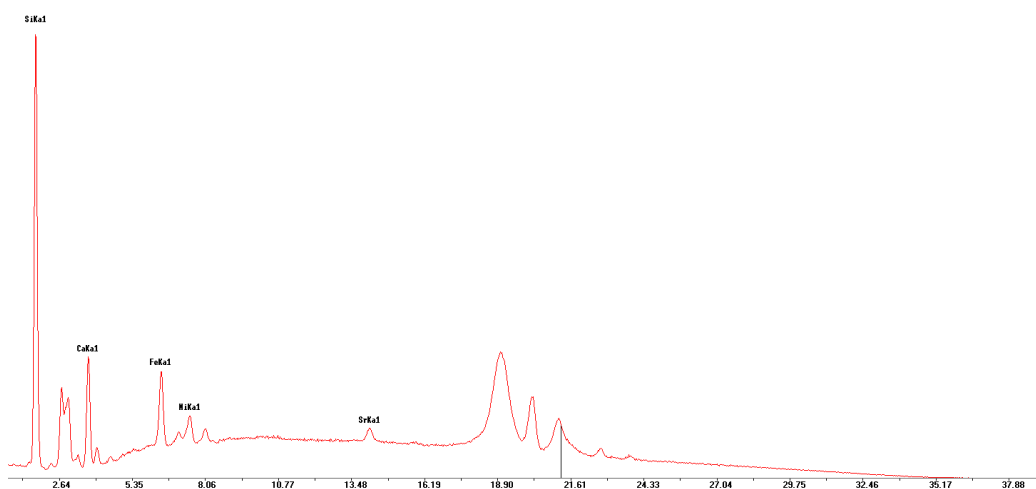


Figure 110: p-XRF spectrum of sample KRD15/S133/L211 from Kordin.

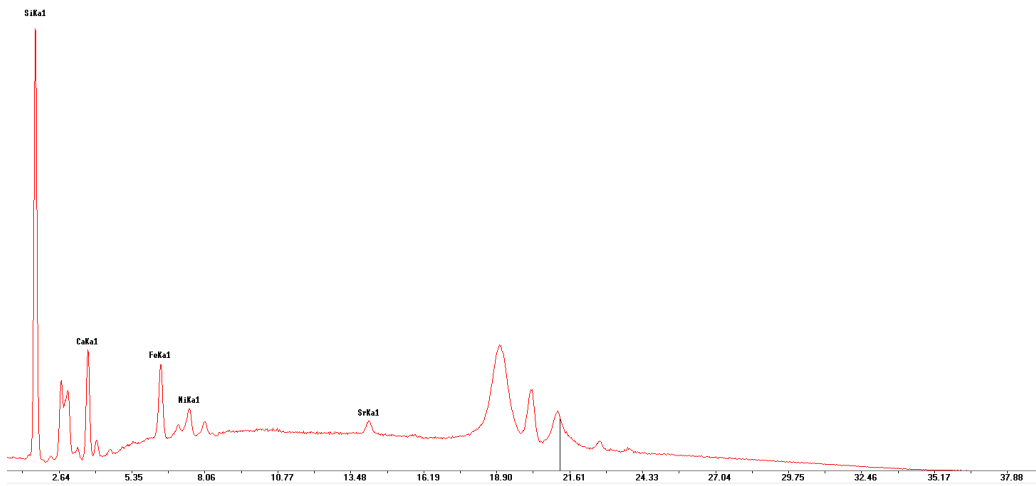


Figure 111: p-XRF spectrum of sample KRD15/S141/L150 from Kordin.

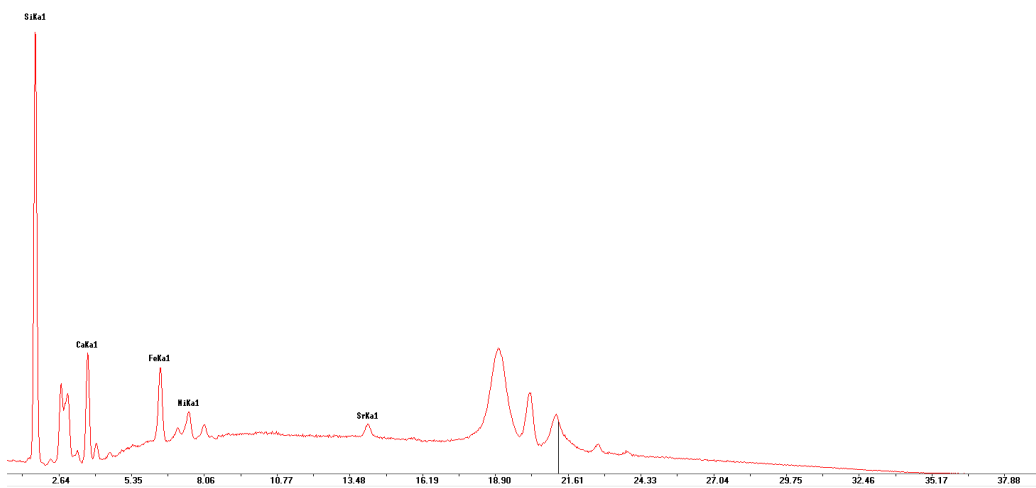


Figure 112: p-XRF spectrum of sample KRD15/S144/L306 from Kordin.

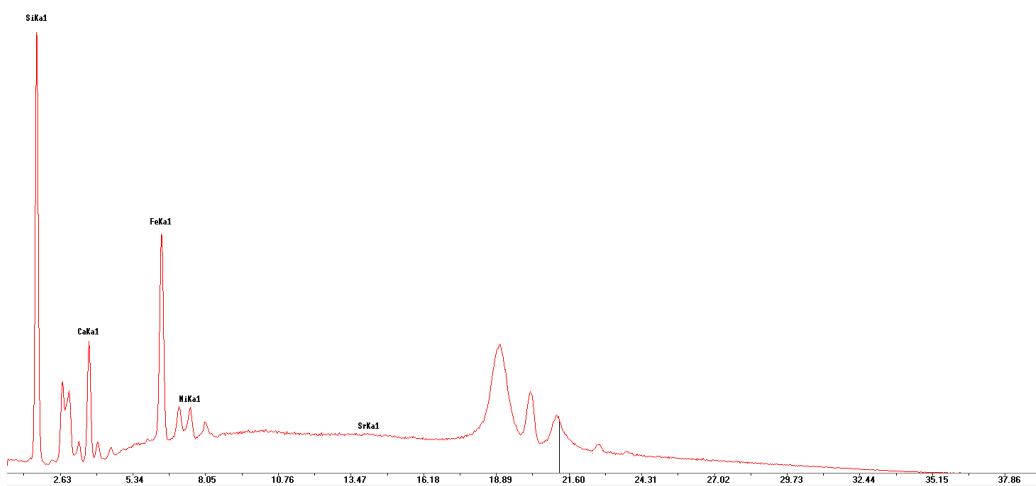


Figure 113: p-XRF spectrum of sample KRD15/S156/L306 from Kordin.

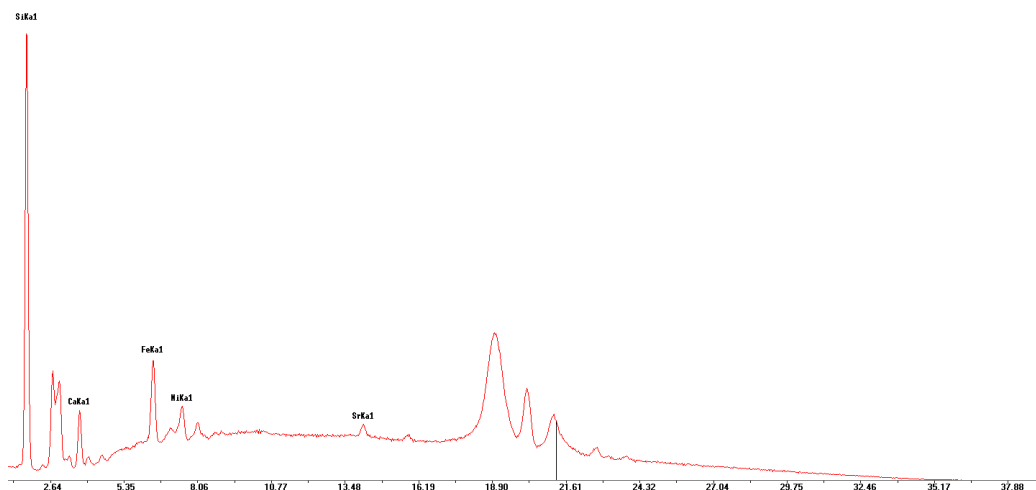


Figure 114: p-XRF spectrum of sample KRD15/ S195/L209 from Kordin.

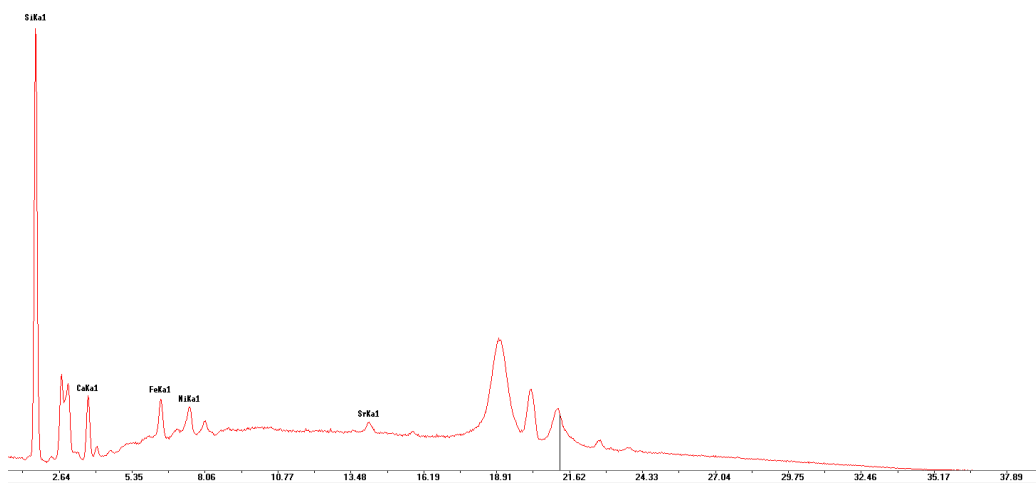


Figure 115: p-XRF spectrum of sample KRD15/ S131/L211 from Kordin.

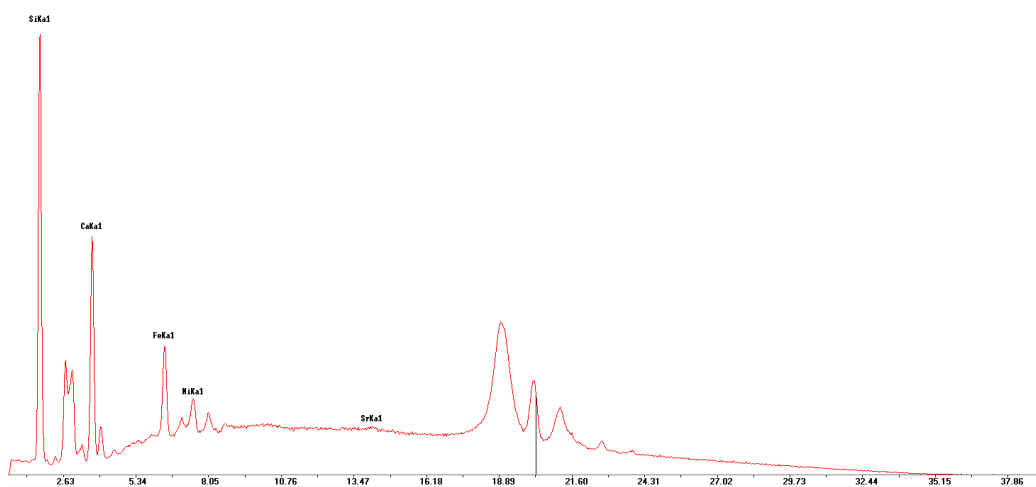


Figure 116: p-XRF spectrum of sample TCC14/S595/L811 from Tać-Ćawla.

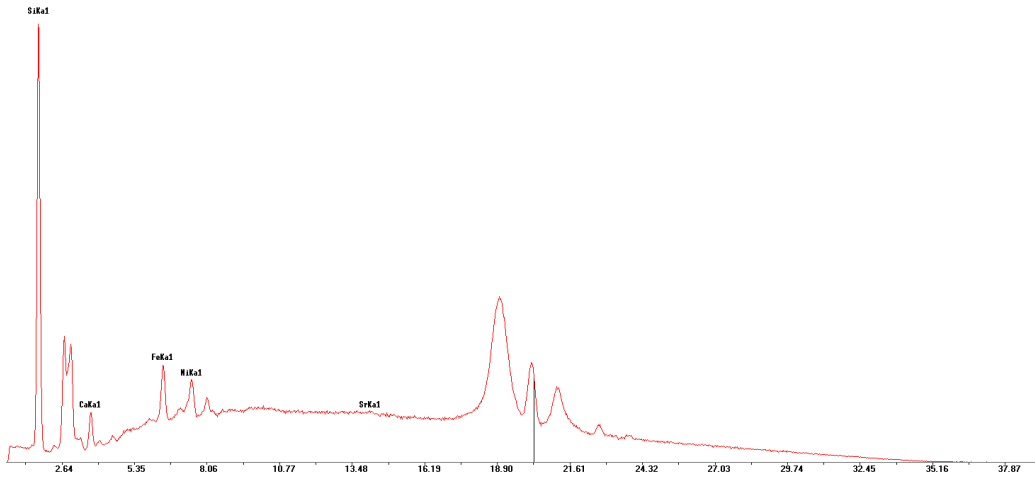


Figure 117: p-XRF spectrum of sample TCC14/S577/L131 from Tač-Ćawla.

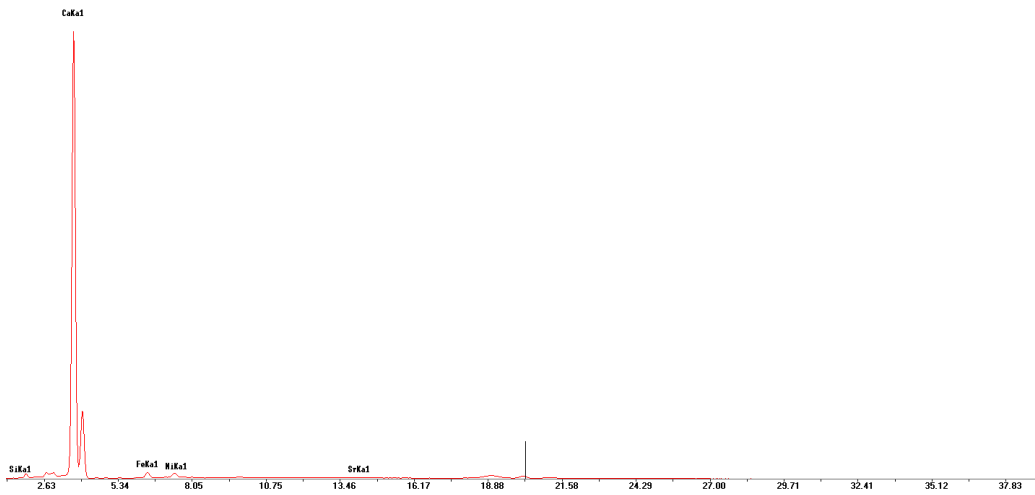


Figure 118: p-XRF spectrum of sample TCC14/S567/L206 from Tač-Ćawla.

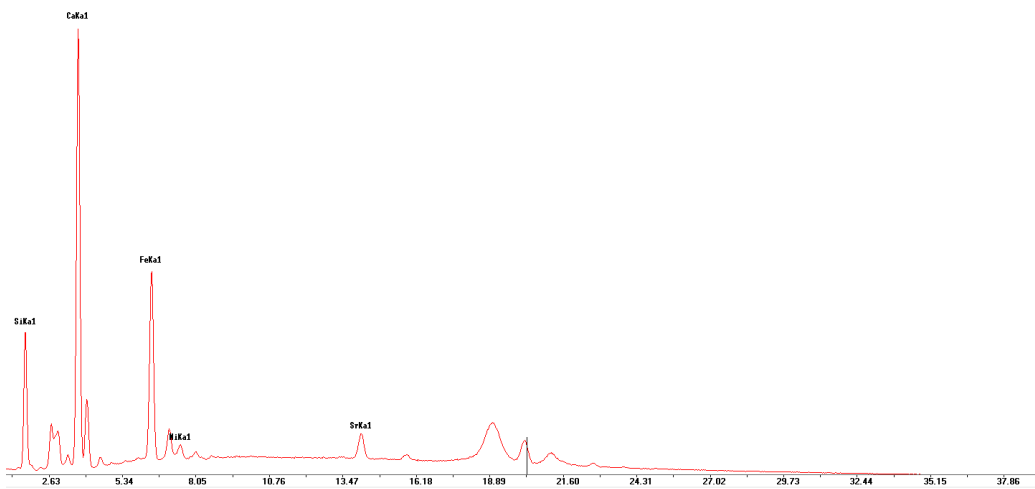


Figure 119: p-XRF spectrum of sample TCC14/S513/L272 from Tač-Ćawla.

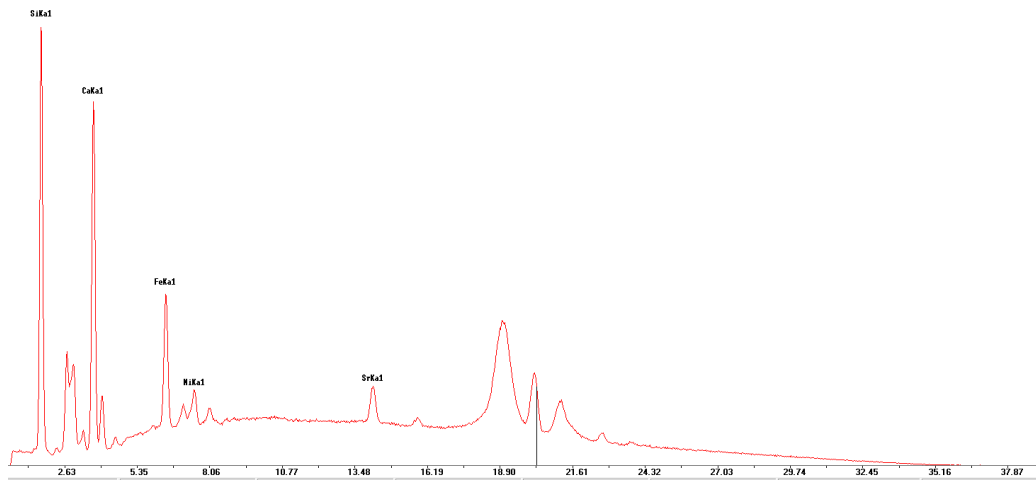


Figure 120: p-XRF spectrum of sample TCC14/S502/L301 from Tač-Čawla.

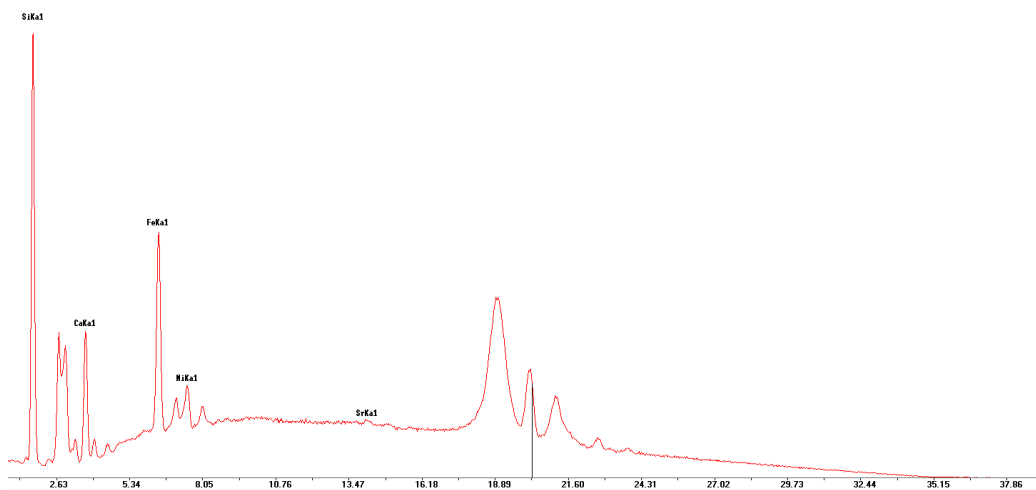


Figure 121: p-XRF spectrum of sample TCC14/S460/L273 from Tač-Čawla.

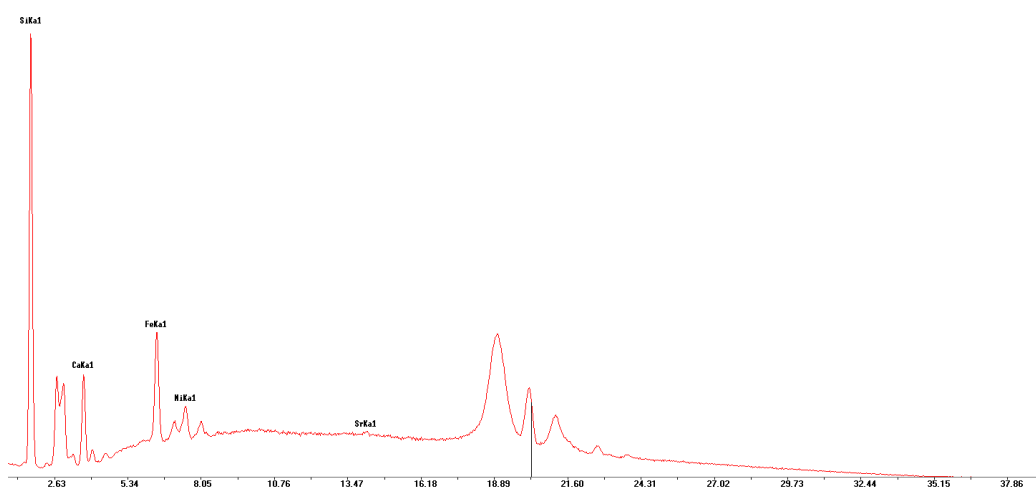


Figure 122: p-XRF spectrum of sample TCC14/S416/L178 from Tač-Čawla.

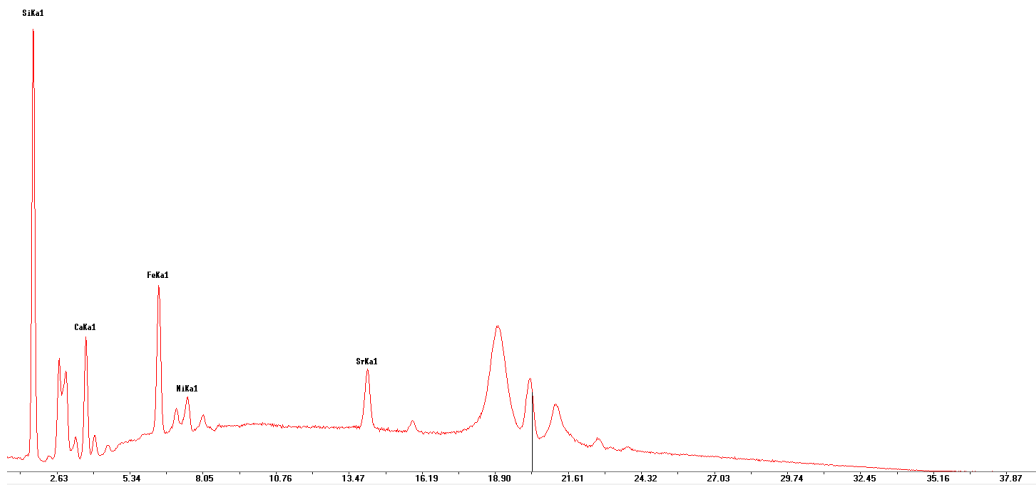


Figure 123: p-XRF spectrum of sample TCC14/S316B/L63 from Tač-Ćawla.

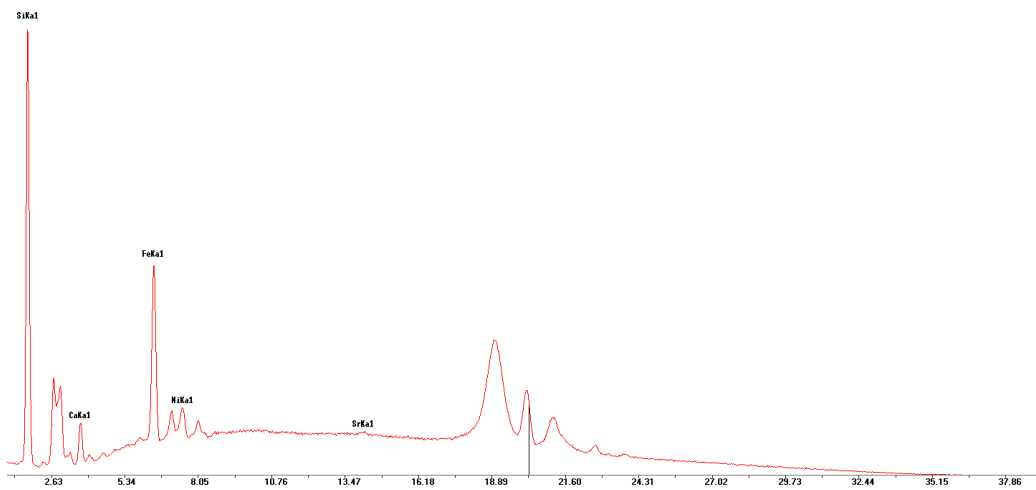


Figure 124: p-XRF spectrum of sample TCC14/S275/L208 from Tač-Ćawla.

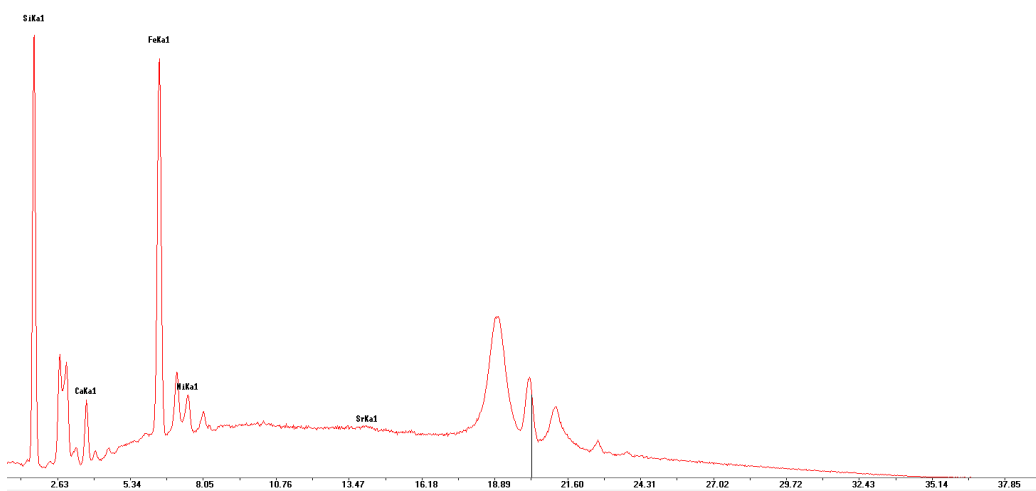


Figure 125: p-XRF spectrum of sample TCC14/S252/L179 from Tač-Ćawla.

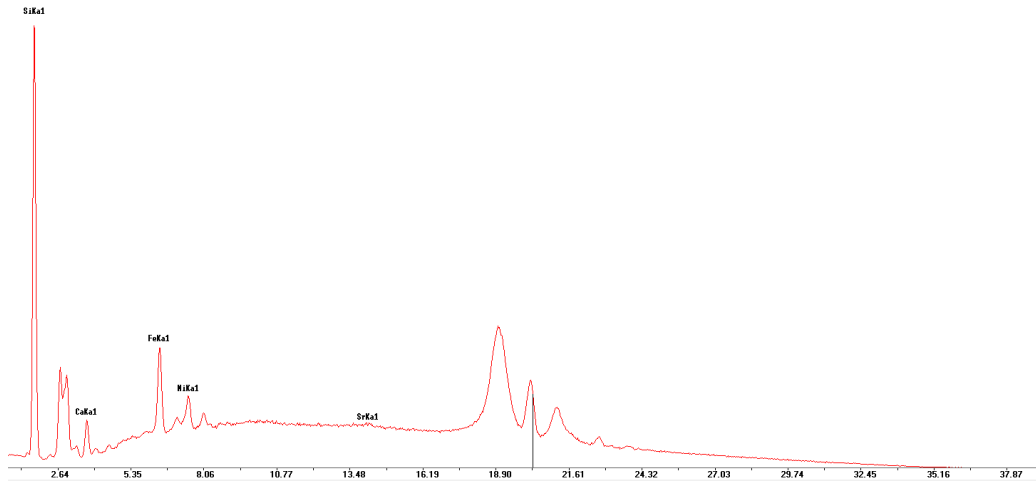


Figure 126: p-XRF spectrum of sample TCC14/S193/L69 from Tač-Čawla.

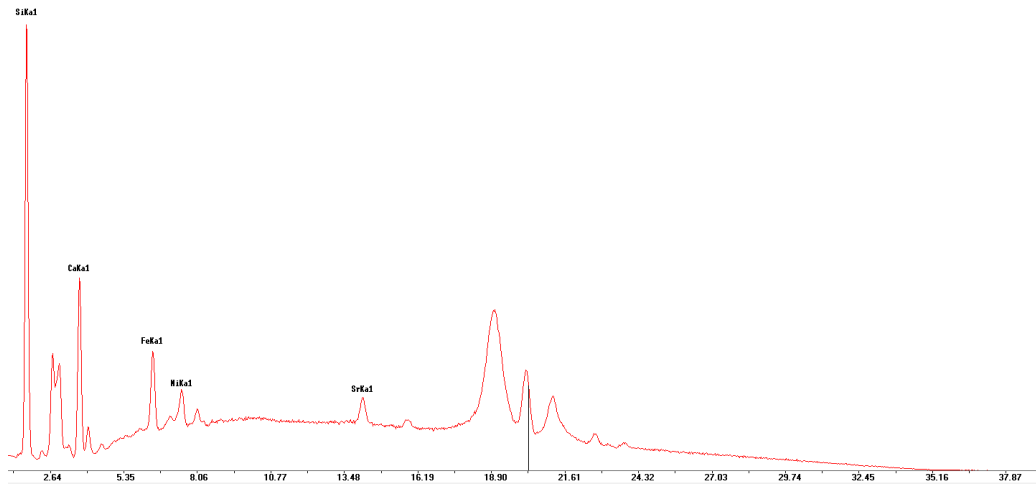


Figure 127: p-XRF spectrum of sample TCC14/S176/L100 from Tač-Čawla.

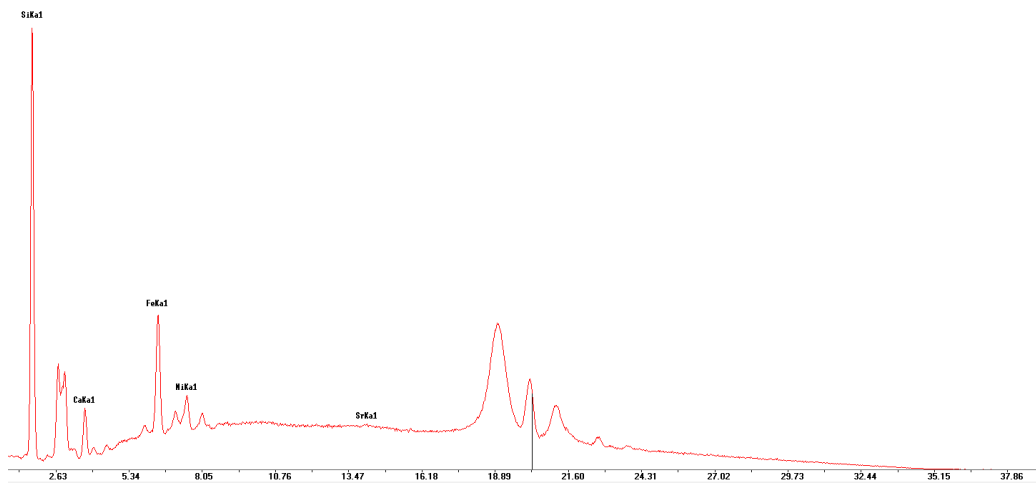


Figure 128: p-XRF spectrum of sample TCC14/S162/L155 from Tač-Čawla.

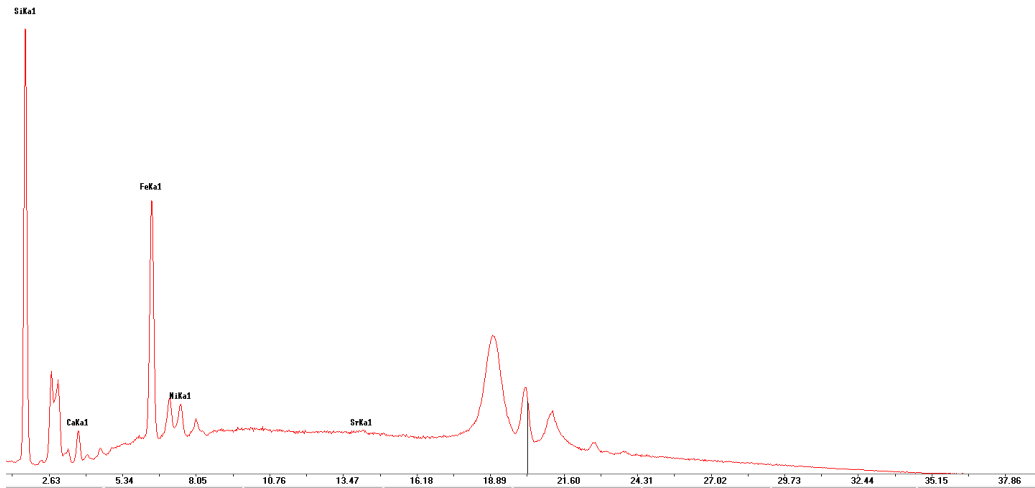


Figure 129: p-XRF spectrum of sample TCC14/S144 from Tač-Ćawla.

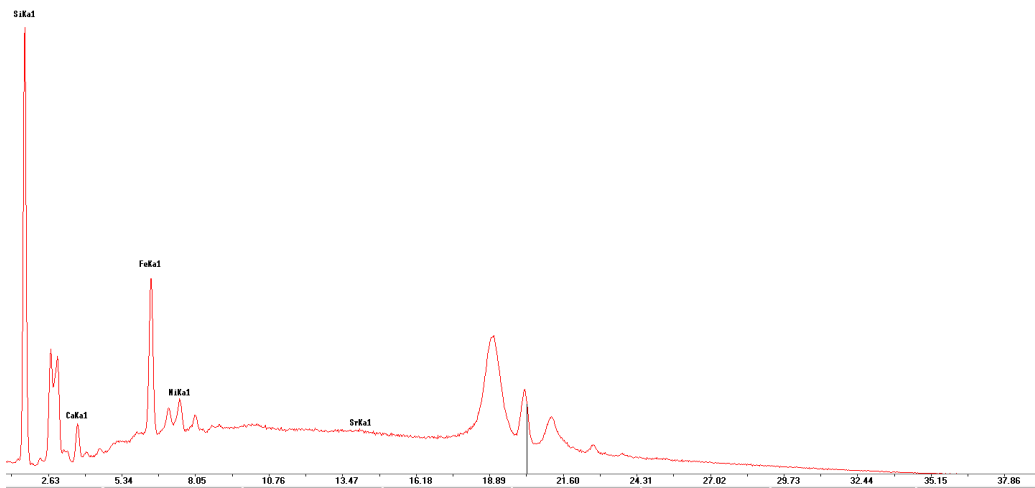


Figure 130: p-XRF spectrum of sample TCC14/S103/L85 from Tač-Ćawla.

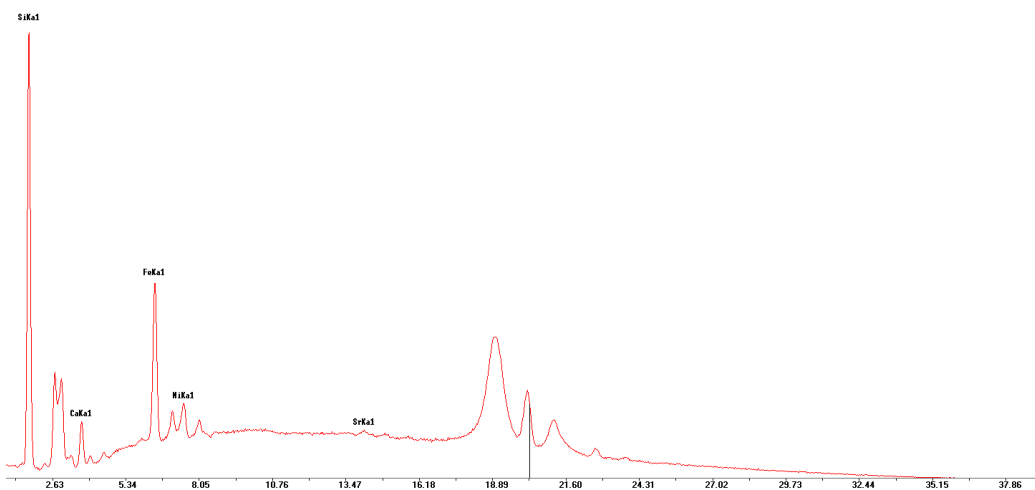


Figure 131: p-XRF spectrum of sample TCC14/S101/L85 from Tač-Ćawla.

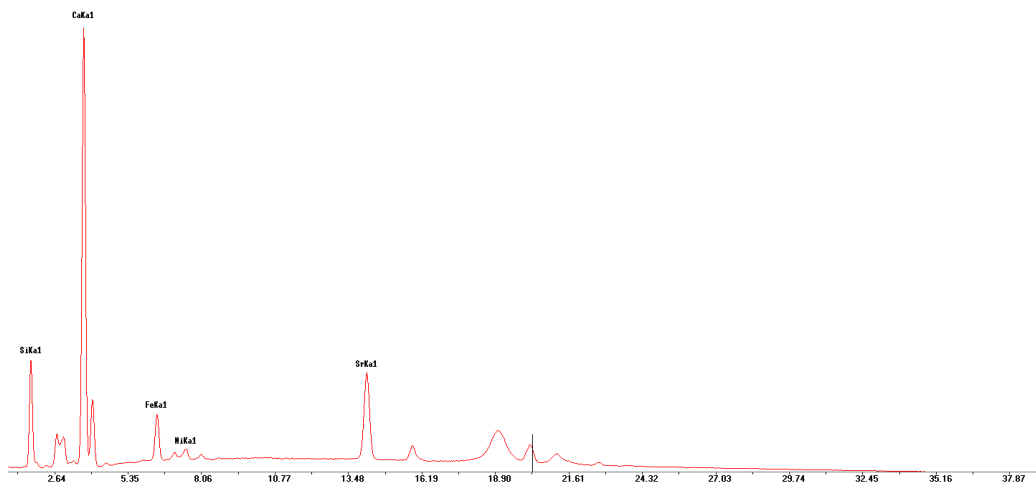


Figure 132: p-XRF spectrum of sample TCC14/S37/L30 from Tač-Ćawla.

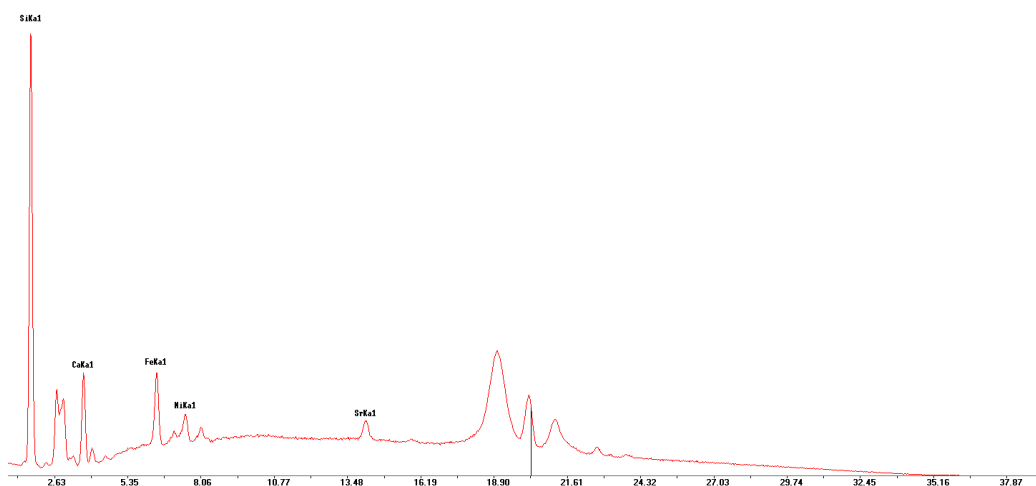


Figure 133: p-XRF spectrum of sample TCC14/S32B/L30 from Tač-Ćawla.

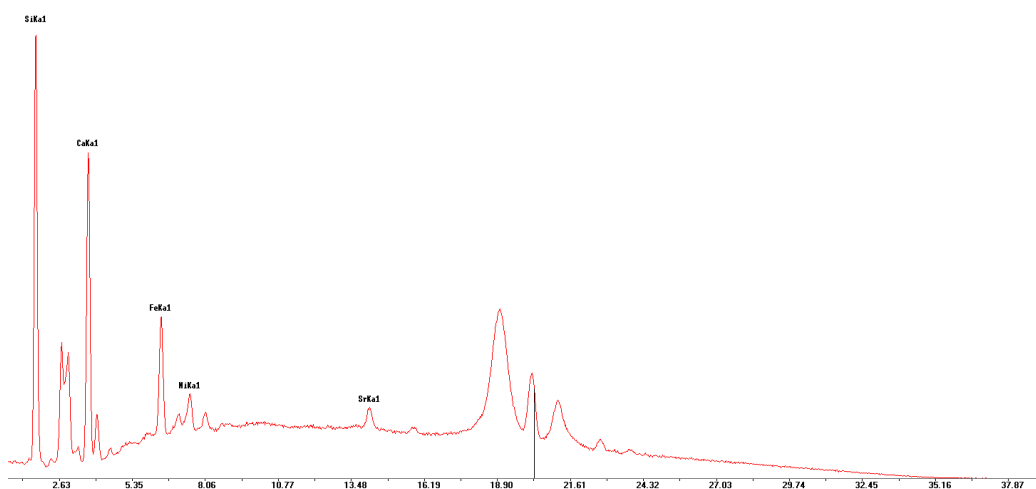


Figure 134: p-XRF spectrum of sample TCC14/S32A/2 from Tač-Ćawla.

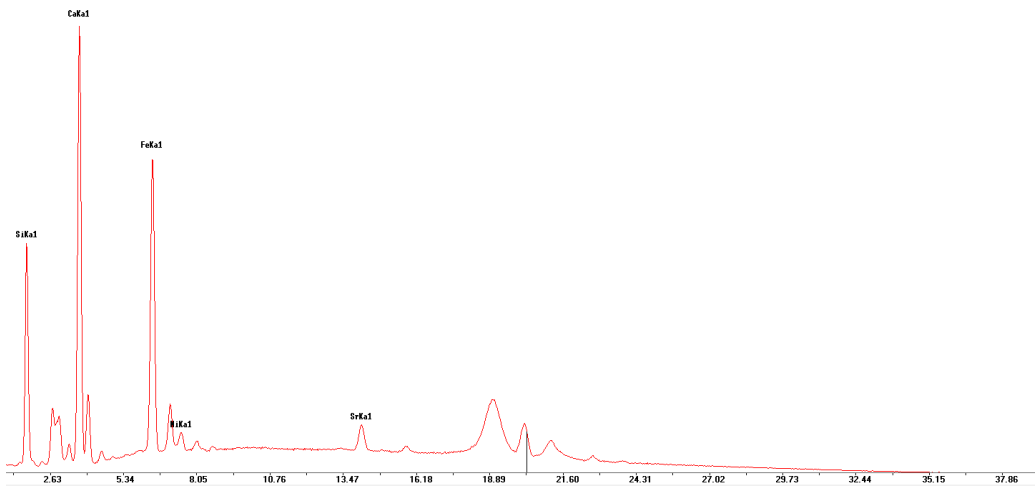


Figure 135: p-XRF spectrum of sample SV15/S144/L42 from Santa Verna.

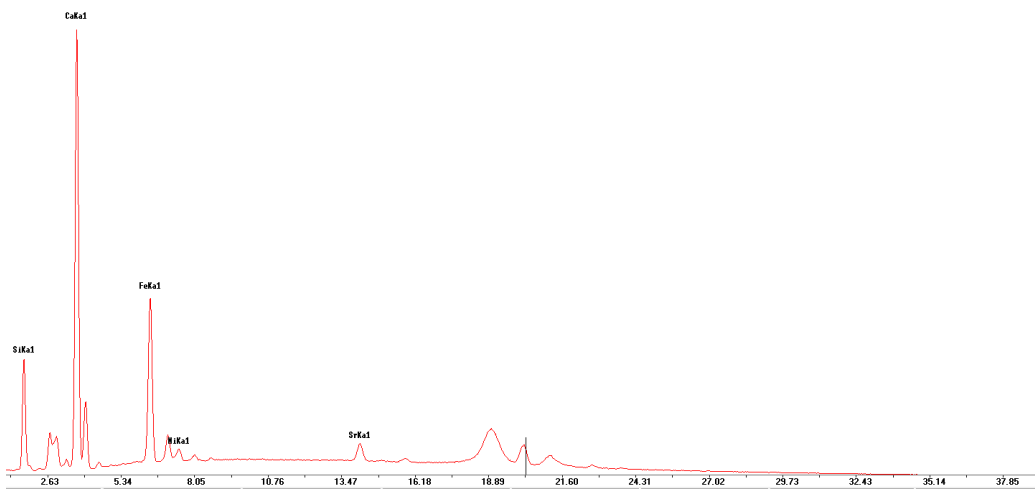


Figure 136: p-XRF spectrum of sample SV15/S134/L58 from Santa Verna.

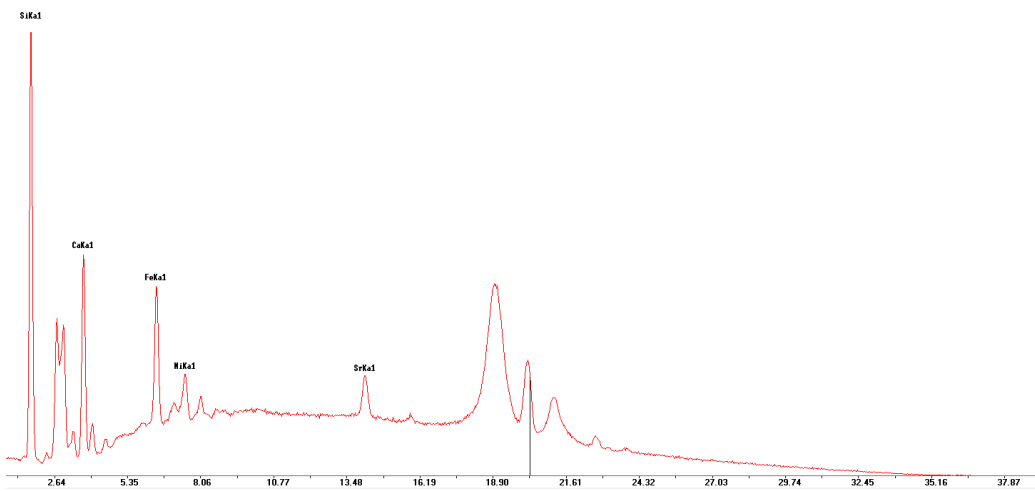


Figure 137: p-XRF spectrum of sample SV15/S67/L34 from Santa Verna.

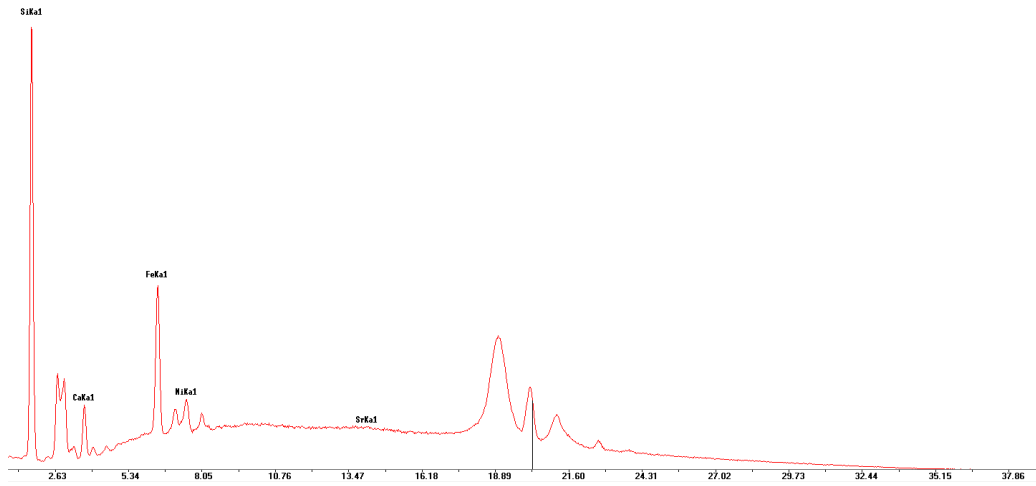


Figure 138: p-XRF spectrum of sample SV15/S38/L8 from Santa Verna.

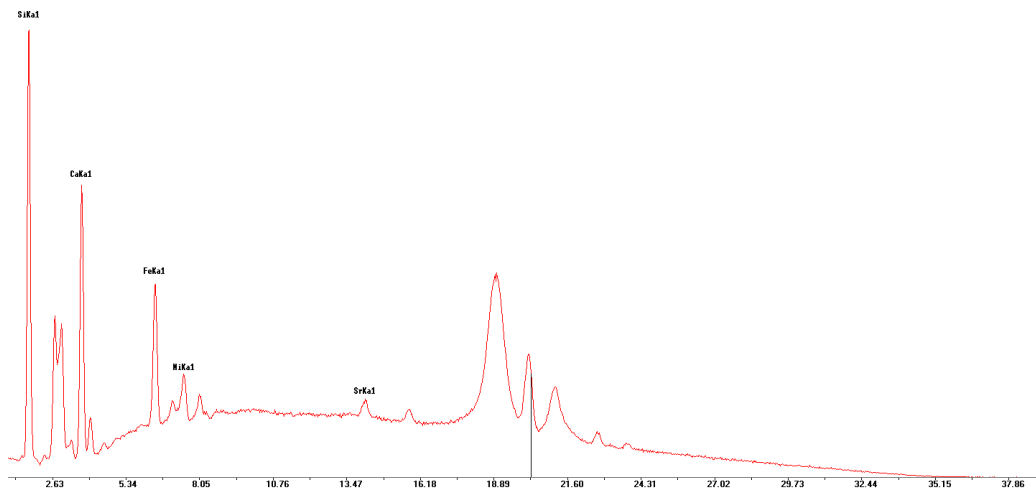


Figure 139: p-XRF spectrum of sample SV15/S32/L5 from Santa Verna.

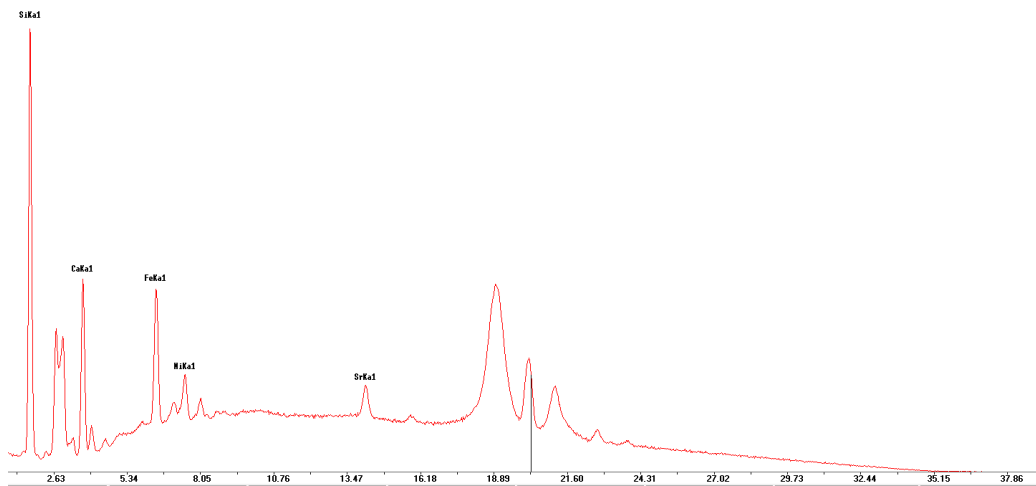


Figure 140: p-XRF spectrum of sample SV15/S1/L98 from Santa Verna.

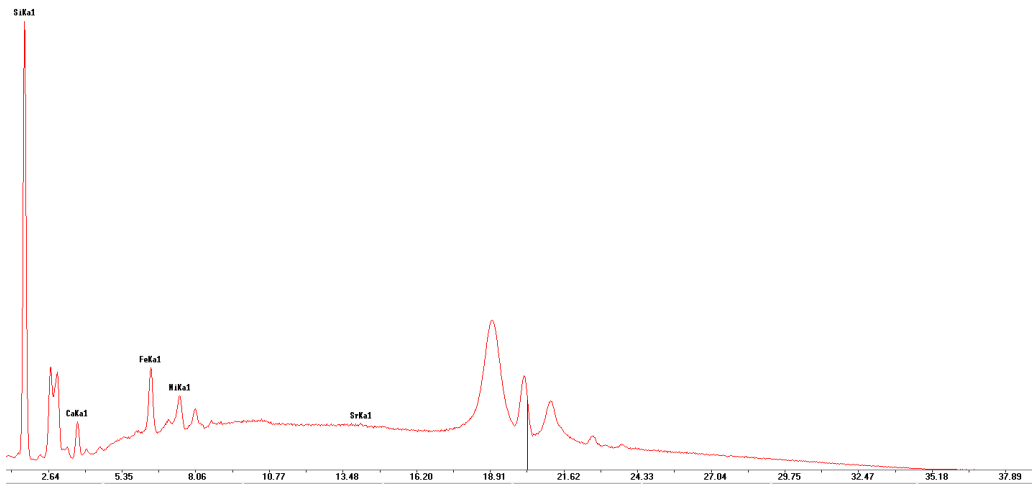


Figure 141: p-XRF spectrum of sample SV15/S1/L80 from Santa Verna.

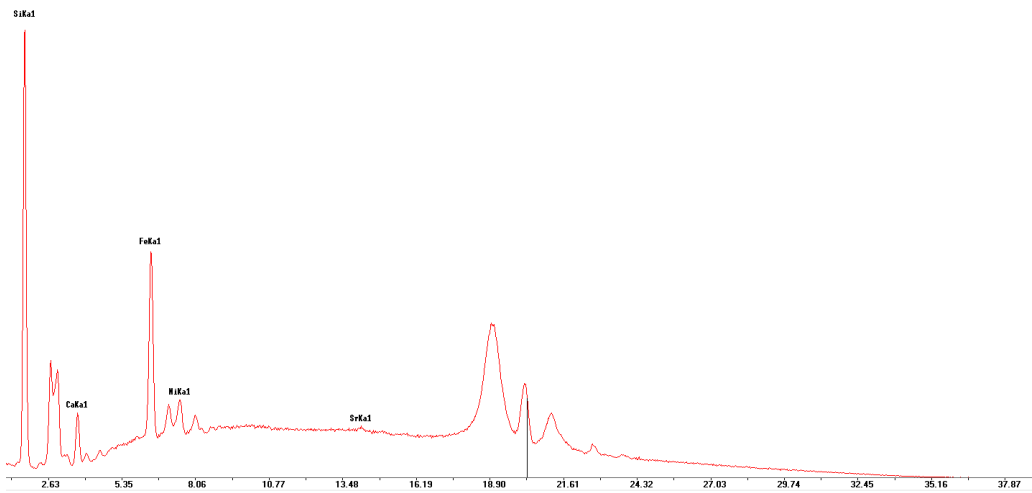


Figure 142: p-XRF spectrum of sample SV15/S1/L68 from Santa Verna.

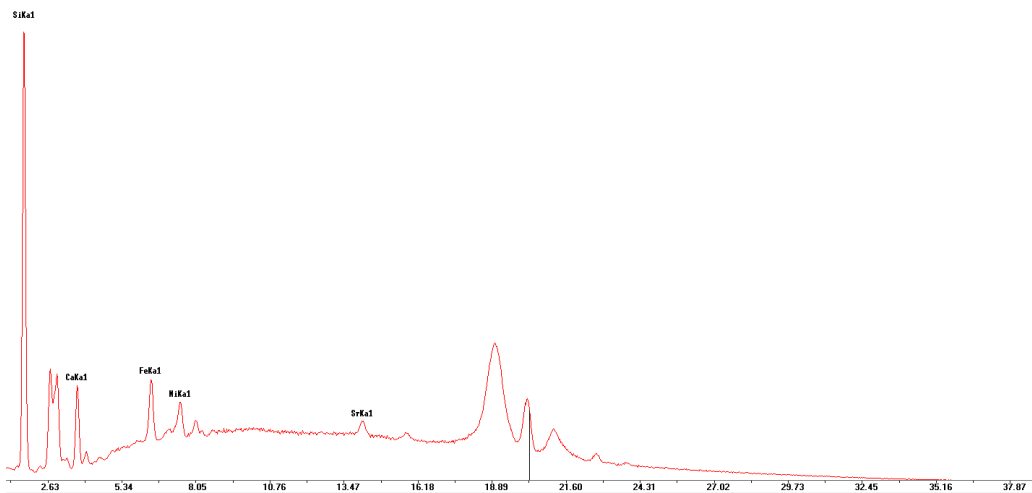


Figure 143: p-XRF spectrum of sample SV15/S1/L61 from Santa Verna.

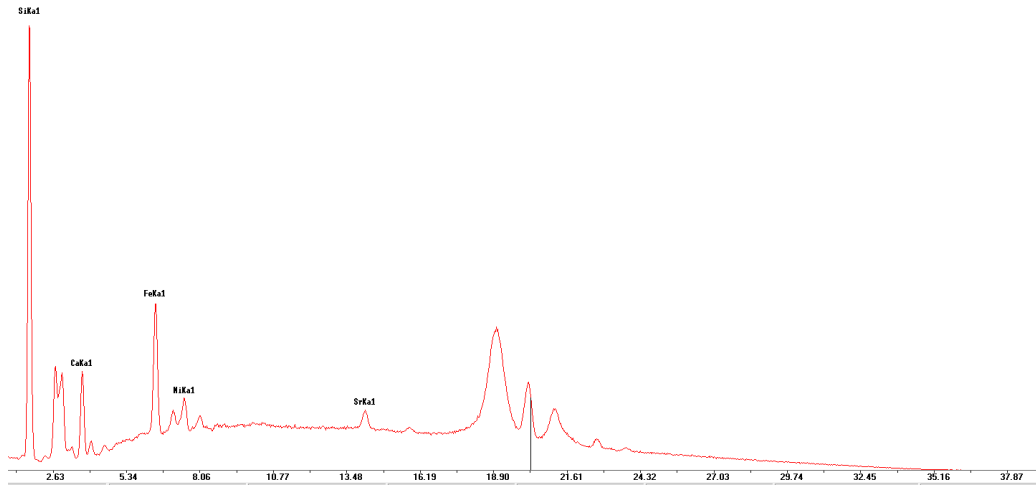


Figure 144: p-XRF spectrum of sample SV15/S1/L52 from Santa Verna.

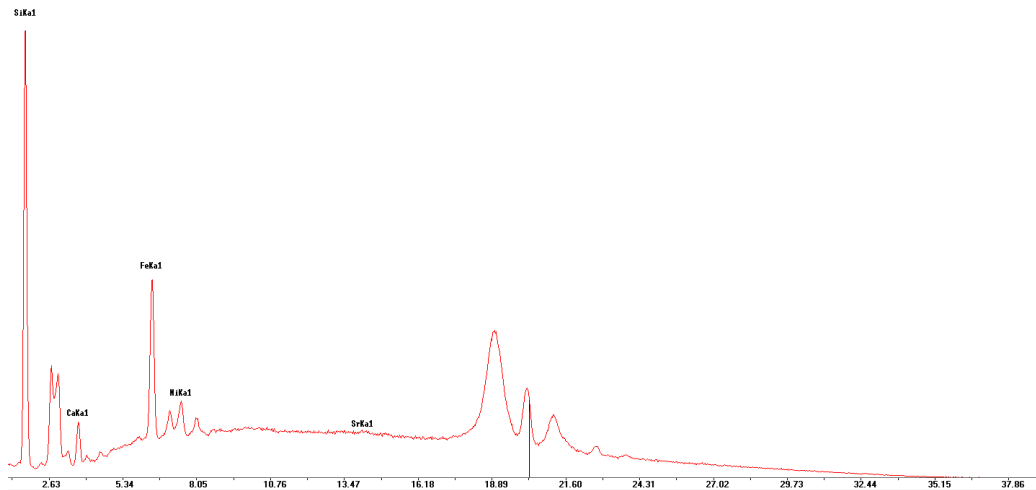


Figure 145: p-XRF spectrum of sample SV15/S3/L41 from Santa Verna.

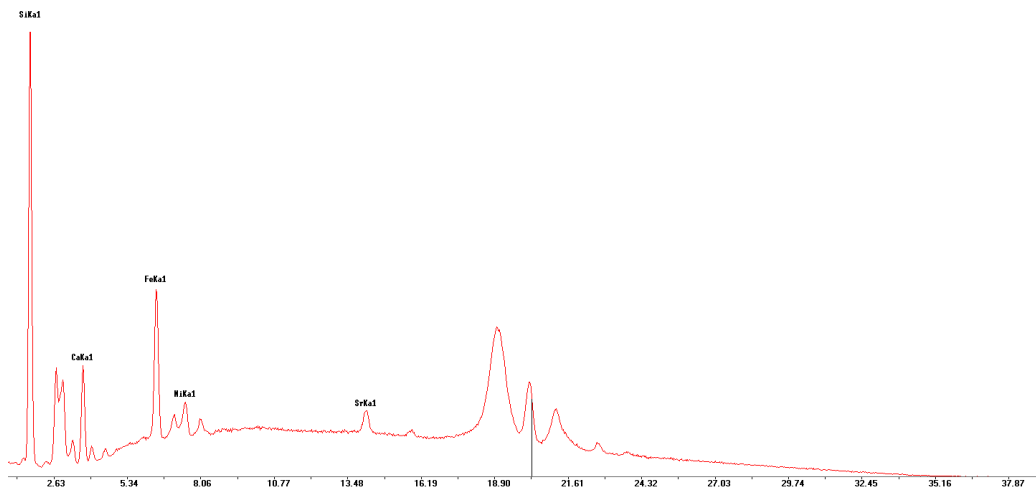


Figure 146: p-XRF spectrum of sample SV15/S2/L41 from Santa Verna.

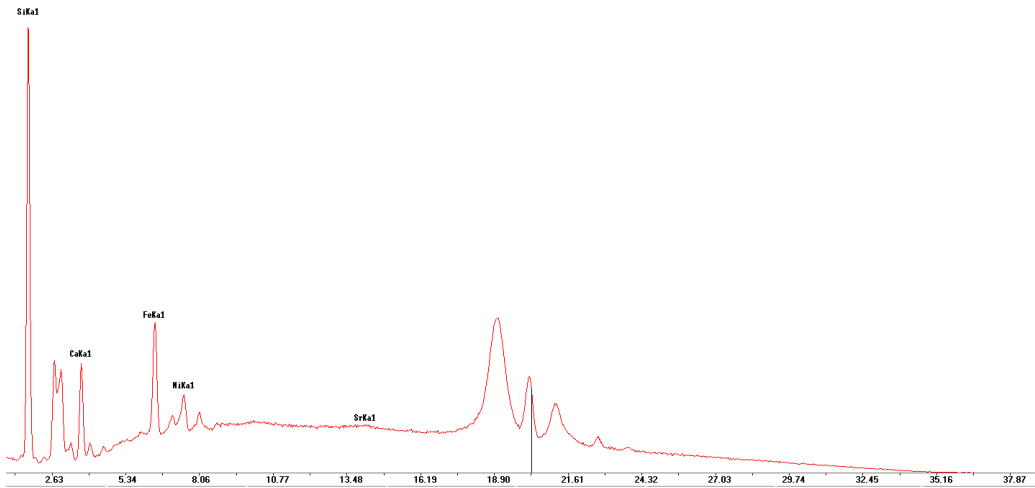


Figure 147: p-XRF spectrum of sample SV15/S1/L41 from Santa Verna.

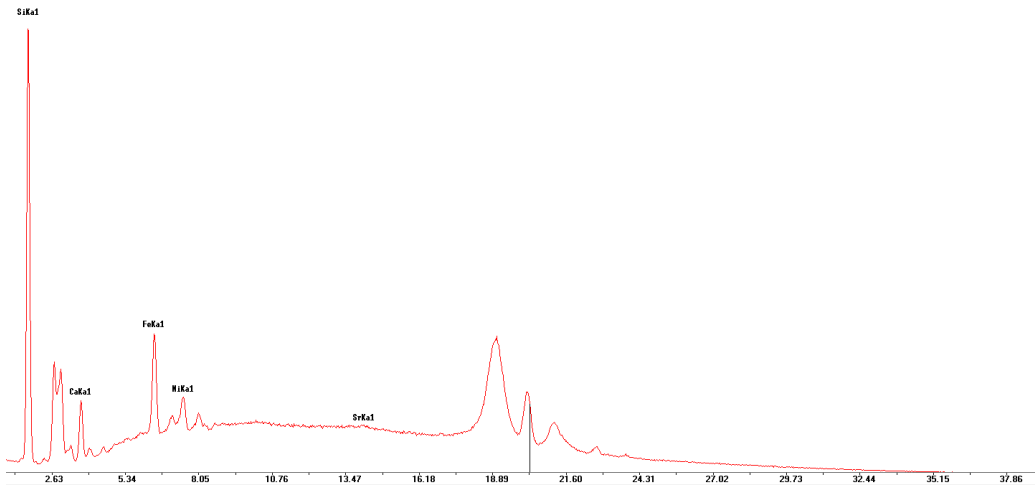


Figure 148: p-XRF spectrum of sample SV15/S1/L36 from Santa Verna.

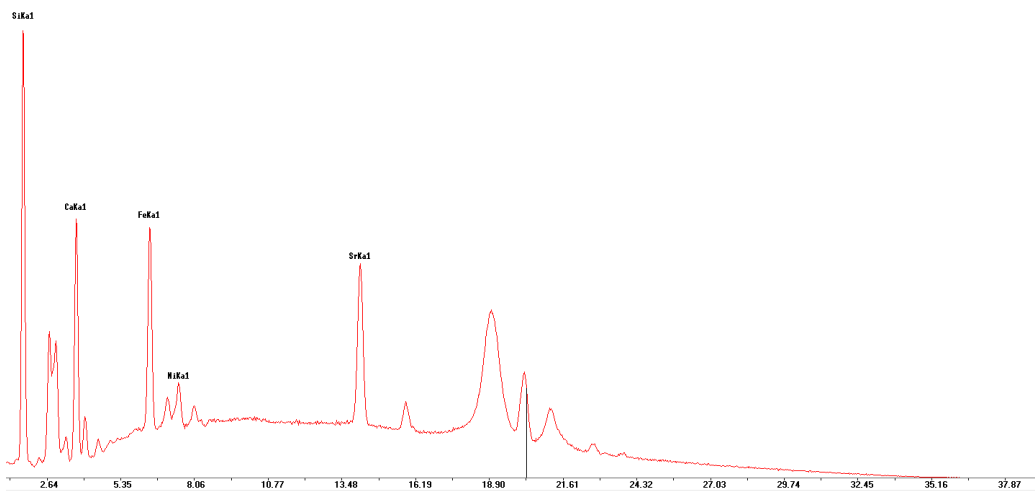


Figure 149: p-XRF spectrum of sample SV15/S1/L34 from Santa Verna.

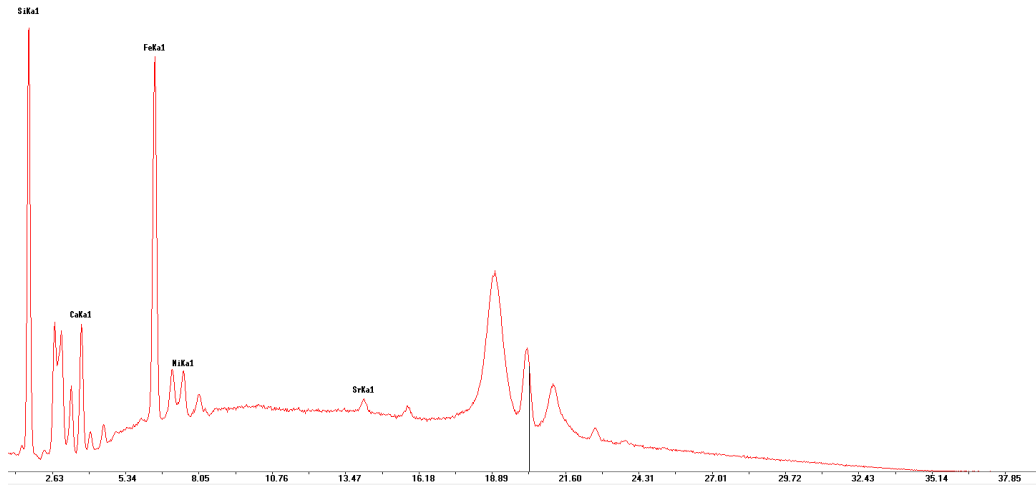


Figure 150: p-XRF spectrum of sample SV15/S1/L33 from Santa Verna.

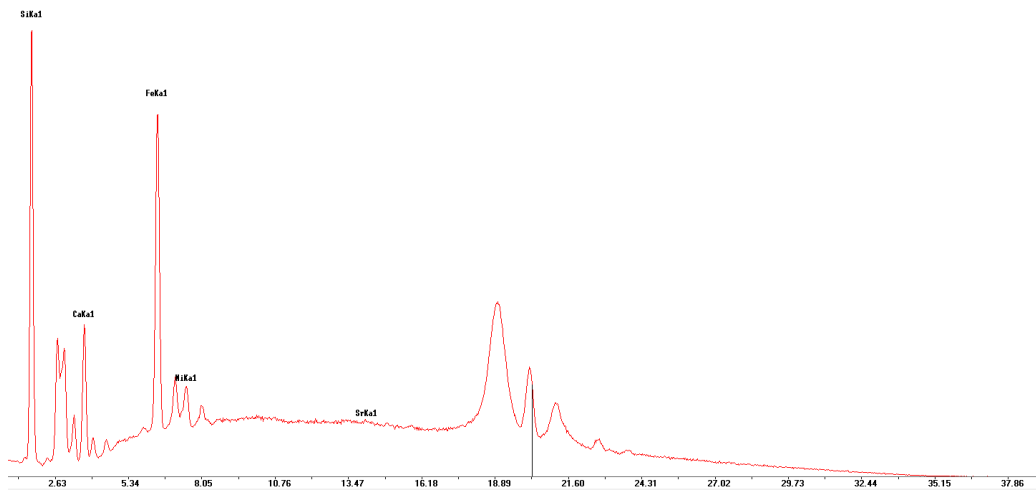


Figure 151: p-XRF spectrum of sample SV15/S2/L22 from Santa Verna.

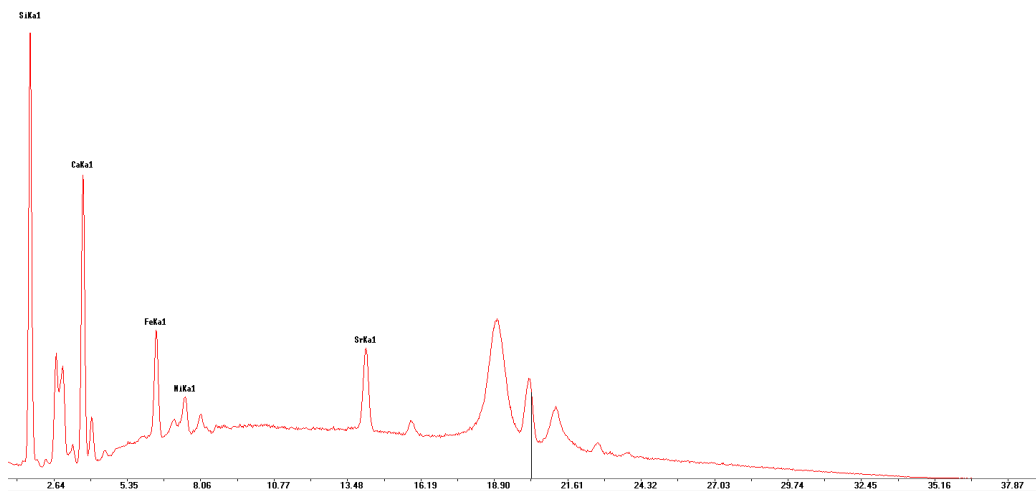


Figure 152: p-XRF spectrum of sample SV15/S1/L22 from Santa Verna.

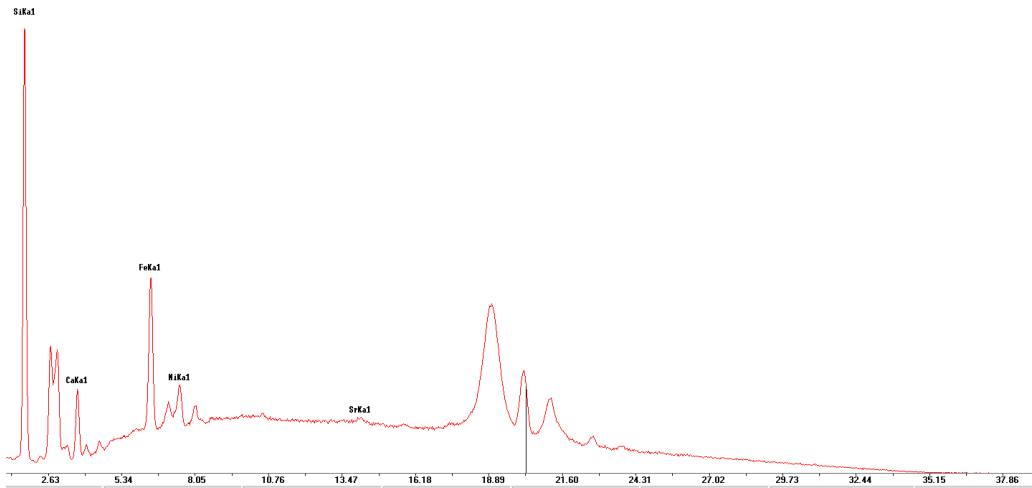


Figure 153: p-XRF spectrum of sample SV15/S1/L17 from Santa Verna.

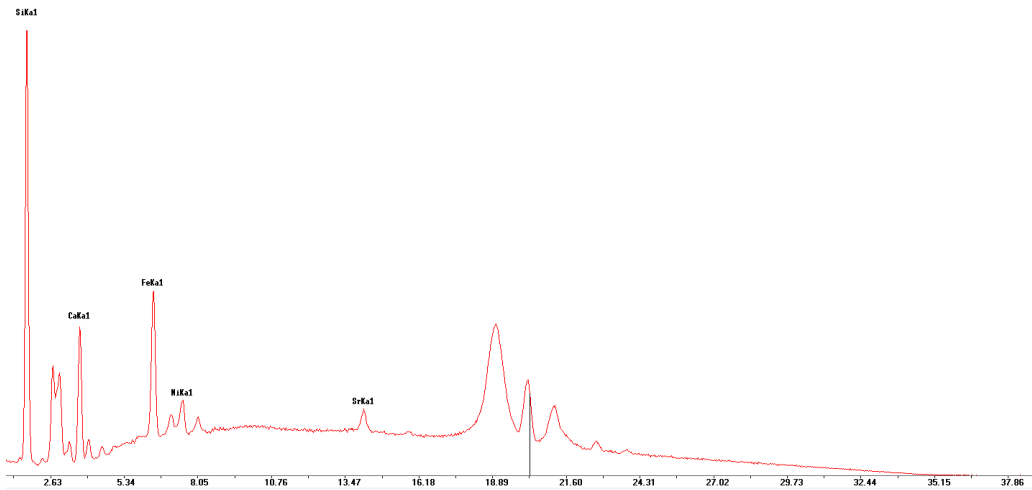


Figure 154: p-XRF spectrum of sample SV15/S1/L16 from Santa Verna.

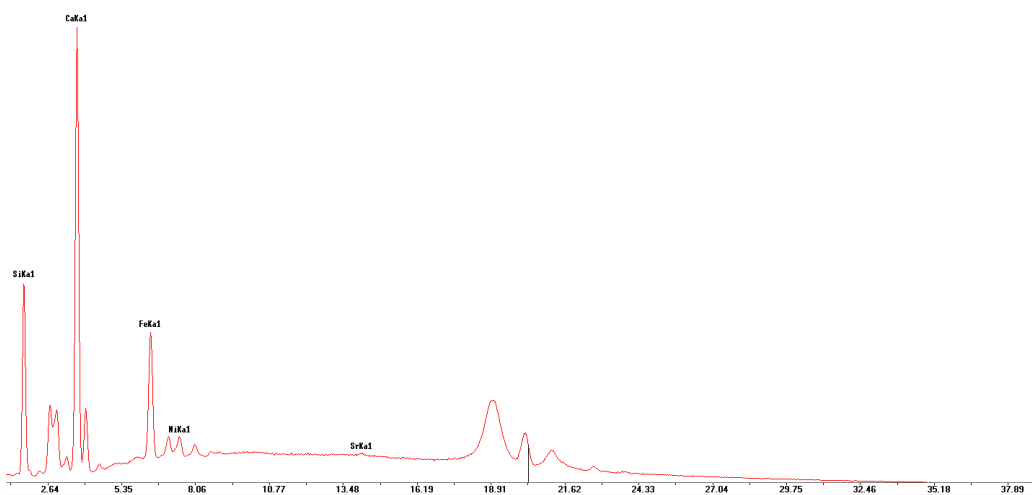


Figure 155: p-XRF spectrum of sample SV15/S1/L4 from Santa Verna.

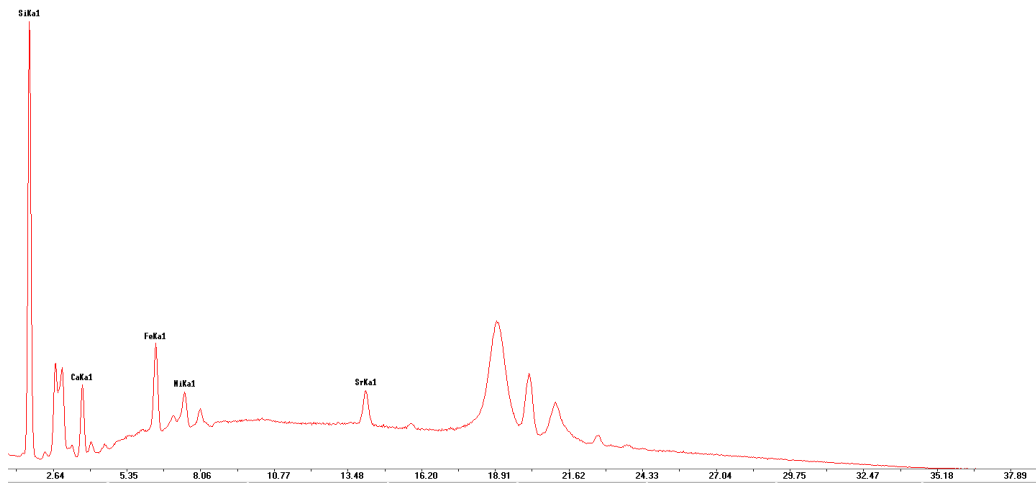


Figure 156: p-XRF spectrum of sample GG15/1004/S1 from Ġgantija.

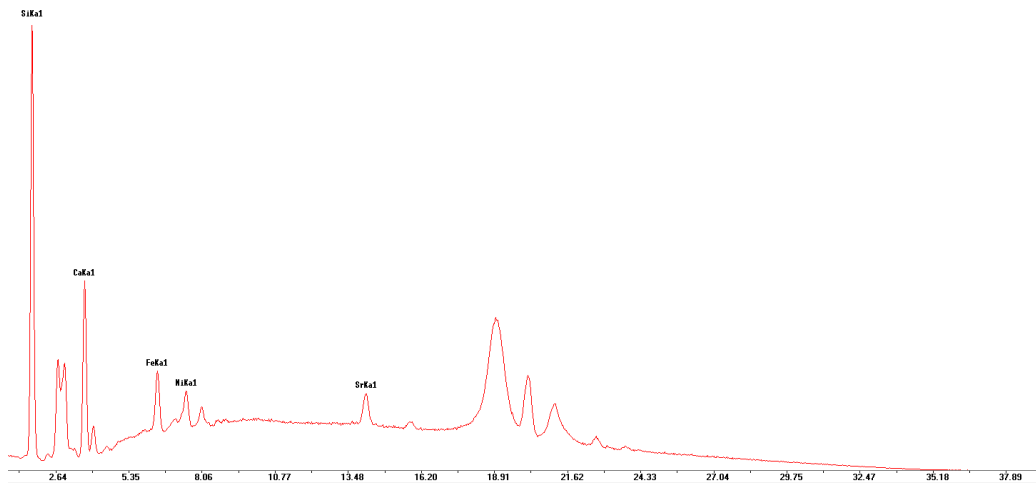


Figure 157: p-XRF spectrum of sample GG15/1004/S2 from Ġgantija.

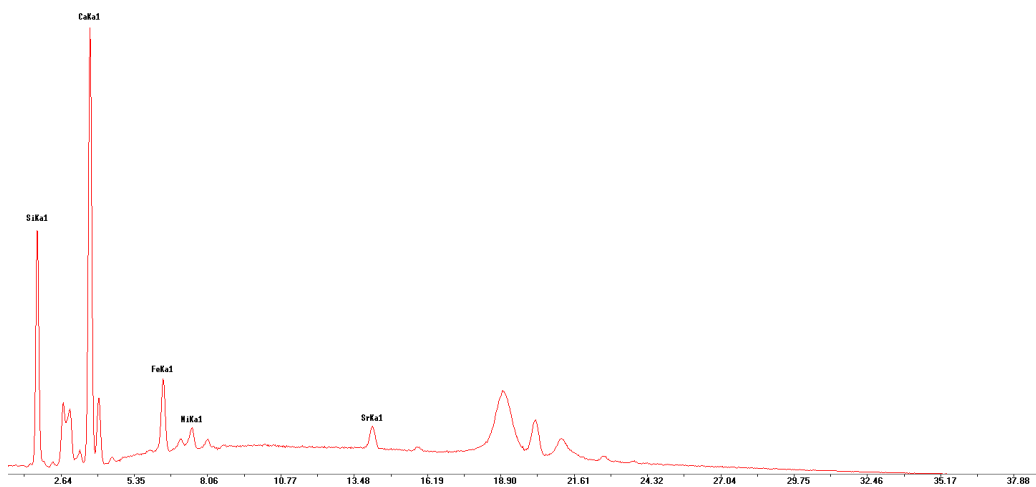


Figure 158: p-XRF spectrum of sample GGWC15/1012/S1 from Ġgantija.

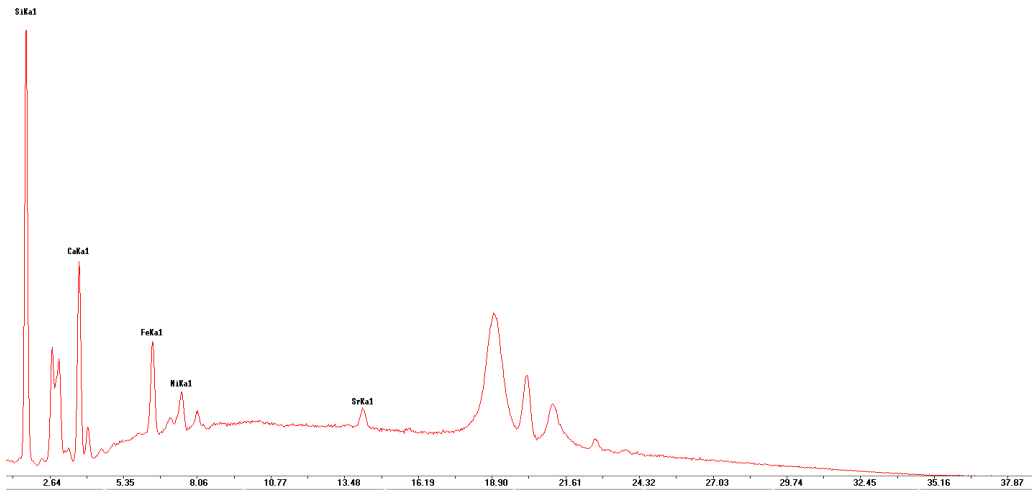


Figure 159: p-XRF spectrum of sample GGWC15/1012/S2 from Ġgantija.

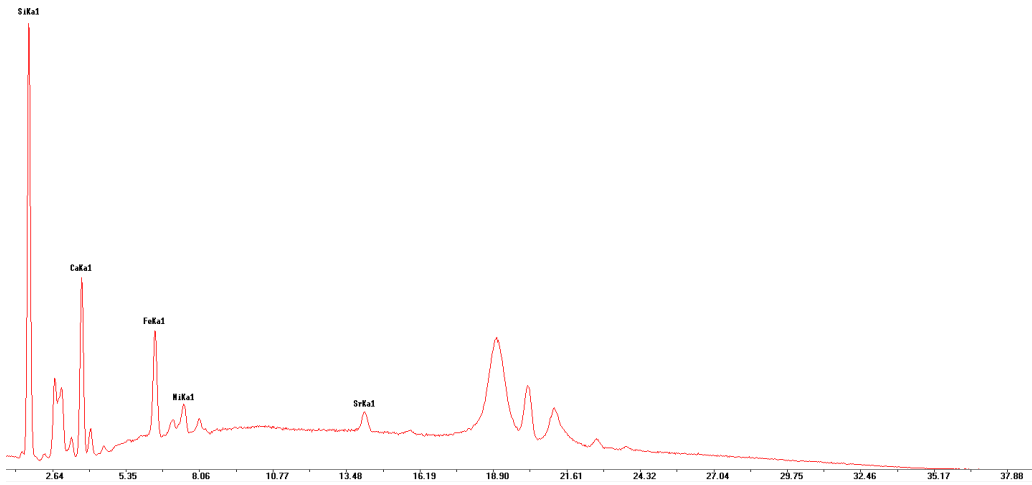


Figure 160: p-XRF spectrum of sample GGWC15/1015/S1 from Ġgantija.

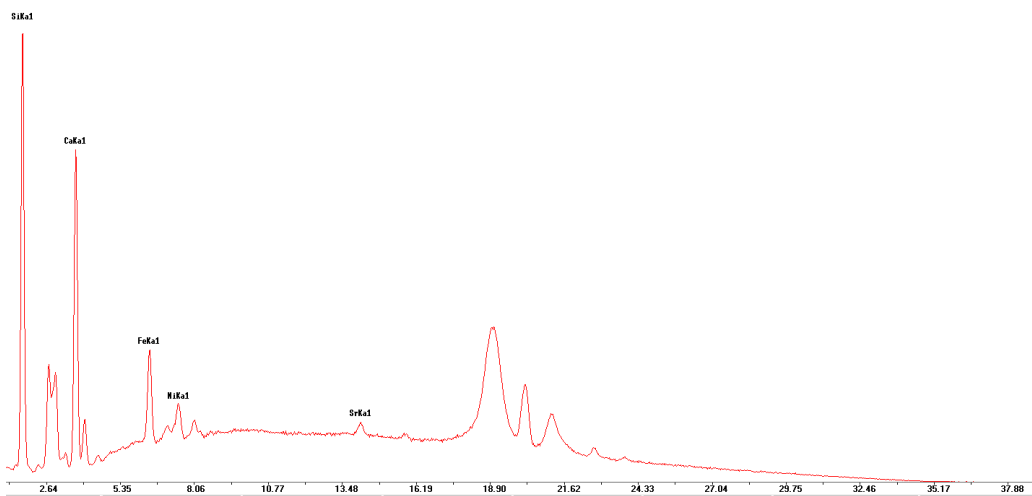


Figure 161: p-XRF spectrum of sample GGWC15/1015/S2 from Ġgantija.

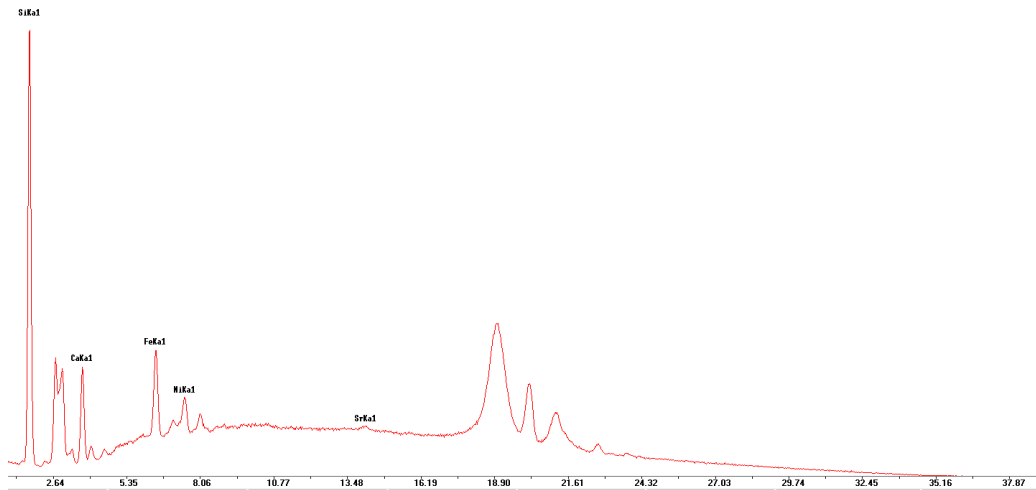


Figure 162: p-XRF spectrum of sample GGWC15/1015/S3 from Ġgantija.

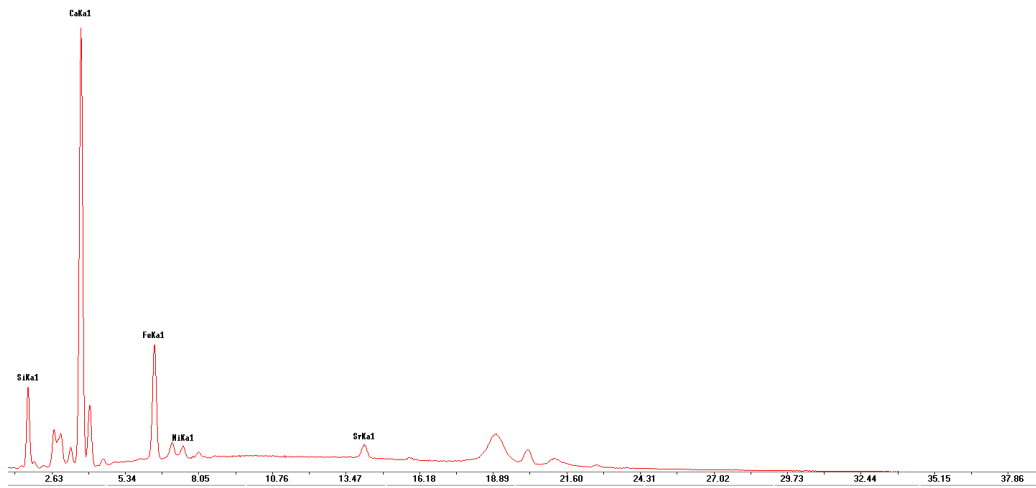


Figure 163: p-XRF spectrum of sample GGWC15/1016/S1 from Ġgantija.

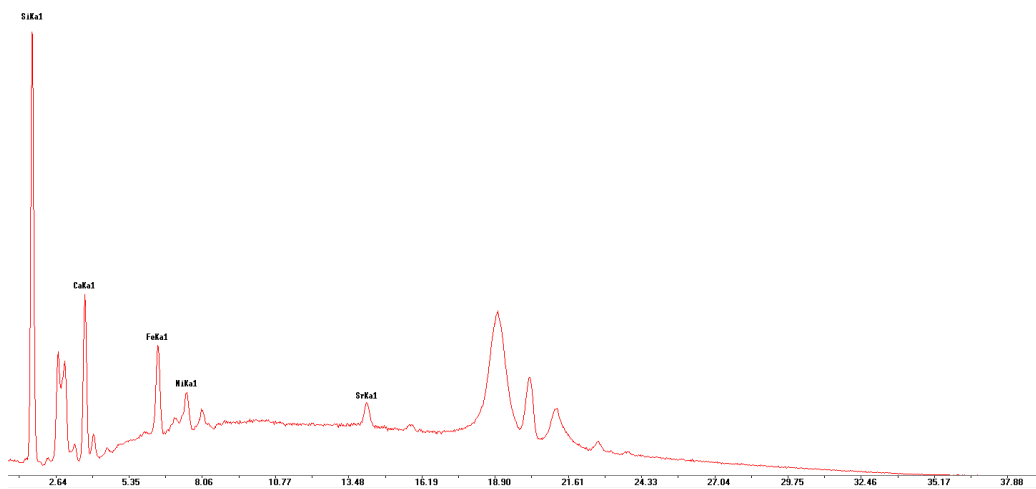


Figure 164: p-XRF spectrum of sample GGWC15/1016/S2 from Ġgantija.

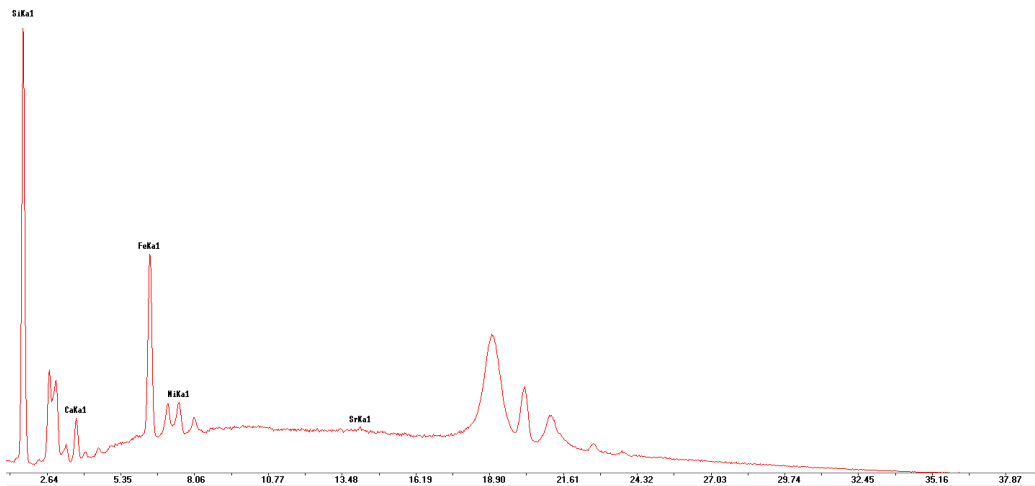


Figure 165: p-XRF spectrum of sample GGWC15/1016/S3 from Ġgantija.

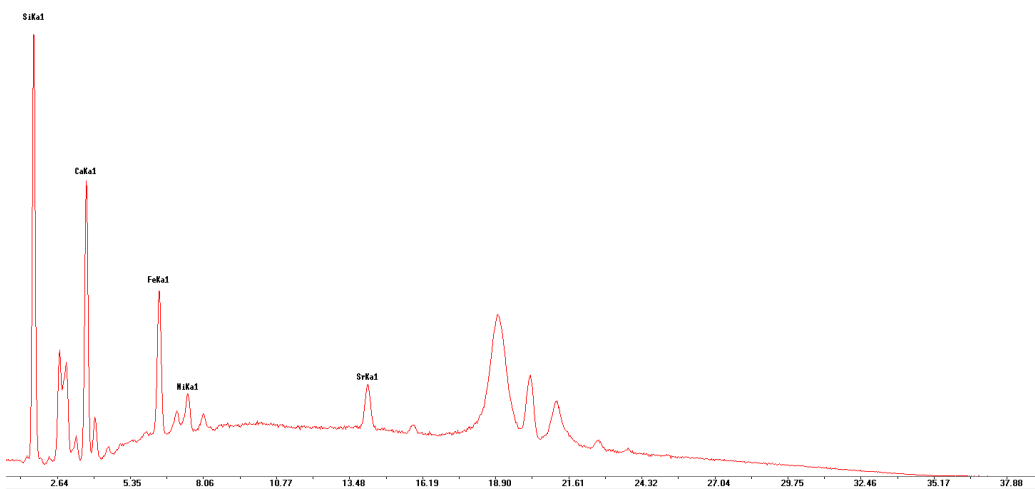


Figure 166: p-XRF spectrum of sample GGWC15/1040/S1 from Ġgantija.

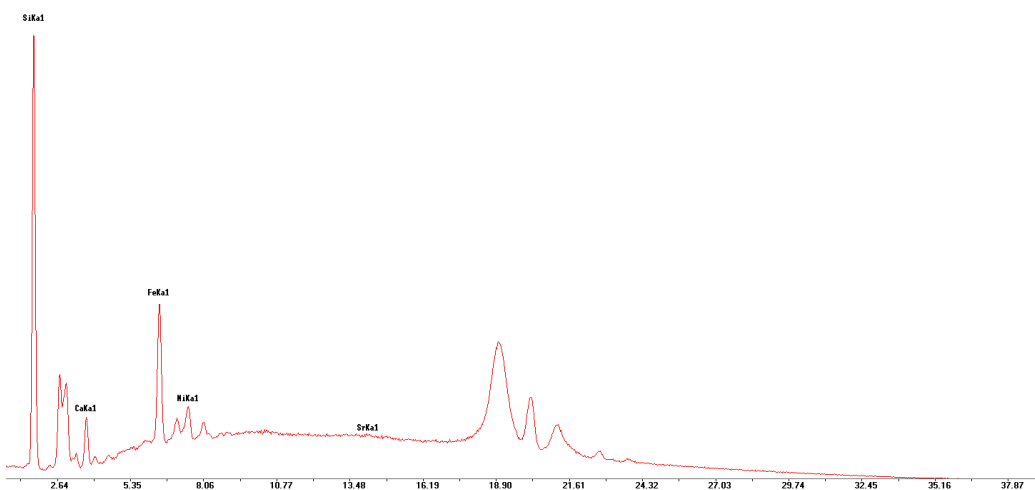


Figure 167: p-XRF spectrum of sample GGWC15/008/S1 from Ġgantija.

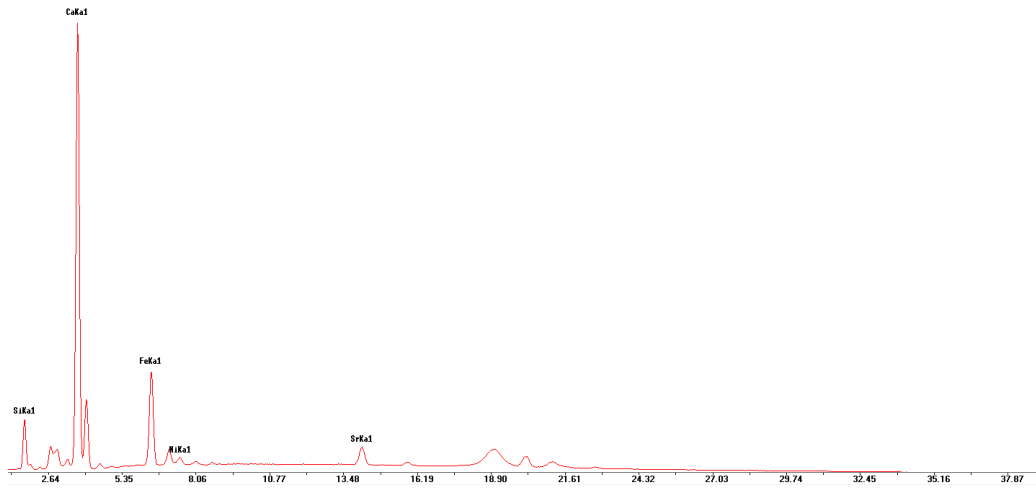


Figure 168: p-XRF spectrum of sample GGWC15/12/S1 from Ġgantija.

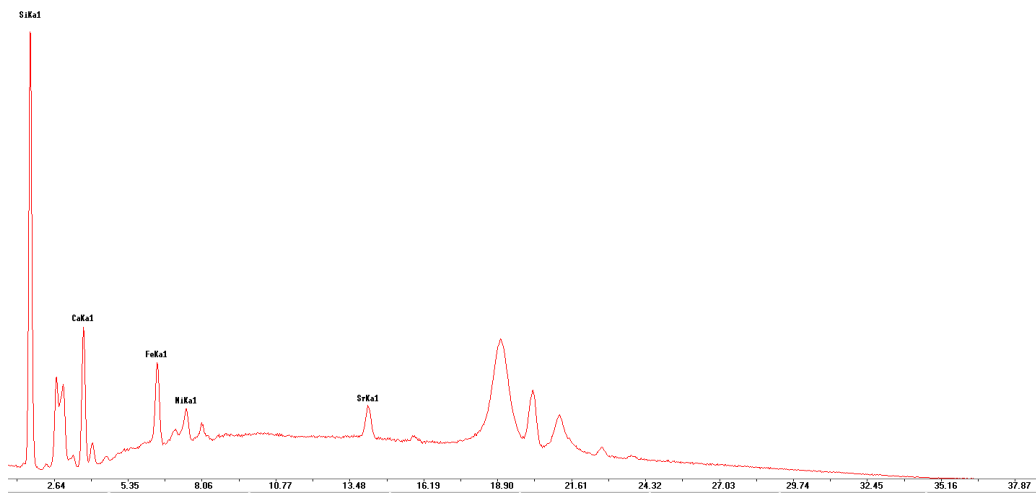


Figure 169: p-XRF spectrum of sample GGWC15/1019/S1 from Ġgantija.

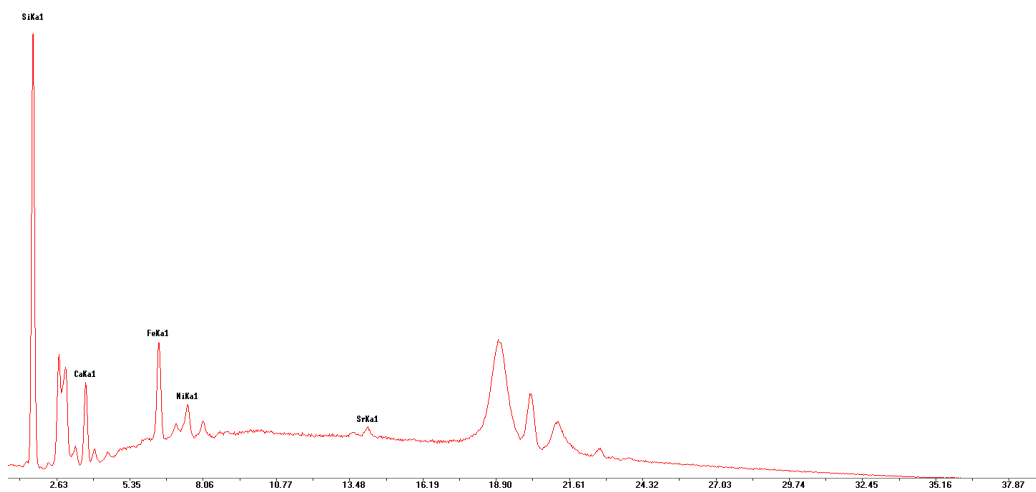


Figure 170: p-XRF spectrum of sample GGWC15/1019/S2 from Ġgantija.

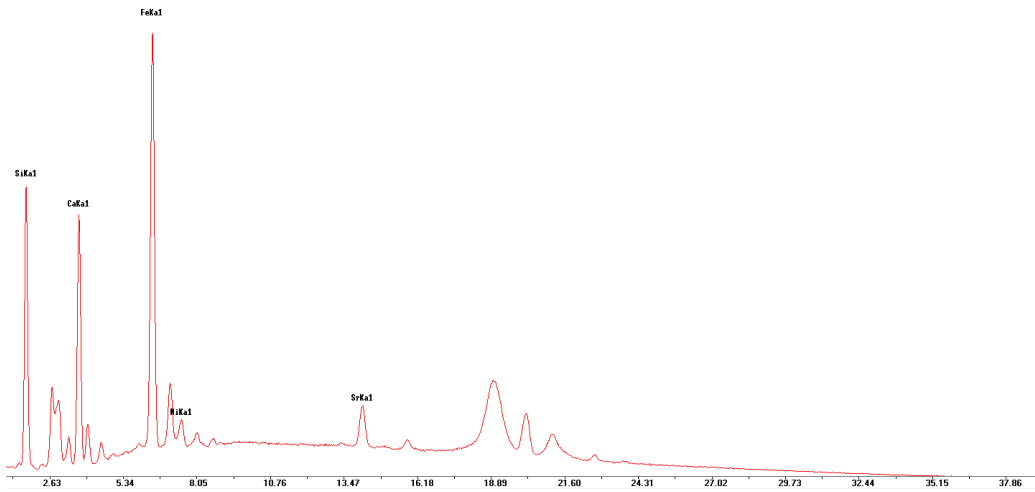


Figure 171: p-XRF spectrum of sample GGWC15/1019/S3 from Ġgantija.

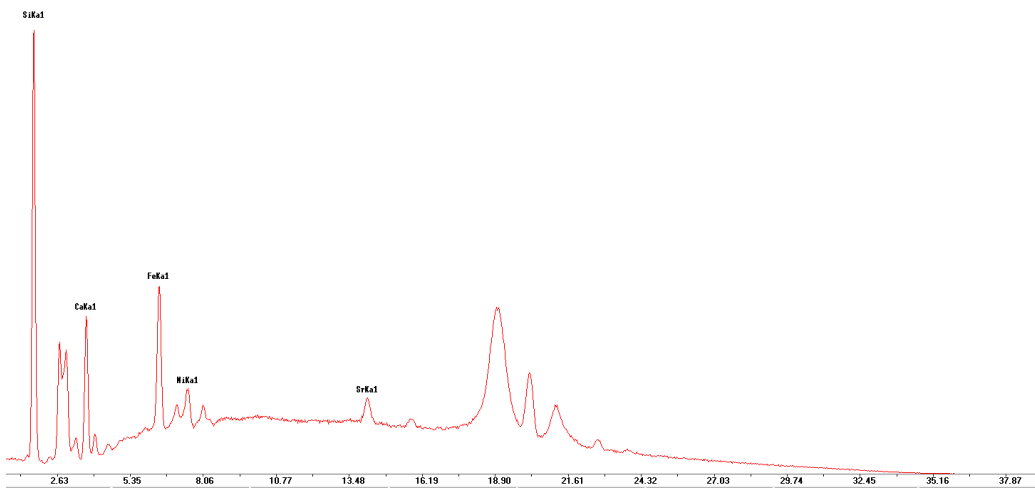


Figure 172: p-XRF spectrum of sample GGWC15/1019/S4 from Ġgantija.

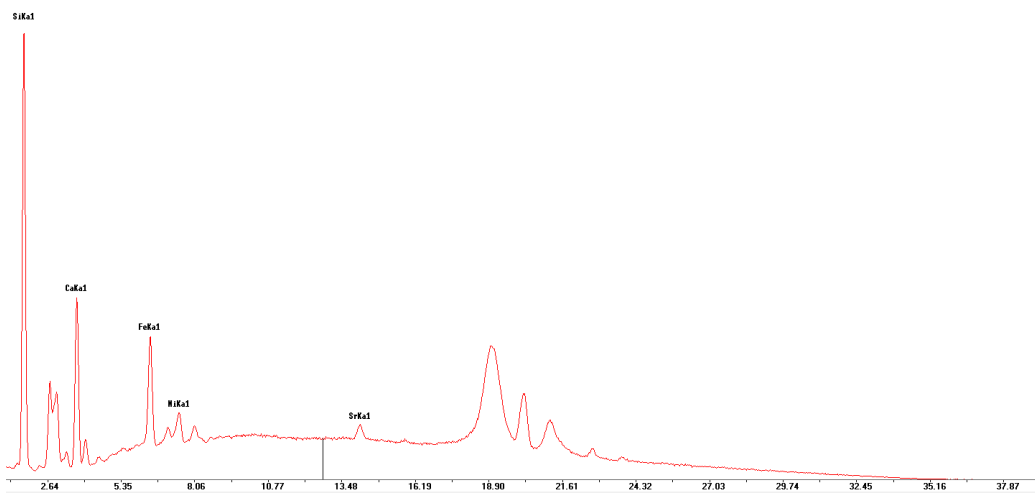


Figure 173: p-XRF spectrum of sample GGWC15/1019/S5 from Ġgantija.

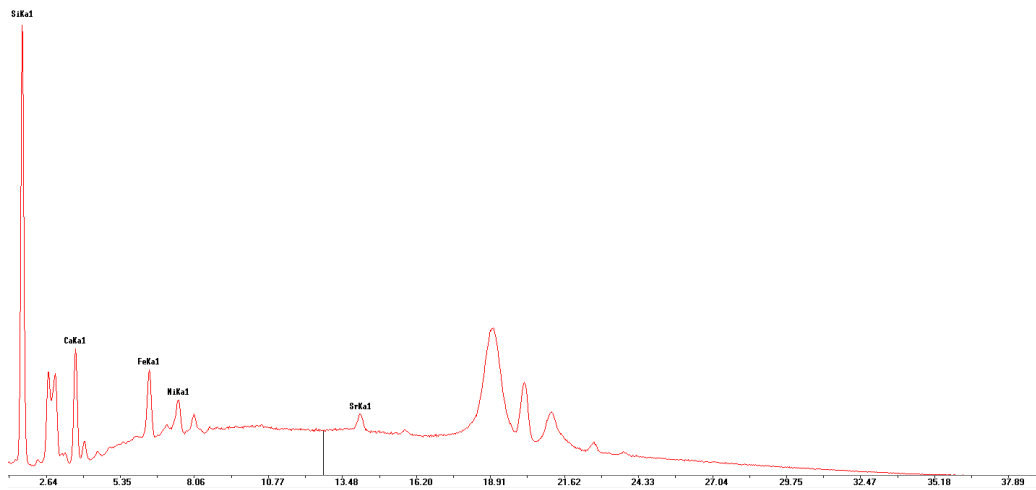


Figure 174: p-XRF spectrum of sample GGWC15/1019/S6/sb from Ġgantija.

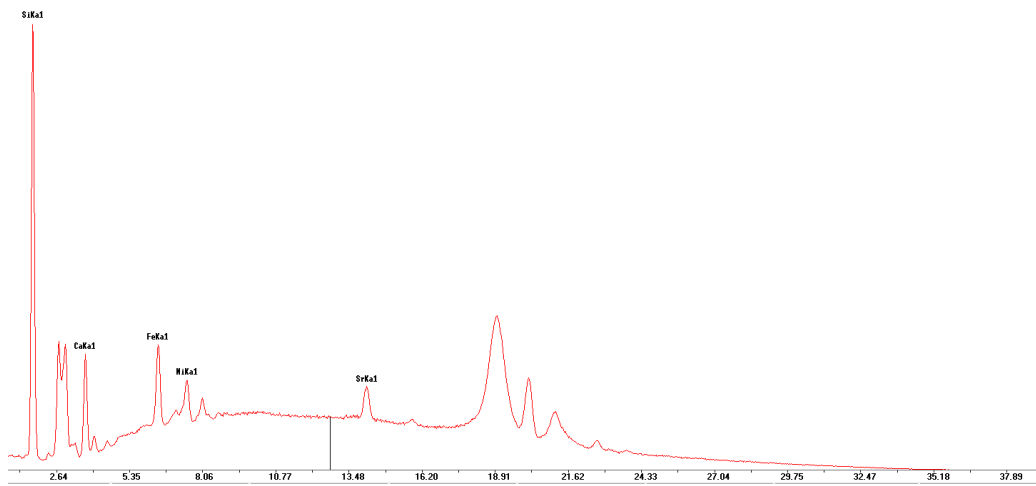


Figure 175: p-XRF spectrum of sample GGWC15/1019/S7/sb from Ġgantija.

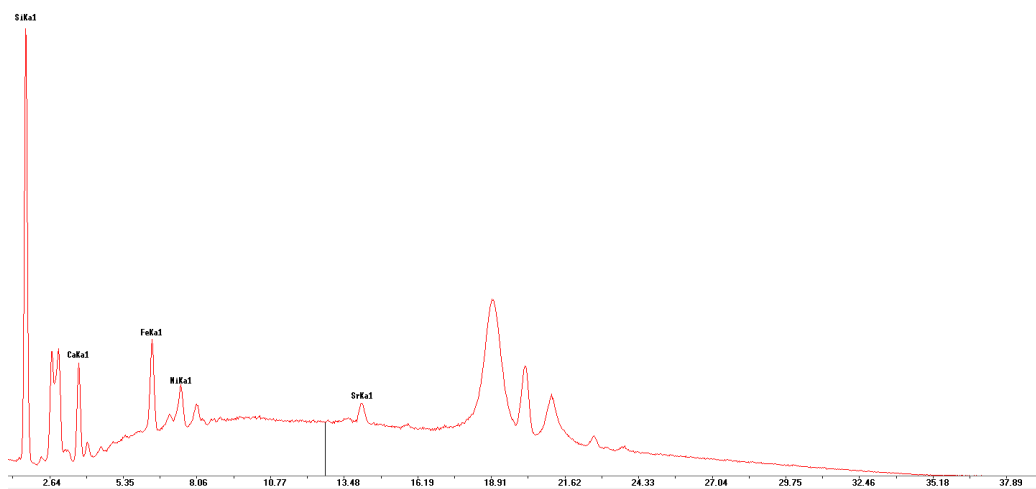


Figure 176: p-XRF spectrum of sample GGWC15/1019/S8/sb from Ġgantija.

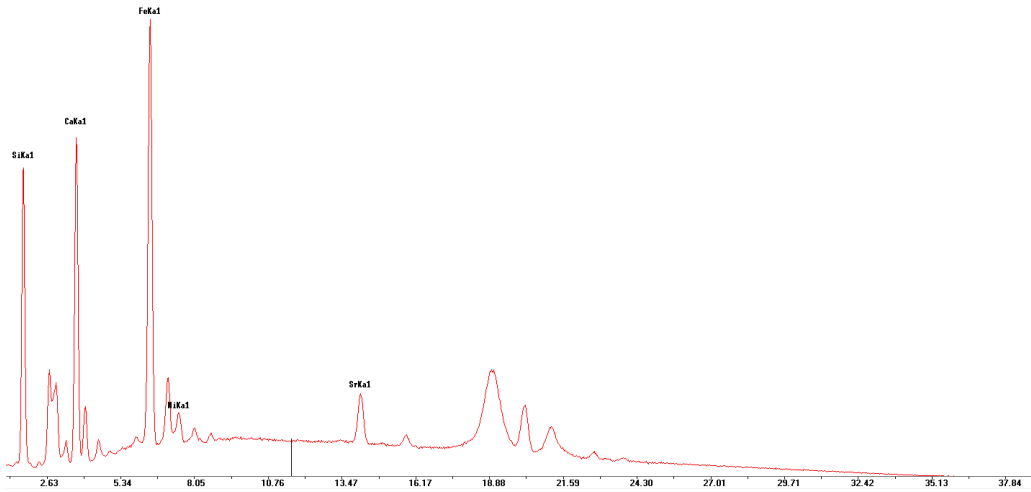


Figure 177: p-XRF spectrum of sample SKB16/S1/L2 from Skorba.

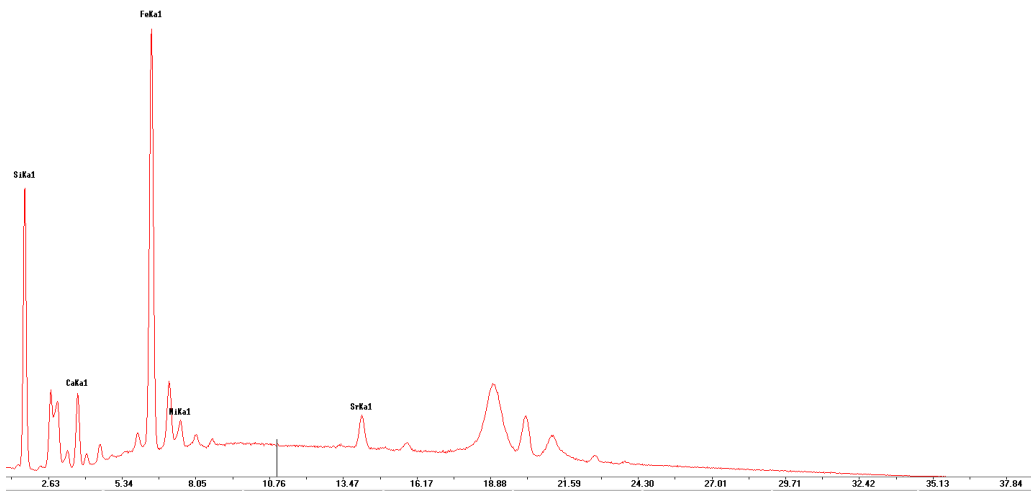


Figure 178: p-XRF spectrum of sample SKB16/S4/L2 from Skorba.

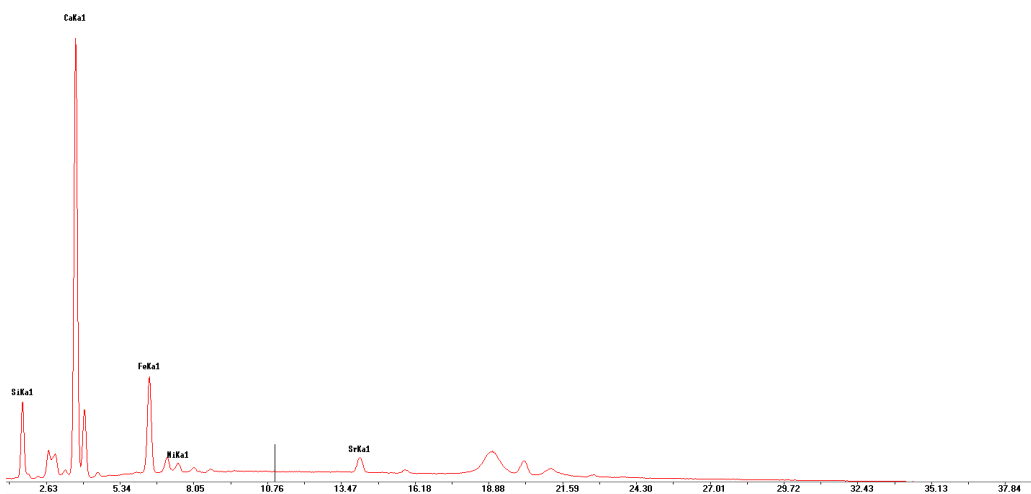


Figure 179: p-XRF spectrum of sample SKB16/S5/L2 from Skorba.

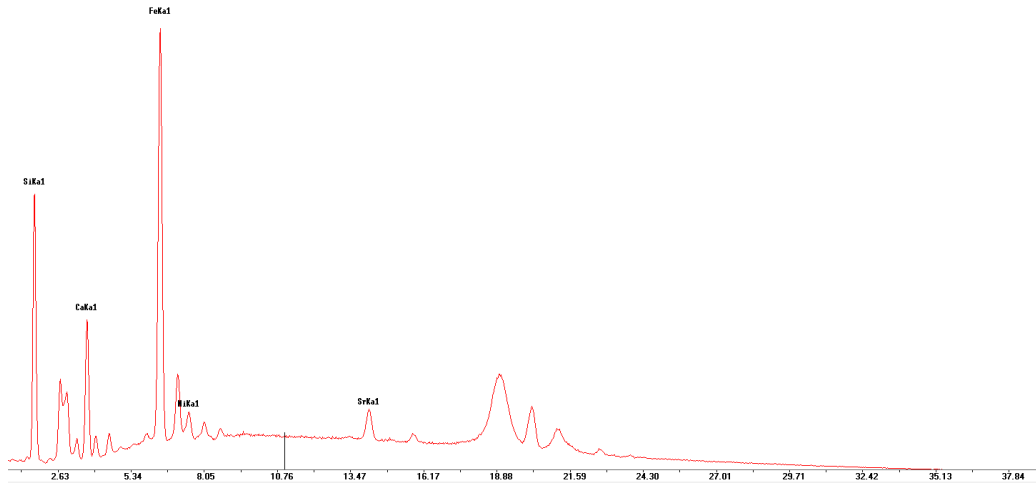


Figure 180: p-XRF spectrum of sample SKB16/S6/L2 from Skorba.

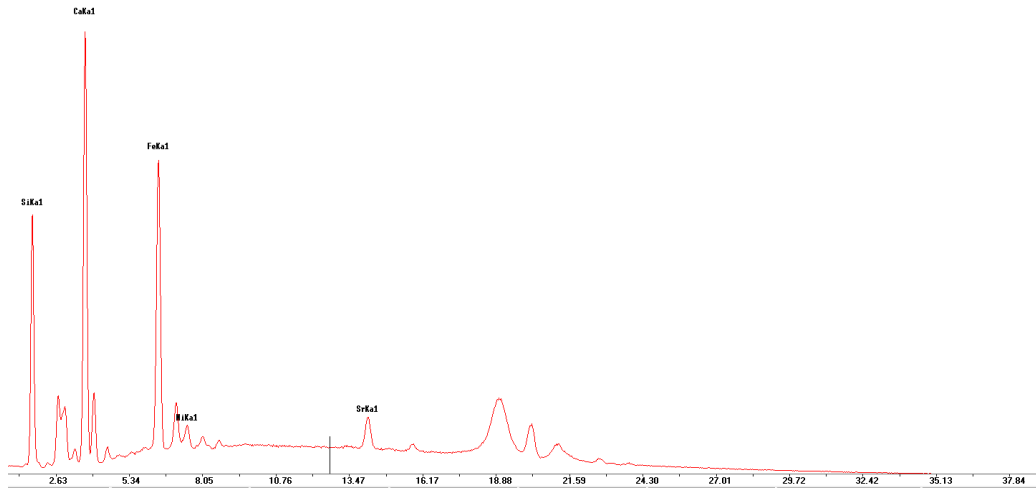


Figure 181: p-XRF spectrum of sample SKB16/S2/L5 from Skorba.

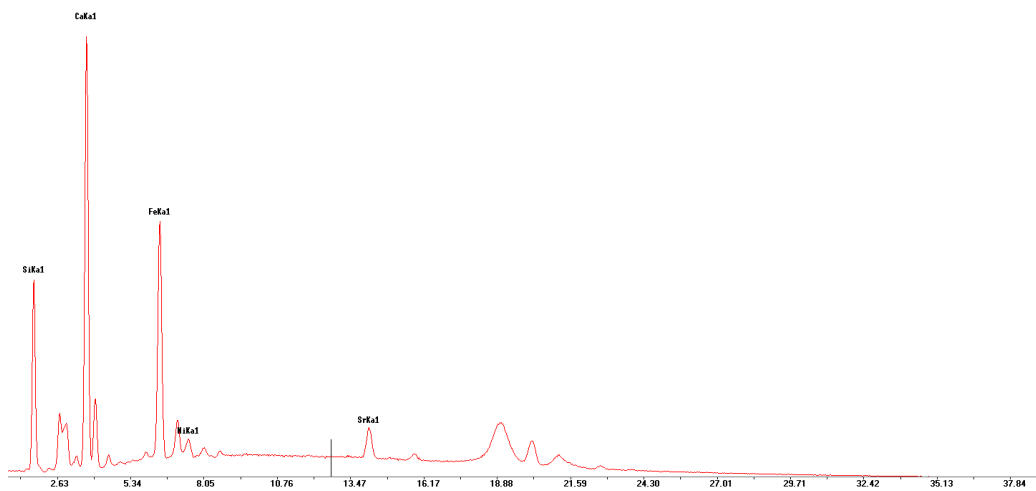


Figure 182: p-XRF spectrum of sample SKB16/S3/L5 from Skorba.

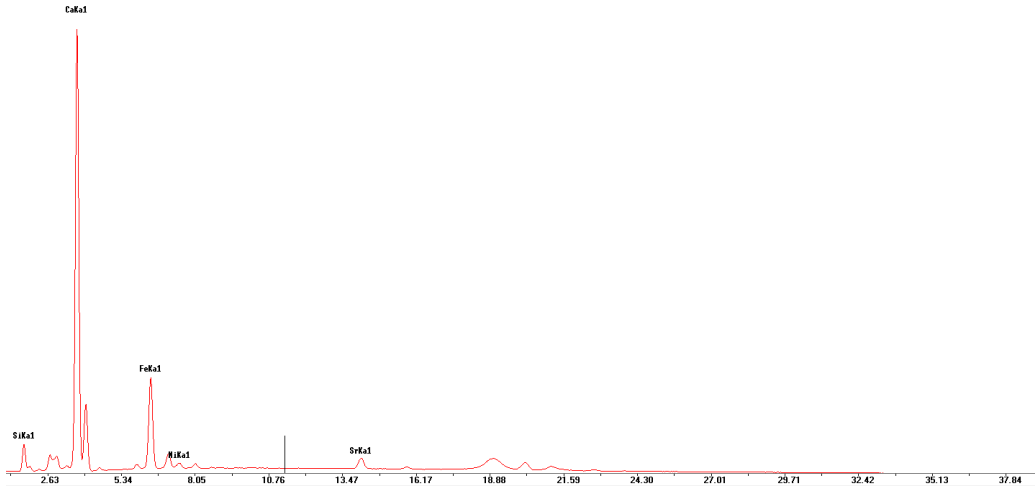


Figure 183: p-XRF spectrum of sample SKB16/S1/L12b from Skorba.

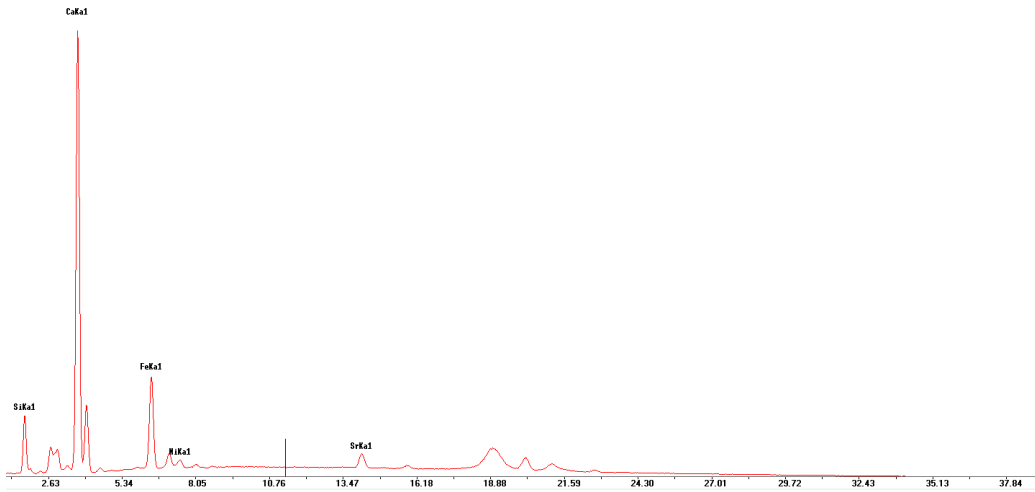


Figure 184: p-XRF spectrum of sample SKB16/S2/L12b from Skorba.

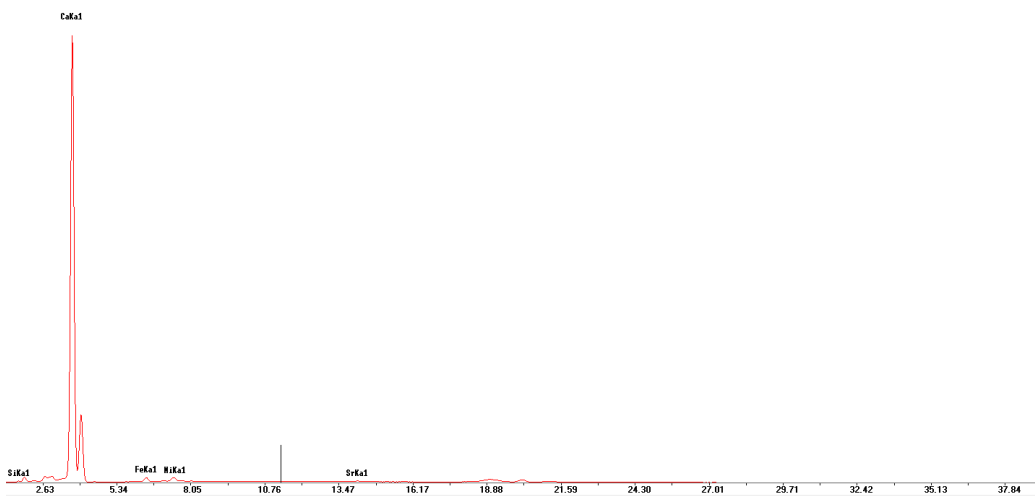


Figure 185: p-XRF spectrum of sample SKB16/S3/L12b from Skorba.

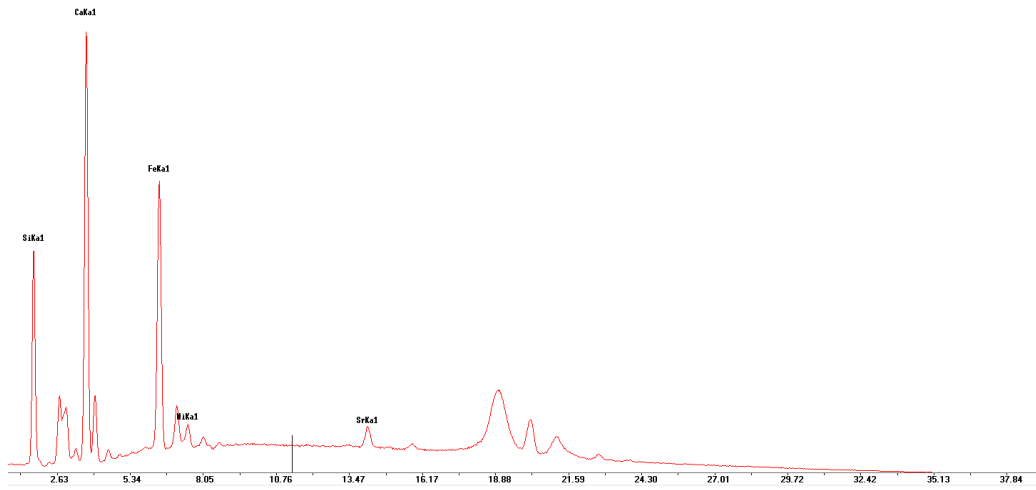


Figure 186: p-XRF spectrum of sample SKB16/S4/L12b from Skorba.

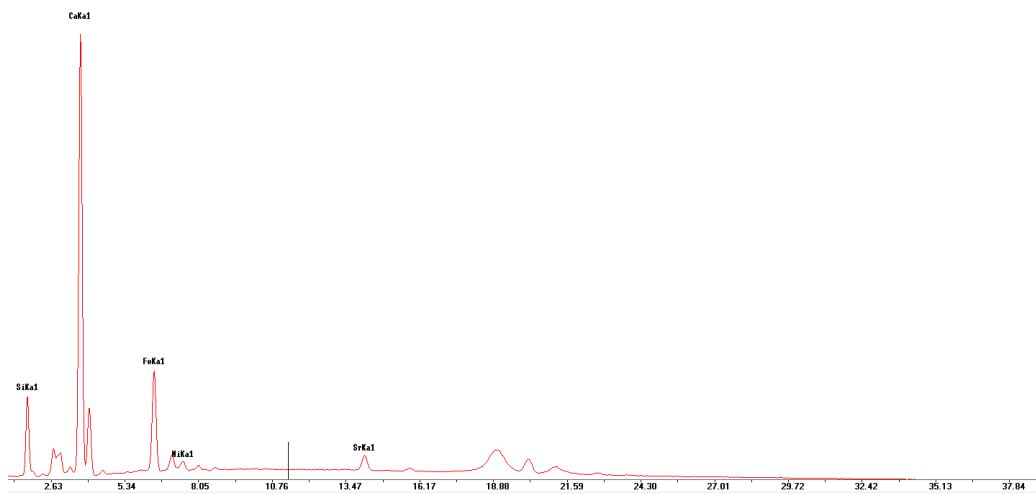


Figure 187: p-XRF spectrum of sample SKB16/S5/L12b from Skorba.

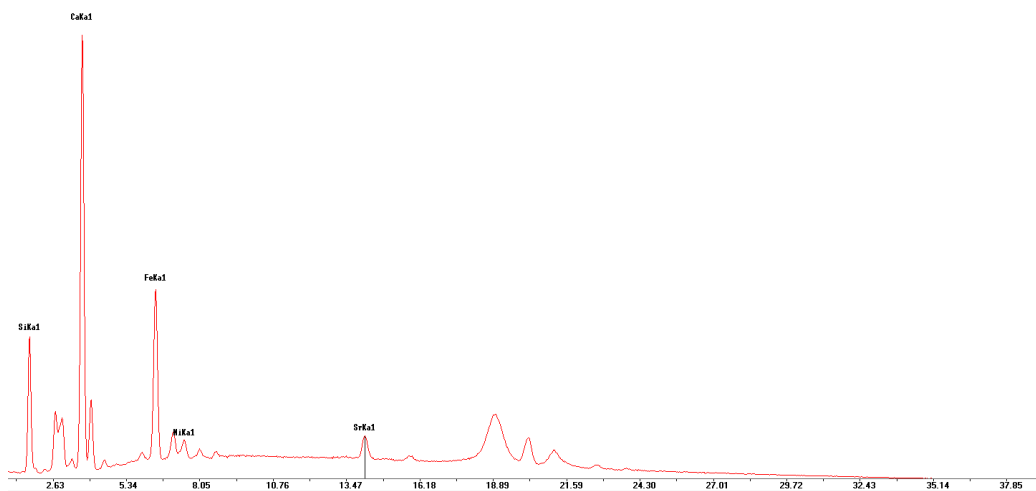


Figure 188: p-XRF spectrum of sample SKB16/S4/L13 from Skorba.

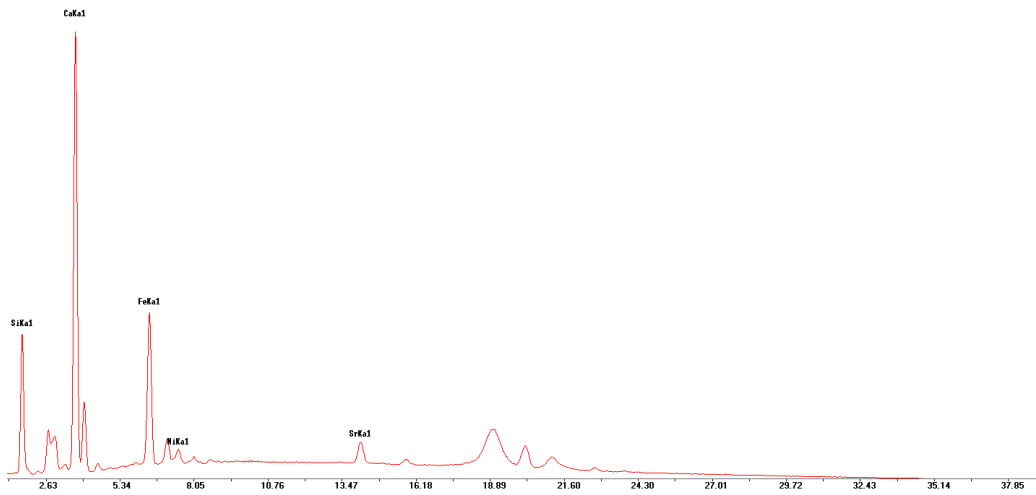


Figure 189: p-XRF spectrum of sample SKB16/S5/L13 from Skorba.

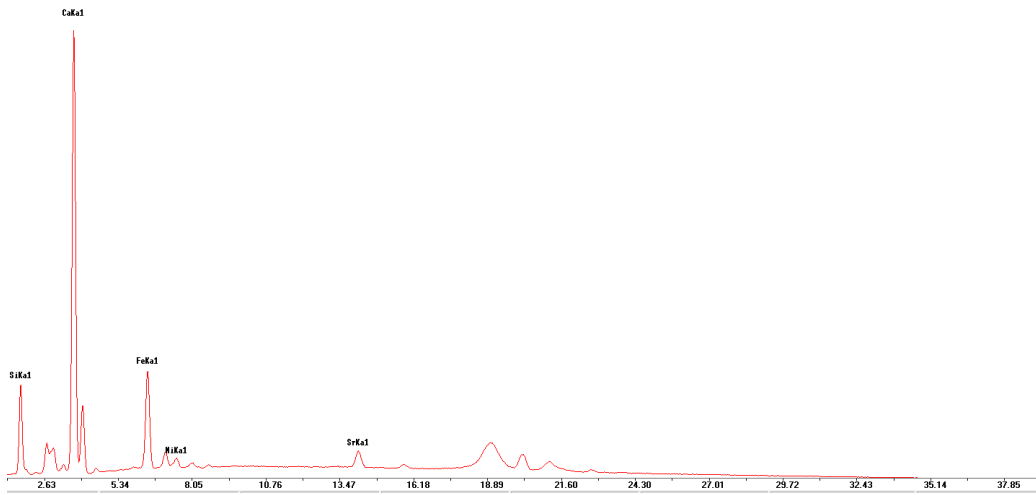


Figure 190: p-XRF spectrum of sample SKB16/S6/L13 from Skorba.

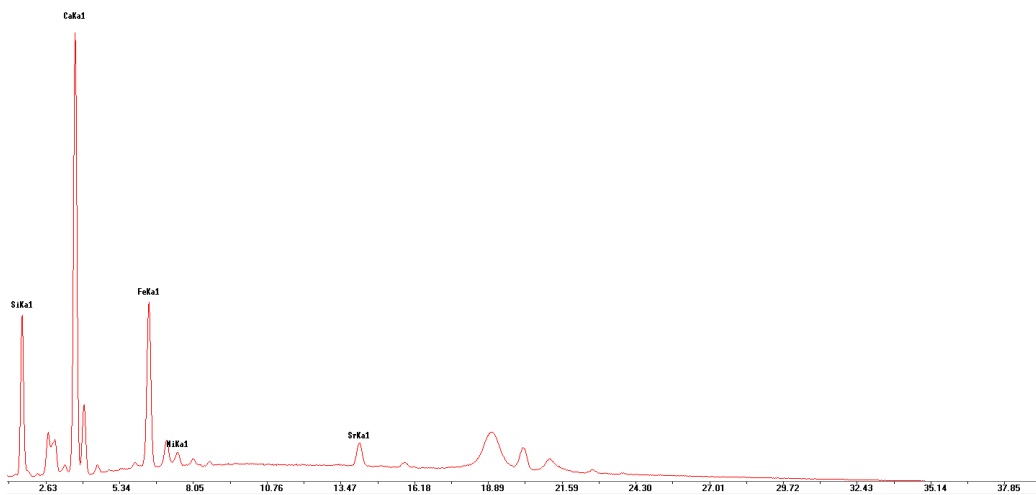


Figure 191: p-XRF spectrum of sample SKB16/S7/L13 from Skorba.

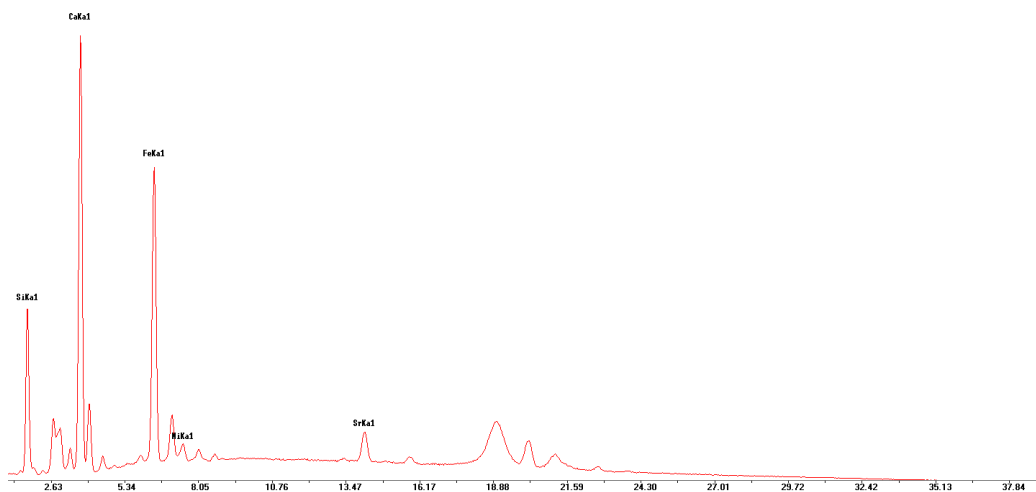


Figure 192: p-XRF spectrum of sample SKB16/S8/L13 from Skorba.



Figure 193: p-XRF spectrum of sample SKB16/S9/L13 from Skorba.



Figure 194: p-XRF spectrum of sample SKB16/S10/L13 from Skorba.

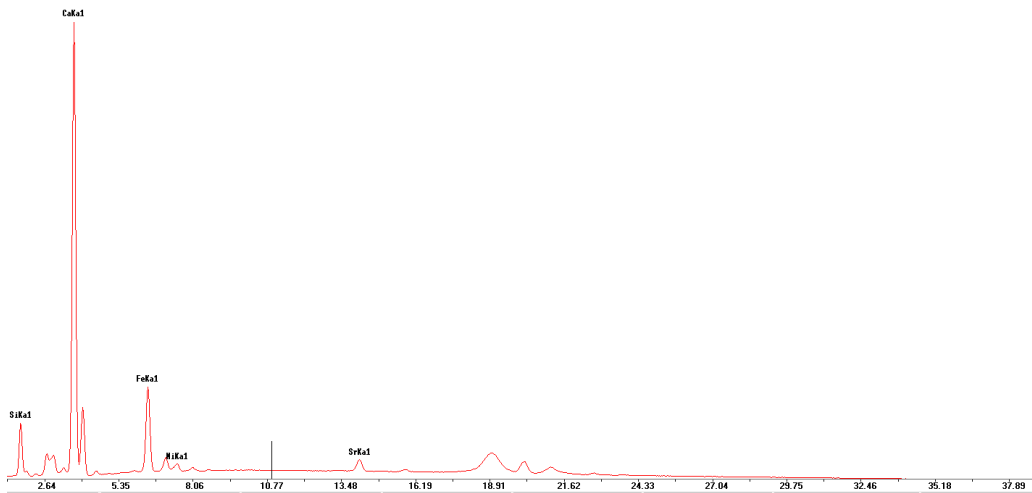


Figure 195: p-XRF spectrum of sample SKB16/S1/L16 from Skorba.

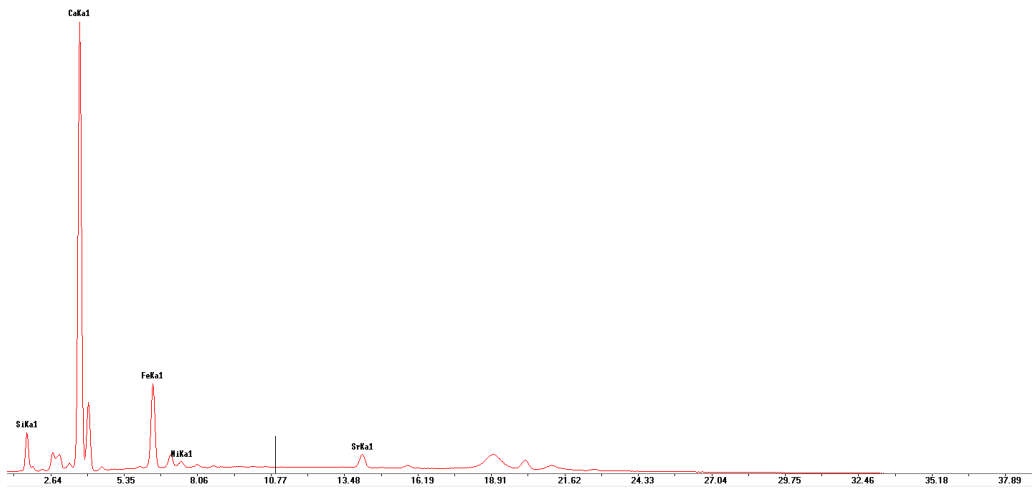


Figure 196: p-XRF spectrum of sample SKB16/S2/L16 from Skorba.

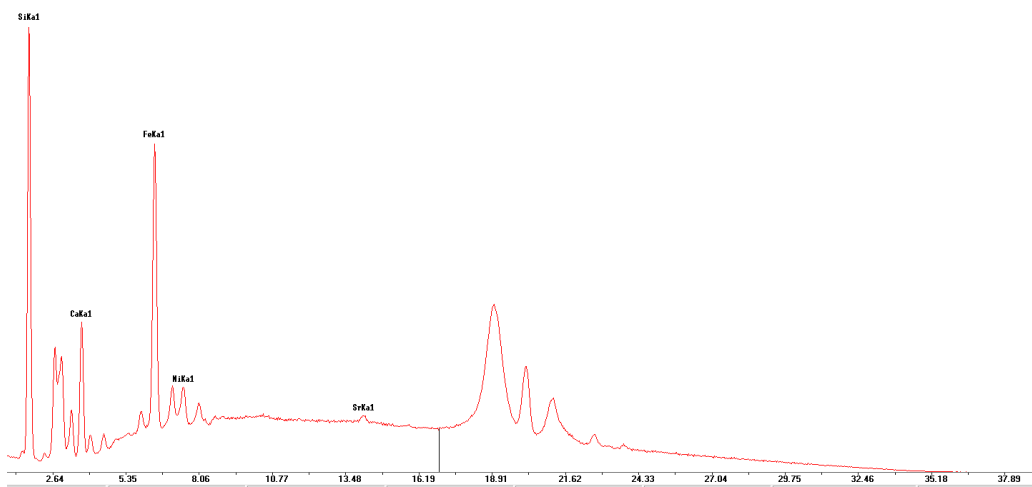


Figure 197: p-XRF spectrum of sample SKB16/S3/L16 from Skorba.

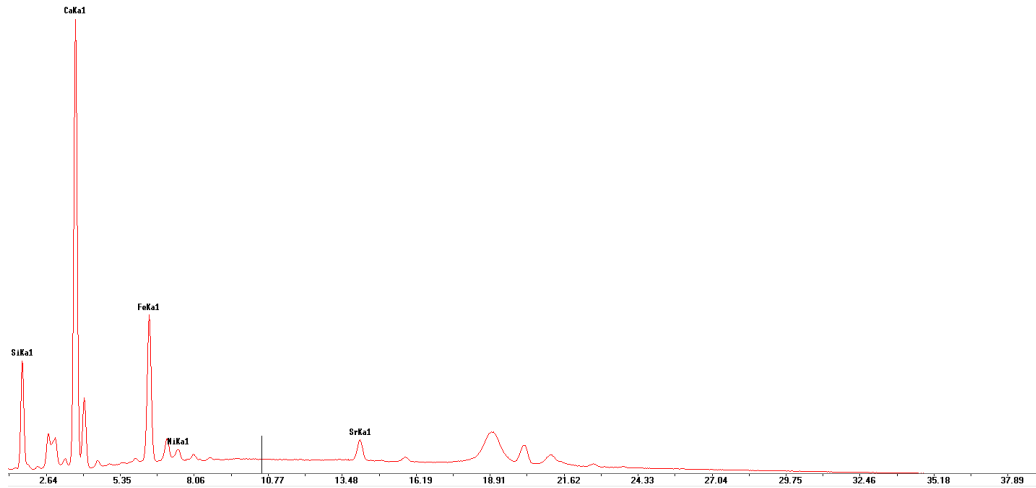


Figure 198: p-XRF spectrum of sample SKB16/S2/L19 from Skorba.

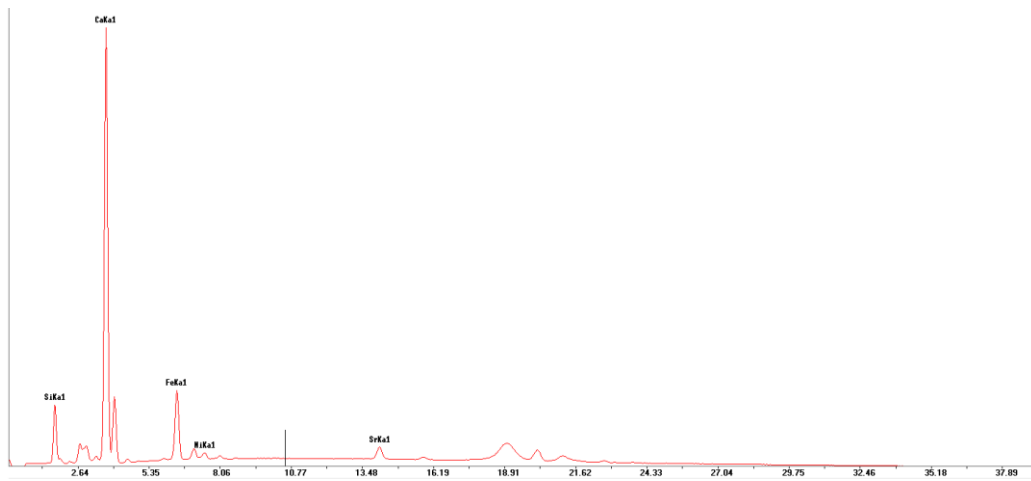


Figure 199: p-XRF spectrum of sample SKB16/S3/L19 from Skorba.

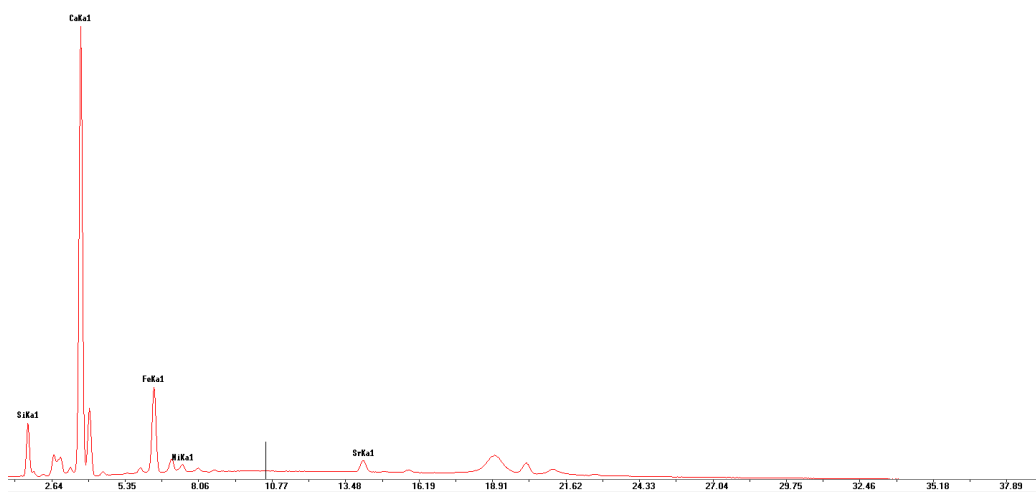


Figure 200: p-XRF spectrum of sample SKB16/S4/L19 from Skorba.

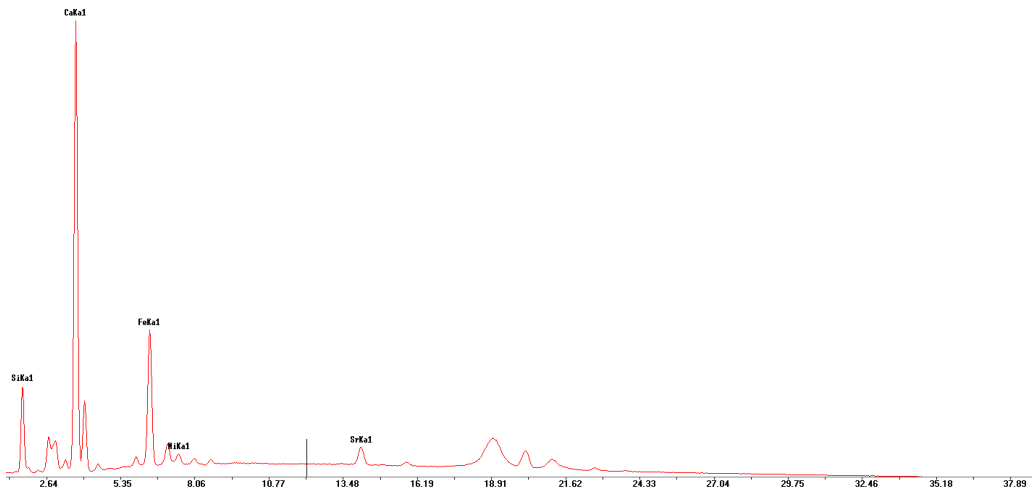


Figure 201: p-XRF spectrum of sample SKB16/S2/L20 from Skorba.

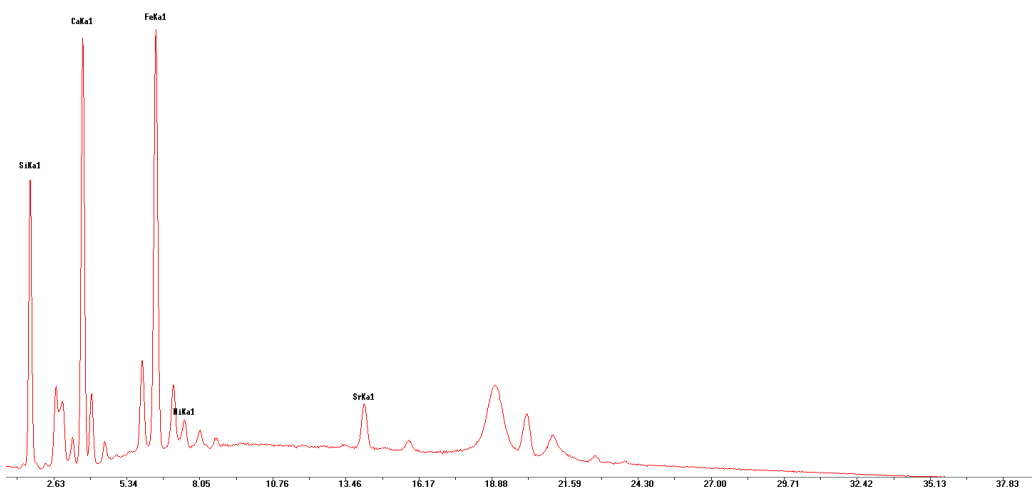


Figure 202: p-XRF spectrum of sample SKB16/S1/L23 from Skorba.

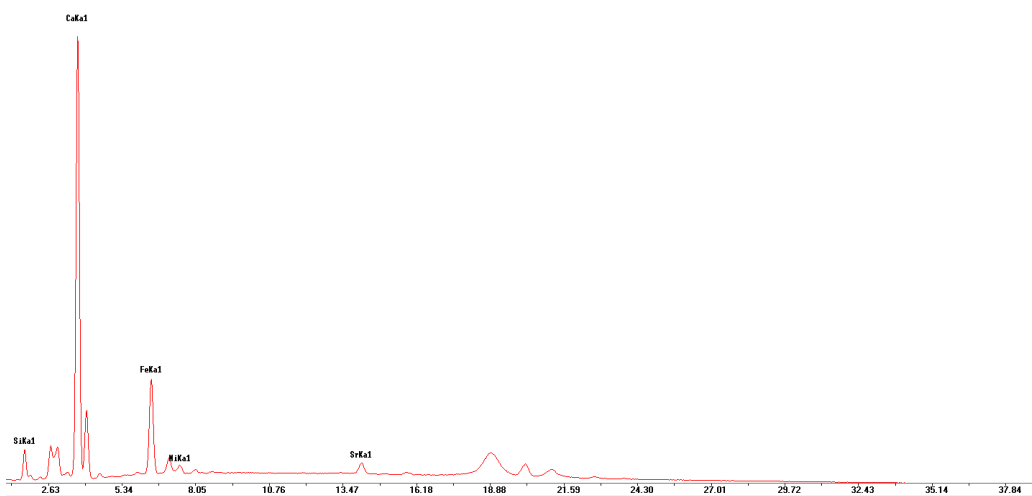


Figure 203: p-XRF spectrum of sample SKB16/S2/L23 from Skorba.

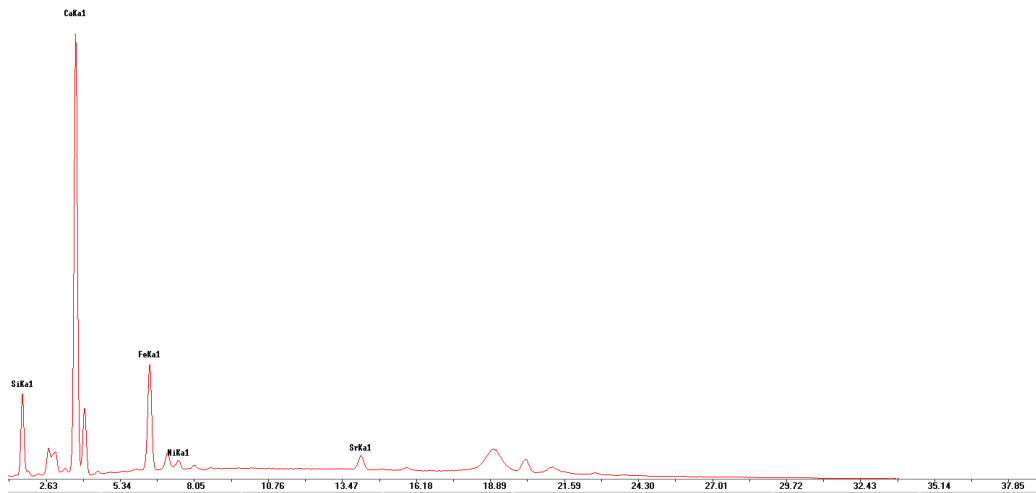


Figure 204: p-XRF spectrum of sample SKB16/S3/L23 from Skorba.

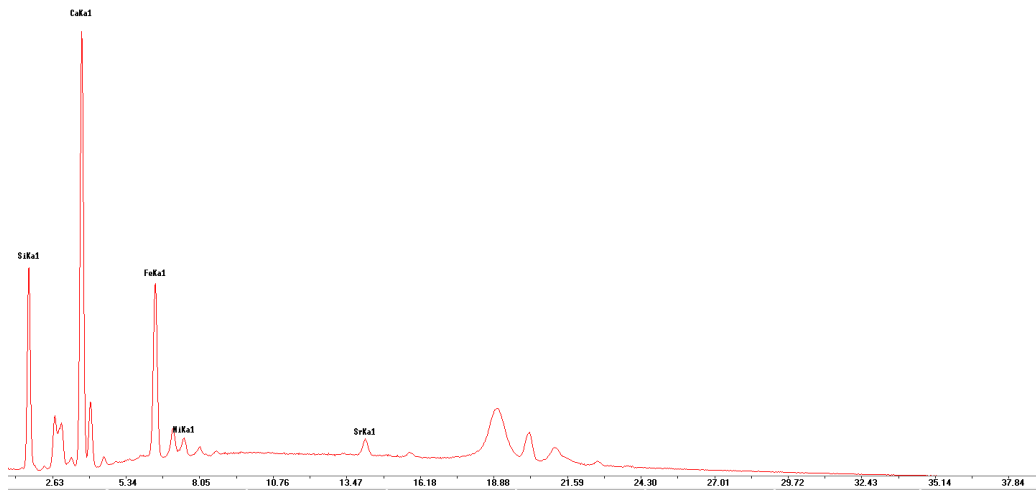


Figure 205: p-XRF spectrum of sample SKB16/S4/L23 from Skorba.

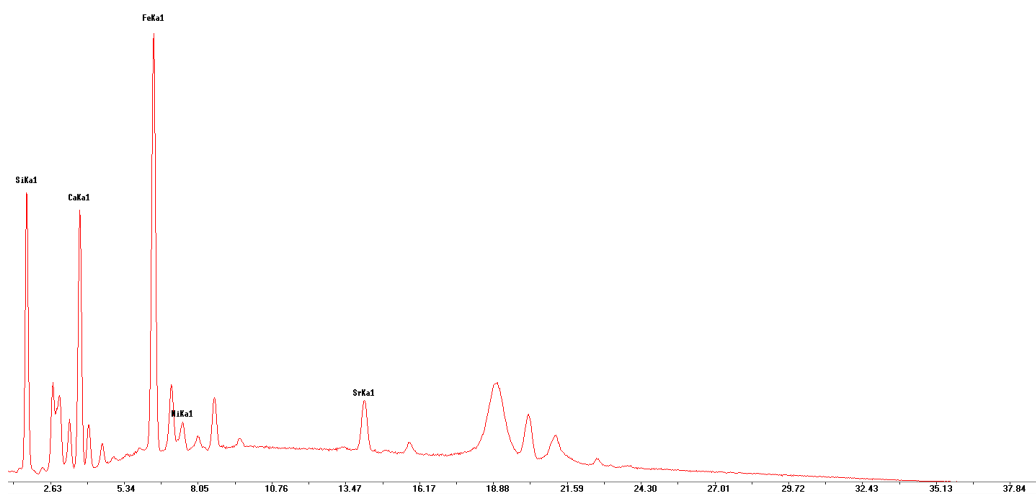


Figure 206: p-XRF spectrum of sample SKB16/S5/L23 from Skorba.

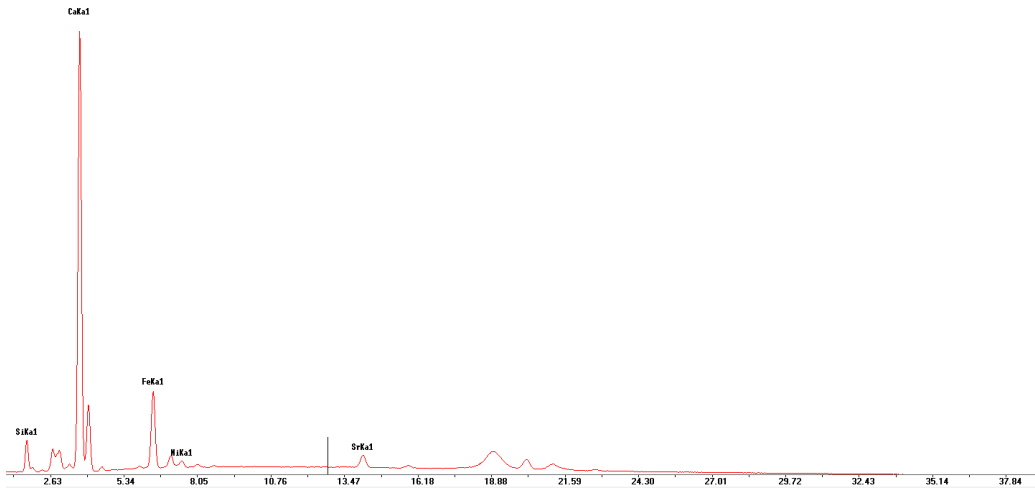


Figure 207: p-XRF spectrum of sample SKB16/S1/L26 from Skorba.

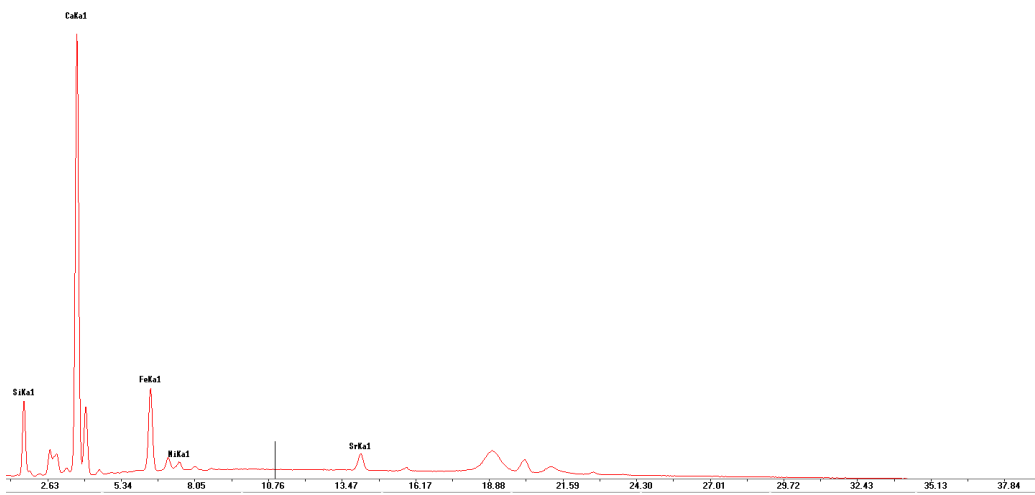


Figure 208: p-XRF spectrum of sample SKB16/S1/L30 from Skorba.

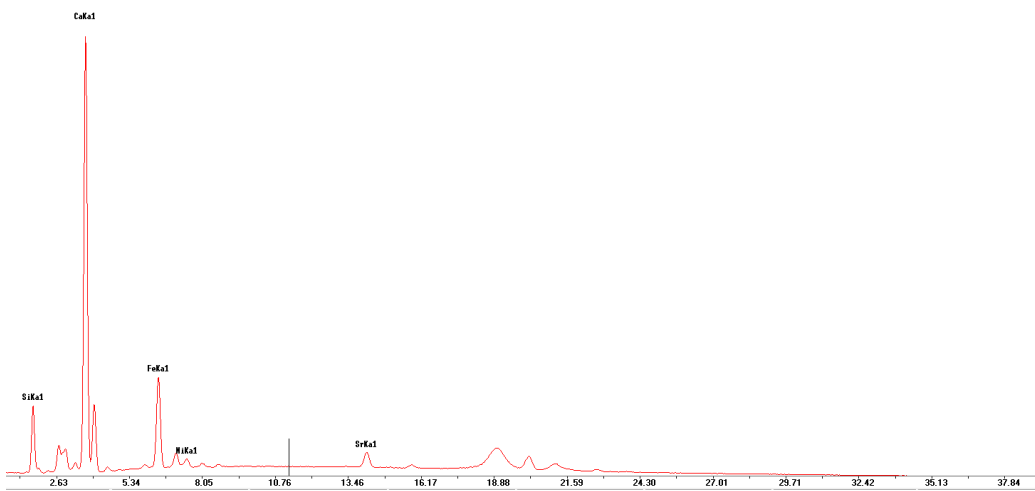


Figure 209: p-XRF spectrum of sample SKB16/S2/L30 from Skorba.

LA-ICP-MS RESULTS ANALYSES

Rock Samples

Table 10: The LA-ICP-MS analyses results of the Maltese rock samples. The elements MgO, Al₂O₃, SiO₂, CaO, TiO₂ and Fe₂O₃ have their values in wt%, while all elements are in part per million (ppm). The N/A (Not Applicable) is imported to indicate that an element was not measured or when a ratio between elements cannot be calculated. Sample G2S6 was measured with the second LA-ICP-MS instrument.

Samples	Location	MgO	Al ₂ O ₃	SiO ₂	CaO	TiO ₂	V	Mn	Fe ₂ O ₃	Ni	Rb	Sr	Y	Ba	Th	U	U/Th	V/(V+Ni)
F1S4	Gozo	2.16	1.68	N/A	23.83	N/A	22.57	32.86	0.72	16.08	11.36	429.52	8.62	N/A	1.09	2.32	2.12	0.58
G1S1	Gozo	0.43	0.55	1.27	71.53	0.02	8.22	11.88	0.27	3.94	3.38	67.67	2.68	N/A	0.52	0.38	0.73	0.67
G1S2	Gozo	0.26	N/A	N/A	68.07	N/A	N/A	N/A	0.01	N/A	N/A	22.45	0.27	N/A	N/A	N/A	N/A	N/A
G2S2	Gozo	2.57	0.92	34.90	13.92	0.04	12.76	22.32	0.24	19.60	6.62	276.50	4.76	N/A	0.56	1.84	3.28	0.39
G2S1	Gozo	1.48	0.85	38.46	12.08	0.03	11.38	15.90	0.25	14.07	6.44	241.66	4.04	N/A	0.59	1.19	2.00	0.45
G2S3	Gozo	1.53	1.40	47.61	19.20	0.07	17.80	25.49	0.52	19.48	8.78	383.50	6.79	N/A	0.88	1.62	1.83	0.48
G2S6	Gozo	0.62	0.46	94.69	4.12	0.01	3.80	4.63	0.08	3.76	2.03	68.21	1.87	2.36	1.41	0.96	0.68	0.50
M1S6	Malta	1.01	0.53	32.01	9.09	0.03	11.44	8.53	0.14	8.06	4.69	162.73	2.78	N/A	0.27	1.58	5.71	0.58
M1S8	Malta	1.00	0.76	41.21	<0.01	0.06	17.46	7.58	0.25	9.50	5.45	131.79	3.56	N/A	0.55	1.94	3.53	0.65
M1S11	Malta	1.02	0.78	39.02	7.69	0.05	11.61	11.24	0.27	8.46	28.26	147.27	3.25	N/A	0.58	1.28	2.21	0.58
M1S9	Malta	1.15	0.65	37.54	6.12	0.04	10.22	8.75	0.19	8.90	5.49	116.62	3.13	N/A	0.43	1.59	3.68	0.53
M1S5v	Malta	0.69	0.69	38.56	6.67	0.07	13.16	8.99	0.21	13.28	4.66	113.75	4.47	N/A	0.71	2.39	3.35	0.50
M2S4	Malta	1.72	0.70	38.04	7.41	0.03	13.41	11.40	0.23	9.28	4.85	150.23	2.28	N/A	0.45	1.81	4.06	0.59
M2S2	Malta	0.47	0.35	25.35	1.94	0.02	17.00	2.28	0.09	4.57	1.96	58.6	1.32	N/A	N/A	1.06	N/A	0.79
F1S2	Malta	1.19	0.87	N/A	9.05	N/A	13.88	13.02	N/A	33.87	0.40	N/A	4.49	N/A	0.69	4.20	6.11	0.29
F1S3	Malta	1.52	N/A	N/A	7.84	N/A	13.82	11.85	N/A	10.10	N/A	166.70	5.22	N/A	0.60	2.28	3.76	0.58
M1S1	Malta	0.94	0.67	39.87	5.06	0.05	9.67	9.29	0.21	7.62	4.18	99.60	1.73	N/A	0.42	1.43	3.41	0.56
M1S1b	Malta	1.30	0.86	47.68	6.17	0.05	13.67	11.29	0.32	7.79	5.52	108.86	5.12	N/A	0.60	2.33	3.88	0.64
M1S2	Malta	1.60	1.14	59.03	11.15	0.06	18.82	15.01	0.43	12.08	7.25	241.00	6.62	N/A	0.78	2.79	3.55	0.61
M1S3	Malta	1.24	0.97	53.11	9.69	0.06	13.68	13.87	0.46	13.54	5.72	168.60	5.44	N/A	0.61	1.75	2.85	0.50
M1S5s	Malta	1.34	0.65	41.13	8.98	0.03	10.87	12.58	0.29	11.81	4.39	152.17	4.12	N/A	0.41	1.86	4.51	0.48
M1S5s2	Malta	1.48	0.89	49.95	11.47	0.05	14.7	14.95	0.26	13.61	5.59	200.33	5.28	N/A	0.65	2.30	3.53	0.52
M1S4	Malta	1.02	0.80	48.96	8.02	0.05	13.93	10.42	0.22	9.44	4.93	143.50	4.281	N/A	0.54	2.62	4.86	0.59
M1S10	Malta	1.81	0.88	47.59	7.80	0.07	16.86	11.89	0.39	11.46	5.33	155.78	4.16	N/A	0.52	2.27	4.33	0.59

Table 11: Second group of the LA-ICP-MS analyses results of the Maltese rock samples. It includes the rare elements and their concentrations in part per million (ppm). The N/A (Not Applicable) is imported to indicate that the values of an element had RSD and %REC outside the accepted values (RSD < 5 and 95% < %REC <105%). Sample G2S6 was measured with the second LA-ICP-MS instrument.

Samples	Location	La	Ce	Pr	Nd	Sm	Eu	Gd	Tb	Dy	Ho	Er	Tm	Yb	Lu
F1S4	Gozo	5.75	7.77	1.21	5	0.97	0.24	1.03	0.15	1.01	0.22	0.65	0.09	0.57	0.09
G1S1	Gozo	1.74	3.04	0.43	1.84	0.41	0.11	0.41	0.06	0.36	0.07	0.20	0.03	0.16	0.02
G1S2	Gozo	N/A	N/A	N/A	N/A	N/A	N/A	N/A	N/A	N/A	N/A	N/A	<0.01	N/A	N/A
G2S2	Gozo	3.26	4.55	0.69	2.85	0.76	0.13	0.57	0.12	0.58	0.13	0.41	0.05	0.38	0.05
G2S1	Gozo	2.27	3.78	0.57	2.09	0.54	0.12	0.49	0.07	0.50	0.09	0.35	0.03	0.24	0.05
G2S3	Gozo	4.83	6.44	1.03	4.19	0.85	0.20	0.84	0.13	0.83	0.18	0.53	0.07	0.46	0.07
G2S6	Gozo	1.24	1.86	0.29	1.10	0.24	0.050	0.22	0.04	0.21	0.05	0.13	0.02	0.11	0.02
M1S6	Malta	1.55	2.52	0.46	1.40	0.30	0.05	0.37	0.06	0.28	0.10	0.19	0.04	0.23	0.04
M1S8	Malta	2.56	4.4	0.57	2.22	0.55	10.24	10.69	0.07	0.32	0.12	0.26	0.05	0.26	0.03
M1S11	Malta	2.34	3.75	0.52	1.96	5.85	0.09	0.45	0.05	0.39	0.08	12.94	0.04	0.22	0.05
M1S9	Malta	1.86	3.10	0.45	1.81	0.47	0.14	9.51	8.57	0.31	0.07	0.29	0.03	0.28	0.02
M1S5v	Malta	2.75	4.12	0.63	2.54	0.52	0.08	0.57	0.04	0.53	0.12	0.37	0.06	9.03	0.05
M2S4	Malta	2.03	3.15	0.33	1.80	0.40	0.12	0.31	0.04	0.41	0.07	0.19	0.04	0.17	0.04
M2S2	Malta	0.84	1.98	0.16	0.72	0.18	0.05	N/A	N/A	0.20	0.04	N/A	N/A	N/A	N/A
F1S2	Malta	0.14	0.85	0.54	0.10	0.08	0.60	5.07	0.14	0.87	0.20	0.56	0.07	0.46	0.07
F1S3	Malta	2.45	3.67	0.53	2.22	0.54	0.14	0.61	0.09	0.58	0.11	0.36	0.04	0.19	0.04
M1S1	Malta	10.06	3.10	0.37	1.02	0.18	0.07	0.34	0.04	0.35	0.11	0.38	0.05	0.29	0.05
M1S1b	Malta	2.87	4.46	0.70	2.84	0.57	0.13	0.58	0.09	0.58	0.13	0.38	0.05	0.32	0.05
M1S2	Malta	3.82	5.46	0.87	3.61	0.70	0.18	0.78	0.12	0.72	0.17	0.49	0.07	0.40	0.06
M1S3	Malta	3.32	5.00	0.74	3.02	0.60	0.15	0.66	0.09	0.63	0.14	0.39	0.05	0.35	0.05
M1S5s	Malta	2.50	3.89	0.55	2.24	0.43	0.11	0.50	0.07	0.45	0.11	0.33	0.04	0.30	0.04
M1S5s2	Malta	3.38	4.81	0.7265	3.04	0.61	0.15	0.64	0.09	0.62	0.14	0.42	0.05	0.34	0.05
M1S4	Malta	2.52	3.70	0.54	2.35	0.49	0.12	0.50	0.08	0.50	0.11	0.34	0.04	0.26	0.05
M1S10	Malta	2.49	3.83	0.57	2.30	0.48	0.11	0.50	0.07	0.48	0.10	0.28	0.04	0.28	0.04

Table 12: The LA-ICP-MS analyses results of the Sicilian chert samples. The elements MgO, Al₂O₃, SiO₂, CaO, TiO₂ and Fe₂O₃ have their values in wt%, while all elements are in part per million (ppm). BDL (Below Detection Limit) signifies a value for oxides or elements where the concentration is below the measured limit. All the Sicilian chert sample were measured with the second LA-ICP-MS instrument.

Samples	Location	MgO	Al ₂ O ₃	SiO ₂	CaO	TiO ₂	V	Mn	Fe ₂ O ₃	Ni	Rb	Sr	Y	Ba	Th	U	U/Th	V/(V+Ni)
S3	Southeast Sicily	0.20	0.12	96.88	2.66	0.01	2.41	3.81	0.13	13.52	0.35	192.16	3.94	3.02	0.28	2.82	9.94	0.15
SD	Valona River	0.03	0.66	98.99	0.05	0.03	2.86	5.87	0.07	1.16	3.72	42.66	0.96	28.14	0.53	0.20	0.38	0.71
S5	Valona River	0.36	0.18	98.85	0.55	<0.01	0.37	6.27	0.05	0.81	0.44	24.71	0.76	8.54	0.08	0.37	4.92	0.31
S6a	Valona River	0.03	0.71	98.99	0.06	0.04	5.18	7.33	0.06	1.01	3.97	42.92	0.61	31.48	0.286	0.151	0.53	0.84
S6b	Valona River	2.15	5.26	87.98	0.36	0.23	54.97	677.26	4.00	66.24	35.95	82.00	4.65	101.14	2.64	0.458	0.17	0.45
S7	Valona River	0.03	0.65	98.99	0.06	0.06	6.29	10.13	0.10	1.35	3.89	32.51	0.68	27.01	0.25	0.23	0.89	0.82
S10	Monte Judica	0.11	0.19	98.99	0.21	0.01	0.32	2.42	0.02	1.05	0.28	21.73	0.19	8.01	0.13	0.17	1.31	0.23
S14	Southeast Sicily	0.60	0.14	97.76	1.29	0.03	1.88	57.98	0.16	11.11	0.54	39.90	2.06	5.96	0.13	0.06	0.44	0.14
S15	Southeast Sicily	0.02	0.26	98.79	0.63	0.02	2.20	11.00	0.24	5.16	1.27	46.90	2.68	535.35	0.80	0.06	0.07	0.30
S16	Southeast Sicily	0.09	0.06	95.12	4.71	<0.01	2.50	35.3	0.01	1.04	0.46	42.14	1.46	34.53	0.05	2.88	57.70	0.71
S17	Southeast Sicily	0.02	0.09	98.68	1.13	0.01	4.18	8.66	0.06	80.09	0.28	13.13	0.46	3.57	2.43	0.30	0.12	0.05
S18	Southeast Sicily	0.01	0.20	98.99	0.12	0.01	4.51	1.55	0.09	2.03	1.86	5.14	1.04	3.75	0.11	2.67	23.18	0.69
S19	Southeast Sicily	0.08	0.26	98.99	BDL	0.07	7.14	142.52	0.57	225.61	2.35	4442.54	6.48	4096.65	12.55	0.56	0.04	0.03
S20	Southeast Sicily	0.01	0.13	98.99	0.12	0.02	2.95	1.48	0.09	16.58	0.44	5.14	1.73	1.77	1.68	0.32	0.19	0.15
S21	Southeast Sicily	0.01	0.16	98.99	0.06	0.02	2.33	0.53	0.02	1.12	0.47	4.35	1.31	43.81	0.39	0.53	1.37	0.67
S22r	West Sicily	0.01	0.29	98.99	0.07	0.02	2.05	2.12	0.16	1.22	1.71	3.48	0.98	19.05	0.25	0.11	0.45	0.63
S22p	West Sicily	0.01	0.20	98.99	0.04	<0.01	0.15	0.22	<0.01	0.43	0.28	3.62	0.08	19.94	0.17	0.15	0.85	0.25
S23	West Sicily	0.03	0.34	98.99	0.10	0.06	3.94	1.99	0.04	2.39	2.01	3.58	0.52	12.27	0.59	0.10	0.16	0.62
S24	West Sicily	0.02	0.21	96.11	0.03	0.01	1.82	5.88	3.58	1.30	1.91	2.43	0.29	4.24	0.16	0.06	0.39	0.58
S25	West Sicily	0.02	0.25	98.99	0.24	0.03	1.72	3.61	0.05	3.37	1.32	4.29	0.90	4.61	35.74	0.05	<0.01	0.34

Table 13: Second group of the LA-ICP-MS analyses results of the Sicilian chert samples. It includes the rare elements and their concentrations in part per million (ppm). All the Sicilian chert sample were measured with the second LA-ICP-MS instrument.

Samples	Location	La	Ce	Pr	Nd	Sm	Eu	Gd	Tb	Dy	Ho	Er	Tm	Yb	Lu
S3	Southeast Sicily	1.95	1.74	0.46	1.91	0.42	0.10	0.46	0.07	0.46	0.10	0.26	0.03	0.20	0.03
SD	Valona River	0.75	1.56	0.13	0.47	0.08	0.02	0.08	0.01	0.11	0.02	0.08	0.01	0.09	0.02
S5	Valona River	0.37	0.22	0.10	0.43	0.11	0.03	0.12	0.02	0.11	0.02	0.07	0.01	0.06	0.01
S6a	Valona River	1.06	3.16	0.29	1.07	0.22	0.04	0.15	0.02	0.13	0.02	0.08	0.01	0.09	0.01
S6b	Valona River	11.29	28.38	2.24	7.33	1.15	0.23	0.83	0.12	0.76	0.18	0.50	0.08	0.59	0.09
S7	Valona River	1.20	3.60	0.27	0.87	0.14	0.03	0.12	0.02	0.11	0.02	0.08	0.02	0.12	0.02
S10	Monte Judica	0.16	0.25	0.05	0.21	0.04	0.01	0.04	<0.01	0.04	0.01	0.02	<0.01	0.01	<0.01
S14	Southeast Sicily	1.66	1.54	0.36	1.01	0.37	0.15	0.15	0.04	0.26	0.05	0.20	0.016	0.13	0.02
S15	Southeast Sicily	1.78	1.37	0.35	1.53	0.31	0.08	0.38	0.06	0.41	0.09	0.25	0.03	0.22	0.03
S16	Southeast Sicily	0.99	0.47	0.14	0.63	0.14	0.04	0.16	0.04	0.20	0.04	0.13	0.02	0.11	0.02
S17	Southeast Sicily	0.45	0.39	0.08	0.32	0.06	0.01	0.06	0.01	0.06	0.01	0.0	<0.01	0.03	<0.01
S18	Southeast Sicily	0.78	0.63	0.15	0.63	0.12	0.03	0.12	0.02	0.10	0.03	0.07	0.01	0.05	0.01
S19	Southeast Sicily	4.86	3.29	0.86	4.24	1.51	0.23	1.60	0.16	0.74	0.18	0.68	0.07	1.67	0.07
S20	Southeast Sicily	1.04	0.95	0.22	0.83	0.17	0.04	0.20	0.02	0.16	0.04	0.09	0.01	0.07	0.01
S21	Southeast Sicily	0.95	0.90	0.20	0.83	0.17	0.04	0.17	0.02	0.14	0.03	0.06	0.01	0.06	0.01
S22r	West Sicily	0.93	0.89	0.25	1.07	0.22	0.06	0.27	0.04	0.26	0.06	0.13	0.02	0.09	0.01
S22p	West Sicily	0.05	0.05	0.01	0.05	0.01	<0.01	0.02	<0.01	0.01	<0.01	0.01	<0.01	0.01	<0.01
S23	West Sicily	0.44	0.52	0.15	0.50	0.11	0.03	0.10	0.02	0.07	0.02	0.04	<0.01	0.04	0.01
S24	West Sicily	0.27	0.53	0.06	0.25	0.05	0.01	0.04	0.01	0.04	0.01	0.02	<0.01	0.03	<0.01
S25	West Sicily	0.75	1.24	0.21	0.73	0.12	0.04	0.13	0.02	0.11	0.02	0.04	0.01	0.06	0.01

Artefact Samples

Table 14: The LA-ICP-MS analyses results of the Xagħra Circle samples (BR). The elements MgO, Al₂O₃, SiO₂, CaO, TiO₂ and Fe₂O₃ have their values in wt%, while all elements are in part per million (ppm). The N/A (Not Applicable) is imported to indicate that the values of an element had RSD and %REC outside the accepted values (RSD < 5 and 95% < %REC < 105%). The samples with blue colour have been measured with the first LA-ICP-MS instrument.

Samples	MgO	Al ₂ O ₃	SiO ₂	CaO	TiO ₂	V	Mn	Fe ₂ O ₃	Ni	Rb	Sr	Y	Ba	Th	U	U/Th	V/(V+Ni)
BR93/ S854/L897	0.23	0.48	98.75	0.15	0.04	7.94	30.31	0.34	10.21	3.62	11.18	3.98	35.35	0.88	3.36	3.82	0.44
BR88/ S110/L274	0.03	0.24	98.99	0.11	0.02	3.35	2.72	0.33	4.11	1.46	11.99	2.40	191.96	2.25	1.50	0.67	0.45
BR91/ S611/L712	0.03	0.28	98.99	0.13	0.03	4.10	6.85	0.22	9.97	1.54	12.19	5.21	104.09	60.47	0.22	<0.01	0.29
BR89/ S291/L334	0.06	0.69	98.50	0.08	0.05	6.05	4.26	0.60	3.04	5.38	7.35	1.90	10.25	0.67	1.38	2.07	0.67
BR93/S843/L41	0.04	0.28	98.99	0.18	0.02	2.55	3.15	0.09	2.77	1.77	3.55	0.48	9.01	22.67	0.58	0.03	0.48
BR89/ S395/L449	0.03	0.20	98.99	0.15	0.01	15.95	2.23	0.08	7.13	1.21	17.90	0.37	10.72	10.08	1.40	0.14	0.69
BR91/ S564/L662	0.01	0.25	98.99	0.09	0.01	2.18	0.77	0.14	1.00	0.48	5.73	2.01	4.36	1.46	0.37	0.26	0.69
BR91/ S745/L845	0.06	0.06	97.77	2.07	<0.01	5.19	1.21	0.02	3.32	0.27	143.25	0.95	2.77	0.91	6.19	6.78	0.61
BR91/ S1142/L1279	0.10	0.17	98.07	1.59	0.01	5.10	2.29	0.05	3.80	1.04	82.43	0.62	9.36	5.06	2.55	0.50	0.57
BR91/ L662/S566	2.04	1.61	62.04	7.59	0.10	20.50	39.7	0.44	13.43	6.19	138.35	6.49	N/A	1.03	2.21	2.14	0.60

Samples	La	Ce	Pr	Nd	Sm	Eu	Gd	Tb	Dy	Ho	Er	Tm	Yb	Lu
BR93/ S854/L897	2.37	2.72	0.55	2.38	0.49	0.10	0.56	0.08	0.50	0.11	0.27	0.03	0.21	0.03
BR88/ S110/L274	1.50	0.98	0.27	1.14	0.21	0.05	0.29	0.04	0.26	0.08	0.17	0.02	0.15	0.02
BR91/ S611/L712	3.42	1.66	0.55	2.22	0.43	0.11	0.64	0.08	0.65	0.12	0.36	0.05	0.36	0.04
BR89/ S291/L334	1.29	1.85	0.31	1.26	0.25	0.05	0.30	0.04	0.26	0.05	0.13	0.02	0.12	0.02
BR93/ S843/L41	0.40	0.66	0.08	0.42	0.08	0.01	0.08	0.01	0.06	0.01	0.03	0.01	0.05	0.01
BR89/ S395/L449	0.29	0.46	0.07	0.23	0.05	0.02	0.04	0.01	0.04	0.01	0.03	0.00	0.02	0.01
BR91/ S564/L662	1.29	0.90	0.26	1.24	0.23	0.05	0.31	0.04	0.26	0.06	0.14	0.01	0.11	0.02
BR91/ S745/L845	0.55	0.58	0.13	0.53	0.10	0.03	0.11	0.01	0.15	0.03	0.04	0.01	0.02	0.01
BR91/ S1142/L1279	0.50	0.60	0.10	0.36	0.08	0.02	0.10	0.01	0.09	0.02	0.04	0.00	0.05	0.01
BR91/L662/S566	5.25	10.40	1.17	5.27	1.35	0.22	0.87	0.13	0.84	0.18	0.52	0.07	0.43	0.08

Table 15: The LA-ICP-MS analyses results of the Kordin samples. The elements MgO, Al₂O₃, SiO₂, CaO, TiO₂ and Fe₂O₃ have their values in wt%, while all elements are in part per million (ppm). The N/A (Not Applicable) is imported to indicate that the values of an element had RSD and %REC outside the accepted values (RSD < 5 and 95% < %REC < 105%). The samples with blue colour have been measured with the first LA-ICP-MS instrument.

Samples	MgO	Al ₂ O ₃	SiO ₂	CaO	TiO ₂	V	Mn	Fe ₂ O ₃	Ni	Rb	Sr	Y	Ba	Th	U	U/Th	V/(V+Ni)
KRD15/S141 /L150	1.66	0.49	93.55	4.06	0.02	4.33	17.96	0.20	5.07	3.77	330.52	1.52	10.98	8.08	0.78	0.10	0.46
KDR15/ S42/L304	0.04	0.22	98.53	1.13	0.01	1.66	4.92	0.06	1.08	1.31	10.89	0.89	2.21	0.94	0.42	0.45	0.61
KDR15/ L201/S9	0.18	0.25	97.61	1.82	0.01	8.24	4.49	0.11	4.28	1.55	57.44	0.79	6.36	6.06	7.02	1.16	0.66
KDR15/ S195/L209	0.05	0.13	98.99	0.58	<0.01	4.49	2.04	0.05	1.41	0.80	17.69	0.54	1.47	0.17	11.97	71.55	0.76
KRD15/ S69/L211	0.04	0.11	97.85	1.93	<0.01	4.95	2.02	0.04	2.19	0.56	71.90	1.95	2.38	0.55	7.83	14.27	0.69
KDR15/ S27/L203	0.09	0.20	97.73	1.84	0.01	4.84	6.95	0.12	3.97	2.14	73.34	1.09	9.06	2.17	3.23	1.49	0.55
KRD15/ S144/L306	0.10	0.47	98.16	0.77	0.04	8.31	33.10	0.44	5.46	5.09	9.66	2.50	9.84	49.62	1.28	0.03	0.60
KRD15/S27/L207	0.04	0.11	98.99	0.54	0.01	9.00	2.57	0.06	4.06	1.00	28.93	0.73	3.27	1.22	16.24	13.34	0.69
KRD15/L71	0.03	0.27	98.99	0.07	0.01	3.23	4.05	0.11	2.60	3.21	3.35	3.53	4.21	1.36	1.39	1.02	0.55
KRD15/ S34/L207	0.02	0.15	98.99	0.35	<0.01	4.51	1.53	0.03	2.76	0.68	38.95	1.21	3.60	1.95	3.30	1.69	0.62
KRD15/L22/S1	0.94	1.48	61.45	10.03	0.07	16.30	12.50	0.40	8.25	7.43	211.33	4.30	N/A	0.70	2.43	3.50	0.66

Samples	La	Ce	Pr	Nd	Sm	Eu	Gd	Tb	Dy	Ho	Er	Tm	Yb	Lu
KRD15/S141 /L150	1.33	1.98	0.30	1.20	0.24	0.06	0.18	0.03	0.23	0.04	0.11	0.01	0.12	0.01
KDR15/ S42/L304	0.66	0.77	0.17	0.77	0.15	0.04	0.18	0.02	0.13	0.03	0.08	0.01	0.10	0.02
KDR15/ L201/S9	0.46	0.68	0.11	0.54	0.11	0.02	0.10	0.02	0.11	0.02	0.06	0.01	0.05	0.01
KDR15/ S195/L209	0.33	0.49	0.08	0.34	0.07	0.02	0.09	0.01	0.06	0.02	0.05	0.01	0.04	0.01
KRD15/ S69/L211	0.58	0.68	0.14	0.57	0.18	0.04	0.23	0.04	0.26	0.05	0.13	0.02	0.08	0.01
KDR15/ S27/L203	0.63	1.22	0.16	0.68	0.18	0.03	0.15	0.02	0.14	0.03	0.08	0.01	0.06	0.01
KRD15/ S144/L306	2.31	3.48	0.52	2.03	0.47	0.10	0.47	0.05	0.31	0.07	0.19	0.03	0.25	0.04
KRD15/S27/L207	0.51	0.78	0.12	0.50	0.10	0.02	0.11	0.02	0.19	0.04	0.06	0.01	0.05	0.01
KRD15/L71	2.96	2.32	0.60	2.32	0.44	0.09	0.40	0.06	0.49	0.09	0.23	0.04	0.23	0.04
KRD15/ S34/L207	0.27	0.48	0.07	0.25	0.07	0.02	0.13	0.02	0.16	0.04	0.14	0.02	0.18	0.03
KRD15/L22/S1	8.77	7.91	1.14	2.77	1.46	0.18	0.53	0.11	1.29	0.13	0.86	0.13	0.35	0.05

Table 16: The LA-ICP-MS analyses results of the Tač-Čawla samples. The elements MgO, Al₂O₃, SiO₂, CaO, TiO₂ and Fe₂O₃ have their values in wt%, while all elements are in part per million (ppm). The N/A (Not Applicable) is imported to indicate that the values of an element had RSD and %REC outside the accepted values (RSD < 5 and 95% < %REC <105%) or when a ration cannot be calculated. The samples with blue colour have been measured with the first LA-ICP-MS instrument.

Samples	MgO	Al ₂ O ₃	SiO ₂	CaO	TiO ₂	V	Mn	Fe ₂ O ₃	Ni	Rb	Sr	Y	Ba	Th	U	U/Th	V/(V+Ni)
TCC14/S252/L179	0.05	0.46	98.42	0.53	0.03	4.43	10.94	0.50	2.77	3.83	8.69	2.51	7.81	3.45	1.03	0.30	0.62
TCC14/S101/L85	0.09	0.44	98.83	0.34	0.03	6.70	8.99	0.25	5.55	4.36	10.17	7.19	18.19	1.12	3.67	3.28	0.55
TCC14/S275/L208	0.04	0.44	98.84	0.18	0.03	10.63	54.41	0.46	3.35	3.34	7.05	0.87	6.62	2.97	4.50	1.51	0.76
TCC14/S193/L69	0.22	1.11	97.96	0.18	0.03	23.82	15.30	0.49	6.24	6.82	8.52	0.52	12.60	66.86	2.61	0.04	0.79
TCC14/S144	0.06	0.48	98.65	0.27	0.05	5.55	5.16	0.47	2.55	4.73	6.37	0.84	10.27	1.82	0.34	0.19	0.69
TCC14/S416/L178	0.04	0.35	97.89	0.47	0.03	3.98	4.48	0.20	2.65	1.95	7.12	1.39	8.42	15.50	3.39	0.22	0.60
TCC14/S577/L131	0.07	0.54	98.99	0.11	0.03	3.61	3.62	0.12	4.78	3.02	3.78	2.42	8.30	60.07	0.07	0.00	0.43
TCC14/S162/L155	0.16	0.63	97.66	0.86	0.09	7.52	93.64	0.60	4.92	5.88	17.30	1.03	22.89	55.00	3.94	0.07	0.60
TCC14/S103/L85	0.05	0.33	98.90	0.32	0.02	3.89	4.24	0.35	3.37	3.61	11.11	21.08	6.67	8.21	0.31	0.04	0.54
TCC14/S316B/L63	2.09	0.24	94.09	3.40	0.02	3.33	8.72	0.15	6.05	2.92	106.34	2.67	9.66	1.76	1.18	0.67	0.36
TCC14/S460/L273	0.16	0.38	98.51	0.50	0.05	9.57	18.71	0.38	5.79	6.20	14.14	6.32	24.78	2.99	0.51	0.17	0.62
TCC14/S176/L100	0.51	0.58	81.88	15.91	0.12	28.33	58.66	0.99	15.34	18.59	116.73	4.32	39.28	15.02	4.29	0.29	0.65
TCC14/S32B/L30	0.13	0.14	97.81	1.81	0.01	25.80	3.80	0.09	5.75	0.93	77.73	0.94	4.04	1.91	10.94	5.74	0.82
TCC14/S567/L206	0.10	N/A	N/A	61.57	N/A	N/A	N/A	0.01	N/A	N/A	28.69	N/A	N/A	N/A	0.31	N/A	N/A
TCC14/S513/L272	9.83	0.63	21.33	19.70	0.03	17.60	28.80	0.22	4.11	8.10	314.00	4.13	N/A	0.80	2.09	2.59	0.81
TCC14/S502/L301	N/A	N/A	N/A	N/A	<0.01	N/A	N/A	N/A	N/A	N/A	N/A	N/A	N/A	N/A	0.28	N/A	N/A
TCC14/L30/S37	3.85	0.19	47.92	9.61	<0.01	1.38	3.60	0.02	N/A	0.43	790.00	1.08	N/A	N/A	0.54	N/A	N/A

Table 17: Second group of the LA-ICP-MS analyses results of the Tač-Čawla samples. It includes the rare elements and their concentrations in part per million (ppm). The N/A (Not Applicable) is imported to indicate that the values of an element had RSD and %REC outside the accepted values (RSD < 5 and 95% < %REC <105%). BDL (Below Detection Limit) signifies a value for oxides or elements where the concentration is below the measured limit. The samples with blue colour have been measured with the first LA-ICP-MS instrument.

Samples	La	Ce	Pr	Nd	Sm	Eu	Gd	Tb	Dy	Ho	Er	Tm	Yb	Lu
TCC14/ S252/L179	4.72	5.38	1.24	5.01	1.04	0.19	0.86	0.11	0.59	0.10	0.24	0.04	0.23	0.03
TCC14/ S101/L85	3.98	2.93	0.80	3.61	0.78	0.20	0.92	0.13	0.91	0.20	0.58	0.08	0.46	0.07
TCC14/ S275/L208	1.16	1.38	0.16	0.72	0.12	0.03	0.13	0.02	0.11	0.02	0.06	0.01	0.07	0.01
TCC14/ S193/L69	0.62	1.31	0.15	0.35	BDL	0.05	0.06	0.00	0.15	0.02	0.05	0.01	0.10	0.01
TCC14/S144	0.80	1.28	0.23	0.95	0.21	0.03	0.18	0.03	0.14	0.04	0.08	0.01	0.12	0.02
TCC14/ S416/L178	1.00	1.25	0.26	1.05	0.23	0.05	0.26	0.03	0.20	0.04	0.11	0.01	0.11	0.01
TCC14/ S577/L131	1.17	1.79	0.33	1.23	0.28	0.05	0.46	0.05	0.43	0.07	0.18	0.03	0.15	0.04
TCC14/ S162/L155	1.08	3.36	0.46	1.17	0.12	0.04	0.15	0.02	0.16	0.05	0.07	0.01	0.15	0.01
TCC14/ S103/L85	9.51	7.49	1.91	8.95	2.10	0.42	2.81	0.35	2.21	0.51	1.30	0.18	0.90	0.12
TCC14/ S316B/L63	1.96	2.51	0.50	2.14	0.50	0.11	0.54	0.07	0.46	0.08	0.20	0.03	0.16	0.02
TCC14/ S460/L273	4.41	2.90	0.69	2.92	0.61	0.14	0.81	0.10	0.72	0.16	0.53	0.09	0.48	0.07
TCC14/ S176/L100	5.23	9.90	1.03	3.72	0.95	0.22	1.20	0.10	0.61	0.13	0.75	0.04	0.32	0.04
TCC14/ S32B/L30	0.73	1.42	0.18	0.71	0.14	0.03	0.16	0.02	0.13	0.02	0.08	0.01	0.05	0.01
TCC14/L206/S567	N/A	N/A	N/A	N/A	N/A	N/A	N/A	N/A	N/A	N/A	N/A	N/A	N/A	N/A
TCC14/L272/S513	3.21	5.30	0.74	N/A	N/A	N/A	0.60	N/A	N/A	0.11	N/A	N/A	0.31	N/A
TCC14/L301/S502	0.14	N/A	N/A	N/A	N/A	N/A	N/A	N/A	N/A	N/A	N/A	N/A	N/A	N/A
TCC14/L30/S37	0.72	0.30	0.15	N/A	N/A	N/A	N/A	N/A	N/A	0.06	N/A	N/A	N/A	N/A

Table 18: The LA-ICP-MS analyses results of the Santa Verna samples. The elements MgO, Al₂O₃, SiO₂, CaO, TiO₂ and Fe₂O₃ have their values in wt%, while all elements are in part per million (ppm). The N/A (Not Applicable) is imported to indicate that the values of an element had RSD and %REC outside the accepted values (RSD < 5 and 95% < %REC <105%) or when a ratio cannot be calculated. BDL (Below Detection Limit) signifies a value for oxides or elements where the concentration is below the measured limit. The samples with blue colour have been measured with the first LA-ICP-MS instrument.

Samples	MgO	Al ₂ O ₃	SiO ₂	CaO	TiO ₂	V	Mn	Fe ₂ O ₃	Ni	Rb	Sr	Y	Ba	Th	U	U/Th	V/(V+Ni)
SV15/L80/S1	0.02	0.04	98.99	0.15	0.04	4.55	18.15	0.08	1.55	0.34	1.18	0.38	0.82	20.33	1.36	0.07	0.75
SV15/L4/S1	0.06	0.45	98.39	0.77	0.03	5.43	14.96	0.30	2.26	3.91	7.50	1.56	6.96	0.40	0.56	1.41	0.71
SV15/ L61/S1	0.12	0.36	98.35	0.97	0.02	8.46	8.41	0.17	5.64	2.81	48.53	0.85	4.82	7.32	1.43	0.20	0.60
SV15/ L41/S3	0.06	0.43	98.99	0.18	0.04	6.55	26.01	0.30	4.98	6.36	4.37	0.60	4.81	1.49	0.60	0.40	0.57
SV15/ L68/S1	0.04	0.33	98.99	0.28	0.02	3.10	5.34	0.24	2.38	1.98	8.60	4.45	5.23	0.97	2.30	2.38	0.57
SV15/ L36/S1	0.15	0.55	98.49	0.44	0.01	6.33	12.48	0.33	3.55	3.72	11.19	4.02	6.17	79.62	2.19	0.03	0.64
SV15/ S38/L8	0.03	0.38	98.99	0.12	0.03	6.83	8.66	0.24	3.52	3.38	5.85	9.46	4.87	8.07	0.93	0.12	0.66
SV15/ L52/S1	2.11	16.46	68.70	5.93	0.39	154.18	386.99	6.33	179.85	211.81	186.94	16.36	204.13	6.36	2.88	0.45	0.46
SV15/ L16/S1	0.24	0.08	90.00	9.15	<0.01	9.41	5.01	0.04	4.25	0.31	264.60	1.21	3.83	0.35	6.51	18.65	0.69
SV15/ L98/S1	0.12	0.54	97.79	1.23	0.01	8.33	30.46	0.29	5.98	3.25	42.05	1.34	10.96	7.44	6.33	0.85	0.58
SV15/ S1/L33	0.09	0.38	96.84	2.50	0.01	11.59	6.14	0.17	6.45	2.44	99.13	0.73	7.49	7.27	9.10	1.25	0.64
SV15/ L41/S2	0.28	0.17	97.09	2.11	0.03	30.63	16.93	0.29	13.35	4.46	108.54	1.18	8.46	2.53	9.04	3.58	0.70
SV15/L41/S1	0.16	0.39	98.39	0.70	0.03	5.96	17.92	0.31	3.49	5.36	12.67	1.15	6.06	39.91	1.22	0.03	0.63
SV15/ L17/S1	0.05	0.41	98.90	0.19	0.08	9.27	6.12	0.33	9.41	2.30	12.78	3.81	37.80	5.90	1.15	0.19	0.50
SV15/ S32/L5	0.16	0.33	98.40	0.91	0.02	14.51	9.14	0.17	9.60	3.17	59.39	0.96	6.23	3.54	4.92	1.39	0.60
SV15/L34/S1	0.45	0.10	34.66	4.93	N/A	1.73	4.91	N/A	N/A	N/A	291.33	0.88	N/A	0.06	0.30	4.72	N/A
SV15/S58/L134	1.06	1.15	55.62	8.63	0.04	10.48	16.30	0.30	5.01	7.00	N/A	4.58	N/A	0.38	1.34	3.52	0.68
SV15/L42/S144	1.12	0.16	N/A	N/A	0.01	4.88	N/A	N/A	N/A	1.94	N/A	1.10	N/A	N/A	0.25	N/A	N/A

Samples	La	Ce	Pr	Nd	Sm	Eu	Gd	Tb	Dy	Ho	Er	Tm	Yb	Lu
SV15/L80/S1	0.09	0.05	0.02	0.06	0.05	0.01	BDL	0.01	0.03	0.01	0.03	N/A	0.01	0.02
SV15/L4/S1	1.83	2.55	0.48	2.02	0.39	0.10	0.39	0.05	0.36	0.06	0.18	0.02	0.19	0.02
SV15/ L61/S1	0.80	1.23	0.15	0.76	0.16	0.03	0.16	0.02	0.12	0.02	0.06	0.01	0.04	0.01
SV15/ L41/S3	0.79	1.34	0.17	0.59	0.09	0.02	0.08	0.01	0.11	0.02	0.06	0.01	0.11	0.02
SV15/ L68/S1	2.90	1.88	0.53	2.36	0.47	0.10	0.66	0.10	0.59	0.12	0.37	0.04	0.27	0.04
SV15/ L36/S1	3.19	2.23	0.60	2.41	0.35	0.14	0.48	0.06	0.42	0.11	0.24	0.05	0.16	0.05
SV15/ S38/L8	5.19	3.98	1.04	4.48	0.86	0.20	1.18	0.18	1.09	0.25	0.73	0.08	0.47	0.07
SV15/ L52/S1	21.14	37.05	4.81	20.00	3.60	2.13	8.15	1.07	3.71	N/A	1.62	N/A	N/A	0.54
SV15/ L16/S1	0.84	0.97	0.18	0.71	0.13	0.03	0.16	0.02	0.15	0.03	0.08	0.01	0.08	0.01
SV15/ L98/S1	1.90	6.65	0.50	1.72	0.70	0.20	0.73	0.01	0.07	0.13	0.16	0.15	0.44	0.10
SV15/ S1/L33	0.98	1.68	0.21	0.77	0.14	0.02	0.14	0.02	0.12	0.03	0.06	0.01	0.04	0.01
SV15/ L41/S2	1.03	2.03	0.24	0.96	0.22	0.04	0.18	0.02	0.14	0.04	0.10	0.01	0.10	0.01
SV15/L41/S1	1.14	2.38	0.25	0.81	0.20	0.05	0.24	0.03	0.14	0.02	0.13	0.02	0.11	0.02
SV15/ L17/S1	2.22	1.96	0.61	2.77	0.56	0.14	0.65	0.08	0.50	0.11	0.28	0.04	0.21	0.03
SV15/ S32/L5	0.78	1.60	0.22	0.84	0.19	0.02	0.10	0.02	0.13	0.03	0.06	0.01	0.08	0.01
SV15/L34/S1	0.61	0.68	0.15	1.02	0.18	N/A	0.16	N/A	N/A	N/A	0.09	N/A	N/A	N/A
SV15/S58/L134	1.96	2.35	0.45	1.86	0.36	N/A	0.51	0.04	0.52	0.13	0.36	0.05	0.24	0.04
SV15/L42/S144	0.53	1.36	0.27	1.10	N/A	N/A	N/A	N/A	N/A	N/A	0.09	N/A	N/A	N/A

Table 19: The LA-ICP-MS analyses results of the Ġgantija samples. The elements MgO, Al₂O₃, SiO₂, CaO, TiO₂ and Fe₂O₃ have their values in wt%, while all elements are in part per million (ppm). The N/A (Not Applicable) is imported to indicate that the values of an element had RSD and %REC outside the accepted values (RSD < 5 and 95% < %REC <105%). The samples with blue colour have been measured with the first LA-ICP-MS instrument.

Samples	MgO	Al ₂ O ₃	SiO ₂	CaO	TiO ₂	V	Mn	Fe ₂ O ₃	Ni	Rb	Sr	Y	Ba	Th	U	U/Th	V/(V+Ni)
GG15/1019/S5	0.03	0.16	98.99	0.66	0.01	8.63	4.55	0.07	2.83	2.45	4.66	0.57	4.40	8.12	5.53	0.68	0.75
GG15/1019/S6	0.15	0.04	97.99	1.70	<0.01	11.63	0.84	0.02	3.11	0.23	61.36	0.54	1.08	4.32	13.57	3.14	0.79
GG15/1019/S7	0.07	0.04	98.79	1.08	<0.01	3.77	1.10	0.01	1.44	0.15	94.55	0.66	2.81	1.30	4.72	3.63	0.72
GG15/1019/S8	0.04	0.04	98.84	1.05	<0.01	7.02	0.45	0.01	2.03	0.18	56.73	0.57	1.59	3.67	16.47	4.49	0.78
GG15/1004/S1	0.07	0.04	98.19	1.65	<0.01	4.43	1.00	0.02	1.89	0.17	88.40	0.43	2.34	1.27	11.53	9.08	0.70
GG15/1004/S2	0.11	0.05	98.00	1.73	<0.01	5.45	1.01	0.01	1.34	0.22	75.22	0.35	1.60	0.16	2.55	15.48	0.80
GG15/L1016/S3	0.07	0.54	98.79	0.21	0.04	6.07	8.03	0.33	3.10	4.89	12.36	7.48	57.41	3.76	1.60	0.43	0.66
GG15/L008/S1	0.06	0.59	98.79	0.15	0.03	4.08	17.78	0.30	3.27	5.95	3.84	1.83	7.86	3.56	0.52	0.14	0.55
GG15/L1015/S3	0.16	0.86	96.34	1.67	0.05	193.48	44.18	0.96	54.65	7.27	16.85	2.69	16.02	68.19	1.71	0.03	0.78
GG15/L12/S1	2.18	1.80	61.18	13.81	0.06	31.50	22.00	0.39	17.50	11.40	271.00	7.57	N/A	1.02	3.35	3.28	0.64

Samples	La	Ce	Pr	Nd	Sm	Eu	Gd	Tb	Dy	Ho	Er	Tm	Yb	Lu
GG15/1019/S5	0.41	0.32	0.06	0.32	0.05	0.01	0.08	0.01	0.07	0.02	0.04	0.01	0.05	0.01
GG15/1019/S6	0.29	0.49	0.07	0.33	0.08	0.01	0.06	0.01	0.06	0.02	0.04	0.01	0.03	0.00
GG15/1019/S7	0.46	0.49	0.11	0.46	0.09	0.02	0.11	0.01	0.07	0.01	0.05	0.00	0.03	0.00
GG15/1019/S8	0.34	0.37	0.08	0.37	0.05	0.01	0.09	0.01	0.07	0.02	0.02	0.01	0.05	0.00
GG15/1004/S1	0.41	0.49	0.12	0.59	0.12	0.02	0.11	0.01	0.09	0.02	0.04	0.01	0.03	0.01
GG15/1004/S2	0.18	0.21	0.04	0.20	0.03	0.01	0.04	0.01	0.05	0.01	0.03	0.00	0.02	0.01
GG15/L1016/S3	5.39	3.86	1.09	5.15	1.09	0.24	1.13	0.16	1.06	0.20	0.55	0.08	0.47	0.07
GG15/L008/S1	0.99	1.58	0.23	0.94	0.19	0.04	0.21	0.03	0.28	0.05	0.14	0.02	0.13	0.02
GG15/L1015/S3	1.13	2.31	0.26	0.84	0.13	0.06	0.24	0.02	0.23	0.04	0.11	0.02	0.14	0.03
GG15/L12/S1	5.49	8.30	1.21	3.89	1.10	0.24	0.88	0.14	1.03	0.20	0.56	0.08	0.50	0.09

Table 20: The LA-ICP-MS analyses results of the Skorba samples. The elements MgO, Al₂O₃, SiO₂, CaO, TiO₂ and Fe₂O₃ have their values in wt%, while all elements are in part per million (ppm). The N/A (Not Applicable) is imported to indicate that the values of an element had RSD and %REC outside the accepted values (RSD < 5 and 95% < %REC < 105%) or when a ratio cannot be calculated. BDL (Below Detection Limit) signifies a value for oxides or elements where the concentration is below the measured limit. The samples with blue colour have been measured with the first LA-ICP-MS instrument.

Samples	MgO	Al ₂ O ₃	SiO ₂	CaO	TiO ₂	V	Mn	Fe ₂ O ₃	Ni	Rb	Sr	Y	Ba	Th	U	U/Th	V/(V+Ni)
SKD15/ S131/L211	0.11	0.13	98.90	0.84	<0.01	5.21	1.62	0.02	3.19	0.76	46.02	0.55	5.14	1.49	5.39	3.62	0.62
SKB16/L2/S1	0.38	1.28	52.41	0.97	0.05	10.90	27.00	0.34	3.21	7.29	26.60	1.40	N/A	0.49	0.26	0.54	0.77
SKB16/L2/S4	1.11	1.13	47.83	0.39	0.05	11.90	5.85	0.27	5.71	6.37	26.24	4.38	N/A	0.58	0.64	1.10	0.68
SKB16/L2/S5	0.62	1.06	48.51	0.91	0.04	9.52	24.60	0.30	5.15	7.02	21.75	0.68	N/A	0.18	0.38	2.15	0.65
SKB16/L2/S6	1.25	1.18	48.77	9.39	0.04	11.52	12.70	0.29	4.86	7.64	177.67	3.57	N/A	0.53	1.54	2.92	0.70
SKB16/L2/S7	0.86	0.98	51.77	7.68	0.04	1.54	14.40	0.25	12.50	5.25	106.40	0.78	N/A	0.09	0.47	5.40	0.11
SKB16/L2/S8	0.03	0.11	98.40	1.38	0.03	8.08	14.87	0.03	1.07	0.99	98.50	0.46	6838.27	5.63	0.50	0.09	0.88
SKB16/L5/S2	0.46	1.10	62.61	5.14	0.06	11.92	13.91	0.31	7.48	7.31	83.20	4.74	N/A	0.51	1.32	2.60	0.61
SKB16/L5/S3	0.80	1.06	48.18	5.97	0.05	9.49	20.85	0.25	5.30	4.81	87.60	2.19	N/A	0.54	1.68	3.14	0.64
SKB16/L5/S4	1.31	1.06	44.74	7.47	0.04	14.33	36.10	0.21	3.43	5.24	127.63	5.34	N/A	0.65	1.53	2.33	0.81
SKB16/L5/S5	0.26	1.03	47.50	0.45	0.05	11.20	7.80	0.46	N/A	6.42	18.68	0.39	N/A	0.24	0.41	1.76	1.00
SKB16/L10/S7	0.28	1.36	50.70	2.33	0.01	13.56	10.65	0.43	9.86	7.30	N/A	2.22	N/A	0.59	0.24	0.41	0.58
SKB16/L10/S8	0.75	1.22	55.41	7.04	0.01	22.35	12.14	0.33	10.45	5.94	82.00	3.95	N/A	0.54	1.95	3.58	0.68
SKB16/L10/S9	0.88	1.42	65.11	11.41	0.02	19.49	397.00	0.31	13.17	7.44	96.00	3.55	N/A	0.46	2.04	4.41	0.60
SKB16/L10/S10	0.68	1.47	73.37	8.91	0.01	16.32	N/A	0.39	11.66	5.55	82.00	3.53	N/A	0.63	2.13	3.37	0.58
SKB16/L10/S11	0.85	1.64	60.97	12.27	0.02	31.62	15.10	0.43	8.67	8.63	152.50	5.60	N/A	0.95	3.16	3.32	0.78
SKB16/L10/S12	0.95	1.81	58.51	5.81	0.02	30.67	960.00	0.62	10.99	9.54	N/A	6.23	N/A	0.75	1.68	2.25	0.74
SKB16/L10/S13	0.57	0.99	58.83	1.34	0.01	9.81	13.31	0.26	6.58	4.28	N/A	2.30	N/A	0.58	0.90	1.56	0.60
SKB16/L10/S14	0.58	0.99	77.87	3.78	0.01	32.50	11.7	0.24	8.40	6.28	N/A	6.17	N/A	0.66	3.57	5.39	0.79
SKB16/L10/S15	0.39	N/A	N/A	59.68	0.03	6.80	37.9	N/A	N/A	N/A	76.67	4.40	0.19	0.14	1.24	8.72	N/A
SKB16/L10/S16	1.20	1.07	44.92	7.95	0.01	17.10	16.2	0.51	11.30	7.36	100.00	5.30	N/A	0.56	1.77	3.18	0.60
SKB16/L10/S18	0.53	2.06	N/A	55.13	0.03	6.63	N/A	0.21	2.74	2.86	121.00	4.65	N/A	0.32	0.55	1.73	0.71
SKB16/L12/S6	0.01	0.13	98.99	BDL	0.01	1.22	BDL	0.32	0.69	1.34	6.44	0.66	0.60	2.17	1.49	0.69	0.64
SKB16/L12b/S1	1.04	1.10	57.76	12.09	0.04	10.60	340.00	0.30	9.49	5.92	236.47	5.05	N/A	0.51	1.59	3.11	0.53
SKB16/L12b/S2	0.89	1.16	44.60	7.78	0.04	10.76	11.18	0.27	5.10	5.11	148.20	3.94	N/A	0.53	1.43	2.70	0.68
SKB16/L12b/S3	0.60	0.02	N/A	66.33	<0.01	0.69	16.00	0.02	N/A	N/A	184.61	N/A	N/A	N/A	1.20	N/A	N/A
SKB16/L12b/S4	0.39	0.60	41.19	1.27	0.03	8.19	5.02	0.17	4.83	3.51	28.48	1.88	N/A	0.26	0.63	2.39	0.63
SKB16/L12b/S5	1.11	1.21	52.52	11.87	0.06	11.19	15.53	0.30	8.71	7.04	202.63	5.03	N/A	0.77	1.67	2.16	0.56
SKB16/L13/S4	0.67	0.93	51.49	5.06	0.03	9.07	N/A	0.21	9.21	4.66	68.77	2.89	N/A	0.44	0.90	2.06	0.50
SKB16/L13/S5	1.87	1.27	50.08	10.52	0.06	13.12	22.60	0.35	9.53	6.28	204.50	20.50	N/A	0.71	1.16	1.64	0.58
SKB16/L13/S6	1.66	1.08	51.34	5.97	0.05	16.54	19.30	0.28	6.55	7.65	131.53	3.51	N/A	0.49	1.44	2.93	0.72

SKB16/L13/S7	0.28	1.11	49.01	4.79	0.04	10.59	14.74	0.29	7.67	5.57	103.80	6.83	N/A	N/A	1.10	N/A	0.58
SKB16/L13/S8	0.49	1.34	54.41	4.99	0.06	11.69	20.17	0.31	7.79	9.07	56.80	1.08	N/A	0.54	0.37	0.69	0.60
SKB16/L13/S9	0.40	0.06	N/A	65.95	N/A	1.25	24.50	0.04	N/A	N/A	120.43	2.44	N/A	0.11	0.41	3.86	N/A
SKB16/L13/S10	0.35	0.01	N/A	65.16	N/A	0.68	4.69	0.01	N/A	N/A	132.03	14.49	N/A	N/A	0.77	N/A	N/A
SKB16/L13/S11	0.07	0.28	43.21	1.92	0.02	8.03	N/A	0.15	4.11	2.24	34.95	1.25	N/A	0.15	0.53	3.50	0.66
SKB16/L13/S12	0.02	0.23	98.99	0.04	0.01	3.22	8.23	0.14	0.90	1.78	2.69	0.79	11.19	1.88	0.67	0.35	0.78
SKB16/L13/S13	0.04	0.04	97.70	2.11	<0.01	35.38	2.17	0.08	5.23	0.16	100.26	0.54	3.56	0.86	5.55	6.43	0.87
SKB16/L16/S1	0.85	0.81	44.85	7.69	0.03	10.79	12.34	0.27	5.76	4.94	140.64	3.65	N/A	0.48	1.29	2.68	0.65
SKB16/L16/S2	1.39	1.68	48.70	22.56	0.08	18.23	42.97	0.47	9.93	9.27	385.00	7.71	N/A	1.07	2.18	2.03	0.65
SKB16/L16/S3	0.01	0.08	98.99	0.07	<0.01	2.68	1.90	0.02	1.03	0.39	2.58	0.41	0.79	0.43	1.79	4.14	0.72
SKB16/L19/S2	0.54	1.34	89.03	8.69	0.02	16.37	23.00	0.38	5.27	7.96	124.00	5.84	N/A	0.65	1.34	2.05	0.76
SKB16/L19/S4	0.63	0.99	34.43	9.89	0.02	12.05	100.00	0.19	4.19	7.67	132.60	2.18	N/A	0.58	1.15	1.98	0.74
SKB16/L19/S3	0.92	0.77	33.28	13.57	0.02	15.61	11.04	0.32	8.00	5.63	151.00	4.84	N/A	0.46	0.87	1.88	0.66
SKB16/L20/S2	0.62	1.26	81.50	8.77	0.02	13.90	26.80	0.26	12.25	6.99	147.00	4.48	N/A	0.64	1.85	2.91	0.53
SKB16/L23/S1	0.17	0.68	24.57	0.32	0.03	6.91	158.52	0.19	9.93	6.00	18.04	N/A	N/A	N/A	0.08	N/A	0.41
SKB16/L23/S2	0.56	0.70	28.90	3.78	0.05	9.66	N/A	0.18	4.46	5.77	76.60	2.77	N/A	0.40	0.91	2.25	0.68
SKB16/L23/S3	0.44	0.39	24.97	4.03	0.01	6.66	44.07	0.14	3.44	2.13	77.47	1.53	N/A	0.19	0.99	5.13	0.66
SKB16/L23/S4	0.30	0.45	25.63	3.46	0.02	6.88	4.08	0.14	3.38	2.89	64.20	2.06	N/A	0.26	0.73	2.81	0.67
SKB16 L23/S5	0.08	0.30	36.15	0.27	0.02	3.60	3.83	0.12	3.77	2.47	26.70	1.51	N/A	0.23	0.32	1.40	0.49
SKB16/L23/S7	0.02	0.27	98.99	0.09	0.03	4.27	7.19	0.23	1.40	1.96	3.18	0.56	17.82	7.09	0.81	0.11	0.75
SKB16/L23/S8	0.03	0.35	98.99	0.07	0.03	5.01	3.40	0.20	1.91	3.20	3.96	2.10	8.78	0.20	0.46	2.28	0.72
SKB16/L26/S1	1.23	1.47	69.63	11.45	0.02	18.55	20.27	0.36	13.28	10.26	105.00	5.91	N/A	0.70	2.41	3.47	0.58
SKB16/L26/S6	1.13	1.15	53.12	9.68	0.02	17.36	11.60	0.33	8.53	6.73	155.50	6.41	N/A	0.65	1.76	2.71	0.67
SKB16/L26/S7	0.86	0.81	70.38	9.29	0.01	12.93	12.32	0.23	7.91	6.25	108.00	3.70	N/A	0.46	1.10	2.41	0.62
SKB16/L26/S8	0.71	1.37	83.42	14.13	0.03	15.00	16.80	0.33	5.34	6.60	82.00	5.24	N/A	0.58	1.12	1.92	0.74
SKB16/L30/S1	0.99	0.83	43.68	9.89	0.06	12.86	9.82	0.25	7.34	5.31	173.20	3.35	N/A	0.38	1.46	3.79	0.64
SKB16/L30/S2	1.12	0.99	47.70	9.93	0.04	10.07	15.19	0.28	7.60	6.93	184.35	3.77	N/A	0.54	1.63	3.04	0.57
SKB16/L30/S3	0.98	1.13	55.12	11.22	0.07	18.55	16.50	0.53	9.27	13.20	171.00	6.14	N/A	0.78	1.64	2.09	0.67
Skb16/L30/S4	0.09	0.42	98.96	0.27	0.05	4.58	16.94	0.21	3.32	1.96	6.03	1.81	1.45	12.48	0.44	0.04	0.58

Table 21: Second group of the LA-ICP-MS analyses results of the Skorba samples. It includes the rare elements and their concentrations in part per million (ppm). The N/A (Not Applicable) is imported to indicate that the values of an element had RSD and %REC outside the accepted values (RSD < 5 and 95% < %REC <105%). The samples with blue colour have been measured with the first LA-ICP-MS instrument.

Samples	La	Ce	Pr	Nd	Sm	Eu	Gd	Tb	Dy	Ho	Er	Tm	Yb	Lu
SKD15/ S131/L211	0.32	0.47	0.08	0.29	0.08	0.01	0.08	0.01	0.06	0.02	0.04	0.01	0.04	0.01
SKB16/L2/S1	2.06	3.59	0.50	1.84	0.35	0.10	0.32	0.04	0.26	0.05	0.23	0.03	0.13	0.01
SKB16/L2/S4	2.78	4.75	0.68	2.76	0.55	0.15	0.62	0.08	0.54	0.12	0.35	0.05	0.27	0.04
SKB16/L2/S5	1.06	1.69	0.22	0.87	0.12	0.03	N/A	N/A	0.09	0.02	0.05	N/A	N/A	0.01
SKB16/L2/S6	2.21	3.84	0.58	1.94	0.40	0.13	0.53	0.07	0.46	0.10	0.28	0.04	0.32	0.05
SKB16/L2/S7	0.42	0.70	0.10	0.47	0.56	N/A	0.62	0.10	0.43	0.09	0.31	0.03	N/A	0.05
SKB16/L2/S8	0.56	0.34	0.06	0.15	0.10	0.09	0.10	0.01	0.04	0.01	0.02	0.02	0.05	0.01
SKB16/L5/S2	3.21	4.92	0.75	3.66	0.61	0.15	0.62	0.12	0.59	0.12	0.38	0.06	0.31	0.06
SKB16/L5/S3	1.72	3.44	0.44	1.77	0.32	0.08	0.33	0.05	0.31	0.06	0.18	0.03	0.15	N/A
SKB16/L5/S4	3.46	5.30	0.80	3.31	0.81	0.16	0.65	0.10	0.64	0.14	0.41	0.07	0.43	0.06
SKB16/L5/S5	1.04	1.82	0.23	0.83	0.27	0.08	0.27	0.02	0.10	0.02	0.11	N/A	0.12	N/A
SKB16/L10/S7	2.88	6.00	0.64	2.68	0.56	0.12	0.44	0.07	0.40	0.08	0.22	0.03	N/A	N/A
SKB16/L10/S8	3.13	4.47	0.62	2.72	0.54	0.14	0.60	0.08	0.48	0.11	0.30	0.04	0.29	0.04
SKB16/L10/S9	3.67	5.95	0.82	2.73	0.61	0.11	0.47	0.06	0.26	0.13	0.28	0.05	0.39	0.05
SKB16/L10/S10	1.97	3.04	0.45	2.31	0.40	0.14	0.38	0.07	0.57	0.09	0.27	0.04	0.24	0.05
SKB16/L10/S11	4.67	7.50	1.13	3.03	0.90	0.20	0.56	0.10	0.55	0.16	0.44	0.07	0.35	0.06
SKB16/L10/S12	4.54	9.36	1.23	4.67	0.90	0.24	0.96	0.13	0.76	0.17	0.50	0.07	0.48	0.06
SKB16/L10/S13	1.85	2.79	0.46	1.93	0.35	0.08	0.26	0.05	0.33	0.06	0.15	0.03	0.17	0.02
SKB16/L10/S14	3.73	5.63	0.82	3.64	0.75	0.14	0.80	0.11	0.57	0.16	0.44	0.03	0.26	0.05
SKB16/L10/S15	2.15	N/A	0.32	1.70	0.43	0.14	0.31	0.05	0.34	0.09	0.27	0.03	0.30	0.05
SKB16/L10/S16	3.01	5.43	0.81	2.92	0.47	0.17	0.66	0.10	0.53	0.12	0.36	0.06	0.36	0.06
SKB16/L10/S18	1.96	5.43	0.35	1.74	0.24	0.09	0.43	0.05	0.34	0.13	0.22	0.03	0.22	0.04
SKB16/L12/S6	0.26	0.46	0.09	0.29	0.15	0.01	0.06	0.02	0.11	0.02	0.07	0.01	0.08	0.01
SKB16/L12b/S1	3.55	5.13	0.75	1.84	0.65	0.14	0.66	0.09	0.63	0.13	0.38	0.06	0.34	0.05
SKB16/L12b/S2	2.75	4.05	0.62	2.44	0.52	0.12	0.56	0.07	0.47	0.10	0.30	0.04	0.27	0.04
SKB16/L12b/S3	N/A	N/A	N/A	N/A	N/A	N/A	N/A	N/A	N/A	N/A	N/A	N/A	N/A	N/A
SKB16/L12b/S4	1.69	2.53	0.32	1.65	0.36	0.08	0.37	0.04	0.35	0.08	0.22	0.03	0.17	0.03
SKB16/L12b/S5	3.27	5.21	0.81	3.42	0.74	0.14	0.73	0.10	0.63	0.14	0.35	0.05	0.32	0.05
SKB16/L13/S4	2.25	3.36	0.53	2.19	0.56	0.07	0.46	0.07	0.41	0.10	0.35	0.05	0.23	0.05
SKB16/L13/S5	6.16	13.10	2.25	9.90	0.67	0.50	2.30	0.22	1.39	0.32	0.35	0.12	0.28	0.04
SKB16/L13/S6	2.31	3.21	0.46	1.88	0.34	0.09	0.39	0.07	0.40	0.09	0.22	0.04	0.28	0.03
SKB16/L13/S7	0.94	1.67	1.05	0.81	0.13	0.03	0.93	0.13	0.11	0.18	0.57	0.07	0.43	0.07

SKB16/L13/S8	1.59	2.63	0.37	1.04	0.31	0.07	0.18	0.04	0.15	0.05	0.09	N/A	N/A	0.01
SKB16/L13/S9	1.60	1.92	0.33	1.43	0.29	0.07	0.25	0.04	0.30	0.06	0.18	N/A	0.22	N/A
SKB16/L13/S10	5.73	0.90	0.91	3.53	1.21	0.21	1.16	0.14	0.85	0.23	0.65	0.07	0.47	0.05
SKB16/L13/S11	N/A	N/A	N/A	N/A	0.17	N/A	0.17	0.03	0.20	0.04	0.10	N/A	0.08	N/A
SKB16/L13/S12	0.53	0.48	0.10	0.38	0.06	0.02	0.08	0.01	0.10	0.02	0.05	0.01	0.06	0.01
SKB16/L13/S13	0.46	0.93	0.10	0.39	0.09	0.03	0.08	0.01	0.07	0.02	0.05	0.00	0.04	0.01
SKB16/L16/S1	2.85	4.02	0.65	2.64	0.52	0.12	0.56	0.08	0.53	0.09	0.27	0.05	0.34	0.03
SKB16/L16/S2	5.22	7.82	1.18	4.85	1.05	0.23	1.02	0.15	0.96	0.21	0.61	0.08	0.54	0.08
SKB16/L16/S3	0.34	0.25	0.07	0.28	0.05	0.01	0.05	0.01	0.04	0.01	0.02	0.00	0.02	0.00
SKB16/L19/S2	3.57	4.95	0.95	3.92	1.00	0.14	0.99	0.08	0.88	0.19	0.54	0.07	0.40	0.07
SKB16/L19/S4	2.04	4.02	0.50	N/A	0.42	0.11	0.43	0.05	0.45	0.09	0.10	0.03	0.60	0.03
SKB16/L19/S3	4.07	4.04	0.60	3.71	0.45	0.12	0.63	0.03	0.61	0.10	0.40	0.06	0.12	0.04
SKB16/L20/S2	3.31	5.19	0.67	3.07	0.70	0.16	0.67	0.10	0.52	0.16	0.42	0.06	0.32	0.06
SKB16/L23/S1	0.39	1.31	0.06	0.29	N/A	N/A	N/A	N/A	N/A	N/A	N/A	N/A	N/A	N/A
SKB16/L23/S2	2.14	3.39	0.47	1.81	0.37	0.08	0.38	0.08	0.33	0.07	0.22	0.04	0.21	0.03
SKB16/L23/S3	0.71	1.29	0.17	0.60	0.14	N/A	N/A	0.03	0.17	0.04	0.11	0.03	0.13	N/A
SKB16/L23/S4	1.50	2.35	0.30	1.36	0.25	0.06	0.25	0.03	0.23	0.04	0.16	0.02	0.10	0.02
SKB16 L23/S5	1.07	1.37	0.25	1.05	0.23	0.05	0.21	0.03	0.22	0.05	0.12	0.02	0.07	0.01
SKB16/L23/S7	0.31	0.32	0.10	0.59	0.03	0.02	0.09	0.01	0.05	0.02	0.06	0.01	0.03	0.01
SKB16/L23/S8	1.16	1.06	0.21	0.82	0.14	0.04	0.19	0.03	0.17	0.04	0.12	0.01	0.10	0.01
SKB16/L26/S1	3.43	4.76	0.80	3.00	0.72	0.17	0.73	0.09	0.72	0.16	0.40	0.05	0.40	0.07
SKB16/L26/S6	4.05	5.38	0.92	3.77	0.89	0.25	0.82	0.09	0.72	0.15	0.43	0.07	0.42	0.05
SKB16/L26/S7	2.37	3.93	0.57	2.10	0.43	0.11	0.51	0.07	0.39	0.10	0.24	0.03	0.27	0.04
SKB16/L26/S8	5.08	4.43	1.13	2.60	0.95	0.32	0.54	0.08	0.74	0.17	0.32	0.05	0.54	0.08
SKB16/L30/S1	2.26	2.68	0.53	2.05	0.44	0.09	0.47	0.06	0.40	0.09	0.27	0.03	0.20	0.03
SKB16/L30/S2	1.77	3.52	0.40	1.58	0.31	0.14	0.32	0.07	0.29	0.07	0.21	0.03	0.26	0.02
SKB16/L30/S3	4.05	5.75	0.87	3.70	0.71	0.16	0.79	0.11	0.72	0.16	0.38	0.06	0.40	0.06
Skb16/L30/S4	1.47	0.99	0.22	0.99	0.16	0.04	0.29	0.02	0.20	0.05	0.10	0.03	0.07	0.01

Table 22: The ratios representing the relative fractionations of the rare earth elements (REE) in the chert samples. The N/A (Not Applicable) is imported when a ration between elements cannot be calculated.

Sample	Ce/Ce*	La _n /Ce _n	La _n /Lu _n
Ridge	~0.29	>3.5	~0.65
Oceanic	~0.58	2 < > 3	~2.7
Continental	~1.03	~1	~1.15
F1S4	0.72	1.50	0.93
G1S1	0.86	1.16	1.04
G1S2	N/A	N/A	N/A
G2S2	0.74	1.45	0.87
G2S1	0.81	1.21	0.71
G2S3	0.71	1.52	1.04
G2S6	0.76	1.35	1.11
M1S6	0.73	1.24	0.62
M1S8	0.90	1.16	1.33
M1S11	0.83	1.27	0.75
M1S9	0.83	1.21	1.41
M1S5v	0.76	1.35	0.89
M2S4	0.92	1.30	0.83
M2S2	1.31	0.86	N/A
F1S2	0.36	0.33	0.03
F1S3	0.79	1.35	0.88
M1S1	0.26	6.57	3.18
M1S1b	0.77	1.30	0.89
M1S2	0.74	1.41	0.97
M1S3	0.78	1.34	0.95
M1S5s	0.81	1.30	0.87
M1S5s2	0.75	1.42	0.94
M1S4	0.78	1.37	0.75
M1S10	0.79	1.32	0.90
S3	0.45	2.26	1.06
SD	1.19	0.98	0.59
S5	0.28	3.45	0.66
S6a	1.39	0.68	1.12
S6b	1.37	0.80	1.91
S7	1.55	0.67	1.01
S10	0.69	1.26	0.91
S14	0.48	2.18	1.26
S15	0.42	2.63	0.83
S16	0.29	4.32	0.81
S17	0.50	2.37	1.14
S18	0.44	2.49	1.22
S19	0.39	2.99	1.06
S20	0.49	2.21	1.12
S21	0.50	2.13	2.04
S22r	0.45	2.12	1.38
S22p	0.48	2.18	0.54
S23	0.50	1.70	0.76

S24	1.01	1.01	1.28
S25	0.77	1.22	1.37

Table 23: The ratios representing the relative fractionations of the rare earth elements (REE) in the artefact samples. The N/A (Not Applicable) is imported when a ration between elements cannot be calculated.

Sample	Ce/Ce*	La _n /Ce _n	La _n /Lu _n
Ridge	0.29	>3.5	0.65
Oceanic	0.58	2 < > 3	2.7
Continental	~1.03	~1	~1.15
BR93/ S854/L897	0.58	1.77	1.10
BR88/ S110/L274	0.37	3.10	1.22
BR91/ S611/L712	0.29	4.16	1.17
BR89/ S291/L334	0.71	1.42	1.16
BR93/ S843/L41	0.89	1.22	0.61
BR89/ S395/L449	0.78	1.29	0.40
BR91/ S564/L662	0.38	2.91	1.28
BR91/ S745/L845	0.54	1.92	0.82
BR91/ S1142/L1279	0.65	1.68	1.17
BR91/L662/S566	1.03	1.02	1.01
KRD15/S141 /L150	0.76	1.36	1.39
KDR15/ S42/L304	0.57	1.72	0.53
KDR15/ L201/S9	0.74	1.37	1.00
KDR15/ S195/L209	0.73	1.36	0.72
KRD15/ S69/L211	0.59	1.75	0.66
KDR15/ S27/L203	0.95	1.04	1.08
KRD15/ S144/L306	0.78	1.34	0.83
KDR15/ S27/L203	0.77	1.33	0.85
KRD15/L71	0.43	2.58	1.24
KRD15/ S34/L207	0.83	1.13	0.15
KRD15/L22/S1	0.58	2.24	2.46
TCC14/ S252/L179	0.54	1.78	2.07
TCC14/ S101/L85	0.40	2.75	0.79
TCC14/ S275/L208	0.76	1.70	1.69
TCC14/ S193/L69	1.07	0.96	0.88
TCC14/S144	0.73	1.27	0.67
TCC14/ S416/L178	0.60	1.61	1.27
TCC14/ S577/L131	0.71	1.32	0.47
TCC14/ S162/L155	1.13	0.65	1.25
TCC14/ S103/L85	0.43	2.57	1.17
TCC14/ S316B/L63	0.62	1.58	1.45
TCC14/ S460/L273	0.40	3.08	1.01
TCC14/ S176/L100	1.04	1.07	2.06
TCC14/ S32B/L30	0.95	1.04	1.06
TCC14/L206/S567	N/A	N/A	N/A
TCC14/L272/S513	0.84	1.23	N/A
TCC14/L301/S502	N/A	N/A	N/A
TCC14/L30/S37	0.23	4.79	N/A
SV15/L80/S1	0.30	3.77	0.07
SV15/L4/S1	0.66	1.45	1.60
SV15/ L61/S1	0.86	1.32	1.73
SV15/ L41/S3	0.91	1.19	0.66
SV15/ L68/S1	0.37	3.13	1.15
SV15/ L36/S1	0.39	2.90	1.00
SV15/ S38/L8	0.42	2.64	1.04
SV15/ L52/S1	0.90	1.15	0.59
SV15/ L16/S1	0.62	1.76	1.95
SV15/ L98/S1	1.67	0.58	0.29
SV15/ S1/L33	0.92	1.18	2.23
SV15/ L41/S2	1.00	1.02	1.47
SV15/L41/S1	1.08	0.97	0.70

SV15/ L17/S1	0.41	2.29	1.05
SV15/ S32/L5	0.94	0.98	0.91
SV15/L34/S1	0.56	1.82	N/A
SV15/S58/L134	0.62	1.69	0.76
SV15/L42/S144	0.84	0.79	N/A
GG15/ 1019/S5	0.47	2.60	0.83
GG15/1019/S6	0.84	1.19	0.95
GG15/ 1019/S7	0.53	1.90	1.61
GG15/ 1019/S8	0.55	1.84	1.59
GG15/ 1004/S1	0.55	1.69	0.52
GG15/ 1004/S2	0.61	1.73	0.49
GG15/ L1016 /S3	0.39	2.83	1.21
GG15/ L008/S1	0.82	1.27	0.81
GG15/ L1015/S3	1.04	0.99	0.56
SKD15/ S131/L211	0.75	1.37	0.92
SKB16/L2/S1	0.86	1.16	2.29
SKB16/L2/S4	0.85	1.18	1.04
SKB16/L2/S5	0.85	1.27	2.05
SKB16/L2/S6	0.83	1.17	0.71
SKB16/L2/S7	0.84	1.22	0.14
SKB16/L2/S8	0.41	3.35	0.77
SKB16/L5/S2	0.78	1.32	0.82
SKB16/L5/S3	0.97	1.01	N/A
SKB16/L5/S4	0.78	1.32	0.92
SKB16/L5/S5	0.91	1.16	N/A
SKB16/L10/S7	1.08	0.97	N/A
SKB16/L10/S8	0.78	1.42	1.05
SKB16/L10/S9	0.84	1.25	1.10
SKB16/L10/S10	0.79	1.31	0.65
SKB16/L10/S11	0.80	1.26	1.16
SKB16/L10/S12	0.97	0.98	1.06
SKB16/L10/S13	0.74	1.34	1.29
SKB16/L10/S14	0.79	1.34	1.13
SKB16/L10/S15	N/A	N/A	0.67
SKB16/L10/S16	0.85	1.12	0.72
SKB16/L10/S18	1.58	0.73	0.71
SKB16/L12/S6	0.75	1.13	0.30
SKB16/L12b/S1	0.77	1.40	1.10
SKB16/L12b/S2	0.76	1.38	1.00
SKB16/L12b/S3	N/A	N/A	N/A
SKB16/L12b/S4	0.84	1.36	0.98
SKB16/L12b/S5	0.79	1.27	0.94
SKB16/L13/S4	0.76	1.35	0.72
SKB16/L13/S5	0.85	0.95	2.12
SKB16/L13/S6	0.76	1.45	1.06
SKB16/L13/S7	0.32	1.14	0.21
SKB16/L13/S8	0.84	1.22	2.85
SKB16/L13/S9	0.64	1.68	N/A
SKB16/L13/S10	0.09	12.83	1.74
SKB16/L13/S11	N/A	N/A	N/A
SKB16/L13 /S12	0.51	2.24	0.77
SKB16/L13/S13	1.09	0.99	0.88
SKB16/L16/S1	0.72	1.44	1.57
SKB16/L16/S2	0.77	1.35	0.97
SKB16/L16/S3	0.39	2.79	1.91
SKB16/L19/S2	0.66	1.46	0.75
SKB16/L19/S4	0.97	1.03	1.16
SKB16/L19/S3	0.61	2.04	1.38
SKB16/L20/S2	0.85	1.29	0.87
SKB16/L23/S1	2.04	0.61	N/A
SKB16/L23/S2	0.83	1.27	0.95
SKB16/L23/S3	0.90	1.11	N/A

SKB16/L23/S4	0.86	1.29	0.97
SKB16 L23/S5	0.64	1.58	1.34
SKB16/L23/S7	0.45	1.96	0.37
SKB16/L23/S8	0.52	2.22	1.25
SKB16/L26/S1	0.71	1.46	0.78
SKB16/L26/S6	0.68	1.52	1.17
SKB16/L26/S7	0.83	1.22	0.79
SKB16/L26/S8	0.45	2.32	0.91
SKB16/L30/S1	0.60	1.71	1.21
SKB16/L30/S2	1.03	1.02	1.06
SKB16/L30/S3	0.75	1.43	0.99
Skb16/L30/S4	0.41	2.99	1.85

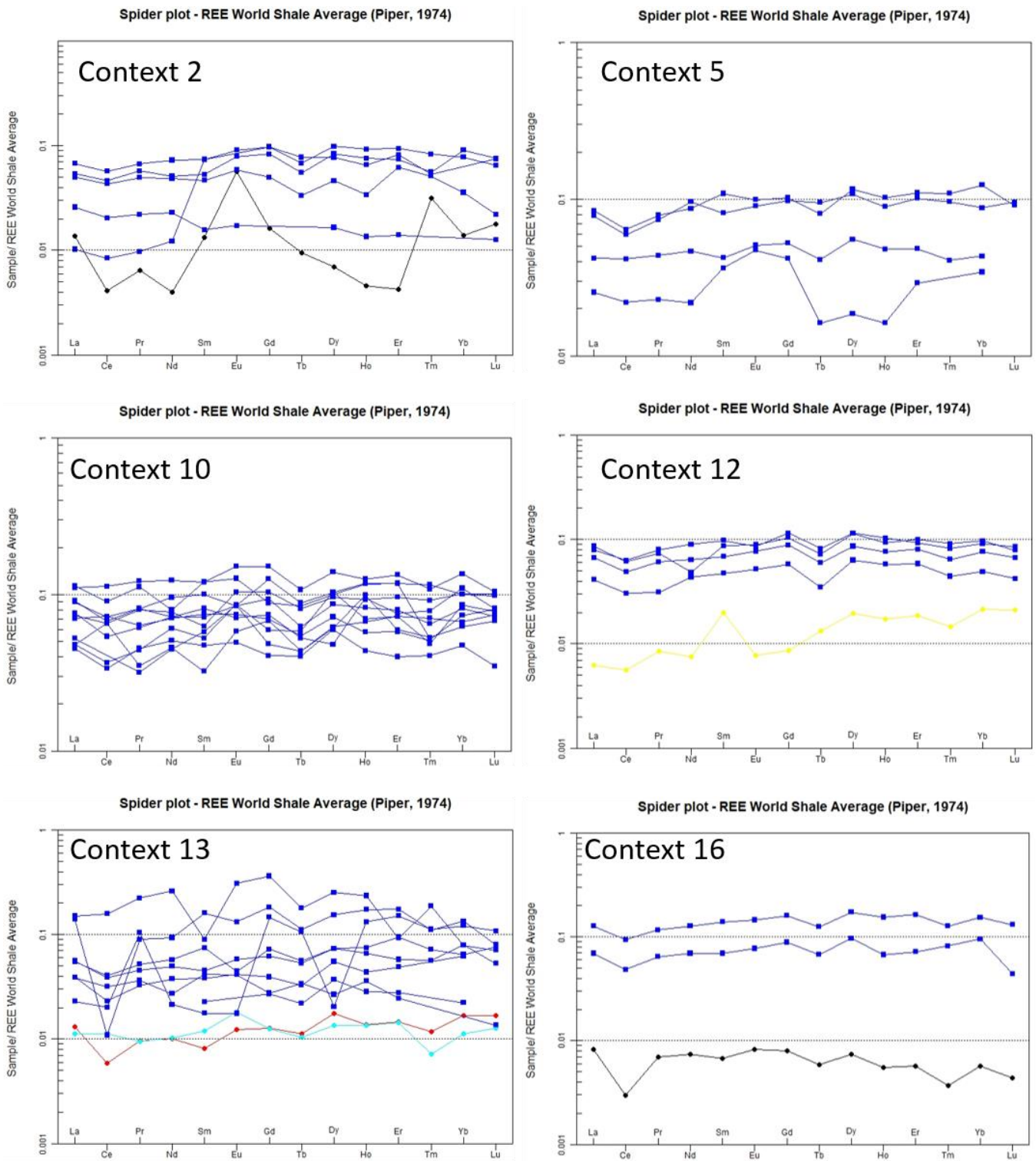


Figure 210: The normalised patterns of rare earth elements of the Skorba artefact samples from context2 to 16.

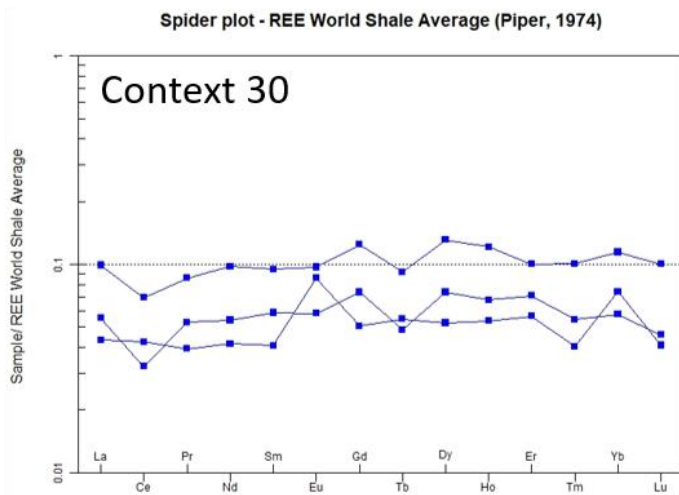
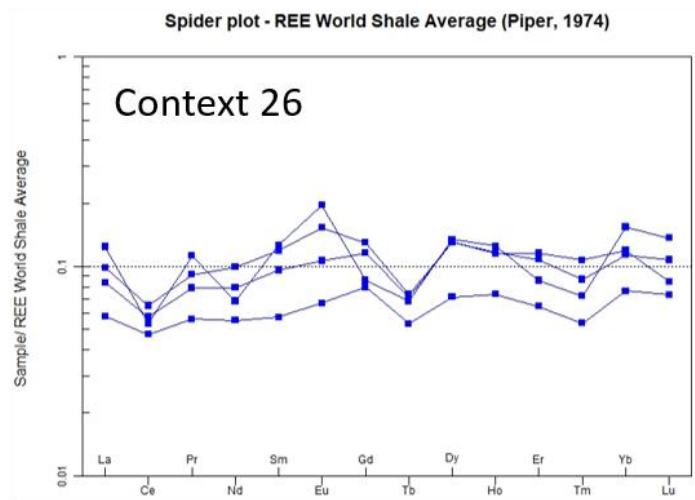
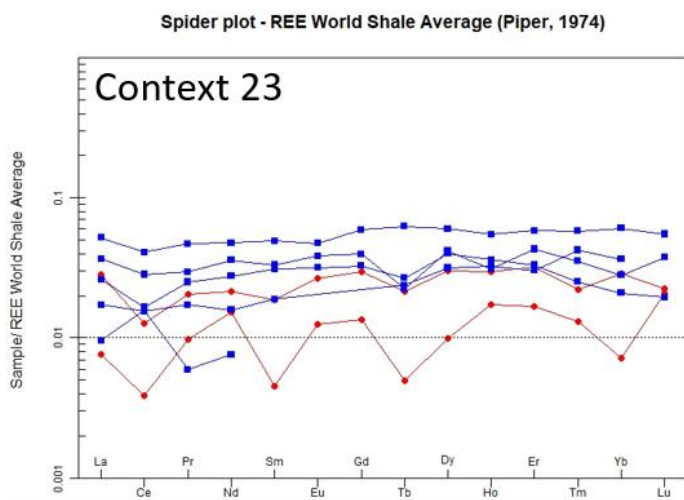
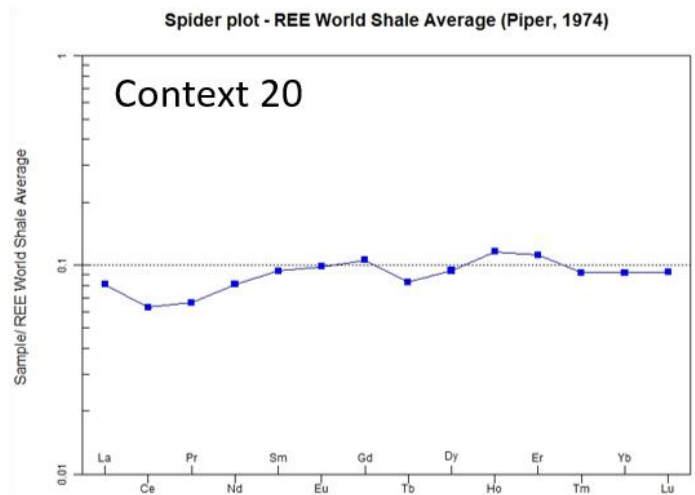
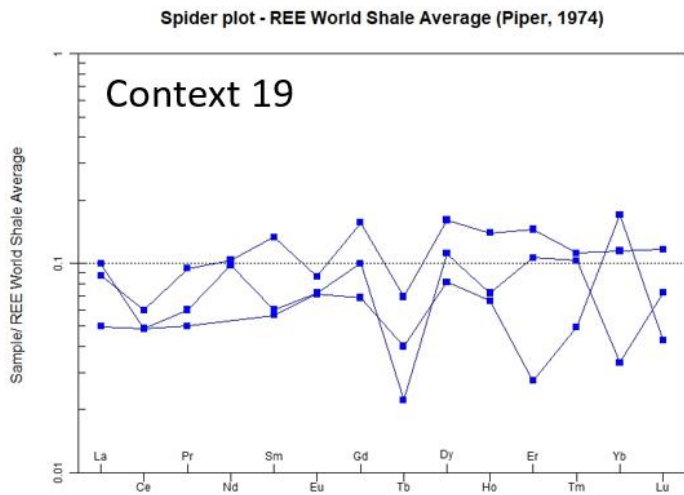


Figure 211: The normalised patterns of rare earth elements of the Skorba artefact samples from context 19 to 30.

APPENDIX II
(Protocols)

FTIR Laboratory Protocol

McBurney Laboratory

David Friesem (3/02/2017)

Equipment required

- Computer with OMNIC software
- FTIR instrument iS5
- Measurement accessory iD1 (for KBr method)
- Measurement accessory iD7 ATR (for ATR method)
- Hydraulic press
- Sample holder
- Agate mortar and pestle
- 7mm die holder (2 pieces)
- Weighing paper
- Kimwipes
- 2x Stainless spatula – micro-spoon
- Infrared red lamp (250W 230-250V)
- Few micrograms of Potassium Bromide (KBr – IR grade)
- Few drops of Hydrochloride acid (HCl 1N) (obtain from Pitt-Rivers Laboratory, Courtyard Building)
- Few drops of distilled water (H₂O) (re-fill available in Pitt-Rivers Laboratory, Courtyard Building)
- Few drops of Acetone (obtain from WB B5 thin section prep lab)

FTIR analysis procedure

- Place the measurement accessory [iD1 Transmission / iD7 ATR] in the middle of the iS5 instrument and make sure it is clear from any sample
- Open OMNIC in the computer
- Experiment setup should be
 - o For KBr method: iD1_Transmission.exp
 - o For ATR method: iD7_ATR_Diamond KBr iS5.exp
- Check that the system status system status in the upper right side of screen is green
 - o If it is red, please do not use the instrument and contact Tonko, Charly or David (df360@cam.ac.uk)
- Press “Col Bkg” in the left side of the upper toolbar to collect background
- Make sure there is no sample in the measurement accessory then press “OK”
- Wait for the instrument to measure
- Press “No” for not adding the background to your window
- Prepare sample (see below)
- Put the sample for measurement in the measurement accessory
- Press “Col Smp” in the left side of the upper toolbar
- Insert the sample name, then press “OK”
- Make sure your sample is placed correctly and press “OK”
- Wait for the instrument to measure
- Press “Yes” for adding the spectrum to the window
- Press “Save” to save the spectrum in your personal folder
- You can now run some macro and print your spectrum by using the icons in the upper toolbar
- Press “Clear” to remove the spectrum from display

Sample preparation (KBr method)

- Take about one gram of material
- Grind it gently into powder using the agate mortar and pestle
- Wipe of the material from the mortar using Kimwipes leaving few micrograms
- Turn on the red lamp

RED LAMP – DURATION: 15min MAX. use / DISTANCE: 30cm MIN.

- Open the glass vial with KBr and leave it open under the red lamp
- Take few micrograms of KBr into the mortar and mix it with the sample using the pestle
- Take the bottom die holder (the one with a rim at the bottom) and place it on the table
- Insert the die on the die holder pin
- Using a weight paper take the sample with the KBr and fill the die hole
- Place the top die holder (with a flat top) on top with its pin pressing the sample
- Carefully take the die and die holders and place them together on the press
- Close the top knob
- Screw in the front knob until the meter reach 1.8 tone
- Wait 5 seconds
- Release the front knob and check pressure is reduced
- Open the top knob and take the die and die holders
- Remove the die from the holders
- Place the die in the sample holder inside the measurement accessory (iD1)
- MEASURE SAMPLE (see above)
- Once finished, take out the die from the sample holder
- Remove the sample from the die using a spatula
- Make sure the die is completely clean from any sample remains using a Kimwipe
- Clean the mortar and pestle with few drops of HCl 1N
- Wash the mortar and pestle with distilled water (H₂O)
- Wipe with Kimwipe the mortar and pestle
- Apply few drops of Acetone to the mortar
- Place it under the red lamp to dry

Do not forget in the end to close the KBr and turn off the red lamp

Do not forget to leave the die, die holders, mortar and pestle clean from any sample residues

Sample preparation (ATR method)

- Take about one gram of material
- Grind it gently into powder using the agate mortar and pestle
- Make sure the silver round measurement platform is located in the centre of the measurement accessory (iD7)
- Using a spatula put the sample on the crystal in the centre of the measurement platform
- Make sure the pin attached to the screw is above the sample
- Close the screw down with the knob until it 'clicks'
- MEASURE SAMPLE (see above)
- Once finished, release the screw up using the knob
- Remove the sample from measurement platform using Kimwipes
- Clean the crystal with wet Kimwipe of few drops of HCl 1N
- Use another wet Kimwipe with distilled water (H₂O)
- Wipe with dry Kimwipe

Do not forget to leave the measurement platform and sink clean from any sample residues